

BELARUSIAN STATE UNIVERSITY  
VIENNA UNIVERSITY OF TECHNOLOGY  
RESEARCH INSTITUTE FOR APPLIED PROBLEMS  
OF MATHEMATICS AND INFORMATICS  
BELARUSIAN REPUBLICAN FOUNDATION  
FOR FUNDAMENTAL RESEARCH  
BELARUSIAN STATISTICAL ASSOCIATION

# COMPUTER DATA ANALYSIS AND MODELING

## STOCHASTICS AND DATA SCIENCE

PROCEEDINGS OF THE TWELFTH INTERNATIONAL CONFERENCE  
MINSK, SEPTEMBER 18–22, 2019

Minsk  
BSU  
2019

UDC 519.2

E D I T O R S:

Prof. Dr. *P. Filzmoser*, Prof. Dr. *Yu. Kharin*

Computer Data Analysis and Modeling: Stochastics and Data Science : Proc. of the Twelfth Intern. Conf., Minsk, Sept. 18–22, 2019. — Minsk : BSU, 2019. — 355 p. ISBN 978-985-566-811-5.

This collection of papers includes proceedings of the Twelfth International Conference “Computer Data Analysis and Modeling: Stochastics and Data Science” organized by the Belarusian State University and held in September 2019 in Minsk. Papers are reviewed by qualified researchers from Austria, Belarus, Lithuania, Russia, Ukraine.

The papers are devoted to the topical problems: robust and nonparametric data analysis; statistical analysis of time series and forecasting; multivariate data analysis; design of experiments; probability and statistical analysis of discrete data; econometric analysis and modeling; survey analysis and official statistics; computer intensive methods, algorithms and software; computer data analysis in applications.

For specialists who work in the fields of mathematical statistics and its applications, computer data analysis, data science and statistical software development.

**UDC 519.2**

ISBN 978-985-566-811-5

© BSU, 2019

# PROGRAM COMMITTEE

## Honorary Chair

**A. Karol** — Rector of the Belarusian State University (Minsk, Belarus)

## Co-Chairs

Prof. Dr. P. Filzmoser (Vienna, Austria)

Prof. Dr. Yu. Kharin (Minsk, Belarus)

## Conference Secretary

V. Malugin (Minsk, Belarus)

## Members

S. Aivazian (Moscow, Russia)	K. Kubilius (Vilnius, Lithuania)
W. Charemza (Leicester, UK)	A. Kukush (Kiev, Ukraine)
D. Chibisov (Moscow, Russia)	B. Lemeshko (Novosibirsk, Russia)
C. Croux (Leuven, Belgium)	Yu. Mishura (Kiev, Ukraine)
K. Ducinkas (Klaipeda, Lithuania)	V. Mkhitarian (Moscow, Russia)
G. Dzemyda (Vilnius, Lithuania)	S. Morgenthaler (Lausanne, Switzerland)
A. Egorov (Minsk, Belarus)	V. Mukha (Minsk, Belarus)
R. Fried (Dortmund, Germany)	H. Oja (Turku, Finland)
K. Fokianos (Lancaster, UK)	Yu. Pavlov (Petrozavodsk, Russia)
K. Hron (Olomouc, Czech Republic)	G. Shevlyakov (St.-Petersburg, Russia)
T. Kollo (Tartu, Estonia)	E. Stoimenova (Sofia, Bulgaria)
A. Kharin (Minsk, Belarus)	M. Templ (Winterthur, Switzerland)
V. Krasnoproshin (Minsk, Belarus)	N. Trough (Minsk, Belarus)
M. Krzysko (Poznan, Poland)	A. Zubkov (Moscow, Russia)

## Local Organizing Committee

### Chair

T. Soboleva, Vice Dean of the Faculty of Applied Mathematics and Informatics

### Co-Chairs

A. Kharin, Head of the Department of Probability Theory and Mathematical Statistics

I. Badziahin, Head of the Department of Mathematical Modeling and Data Analysis

### Members

O. Dernakova, T. Tsekhavaya, M. Kislach, U. Palukha, Ya. Viachorka, O. Golos,  
S. Staleuskaya, T. Varatnitskaya, I. Pirshtuk, V. Voloshko

*To the 70-years Jubilee  
of Prof. Dr. Yuriy Kharin,  
Correspondent Member  
of the National Academy of Sciences of Belarus,  
the Principal Organizer  
of the Conference Series on Computer Data Analysis and Modeling*



# Yuriy S. Kharin

born in Zyrianskoe village, Tomsk Region, Russian Federation 17.09.1949

## Education

Secondary School, Tomsk (Medal in Gold) 1966  
Tomsk State University (Honours Diploma) 1971  
Ph.D. in Physics and Mathematics, Tomsk State University 1974  
Dr.Sc. in Physics and Mathematics, Keldysh Institute  
for Applied Mathematics, Russian Academy of Sciences, Moscow 1986

## Academic Titles

Associate Professor 1978  
Full Professor 1990  
Correspondent Member, National Academy of Sciences 2004

## Positions

Senior Lecturer, then Associate Professor,  
Department of Applied Mathematics, Tomsk State University 1974–1976  
Associate Professor, then Professor,  
Department of Probability Theory & Mathematical Statistics,  
Belarusian State University (BSU), Minsk 1976–1988  
Organizer and Head  
of the Dept. of Mathematical Modeling & Data Analysis, BSU, Minsk 1988–2018  
Organizer and Director of the Research Institute  
for Applied Problems of Mathematics and Informatics, BSU, Minsk 2000–present

## Memberships

Belarusian Statistical Association (Organizer and Head in 1998–2009) 1998–present  
Belarusian Mathematical Society 2001–present  
American Mathematical Society 1996–present  
International Institute of Mathematical Statistics 1996–present  
International Statistical Institute 1996–present  
Bernoulli Society 2000–present  
Association for Computing Machinery 2001–present

## Honours

A.N. Sevchenko Prize Laureate 1997  
Excellence in Education of the Republic of Belarus 1999  
State Prize Laureate in Science and Engineering, Republic of Belarus 2002  
Honoured Scientist of Belarus 2010  
Honoured Worker of the Belarusian State University 2013

## Publications

Monographs and Textbooks 35  
Papers in scientific journals > 300

## Teaching

Ph. D. and Dr. Hab. dissertations supervised 34

# PREFACE

The Twelfth International Conference “Computer Data Analysis and Modeling: Stochastics and Data Science” (CDAM’2019) organized by the Belarusian State University on September 18-22, 2019, is devoted to the topical problems in computer data analysis and modeling. Methods of computer data analysis and modeling are widely used in variety of fields: computer support of scientific research; decision making in economics, business, engineering, medicine and ecology; statistical modeling of complex systems of different nature and purpose. In the Republic of Belarus computer data analysis and modeling have been developed successfully for more than 30 years. Scientific conferences CDAM were held in September 1988, December 1990, December 1992, September 1995, June 1998, September 2001, September 2004, September 2007, September 2010, September 2013, and September 2016 in Minsk.

The Proceedings of the CDAM’2019 contain 73 papers. The topics of the papers correspond to the following scientific problems: robust and nonparametric statistical analysis of time series and forecasting, multivariate data analysis, statistical classification and pattern recognition, signal processing, statistical modeling, modeling of complex systems in different applications, statistics in economics, finance and other fields, software for data analysis and statistical modeling.

The Organizing Committee of the CDAM’2019 makes its acknowledgements to Belarusian State University, Research Institute for Applied Problems of Mathematics and Informatics, Belarusian Republican Foundation for Fundamental Research, Vienna University of Technology, Belarusian Science and Technology Association “Infopark”, SDC “Itransition”, and BSB Bank for financial support.

Peter Filzmoser  
Alexey Kharin  
Vladimir Malugin

# CONTENTS

## INVITED PLENARY PAPERS

<b>Barbiero A.</b> Inducing a target association between ordinal variables by using a parametric copula family . . . . .	13
<b>Dučinskas K., Dreiziene L.</b> Spatial model selection based on hybrid performance measure of linear classifier . . . . .	17
<b>Dürre A., Fried R.</b> Detecting changes in the dependence structure of a time series . . . . .	21
<b>Dzemyda G., Sabaliauskas M.</b> New method to minimize the stress in multidimensional scaling . . . . .	29
<b>Filzmoser P., Brodinová Š., Ortner T., Breitender C., Rohm M.</b> Robust and sparse k-means clustering for high-dimensional data . . . . .	32
<b>Gammerman A.</b> Conformal predictors for reliable pattern recognition . . . . .	33
<b>Grimes T., Datta S.</b> A random graph generation model for transcription networks and nonparametric simulator for RNA-seq expression data . . . . .	37
<b>Groenen P.J.F., van den Burg G.J.J.</b> Multiclass support vector machines with GenSVM . . . . .	43
<b>Kharin Yu.S.</b> Discrete-valued time series analysis by parsimonious high-order Markov chains . . . . .	51
<b>Kollo T., von Rosen D., Valge M.</b> Testing structure of the covariance matrix: a non-normal approach . . . . .	65
<b>Kubilius K.</b> Hurst parameter estimation in fractional diffusion models . . . . .	68
<b>Li P., Maiti T.</b> Functional graphical model classification . . . . .	71
<b>Lietzén N., Virta J., Nordhausen K., Ilmonen P.</b> Minimum distance index for non-square complex valued mixing matrices . . . . .	79
<b>Machalová J., Talská R., Hron K.</b> Approximation of density functions using simplicial splines . . . . .	87
<b>Mishura Yu.</b> Fractional stochastic volatility: F-Ornstein–Uhlenbeck and F-CIR processes . . . . .	94
<b>Orsingher E.</b> Some results on the Brownian meander . . . . .	102
<b>Rattihalli R.N., Raghunath M.</b> Power skew symmetric distributions: tests for symmetry . . . . .	104

<b>Sakhno L.M.</b> Investigation of conditions for asymptotic normality of spectral estimates .....	115
<b>Shevlyakov G.L., Shirokov I.S., Litvinova V.G.</b> Robust analogs of the $Q_n$ -estimate of scale for the Student distributions .....	117
<b>Stoimenova E.</b> On the upper bound of the risk in selection of the $T$ best items .	123
<b>Zubkov A.M.</b> Recent results on the total variation distance .....	128

## CONTRIBUTED PAPERS

<b>Abdushukurov A.A.</b> Estimation of conditional survival function under dependent random censored data.....	133
<b>Abramovich M.S., Kozlovsky V.V., Stelmashok V.I., Polonetsky O.L.</b> Predicting the success of antegrade chronic total occlusion recanalization using machine learning .....	138
<b>Badziahin I.A.</b> On parameter estimation of double-censored stationary Gaussian time series .....	142
<b>Belovas I.</b> Modeling baltic market indices: a comparison of models.....	144
<b>Bokun N.</b> Tourism in Belarus: indicators, satellite account and surveys .....	148
<b>Dermenzhy I., Vostrov G.</b> Probabilistic approach in factorization by elliptic curve method .....	154
<b>Egorov A.D., Zherelo A.V.</b> Approximate formulas for expectation of functionals from solution to linear Skorohod stochastic differential equation .....	158
<b>Fedotkin M.A., Kudryavtsev E.V.</b> Simulation of adaptive control system with conflict flows of non-homogeneous requests .....	163
<b>Hubin A., Storvik G., Grini P., Butenko M.</b> Bayesian binomial regression model with a latent Gaussian field for analysis of epigenetic data .....	167
<b>Karaliutė M., Dučinskas K., Šaltytė-Vaisiauskė L.</b> Expected error rate in linear discrimination of balanced spatial Gaussian time series .....	172
<b>Kharin Yu.S., Dernakova O.V.</b> On statistical estimation of transition probabilities matrix for Markov chain under incomplete observations .....	176
<b>Kharin Yu.S., Kislach M.I.</b> Statistical analysis of count conditionally nonlinear autoregressive time series by frequencies-based estimators .....	183
<b>Kharin A.Yu., Ton That Tu</b> Performance and robustness in sequential testing of hypotheses .....	187

<b>Kolchin A.V., Ionkina H.G.</b> On some new aspects in acquisition and analysis of brain electrical activity .....	191
<b>Kopats D., Matalytski M.</b> Application of open Markov networks with various features at modeling real objects .....	194
<b>Kornet M.E., Medvedev A.V., Mihov E.D.</b> About the processes in the changing fractional dimension space.....	199
<b>Kostogryzov A., Nistratov A., Nistratov G.</b> Probabilistic data analysis for predicting mean time before critical integrity losses of complex system when explicit quantitative requirements to integrity are not specified .....	203
<b>Krasnoproshin V.V., Matskevich V.V.</b> Statistical approach to image compression based on a restricted Boltzmann machine .....	207
<b>Kulyukin V.A., Mukherjee S., Vats P., Tiwari A., Burkatovskaya Y.B.</b> Classification of Motion Regions with Convolutional Networks, Support Vector Machines, and Random Forests in Video-Based Analysis of Bee Traffic..	214
<b>Levakov A.A., Vaskouski M.M., Kachan I.V.</b> Asymptotic expansions of solutions of mixed type SDE driven by fractional Brownian motions for small times .....	219
<b>Lohvinenko S.S.</b> Statistical properties of parameter estimators in the fractional Vasicek model.....	224
<b>Malugin V.I., Novopoltsev A.Yu., Hryn N.V.</b> Analysis of financial stability of the Belarusian economy based on microdata and expert information .....	228
<b>Mangalova E., Chubarova O., Melekh D.</b> Influence of the training set on the prediction stability in estimation of acute pancreatitis severity .....	232
<b>Medvedev A.V., Tereshina A.V., Yaresenko D.I.</b> Nonparametric modelling of multidimensional memoryless processes .....	237
<b>Mihov E.D.</b> Finding significant variables in the problems of modelling less memory processes.....	242
<b>Mikšová D., Rieser C., Filzmoser P.</b> Identification of mineralization in geochemistry based on the spatial curvature of log-ratios.....	246
<b>Minkevičius S.</b> Fluid limits for the waiting time of a customer in multiphase queues .....	249
<b>Mukha V.S., Kako N.F.</b> Integrals related to the multidimensional-matrix Gaussian distribution .....	253
<b>Navickas G., Korvel G., Bernatavičienė J.</b> Overview of speech synthesis using LSTM neural networks.....	257
<b>Nikitionak V.I., Vetokhin S.S., Bakhar A.M., Tereshko E.V.</b> Comparative analysis of optimal algorithms treatment of stationary Poisson fluxes .....	262

<b>Novopoltsev A.Yu.</b> Using credit history data to monitor financial stability of the Belarusian economy .....	267
<b>Podolskiy V.A., Turovskiy Ya.A., Alekseev A.V., Mikhalskii A.I.</b> Use of variability of the heart rhythm for predicting the success of the operator's work when using human-machine interfaces.....	271
<b>Poleshchuk E.A.</b> Problems of the formation of the system of environmental-economic accounting .....	276
<b>Radavičius M.</b> Structural distribution estimation.....	280
<b>Ralchenko K.</b> Drift parameter estimation in Gaussian regression model by continuous and discrete observations.....	285
<b>Savelov M.P.</b> A set of asymptotically independent statistics of polynomial frequencies containing the Pearson statistic .....	289
<b>Serov A.A., Zubkov A.M.</b> Testing the NIST Statistical Test Suite on artificial pseudorandom sequences .....	291
<b>Soshnikova L.A.</b> Adaptive methods for forecasting currency courses .....	295
<b>Starodubtsev I.E., Kharin Yu.S., Starodubtseva M.N.</b> Statistical classification of the states of biological cells treated with carbon nanotubes based on AFM-images of cell surface.....	298
<b>Tsekhavaya T.V., Trough N.N.</b> Internally homogeneous random fields analysis	302
<b>Venskus J., Treigys P.</b> Meteorological data influence on missing vessel type detection using deep multi-stacked LSTM neural network.....	307
<b>Voloshko V.A., Vecherko E.V.</b> On some upper bounds for noncentral chi-square cdf.....	311
<b>Vorobeychikov S.E., Burkatovskaya Yu.B.</b> Non-asymptotic confidence estimation of the autoregressive parameter in AR(1) process with an unknown noise variance.....	315
<b>Vostrov G., Opiata R.</b> A generalized probabilistic model of computer proof of the Artin hypothesis .....	319
<b>Vostrov G., Ponomarenko O.</b> Stochastic analysis of the smooth number properties and their search.....	326
<b>Yanovich L.A., Ignatenko M.V.</b> Some formulas of operator interpolation on the set of random processes .....	330
<b>Zakhidov D.G., Iskandarov D.Kh.</b> Empirical likelihood confidence intervals for censored integrals.....	335
<b>Zhuk E.E.</b> Principle components method in statistical classification and its efficiency.....	337

<b>Zikarienė E., Dučinskas K.</b> Implementation of generalized additive models for spatial beta regression.....	341
<b>Zorine A.V.</b> Regenerative simulation of time-sharing queueing system in random environment .....	344
<b>Zubkov A.M., Kruglov V.I.</b> Number of pairs of identically marked templates in $q$ -ary tree .....	348
<b>Zuev N.M.</b> Formula for European options costs calculation .....	352
<b>Index</b> .....	354

# **INVITED PLENARY PAPERS**

# INDUCING A TARGET ASSOCIATION BETWEEN ORDINAL VARIABLES BY USING A PARAMETRIC COPULA FAMILY

A. BARBIERO

*Università degli Studi di Milano*

*Milan, ITALY*

e-mail: `alessandro.barbiero@unimi.it`

## Abstract

The need for building and generating statistically dependent random variables arises in various fields of study where simulation has proven to be a useful tool. In this work, we present an approach for constructing ordinal variables with arbitrary marginal distributions and association, expressed in terms of either Goodman and Kruskal's gamma or Pearson's linear correlation.

**Keywords:** data science, ordinal variables, copula

## 1 Introduction

The need for building and generating statistically dependent random variables arises in various fields of study where simulation has proven to be a useful tool. The ability to simulate data resembling observed data is fundamental to compare and investigate the behaviour of statistical procedures when analytical results are not derivable or are cumbersome to derive.

Many datasets, especially those arising in the social sciences, often contain ordinal variables. Sometimes they are genuine ordered assessments (judgements, preferences, degree of liking, etc.) whereas in other circumstances they are discretized or categorized for convenience (e.g., age of people in classes or education achievement). There are several statistical models and techniques that can be employed for handling multivariate ordinal data without trying to quantify their ordered categories: [1] gives a thorough treatment. Among them, correlation models and association models both study departures from independence in contingency tables and involve the assignment of scores to the categories of the row and column variables in order to maximize the relevant measure of relationship (the correlation coefficient in the correlation models or the measure of intrinsic association in association models [5]). Alternatively, one can code the ordered categories as integers numbers  $(1, 2 \dots, m)$ : This amounts to assuming that the categories are evenly spaced.

In this work, we present an approach for constructing ordinal variables with arbitrary marginal distributions and association, expressed in terms of either Goodman and Kruskal's gamma or Pearson's linear correlation. Similar proposals have been already suggested by [7], when dealing with ordinal variables and Goodman and Kruskal's gamma, and by [2, 8, 4] for ordinal (and count) variables and Pearson's correlation.

## 2 Statement of the problem

We consider two ordinal random variables (rvs),  $X$  and  $Y$ , with  $h$  and  $k$  ordered categories, respectively, with marginal distributions  $p_i = P(X = x_i), i = 1, \dots, h$ , and  $p_j = P(Y = y_j), j = 1, \dots, k$ . We want to determine *some* joint probability distribution  $p_{ij} = P(X = x_i, Y = y_j), i = 1, \dots, h, j = 1, \dots, k$ , such that its margins are actually  $p_i$  and  $p_j$ , and with an assigned level of association.

Being  $X$  and  $Y$  ordinal variables, the association can be naturally expressed through the Goodman and Kruskal's gamma [6]. Considering two independent realizations  $(X_s, Y_s)$  and  $(X_t, Y_t)$  of  $(X, Y)$ , Goodman and Kruskal's gamma is defined as

$$\gamma = \frac{\Pi_c - \Pi_d}{\Pi_c + \Pi_d},$$

where  $\Pi_c$  is the probability of concordance:

$$\Pi_c = Pr \{X_s < X_t \text{ and } Y_s < Y_t\} + Pr \{X_s > X_t \text{ and } Y_s > Y_t\}$$

and  $\Pi_d$  the probability of discordance:

$$\Pi_d = Pr \{X_s < X_t \text{ and } Y_s > Y_t\} + Pr \{X_s > X_t \text{ and } Y_s < Y_t\}.$$

$\Pi_c$  and  $\Pi_d$  can be expressed in terms of the joint probabilities  $p_{ij}$ .  $\gamma$  take values in the  $[-1, +1]$  interval; in particular, the values  $-1, 0$ , and  $+1$  are attained when  $\Pi_c = 0, \Pi_c = \Pi_d, \Pi_d = 0$ , respectively.

If we treat  $X$  and  $Y$  as point-scale discrete variables, by assigning the first  $h$  and  $k$  positive integers, respectively, to their ordered categories, then we can use Pearson's correlation coefficient as a measure of association:

$$\rho = (\mathbb{E}(XY) - \mathbb{E}(X)\mathbb{E}(Y))(\text{Var}(X)\text{Var}(Y))^{-1/2}$$

with  $\mu_X = \mathbb{E}(X) = \sum_{i=1}^h ip_i$ ,  $\text{Var}(X) = \sum_{i=1}^h (i - \mu_X)^2 p_i$ . (analogous results hold for  $Y$ ), and  $\mathbb{E}(XY) = \sum_{i=1}^h \sum_{j=1}^k ij p_{ij}$ . Like  $\gamma$ , also Pearson's correlation takes values in the  $[-1, +1]$  interval; however, given two marginal distributions and a value  $\rho \in [-1, +1]$ , it is not always possible to construct a joint distribution with those assigned margins, whose correlation is equal to the assigned  $\rho$  [9]. In more detail, the attainable correlations form a closed interval  $[\rho_{\min}, \rho_{\max}]$  with  $\rho_{\min} < 0 < \rho_{\max}$ . The minimum correlation  $\rho = \rho_{\min}$  is attained if and only if  $X$  and  $Y$  are countermonotonic; the maximum correlation  $\rho = \rho_{\max}$  is attained if and only if  $X$  and  $Y$  are comonotonic. Moreover,  $\rho_{\min} = -1$  if and only if  $X_1$  and  $-X_2$  are of the same type, and  $\rho_{\max} = 1$  if and only if  $X_1$  and  $X_2$  are of the same type. Given the two margins, a correlation  $\rho$  is said "feasible" if it falls within  $[\rho_{\min}, \rho_{\max}]$ .

## 3 A solution to the problem employing copulas

Finding a joint probability distribution with assigned margins and a desired (feasible) value of association is equivalent to solving a system in  $h \times k$  unknowns, the  $p_{ij}$ ,

belonging to the standard simplex, subject to  $h + k - 1$  constraints corresponding to the assigned margins and one further constraint dictated by the desired association. This system, when  $h$  or  $k$  is greater than 2, has infinite solutions, which can be recovered more easily when using Pearson's correlation as a measure of association, being it a linear function in the  $p_{ij}$ .

Here we propose an approach to identify just one solution, i.e., one joint distribution. This procedure relies on one-parameter bivariate copulas, which allow to split the original problem into two sequential steps: first, identifying a class of joint distributions respecting the assigned margins; then, within this class, finding the joint distribution matching the desired level of association.

### 3.1 Selecting a class of joint distributions having the pre-specified margins

As for the first step, if  $F_1$  and  $F_2$  are the distribution functions of two rvs  $X$  and  $Y$ , and  $C(u, v; \theta)$  is a bivariate parametric copula family, characterized by some scalar parameter  $\theta$ , the function

$$F(x, y) = C(F_1(x), F_2(y); \theta), \quad x, y \in \mathbb{R}, \quad (1)$$

defines a valid joint distribution function, whose margins are exactly  $F_1$  and  $F_2$ . This result keeps holding if  $X$  and  $Y$  are discrete; in this case, the joint probabilities can be derived from (1) as:

$$p_{ij} = F(i, j) - F(i - 1, j) - F(i, j - 1) + F(i - 1, j - 1),$$

for  $i = 1, \dots, h; j = 1, \dots, k$ . In order to induce any feasible value of association between the two discrete margins, we have further to impose that the copula  $C(u, v; \theta)$  is able to encompass the entire range of dependence, from perfect negative dependence to perfect positive dependence.

### 3.2 Inducing the desired value of association

As for the second step, the association between  $X$  and  $Y$  now depends only on the copula parameter  $\theta$ ; this relationship may be written in an analytical or numerical form, say  $\gamma = f(\theta)$ , or  $\rho = g(\theta)$ . Since the function  $f$  (or  $g$ ) is not usually analytically invertible, inducing a desired feasible value of association, by setting an appropriate value of  $\theta$ , is a task that can be generally done only numerically, by finding the (unique) root of the equation  $f(\theta) - \gamma = 0$  (or  $g(\theta) - \rho = 0$ ). If  $\gamma$  (or  $\rho$ ) is a monotone increasing function of the copula parameter, and this is often the case (e.g., for the Gauss, Frank, and Plackett copulas), one can implement some iterative procedure that is more efficient than the standard bisection method. For discrete random variables, several proposals have been suggested for matching a desired value of Pearson's correlation, see [2, 8, 4].

Simulating from the selected joint distribution is straightforward, by resorting to preliminary simulation of copulas or more easily to a direct inversion algorithm [3, 7].

## References

- [1] Agresti A. (2010). *Analysis of ordinal categorical data*. John Wiley & Sons, New York.
- [2] Demirtas H. (2006). A method for multivariate ordinal data generation given marginal distributions and correlations. *Journal of Statistical Computation and Simulation*. Vol. **76(11)**, pp. 1017-1025.
- [3] Devroye L. (1986). *Non-Uniform Random Variate Generation*. Springer, New York.
- [4] Ferrari P.A., Barbiero A. (2012). Simulating ordinal data. *Multivariate Behavioral Research*. Vol. **47(4)**, pp. 566-589.
- [5] Faust K., Wasserman S. (1993). Correlation and Association Models for Studying Measurements on Ordinal Relations. *Sociological Methodology*. Vol. **23**, pp. 177-215.
- [6] Goodman L.A., Kruskal W.H. (1954). Measures of association for cross classifications. *Journal of the American Statistical Association*. Vol. **49**, pp. 732-764.
- [7] Lee A.J. (1997). Some methods for generating correlated categorical variates. *Computational Statistics and Data Analysis*. Vol. **26**, pp. 133-148.
- [8] Madsen L., Dalthorp D. (2007). Simulating correlated count data. *Environmental and Ecological Statistics*. Vol. **14(2)**, pp. 129-148.
- [9] McNeil A., Frey R., Embrechts P. (2005). *Quantitative risk management. Concepts, Techniques and Tools*. Princeton Series in Finance, Princeton.

# SPATIAL MODEL SELECTION BASED ON HYBRID PERFORMANCE MEASURE OF LINEAR CLASSIFIER

K. DUČINSKAS<sup>1,2</sup>, L. DREIZIENE<sup>1,3</sup>

<sup>1</sup>*Klaipeda University*

<sup>2</sup>*Vilnius University*

<sup>3</sup>*Lithuanian Maritime Academy*

*Klaipeda, Vilnius, LITHUANIA*

e-mail: k.ducinkas@gmail.com, l.dreiziene@gmail.com

## Abstract

Assuming that spatial data is generated by Gaussian random field (GRF), the problem of classifying its observation into one of two populations is considered. Populations are specified by the common regressors but different regression parameters. Authors concern with classification procedures associated with Bayes discriminant function (BDF) and its sample version (SDF). The average of plug-in and apparent correct classification rates is considered as performance measure of classifier based on SDF. Various types of spatial data models for invasive species (*zebra mussels*) distributed in the Curonian Lagoon are considered and ranked by the defined criterion. Advanced models are proposed to the mapping of presence and absence of zebra mussels in the Curonian Lagoon.

**Keywords:** spatial model, data science, linear classifier, Gaussian random field

## 1 Introduction

Classification of spatial data has been mentioned in the ecological literature, but lacks full mathematical treatment and easily available algorithms and software. This paper fills this gap by defining the method of statistical classification based on BDF by providing novel formulas and algorithms, which allows to evaluate the influence of spatial information to the performance of proposed classifier. Performance of the classifier based on SDF in the complete parametric uncertainty case is implemented by Ducinkas and Dreiziene (2011). Numerical comparison of the performances for different spatial classification rules is performed by Berrett and Calder (2016). In the present paper we focus on linear classification problem of GRF observation for the so-called geostatistical model (GS) with continuous spatial index and directly specified parametric covariance functions. It should be noted that classification of spatial lattice data modeled by conditionally autoregressive models is recently explored by Ducinkas and Dreiziene (2018). The average of the plug-in and apparent correct classification rates (AVER) is considered as an hybrid estimator for the classifiers based on SDF. These are used in comparison and selection of the spatial linear models for spatial ecological data. Spatial distribution and spread of invasive species (*zebra mussels*) in lagoons and bays are interested a lot of ecologists (see, e.g. Zaiko, Daunys 2015). In the present paper three spatial linear models for zebra mussels distributed in the Curonian Lagoon are considered and compared by proposed performance measure.

## 2 The Main Concepts and Definitions

In this paper we focus on classification of a single scalar GRF  $\{Z(s) : s \in D \subset R^2\}$  observation, when training sample is given. The model of observation  $Z(s)$  in population  $\Omega_l$  is  $Z(s) = x'(s)\beta_l + \varepsilon(s)$ , where  $x(s)$  is a  $q \times 1$  vector of non-random regressors and  $\beta_l$  is a  $q \times 1$  vector of parameters,  $l = 1, 2$ , and  $\beta_1 \neq \beta_2$ . The error term  $\varepsilon(s)$  is generated by zero-mean GRF  $\{\varepsilon(s) : s \in D\}$  with covariance function  $\sigma(s, t) = cov(\varepsilon(s), \varepsilon(t))$ , for  $s, t \in D$ .

Suppose that  $\{s_i \in D, i = 0, 1, \dots, n\}$  is the set of spatial sites where the observations of GRF are taken. Indexing spatial sites by integers i.e.  $s_i = i, i = 0, 1, \dots, n$ , denote the set of training sites by  $S_n = S^{(1)} \cup S^{(2)}$ , where  $S^{(1)} = \{1, 2, \dots, n_1\}$  and  $S^{(2)} = \{n_1 + 1, \dots, n_1 + n_2\}$ ,  $n = n_1 + n_2$ , are the subsets of  $S_n$  that contains  $n_l$  observations of  $Z(s)$  from  $\Omega_l, l = 1, 2$ . The location of the observation to be classified is indexed by  $\{0\}$ .

In what follows we use the notations  $Z(i) = Z_i, \varepsilon(i) = \varepsilon_i, x(i) = x_i, \sigma_{ij} = cov(Z_i, Z_j), i, j = 0, 1, \dots, n$  and  $\varepsilon = (\varepsilon_1, \dots, \varepsilon_n)'$ ,  $Z = (Z_1, \dots, Z_n)'$ . Define n-vector  $c_0$  and  $n \times n$  matrix  $\Sigma$  by  $c_0 = (\sigma_{01}, \sigma_{02}, \dots, \sigma_{0n})'$  and  $\Sigma = (\sigma_{ij}, i, j = 1, \dots, n)$ .

Put  $\beta' = (\beta'_1, \beta'_2)$ ,  $\alpha_0 = \Sigma^{-1}c_0$ , and denote by  $X$  the  $n \times 2q$  design matrix of training sample  $Z$ . Then the training sample  $Z$  has multivariate Gaussian distribution  $Z \sim N_n(X\beta, \Sigma(\theta))$ .

The main objective of this paper is to classify the single observation of scalar GRF  $\{Z(s) : s \in D \subset R^2\}$  at location  $s_0$  given training sample  $Z$ . Let  $z$  denote the realization of  $Z$ . Then the conditional distribution of  $Z_0$  given  $Z = z$  in  $\Omega_l$  is Gaussian with mean and variance

$$\mu_{lz}^0 = E(Z_0|Z = z; \Omega_l) = x'_0\beta_l + \alpha'_0(z - X\beta), \quad (1)$$

$$\sigma_{0z}^2(\theta) = \sigma_{00} - c'_0\Sigma^{-1}c_0. \quad (2)$$

For geostatistical data, spatial index  $s$  is assumed to vary continuously throughout the set  $D$ . Let  $\Psi = (\beta', \theta')$  denote the combined vector of population parameters. Under the assumption of complete parametric certainty of populations and for known prior probabilities of the populations the BDF maximizing the probability of correct classification is formed by log ratio of conditional likelihoods of  $Z_0$  at location  $s_0$ . Then BDF is specified by

$$W_z(Z_0, \Psi) = \left( Z_0 - 1/2(\mu_{1z}^0 + \mu_{2z}^0) \right) (\mu_{1z}^0 - \mu_{2z}^0) / \sigma_{0z}^2 + \gamma_0, \quad (3)$$

where  $\gamma_0 = \ln(\pi_1^0/\pi_2^0)$ .  $\pi_1^0$  and  $\pi_2^0$  are prior probabilities, and  $\pi_1^0 + \pi_2^0 = 1$ . Suppose that for  $l = 1, 2$ , the probability measure  $P_{lz}$  based on conditional Gaussian distribution of  $Z_0$  given  $Z = z, \Omega_l$  i.e.  $Z_0|Z = z, \Omega_l \sim N_l(\mu_{0z}^l, \sigma_{0z}^2)$ .

**Definition 1.** The probability of correct classification for the BDF  $W_z(Z_0, \Psi)$  is defined as  $PC(\Psi) = \sum_{l=1}^2 \pi_l P_l$ , where, for  $l = 1, 2, P_l = P_{lz}((-1)^l W_z(Z_0, \Psi) < 0)$ .

As it follows,  $PC(\Psi)$  will be called Bayes probability of correct classification (BPCC).

**Lemma 1.** Closed-form expression for BPCC is  $PC(\Psi) = \sum_{l=1}^2 \pi_l^0 \Phi(\Delta_0/2 - (-1)^l \gamma_0/\Delta_0)$ , where  $\Phi(\cdot)$  is the standard Gaussian distribution function and  $\Delta_0$  stands for conditional Mahalanobis distance between conditional distributions of  $Z_0$ , given  $Z = z$ .

Proof of Lemma 1 follows from Definition 1 and properties of Gaussian distribution.

In practice it is rarely the case that regression parameters vector  $\beta$  and covariance parameter vector  $\theta$  are known, and often we need to estimate these parameters from the training data. Here we use maximum likelihood (ML) method for estimation and corresponding estimators are denoted by  $\hat{\beta}$ ,  $\hat{\theta}$ , and  $\hat{\Psi} = (\hat{\beta}', \hat{\theta}')$ .

Then using (1), (2) we get the estimators of conditional mean and conditional variance

$$\hat{\mu}_{lz}^0 = E(Z_0|Z = z; \Omega_l) = x'_0 \hat{\beta}_l + \hat{\alpha}'_0(z - X \hat{\beta}), l = 1, 2, \hat{\sigma}_{0z}^2 = \sigma_{0z}^2(\hat{\theta}).$$

By replacing the parameters with their ML estimators in (3) we form the SDF  $W_z(Z_0, \hat{\Psi})$ .

Set for  $l = 1, 2$ ,  $\hat{P}_{lz}((-1)^l W_z(Z_0, \hat{\Psi}) < 0)$ . Then the actual correct classification rate for SDF  $W_z(Z_0, \hat{\Psi})$  is  $AR = \sum_{l=1}^2 \pi_l^0 \hat{P}_l$ .

Closed-form expression for AR is derived in Ducinkas and Dreiziene (2011).

**Definition 2.** Plug-in correct classification rates for the AR based on SDF is

$$PR = \sum_{l=1}^2 \left( \pi_l^0 \Phi(\hat{\Delta}_0/2 - (-1)^l \gamma_0/\hat{\Delta}_0) \right).$$

**Definition 3.** Apparent correct classification rates are defined by

$APR = \left( \sum_{i=1}^{n_l} H(W_z(Z_i, \hat{\Psi})) + \sum_{i=n_l+1}^n H(-W_z(Z_i, \hat{\Psi})) \right) / n$ , where  $H(\cdot)$  is the Heaviside step function.

We propose  $AVER = (PR + APR)/2$  consider as hybrid estimator of AR based on SDF for different linear models of spatial ecological data.

### 3 Model selection

In this section the application of the proposed estimators for model selection is considered. We use a real dataset of zebra mussels observed over the Curonian Lagoon, a large, shallow coastal waterbody connected to the Baltic Sea by the narrow Klaipeda Strait. Zebra mussels (*Dreissena polymorpha*) are one of the most widespread invasive freshwater animals in the world. Currently, zebra mussels are highly abundant in the Curonian Lagoon, occupying the littoral zone down to 3-4m depth and occurring on both hard substrates and soft bottoms (Zaiko, Daunys 2015). We have 39 spatial sites in Curonian Lagoon where salinity, depth and water renewal time were observed. We also have information about the absence and presence of zebra mussels at those sites. We treat water renewal time as dependent variable and the remaining two as explanatory variables. The main purpose is to select the most appropriate model to the mapping of presence and absence of zebra mussels in the Curonian Lagoon, that is, to build a model with the greatest correct classification probability.

Let  $M_T$ ,  $M_R$ ,  $M_M$  denote three candidate models with different mean structure, that is, a different mean component  $X\beta$ :  $M_T$  - 1st order trend surface model;  $M_R$  - regression model, that is represented as a function of two explanatory variables;  $M_M$  - mixed model which combines  $M_T$  and  $M_R$ . The design matrix for this model consists of intercept, coordinates of spatial sites and explanatory variables.

A different number of neighbours are used for the specifying the prior probabilities. Spatial correlation is modelled by isotropic exponential covariance function given by  $\sigma(h) = \sigma^2 \exp(-h/\eta) + \tau^2 \delta(h)$ , where  $h$  is a distance between spatial sites,  $\eta$  is a parameter of spatial correlation,  $\tau^2$  is a nugget effect, and  $\delta(h) = 1$ , if  $h = 0$ , and  $\delta(h) = 0$ , if  $h \neq 0$ .

The results show that the mixed model ( $M_M$ ), including the set of closest neighbors for estimation of priors, gives the maximum of AVER (AVER=0.757). Salinity, depth and the coordinates of spatial sites are considered as covariates in the mean model.

## 4 Conclusions

This work describes a novel approach for spatial linear model selection, applicable to classified spatial data. This has several attractive features that make it compare favourably against other model selection approaches. First, it essentially incorporates the spatial information into data model and classification rule specification. Second, the approach provides an easily interpretable criterion of how strongly the data support each of the competing models. The best model has a mixed mean structure which includes coordinates of spatial sites and explanatory variables salinity and depth as covariates. The highest probability of correct classification could be approached using the set of nearest neighbours for estimating the prior probabilities.

## References

- [1] Berret C., Calder C.A. (2016). Bayesian spatial binary classification. *Spatial Statistics*. Vol. **16**, pp. 72-102.
- [2] Ducinkas K., Dreiziene L. (2018). Risk of classification of the Gaussian Markov random field observations. *Journal of Classification*. Vol. **35**, pp. 422-436.
- [3] Ducinkas K., Dreiziene L. (2011). Supervised classification of the scalar Gaussian random field observations under a deterministic spatial sampling design. *Austrian Journal of Statistics*. Vol. **40(1&2)**, pp. 25-36.
- [4] Zaiko A., Daunys D. (2015). Invasive ecosystem engineers and biotic indices: giving a wrong impression of water quality improvement. *Ecological Indicators*. Vol. **52**, pp. 292-299.

# DETECTING CHANGES IN THE DEPENDENCE STRUCTURE OF A TIME SERIES

A. DÜRRE, R. FRIED  
*Technische Universität Dortmund*  
*Dortmund, GERMANY*  
e-mail: alexander.duerre@udo.edu

## Abstract

We propose a new robust test to detect changes in the dependence structure of a time series. The test is based on empirical autocovariances of a robust transformation of the original time series. Because of the transformation we do not require any finite moments of the original time series making the test especially suitable for heavy tailed time series. We furthermore propose a lag weighting scheme which puts emphasis on changes of the autocorrelation at smaller lags. Our approach is compared to existing ones in some simulations.

**Keywords:** data science, dependence structure, changes detection, time series

## 1 Introduction

Detecting changes in the dependence structure of a time series goes back to [34] and [22]. To the best of our knowledge the first test to detect a change in the dependence structure where the possible time of change is not known a priori can be found in [33]. Since then a lot of alternatives have been proposed. In [23] estimated autocovariances of subsamples are compared to the estimation based on the whole time series. For linear models several tests have been proposed, see [3], [4], [2], [13] and [1]. CUSUM-type tests to detect changes in one or several autocovariances have been derived in [5], [24] and [14]. A test based on the auto-copula has been proposed in [7]. Tests which check stationarity of the spectrum are presented in [30], [17] and [36] and a wavelet periodogram is used in [26] and [8]. There are also proposals which compare local estimates of the spectrum with a global estimation, see [37], [28], [29] [15] and [32]. Surprisingly little attention has been paid to robustness. We want to fill the gap with a CUSUM type test based on robustified autocovariances. The testing procedure is described in Section 2 and a small simulation study in Section 3 indicates the usefulness of the proposed test.

## 2 Testing procedure

Denote  $\mathbb{X} = X_1, \dots, X_T$  a one dimensional time series which is stationary under the null-hypothesis. We assume in the following that  $\mathbb{X}$  has a continuous marginal distribution and is strongly mixing with mixing coefficients  $(a_k)_{k \in \mathbb{N}}$  fulfilling  $a_k = O(k^{-1-\epsilon})$  for some  $\epsilon > 0$ . Strong mixing was first introduced in [35] and describes how fast the dependence between two observations decreases as the time lag between them increases,

see [6] for more details. We only want to emphasize here that a broad class of time series models is strongly mixing, like linear and GARCH processes with continuously distributed innovations, see [9] and [25].

We want to test whether the autocorrelation function of  $\mathbb{X}$  stays the same, concentrating on the first  $p$  lags. We follow the approach of [16] and use bounded transformations. Before using them, the observations need to be properly standardized. Denote therefore by  $\hat{\mu}$  the sample median and by  $\hat{\sigma}$  the sample MAD of  $\mathbb{X}$ , and  $\mu$  and  $\sigma$  their theoretical counterparts. Then we define

$$\hat{Y}_i = \psi\left(\frac{X_i - \hat{\mu}}{\hat{\sigma}}\right) \quad \text{and} \quad Y_i = \psi\left(\frac{X_i - \mu}{\sigma}\right), \quad \text{where} \quad \psi = \begin{cases} -k & x < -k \\ x & |x| \leq k \\ k & x > k \end{cases}$$

denotes the Huber- $\psi$  function. This function was originally introduced for location estimation in [18] and basically downweights the influence of observations with large absolute values by shrinking them to more plausible values, namely  $-k$  respectively  $k$ . The tuning-coefficient  $k$  determines the robustness of the test. A larger value of  $k$  is favourable under Gaussian time series whereas a smaller  $k$  is needed if the data is corrupted or heavy tailed. In [19]  $k = 1.5$  is recommended as a compromise.

In the following we derive a CUSUM type test based on the Huber-transformed time series. Denote therefore  $S_k^{(l)} = \sum_{t=1}^k \hat{Y}_i \hat{Y}_{i+l}$ , then we look at

$$R_T = \max_{k=1, \dots, \tilde{T}} \frac{1}{\tilde{T}} \begin{pmatrix} S_k^{(1)} - \frac{k}{\tilde{T}} S_{\tilde{T}}^{(1)} \\ \vdots \\ S_k^{(p)} - \frac{k}{\tilde{T}} S_{\tilde{T}}^{(p)} \end{pmatrix}^T \begin{pmatrix} w_1 & 0 & \dots & 0 \\ 0 & \ddots & \ddots & \vdots \\ \vdots & \ddots & \ddots & 0 \\ 0 & \dots & 0 & w_p \end{pmatrix} \begin{pmatrix} S_k^{(1)} - \frac{k}{\tilde{T}} S_{\tilde{T}}^{(1)} \\ \vdots \\ S_k^{(p)} - \frac{k}{\tilde{T}} S_{\tilde{T}}^{(p)} \end{pmatrix}$$

where  $w_1, \dots, w_p > 0$  and  $\tilde{T} = T - p$ . Here are some remarks with regard to  $R_T$ :

- Technically  $R_T$  tests the following hypothesis

$$H_0 : \begin{pmatrix} \text{Cov}(Y_1, Y_2) \\ \vdots \\ \text{Cov}(Y_1, Y_{p+1}) \end{pmatrix} = \dots = \begin{pmatrix} \text{Cov}(Y_{T-p}, Y_{T-p+1}) \\ \vdots \\ \text{Cov}(Y_{T-p}, Y_T) \end{pmatrix} \quad \text{vs.} \\ H_1 : \exists k < T : \begin{pmatrix} \text{Cov}(Y_{k-p}, Y_{k-p+1}) \\ \vdots \\ \text{Cor}(Y_{k-p}, Y_k) \end{pmatrix} \neq \begin{pmatrix} \text{Cor}(Y_k, Y_{k+1}) \\ \vdots \\ \text{Cor}(Y_k, Y_{p+k}) \end{pmatrix}.$$

This is not equivalent to a test for a stationary dependence structure. For example  $R_T$  will have problems to detect changes in the tail dependence, since extreme values are downweighted by  $\psi$ .

- We decided against calculating real robust correlations by standardizing  $S_k^{(j)}$  by  $S_k^{(0)}$  respectively  $S_{\tilde{T}}^{(0)}$  for  $j = 1, \dots, p$ . Note that we already standardize our observations by  $\hat{\sigma}$ . So there is no mandatory need to standardize  $S_k^{(j)}$ , too.

- The choice of  $p$  is crucial for the power of the test. If there is only a change in the first lag a large  $p$  only adds noise and can mask the change point. On the other hand if one chooses  $p$  to small one cannot detect changes in the higher lags. Furthermore one has to keep in mind that the estimation of  $\Sigma$  gets very poor if  $p$  is large compared to  $\tilde{T}$ . As a rule of thumb use  $p < \lfloor \tilde{T}/20 \rfloor$ .
- In the multivariate context it is common and beneficial to use the quadratic form with respect to  $\Sigma$ , the asymptotic long run variance covariance matrix of  $S_{\tilde{T}}^{(1)}, \dots, S_{\tilde{T}}^{(p)}$ . In this case  $R_T$  gets affine invariant. However, in the time series context this property is not desirable. The weights  $w_1, \dots, w_p$  gives us more flexibility. Usually one would choose descending weights to smooth the transition between lags of the acf where one can detect a change  $j = 1, \dots, p$  to those neglected  $j > p$ . If there is only a change in the first autocorrelation and one chooses  $p$  to large the change could be masked by the noise from the other autocorrelations. Descending weights somehow counteract this problem. Without further knowledge we suggest using  $w_i = 1 - (i - 1)/p$  for  $i = 1, \dots, p$ . A disadvantage of using weights instead of  $\Sigma$  is that  $R_T$  depends on the actual dependence structure of  $\mathbb{X}$ . Therefore one cannot use tabulated asymptotical critical values. However, one can approximate the distribution of  $R_T$  by sampling Gaussian processes with the estimated covariance structure.

Now we describe how one can approximate the distribution of  $R_T$  under the null-hypothesis. Under the above assumptions one can use Theorem 1 of [16]. It is not explicitly stated there but effectively proved in Proposition 1 and 2 that

$$\frac{1}{\sqrt{\tilde{T}}} \left[ S_{\lfloor \tilde{T}x \rfloor}^{(1)} - \frac{\lfloor \tilde{T}x \rfloor}{\tilde{T}} S_{\tilde{T}}^{(1)}, \dots, S_{\lfloor \tilde{T}x \rfloor}^{(p)} - \frac{\lfloor \tilde{T}x \rfloor}{\tilde{T}} S_{\tilde{T}}^{(p)} \right]_{x \in [0,1]} \xrightarrow{w} [\mathbf{B}\mathbf{B}(x)]_{x \in [0,1]}$$

where  $[\mathbf{B}(x)]_{x \in [0,1]}$  is a Gaussian process with mean function  $g(x) = \mathbf{0}$  and covariance function  $\gamma(x, y) = x(1 - y)\Sigma$  for  $0 \leq x \leq y \leq 1$ . Here,  $\Sigma$  is the asymptotic long run covariance matrix defined by

$$\Sigma = \sum_{h=-\infty}^{\infty} \text{Cov} \left( \begin{bmatrix} Y_1 Y_2 \\ \vdots \\ Y_1 Y_{1+p} \end{bmatrix}, \begin{bmatrix} Y_{1+h} Y_{2+h} \\ \vdots \\ Y_{1+h} Y_{1+p+h} \end{bmatrix} \right).$$

Proposition 3 in [16] states that  $\Sigma$  can be consistently estimated by a kernel estimator. Denote therefore  $b_{\tilde{T}} \geq 0$  a bandwidth and  $k : \mathbb{R} \rightarrow [-1, 1]$  a kernel function. Then  $\hat{\Sigma}$  with the elements

$$\hat{\Sigma}_{[i,j]} = \frac{1}{T} \sum_{t=1}^{\tilde{T}} \sum_{s=1}^{\tilde{T}} (\hat{Y}_s \hat{Y}_{s+i} - S_{\tilde{T}}^{(i)}) (\hat{Y}_t \hat{Y}_{t+j} - S_{\tilde{T}}^{(j)}) k \left( \frac{|s-t|}{b_{\tilde{T}}} \right)$$

is the related kernel estimator. Simulations indicate that the flat-top kernel

$$k(x) = \begin{cases} 1 & 0 \leq |x| \leq 0.5 \\ 2 - 2|x| & 0.5 < |x| \leq 1 \\ 0 & |x| > 1 \end{cases}$$

proposed [31] in works well together with  $b_T = \tilde{T}^{\frac{1}{3}}$  under autoregressive processes of order 1. One can generate random variables  $\tilde{R}_T^{(i)}$ ,  $i = 1, \dots, m$ , which have asymptotically the same distribution as  $R_T$  under the null-hypothesis by the following algorithm:

- generate  $p \cdot \tilde{T}$  independent standard normal random variables and store them in a  $\tilde{T} \times p$  matrix  $Z$
- reproduce the cross sectional dependence by multiplying  $Z$  with  $L$  of the Cholesky decomposition  $\hat{\Sigma} = LL^T$ : Set  $V = Z \cdot L$
- calculate the weighted test statistic

$$\tilde{R}_T = \frac{1}{\tilde{T}} \max_{k=1, \dots, \tilde{T}} \left( \sum_{t=1}^k V_{[t,]} - \frac{k}{\tilde{T}} \sum_{t=1}^T V_{[t,]} \right) W \left( \sum_{t=1}^k V_{[t,]} - \frac{k}{\tilde{T}} \sum_{t=1}^T V_{[t,]} \right)^T$$

By this algorithm one can generate random variables to calculate approximate p-values very fast. We recommend using a modified Cholesky decomposition to safeguard against numeric instabilities which could arise especially if  $T$  is small compared to  $p$ . In our simulations we used the algorithm proposed in [38].

### 3 Simulations

We want to assess our approach in a small simulation study. We compare our method with tests for second order stationarity which are available in R, namely two wavelet based tests [26] and [10], which are implemented in the packages [27] respectively [11], and a revised version of the ANOVA test originally proposed in [33], which is implemented in the package [12]. We abbreviate these tests by *Wav*, *Rpar* and *Anova*. Note that all these methods are constructed with multiple break points in mind, so we expect our method to perform comparatively well in the one change-point setting. Usually we set  $p = 3$  and use the abbreviation *HCov* if we use  $k = 1.5$  and *Cov* if we use  $k = 1000$ , which is effectively a covariance based test and not robust.

First we evaluate the behaviour under the null hypotheses. We look at AR(1) models  $X_t = \rho X_{t-1} + \epsilon_t$  for  $t = 1, \dots, T$  with parameters  $\rho \in \{0, 0.8\}$ , different distributions for the innovations  $(\epsilon_t)_{t=1, \dots, T}$ , namely the standard normal and a t-distribution with 3 degrees of freedom, and different length  $T \in \{128, 256, 512\}$ . Results are based on 10000 repetitions and summarized in Table 1. We can see that *HCov* holds its size very well under serial dependence and heavy tails, whereas *Wave*, *Rpar* and to some degree also *Cov* have problems in the later case. Surprisingly *Anova* needs at least  $T = 256$  to work well.

To assess power under  $H_1$  we look at  $X_t = \begin{cases} \epsilon_t, & t = 1, \dots, 128 \\ 0.3X_{t-1} + \epsilon_t, & t = 129, \dots, 256 \end{cases}$ . Here the autocorrelation function changes from  $\rho(k) = 0$  to  $\rho(k) = 0.3^k$  for  $k \in \mathbb{N}$ . We use  $t$ -distributions with different degrees of freedom to investigate the influence of heavy tails. Results based on 16000 repetitions can be seen in Figure 1 on the left. The

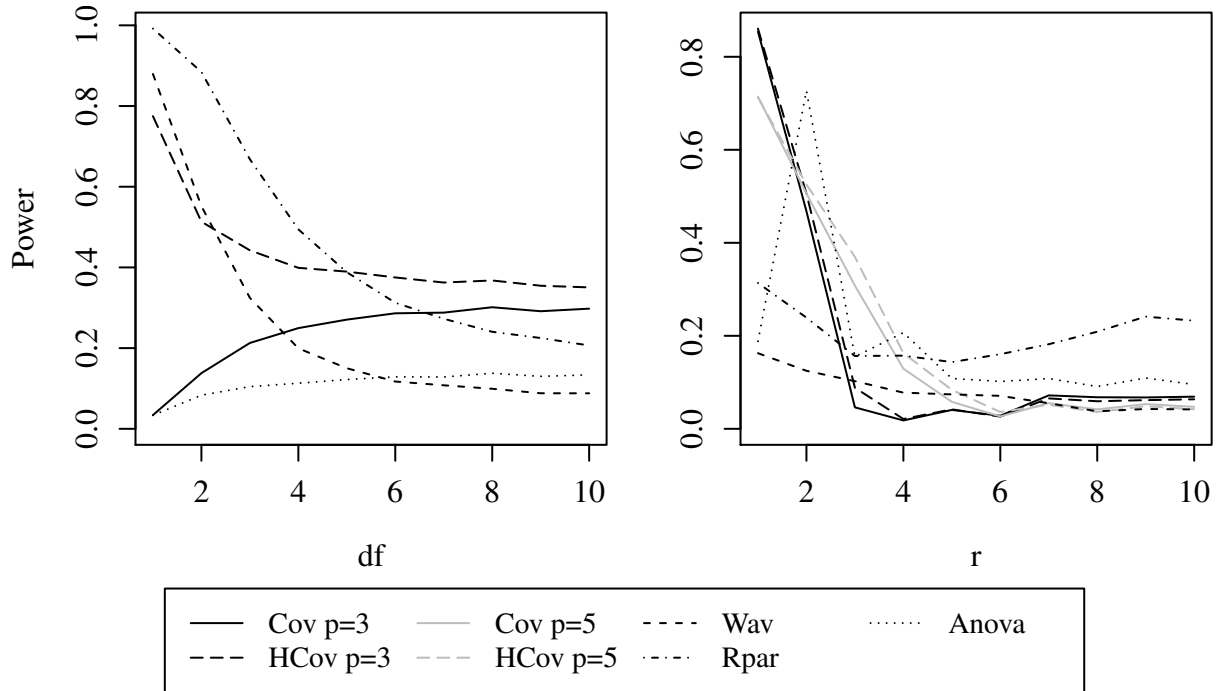


Figure 1: Empirical power under a change from independent observations to an AR(1) model with  $t$  distributed innovations with various degrees of freedom (left) and a change to an MA( $r$ ) model with normal innovations (right).

Table 1: Empirical size in percent under AR(1) models with different  $\rho$ , normal and  $t_3$  distributed innovations and various time series lengths  $T$  at a nominal level of 0.05.

$\rho$	N(0,1)						$t_3$					
	0			0.8			0			0.8		
$T$	128	256	512	128	256	512	128	256	512	128	256	512
Cov	3	4	5	2	3	4	4	6	7	2	2	3
HCov	3	4	5	3	4	4	3	4	5	3	3	4
Wav	1	3	4	2	4	4	8	29	34	6	23	27
Rpar	5	6	7	5	6	6	46	62	76	44	61	76
Anova	67	6	6	52	14	10	53	3	3	54	11	7

robust test  $HCov$  dominates its competitors for  $df = 10$  and even gains power as  $df$  decreases. This could be a result of good leverage points. We see that the wavelet based tests have a higher power at some point, though this is completely driven by their anticonservatism under the null-hypothesis.

Finally we want to evaluate the influence of the time-lag where the autocorrelation function changes and look at  $X_t = \begin{cases} \epsilon_t & t = 1, \dots, 128 \\ \epsilon_t + 0.8\epsilon_{t-r} & t = 129, \dots, 256 \end{cases}$ . Here the acf changes

from  $\rho(k) = 0$  to  $\rho(k) = 0.8/(1 + 0.8^2)I_{\{k=r\}}$  for  $k \in \mathbb{N}$ . Results under normal innovations and 16000 repetitions can be seen in Figure 1 at the right. Our tests with the choice  $p = 3$  can only detect changes of the acf at lag 1 and 2. We also run our tests with  $p = 6$  and noticed that the power for smaller lags deteriorates a little while we can now detect changes up to lag 4. Apart from  $Rpar$  all tests loose power as the lag of change  $r$  increases.

In summary our robust change-point test behaves well under linear models with and without heavy tails. The choice of  $p$  is crucial and determines up to which lag changes in the acf can be detected. In case of doubt one should choose it rather larger than smaller to be able to detect changes in the acf at higher lags.

## References

- [1] Akashi F., Dette H., Liu Y. (2018). Change point detection in autoregressive models with no moment assumptions. *Journal of Time Series Analysis*. Vol. **39**, pp. 763-786.
- [2] Andrews D.W.K. (1993). Tests for Parameter Instability and Structural Change with unknown Change Point. *Econometrica*. Vol. **61**, pp. 821-856.
- [3] Bai J. (1993). On the partial sums of residuals in autoregressive and moving average models. *Journal of Time Series Analysis*. Vol. **14**, pp. 247-260.
- [4] Bai J. (1994). Weak convergence of the sequential empirical processes of residuals in ARMA models. *The Annals of Statistics*. Vol. **22**, pp. 2051-2061.
- [5] Berkes I., Gombay E., Horvath, L. (2009). Testing for changes in the covariance structure of linear processes. *Journal of Statistical Planning and Inference*. Vol. **139**, pp. 2044-2063.
- [6] Bradley R.C. (2005). Basic properties of strong mixing conditions. a survey and some open questions. *Probability Surveys*. Vol. **2**, pp. 107-144.
- [7] Bucher A., Fermanian J.D., Kojadinovic I. (2019). Combining Cumulative Sum Change-Point Detection Tests for Assessing the Stationarity of Univariate Time Series. *Journal of Time Series Analysis*. Vol. 40, pp. 124-150.
- [8] Cardinali A., Nason G. (2018). Practical powerful wavelet packet tests for second-order stationarity. *Applied and Computational Harmonic Analysis*. Vol. **44**, pp. 558-583.

- [9] Chanda K.C. (1974). Strong mixing properties of linear stochastic processes. *Journal of Applied Probability*. Vol. **11**, pp. 401-408.
- [10] Cho H. (2016). A test for second-order stationarity of time series based on unsystematic sub-samples. *Stat*. Vol. **5**, pp. 262-277.
- [11] Cho H. (2018). unsystation - Stationarity Test Based on Unsystematic Sub-Sampling. *R-Package*, Version 0.2.0.
- [12] Constantine W., Percival D. (2017). fractal - A Fractal Time Series Modeling and Analysis Package. *R-Package*, Version 2.0.4.
- [13] Davis R.A., Huang D., Yao, Y. (1995). Testing for a Change in the Parameter Values and Order of an Autoregressive Model. *The Annals of Statistics*. Vol. **23**, pp. 282-304.
- [14] Dette H., Wu W., Zhou, Z. (2015). Change point analysis of second order characteristics in non-stationary time series. *arXiv e-prints*. arXiv:1503.08610.
- [15] Dette H., Preuß P., Vetter M. (2011). A measure of stationarity in locally stationary processes with applications to testing. *Journal of the American Statistical Association*. Vol. **106**, pp. 1113-1124.
- [16] Dürre A., Fried R. (2019). Robust change point tests by bounded transformations. *arXiv e-prints*. arXiv:1905.06201.
- [17] Giraitis L., Leipus R. (1992). Testing and estimating in the change-point problem of the spectral function. *Lithuanian Mathematical Journal*. Vol. **32**, pp. 15-29.
- [18] Huber P.J. (1964). Robust estimation of a location parameter. *The Annals of Mathematical Statistics*. Vol. **35**, pp. 73-101.
- [19] Huber P.J., (2011). Robust Statistics. In *International Encyclopedia of Statistical Science*. Springer, pp. 1248-1251.
- [20] Huskova M., Kirch C., Praskova Z., Steinebach, J. (2007). On the detection of changes in autoregressive time series I. Asymptotics. *Journal of Statistical Planning and Inference*. Vol. **137**, pp. 1243-1259.
- [21] Huskova M., Kirch C., Praskova Z., Steinebach, J. (2007). On the detection of changes in autoregressive time series II. Resampling Procedures. *Journal of Statistical Planning and Inference*. Vol. **138**, pp. 1697-1721.
- [22] Jenkins G.M. (1961). The comparison of correlations in time series. *Journal of the Royal Statistical Society: Series B (Methodological)*. Vol. **20**, pp. 158-164.
- [23] Jin L., Wang S. Wang H. (2015). A new non-parametric stationarity test of time series in the time domain. *Journal of the Royal Statistical Society: Series B (Methodological)*. Vol. **77**, pp. 893-922.

- [24] Lee S., Ha J. Na O., Na, S. (2015). The Cusum Test for Parameter Change in Time Series Models. *Scandinavian Journal of Statistics*. Vol. **30**, pp. 781-796.
- [25] Lindner A.M. (2009). Stationarity, mixing, distributional properties and moments of GARCH (p, q)-processes. In *Handbook of financial time series*. Springer, pp. 43-69.
- [26] Nason G. (2013). A test for second-order stationarity and approximate confidence intervals for localized autocovariances for locally stationary time series. *Journal of the Royal Statistical Society: Series B (Statistical Methodology)*. Vol. **75**, pp. 879-904.
- [27] Nason G. (2016). Locits - Test of Stationarity and Localized Autocovariance. *R-Package*, Version 1.7.3.
- [28] Paparoditis E. (2009). Testing temporal constancy of the spectral structure of a time series. *Bernoulli*. Vol. **15**, pp. 1190-1221.
- [29] Paparoditis E. (2010). Validating stationarity assumptions in time series analysis by rolling local periodograms. *Journal of the American Statistical Association*. Vol. **105**, pp. 839-851.
- [30] Picard D. (1985). Testing and estimating change-points in time series. *Advances in applied probability*. Vol. **17**, pp. 841-867.
- [31] Politis D.N, Romano J.P. (1993). On a family of smoothing kernels of infinite order. {Computing Science and Statistics, Proceedings of the 25th Symposium on the Interface}, pp.141-145.
- [32] Preuß P., Vetter M., Dette H. (2013). A test for stationarity based on empirical processes. *Bernoulli*. Vol. **19**, pp. 2715-2749.
- [33] Priestley M.B., Rao T.S. (1969). A test for non-stationarity of time-series. *Journal of the Royal Statistical Society: Series B (Methodological)*. Vol. **31**, pp. 140-149.
- [34] Quenouille M.H. (1958). The comparison of correlations in time series. *Journal of the Royal Statistical Society: Series B (Methodological)*. Vol. **20**, pp. 158-164.
- [35] Rosenblatt M. (1956). A central limit theorem and a strong mixing condition. *Proceedings of the National Academy of Sciences of the United States of America*. Vol. **42**, pp. 43-47.
- [36] Rosenholc Y. (2001). Nonparametric Tests of Change-Points with Tapered Data. *Journal of Time Series Analysis*. Vol. **22**, pp. 13-43.
- [37] Von Sachs R., Neumann M.H. (2000). A wavelet-based test for stationarity. *Journal of Time Series Analysis*. Vol. **21**, pp. 597-613.
- [38] Schnabel R.B., Eskow E. (1999). A revised modified Cholesky factorization algorithm. *SIAM Journal on Optimization*. Vol. **9**, pp. 1135-1148.

# NEW METHOD TO MINIMIZE THE STRESS IN MULTIDIMENSIONAL SCALING

G. DZEMYDA, M. SABALIAUSKAS

*Vilnius University Institute of Data Science and Digital Technologies*

*Vilnius, LITHUANIA*

e-mail: gintautas.dzemyda@mii.vu.lt, martynas.sabalaiuskas@mii.vu.lt

## Abstract

A novel geometric interpretation of the stress function and multidimensional scaling in general (GMDS) has been discussed. Following this interpretation, the step size and direction forward the minimum of the stress function are found analytically for a separate point without reference to the analytical expression of the stress function, numerical evaluation of its derivatives and the linear search.

**Keywords:** data science, multidimensional scaling, stress function

## 1 Multidimensional scaling

The human being can comprehend visual information more quickly and deeply than textual one. The goal of the projection (visualization) methods is to represent the input data items in a lower-dimensional space so that certain properties of the structure of the data set were preserved as faithfully as possible. Example of such visualization is given in Fig. 1. Numerical 6-dimensional data is on the left, and its projection on a plane is on the right.

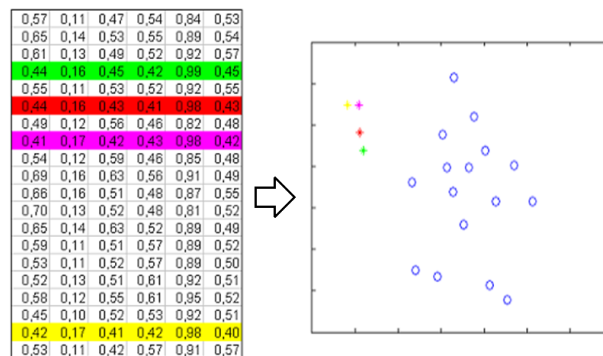


Figure 1: Example of 2D projection

Multidimensional scaling (MDS) is one of the most popular methods for a visual representation of multidimensional data [1], [2]. Suppose, we have a set  $X = \{X_i = (x_{i1}, \dots, x_{in}), i = 1, \dots, m\}$  of  $n$ -dimensional data points  $X_i \in \mathbb{R}^n$ ,  $n \geq 3$ .

Dimensionality reduction and visualization requires estimating the coordinates of new points  $Y_i = (y_{i1}, \dots, y_{id}), i = 1, \dots, m$ , in a lower-dimensional space ( $d < n$ ) by holding proximities (e. g. distances  $d_{ij}$ ) between multidimensional points  $X_i$  and  $X_j$ ,  $i, j = 1, \dots, m$ , as much as possible. MDS finds the coordinates of new points  $Y_i$

representing  $X_i$  in a lower-dimensional space  $\mathbb{R}^d$  by minimizing the multimodal stress function depending on  $Y_1, \dots, Y_m$ . We consider stress equal to squared differences between pairs of distances of corresponding points in original and projected spaces.

## 2 Peculiarities of GMDS

Following the new interpretation of MDS stress (denote it by GMDS), the step size and direction forward the minimum of the stress function are found analytically for a separate point in a projected space without reference to the analytical expression of the stress function, numerical evaluation of its derivatives and the linear search. It is proved theoretically that the direction coincides with the steepest descent direction, and the analytically found step size guaranties almost the optimal step in this direction. The discovered option to minimize the stress function is examined on the simple realization of GMDS.

Simple realizations of GMDS are based on fixing some initial positions of points  $Y_i = (y_{i1}, \dots, y_{id})$ ,  $i = 1, \dots, m$  (at random, using principal component analysis, etc.), and further changing the positions of  $Y_j$  (once or several times) in consecutive order from  $j = 1$  to  $j = m$  many times till some stop condition is met: e.g. number of runs from  $j = 1$  to  $j = m$  reaches some limit or the decrease of stress function  $S(\cdot)$  becomes less than some small constant after two consecutive runs.

The essence of the proposed method lies in computing of new point  $Y_j^*$  for current point  $Y_j$  as average of points  $A_{ij}$ ,  $i = 1, \dots, m$ ,  $i \neq j$ , where  $A_{ij}$  are points lying on the line between point  $Y_j$  and  $Y_i$  on the distance  $d_{ij}$  from  $Y_i$ . See Fig. 2 for graphical illustration.

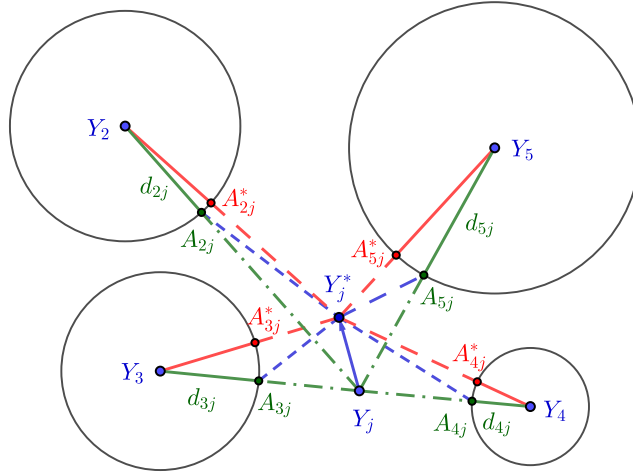


Figure 2: An example of a single iteration of GMDS method

## References

- [1] Dzemyda, G., Kurasova, O., Žilinskas, J. (2013). *Multidimensional Data Visualization: Methods and Applications*. Series: *Springer Optimization and its Applications*, Vol. 75, Springer.
- [2] Borg, I., Groenen, P.J.F., Mair, P. (2018). *Applied Multidimensional Scaling and Unfolding*. 2nd ed., Springer.

# ROBUST AND SPARSE K-MEANS CLUSTERING FOR HIGH-DIMENSIONAL DATA

P. FILZMOSER, Š. BRODINOVÁ, T. ORTNER, C. BREITENDER, M. ROHM  
*TU Wien*  
*Vienna, AUSTRIA*  
e-mail: Peter.Filzmoser@tuwien.ac.at

## Abstract

We introduce a robust  $k$ -means-based clustering method for high-dimensional data where not only outliers but also a large number of noise variables are very likely to be present [4]. Although Kondo et al. [2] already addressed such an application scenario, our approach goes even further. Firstly, the introduced method is designed to identify clusters, informative variables, and outliers simultaneously. Secondly, the proposed clustering technique additionally aims at optimizing required parameters, e.g. the number of clusters. This is a great advantage over most existing methods. Moreover, the robustness aspect is achieved through a robust initialization [3] and a proposed weighting function using the Local Outlier Factor [1]. The weighting function provides a valuable source of information about the outlyingness of each observation for a subsequent outlier detection. In order to reveal both clusters and informative variables properly, the approach uses a lasso-type penalty [5]. The method has thoroughly been tested on simulated as well as on real high-dimensional datasets. The conducted experiments demonstrated a great ability of the clustering method to identify clusters, outliers, and informative variables.

**Keywords:** k-means clustering, high-dimensional data, robustness, data science

## References

- [1] Breunig M.M., Kriegel H.P., Ng R.T., Sander J. (2000). LOF: Identifying density-based local outliers. *ACM Sigmod Record*. Vol. **29**, pp. 93-104.
- [2] Kondo Y., Salibian-Barrera M., Zamar R. (2016). RSKC: An R package for a robust and sparse k-means clustering algorithm. *Journal of Statistical Software*. Vol. **72**, pp. 1-26.
- [3] Mohammad A.H., Vineet C., Saeed S., Mohammed J.Z. (2009). Robust partitional clustering by outlier and density insensitive seeding. *Pattern Recognition Letters*. **30(11)**, pp. 994-1002.
- [4] Brodinova S., Filzmoser P., Ortner T., Breiteneder C., Rohm M. (2019). Robust and sparse k-means clustering for high-dimensional data. *Advances in Data Analysis and Classification*. To appear.
- [5] Witten D.M., Tibshirani R. (2010). A framework for feature selection in clustering. *Journal of the American Statistical Association*. **105(490)**, pp. 713-726.

# CONFORMAL PREDICTORS FOR RELIABLE PATTERN RECOGNITION

A. GAMMERMAN

*Royal Holloway, University of London*

*London, UNITED KINGDOM*

e-mail: a.gammerman@rhul.ac.uk

## Abstract

The talk reviews a modern machine learning technique called Conformal Predictors. The approach has been motivated by algorithmic notion of randomness and allows us to make reliable predictions with valid measures of confidence for individual examples. The developed technique guarantees that the overall accuracy can be controlled by a required confidence level. Unlike many conventional techniques the approach does not make any additional assumption about the data beyond the i.i.d. assumption: the examples are independent and identically distributed. The way to test this assumption is described. The talk also outlines some generalisations of Conformal Predictors and their applications to many different fields including medicine, cheminformatics, information security, environment, plasma physics, home security and others.

**Keywords:** conformal predictors, pattern recognition, data science

## 1 Background

The talk reviews a modern machine learning technique called Conformal Predictors [1, 2]. Given a set of training examples  $(x_1, y_1), \dots, (x_l, y_l)$ , where each example consists of an object and a label, the problem of classification or regression can be considered as assigning a label  $y_{l+1}$  to a new object  $x_{l+1}$ , so that an example  $(x_{l+1}, y_{l+1})$  does not look *strange* among the training examples. Or, in other words, how well the new example fits with the training set. In order to measure the *strangeness* of the new example in comparison with the training set, we introduced so-called *non-conformity measure* (NCM). This leads to a novel way to quantify the uncertainty of the prediction under rather general assumption. A non-conformity measure can, in principle, be extracted from any machine learning algorithm, such as SVM, logistic regression, neural networks, etc. We shall call the algorithm used for the extraction of an NCM as an underlying model.

Once an NCM is developed, it is possible to compute for any example  $(x, y)$  a *p*-value that reflects how good the new example from the test set fits (or conforms with the i.i.d. assumption) with the training set. A more accurate and formal statement is this: chosen a significance level  $\epsilon \in [0, 1]$  it is possible to compute *p*-values for the test examples so that they are (in the long run) smaller or equal than  $\epsilon$  with probability at most  $\epsilon$ . Note that the key assumption here is that the examples in the training set and the test objects are independent and identically distributed (although a weaker requirement of exchangeability is sufficient). The idea is then to compute for a test

object  $x$  a  $p$ -value for every possible choice of the label  $y$  and make a prediction by choosing a label with the largest  $p$ -value and the confidence as (1 - 2nd largest  $p$ -value). Once the  $p$ -values are computed, they can be used in one of the following ways: a) to allow a user to specify a confidence level (or an error rate) so that the correct prediction rate is not worse than pre-specified confidence level; or b) to provide prediction with confidence for each individual example. More precisely:

- Given a significance level,  $\epsilon$ , the predictor outputs a *region set* of possible labels for each test object such that the actual label appears no more than  $\epsilon$  times in the set. This property is called *validity* of conformal predictors and it follows from the observations that in the online prediction protocol, the errors made  $err_1^\epsilon, err_2^\epsilon, \dots$  are independent and take value 1 with probability  $\epsilon$ . Naturally, the narrower the prediction region is, the more *efficient* our prediction is

$$\Gamma^\epsilon = \{y \in Y : p(y) > \epsilon\},$$

where  $\Gamma^\epsilon$  is a prediction region, and the output provides the user with all labels  $y$  where  $p$ -value is greater than  $\epsilon$ .

- Another way is to supply a prediction for a new test object with two numbers: the **confidence**

$$\sup \{1 - \epsilon : |\Gamma^\epsilon| \leq 1\}$$

and the **credibility**

$$\inf \{\epsilon : |\Gamma^\epsilon| = 0\}.$$

Low credibility, for example, implies either the training set is non-random or the test object is not representative of the training set.

## 2 Conformal and Probabilistic Predictors

This method described above is so-called *transductive* conformal prediction (CP). It requires to retrain underlying model for each new test example. To make the method computationally more efficient, it has been generalised for *inductive* conformal predictor. In fact, there are now a number of various generalisations. Among them:

- *Inductive CP* (for computational efficiency). The inductive conformal predictors require the underlying model to be trained only once. The dataset is divided into *proper training* set, *calibration* set and *test* set. The proper training set is used only to calculate NCM scores ( $\alpha$ 's) of calibration and testing examples. Then  $p$ -values are calculated using only those  $\alpha$ 's.
- *Mondrian CP* (for imbalanced data). In transductive and inductive CPs the examples we usually deal with belong to different classes or categories. Conformal predictors do not guarantee *validity* within the categories. The fraction of errors can be much larger than the pre-specified significance level for some categories, if

this is compensated by a smaller fraction of errors in other categories. This validity within the categories is the main property of Mondrian conformal predictors<sup>1</sup>. Mondrian CP allows to have separate guarantees of the errors of different types. CP prediction set covers the true label with probability  $1 - \epsilon$ . In Mondrian CP: if the true label is 1, then the prediction set contains 1 with probability  $1 - \epsilon_1$ ; if the true label is 0, then the prediction set contains 1 with probability  $1 - \epsilon_0$ .

- *Probabilistic predictor* (produces reliable two-sided probabilistic estimates instead of p-values). Conformal predictors output *p-values*, but sometimes *p-values* are more difficult to interpret than probabilities. In Bayesian decision theory: probabilities (but not the *p-values*) can be combined with utilities to arrive at optimal decisions. We have also developed a method of probabilistic prediction [1, 2] that is related to conformal prediction – so called Venn machine – that also has a guaranteed property of *validity*. It outputs multiprobabilistic predictions; for example, in the classification problem it provides a lower and upper bounds of probabilistic predictions.

Several other techniques have been developed such as *Cross-conformal* predictors (a hybrid of inductive CP and cross-validation); *On-line Compression Model* (for assumptions other than i.i.d.); *Conformal Predictive distribution* (provides the whole distribution and can be used for decision-making); *Ridge Regression Confidence Machine* and others.

The main point is that in all these generalisations the property of **validity** is preserved.

### 3 Applications

The conformal predictors techniques have been successfully applied in many fields: in medicine for diagnostic of ovarian and breast cancers; in neurosciences for diagnostic and treatment of depression; in information security in identifying various bots; in environment for assessing a level of pollution and many others. One of the most recent application is in pharmaceutical industry to find chemical compound activity using publicly available data [3]. A version of conformal predictors called Inductive Mondrian Predictor that keeps validity guarantees for each class has been applied for the large, high-dimensional, sparse and imbalanced pharmaceutical data. The experiments were conducted using several non-conformity measures extracted from underlying algorithms such as SVM, Nearest Neighbours and Naive Bayes. The results show that Inductive Conformal Mondrian Prediction framework allows to rank the compound activities and to find potentially useful molecules for drug developments.

---

<sup>1</sup>Called Mondrian because the categories resemble a Mondrian paintings by Piet Mondrian (1872-1944).

## References

- [1] Vovk V., Gammerman A., Shafer G. (2005). *Algorithmic learning in a random world*. Springer, New York.
- [2] Gammerman A., Vovk V. (2007). Hedging prediction in machine learning. *The Computer J.* Vol. 50, pp. 151–163.
- [3] Toccaceli P., Gammerman A. (2018). Combination of inductive mondrian conformal predictors. *Machine Learning*. Vol. 50, pp. 1–22.

# A RANDOM GRAPH GENERATION MODEL FOR TRANSCRIPTION NETWORKS AND NONPARAMETRIC SIMULATOR FOR RNA-SEQ EXPRESSION DATA

T. GRIMES, S. DATTA

*University of Florida*

*Gainesville, USA*

e-mail: somnath.datta@ufl.edu

## Abstract

With the advent of high-throughput sequencing and continually decreasing costs, an abundance of gene expression data has been generated and is available for analysis. These data provide a rich resource for inferring connections in gene regulatory networks. A vast collection of methodologies have been developed, but a challenge remains in assessing and benchmarking their performance. Gold-standard datasets are scarce, and commonly-used simulators are not designed to resemble the data generated from RNA-seq experiments. The present study provides a novel random graph generator that produces networks having comparable topology to transcription networks. In addition, a nonparametric simulator is proposed that generates conditionally dependent expression data; the conditional dependencies are based on an underlying network structure, and the marginal distribution of gene expression profiles are based on a reference RNA-seq dataset. These methods provide tools for creating *in silico* RNA-seq data for benchmarking and assessing gene network inference methods.

**Keywords:** data science, random graph, transcription network, RNA expression

## 1 Introduction

Gene regulatory networks (GRN) describe systems of gene-gene interactions that regulate gene expression. Using RNA-sequencing to measure simultaneous gene expression is an effective avenue for inferring these networks. A vast collection of methods have been developed for reverse engineering the network structure from gene expression data [7, 14, 13]. Frameworks for GRN inference extend from Bayesian networks to regression-based models and information-theoretic approaches. [3] These frameworks have shown success in identifying well-known regulatory interactions, and many methods have identified new interactions that were later validated [12].

A major challenge remains in assessing the relative performance of different methods. Assessing network inference is difficult because the true underlying network of real expression data is unknown, and validating GRNs experimentally is not a simple task [17]. The Dialogue for Reverse Engineering Assessment and Methods (DREAM) was an early effort for tackling this challenge [10]. However, there remains limited resources for next-generation sequencing technologies and assessing performance on RNA-seq expression data.

Evaluating the performance of GRN methods requires two components: (1) knowledge of the underlying network structure, and (2) expression data generated from the network. The first can be obtained from well-studied regulatory interactions, such as those in the *E. coli* transcription network [15]. Gene expression data are obtained either experimentally or through simulations. Real data have been curated from the Gene Expression Omnibus (GEO) database for *E. coli* and are publicly available through the Many Microbe Microarray Database [6]. Simulated data are commonly generated using dynamic models of gene expression [5]; this produces continuous expression values that resemble data from microarray experiments. Alternatively, simulators can use a probabilistic model to generate correlated expression data; Gaussian models are often used in modern methodology papers for assessing GRN inference performance [4, 8, 18, 20]. And while several tools exist for simulating RNA-seq data, none of them address the problem of simulating RNA-seq expression data from gene co-expression networks.

In this study, we address two major challenges: (1) generating random networks that have a topology similar to real transcription networks, and (2) simulated RNA-seq expression data with conditional dependencies defined by an underlying network structure. The network generator is able to produce a rich distribution of network topologies, and we demonstrate its ability to replicate the structure of the *E. coli* transcription network. The RNA-seq expression simulator uses a reference dataset to generate realistic data, and we show that the marginal profiles of gene expression are comparable between simulated and real datasets. In an application of these simulation tools, a robust evaluation of twelve GRN inference methods is performed by varying the underlying network structure and comparing different sources of reference datasets.

## 2 Methods

The proposed simulator consists of three separate components: the network generator, a Gaussian graphical model (GGM), and a converter from GGM values to RNA-seq expression data. The network generator decomposes the network into individual gene modules that specify local connectivity among subsets of genes. The collective dynamics of the local modules result in a global structure resembling real transcription networks. Weights for the local connections are generated under the framework of a GGM. In the final step, Gaussian values are converted into RNA-seq data while maintaining the dependence structure among the gene expression profiles.

The local network structures model individual regulatory pathways; each pathway has its own gene-gene co-expression pattern. As with biological pathways, the network modules are allowed to overlap. The network generator also incorporates link nodes used to connect modules together. This models the behavior of transcription factors that regulate genes across multiple pathways. Within each module, the network structure is generated using a novel algorithm. Similar to the Watts-Strogatz algorithm [19], the procedure begins with a ring lattice structure. The connections are then rewired, each with a constant probability. However, rewiring is performed with preferential attachment. The approach is similar to the Barabasi-Albert model [1], but the preference in the proposed model does not scale linearly with node degree. Instead, the rankings

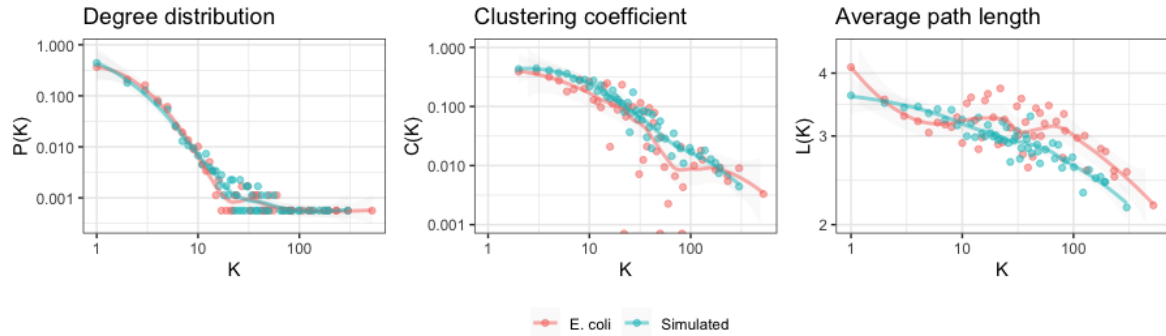


Figure 1: Comparison of a generated network and the *E. coli* transcription network. The degree distribution (left), clustering coefficient (middle), and average path length (right), are shown as a function of node degree with the axes drawn on a log scale.

of the node degree are used in combination with a Beta distribution function. The end result produces global networks with much larger hub genes than expected under scale-free network models.

Once the local network structure is created, edges weights are added to each connection. These weights are generated under the guise of a GGM. The Gaussian model imposes certain constraints to the edge weights, but the overall structure is preserved. Expression values are generated from the GGM, and the final step of the simulator converts these Gaussian values into RNA-seq data. This is done by incorporating a reference dataset and using the inverse-CDF method for transforming Gaussian values into RNA-seq expression values derived from the empirical distribution of expression profiles.

### 3 Results

The random graph generation model is assessed using three topological measures, including the degree distribution, clustering coefficient, and average path length [2]. Each of these measures are considered at a local level as a function of node degree, and at a global level averaged over the entire network.

The topology of a simulated network is compared to the *E. coli* transcription network. Figure 1 shows a comparison of the local topologies of both networks. These plots are shown on a log scale, and both networks show very similar properties. Notably, the degree distribution of these networks differ from scale-free networks or small-world graphs, which would tend to show a linear relationship. This indicate that the Barabasi-Watts model and Strogatz-Watts algorithm are insufficient for replicating the structure of the transcription network. However, the proposed model is able to captures its properties. In particular, it's able to create the exceedingly high-degree genes found in *E. coli*.

In addition to generating gene-gene networks, a nonparametric model for simulating RNA-seq expression data is proposed. This simulator is able to generate expression

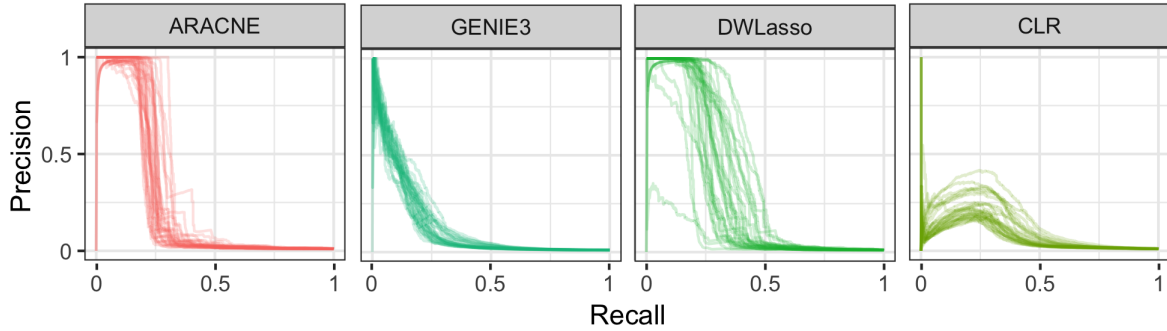


Figure 2: Precision-recall curves for four GRN inference methods on 30 simulated datasets.

profiles with marginal distributions that are similar to a reference dataset (results not shown). In an application, simulated data are used to assess the performance of 12 co-expression networks in various settings; these settings include various topologies for the underlying network and different marginal distributions for the expression data. The receiver operating characteristic (ROC) and precision-recall (PR) curves are used to summarize method performance, along with their respective area under the curve (AUC) metrics.

Results for four methods are shown in Figure 2 in terms of their PR-curves from 30 simulations. The methods shown include ARACNE [11], GENIE3 [9], DWLasso [16], and CLR [6]. The underlying network was generated from the proposed graph generating algorithm, and the expression data were modeled from a breast cancer reference dataset. These results suggest that DWLasso and ARANCE have relatively better performance for inferring gene-gene connections compared to GENIE3 and CLR. However, the relative performance will change depending on the underlying network structure and the performance metric considered (results not shown).

## 4 Discussion

The proposed methods fill two voids that are present in the current literature. The first is a random graph generation model that is able to capture the topological properties found in real transcription networks. The topology of the *E. coli* transcription network diverges from those expected under a scale-free model, where the node degree follows a power-law distribution. This highlights the need for new generators that extend beyond classical approaches like the Watts-Strogatz algorithm and Barabasi-Albert model, and the proposed method achieves in this regard. The second void filled is a simulator for expression data that can mirror the marginal expression profiles found in RNA-seq datasets. The proposed method takes a nonparametric approach that is applicable to any reference dataset.

Taken together, these methods can be used in a variety of applications: for example, (1) to compare the performance of various co-expression methods in a particular setting; (2) to explore how robust a method is to assumptions on network topology or

distribution of gene expression; (3) to determining whether different transformations of the data improve performance; (4) to display the estimated network and visually compare it to the true underlying network; (5) to determine if a method is able to identify certain motifs in the underlying network; and (6) to assess the performance of differential network analysis methods.

## References

- [1] Barabási A. L., Albert R. (1999). Emergence of scaling in random networks. *Science*. Vol. 286, No. 5439, pp. 509–512.
- [2] Barabasi A. L., Oltvai Z. N. (2004). Network biology: understanding the cell’s functional organization. *Nature Reviews Genetics*. Vol. 5, No. 2, pp. 101.
- [3] Barbosa S. [et al.] (2018). A guide to gene regulatory network inference for obtaining predictive solutions: underlying assumptions and fundamental biological and data constraints. *Biosystems*.
- [4] Danaher P., Wang P., Witten D. M. (2014). The joint graphical lasso for inverse covariance estimation across multiple classes. *J. Royal Statistical Society B*. Vol. 76, No. 2, pp. 373–397.
- [5] de Jong H. (2002). Modeling and simulation of genetic regulatory systems: a literature review. *J. Computational Biology*. Vol. 9, No. 1, pp. 67–103.
- [6] Faith J. J. [et al.] (2007). Large-scale mapping and validation of escherichia coli transcriptional regulation from a compendium of expression profiles. *PLoS Biology*. Vol. 5, No. 1, pp. e8.
- [7] Featherstone D. E., Broadie K. (2002). Wrestling with pleiotropy: genomic and topological analysis of the yeast gene expression network. *Bioessays*. Vol. 24, No. 3, pp. 267–274.
- [8] Ha M. J., Baladandayuthapani V., Do K. A. (2015). DINGO: differential network analysis in genomics. *Bioinformatics*. Vol. 31, No. 21, pp. 3413–3420.
- [9] Huynh-Thu V. A. [et al.] (2010). Inferring regulatory networks from expression data using tree-based methods. *PloS ONE*. Vol. 5, No. 9, pp. e12776.
- [10] Marbach D. [et al.] (2010). Revealing strengths and weaknesses of methods for gene network inference. *Proc. National Academy of Sciences*. Vol. 107, No. 14, pp. 6286–6291.
- [11] Margolin A. A. [et al.] (2006). ARACNE: an algorithm for the reconstruction of gene regulatory networks in a mammalian cellular context. *BMC Bioinformatics*. Vol. 7, pp. S7.

- [12] Modi S. R. [et al.] (2011). Functional characterization of bacterial sRNAs using a network biology approach. *Proc. National Academy of Sciences*. Vol. 108, No. 37, pp. 15522–15527.
- [13] Pesonen M. [et al.] (2018). A combined PLS and negative binomial regression model for inferring association networks from next-generation sequencing count data. *IEEE/ACM Trans. Computational Biology and Bioinformatics (TCBB)*. Vol. 15, No. 3, pp. 760–773.
- [14] Pihur V., Datta S., Datta S. (2008). Reconstruction of genetic association networks from microarray data: a partial least squares approach. *Bioinformatics*. Vol. 24, No. 4, pp. 561–568.
- [15] Santos-Zavaleta A. [et al.] (2018). RegulonDB v 10.5: tackling challenges to unify classic and high throughput knowledge of gene regulation in *E. coli* K-12. *Nucleic acids research*. Vol. 47, No. D1, pp. D212–D220.
- [16] Sulaimanov N. (2018). Inferring gene expression networks with hubs using a degree weighted Lasso approach. *Bioinformatics*. Vol. 35, No. 6, pp. 987–994.
- [17] Walhout A. J. (2011). What does biologically meaningful mean? a perspective on gene regulatory network validation. *Genome Biology*. Vol. 12, No. 4, pp. 109.
- [18] Wang Z. [et al.] (2017). VCNet: vector-based gene co-expression network construction and its application to RNA-seq data. *Bioinformatics*. Vol. 33, No. 14, pp. 2173–2181.
- [19] Watts D. J., Strogatz S. H. (1998). Collective dynamics of “small-world” networks. *Nature*. Vol. 393, No. 6684, pp. 440.
- [20] Xu T. [et al.] (2018). Identifying gene network rewiring by integrating gene expression and gene network data. *IEEE/ACM Trans. Computational Biology and Bioinformatics*. Vol. 15, No. 6, pp. 2079–2085.

# MULTICLASS SUPPORT VECTOR MACHINES WITH GENSVN

P.J.F. GROENEN, G.J.J. VAN DEN BURG  
*Econometric Institute, Erasmus University Rotterdam*  
*Rotterdam, THE NETHERLANDS*  
e-mail: groenen@ese.eur.nl

## Abstract

Binary support vector machines (SVM) have become a standard tool for supervised machine learning. Attractive features of the SVM are that its solution only depends on badly fitting observations, it combats overfitting through regularization, can handle high dimensionality (thus many predictors), allows for nonlinear predictions, and is robust against outliers. Much less attention has been given to classification problems with more than two classes. In the machine learning literature, such multiclass problems tend to be solved by repeatedly applying binary SVMs, for example, through one-versus-one (OvO) or one-versus-all (OvA). Although such approaches are generally fast, they can lead to regions that are inconclusive in their prediction. As an alternative, the present authors have proposed a single machine classifier, called GenSVM (see, [1]). In this paper, we present its main properties and discuss examples of its implementations in the R and Python packages.

**Keywords:** data science, support vector machine, multiclass classification

## 1 Introduction

Multiclass classification is abundant in many areas of empirical science. In medicine, the task could be to predict cancer stages out of blood values, in epidemiology to predict college degree out of genetic variables, and in marketing to predict buyers from nonbuyers out of previous shopping behavior. All these cases are examples of the multiclass classification problem that has  $K$  (two or more) response categories, with usually one or more predictor variables. Often, the goal is to find a linear combination of the predictor variables that separates the predictor space into  $K$  polyhedral sets. Then the decision rule is to assign the observation to the class of the polyhedral set it falls in. Some multiclass classification techniques include: Fisher discriminant analysis, multinomial regression, classification trees, and neural networks.

Here, we focus on the supervised learning technique of support vector machines (SVMs). The binary SVM is quite popular in computer science. The advantage of the binary SVM is that it only depends on observations that are not perfectly predicted, it is robust against outliers, and has a provision against overfitting by using regularisation term. Multiclass classification is often performed through repeated binary SVMs, either through one-versus-one (OvO, doing binary SVMs between all pairs of classes, or through one-versus-all (OvA, for each class doing a binary SVMs between itself against the remaining classes). OvO has the advantage that each binary SVM solves a small subproblem, whereas OvA only needs to solve  $K$  problems. Both approaches can make

use of standard binary SVM implementations. However, there are also disadvantages of OvO and OvA. For example, OvO needs to solve  $K(K - 1)/2$  problems which can become large as  $K$  grows. OvA can be expected to be slower than OvO because for each class the binary SVM problem is as large as the full data set. More importantly, the binary SVM is not designed for the multiclass problem. Both OvO and OvA can have ambiguity in prediction regions.

To overcome these problems, Van den Burg and Groenen (2016) [2] proposed a novel single machine multiclass SVM called GenSVM. It is specifically designed for the multiclass problem, it is a direct extension of the binary SVM, it is flexible through different weightings and hyperparameters, is fast and accurate. In this paper, we explain the main properties of GenSVM and show an example from the R package (see [3]) and Python package of GenSVM.

## 2 GenSVM

The basic idea of GenSVM is as follows. Let the  $n \times m$  matrix  $\mathbf{X}$  contain  $m$  predictor variables from the training set. In addition, let  $\mathbf{y}$  be an  $n$  vector with class labels  $\{1, 2, \dots, K\}$  for each of the  $i$  objects. Also, let the  $K \times (K - 1)$  matrix  $\mathbf{U}$  contain coordinates of a regular simplex in  $K - 1$  dimensions. For example, for  $K = 3$  classes, the simplex is an equilateral triangle in two dimensions. Then, the goal of GenSVM is to (non)linearly map the  $n$  objects in the  $p$  dimensional space given by  $\mathbf{X}$  to the  $K - 1$  dimensional space of the simplex such that each object  $i$  is in or as close as possible to the prediction region of its class  $y_i$  according to some missclassification error. Figure 1 gives an example of a multiclass classification problem with  $K = 3$  classes and  $m = 2$  predictor variables. The left panel shows the  $n$  objects as points labeled by their class in the space of the predictor variables in  $\mathbf{X}$ . The middle panel show the  $K - 1 = 2$  dimensional simplex space with the boundaries (solid lines) of the predictor regions. The right panel shows the nonlinear boundaries of the prediction regions in the original space of  $\mathbf{X}$ .

Important aspects of GenSVM are (a) how exactly the mapping is being done from the original space of  $\mathbf{X}$  to the simplex space  $\mathbf{S}$  and (b) how the errors are being defined. We will discuss linear mappings only. For an explanation on how nonlinear mappings can be obtained through kernels, we refer to the appendix of [2]. The linear mapping of  $\mathbf{X}$  to the simplex space  $\mathbf{S}$  is obtained by

$$\mathbf{S} = \mathbf{X}\mathbf{W} + \mathbf{1}\mathbf{c}^\top$$

with  $\mathbf{W}$  the  $m \times (K - 1)$  matrix with unknown weights and  $\mathbf{c}$  the  $(K - 1) \times 1$  translation vector.

Once the mapping is obtained, GenSVM needs to determine how good or bad an object is placed. Consider Figure 4 where object  $A$  is shown as a point in the simplex space corresponding to one of the rows of  $\mathbf{S}$ . Assume that  $A$  has  $y_A = 2$  so that ideally  $A$  should be located in the shaded area around vertex  $\mathbf{u}_2$ .

To measure the error in classification, GenSVM uses a measure of distance to the shaded area. In particular, consider the projection  $q_A^{21}$  of point  $A$  onto difference vector

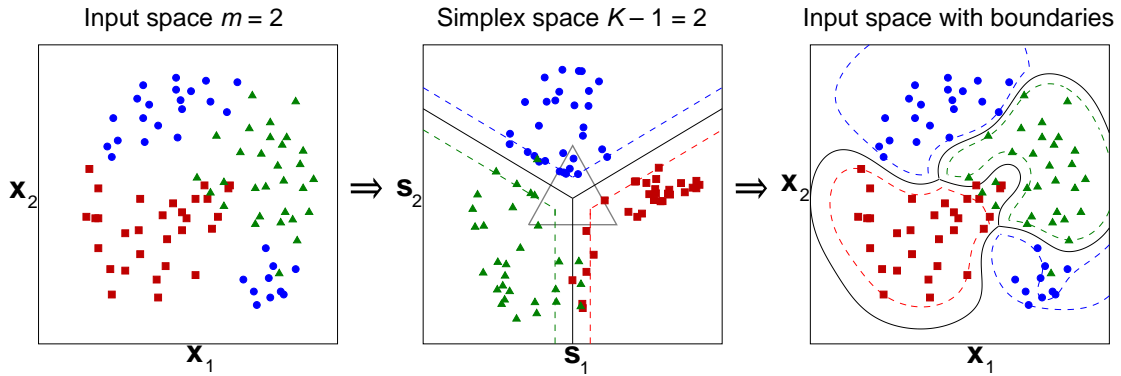


Figure 1: Example of objects in  $K = 3$  classes in the original  $p = 2$  dimensional space of  $\mathbf{X}$  (left panel), their mapping in the  $K - 1 = 2$  dimensional simplex space, the simplex, and the prediction regions (middle panel), and the resulting nonlinear prediction regions for the classes in the original space of  $\mathbf{X}$  (right panel). This figure is reproduced from [2].

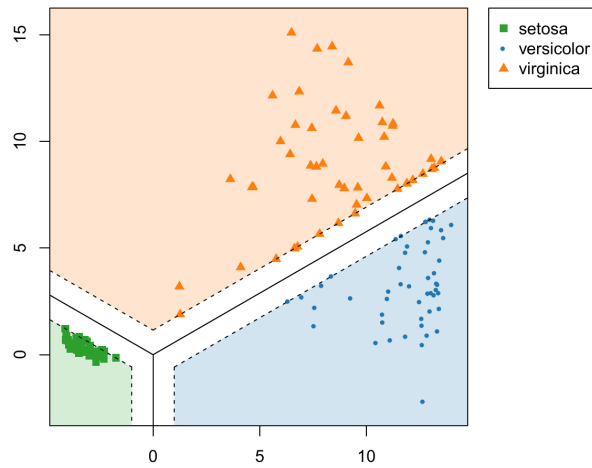


Figure 2: The simplex space with misclassified object  $A$  that ideally should have been positioned in the shaded prediction region of its class 2. The projections  $q_A^{21}$  and  $q_A^{23}$  show how far  $A$  is from the boundaries separating vertices  $\mathbf{u}_2$  and  $\mathbf{u}_1$  and vertices  $\mathbf{u}_2$  and  $\mathbf{u}_3$ . This figure is reproduced from [2].

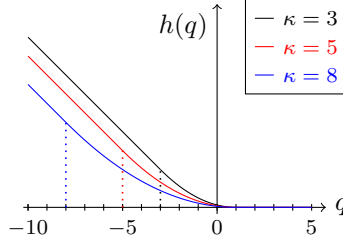


Figure 3: The huberized hinge error  $h(q)$ .

$\mathbf{u}_2 - \mathbf{u}_1$  that measures the distance of  $A$  to the boundary separating class 2 from 1. Here, this boundary coincides with the vertical axis, thus all points with  $s_1 = 0$ . Let the values on the predictor variables for  $A$  be in the vector  $\mathbf{x}_A^\top$ . Then, the position of  $A$  in the simplex space is given by  $\mathbf{s}_A^\top = \mathbf{x}_A^\top \mathbf{W} + \mathbf{c}^\top$  and its projections onto the difference vectors separating class 2 from 1 and 3 by

$$\begin{aligned} q_A^{(21)} &= \mathbf{s}_A^\top (\mathbf{u}_2 - \mathbf{u}_1) && (< 0 \text{ when misclassified}) \\ q_A^{(23)} &= \mathbf{s}_A^\top (\mathbf{u}_2 - \mathbf{u}_3) && (< 0 \text{ when misclassified}). \end{aligned}$$

The seriousness of the misclassification is given by the Huberized hinge error

$$h(q) = \begin{cases} 1 - q - (\kappa + 1)/2 & \text{if } q \leq -\kappa \\ (1 - q)^2 / (2(\kappa + 1)) & \text{if } q \in (-\kappa, 1] \\ 0 & \text{if } q > 1 \end{cases}$$

as shown in Figure 3. Finally, a rule is needed to combine the misclassification errors. For this, GenSVM uses the  $L_p$  norm

$$h\left(q_i^{(y_i,j)}\right) = \left( \sum_{j \neq y_i} h^p\left(q_i^{(y_i,j)}\right) \right)^{1/p}$$

where  $1 \leq p \leq 2$ . The effect for this error function is shown in Figure 4 for  $p = 2$  and  $\kappa = -0.95$ . In this case, one can easily see that this error is a function of the Euclidean distance of the point to the boundary. As  $\kappa$  grows larger, the sharp bend becomes more smooth (quadratic). If  $p = 1$ , the  $L_1$  norm is used, implying that misclassification with respect to multiple classes receives a higher error than misclassification with respect to a single class only.

With these definitions, the GenSVM loss function can be defined as

$$L_{\text{MSVM}}(\mathbf{W}, \mathbf{c}) = \frac{1}{n} \sum_{i=1}^n \rho_i \left( \sum_{j \neq y_i} h^p\left(q_i^{(y_i,j)}\right) \right)^{1/p} + \lambda \text{tr } \mathbf{W}'\mathbf{W} \quad (1)$$

with  $\rho_i \geq 0$  prespecified object weights and  $\lambda > 0$  a given penalty strength parameter. Note that the term  $\text{tr } \mathbf{W}'\mathbf{W}$  is quadratic in  $\mathbf{W}$  and penalizes nonzero  $w_{kl}$ . The GenSVM

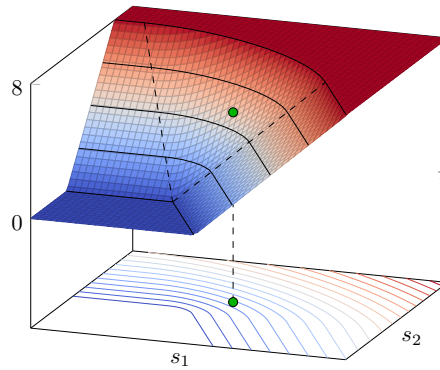


Figure 4: The combined hinge error by  $h\left(q_i^{(y_i,j)}\right)$  for  $p = 2$  and  $\kappa = -0.95$ .

loss function has several nice properties. First, it is a convex function in  $\mathbf{W}$  and  $\mathbf{c}$  as it is a sum of convex functions. Consequently, its minimum is global. Secondly, (1) simplifies into standard binary SVM if  $K = 2$  and  $\kappa = -1$ . Finding optimal values for  $\lambda$ ,  $p$ , and  $\kappa$  can be done through  $K$ -fold cross validation.

The GenSVM algorithm developed in [2] and implemented in [3] that optimizes  $L_{\text{MSVM}}(\mathbf{W}, \mathbf{c})$  is based on the MM (minimization by majorization principle, see [1]). One of the main advantages of MM is that for a given  $\lambda$ ,  $p$ , and  $\kappa$  the function value decreases until a minimum is reached. In  $K$ -fold cross validation, (1) needs to be minimized for many combinations of  $\lambda$ ,  $p$ , and  $\kappa$ . The advantage of the MM algorithm is that warm starts can be used, for example, if two subsequent  $\lambda$  values are only slightly different, then the  $\mathbf{W}$  and  $\mathbf{c}$  obtained can be used as start values for the run of the next  $\lambda$ . Often only a very few iterations are needed thereby greatly reducing the computational efforts.

### 3 The GenSVM package in R

The GenSVM package in R implements the loss function and minimization procedure discussed above.<sup>1</sup> The core of the package is written in C so that it tends to run fast. The linear algebra routines used by GenSVM use the optimized BLAS and LAPACK libraries shipped with R, and therefore automatically takes advantage of multi-core architectures.

Below is a simple example of a nonlinear GenSVM applied to the Fisher Iris data using the radial basis function (RBF) kernel. Because the Iris data only has  $K = 3$  classes, the simplex space can be visualized in 2D in Figure 5.

```
R> library(gensvm)
R> x <- iris[, -5]
R> y <- iris[, 5]
R> # Fit a nonlinear GenSVM through the RBF kernel
R> fit <- gensvm(scale(x), y, kernel='rbf', max.iter=10000)
```

<sup>1</sup>The gensvm package is available on CRAN.

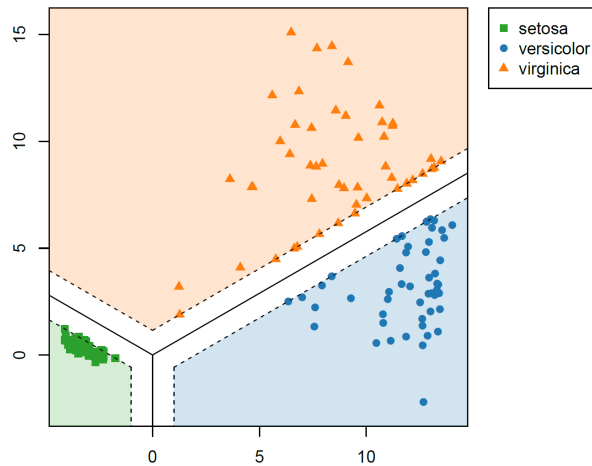


Figure 5: Simplex space of the GenSVM solution on the iris data set.

```
R> plot(fit)
```

The R package includes code for efficiently running cross validation and grid search over the hyperparameters. This code ensures that warm starts are used throughout, thereby increasing the efficiency of the MM algorithm. For GenSVM and SVMs in general, optimizing the hyperparameters is an important step for obtaining high classification accuracy. GenSVM is flexible through three different hyperparameters ( $\kappa$ ,  $p$ , and  $\lambda$ ) and optimizing these through grid search can be a time-consuming task for the user. To facilitate this, the GenSVM R package contains three pre-defined parameter grids in the function `gensvm.grid` that are designed to obtain high out-of-the-box classification accuracy. These parameter grids were constructed from the best hyperparameter configurations found in the large experimental study of [2]. For instance, the following code illustrates running a grid search with a very small hyperparameter grid:

```
R> fit <- gensvm.grid(x, y, param.grid = 'tiny')
```

A convenient feature of this grid search function is that the resulting object can directly be used with common R functions such as `plot` and `predict`, for which the best performing model will be used. Moreover, the object contains a `cv.results` attribute that holds a data frame with the complete results of the grid search.

Another common task in fitting SVMs is scaling the data and creating a training and test dataset. Scaling the features is necessary to ensure that the regularization term works equally on all features. To facilitate this, the GenSVM R package contains the `gensvm.maxabs.scale` function that scales the features to the interval  $[-1, 1]$  while preserving sparsity. Furthermore, the R package also includes a function for creating a train and test dataset called `gensvm.train.test.split`. These functions can be combined as follows:

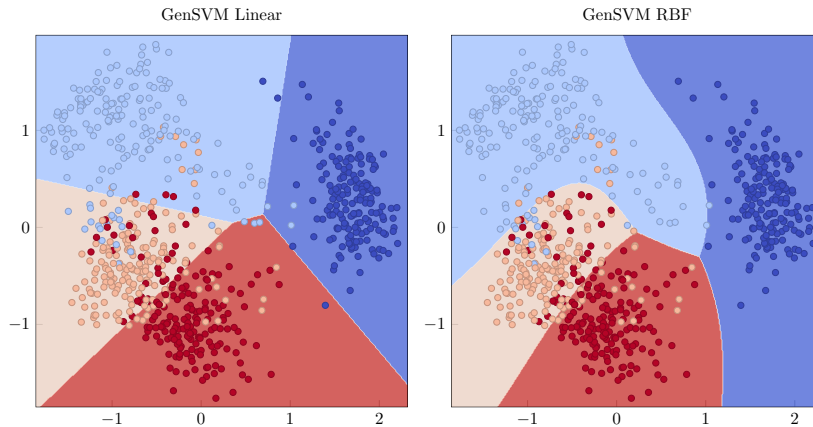


Figure 6: Illustration of linear and nonlinear GenSVM for a subset of the handwritten digits dataset using the Python package for GenSVM. Dimensionality reduction was applied to obtain two input dimensions for easy visualization, but this is not a requirement for GenSVM.

```
R> split <- gensvm.train.test.split(x, y, random.state=123)
R> x.train <- split$x.train; y.train <- split$y.train;
R> x.test <- split$x.test; y.test <- split$y.test;
R> scaled <- gensvm.maxabs.scale(x.train, x.test)
R> fit <- gensvm(scaled$x, y.train, kernel='rbf', max.iter=1000, random.seed=123)
R> gensvm.accuracy(predict(fit, scaled$x.test), y.test)

[1] 0.921
```

## 4 The GenSVM package in Python

The Python package for GenSVM has similar functionality to the R package, but is based on the object-oriented framework for machine learning methods used in Scikit-Learn [4].<sup>2</sup> This allows for straightforward interoperability with existing code that uses methods from the Scikit-Learn package. The computational routines in the Python package are again implemented in C (in fact, both packages share the same C library) and are linked to Python through Cython. An example of fitting and predicting a GenSVM model with the Python package is as follows:

```
from gensvm import GenSVM

clf = GenSVM(kernel='rbf', verbose=1)
clf.fit(x, y)
```

Note that due to the object-oriented nature of the code, parameters that determine the kernel and affect the loss function are provided in the constructor of the `GenSVM` object.

<sup>2</sup>The Python package for GenSVM is available on PyPI.

While previously we have illustrated the *simplex space* of a GenSVM solution, we now illustrate the decision boundaries in the *input space*. We use a subset of the handwritten digits dataset from the UCI repository [5] and illustrate the decision boundaries in the original space in Figure 6. Notice that the dataset is not separable with either a linear or nonlinear kernel. However, GenSVM with the RBF kernel achieves better separation of the classes.

## References

- [1] Hunter, D.R. & Lange, K. (2004). A tutorial on MM algorithms. *The American Statistician*, 58 (1):30–37.
- [2] Van den Burg, G.J.J. & Groenen, P.J.F. (2016). GenSVM: A generalized multiclass support vector machine. *Journal of Machine Learning Research*, 17, 1-42.
- [3] Van den Burg, G.J.J. & Groenen, P.J.F. (2018). *GenSVM: A generalized multiclass support vector machine*. <https://cran.r-project.org/package=gensvm>, R-package.
- [4] Pedregosa, F. et al. (2011). Scikit-learn: Machine learning in Python. *Journal of Machine Learning Research*, 12 (Oct):2825–2830.
- [5] Bache, K. & Lichman, M. (2013). UCI Machine Learning Repository. *University of California, Irvine*. <http://archive.ics.uci.edu/ml>

# DISCRETE-VALUED TIME SERIES ANALYSIS BY PARSIMONIOUS HIGH-ORDER MARKOV CHAINS

YU.S. KHARIN

*Research Institute for Applied Problems of Mathematics and Informatics  
Belarusian State University  
Minsk, BELARUS  
e-mail: Kharin@bsu.by*

## Abstract

Problems of statistical analysis of discrete-valued time series are considered. A family of parsimonious (small-parametric) models for observed data are proposed based on high-order Markov chains. Consistent statistical estimators for parameters of the proposed models and some known models, and also statistical tests on the values of parameters are constructed. Probabilistic properties of the constructed statistical inferences are given. The developed approach is also applied for statistical analysis of spatio-temporal data. Theoretical results are illustrated by results of computer experiments on real statistical data.

**Keywords:** data science, parsimonious model, Markov chain, discrete data

## 1 Introduction

Time series analysis is deep developed [1] for “continious” data when the observation space  $\mathbf{A}$  is some Euclidean space or its subspace of nonzero Lebesgue measure:  $\mathbf{A} \subseteq R^m$ ,  $\text{mes}(\mathbf{A}) > 0$ . In practice, however, (because of “digitalization” of our real world) the statisticians need to use discrete-valued models of time series, when the observation space  $\mathbf{A}$  is some discrete set with cardinality  $N = |\mathbf{A}|$ ,  $\text{mes}(\mathbf{A}) = 0$ . Give some applied areas where discrete-valued time series models are extremely helpful [2]: bioinformatics for analysis of genetic sequences ( $N=4$ ); information systems for information protection ( $N = 2$ ); meteorology for weather prediction; social science for modelling of dynamics in social behavior; public health and personalized medicine; prediction of environmental processes; financial engineering; telecommunications; alarm systems.

Discrete-valued time series is a random process  $x_t \in \mathbf{A}$  on some probability space  $(\Omega, \mathbf{F}, \mathbf{P})$  with discrete time  $t \in \mathbf{N}_0 = \{0, 1, 2, \dots\}$  and a discrete state space  $\mathbf{A}$  with the cardinality  $N = |\mathbf{A}|$ ,  $2 \leq N \leq +\infty$ . Much attention to discrete-valued time series considered as categorical time series was paid by B. Kedem and K. Fokianos [3].

If  $\mathbf{A}$  is any countable set ( $N = +\infty$ ), then we have a countable valued time series  $x_t$ . If  $\mathbf{A}$  is any finite set ( $N < +\infty$ ), then we have a finitely valued time series, also called categorical time series [3]. We will consider here these cases both, and, without loss of generality, we will assume that  $\mathbf{A} = \{0, 1, \dots, N - 1\}$ .

An universal base model for discrete-valued time series  $x_t \in \mathbf{A}$  is the homogeneous Markov chain  $\text{MC}(s)$  of some order  $s \in \mathbf{N}_0$ , determined by the generalized Markov property ( $t > s$ ):

$$\mathbf{P}\{x_t=i_t|x_{t-1}=i_{t-1}, \dots, x_1=i_1\}=\mathbf{P}\{x_t=i_t|x_{t-1}=i_{t-1}, \dots, x_{t-s}=i_{t-s}\}=p_{i_{t-s}, \dots, i_{t-1}, i_t}, \quad (1)$$

where  $s$  is the memory depth;  $i_1, i_2, \dots, i_t \in \mathbf{A}$  are values of the process at the time moments  $1, 2, \dots, t$  respectively;  $\mathbf{P} = (p_{i_{t-s}, \dots, i_{t-1}, i_t})$  is an  $(s+1)$ -dimensional matrix of one-step transition probabilities. Number of independent parameters for the MC( $s$ ) model increases exponentially w.r.t. the memory depth  $s$ :  $D_{\text{MC}(s)} = N^s(N-1)$ .

To identify this model (1) we need to have huge data sets and the computation work of size  $O(N^{s+1})$ . To avoid this ‘‘curse of dimensionality’’ we propose to use the parsimonious (‘‘small-parametric’’) models of high-order Markov chains that are determined by small number of parameters  $d \ll D_{\text{MC}(s)}$  [4].

## 2 Approaches to construction of parsimonious high-order Markov chains

According to what has been said in Introduction, parsimonious high-order Markov chain is determined by parsimonious representation of the one-step transition probabilities matrix  $\mathbf{P}$ , defined by (1). Number of independent parameters  $d$  of the parsimonious matrix is much smaller than the total number of independent parameters and is determined by the parsimony coefficient:

$$\varkappa ::= \frac{d}{D_{\text{MC}(s)}} \ll 1. \quad (2)$$

In our opinion, there are two main approaches to construction of parsimonious matrix  $\mathbf{P}$ :

- 1) squeezing of the set of different values of elements in matrix  $\mathbf{P}$ ;
- 2) using of some generation equation for the conditional probability distribution (1) of the future state  $x_t$  under its prehistory.

To explain **the first approach** let us introduce some notations:  $Q = (q_{j_1, \dots, j_r, j_{r+1}})$  is some stochastic  $(r+1)$ -dimensional matrix,  $1 \leq r < s$ ,  $\sum_{j_{r+1} \in \mathbf{A}} q_{j_1, \dots, j_r, j_{r+1}} \equiv 1$ ,  $0 \leq q_{j_1, \dots, j_r, j_{r+1}} \leq 1$ ,  $j_1, \dots, j_{r+1} \in \mathbf{A}$ ;  $B(\cdot) : \mathbf{A}^s \rightarrow \mathbf{A}^r$  is some discrete function. The  $(s+1)$ -dimensional matrix  $\mathbf{P}$  is squeezed to the  $(r+1)$ -dimensional matrix  $Q$  by the general transformation:

$$p_{i_1, \dots, i_s, i_{s+1}} = q_{B(i_1, \dots, i_s), i_{s+1}} \quad (3)$$

with the parsimony coefficient (2) equal to

$$\varkappa = N^{r-s} \leq 1. \quad (4)$$

Illustration of the squeezing approach (3) for the case of  $N = 2$ ,  $s = 4$ ,  $r = 2$  is given by Figure 1 and Figure 2. As it is seen from these figures and from (3), matrix  $\mathbf{P}$  has many identical rows (they are marked by identical colors).

Give a list of known parsimonious high-order Markov chains correspondent to **the first approach**: Markov chain of order  $s$  with  $r$  partial connections MC( $s, r$ ) [5, 6], Markov chain of conditional order MCCO( $s, r$ ) [7], variable length Markov chain [8].

$$\mathbf{P} = \begin{matrix}
0 & 0 & 0 & 0 \\
0 & 0 & 0 & 1 \\
0 & 0 & 1 & 0 \\
0 & 0 & 1 & 1 \\
0 & 1 & 0 & 0 \\
0 & 1 & 0 & 1 \\
0 & 1 & 1 & 0 \\
0 & 1 & 1 & 1 \\
1 & 0 & 0 & 0 \\
1 & 0 & 0 & 1 \\
1 & 0 & 1 & 0 \\
1 & 0 & 1 & 1 \\
1 & 1 & 0 & 0 \\
1 & 1 & 0 & 1 \\
1 & 1 & 1 & 0 \\
1 & 1 & 1 & 1
\end{matrix} \begin{pmatrix}
0 & 1 \\
q_{000} & 1-q & 000 \\
q_{000} & 1-q & 000 \\
q_{010} & 1-q & 010 \\
q_{010} & 1-q & 010 \\
q_{000} & 1-q & 000 \\
q_{000} & 1-q & 000 \\
q_{010} & 1-q & 010 \\
q_{010} & 1-q & 010 \\
q_{100} & 1-q & 100 \\
q_{100} & 1-q & 100 \\
q_{110} & 1-q & 110 \\
q_{110} & 1-q & 110 \\
q_{100} & 1-q & 100 \\
q_{100} & 1-q & 100 \\
q_{110} & 1-q & 110 \\
q_{110} & 1-q & 110
\end{pmatrix}$$

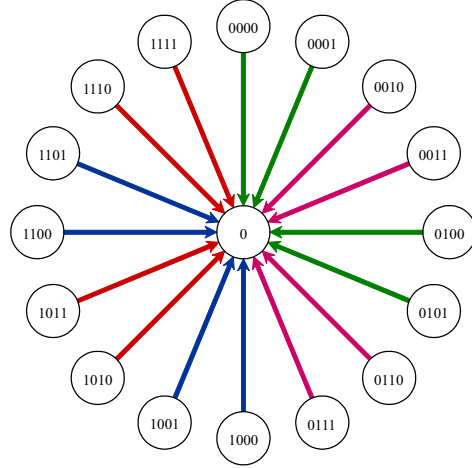


Figure 1: Parsimonious matrix  $\mathbf{P}$ :  $N=2, s=4, r=2, \varkappa=0.25$       Figure 2: Visualization of the parsimonious matrix from Figure 1

**The second approach** to construction of parsimonious high-order Markov chain is based on some generation equation for the conditional probability distribution of the future state  $x_t \in \mathbf{A}$  under its prehistory  $X_{t-s}^{t-1} = (x_{t-1}, \dots, x_{t-s})'$ :

$$p_{i_1, \dots, i_s, i_{s+1}} = q_{i_{s+1}}(\theta(i_1, \dots, i_s; a)), \quad i_1, \dots, i_{s+1} \in \mathbf{A}, \quad (5)$$

where  $\{q_j(\theta) : j \in \mathbf{A}\}$  is some discrete probability distribution on  $\mathbf{A}$  that is dependent on the parameter  $\theta = (\theta_j) \in \Theta \subseteq R^L$ ,  $\theta(i_1, \dots, i_s; a)$  is some parametric function a priori known up to some unknown vector parameter  $a = (a_k) \in R^m$ .

The parsimony coefficient for this approach is

$$\varkappa = \frac{m}{N^s(N-1)} \leq 1. \quad (6)$$

List of known parsimonious high-order Markov chains correspondent to **the second approach** is longer: Jakobs – Lewis model [9], MTD-model [10], DAR( $s$ ) [11], BCNAR( $s$ ) [12], BiCNAR( $s$ ) [13], PCNAR( $s$ ) [14].

### 3 Statistical analysis for parsimonious models constructed by the first approach

#### 3.1 Markov chain MC( $s, r$ ) of order $s$ with $r$ partial connections

The MC( $s, r$ ) proposed by Yu. Kharin in 2004 [5] is determined by the following parsimonious reparametrization of the  $(s+1)$ -dimensional transition probability matrix:

$$p_{J_1^{s+1}} = p_{j_1, \dots, j_s, j_{s+1}} = q_{j_m^0, \dots, j_m^0, j_{s+1}}, \quad (7)$$

where  $J_1^{s+1} = (j_1, \dots, j_{s+1}) \in \mathbf{A}^s$  is the  $(s+1)$ -dimensional index vector;  $r$  is the number of connections ( $1 \leq r \leq s$ );  $M_r^0 = (m_1^0, \dots, m_r^0) \in M$  is some integer-valued vector with  $r$  ordered components,  $1 = m_1^0 < m_2^0 < \dots < m_r^0 \leq s$ , called the template of connections;  $Q = \left( q_{J_1^{r+1}} \right)_{J_1^{r+1} \in \mathbf{A}^{r+1}}$  is an  $(r+1)$ -dimensional stochastic matrix. If  $r = s$ , we have the general MC( $s$ )-model.

In [4, 5, 6] the following probabilistic properties of the MC( $s, r$ )-model are found.

**Theorem 1.** *The MC( $s, r$ ) defined by (7) is an ergodic Markov chain iff there exists*

*$i \in N$  such that  $\min_{J_1^s, J_{s+i+1}^{2s+i} \in \mathbf{A}^s} \sum_{J_{s+1}^{s+i} \in \mathbf{A}^i} \prod_{k=1}^{s+i} q_{j_{k+m_1^0-1}, \dots, j_{k+m_r^0-1}, j_{k+s}} > 0$ . Stationary probability*

*distribution  $\pi_{J_1^s}^*$  satisfies the equations:  $\pi_{J_2^{s+1}}^* = \sum_{j_1 \in \mathbf{A}} \pi_{J_1^s}^* q_{j_{m_1^0}, \dots, j_{m_r^0}, j_{s+1}}$ ,  $J_1^{s+1} \in \mathbf{A}^s$ .*

**Corollary 1.** *For a stationary Markov chain the stationary probability distribution has*

*the multiplicative form:  $\pi_{J_1^s}^* = \prod_{i=1}^s \pi_{j_i}^*$ ,  $J_1^s \in \mathbf{A}^s$ , if  $\pi_{J_{r+1}^r}^* = \sum_{j_1 \in \mathbf{A}} \pi_{j_1}^* q_{J_1^{r+1}}$ ,  $J_2^{r+1} \in \mathbf{A}^r$ .*

**Corollary 2.** *If  $Q$  is doubly stochastic:  $\sum_{j_1 \in \mathbf{A}} q_{J_1^{r+1}} \equiv 1$ ,  $\sum_{j_{r+1} \in \mathbf{A}} q_{J_1^{r+1}} \equiv 1$ , then the stationary probability distribution is uniform:  $\pi_{J_1^s}^* \equiv N^{-s}$ .*

Introduce the notation:  $\delta_{ij}$  is Kronecker symbol;  $F(J_i^{i+s-1}; M_r) = (j_{i+m_1-1}, \dots, j_{i+m_r-1})$  is the selector-function;

$$\nu_{J_1^{r+1}}(X_1^n; M_r) = \sum_{t=1}^{n-s} \delta_{F(X_t^{t+s-1}; M_r), J_1^r} \delta_{x_{t+s}, j_{r+1}} \quad (8)$$

is the frequency statistic for the template  $M_r \in M$ ;  $\mu_{J_1^{r+1}}(M_r) = \mathbf{P}\{F(X_t^{t+s-1}; M_r) = J_1^r, x_{t+s} = j_{r+1}\}$  is the probability distribution of the  $(r+1)$ -tuple; the dot used instead of any index means summation on all its values:  $\mu_{J_1^r \bullet}(M_r) = \sum_{j_{r+1} \in \mathbf{A}} \mu_{J_1^{r+1}}(M_r)$ ;

$\hat{\mu}_{J_1^{r+1}}(M_r) = \nu_{J_1^{r+1}}(X_1^n; M_r) / (n-s)$  is the frequency estimator for the probability  $\mu_{J_1^{r+1}}(M_r)$ ,  $J_1^{r+1} \in \mathbf{A}^{r+1}$ ,  $M_r \in M$ .

**Theorem 2.** *If the template of connections  $M_r^0$  is known, then the maximum likelihood estimator (MLE) for the matrix  $Q$  is  $\hat{Q} = \left( \hat{q}_{J_1^{r+1}} \right)_{J_1^{r+1} \in \mathbf{A}^{r+1}}$ :*

*$\hat{q}_{J_1^{r+1}} = \left\{ \hat{\mu}_{J_1^{r+1}}(M_r^0) / \hat{\mu}_{J_1^r \bullet}(M_r^0), \text{ if } \hat{\mu}_{J_1^r \bullet}(M_r^0) > 0; 1/N \text{ else} \right\}$ . Under the stationarity condition,  $\left\{ \hat{q}_{J_1^{r+1}} : J_1^{r+1} \in \mathbf{A}^{r+1} \right\}$  are asymptotically ( $n \rightarrow \infty$ ) unbiased and consistent with covariances  $\text{Cov} \left\{ \hat{q}_{J_1^{r+1}}, \hat{q}_{K_1^{r+1}} \right\} = \sigma_{J_1^{r+1}, K_1^{r+1}}^{\hat{q}} / (n-s) + O(1/n^2)$ ,*

$$\sigma_{J_1^{r+1}, K_1^{r+1}}^{\hat{q}} = \delta_{J_1^r, K_1^r} q_{J_1^{r+1}} \left( \delta_{j_{r+1}, k_{r+1}} - q_{K_1^{r+1}} \right) / \mu_{J_1^r \bullet}(M_1^0), \quad J_1^{r+1}, K_1^{r+1} \in \mathbf{A}^{r+1}.$$

Moreover, the probability distribution of the  $N^{r+1}$ -dimensional composed random vector  $\left(\sqrt{n-s} \left(\hat{q}_{J_1^{r+1}} - q_{J_1^{r+1}}\right)\right)_{J_1^{r+1} \in \mathbf{A}^{r+1}}$  at  $n \rightarrow \infty$  converges to the normal probability distribution with zero mean and the covariance matrix  $\Sigma^{\hat{q}} = \left(\sigma_{J_1^{r+1}, K_1^{r+1}}^{\hat{q}}\right)$ .

The consistent statistical test for the hypotheses  $H_0 = \{Q = Q^0\}$ , where  $Q^0 = \left(q_{J_1^{r+1}}^0\right)_{J_1^{r+1} \in \mathbf{A}^{r+1}}$  is some given matrix;  $H_1 = \overline{H_0}$ , consists of the following steps.

1. Computation of the statistics  $\nu_{J_1^{r+1}}(X_1^n; M_r^0)$ ,  $J_1^{r+1} \in \mathbf{A}^{r+1}$ , by (8).

2. Computation of the statistic  $\left(D_{J_1^r} = \left\{j_{r+1} \in \mathbf{A} : q_{J_1^{r+1}}^0 > 0\right\}\right)$

$$\rho = \sum_{J_1^r \in \mathbf{A}^r, j_{r+1} \in D_{J_1^r}} \nu_{J_1^{\bullet}}(X_1^n; M_r^0) \left(\hat{q}_{J_1^{r+1}} - q_{J_1^{r+1}}^0\right)^2 / q_{J_1^{r+1}}^0.$$

3. Computation of the  $P$ -value:  $P = 1 - G_U(\rho)$ , where  $G_U(\cdot)$  is the standard  $\chi^2$ -distribution function with  $U = \sum_{J_1^r \in \mathbf{A}^r} (|D_{J_1^r}| - 1)$  degrees of freedom.

4. The decision rule with an asymptotic significance level  $\varepsilon$ : if  $P \geq \varepsilon$ , then to conclude that the hypothesis  $H_0$  is true; otherwise, the alternative  $H_1$  is true.

**Corollary 3.** Under stationary  $MC(s, r)$  and contigual family of alternatives  $H_{1n} = \{Q = Q^{1n}\}$ , where  $Q^{1n} = \left(q_{J_1^{r+1}}^{1n}\right)_{J_1^{r+1} \in \mathbf{A}^{r+1}}$ ,  $q_{J_1^{r+1}}^{1n} = q_{J_1^{r+1}}^0 \frac{1 + d_{J_1^{r+1}}}{\sqrt{n-s}}$ ,  $\sum_{j_{r+1} \in \mathbf{A}} d_{J_1^{r+1}} q_{J_1^{r+1}}^0 = 0$ ,

$\sum_{J_1^{r+1} \in \mathbf{A}^{r+1}} |d_{J_1^{r+1}}| > 0$ , if  $H_{1n}$  is true, then at  $n \rightarrow \infty$  the power of the developed test

$w \rightarrow 1 - G_{U,a}(G_U^{-1}(1 - \varepsilon))$ , where  $G_{U,a}(\cdot)$  is the probability distribution function of the noncentral  $\chi^2$ -distribution with  $U$  degrees of freedom and the noncentrality parameter

$$a = \sum_{J_1^{r+1} \in \mathbf{A}^{r+1}} \mu_{J_1^{r+1}}(M_r^0) d_{J_1^{r+1}}^2.$$

Introduce the notation:  $M$  is the set of all admissible templates  $M_r$ ;

$$H(M_r) = - \sum_{J_1^{r+1} \in \mathbf{A}^{r+1}} \mu_{J_1^{r+1}}(M_r) \ln \left( \mu_{J_1^{r+1}}(M_r) / \mu_{J_1^{r+1}, \bullet}(M_r) \right) \geq 0 \quad (9)$$

is the conditional entropy of the future symbol  $x_{t+s} \in \mathbf{A}$  relative to the past derived by the selector  $F(X_t^{t+s-1}; M_r) \in \mathbf{A}^r$ ,  $M_r \in M$ ;  $\hat{H}(M_r)$  is the ‘‘plug-in’’ estimator of the conditional entropy, which is generated by substitution of the estimators  $\hat{\mu}_{J_1^{r+1}}(M_r)$  instead of true probabilities  $\mu_{J_1^{r+1}}(M_r)$  in (9).

**Theorem 3.** If the order  $s$  and the number of connections  $r$  are known, then the MLE  $\hat{M}_r = \arg \min_{M_r \in M} \hat{H}(M_r)$ . Under the stationarity condition of the  $MC(s, r)$  the estimator

$\hat{M}_r$  at  $n \rightarrow \infty$  is consistent:  $\hat{M}_r \xrightarrow{\mathbf{P}} M_r^0$ .

Let  $s \in [s_-, s_+]$ ,  $r \in [r_-, r_+]$ ,  $1 \leq s_- < s_+ < \infty$ ,  $1 \leq r_- < r_+ < s_+$ . To estimate parameters  $r, s$  we use the Bayesian Information Criterion (BIC) [5]:

$$BIC(s, r) = 2(n - s)\hat{H}(\hat{M}_r) + U \ln(n - s), \quad (10)$$

where  $U = \sum_{J_1^r \in \mathbf{A}^r} \left( |D_{J_1^r}| - 1 + \delta_{\hat{\mu}_{J_1^r}(\hat{M}_r), 0} \right)$ ,  $D_{J_1^r} = \left\{ j_{r+1} \in \mathbf{A} : \hat{\mu}_{j_{r+1}}(\hat{M}_r) > 0 \right\}$ .

Consistent estimators  $\hat{s}, \hat{r}$  are determined by minimization:  $BIC(s, r) \rightarrow \min_{s, r}$ .

**Theorem 4.** *If  $MC(s, r)$  is stationary, then the BIC-estimators  $\hat{r}, \hat{s}$  at  $n \rightarrow \infty$ , are consistent.*

### 3.2 Markov chain of conditional order MCCO( $s, L$ )

Introduce the notation:  $l \in \{1, 2, \dots, s - 1\}$  is some positive integer,  $K = N^l - 1$ ;  $Q^{(1)}, \dots, Q^{(M)}$  are  $M$  ( $1 \leq M \leq K + 1$ ) different square stochastic matrices of the order  $N$ :

$$Q^{(m)} = \left( q_{i,j}^{(m)} \right), \quad 0 \leq q_{i,j}^{(m)} \leq 1, \quad \sum_{j \in \mathbf{A}} q_{i,j}^{(m)} \equiv 1, \quad i, j \in \mathbf{A}, \quad 1 \leq m \leq M;$$

$\langle J_n^m \rangle = \sum_{k=n}^m N^{k-n} j_k \in \{0, 1, \dots, N^{m-n+1} - 1\}$  is the numeric representation of the multiindex  $J_n^m \in \mathbf{A}^{m-n+1}$ ;  $I\{C\}$  is the indicator function of the event  $C$ ;  $1 \leq m_k \leq M$ ,  $1 \leq b_k \leq s - L$ ,  $0 \leq k \leq K$ . It is assumed that sequences  $\{m_k\}$  and  $\{b_k\}$  are fixed,  $\min_{0 \leq k \leq K} b_k = 1$  and all elements of the set  $\{1, 2, \dots, M\}$  are present in the sequence  $m_0, \dots, m_K$ .

Markov chain  $\{x_t \in \mathbf{A} : t \in \mathbb{N}\}$  is called [7] the Markov chain of conditional order (MCCO( $s, L$ )), if its one-step transition probabilities have the following parsimonious form:

$$p_{J_1^{s+1}} = \sum_{k=0}^K I\{\langle J_{s-L+1}^s \rangle = k\} q_{j_{b_k}, j_{s+1}}^{(m_k)}.$$

The sequence of elements  $J_{s-L+1}^s$  is called the base memory fragment (BMF) of the random sequence;  $L$  is the length of BMF; the value  $s_k = s - b_k + 1$  is called the conditional order of Markov chain. Thus the conditional probability distribution of the state  $x_{t+1}$  at time point  $t + 1$  depends not on all  $s$  previous states, but it depends only on  $L + 1$  selected states ( $j_{b_k}, J_{s-L+1}^s$ ). Note that if  $L = s - 1$ ,  $s_0 = s_1 = \dots = s_K = s$ , we have the full-connected Markov chain of the order  $s$ :  $MC(s)$ . If  $M = K + 1$ , then each transition matrix corresponds to only one value of the BMF, otherwise there exists a common matrix which corresponds to several values of BMF.

Hence the transition matrix  $\mathbf{P}$  of the Markov chain of conditional order is determined by  $d = 2(N^L + 1) + MN(N - 1)$  independent elements, and the parsimony coefficient (2) is

$$\varkappa = \frac{2(N^L + 1) + MN(N - 1)}{N^s} \leq 1.$$

Methods and algorithms of statistical analysis for MCCO( $s, L$ ) are presented in [11].

## 4 Statistical analysis for parsimonious models constructed by the second approach

### 4.1 Jacobs – Lewis model

Jacobs – Lewis model is determined by a stochastic difference equation [9] ( $t > s$ ):

$$x_t = \mu_t x_{t-\eta_t} + (1 - \mu_t) \xi_t, \quad (11)$$

where  $\{\xi_t, \eta_t, \mu_t\}$  are independent random variables with probability distributions:

$$\begin{aligned} \mathbf{P}\{\mu_t = 1\} = 1 - \mathbf{P}\{\mu_t = 0\} = \rho; \quad \mathbf{P}\{\xi_t = k\} = \pi_k, \quad k \in \mathbf{A}, \quad \sum_{k \in \mathbf{A}} \pi_k = 1; \\ \mathbf{P}\{\eta_t = i\} = \lambda_i, \quad i \in \{1, 2, \dots, s\}, \quad \sum_{i=1}^s \lambda_i = 1, \quad \lambda_s \neq 0. \end{aligned} \quad (12)$$

Number of parameters depends linearly on  $s$ :  $D_{\text{JL}} = N + s - 1$ ;  $\varkappa = (N + s - 1)/N^s \leq 1$ .

In [9] only moments and stationary distributions were analyzed. We proved [4] probabilistic and statistical properties of the model (11), (12) by the MC( $s$ )-model.

**Theorem 5.** *Discrete-valued time series  $x_t$  determined by (11), (12) is a homogeneous Markov chain of the order  $s$  with the initial probability distribution  $\pi_{i_1, \dots, i_s} = \pi_{i_1} \cdot \dots \cdot \pi_{i_s}$  and the  $(s + 1)$ -dimensional matrix of transition probabilities  $\mathbf{P}(\pi, \lambda, \rho) = (p_{i_1, \dots, i_{s+1}})$ :*

$$p_{i_1, \dots, i_s, i_{s+1}} = (1 - \rho) \pi_{i_{s+1}} + \sum_{j=1}^s \lambda_j \delta_{i_{s-j+1}, i_{s+1}}, \quad i_1, \dots, i_{s+1} \in \mathbf{A}.$$

**Corollary 4.** *Maximum likelihood estimators  $\hat{\pi}, \hat{\lambda}, \hat{\rho}$  by the data  $X_1^n = (x_1, \dots, x_n)'$  are determined by the solution of the maximization problem:*

$$l(\pi, \lambda, \rho) = \sum_{t=1}^s \ln \pi_{x_t} + \sum_{t=s+1}^n \ln \left( (1 - \rho) \pi_{x_t} + \rho \sum_{j=1}^s \lambda_j \delta_{x_{t-j}, x_t} \right) \rightarrow \max_{\pi, \lambda, \rho}.$$

Using these MLEs we had constructed [4] a consistent generalized probability ratio test for hypotheses on the true values of parameters  $\rho, \lambda, \pi$  in (12).

### 4.2 Raftery model

Mixture Transition Distribution-model (MTD-model) was proposed in 1985 by A. Raftery [10] as a special parsimonious representation of the matrix  $\mathbf{P}$ :

$$p_{i_1, \dots, i_s, i_{s+1}} = \sum_{j=1}^s \lambda_j q_{i_j, i_{s+1}}, \quad i_1, \dots, i_{s+1} \in \mathbf{A}, \quad (13)$$

where  $Q = (q_{i,k})$  is a stochastic  $(N \times N)$ -matrix,  $0 \leq q_{i,k} \leq 1$ ,  $\sum_{k \in \mathbf{A}} q_{i,k} \equiv 1$ ,  $i, k \in \mathbf{A}$ ,  $\lambda = (\lambda_1, \dots, \lambda_s)'$  is a discrete probability distribution,  $\lambda_1 > 0$ .

The MTDg (generalized MTD)-model:

$$p_{i_1, \dots, i_s, i_{s+1}} = \sum_{j=1}^s \lambda_j q_{i_s-j+1, i_{s+1}}^{(j)}, \quad i_1, \dots, i_{s+1} \in \mathbf{A}, \quad (14)$$

where  $Q^{(j)} = (q_{i,k}^{(j)})$  is a stochastic matrix for the  $j$ -th lag.

Number of parameters for the MTDg:  $D_{\text{MTDg}} = s(N(N-1)/2 + 1) - 1$ ;  $\varkappa = O(s \cdot N^{2-s})$ .

We have constructed a simple criterion for the ergodicity of the MTD-model and found a useful property of the stationary probability distribution [4].

**Theorem 6.** *For the MTDg-model (14), if  $\exists k \in N : \left( (Q^{(1)})^K \right)_{ij} > 0$ ,  $\forall i, j \in \mathbf{A}$ , then the  $s$ -dimensional stationary probability distribution satisfies the equation  $(i_1, \dots, i_s \in \mathbf{A})$ :*

$$\pi_{i_1, \dots, i_s}^* = \prod_{l=0}^{s-1} \left( \pi_{i_s-l}^* + \sum_{j=l+1}^s \lambda_j \left( q_{i_{j-l}, i_{s-l}}^{(j)} - \sum_{r=0}^{N-1} q_{r, i_{s-l}}^{(j)} \pi_r^* \right) \right).$$

**Corollary 5.** *For the ergodic MTD-model (13) the 2-dimensional stationary probability distribution of the random vector  $(x_{t-m}, x_t)'$  is  $\pi_{ki}^*(m) = \pi_k^* \pi_i^* + \pi_k^* \lambda_{s-m+1} (q_{ki} - \pi_i^*)$ ,  $i, k \in \mathbf{A}$ ,  $1 \leq m \leq s$ .*

Based on Corollary 5 we have constructed statistical estimators  $\tilde{\lambda}$ ,  $\tilde{Q}$  by an observed time series  $X_1^n = (x_1, \dots, x_n)'$  of the length  $n$ :

$$\tilde{\pi}_i = \frac{1}{n - 2s + 1} \sum_{t=s+1}^{n-s+1} \delta_{x_t, i}; \quad \tilde{\pi}_{ki}(j) = \frac{1}{n - 2s + 1} \sum_{t=s+j}^{n-s+j} \delta_{x_{t-j}, k} \delta_{x_t, i};$$

$$z_{ki}(j) = \tilde{\pi}_{ki}(s-j) / \tilde{\pi}_k - \tilde{\pi}_i, \quad d_{ki} = \tilde{q}_{ki} - \tilde{\pi}_i, \quad i, k \in \mathbf{A}; \quad \tilde{\lambda}_j = \sum_{i, k \in \mathbf{A}} z_{ki}(s-j) d_{ki} / \sum_{i, k \in \mathbf{A}} d_{ki}^2, \quad j=1, \dots, s;$$

$$\tilde{q}_{ki} = \left\{ \begin{array}{l} \sum_{j=1}^s \tilde{\pi}_{ki}(j) / \tilde{\pi}_k - (s-1) \tilde{\pi}_i, \quad \text{if } \tilde{\pi}_k > 0; \\ N^{-1} \quad \text{else} \end{array} \right\}. \quad (15)$$

**Theorem 7.** *For the ergodic MTD-model (13) the estimators  $\tilde{Q}$ ,  $\tilde{\lambda}$  determined by (15) at  $n \rightarrow \infty$  are consistent and asymptotically unbiased.*

MLE  $\hat{Q}$ ,  $\hat{\lambda}$  are solutions of the nonlinear maximization problem:

$$l(Q, \lambda) = \sum_{t=s+1}^n \ln \sum_{j=1}^s \lambda_j q_{x_{t-s+j-1}, x_t} \rightarrow \max_{Q, \lambda}. \quad (16)$$

The estimators  $\tilde{Q}$ ,  $\tilde{\lambda}$  are used as initial values in the iterative computation of the MLEs  $\hat{Q}$ ,  $\hat{\lambda}$  in (16). Generalized probability ratio test of the asymptotic size  $\varepsilon \in (0, 1)$  for  $H_0 = \{Q = Q^0, \lambda = \lambda^0\}$ ,  $H_1 = \overline{H_0}$  is constructed as in the previous subsection.

### 4.3 Binomial conditionally nonlinear autoregressive model BiCNAR( $s$ )

This model [13] is determined by the special (binomial) case of equation (5):

$$p_{i_1, \dots, i_s, i_{s+1}} = C_{N-1}^{i_{s+1}} \theta^{i_{s+1}} (1 - \theta)^{N-1-i_{s+1}}, \quad i_{s+1} \in \mathbf{A} = \{0, 1, \dots, N-1\}, \quad (17)$$

$$\theta = \theta(\mathbf{I}_1^s) = F(a' \Psi(\mathbf{I}_1^s)), \quad \mathbf{I}_1^s = (i_1, \dots, i_s)' \in \mathbf{A}^s.$$

Here  $\Psi(\mathbf{I}_1^s) = (\psi_1(\mathbf{I}_1^s), \dots, \psi_m(\mathbf{I}_1^s))' : \mathbf{A}^s \rightarrow R^m$  is a column-vector of  $m \leq N^s$  linearly independent functions, e.g. polynomials,  $F(\cdot) : R^1 \rightarrow [0, 1]$  is some fixed cumulative distribution function, e.g. logistic, normal or Cauchy:

$$\Lambda(\zeta) = \frac{1}{1 + e^{-\zeta}}, \quad \Phi(\zeta) = \frac{1}{\sqrt{2\pi}} \int_{-\infty}^{\zeta} e^{-\frac{x^2}{2}} dx, \quad C(\zeta) = \frac{1}{2} + \frac{\arctan(\zeta)}{\pi}, \quad \zeta \in R^1,$$

$a = (a_1, \dots, a_m)'$  is a column-vector of  $m$  unknown model parameters. Parsimony coefficient for this model  $\varkappa = m(N^s(N-1))^{-1} \leq 1$ .

Introduce the notation:  $F^{-1}(\cdot)$  is the quantile function;  $X_1^T = (x_1, \dots, x_T)' \in \mathbf{A}^T$  is the observed time series of length  $T$ ;

$$\hat{\theta}(J) = \frac{1}{N-1} \cdot \frac{\sum_{t=s+1}^T x_t \mathbf{I}\{X_{t-s}^{t-1} = J\}}{\sum_{t=s+1}^T \mathbf{I}\{X_{t-s}^{t-1} = J\}}, \quad J \in \mathbf{A}^s;$$

$B = (b_J)$  is  $(N^s \times 1)$  - vector-column,  $b_J = F^{-1}(\hat{\theta}(J))$ ;  $H = (h_{J,J'})$  is some fixed  $(N^s \times N^s)$  - symmetrical nonnegatively defined matrix;  $\Psi = (\Psi(J))$  is  $(m \times N^s)$  matrix;  $O_m$  is the zero  $m$ -vector.

**Theorem 8.** *If  $F(\cdot)$  satisfies the smoothness assumptions:  $0 < F(\zeta) < 1$ ,  $0 < F'(\zeta) < +\infty$ ,  $F(\cdot)$  and  $F^{-1}(\cdot)$  are twice differentiable, and  $|\Psi H \Psi'| \neq 0$ , then the Frequencies Based Estimator (FBE)*

$$\hat{a} = (\Psi H \Psi')^{-1} \Psi H B \quad (18)$$

*is consistent and asymptotically normal at  $T \rightarrow +\infty$ :*

$$\hat{a} \xrightarrow{\mathbf{P}} a, \quad \sqrt{T}(\hat{a} - a) \xrightarrow{\mathbf{D}} \mathcal{N}_m(O_m, \Sigma_H),$$

$$\Sigma_H = (\Psi H \Psi')^{-1} \Psi H J^{-1} H (\Psi H \Psi')^{-1},$$

*where  $J$  is the Fisher information matrix.*

**Corollary 6.** *For the weight matrix  $H = J$  the FBE (18) is asymptotically efficient (it attains the Cramer - Rao boundary at  $T \rightarrow +\infty$ ).*

Proofs of Theorem 8 and its corollary are given in [13].

FBE (17) has the following significant advantages w.r.t. the MLE: 1) explicit expression of FBE w.r.t. the iterative computation of MLE; 2) fast iterative computation of FBE if we extend the basis  $\{\psi_i(\cdot)\}$ ; 3) possibility to control the computational complexity of FBE by variation of the matrix  $H$ .

Note in conclusion, that the developed method of FBE construction for the BiCNAR is successively used for some other models of discrete-valued time series [14]: semibinomial, Poisson, geometric, negative binomial conditionally nonlinear autoregressive time series. The Binomial and Poisson conditional nonlinear autoregressive models are also extended for discrete-valued spatio-temporal data [15].

Note also one more known parsimonious model constructed by the second approach [16] – INAR( $p$ ) time series.

## 5 Application of the developed algorithms of computer data analysis

All algorithms developed in Sections 2-4 were tested on simulated data and illustrated accordance with the proved theoretical properties. Here we give some results of computer experiments with the developed algorithms on real data from applications. We present here 4 examples.

### 5.1 Modeling of wind direction

The discrete-valued time series of the daily average wind speed at Malin Head (North of Ireland) during the period 1961 – 1978 [9]  $x_t \in \{0, 1, 2\}$ ,  $N = 3$ , of the length  $T = 6574$  was fitted by the MC( $s, r$ )-model for  $s = \{1, 2, \dots, 7\}$ ,  $r = \{1, 2, \dots, 7\}$ . Table 1 presents the values of the BIC for different pairs  $(s, r)$ .

The best fitted model is the MC(3,2) with  $\hat{M}_r = (1, 3)$  and the transposed matrix

$$\hat{Q}' = \begin{pmatrix} 0.27 & 0.08 & 0 & 0.22 & 0.04 & 0 & 0.21 & 0.02 & 0 \\ 0.73 & 0.86 & 0.63 & 0.78 & 0.82 & 0.52 & 0.79 & 0.72 & 0.43 \\ 0 & 0.06 & 0.37 & 0 & 0.14 & 0.48 & 0 & 0.26 & 0.57 \end{pmatrix}.$$

The fitted model MC(3, 2) detects significant dependencies in this data.

Table 1: Modelling of the wind speed data

Model	BIC	Model	BIC	Model	BIC	Model	BIC
MC(1,1)	8127.52	MC(4,2)	8139.12	MC(5,5)	8621.97	MC(7,1)	9041.43
MC(2,1)	8777.63	MC(4,3)	8164.79	MC(6,1)	9016.23	MC(7,2)	8163.07
MC(2,2)	8096.08	MC(4,4)	8332.77	MC(6,2)	8148.48	MC(7,3)	8197.91
MC(3,1)	8849.90	MC(5,1)	8984.10	MC(6,3)	8190.78	MC(7,4)	8323.19
<b>MC(3,2)</b>	<b>8079.81</b>	MC(5,2)	8129.83	MC(6,4)	8350.82	MC(7,5)	8599.09
MC(3,3)	8143.13	MC(5,3)	8177.92	MC(6,5)	8576.92	MC(7,6)	8973.15
MC(4,1)	8956.11	MC(5,4)	8349.62	MC(6,6)	8969.54	MC(7,7)	9575.64

## 5.2 Genomic sequencing

We used the drosophila genome sequence ([www.fruitfly.org](http://www.fruitfly.org)):  $N=4$ ,  $T=5 \cdot 10^5$ ,  $s_- = 1$ ,  $s_+ = 8$ ,  $r_- = 1$ ,  $r_+ = 8$ . The best fitted model is the MC(6,3) with the template  $\hat{M}_r = (1, 5, 6)$  and the matrix  $\hat{Q}$  visualized in Figure 3. Here on “ $x$ -axis” the values of  $\hat{M}_r$ -prehistory are indicated, “ $y$ -axis” gives the values of one-step transition probabilities to four states indicated by different levels of color.

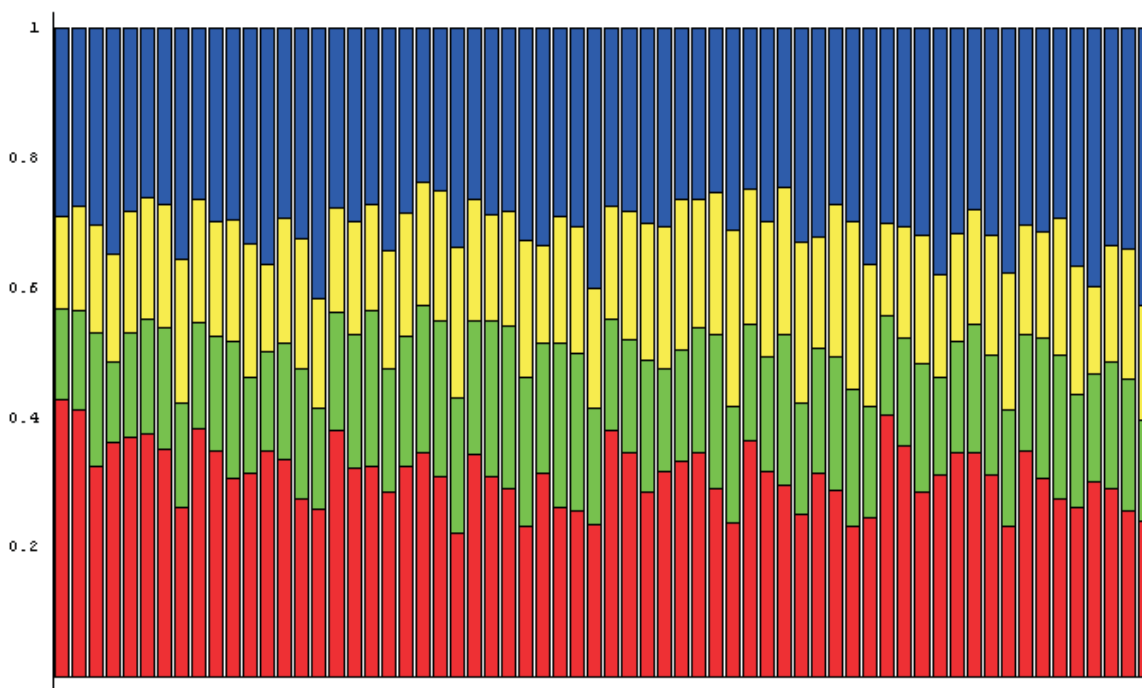


Figure 3: The matrix  $\hat{Q}$  for the genomic sequencing

### 5.3 Analysis of CG-patterns in genome

We took the complete *Panthera tigris* mitochondrion genome of the length  $T = 16990$  (available from NCBI Nucleotide data base, ID EF551003.1) and extracted the binary sequence  $x_t$  of its CG-indicators:  $x_t = 1$  iff the  $t$ 'th nucleotide is Guanine or Cytosine,  $t = 1, \dots, T$ . Portion of "1" in  $X_1^T$  is known as CG-content and plays important role in bioinformatics [11].

In order to evaluate individual and pairwise impact of the lagged variables  $X_{t-s}^{t-1}$  on  $x_t$  we fitted the BCNAR( $s$ )-model (up to  $s = 15$ ) for  $N = 2$  with the bilinear bases  $\{\psi_i(\cdot)\}$  and the Gaussian c.d.f.  $\Phi(\cdot)$ .

Two fitted BCNAR-models for  $s = 10$ ; 15 respectively, are ( $\zeta_t = (-1)^{x_t}$ ):

$$\begin{aligned} \mathbf{P}\{x_t|x_{t-1}, \dots\} &= \Phi(-0.3962 + 0.0313\zeta_{t-1} + 0.0241\zeta_{t-3} + 0.033\zeta_{t-10} + \\ &\quad + 0.045\zeta_{t-3}\zeta_{t-6} - 0.0576\zeta_{t-3}\zeta_{t-10}), \\ \mathbf{P}\{x_t|x_{t-1}, \dots\} &= \Phi(-0.1319 + 0.022\zeta_{t-1} + 0.0269\zeta_{t-6} + 0.0248\zeta_{t-15} - \\ &\quad - 0.0434\zeta_{t-6}\zeta_{t-15}), \end{aligned} \tag{19}$$

that are adequate according to BIC. It is seen that in the two fitted models of high orders  $s = 10$  and  $s = 15$  the future state  $x_t$  is significantly influenced by the past states  $x_{t-i}$  lagged by multiples of three ( $i = 3j$ ), and even the closest predecessor  $x_{t-1}$  has a weaker impact on  $x_t$ . Note also that the pairs of the lagged variables in these two models are more influential than the single lagged variables, i.e. the bilinear basis caught some essential high-order statistical dependencies invisible to the linear one. These identified properties of the bilinear models confirm the known in genetics effect of statistical 3-periodicity of protein-coding fragments [11]; this fact indicates the usefulness of the developed theory for statistical analysis of genetic sequences.

### 5.4 Dynamics analysis for the incidence rate of children leukemia

Real medical data describes the incidence rate of children leukemia in  $n = 3$  cites of Belarus for  $T = 25$  years after Chernobyl (normalization of the data was made by the number of residents at the group of risk). We used the Poisson conditionally nonlinear autoregressive spatio-temporal model [15].

Statistical estimators of the parameters obtained by  $T = 25$  observations:

$$\hat{\theta}_1 = (-0.06, 0.15)', \hat{\theta}_2 = (-0.01, -0.02, 1.51)', \hat{\theta}_3 = (0.07, 0.05, 0.82)', \tag{20}$$

e.g. for the site number  $s = 3$  the estimator of expected incidence rate is

$$\hat{\lambda}_{3,t} = \exp(0.07x_{3,t-1} \cdot \mathbf{I}\{t > 1\} + 0.05x_{2,t} + 0.82). \tag{21}$$

Forecasting results are presented in Figures 4-6.

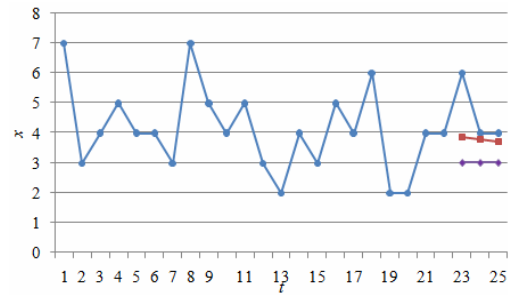
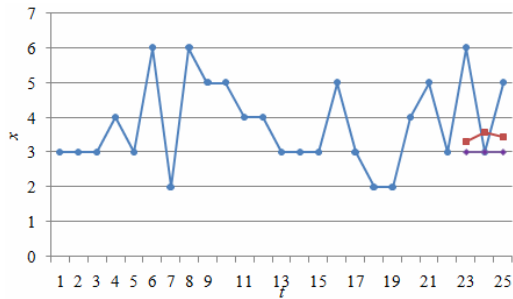


Figure 4: Forecasting results for the site  $s=1$

Figure 5: Forecasting results for the site  $s=2$

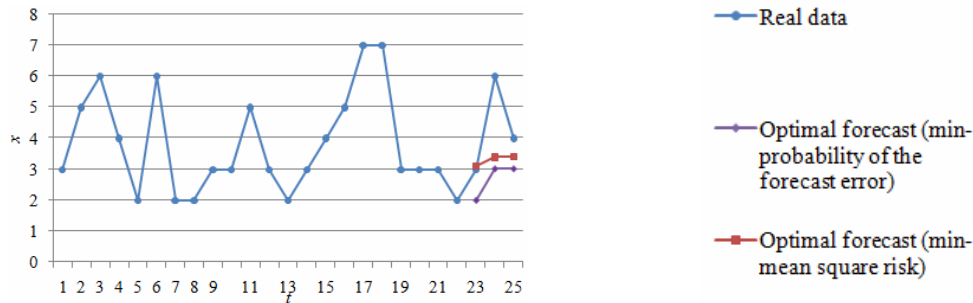


Figure 6: Forecasting results for the site  $s = 3$

## References

- [1] Anderson T. (2003). *An introduction to multivariate Statistical Analysis*. Wiley, N.Y.
- [2] Weiss C.H. (2018). *An Introduction to Discrete-Valued Time Series*. Wiley, N.Y.
- [3] Kedem B., Fokianos K. (2002). *Regression Models for Time Series Analysis*. Wiley, N.Y.
- [4] Kharin Yu. (2013). *Robustness in Statistical Forecasting*. Springer, N.Y.
- [5] Kharin Yu.S. (2004). Markov chains with  $r$ -partial connections and their statistical estimators. *Trans. Nat. Acad. Sci. Belarus*. Vol. **48**, No. 1, pp. 40-44.
- [6] Kharin Yu.S., Piatlitski A.I. (2007). A Markov chain of order  $s$  with  $r$  partial connections and statistical inference on its parameters. *Discrete Mathematics and Applications*. Vol. **17**, No. 3, pp. 295-317.

- [7] Kharin Yu., Maltsev M. (2014). Markov chain of conditional order: Properties and Statistical Analysis. *Austrian Journal of Statistics*. Vol. **43**, No. 3-4, pp. 205-217.
- [8] Buhlmann P., Wyner A.J. (1999). Variable length Markov chains. *The Annals of Statistics*. Vol. **27**, No. 2, pp. 480-513.
- [9] Jacobs P.A., Lewis P.A.W. (1978). Discrete time series generated by mixtures I: correlational and runs properties. *Journal of the Royal Statistical Society. Ser. B*. Vol. **40**, No. 1, pp. 94-105.
- [10] Raftery A. (1985). A model for high-order Markov chains. *Journal of the Royal-Statistical Society. Ser. B*. Vol. **47**, No. 3, pp. 528-539.
- [11] Kharin Yu., Maltsev M. (2017). Statistical analysis of high-order dependencies. *Acta et Commentationes Universitetas Tartuensis de Mathematica*. Vol. **21**, No. 1, pp. 37-45.
- [12] Kharin Yu.S., Voloshko V.A., Medved E.A. (2019). Statistical estimation of parameters for binary conditionally nonlinear autoregressive time series. *Mathematical Methods of Statistics*. Vol. **26**, No. 2, pp. 103-118.
- [13] Kharin Yu.S., Voloshko V.A. (2019). Binomial conditionally nonlinear autoregressive model of discrete-valued time series and its probabilistic and statistical properties. *Transactions of the Institute of Mathematics of NAS Belarus*. Vol. **26**, No. 1, pp. 95-105.
- [14] Kharin Y., Kislach M. (2019). Statistical analysis of Poisson conditionally nonlinear autoregressive time series by frequencies-based estimators. *Proceedings of the 14-th International Conference. Minsk, Belarus "Pattern Recognition and Information Processing"*, pp. 233-236.
- [15] Kharin Yu., Zhurak M. (2015). Statistical analysis of spatio-temporal data based on Poisson conditional autoregressive model. *INFORMATICA*. Vol. **26**, No. 1, pp. 67-87.
- [16] Alzaid A.A., Al-Osch M. (1990). An integer-valued  $p$ th-order autoregressive structure (INAR( $p$ )) process. *Journal of Applied Probability*. Vol. **27**, pp. 314-324.

# TESTING STRUCTURE OF THE COVARIANCE MATRIX: A NON-NORMAL APPROACH

T. KOLLO, D. VON ROSEN, M. VALGE  
*Institute of Mathematics and Statistics*  
*Tartu, ESTONIA*  
 e-mail: tonu.kollo@ut.ee

## Abstract

Classical tests about covariance structure are examined in the situation when the population distribution is non-normal and existence of the fourth order moments is assumed. Asymptotic distributions for test statistics are derived and speed of convergence to the asymptotic distributions examined in a simulation experiment.

**Keywords:** data science, covariance matrix, non-normality

Let  $\mathcal{X} = (\mathbf{x}_1, \dots, \mathbf{x}_n)$  be a sample of size  $n$  from a  $p$ -dimensional population  $\mathbf{x}_i \sim P_{\mathbf{x}}$  with

$$E\mathbf{x}_i = \boldsymbol{\mu}; \quad D\mathbf{x}_i = \boldsymbol{\Sigma}; \quad M_4(\mathbf{x}_i) < \infty.$$

Denote

$$\bar{\mathbf{x}} = \frac{1}{n} \sum_{i=1}^n \mathbf{x}_i; \quad \mathbf{S} = \frac{1}{n-1} \sum_{i=1}^n (\mathbf{x}_i - \bar{\mathbf{x}})(\mathbf{x}_i - \bar{\mathbf{x}})'$$

We are interested in testing hypotheses about the covariance structure:

$$H_0 : \boldsymbol{\Sigma} = \boldsymbol{\Sigma}_0, \tag{1}$$

with a special interest to the hypotheses

$$H_{01} : \boldsymbol{\Sigma} = \mathbf{I}_p, \tag{2}$$

$$H_{02} : \boldsymbol{\Sigma} = \sigma^2 \mathbf{I}_p, \tag{3}$$

$$H_{03} : \boldsymbol{\Sigma} = \boldsymbol{\Lambda}, \quad \boldsymbol{\Lambda} - \text{diagonal}. \tag{4}$$

Test  $H_{02}$  is called the sphericity test while  $H_{03}$  is the uncorrelatedness test. John (1971,1972) proved that the test based on

$$U = \frac{1}{p} \text{tr} \left[ \left( \frac{\mathbf{S}}{(1/p)\text{tr}\mathbf{S}} - \mathbf{I}_p \right)^2 \right]$$

is locally most powerful invariant test for sphericity  $H_{02}$ . Nagao (1973) suggested test statistics for  $H_{02}$

$$T_2 = \frac{v^2}{2} \text{tr} \left[ \left( \frac{\mathbf{S}}{\text{tr}\mathbf{S}} - \frac{1}{p} \mathbf{I}_p \right)^2 \right]$$

and for  $H_{03}$

$$T_3 = \frac{n}{2} \text{tr} \left[ \left( \mathbf{S}\mathbf{S}_d^{-1} - \mathbf{I}_p \right)^2 \right],$$

where  $\mathbf{S}_d$  is the diagonalized matrix  $\mathbf{S}$ . In high-dimensional set-up (  $p \geq n$  ) several papers were published in the beginning of 2000-s for a normal population. Ledoit, Wolf (2002) suggested for  $H_{01}$  the statistic

$$W = \frac{1}{p} \text{tr} \left[ (\mathbf{S} - \mathbf{I}_p)^2 \right] - \frac{p}{n} \left( \frac{1}{p} \text{tr} \mathbf{S} \right)^2 + \frac{p}{n}.$$

For the tests (2)-(4) Srivastava (2005, 2006) constructed test statistics in high-dimensional set-up for a normal population. We are going to construct test statistics for non-normal populations in the situation when both, the number of variables  $p$  and the sample size  $n$  are growing:  $p, n \rightarrow \infty$ ,  $p/n < 1$ . The last assumption makes it possible to rely on asymptotic normality and asymptotic chi-square distributions. Non-normal populations have got much attention in last years. Yuan, Bentler (1999) study robustness of likelihood ratio statistic for two non-normal populations, including elliptical distributions. Srivastava et al (2011) consider some tests for the covariance matrices with fewer observations than the dimension under non-normality, Harrar (2009) examines asymptotics for several tests under non-normality. Srivastava, Singull (2017) consider tests in high-dimensional set-up using  $U$ -statistics. We derive expressions of test-statistics for sphericity and uncorrelatedness tests and examine empirically speed of convergence to the asymptotic distributions in simulation experiments.

## References

- [1] Harrar, S. W. (2009). Asymptotics for tests on mean profiles, additional information and dimensionality under non-normality. *JSPI*. Vol. **139**, pp. 2685-2705.
- [2] John, S. (1971). Some optimal multivariate tests. *Biometrika*. Vol. **58**, pp. 123-127.
- [3] John, S. (1972). The distribution of a statistic used for testing sphericity. *Biometrika*. Vol. **59**, pp. 169-173.
- [4] Ledoit, O., Wolf, M. (2002). Some hypothesis tests for the covariance matrix when the dimension is large. *Ann. Statist.*. Vol. **30**, pp. 1081-1102.
- [5] Nagao, H. (1973). On some test criteria for covariance matrix. *Ann. Statist.*. Vol. **1**, pp. 700-709.
- [6] Srivastava, M. S. (2005). Some tests concerning the covariance matrix in high dimensional data. *Japan Statist. Soc.*. Vol. **35**, pp. 251-272.
- [7] Srivastava, M. S. (2006). Some test criteria for the covariance matrix with fewer observations than the dimension. *J. Multivariate Anal.*. Vol. **102**, pp. 1090-1103.
- [8] Srivastava, M. S., Kollo, T., von Rosen, D. (2011). Some tests for the covariance matrix with fewer observations than the dimension under non-normality. *J. Multivariate Anal.*. Vol. **102**, pp. 1090-1103.

- [9] Srivastava, M. S. and Singull, M. (2017). Testing sphericity and intraclass covariance structures under a Growth Curve model in high dimension. *Communications in Statistics - Simulation and Computation*. Vol. **46**, pp. 5740-5751.
- [10] Yuan, K.-H., Bentler, P. M. (1999). On normal theory and associated teststatistics in covariance structure analysis under two classes of nonnormal distributions. *Statistica Sinica*. Vol. **9**, pp. 831-853.

# HURST PARAMETER ESTIMATION IN FRACTIONAL DIFFUSION MODELS

K. KUBILIUS

*Vilnius University, Faculty of Mathematics and Informatics*

*Vilnius, LITHUANIA*

e-mail: `kestutis.kubilius@mii.vu.lt`

## Abstract

We consider the problem of Hurst index estimation for solutions of stochastic differential equations driven by fractional Brownian motion or mixed fractional Brownian motion.

**Keywords:** data science, fractional Brownian motion, Hurst parameter

## 1 Introduction

Many modern models are described using stochastic differential equations (SDE) driven by fractional Brownian motion or mixed fractional Brownian motion

$$X_t = X_0 + \int_0^t f(s, X_s) ds + \int_0^t g_1(s, X_s) dW_s + \int_0^t g_2(s, X_s) dB_s^H, \quad t \in [0, T], \quad (1)$$

where  $T > 0$  is fixed,  $X_0$  is an initial r.v.,  $f$ ,  $g_1$ , and  $g_2$  are continuous functions satisfying some regularity conditions,  $B^H$  is a fBm with the Hurst index  $1/2 < H < 1$  and  $W$  is a standard Brownian motion. More results on parameter estimations for stochastic differential equation (1) with  $g_1 = 0$  can be found in the book [4].

We focus on estimators of the Hurst index. Our goal is to construct strongly consistent and asymptotically normal estimators of the Hurst parameter  $H$  from discrete observations of a single sample path.

## 2 SDE driven by mixed fractional Brownian motion

Consider stochastic differential equation

$$X_t = x_0 + \theta \int_0^t X_s ds + M_t^H, \quad t \in [0, T], \quad (2)$$

where  $0 < H < 1$  and

$$M_t^H = \sigma_1 W_t + \sigma_2 B_t^H, \quad \sigma_1, \sigma_2 \in \mathbf{R}. \quad (3)$$

The process (3) is frequently called a mixed fractional Brownian motion. Moreover, assume that  $W$  and  $B^H$  are independent. Then equation (2) has unique strong solution.

The type of estimators depend on the value of  $H$ . If the Hurst index  $H$  is less than  $1/2$  we construct one type estimators, if  $H$  is over  $1/2$  we construct another type estimators.

One can check that

$$V_{n,T}^{(1)X} = \sum_{i=1}^n \left( X_{\frac{T_i}{n}} - X_{\frac{T(i-1)}{n}} \right)^2 \xrightarrow{n \rightarrow \infty} \begin{cases} +\infty & \text{if } H < 1/2, \\ \sigma_1^2 T & \text{if } H > 1/2. \end{cases}$$

This test allows us to decide to which interval belongs  $H$ . Thus, for  $H < 1/2$  we set

$$\widehat{H}_n^{(1)} = \varphi_{n,T}^{-1} \left( \frac{1}{n} V_{n,T}^{(2)X} \right) \quad \text{for } n > T, \quad \widehat{H}_n^{(2)} = \frac{1}{2} - \frac{1}{2 \ln 2} \ln \left( \frac{V_{2n,T}^{(2)X}}{V_{n,T}^{(2)X}} \right),$$

where

$$\varphi_{n,T}(x) = \sigma_2^2 \left( \frac{T}{n} \right)^{2x} (4 - 2^{2x}), \quad x \in (0, 1),$$

and  $\varphi_{n,T}^{-1}$  is inverse of  $\varphi_{n,T}$ ,  $x \in (0, 1)$ ,  $n > T$ . Then

$$\widehat{H}_n^{(i)} \xrightarrow{a.s.} H \quad \text{for } i = 1, 2.$$

When the Hurst index  $H$  belongs to the interval  $[\frac{1}{2}, 1)$  the influence of Brownian motion becomes too strong and the estimators  $\widehat{H}_n^{(1)}, \widehat{H}_n^{(2)}$  stop converging. Therefore, this Brownian motion effect should be reduced.

Thus, for  $H \in (\frac{1}{2}, \frac{3}{4})$  we apply statistics

$$\begin{aligned} \widetilde{H}_n^{(1)} &= \varphi_{n,T}^{-1} \left( \frac{1}{n} \sum_{k=1}^{n-1} \left[ (\Delta_{n,k}^{(2)} X)^2 - \frac{1}{2} \sum_{j=1-n^2}^{n^2-1} (\Delta^{(2)} X_{s_j^n + t_k^n})^2 \right] \right), \quad n > T, \\ \widetilde{H}_n^{(2)} &= \frac{1}{2} - \frac{1}{2 \ln 2} \ln \left( \frac{\sum_{k=1}^{2n-1} [(\Delta_{n,k}^{(2)} X)^2 - \frac{1}{2} \sum_{j=1-n^2}^{n^2-1} (\Delta^{(2)} X_{s_j^n + t_k^n})^2]}{\sum_{k=1}^{n-1} [(\Delta_{n,k}^{(2)} X)^2 - \frac{1}{2} \sum_{j=1-n^2}^{n^2-1} (\Delta^{(2)} X_{s_j^n + t_k^n})^2]} \right), \end{aligned}$$

where

$$\begin{aligned} \Delta_{n,k}^{(2)} X &= X_{t_{k+1}^n} - 2X_{t_k^n} + X_{t_{k-1}^n}, \quad t_k^n = \frac{k}{n} T, \quad 1 \leq k \leq n-1, \\ \Delta^{(2)} B_{s_j^n + t_k^n}^H &= B_{s_{j+1}^n + t_k^n}^H - 2B_{s_j^n + t_k^n}^H + B_{s_{j-1}^n + t_k^n}^H, \quad s_j^n = \frac{j}{n^3} T, \quad j = 1 - n^2, \dots, n^2 - 1. \end{aligned}$$

Then

$$\widetilde{H}_n^{(i)} \xrightarrow{a.s.} H, \quad \text{for } i = 1, 2.$$

In the paper [2], the authors construct strongly consistent estimators of parameters  $H$  and study asymptotic normality of the estimators of  $H$ . They used completely different statistics to estimate the Hurst index  $0 < H < \frac{3}{4}$ .

### 3 Fractional model of type of Ait-Sahalia

Let us consider SDE

$$X_t = X_0 + \int_0^t (a_1 X_s^{-1} + a_2 + a_3 X_s + a_4 X_s^r) ds + \sigma \int_0^t X_s^\beta dB_s^H, \quad t \geq 0 \quad (4)$$

with the initial value  $X_0 > 0$ ,  $r \in (-1, 1)$ ,  $H \in (\frac{1}{2}, 1)$ , deterministic constants  $a_1, a_2, a_4 \geq 0$ ,  $a_3 \in \mathbf{R}$ ,  $\sigma > 0$  and  $\beta \in [1/2, 1)$ . The original Ait-Sahalia interest rate model was proposed first by Ait-Sahalia [1] with  $H = \frac{1}{2}$ . The special case of (4) is CIR model. The conditions under which the CIR model has unique positive solution were obtained in [3], [5, 6].

For the construction of the estimators of the Hurst index, we need this equation to have a strongly positive solution. The existence of strongly positive solution of this equation come down to the existence of strongly positive solution of equation

$$Y_t = Y_0 + (1 - \beta) \int_0^t \left( \frac{a_1}{Y_s^{\frac{1+\beta}{1-\beta}}} + \frac{a_2}{Y_s^{\frac{\beta}{1-\beta}}} + a_3 Y_s + \frac{a_4}{Y_s^{\frac{\beta-r}{1-\beta}}} \right) ds + (1 - \beta) \sigma B_t^H, \quad t \geq 0 \quad (5)$$

with  $Y_0 > 0$ . Under conditions on coefficients mentioned above, equation (5) has a strongly positive Hölder continuous of order  $H$  solution  $Y$ . Moreover, the process  $Y_t^{\frac{1}{1-\beta}}$  is the solution of equation (4).

The equality  $X_t = Y_t^{\frac{1}{1-\beta}}$  allows us to construct estimators that are strongly consistent and asymptotically normal.

## References

- [1] Ait-Sahalia Y. (1996). Testing continuous-time models of the spot interest rate. *Rev. Financ. Stud.* Vol. **9**, pp. 385-426.
- [2] Dozzi M., Mishura Y., Shevchenko, G. (2015). Asymptotic behavior of mixed power variations and statistical estimation in mixed models. *Stat. Inference Stoch. Process.* Vol. **18**, pp. 151-175.
- [3] Hu Y., Nualart D. and Song X. (2008). A singular stochastic differential equation driven by fractional Brownian motion. *Statistics and Probability Letters.* Vol. **78**, pp. 2075-2085.
- [4] Kubilius K., Mishura Yu., Ralchenko K. (2017). Parameter Estimation in Fractional Diffusion Models, Springer (Bocconi & Springer Series).
- [5] Lepinette E., Mehroudfou F. (2017). A fractional version of the Heston model with hurst parameter  $H \in (1/2, 1)$ . *Dynamic Systems and Applications.* Vol. **26**, pp. 535-548.
- [6] Mishura Yu., Yurchenko-Tytarenko A. (2018). Fractional Cox-Ingersoll-Ross process with non-zero mean. *Modern Stochastics: Theory and Applications.* Vol. **5**, pp. 99-111

# FUNCTIONAL GRAPHICAL MODEL CLASSIFICATION

P. LI, T. MAITI  
*Michigan State University*  
*East Lansing, USA*  
e-mail: maiti@msu.edu

## Abstract

The functional magnetic resonance imaging (fMRI) records signals coming from human brains, which show activities and states of brains. This measurements result in a high-dimensional time series, and each dimension represents a region of brains. In this paper, we propose a functional Gaussian graphical model to describe the distribution and the correlation structure for this type of high-dimensional time series data, and we find a quadratic discriminant analysis can be effective on functional graphical model. There are two kernel estimators introduced in our work to estimate the node set and the edge set of the functional graphical model, and they are used in our discriminant functions. The simulation study showed that this classification method outperforms other existing methods, and it demonstrated the idea of choosing tuning parameters with different simulated data set. In addition, we present two real data applications. One is an alcoholic condition detection with Electroencephalography (EEG) data collected from electrodes placed on subject's scalps, and the other is a resting state detection using resting state fMRI data from the OpenfMRI database. In both applications, our proposed methodology performs better than other competitive methodologies.

**Keywords:** data science, classification, functional graphical model

## 1 Introduction

The advent of functional graphical model [1] has provided a new statistical model for high-dimensional time series data such as Electroencephalography (EEG) data and functional magnetic resonance imaging (fMRI) data. While these two types of data have different features, however, both of them are collected in a sequential form and have high dimensions. To analyze these data, we need to consider the data collected at a specific time point as a structured object and explore the correlation structure of these data. Graphical model turns out to be an appropriate tool to describe the distribution of the data, since the model can contain both vertex information as well as the conditional correlation structure. This can significantly help us, for example, to study the whole brain instead of separating it to different regions.

The classification problem then becomes significant once we can study the brain as a whole object. Since both EEG data and fMRI data record signals from human brain under different conditions, we may be interested about detecting human brain activities or states via these data. Currently, some algorithms, both regression based algorithm and optimization based algorithm, have been proposed to solve this problem. From the

regression part, some logistic regression and sparse logistic regression model have been applied for the whole brain classification problem. In the statistical learning aspect, for example, [2] proposed a support vector machine for temporal classification in fMRI data, and [6] has further developed a sparse version of support vector machine for the whole brain classification problem. Moreover, [7] tried to design feature vectors of the brain image data using independent component analysis and apply support vector machine to this feature vector for classification. All these algorithms work well in their application. However, there are some issues remaining unclear in all these methods. The first one is how to vectorize and reduce the rank of the data. As we know, the brain image data, especially fMRI data, usually come in a form of high dimensional time sequence. At each scan, the data we can get is a 3 dimensional real-valued matrix, which cannot be applied to support vector machine model directly. Vectorization is the only way we can do to handle it, but it will lose the temporal information contained in the original data and will result in a super high dimensional vector. Simply reduce the rank of this vector with principle component analysis or independent component analysis will be difficult to interpret. Second, all these classification methods treat the high dimensional time sequence as repeated observation. This restricts the classification can only be made at certain discrete time point. However, the brain activity is a continuous procedure, so we should be able to do classification at any arbitrary time point.

In this paper, we proposed a new classification method, primly for brain image data but also fine for EEG data, to remedy the issues mentioned above. We tried to capture the time varying property of these data by estimating a functional graphical model with two Nadaraya-Waston estimators. These estimates are consistent in non-parametric statistics according to [5] and [4]. We then constructed a discriminant analysis classification with the estimators. The innovation of this work is that we preserved the spatial temporal information in model estimation. The dynamic of the model can help to improve the performance of classification. To compare our classification performance, we select two support vector machine based methods as benchmarks.

- **Sparse SVM:** Refer [6]
- **ICA SVM:** Refer [7]

The paper is formed in the following way. First, we introduce our functional graphical model, and present our estimators for this model. Then, we propose a classification basing on Bayes Classifier and Graphical Lasso. In simulation part, we use data generated from two different Brownian Motions to validate our method. Finally, we compare our method with two other methods in two different real data analysis, one is EEG data and the other is resting state fMRI data.

## 2 Methodology

### 2.1 Functional Gaussian Graphical Model

We shall start describing our methodology from the extension of Gaussian Graphical Model. Graphical model is a popular tool to present the distribution of some high-dimensional data, especially some data having complicate correlation structures. We refer [8] for the introduction of graphical models. A graphical model,  $G$ , consists of two components, the node set  $V$  and the edge set  $E$ . While the node set contains all the data information we observed, the edge set describes the underlying correlation between each nodes. Besides the data distribution, we are more eager to know the conditional correlation between each node. At this stage, Gaussian Graphical model is the most popular option, since the edge set becomes to be the precision matrix of the Gaussian distribution with the property that node  $i$  and  $j$  are conditionally independent if and only if  $(i, j)$  th element of the precision matrix is 0. What we are going to do here is extending the Gaussian graphical model into a functional setup.

Assume the graphical model  $G(t) = (V(t), E(t))$  is changing smoothly with time  $t$ . At a fixed time point  $t$ , our observation  $X \in \mathbb{R}^p$  is a  $p$ -dimensional random vector, representing the observations from each part of the model at this specific time point. Further, we assume this vector,  $X$ , is coming from a multivariate normal distribution  $\mathcal{N}(\mu(t), \Sigma(t))$ . Here, both  $\mu(t)$  and  $\Sigma(t)$  are continuous functions with respect to time. As a result,  $X(t)$  will be our node set  $V(t)$ , and the inverse matrix of  $\Sigma(t)$  decides the conditional correlation structure,  $E(t)$ , at this time point since the model is basing on the Gaussian assumption. We call  $G(t)$  is our functional Gaussian graphical model defined on the continuous time interval. In the next part, we will present our methods for estimating this functional graphical model with data observed at several time points.

### 2.2 Kernel Estimator

Before the description of methodology, let's define the high-dimensional time series data with the following notation. Suppose  $i = 1, \dots, n$  and  $j = 1, \dots, n_i$ , which means there are  $n$  total individuals and each individual has  $n_i$  different observations. We also assume the observations are taken at time point  $t_1, t_2, \dots, t_d \in [0, 1]$ . At each time point  $t_k, k = 1, \dots, d$ , we observe a  $p$  dimensional vector,  $X_{ij}(t_k)$ , which represents the  $j$ -th observation from the  $i$ -th individual. More specifically, the  $j$ -th observation from  $i$ -th individual at time point  $k$  can be denoted by  $X_{ij}(t_k) = (X_{ij}^{(1)}(t_k), \dots, X_{ij}^{(p)}(t_k))^T$ ,  $i = 1, \dots, n; j = 1, \dots, n_i; k = 1, \dots, d$ . The table 1 shows the general structure of the data.

To functionalize our model, we introduce a bounded continuous kernel function defined on the interval  $[0, 1]$ . With the observations, we propose two kernel estimators for the mean and covariance of the random vector  $X$  at any arbitrary time point  $t$ . Here are some necessary notations:

$$\bar{X}(t_k) = \frac{1}{\sum_i n_i} \sum_{i,j} X_{ij}(t_k), \quad \Sigma(t_k) = \frac{1}{\sum_i n_i} \sum_{i,j} (X_{ij}(t_k) - \bar{X}(t_k))(X_{ij}(t_k) - \bar{X}(t_k))^T,$$

Table 1: Data Structure

$X_i$	$X_{i1}$	$X_{i1}(t_1) = (X_{i1}^{(1)}(t_1), \dots, X_{i1}^{(p)}(t_1))^T$
		...
	$X_{i1}(t_d) = (X_{i1}^{(1)}(t_d), \dots, X_{i1}^{(p)}(t_d))^T$	
	...	
	...	
	...	
	$X_{in_i}$	$X_{in_i}(t_1) = (X_{in_i}^{(1)}(t_1), \dots, X_{in_i}^{(p)}(t_1))^T$
		...
		$X_{in_i}(t_d) = (X_{in_i}^{(1)}(t_d), \dots, X_{in_i}^{(p)}(t_d))^T$

where  $K(\cdot)$  is the kernel function. Our kernel estimators for mean and covariance matrix are

$$\hat{\mu}(t) = \frac{\sum_{k=1}^d K\left(\frac{|t-t_k|}{h}\right) \bar{X}(t_k)}{\sum_{k=1}^d K\left(\frac{|t-t_k|}{h}\right)}$$

$$\hat{S}_n(t) = \frac{\sum_{k=1}^d K\left(\frac{|t-t_k|}{h}\right) \Sigma(t_k)}{\sum_{k=1}^d K\left(\frac{|t-t_k|}{h}\right)}$$

$h$  is a tuning parameter here, which is approximately  $O(n^{-\frac{1}{5}})$ . These two estimators then can be used to estimate the precision matrices of the functional Gaussian graphical model and classification procedure. The kernel function here are Gaussian kernel, Epanechnikov and Tri-cube kernels. We try all of them in our data applications. Some other kernel functions used in data smoothing can also be considered.

To complete the model fitting procedure, we need to get the precision matrix of the distribution. However, simply computing the inverse matrix of our second estimator does not work well. There are two issues for that, one is the high cost of computation, the other is the singularity of the inverse matrix. Hence, we use graphical lasso instead. The precision matrix will be estimated with the following optimization procedure:

$$\hat{\Theta}(t) = \arg \max \log \det(\Theta(t)) - \text{tr}(\hat{S}_n(t)\Theta(t)) - \lambda |\Theta(t)|_{m \neq l} \quad (1)$$

$|\Theta(t)|_{m \neq l}$  is the L1 norm of the off-diagonal elements in the precision matrix. Among all positive definite matrices, we find the optimizer of the loss function, and it is going to be our estimate for the precision matrix  $\Omega(t)$ .

### 2.3 Binary Classification

Finally, we can describe our classification part. We start with a traditional binary classification set up. Let  $X_{ij}(t_k), i = 1, \dots, n; j = 1, \dots, n_i; k = 1, \dots, d$  and  $Y_{ij}(t_k), i = 1, \dots, m; j = 1, \dots, m_i; k = 1, \dots, d$  be two groups of observations. Suppose we get a new sequence of observations, which is denoted by  $Z(t) = (z(t_1), \dots, z(t_l))$ ,  $l$  is any arbitrary number, not necessarily equal to  $d$ . A quadratic discriminant analysis is applied to this

new observation. Let  $\hat{\mu}^1(t)$  and  $\hat{\Omega}^1(t)$  be the estimated mean and covariance matrix for group X at time  $t$ , and  $\hat{\mu}^2(t)$  and  $\hat{\Omega}^2(t)$  be the estimated mean and covariance matrix for group Y.  $\pi_q$  are the corresponding prior probabilities. The discriminant function for quadratic discriminant is

$$\delta(z(t), q) = \frac{1}{2} \log |\hat{\Omega}^q(t)| - \frac{1}{2} [z(t) - \hat{\mu}^q(t)]^T \hat{\Omega}^q(t) [z(t) - \hat{\mu}^q(t)] + \log \pi_q$$

Then we think  $z(t)$  is from class 1 if  $\delta(z(t), 1) \geq \delta(z(t), 2)$ .

We then can present the posterior probability of the classification result in the following way. Since  $\mathbb{P}(Z \in \text{Class1} | Z = z) = \mathbb{E}[I\{Z \in \text{class1} | Z = z\}]$ , the posterior probability is  $\hat{\mathbb{P}} = \frac{1}{l} \sum_{k=1}^l I\{Z(t_k) \in \text{class1} | Z(t_k) = z(t_k)\}$ .  $I$  is an indicator function here.

### 3 Simulation

In order to demonstrate the performance of our classification method, we apply it to a data set generated from two different Brownian Motions. As time varying Gaussian processes, the mean vectors and covariance matrices of these two Brownian Motions are functions of time. Suppose we use  $\mu^1(t), \mu^2(t)$  and  $\Sigma^1(t), \Sigma^2(t)$  to denote the corresponding mean vectors and covariance matrices of these two Brownian Motions, then

$$\begin{aligned} \mu^1(t) &= \left(\frac{t}{100}, \dots, \frac{t}{100}\right)^T & \mu^2(t) &= \left(\frac{5t}{100}, \dots, \frac{5t}{100}\right)^T \\ \Sigma^1(t) &= \left[\min\left(\frac{it}{500}, \frac{jt}{500}\right)\right]_{100 \times 100} & \Sigma^2(t) &= \left[\min\left(\frac{5it}{500}, \frac{5jt}{500}\right)\right]_{100 \times 100} \end{aligned}$$

For each Brownian Motion, we randomly generate 100 samples at each time point, and the time points are equally spaced between 1 and 2, i.e.  $t = \frac{101}{100}, \frac{102}{100}, \dots, \frac{200}{100}$ . Thus, we have 200 individuals in total. Each individual is a  $100 \times 100$  matrix, whose rows are observations of that individual at a certain time point. The training set consists of 80 individuals from each group, and the remaining individuals are test set. The result in table 2 shows that our method has a much better performance. However, there is no difference between different kernel function in classification performance.

## 4 Real Data Analysis

### 4.1 EEG Data

In this section, we are going to apply our method to the Electroencephalography (EEG) Data from the UCI Machine Learning Repository, <https://archive.ics.uci.edu/ml/machine-learning-databases/eeg-mld/eeg.data.html>. Our EEG data set arises from a large study to examine EEG correlates of genetic predisposition to alcoholism. It contains measurements from 64 electrodes placed on the scalp sampled at 256 Hz (3.9-msec epoch) for 1 second. There were two groups of subjects: alcoholic

Table 2: Classification Performance Comparison

	Kernel	Sensitivity	Specificity	Precision	Accuracy
FGM	Gaussian	0.9	1	1	0.95
	Epanechnikov	0.9	1	1	0.95
	Tri-cube	0.9	1	1	0.95
Sparse SVM	Gaussian	0.75	0.8	0.7894	0.775
	Epanechnikov	0.75	0.8	0.7894	0.775
	Tri-cube	0.75	0.8	0.7894	0.775
ICA SVM		0.523	0.52	0.55	0.53

Table 3: Classification Performance Comparison: EEG Data

	Kernel	Sensitivity	Specificity	Precision	Accuracy
FGM	Gaussian	0.958	0.917	0.92	0.938
	Epanechnikov	0.938	0.938	0.938	0.917
	Tri-cube	0.917	0.917	0.917	0.917
Sparse SVM	Gaussian	0.567	0.833	0.773	0.7
	Epanechnikov	0.833	0.6	0.676	0.716
	Tri-cube	0.833	0.6	0.676	0.716
ICA SVM		0.57	0.55	0.56	0.582

and control. Each subject was exposed to different conditions and their response in terms of EEG data was collected. There were 122 subjects and each subject completed 120 trials. The electrode positions were located at standard sites (Standard Electrode Position Nomenclature, American Electroencephalographic Association 1990). [9] describes in detail the data collection process. We apply our classification method to this data set and record its performance. Further, we compared our results with some other methods to check the efficiency of our functional graphical model.

The original EEG data set contains huge amount of observations, and we randomly select 180 observations to evaluate our classification method. Among these 180 observations, half of them are from alcoholic group and the other half are from the control group. The training set has 60 observations from each class, and the rest 60 observations are used as testing set.

In our results, we compute the sensitivity, specificity, precision and accuracy of our classification research to demonstrate the efficiency of our method. Sensitivity is the true positive rate, specificity is the true negative rate, precision is the positive predictive rate and accuracy is the accuracy rate. The results are in 3. Our functional quadratic discriminant analysis method outperforms the other two methods again. The difference between classification accuracy is pretty similar to the simulation results. We can also find that the choice of kernel function does not make a great difference in classification result, although Gaussian kernel works slightly better in functional QDA.

Table 4: Classification Performance Comparison: fMRI Data

	Kernel	Sensitivity	Specificity	Precision	Accuracy
FGM	Epanechnikov	0.8	0.7	0.727	0.71
	Uniform	0.7	0.6	0.636	0.65
	Tri-cube	0.7	0.7	0.54	0.7
Sparse SVM	Epanechnikov	0.8	0.4	0.57	0.6
	Uniform	0.7	0.5	0.53	0.6
	Tri-cube	0.7	0.5	0.53	0.6
ICA SVM		0.57	0.55	0.56	0.582

## 4.2 fMRI Classification

In this section, we are heading to the most important topic and adopt all our tensor based methods to a fMRI classification task. The data was obtained from the Open-Neuro database. This project is a functional brain imaging study where 48 younger (20-30 years old) and 36 older (65-75 years old) healthy participants underwent magnetic resonance imaging after having adequate sleep or partial deprived sleep in a crossover design. There are three experiments investigating emotional mimicry, empathy for pain, and cognitive reappraisal, as well as resting state functional magnetic resonance imaging (fMRI). It also contains T1- and T2-weighted structural images and diffusion tensor images. On the night before imaging, participants were monitored with ambulatory polysomnography and were instructed to sleep either as usual or only for three hours. Participants came to the scanner the following evening. In this application, we only use the resting state fMRI data, and try to identify whether patients have enough sleeping or are under partial sleep deprivation with the data.

The fMRI data is pre-processed with the pipeline introduced by [7]. Temporal, spatial correction and coregistration have been applied to the original scans with Matlab tool box SPM 12.0. After data pre-processing, there are 70 scans from the group where patients had adequate sleep, and another 70 scans from the group where patients did not. We performed a principle components analysis to reduce the dimension of data. The table 4 shows that our functional graphical model classification works better than others.

## 5 Conclusion

In this work, the functional Gaussian graphical model provides a semi-parametric way to estimate the distribution of high-dimensional functional neuroimage data, while the spatial temporal information contained in the data are well preserved. With some appropriate choices of the tuning parameters and the kernel functions, the model estimates are proved to be consistent. Compared with regularized support vector machine [2], our classification method, which is based on this functional graphical model, works much better with different kernel functions in the simulation as well as the real

data applications.

In future, we are going to optimize our computation steps and speed up the whole classification procedure. Currently, the procedure is not fast enough when the sample size in the training set is too large. We hope to make it capable for big data applications in which both the sample size and the data dimension are huge.

## References

- [1] Qiao X., Guo S., James G.M. (2018). Functional graphical models. *Journal of the American Statistical Association*, 1-12.
- [2] LaConte S., Strother S., Cherkassky V., Anderson J., Hu X. (2005). Support vector machines for temporal classification of block design fMRI data. *NeuroImage*, 26(2), 317-329.
- [3] Kolar M., Xing E. (2011). On time varying undirected graphs. In *Proceedings of the Fourteenth International Conference on Artificial Intelligence and Statistics* (pp. 407-415).
- [4] Ramsay J. (2005). Functional data analysis. *Encyclopedia of Statistics in Behavioral Science*.
- [5] Fan J. (2018). *Local polynomial modelling and its applications: monographs on statistics and applied probability 66*. Routledge.
- [6] Rosa M.J., Portugal L., Hahn T., Fallgatter A.J., Garrido M.I., Shawe-Taylor J., Mourao-Miranda J. (2015). Sparse network-based models for patient classification using fMRI. *Neuroimage*, 105, 493-506.
- [7] Anderson A., Cohen M. (2019). Functional Network Connectivity and SVM Classification of fMRI data using R. *Journal of Statistical Software*.
- [8] Koller D., Friedman N., Bach F. (2009). *Probabilistic graphical models: principles and techniques*. MIT press.
- [9] Gevins A., Brickett P., Costales B., Le J., Reutter B. (1990). Beyond topographic mapping: towards functional-anatomical imaging with 124-channel EEGs and 3-D MRIs. *Brain topography*, 3(1), 53-64.

# MINIMUM DISTANCE INDEX FOR NON-SQUARE COMPLEX VALUED MIXING MATRICES

N. LIETZÉN<sup>1</sup>, J. VIRTA<sup>1</sup>, K. NORDHAUSEN<sup>2</sup>, P. ILMONEN<sup>1</sup>

<sup>1</sup>*Aalto University School of Science*, e-mail: pauliina.ilmonen@aalto.fi

<sup>2</sup>*Institute of Statistics & Mathematical Methods in Economics, TU Wien  
Helsinki, FINLAND; Vienna, AUSTRIA*

## Abstract

We consider complex valued linear blind source separation, where the objective is to estimate a subset of the latent sources. In order to measure the success of the signal separation, we propose an extension of the minimum distance index and establish its properties. Interpretations for the index are derived through connections to signal-to-noise ratios and correlations. The interpretations are novel also for the square real valued (original) case.

**Keywords:** blind source separation, latent source, minimum distance index, data science

## 1 Introduction

In classic linear blind source separation (BSS), one assumes that the observation vectors are linear mixtures of a collection of latent *source* variables. The linearity assumption strikes a good balance between intricacy, mathematical tractability and interpretability, and the model has been used successfully in a wide variety of contexts ranging from signal processing and economics to biomedical applications. See, e.g., [1] for an introduction.

Numerous algorithms for the linear BSS problem under various assumptions on the sources have been proposed over the years, and a natural question is how to compare them. As the theoretical properties of the methods are often difficult to derive, comparisons are often conducted using simulation studies, see for example [4, 7, 8, 10, 12, 14]. To enable the comparisons, a performance measure for the success of the methods, called hereafter an *index*, is required. Popular indices considered in the literature include the Amari index, interference to signal ratio (ISR), mean square error (MSE) and the minimum distance index (MDI), see [9] for a comparative study. MDI has the advantage of both, being affine invariant and having a known asymptotic behavior, in the case of real valued square mixing matrices, see [3, 5]. Therefore, in this paper, our focus is on the minimum distance index.

In this paper, we extend the MDI to the case where only some of the sources, the signals, are of interest to us, and the index should measure how well these signals are recovered. Furthermore, in order to cover applications such as biomedical image processing, where the observed signals can be complex valued, we work under the assumption of complex valued variables. A real valued version of this extension was proposed already in [13]. However, in contrast to the current paper, no theoretical

justification for its properties was given in [13]. Similarly, a complex valued version of the regular MDI (where no distinction between the signal and the noise was made) was introduced in [6]. Moreover, the use of the minimum distance index is complicated by the fact that there is no clear scale attached to its values, making interpretation difficult. We provide a connection between the MDI and two commonly used statistics, SNR and correlation. These interpretations are given in the complex valued case, and the findings are novel also in the real valued case.

## 2 Complex valued blind source separation

Let  $\mathbf{x}$  be an observable  $\mathbb{C}^p$ -valued random vector that obeys the complex valued blind source separation model,

$$\mathbf{x} = \mathbf{\Omega}\mathbf{z} = \mathbf{\Omega} \begin{pmatrix} \mathbf{z}_1^\top & \mathbf{z}_0^\top \end{pmatrix}^\top, \quad (1)$$

where  $\mathbf{\Omega}$  is a full-rank  $\mathbb{C}^{p \times p}$ -matrix and the latent  $\mathbb{C}^p$ -vector  $\mathbf{z} = \begin{pmatrix} \mathbf{z}_1^\top & \mathbf{z}_0^\top \end{pmatrix}^\top$ , consists of two parts. In this model, the  $\mathbb{C}^d$ -vector  $\mathbf{z}_1$  contains the signals of interest that we wish to extract and the  $\mathbb{C}^{d_0}$ -vector  $\mathbf{z}_0$ ,  $d + d_0 = p$ , contains uninteresting noise. Depending on the type of the problem, additional assumptions are imposed on the signal and the noise. For example, independent component analysis (ICA) assumes that  $\mathbf{z}_1$  has independent marginals, second order separation (SOS) assumes that the signals and the noise have some specific temporal structure. In several approaches, some assumptions regarding the existence of the moments of  $\mathbf{z}$  are also made.

The objective in Model (1) is to find a  $\mathbb{C}^{d \times p}$  transformation matrix  $\mathbf{\Gamma}$ , such that the transformed vector corresponds to the signal variables,  $\mathbf{\Gamma}\mathbf{x} = \mathbf{z}_1$ , up to some class of transformations. The goal is to simultaneously extract both, the transformation matrix  $\mathbf{\Gamma}$  and the source signals, by using only the information contained in the observable  $\mathbf{x}$ . Note that usually the transformation matrix  $\mathbf{\Gamma}$  is not unique. For example, in ICA, the independent components stay independent, if we apply heterogeneous scaling, permutations or so-called phase-shifts to them. Thus in general, we have no guarantees that two separate IC estimation procedures estimate the same population quantities, which is something we need to consider when measuring the methods' performances. The minimum distance index discussed in the next section solves the issue by measuring how close the *gain matrix*  $\mathbf{G} = \mathbf{\Gamma}\mathbf{\Omega}$  is to the matrix  $\mathfrak{J}_{d,p} = \begin{pmatrix} \mathbf{I}_d & \mathbf{0} \end{pmatrix} \in \mathbb{R}^{d \times p}$ , up to heterogeneous scaling, permutations and phase-shifts.

## 3 Non-square complex valued MDI

In this section, we provide the mathematical background for the non-square complex valued MDI. We begin with the concept of equivalent matrices in the sense that is relevant in the context of BSS.

**Definition 1.** Let  $\sim$  be a relation on  $\mathbb{C}^{d \times p}$ , defined by  $\mathbf{A} \sim \mathbf{B} \iff \mathbf{A} = (\mathbf{P}\mathbf{J}\mathbf{D})\mathbf{B}$ , for some  $\mathbf{D} \in \mathcal{D}^d$ ,  $\mathbf{J} \in \mathcal{J}^d$  and  $\mathbf{P} \in \mathcal{P}^d$ , where  $\mathcal{P}^d$  is the set of  $\mathbb{R}^{d \times d}$  permutation

matrices,  $\mathcal{D}^d$  is the set of  $\mathbb{R}^{d \times d}$  diagonal matrices with positive real valued diagonal entries and  $\mathcal{J}^d$  is the set of  $\mathbb{C}^{d \times d}$  diagonal matrices with diagonal entries of the form  $\exp(\theta_1 i), \dots, \exp(\theta_d i)$ , where  $i$  is the imaginary unit. Furthermore, we use the notation  $\mathcal{C}^d$  for the set defined as  $\mathcal{C}^d = \{\mathbf{C} \in \mathbb{C}^{d \times d} \mid \mathbf{C} = \mathbf{P}\mathbf{J}\mathbf{D} : \mathbf{P} \in \mathcal{P}^d, \mathbf{J} \in \mathcal{J}^d, \mathbf{D} \in \mathcal{D}^d\}$ .

**Proposition 2.** The relation  $\sim$  is an equivalence relation on  $\mathbb{C}^{d \times p}$ .

The proof of Proposition 2 is omitted here as reflexivity, symmetry and transitivity of the relation  $\sim$  can be verified straightforwardly. We use the relation  $\sim$  to partition  $\mathbb{C}^{d \times p}$  into equivalence classes and denote matrices that are equivalent to the matrix  $\mathbf{A}$  as  $\mathcal{C}_{\mathbf{A}} = \{\mathbf{B} \in \mathbb{C}^{d \times p} \mid \mathbf{A} \sim \mathbf{B}\}$ .

We next consider the shortest squared distance between the equivalence class  $\mathcal{C}_{\mathbf{A}}$  and the matrix  $\mathfrak{J}_{d,p} = (\mathbf{I}_d \ \mathbf{0}) \in \mathbb{R}^{d \times p}$ . The optimization problem can be formulated as,

$$\text{minimize} \quad \|\mathbf{P}\mathbf{J}\mathbf{D}\mathbf{A} - \mathfrak{J}_{d,p}\|_{\text{F}}^2 \quad \text{s.t.} \quad \mathbf{P} \in \mathcal{P}^d, \quad \mathbf{J} \in \mathcal{J}^d \quad \text{and} \quad \mathbf{D} \in \mathcal{D}^d, \quad (2)$$

where  $\|\cdot\|_{\text{F}}$  is the Frobenius norm. Note that this optimization problem is not solvable in general, since the diagonal elements of matrices belonging to  $\mathcal{D}^d$  are in the open interval  $(0, \infty)$ . Hereby, we define the shortest squared distance between the equivalence class  $\mathcal{C}_{\mathbf{A}}$  and the matrix  $\mathfrak{J}_{d,p}$  to be the greatest lower bound, that is,

$$\varrho(\mathbf{A}, \mathfrak{J}_{d,p}) = \inf_{\mathbf{B} \in \mathcal{C}_{\mathbf{A}}} \|\mathbf{B} - \mathfrak{J}_{d,p}\|_{\text{F}}^2 = \inf_{\mathbf{C} \in \mathcal{C}^d} \|\mathbf{C}\mathbf{A} - \mathfrak{J}_{d,p}\|_{\text{F}}^2. \quad (3)$$

The distance  $\varrho(\mathbf{A}, \mathfrak{J}_{d,p})$  defined above can be converted into a more applicable form from the computational point of view, see the following theorem.

**Theorem 3.** Let  $\mathbf{A} \in \mathbb{C}^{d \times p}$  and  $\mathfrak{J}_{d,p} = (\mathbf{I}_d \ \mathbf{0}) \in \mathbb{R}^{d \times p}$ ,  $d \leq p$ . Furthermore, let  $\tilde{\mathbf{A}}_{jk} = |\mathbf{A}_{jk}|^2 / \sum_{h=1}^p |\mathbf{A}_{jh}|^2$ , if  $\mathbf{A}$  has at least one nonzero element in row  $j$  and  $\tilde{\mathbf{A}}_{jk} = 0$  if  $\mathbf{A}$  has only zeros in row  $j$ . Then, the distance  $\varrho(\mathbf{A}, \mathfrak{J}_{d,p})$  defined in Eq. (3), coincides with,

$$d - \max_{\mathbf{P} \in \mathcal{P}^d} \left\{ \text{Trace} \left( \mathbf{P}\tilde{\mathbf{A}} \right) \right\},$$

where the trace of a non-square matrix is the sum of its main-diagonal elements.

*Proof of Theorem 3.* We find the greatest lower bound by allowing the matrix  $\mathbf{D}$  to have also zeros on the diagonal. Then, we combine the optimization variables  $\mathbf{J}$  and  $\mathbf{D}$  by optimizing over a variable  $\mathbf{L} \in \mathcal{L}^d$ , where  $\mathcal{L}^d$  is the set of all  $\mathbb{C}^{d \times d}$  diagonal matrices. Now, since the Frobenius norm is orthogonally invariant, the objective function  $f$  can be reformulated as follows,

$$f(\mathbf{P}, \mathbf{L}, \mathfrak{J}_{d,p}) = \|\mathbf{P}\mathbf{L}\mathbf{A} - \mathfrak{J}_{d,p}\|_{\text{F}}^2 = \|\mathbf{P}(\mathbf{L}\mathbf{A} - \mathbf{P}^{\text{T}}\mathfrak{J}_{d,p})\|_{\text{F}}^2 = \|\mathbf{L}\mathbf{A} - \mathbf{P}^{\text{T}}\mathfrak{J}_{d,p}\|_{\text{F}}^2.$$

Next, write  $\mathbf{A} = \mathbf{V} + i\mathbf{W}$  and  $\mathbf{L} = \mathbf{Q} + i\mathbf{R}$ , where  $\mathbf{Q}, \mathbf{R}, \mathbf{V}, \mathbf{W}$  have real valued elements. Now, since  $\mathbf{L}$  is a diagonal matrix, we obtain the following form for  $f(\mathbf{P}, \mathbf{L}, \mathfrak{J}_{d,p})$ :

$$\sum_{j=1}^d \sum_{k=1}^p [\mathbf{Q}_{jj}^2 (\mathbf{V}_{jk}^2 + \mathbf{W}_{jk}^2) + \mathbf{R}_{jj}^2 (\mathbf{V}_{jk}^2 + \mathbf{W}_{jk}^2)] - 2 \sum_{j,k=1}^d (\mathbf{Q}_{jj}\mathbf{V}_{jk} - \mathbf{R}_{jj}\mathbf{W}_{jk}) \mathbf{P}_{kj} + d.$$

In the above formulation, we have applied the constraints that the off-diagonal elements of  $\mathbf{Q}$  and  $\mathbf{R}$  are zero. Thus, the only remaining constraint is that  $\mathbf{P}$  is a permutation matrix. We proceed to verify the Karush-Kuhn-Tucker necessary conditions.

Assume that  $\mathbf{A}$  has  $\ell$  rows that have at least one nonzero element. The  $d - \ell$  rows that contain only zeros give no contribution to the objective function and we can without loss of generality permute  $\mathbf{A}$  such that the  $\ell$  first rows of  $\mathbf{A}$  are the ones with at least one nonzero element. Regardless of the optimal permutation matrix, the partial derivatives with respect to the first  $\ell$  diagonal elements of  $\mathbf{Q}$  and  $\mathbf{R}$  are,

$$\begin{aligned}\frac{\partial f(\mathbf{P}, \mathbf{L}, \mathcal{J}_{d,p})}{\partial \mathbf{Q}_{jj}} &= \sum_{k=1}^p 2\mathbf{Q}_{jj} (\mathbf{V}_{jk}^2 + \mathbf{W}_{jk}^2) - 2 \sum_{k=1}^d \mathbf{V}_{jk} \mathbf{P}_{kj}, \\ \frac{\partial f(\mathbf{P}, \mathbf{L}, \mathcal{J}_{d,p})}{\partial \mathbf{R}_{jj}} &= \sum_{k=1}^p 2\mathbf{R}_{jj} (\mathbf{V}_{jk}^2 + \mathbf{W}_{jk}^2) + 2 \sum_{k=1}^d \mathbf{W}_{jk} \mathbf{P}_{kj},\end{aligned}$$

from which we can solve the solution candidates  $\mathbf{Q}'_{jj}$  and  $\mathbf{R}'_{jj}$ ,

$$\mathbf{Q}'_{jj} = \frac{\sum_{k=1}^d \mathbf{V}_{jk} \mathbf{P}_{kj}}{\sum_{k=1}^p (\mathbf{V}_{jk}^2 + \mathbf{W}_{jk}^2)} \quad \text{and} \quad \mathbf{R}'_{jj} = \frac{-\sum_{k=1}^d \mathbf{W}_{jk} \mathbf{P}_{kj}}{\sum_{k=1}^p (\mathbf{V}_{jk}^2 + \mathbf{W}_{jk}^2)}, \quad j \leq \ell.$$

Since the last  $d - \ell$  rows of  $\mathbf{A}$  do not contribute to the objective function, we set  $\mathbf{Q}'_{jj} = \mathbf{L}'_{jj} = 0$  and  $\mathbf{P}_{jj} = 1$ , when  $j > \ell$ . Using the property  $\mathbf{V}_{jk}^2 + \mathbf{W}_{jk}^2 = |\mathbf{A}_{jk}|^2$  and since a permutation matrix has exactly one nonzero element 1 in every row and column, we can reformulate the objective function for  $\mathbf{L}' = \mathbf{Q}' + i\mathbf{R}'$  as follows,

$$f(\mathbf{P}, \mathbf{L}', \mathcal{J}_{d,p}) = d - \sum_{j=1}^{\ell} \frac{|\mathbf{A}_{j,\pi(\mathbf{P},j)}|^2 \mathbf{P}_{\pi(\mathbf{P},j),j}}{\sum_{k=1}^p |\mathbf{A}_{j,k}|^2} - \sum_{j=\ell+1}^d 0 = d - \sum_{j=1}^d \tilde{\mathbf{A}}_{j,\pi(\mathbf{P},j)}$$

such that  $\pi : \mathcal{P}^d \times \{1, \dots, d\} \rightarrow \{1, \dots, d\} : \mathbf{P} \times j \mapsto c_j$ , where  $c_j$  is the row-index for the only nonzero element of the permutation matrix  $\mathbf{P}$  in the column  $j$ . An equivalent optimization problem is then to find a permutation for the rows of  $\mathbf{A}$ , such that the sum of the main-diagonal elements is maximized, that is,

$$\min_{\mathbf{P} \in \mathcal{P}^d} \left\{ d - \sum_{j=1}^d \tilde{\mathbf{A}}_{j,\pi(\mathbf{P},j)} \right\} \iff d - \max_{\mathbf{P} \in \mathcal{P}^d} \left\{ \text{Trace}(\mathbf{P}\tilde{\mathbf{A}}) \right\}.$$

□

We next present the minimum distance index (MDI) for non-square complex valued mixing matrices. Note that this is an extension to the cases presented in [3, 5, 6].

**Definition 4.** Let  $\mathbf{\Omega}$  be the mixing matrix of the noisy IC model given in Eq. (1), let  $\hat{\mathbf{\Gamma}}$  be a corresponding unmixing estimate and let  $\hat{\mathbf{G}} = \hat{\mathbf{\Gamma}}\mathbf{\Omega} \in \mathbb{C}^{d \times p}$ . The minimum distance index (MDI) for the estimate  $\hat{\mathbf{\Gamma}}$  is given by,

$$\text{MD}(\hat{\mathbf{\Gamma}}) = \frac{\varrho(\hat{\mathbf{G}}, \mathcal{J}_{d,p})}{\sqrt{d}} = \frac{1}{\sqrt{d}} \inf_{\mathbf{C} \in \mathbb{C}^d} \left\| \mathbf{C}\hat{\mathbf{G}} - (\mathbf{I}_d \ \mathbf{0}) \right\|_{\mathbb{F}}.$$

**Remark 5.** In previous formulations of the MDI in [3, 5, 6], the MDI was defined such that  $\varrho$  was scaled by  $1/\sqrt{d-1}$ . In the corresponding previous work, it was assumed that every row of  $\hat{\mathbf{G}}$  has at least one nonzero element. In this paper, we consider the more general situation allowing zero rows, yielding the scaling factor  $1/\sqrt{d}$ .

As in [5], the trace maximization problem in Theorem 3 can be seen as a linear sum assignment problem (LSAP). It can be solved, e.g., by the Hungarian method [11]. We next establish some key properties of the proposed index.

**Theorem 6.** *Let  $\mathbf{A} \in \mathbb{C}^{d \times p}$ . Then,  $\text{MD}(\mathbf{A}) \in [0, 1]$  and the MDI satisfies,*

$$(i) \text{MD}(\mathbf{A}) = 0 \iff \mathbf{A} \sim (\mathbf{I}_d \ \mathbf{0}) = \mathfrak{J}_{d,p},$$

$$(ii) \text{MD}(\mathbf{A}) = 1 \iff \exists \mathbf{B} \in \mathbb{C}^{d \times (p-d)} : \mathbf{A} = (\mathbf{0} \ \mathbf{B}),$$

(iii) *the function  $f : c \mapsto \text{MD}[(\mathbf{I}_d \ \mathbf{0}) + c \cdot \text{off}(\mathbf{A})]$  is increasing in  $c \in [0, 1]$  for all matrices  $\mathbf{A}$  that satisfy  $|\mathbf{A}_{jk}| < 1$  when  $j \neq k$ . (The function  $\text{off}(\cdot)$  here sets the main-diagonal elements of its argument equal to zero.)*

*Proof of Theorem 6.* By Theorem 3, we have that  $\text{MD}^2(\mathbf{A}) = 1 - \frac{1}{d} \max_{\mathbf{P}} \{\text{Trace}(\mathbf{P}\tilde{\mathbf{A}})\}$ , where the elements of  $\tilde{\mathbf{A}}$  are between zero and one. It follows from this formulation that  $\text{MD}(\mathbf{A}) \in [0, 1]$ . Next, we proceed to verify properties (i)–(iii).

First, assume that  $\mathbf{A} \sim \mathfrak{J}_{d,p}$ . This gives us that  $\tilde{\mathbf{A}}$  is equal, up to a permutation, to  $\mathfrak{J}_{d,p}$ . The maximal trace is then achieved by the permutation that places the only nonzero elements 1 of the matrix  $\tilde{\mathbf{A}}$  to the main-diagonal. Thus,  $\max_{\mathbf{P}} \{\text{Trace}(\mathbf{P}\tilde{\mathbf{A}})\} = d$ , which implies  $\text{MD}(\mathbf{A}) = 0$ . Next, assume that  $\text{MD}(\mathbf{A}) = 0$ . This assumption gives us that  $\max_{\mathbf{P}} \{\text{Trace}(\mathbf{P}\tilde{\mathbf{A}})\} = d$ . The corresponding trace can be  $d$  only when there exists an element  $\tilde{\mathbf{A}}_{jk}$  in every row  $j$  such that  $k \leq d$  and  $\tilde{\mathbf{A}}_{jk} = 1$ . Hereby, there has to be exactly one nonzero element in the first  $d$  columns of  $\mathbf{A}$  and the elements have to be on different rows. Consequently,  $\mathbf{A}$  is equivalent to  $\mathfrak{J}_{d,p}$ . Thus, property (i) holds.

For property (ii), first assume that  $\mathbf{A} = (\mathbf{0} \ \mathbf{B})$ . Then, the main-diagonal of  $\tilde{\mathbf{A}}_{jk}$  contains only zeros, regardless of the permutation and regardless of the matrix  $\mathbf{B}$ . Thus,  $\max_{\mathbf{P}} \{\text{Trace}(\mathbf{P}\tilde{\mathbf{A}})\} = 0$ , which gives us that  $\text{MD}(\mathbf{A}) = 1$ . For the only if part, assume that  $\text{MD}(\mathbf{A}) = 1$ . This assumption gives us that  $\text{Trace}(\mathbf{P}\tilde{\mathbf{A}}) = 0$  for the optimal  $\mathbf{P}$  and consequently for every other  $\mathbf{P}$  as well. Thus,  $\mathbf{A} = (\mathbf{0} \ \mathbf{B})$ , where  $\mathbf{B} \in \mathbb{C}^{d \times (p-d)}$  is arbitrary. Hereby, property (ii) holds.

For the final property (iii), assume that  $0 \leq c_1 \leq c_2 \leq 1$ . The requirement that the absolute values of the off-diagonal elements of  $\mathbf{A}$  are less than one ensures that the permutation matrix that maximizes the trace is the identity matrix. Then,

$$[f(c_2)]^2 - [f(c_1)]^2 = \frac{1}{d} \sum_{k=1}^d \left( \frac{-1}{c_2 \sum_{j \neq k}^p |\mathbf{A}_{kj}|^2 + 1} + \frac{1}{c_1 \sum_{j \neq k}^p |\mathbf{A}_{kj}|^2 + 1} \right) \geq 0,$$

that is, the function  $f$  is increasing under the given conditions.  $\square$

## 4 Interpretation of the minimum distance index

The interpretation of the MDI presented in [3, 5] has been difficult, since its formulation provided no clear way of directly interpreting its numerical values. While the extreme values of 0 and 1 are by Theorem 6, respectively, indicators of a perfect and fully unsuccessful separation, the intermediate values have been complicated to understand.

We next provide connections between the MDI and two easily interpretable statistics, signal-to-noise ratio and correlation. Assume Model (1), where  $\text{Cov}(\mathbf{z}) = \mathbf{I}_p$  (taken without loss of generality as the scales of the sources are confounded with the scales of  $\mathbf{\Omega}$ ). Assume furthermore that our aim is to extract only the  $d$  signal sources  $\mathbf{z}_1 = (z_1, \dots, z_d)$  and for this we have obtained an estimate  $\hat{\mathbf{\Gamma}} \in \mathbb{C}^{d \times p}$ , with the corresponding gain matrix  $\hat{\mathbf{G}} = \hat{\mathbf{\Gamma}}\mathbf{\Omega} \in \mathbb{C}^{d \times p}$ .

The estimates of the signals are then equal to  $\hat{\mathbf{z}}_1 = (\hat{z}_1, \dots, \hat{z}_d)^\top = \hat{\mathbf{G}}\mathbf{z}$  and we define the signal-to-noise ratio (SNR) and the correlation of the  $j$ th signal to be,

$$\text{SNR}_j = \frac{\text{Var}(\hat{z}_j)}{\text{Var}(\hat{z}_j - z_j)} \quad \text{and} \quad \text{Cor}_j = \text{Cor}(\hat{z}_j, z_j).$$

We here use the version of SNR defined in [2]. The following theorem connects the three statistics (MDI, SNR and correlation) under two different models for the gain matrix  $\hat{\mathbf{G}}$ : homogeneous contamination where all of the elements of  $\hat{\mathbf{G}}$  deviate equally from those of  $\mathfrak{J}_{d,p}$ , and heterogeneous contamination where no structure for the contamination is assumed besides the requirement that it applies only to the off-diagonal elements of  $\hat{\mathbf{G}}$ . Let  $\mathbf{A}(c_j) = \mathbf{A}(c_1, \dots, c_d)$  and  $\mathbf{H}(c_j) = \mathbf{H}(c_1, \dots, c_d)$  denote, respectively, the arithmetic and harmonic means of the values  $c_1, \dots, c_d$ .

**Theorem 7.** *Assume Model (1), where  $\text{Cov}(\mathbf{z}) = \mathbf{I}_p$ . Then, under the homogeneous contamination model  $\hat{\mathbf{G}} = \mathfrak{J}_{d,p} + \varepsilon \mathbf{1}_{d,p}$ , where  $\mathbf{1}_{d,p}$  is a  $d \times p$  matrix full of ones and  $\text{Re}(\varepsilon) > -1/2$ ,*

$$\text{MD}^2(\hat{\mathbf{G}}) = \left( \frac{p-1}{p} \right) \text{SNR}_j^{-1} = 1 - |\text{Cor}_j|^2.$$

*Under the heterogenous contamination model  $\hat{\mathbf{G}} = \mathfrak{J}_{d,p} + \mathbf{B}$ , where  $\mathbf{B} \in \mathbb{C}^{d \times p}$  has zero main-diagonal and  $|\mathbf{B}_{jk}| < 1$ ,  $j \neq k$ , we have*

$$\text{MD}^2(\hat{\mathbf{G}}) = \mathbf{H}(\text{SNR}_1, \dots, \text{SNR}_d)^{-1} = 1 - \mathbf{A}(|\text{Cor}_1|^2, \dots, |\text{Cor}_d|^2).$$

*Proof of Theorem 7.* We consider the two models separately. Under the homogeneous one, we have  $\text{MD}^2(\hat{\mathbf{G}}) = 1 - \frac{1}{d} \max_{\mathbf{P}} \{\text{Trace}(\mathbf{P}\hat{\mathbf{G}})\}$ , where the diagonal elements of  $\hat{\mathbf{G}}$  are equal to  $|1 + \varepsilon|^2 / [|1 + \varepsilon|^2 + (p-1)|\varepsilon|^2]$  and the off-diagonal elements are equal to  $|\varepsilon|^2 / [|1 + \varepsilon|^2 + (p-1)|\varepsilon|^2]$ . The requirement that  $\text{Re}(\varepsilon) > -1/2$  ensures that the maximization over  $d \times d$  permutation matrices is solved by  $\mathbf{I}_d$  and we get  $\text{MD}^2(\hat{\mathbf{G}}) = [(p-1)|\varepsilon|^2] / [|1 + \varepsilon|^2 + (p-1)|\varepsilon|^2]$ . Consider then the signal-to-noise ratio  $\text{SNR}_j$  of the  $j$ th signal  $\hat{z}_j = \hat{\mathbf{G}}_{j1}z_1 + \dots + \hat{\mathbf{G}}_{jd}z_p$ . As the sources are uncorrelated and have unit variances, we obtain

$$\text{SNR}_j = \frac{\text{Var}(\hat{z}_j)}{\text{Var}(\hat{z}_j - z_j)} = \frac{\sum_{k=1}^p |\hat{\mathbf{G}}_{jk}|^2}{|\hat{\mathbf{G}}_{jj} - 1|^2 + \sum_{k \neq j}^p |\hat{\mathbf{G}}_{jk}|^2} = \left( \frac{p-1}{p} \right) \text{MD}^{-2}(\hat{\mathbf{G}}). \quad (4)$$

Table 1: Average SNRs and correlations corresponding to certain MDI-values.

MDI	0.1	0.01	0.001	0.0001
$\mathbb{H}(\text{SNR}_j)$	20 dB	40 dB	60 dB	80 dB
$\sqrt{\mathbb{A}( \text{Cor}_j ^2)}$	$1 - 0.5 \cdot 10^{-2}$	$1 - 0.5 \cdot 10^{-4}$	$1 - 0.5 \cdot 10^{-6}$	$1 - 0.5 \cdot 10^{-8}$ .

Similarly, for the correlation, we have  $\text{Var}(z_j) = 1$ ,  $\text{Var}(\hat{z}_j) = |1 + \varepsilon|^2 + (p - 1) |\varepsilon|^2$  and  $\text{Cov}(\hat{z}_j, z_j) = 1 + \varepsilon$ , yielding,

$$|\text{Cor}_j|^2 = \frac{|\text{Cov}(\hat{z}_j, z_j)|^2}{\text{Var}(\hat{z}_j)\text{Var}(z_j)} = \frac{|1 + \varepsilon|^2}{|1 + \varepsilon|^2 + (p - 1) |\varepsilon|^2} = 1 - \text{MD}^2(\hat{\mathbf{G}}),$$

proving the claim under the homogeneous contamination. The proof for the heterogeneous contamination proceeds in exactly the same manner and we provide only the values for the key quantities. The squared MDI equals  $\text{MD}^2(\hat{\mathbf{G}}) = 1 - (1/d) \sum_{j=1}^d (1 + \sum_{k \neq j}^p |\hat{\mathbf{G}}_{jk}|^2)^{-1}$ . Using the general form for signal-to-noise ratio in (4), we get  $1 - (\text{SNR}_j)^{-1} = (1 + \sum_{k \neq j}^p |\hat{\mathbf{G}}_{jk}|^2)^{-1}$  which when combined with the expression for  $\text{MD}^2(\hat{\mathbf{G}})$  yields the claim for SNR. For the correlation we have  $\text{Var}(z_j) = 1$ ,  $\text{Var}(\hat{z}_j) = 1 + \sum_{k \neq j}^p |\hat{\mathbf{G}}_{jk}|^2$  and  $\text{Cov}(\hat{z}_j, z_j) = 1$ , yielding  $|\text{Cor}_j|^2 = (1 + \sum_{k \neq j}^p |\hat{\mathbf{G}}_{jk}|^2)^{-1}$  and establishing the final part of the claim.  $\square$

Table 1 displays the connection between the MDI values and the average signal-to-noise ratios and the correlations under the heterogeneous contamination model. In the table, the signal-to-noise ratios have been converted to the standard decibel scale using the transformation  $10 \log_{10}(\text{SNR})$ . Interestingly, the table shows that the minimum distance index of 0.1 can already be considered extremely good; it corresponds to the high average SNR of 20 dB and to the almost perfect average correlation of 0.995. Similarly, the index value of 0.01 can be considered to correspond to an almost flawless separation.

## 5 Discussion

In recent years BSS has become a popular tool for dimension reduction and thus the interest for models with non-square mixing matrices has grown considerably. To facilitate comparisons of different BSS methods, we extended the popular MDI to the complex valued non-square case. To give a better understanding of the MDI values besides the extremes, we derived a connection between MDI, and SNR and correlations, which provides the opportunity to better judge if a method is of practical use.

In future work, we will derive asymptotic properties of the extended MDI. Moreover, we will explore whether variants of the index can be used in nonlinear BSS.

**Acknowledgements:** N. Lietzén gratefully acknowledges financial support from the Emil Aaltonen Foundation (grant 180144). The authors would also like to thank the anonymous referee.

## References

- [1] Comon P., Jutten C. (2010). *Handbook of Blind Source Separation: Independent component analysis and applications*. Academic Press, Oxford.
- [2] Gonzales R.C., Woods R.E. (2001). *Digital Image Processing, Second Edition*. Prentice Hall, Upper Saddle River, New Jersey.
- [3] Ilmonen P., Nordhausen K., Oja H., Ollila E. (2010). A new performance index for ICA: properties, computation and asymptotic analysis. *International Conference on Latent Variable Analysis and Signal Separation*. pp. 229-236, Springer.
- [4] Ilmonen P., Paindaveine D. (2011). Semiparametrically efficient inference based on signed ranks in symmetric independent component models. *Annals of Statistics*. Vol. **39**, pp. 2448-2476.
- [5] Ilmonen P., Nordhausen K., Oja H., Ollila E. (2012). On asymptotics of ICA estimators and their performance indices. *arXiv preprint arXiv:1212.3953*.
- [6] Lietzén N., Nordhausen K., Ilmonen P. (2016). Minimum distance index for complex valued ICA. *Statistics & Probability Letters*. Vol. **118**, pp. 100-106.
- [7] Matteson D.S., Tsay R.S. (2017). Independent component analysis via distance covariance. *Journal of the American Statistical Association*. Vol. **112**, pp. 623-637.
- [8] Miettinen J., Illner K., Nordhausen K., Oja H., Taskinen S., Theis F.J. (2016). Separation of uncorrelated stationary time series using autocovariance matrices. *Journal of Time Series Analysis*. Vol. **37**, pp. 337-354.
- [9] Nordhausen K., Ollila E., Oja H. (2011). On the performance indices of ICA and blind source separation. *2011 IEEE 12th International Workshop on Signal Processing Advances in Wireless Communications*. pp. 486-490, IEEE.
- [10] Nordhausen K. (2014). On robustifying some second order blind source separation methods for nonstationary time series. *Statistical Papers*. Vol. **55**, pp. 141-156.
- [11] Papadimitriou C., Steiglitz K. (1982). *Combinatorial Optimization: Algorithms and Complexity*. Prentice Hall, Englewood Cliffs.
- [12] Risk B.B., Matteson D.S., Ruppert D., Eloyan A., Caffo B.S. (2014). An evaluation of independent component analyses with an application to resting-state fMRI. *Biometrics*. Vol. **70**, pp. 224-236.
- [13] Virta J., Nordhausen K., Oja H. (2016). Projection pursuit for non-Gaussian independent components. *arXiv preprint arXiv:1612.05445*.
- [14] Virta J., Li B., Nordhausen K., Oja H. (2017). Independent component analysis for tensor-valued data. *Journal of Multivariate Analysis*, Vol. **162**, pp. 172-192.

# APPROXIMATION OF DENSITY FUNCTIONS USING SIMPLICIAL SPLINES

J. MACHALOVÁ, R. TALSKÁ, K. HRON

*Department of Mathematical Analysis and Applications of Mathematics,*

*Faculty of Science, Palacký University Olomouc*

*Olomouc, CZECH REPUBLIC*

e-mail: jitka.machalova@upol.cz

## Abstract

Probability density functions result in practice frequently from aggregation of massive data and their further statistical processing is thus of increasing importance. However, specific properties of density functions prevent from analyzing a sample of densities directly using tools of functional data analysis. Moreover, it is not only about the unit integral constraint, which results from representation of densities within the equivalence class of proportional positive-valued functions, but also about their relative scale which emphasizes the effect of small relative contributions of Borel subsets to the overall measure of the support. For practical data processing, it is popular to approximate first the input (discrete) data with a proper spline representation. Aim of the contribution is to introduce new class of B-splines within the Bayes space methodology which is suitable for representation of density functions. Accordingly, the original densities are expressed as real functions using the centred logratio transformation and optimal smoothing splines with B-spline basis honoring the resulting zero-integral constraint are developed.

**Keywords:** data science, simplicial spline, density function

## 1 Introduction

Probability density functions are non-negative functions, popularly represented with a unit integral constraint. However, in some fields, e.g., in Bayesian statistics density functions are considered in a more general setting, where any representation within the equivalence class of proportional functions can be taken. This reflects better the basic property of densities - their scale invariance. Accordingly, the sample space of densities is formed by a set of equivalence classes of proportional positive functions. In this paper a bounded support  $I = [a, b] \subset \mathbb{R}$  of densities is considered which occurs frequently in practice. Specific properties of density functions are captured by the Bayes space  $\mathcal{B}^2(I)$  of functions with square-integrable logarithm [2, 5]; in a default setting the Lebesgue reference measure is taken. The Bayes space  $\mathcal{B}^2(I)$  has structure of separable Hilbert space which enables to construct an isometric isomorphism between  $\mathcal{B}^2(I)$  and  $L^2(I)$ , the  $L^2$  space restricted to  $I$ . An isometric isomorphism between  $\mathcal{B}^2(I)$  and  $L^2(I)$  is represented by the *centred log-ratio* (clr) transformation [2]. It is defined for a density  $f \in \mathcal{B}^2(I)$  as

$$\text{clr}(f)(x) = f_c(x) = \ln f(x) - \frac{1}{\eta} \int_I \ln f(y) dy,$$

with  $\eta = b - a$ . The clr transformation induces an additional zero-integral constraint that needs to be taken into account for computation and analysis on clr-transformed density functions. As the clr space is clearly a subspace of  $L^2(I)$ , hereafter it is denoted as  $L_0^2(I)$ . Although the clr transformed densities are standard real functions, their constrained character calls for modification of methods for their approximation and further statistical processing using methods of functional data analysis. This is also the case of approximation using splines, described in a detail in the next section.

## 2 Optimal smoothing splines in $L^2(I)$

Firstly we recall the basic knowledge about  $B$ -spline representation of splines, see [3, 4, 12]. Let  $\mathcal{S}_k^{\Delta\lambda}[a, b]$  denote the vector space of polynomial splines of degree  $k > 0$ , defined on a finite interval  $I = [a, b]$  with the sequence of knots  $\Delta\lambda$ , where

$$\Delta\lambda := \lambda_0 = a < \lambda_1 < \dots < \lambda_g < b = \lambda_{g+1}.$$

It is known that  $\dim(\mathcal{S}_k^{\Delta\lambda}[a, b]) = g + k + 1$ . Then every spline  $s_k(x) \in \mathcal{S}_k^{\Delta\lambda}[a, b]$  in  $L^2(I)$  has a unique representation

$$s_k(x) = \sum_{i=-k}^g b_i B_i^{k+1}(x).$$

For this representation it is necessary to add some additional knots, e.g. such that

$$\lambda_{-k} = \dots = \lambda_{-1} = \lambda_0, \quad \lambda_{g+1} = \lambda_{g+2} = \dots = \lambda_{g+k+1}. \quad (1)$$

Vector  $\mathbf{b} = (b_{-k}, \dots, b_g)^\top$  is called *the vector of  $B$ -spline coefficients* of  $s_k(x)$ , functions  $B_i^{k+1}(x)$ ,  $i = -k, \dots, g$  are  *$B$ -splines of degree  $k$*  and form basis in  $\mathcal{S}_k^{\Delta\lambda}[a, b]$ . In matrix notation it can be written as

$$s_k(x) = \mathbf{C}_{k+1}(x)\mathbf{b},$$

where  $\mathbf{C}_{k+1}(x) = (B_i^{k+1}(x))_{i=-k}^g$  is so called *collocation matrix*. It is known that derivative of order  $l$ ,  $l \in \{1, \dots, k-1\}$ , of the spline  $s_k(x) \in \mathcal{S}_k^{\Delta\lambda}[a, b]$  is a spline  $s_{k-l}(x) \in \mathcal{S}_{k-l}^{\Delta\lambda}[a, b]$  with the same knots. Using properties of  $B$ -splines the spline derivatives can be written in matrix notation as

$$s_k^{(l)}(x) = \mathbf{C}_{k+1-l}(x)\mathbf{b}^{(l)},$$

where  $\mathbf{b}^{(l)} \in \mathbb{R}^{g+k+1-l}$  is given by  $\mathbf{b}^{(l)} = \mathbf{D}_l \mathbf{L}_l \mathbf{b}^{(l-1)} = \mathbf{D}_l \mathbf{L}_l \dots \mathbf{D}_1 \mathbf{L}_1 \mathbf{b} = \mathbf{S}_l \mathbf{b}$  and  $\mathbf{b}^{(0)} = \mathbf{b}$ . Upper triangular matrix  $\mathbf{S}_l = \mathbf{D}_l \mathbf{L}_l \dots \mathbf{D}_1 \mathbf{L}_1 \in \mathbb{R}^{g+k+1-l, g+k+1}$  has full row rank. Matrix  $\mathbf{D}_j \in \mathbb{R}^{g+k+1-j, g+k+1-j}$  is diagonal such that

$$\mathbf{D}_j = (k+1-j) \text{diag}(d_{-k+j}, \dots, d_g), \quad d_i = \frac{1}{\lambda_{i+k+1-j} - \lambda_i} \quad \forall i = -k+j, \dots, g$$

and

$$\mathbf{L}_j := \begin{pmatrix} -1 & 1 & & \\ & \ddots & \ddots & \\ & & -1 & 1 \end{pmatrix} \in \mathbb{R}^{g+k+1-j, g+k+2-j}.$$

Now we assume that data  $(x_i, y_i)$ ,  $a \leq x_i \leq b$ , weights  $w_i \geq 0$ ,  $i = 1, \dots, n$ , sequence of knots  $\Delta\lambda$ ,  $n \geq g + 1$ , and a parameter  $\alpha \in (0, 1)$  are given. The optimal smoothing problem, [9, 10], which is in fact generalization of smoothing problem [3, 4], is defined as a task to find a spline  $s_k(x) \in \mathcal{S}_k^{\Delta\lambda}[a, b]$ , which minimizes the functional

$$J_l(s_k) = \int_a^b \left[ s_k^{(l)}(x) \right]^2 dx + \alpha \sum_{i=1}^n w_i [y_i - s_k(x_i)]^2. \quad (2)$$

The choice of parameter  $l$  will affect smoothness of the resulting spline. Let us denote  $\mathbf{x} = (x_1, \dots, x_n)^\top$ ,  $\mathbf{y} = (y_1, \dots, y_n)^\top$ ,  $\mathbf{w} = (w_1, \dots, w_n)^\top$  and  $\mathbf{W} = \text{diag}(\mathbf{w})$ . The functional  $J_l(s_k)$  can be written in a matrix form as

$$J_l(\mathbf{b}) = \mathbf{b}^\top \mathbf{N}_{kl} \mathbf{b} + \alpha [\mathbf{y} - \mathbf{C}_{k+1}(\mathbf{x}) \mathbf{b}]^\top \mathbf{W} [\mathbf{y} - \mathbf{C}_{k+1}(\mathbf{x}) \mathbf{b}],$$

see [9, 10] for details. The matrix  $\mathbf{N}_{kl} = \mathbf{S}_l^\top \mathbf{M}_{kl} \mathbf{S}_l$  is positive semidefinite, where

$$\mathbf{M}_{kl} = \begin{pmatrix} (B_{-k+l}^{k+1-l}, B_{-k+l}^{k+1-l}) & \dots & (B_g^{k+1-l}, B_{-k+l}^{k+1-l}) \\ \vdots & & \vdots \\ (B_{-k+l}^{k+1-l}, B_g^{k+1-l}) & \dots & (B_g^{k+1-l}, B_g^{k+1-l}) \end{pmatrix} \in \mathbb{R}^{g+k+1-l, g+k+1-l}$$

and

$$(B_i^{k+1-l}, B_j^{k+1-l}) = \int_a^b B_i^{k+1-l}(x) B_j^{k+1-l}(x) dx$$

stands for scalar product of  $B$ -splines in  $L^2(I)$  space. Matrix  $\mathbf{M}_{kl}$  is positive definite, because  $B_i^{k+1-l}(x) \geq 0$ ,  $i = -k + l, \dots, g$  are basis functions. Now the task is to find a minimum of function  $J_l(\mathbf{b})$ . It is obvious that this minimum fulfils the condition

$$\frac{\partial J_l(\mathbf{b})}{\partial \mathbf{b}^\top} = 0,$$

which can be written as a system of linear equations  $\mathbf{G} \mathbf{b} = \mathbf{g}$  with

$$\mathbf{G} = \alpha^{-1} \mathbf{N}_{kl} + \mathbf{C}_{k+1}^\top(\mathbf{x}) \mathbf{W} \mathbf{C}_{k+1}(\mathbf{x}), \quad \mathbf{g} = \mathbf{C}_{k+1}^\top(\mathbf{x}) \mathbf{W} \mathbf{y}.$$

If this system is consistent, then there exists a solution which is given by  $\mathbf{b}^* = \mathbf{G}^{-1} \mathbf{g}$ , see [10]. So finally  $s_k^*(x) = \mathbf{C}_{k+1}(x) \mathbf{b}^*$  is resulting optimal smoothing spline, i.e. spline which minimizes functional (2).

### 3 Optimal smoothing splines in $L_0^2(I)$

In this section the case of smoothing clr-transformed density functions is considered. The task is find spline  $s_k(x) \in \mathcal{S}_k^{\Delta\lambda}[a, b]$  which minimizes functional (2) and which satisfies an additional condition

$$\int_a^b s_k(x) dx = 0. \quad (3)$$

There are two possibilities how to deal with this problem. The first approach, which was published in [8], is based on using expression between coefficients of spline and its derivative. The second possibility uses new  $B$ -spline basis functions which satisfy the condition (3). This process is described in [7].

Now the first approach will be described in more details. Note that the spline

$$s_k(x) = \sum_{i=-k}^g b_i B_i^{k+1}(x)$$

is a derivative of spline

$$s_{k+1}(x) = \sum_{i=-k-1}^g c_i B_i^{k+2}(x), \quad (4)$$

if

$$b_i = (k+1) \frac{c_i - c_{i-1}}{\lambda_{i+k+1} - \lambda_i} \quad \forall i = -k, \dots, g. \quad (5)$$

For each spline  $s_k(x) \in \mathcal{S}_k^{\Delta\lambda}[a, b]$  satisfying the condition (3) we have

$$0 = \int_a^b s_k(x) dx = [s_{k+1}(x)]_a^b = s_{k+1}(\lambda_{g+1}) - s_{k+1}(\lambda_0),$$

because  $a = \lambda_0$ ,  $b = \lambda_{g+1}$ . With respect to the definition and properties of  $B$ -splines, the additional knots (1) and notation (4) we get

$$0 = s_{k+1}(\lambda_{g+1}) - s_{k+1}(\lambda_0) = c_g - c_{-k-1},$$

so that  $c_{-k-1} = c_g$ . The relationship (5) between the vector  $\mathbf{b} = (b_{-k}, \dots, b_g)^\top$  of  $B$ -spline coefficients of  $s_k(x)$  and the vector  $\mathbf{c} = (c_{-k-1}, \dots, c_g)^\top$  of  $s_{k+1}(x)$ ,  $\mathbf{c} \in \mathbb{R}^{g+k+2}$  such that  $c_{-k-1} = c_g$ , can be written as

$$\mathbf{b} = \mathbf{DK}\bar{\mathbf{c}},$$

where  $\bar{\mathbf{c}} = (c_{-k}, \dots, c_g)^\top \in \mathbb{R}^{g+k+1}$ . Matrices  $\mathbf{D}$  and  $\mathbf{K}$  are known, see [8]. So with this relationship we are able to rewrite function  $J_l(\mathbf{b})$  as a function  $J_l(\bar{\mathbf{c}})$ . Then we find its minimum  $\bar{\mathbf{c}}^*$  and finally the vector of  $B$ -spline coefficients  $\mathbf{b}^*$  for optimal smoothing spline which has zero integral is obtained by

$$\mathbf{b}^* = \mathbf{DK}\bar{\mathbf{c}}^*.$$

The corresponding spline is given by  $s_k^*(x) = \mathbf{C}_{k+1}(x)\mathbf{b}^*$ .

The second approach for finding optimal smoothing spline with zero integral, which is presented in [7], uses new functions  $Z_i^{k+1}(x)$  for  $k \geq 0$ . They are defined by formula

$$Z_i^{k+1}(x) := \frac{d}{dx} B_i^{k+2}(x).$$

More precisely for  $k = 0$

$$Z_i^1(x) = \begin{cases} 1 & \text{if } x \in [\lambda_i, \lambda_{i+1}) \\ -1 & \text{if } x \in (\lambda_{i+1}, \lambda_{i+2}] \end{cases} \quad (6)$$

and for  $k \geq 1$

$$Z_i^{k+1}(x) = (k+1) \left( \frac{B_i^{k+1}(x)}{\lambda_{i+k+1} - \lambda_i} - \frac{B_{i+1}^{k+1}(x)}{\lambda_{i+k+2} - \lambda_{i+1}} \right). \quad (7)$$

Noteworthy, functions  $Z_i^{k+1}(x)$  have similar properties as  $B$ -splines  $B_i^{k+1}(x)$ , we called them  $ZB$ -splines, for more details see [7]. Example of quadratic  $ZB$ -splines  $Z_i^3(x)$  is displayed in Figure 1.

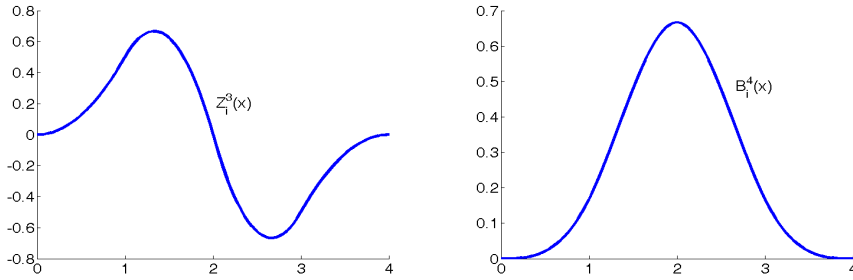


Figure 1: Quadratic  $ZB$ -spline  $Z_i^3(x) = \frac{d}{dx} B_i^4(x)$  with equidistant knots  $0, 1, 2, 3, 4$ .

From the perspective of  $L_0^2(I)$  a crucial point is that integral of  $Z_i^{k+1}(x)$  equals to zero:

$$\begin{aligned} \int_{-\infty}^{+\infty} Z_i^{k+1}(x) dx &= \int_{\lambda_i}^{\lambda_{i+k+2}} Z_i^{k+1}(x) dx = \int_{\lambda_i}^{\lambda_{i+k+2}} \frac{d}{dx} B_i^{k+2}(x) dx = \\ &= [B_i^{k+2}(x)]_{\lambda_i}^{\lambda_{i+k+2}} = 0. \end{aligned}$$

In the following,  $\mathcal{Z}_k^{\Delta\lambda}[a, b]$  denotes the vector space of polynomial splines of degree  $k > 0$ , defined on a finite interval  $[a, b]$  with the sequence of knots  $\Delta\lambda$  and having zero integral on  $[a, b]$ . With respect to the condition of the zero integral it is clear that  $\dim(\mathcal{Z}_k^{\Delta\lambda}[a, b]) = g + k$ , for more details see [7]. With the additional knots (1) we can construct  $g + k$  functions  $Z_{-k}^{k+1}(x), \dots, Z_{g-1}^{k+1}(x)$ , which are basis functions of the space  $\mathcal{Z}_k^{\Delta\lambda}[a, b]$ . Then every spline  $s_k(x) \in \mathcal{Z}_k^{\Delta\lambda}[a, b]$  has a unique representation

$$s_k(x) = \sum_{i=-k}^{g-1} z_i Z_i^{k+1}(x).$$

In matrix notation it can be expressed as

$$s_k(x) = \mathbf{Z}_{k+1}(x) \mathbf{z},$$

where  $\mathbf{Z}_{k+1} = (Z_i^{k+1}(x))_{i=-k}^{g-1}$ ,  $\mathbf{z} = (z_{-k}, \dots, z_{g-1})^\top$ . Next steps are similar as we used in the first approach, the functional (2) is expressed as a function of variable  $\mathbf{z}$ . Then we find its minimum  $\mathbf{z}^*$  and finally the optimal smoothing spline with zero integral is given by formula  $s_k^*(x) = \mathbf{Z}_{k+1}(x)\mathbf{z}^*$ .

Reduction of dimension for splines in  $L_0^2(I)$  by one is a very natural consequence of clr transformation of density functions. Note that this feature is present also for clr coefficients of compositional data [1].

## 4 Simplicial splines in the Bayes space

Construction of splines directly in  $L_0^2(I)$  has important practical consequences, however, it is important also from theoretical perspective. Expressing  $B$ -splines as functions in  $L_0^2(I)$  enables to back-transform them to the original Bayes space  $\mathcal{B}^2(I)$  using inverse clr transformation [2]. It results in *simplicial B-splines (SB-splines)*, obtained from (6), (7) as

$$\zeta_i^{k+1}(x) = \frac{\exp[Z_i^{k+1}(x)]}{\int_I \exp[Z_i^{k+1}(y)] dy}, \quad i = -k, \dots, g-1, k \geq 0.$$

Note that  $SB$ -splines  $\zeta_i^{k+1}(x)$  fulfill the unit integral constraint. As a consequence, it is immediate to define vector space  $\mathcal{C}_k^{\Delta\lambda}[a, b]$  of simplicial polynomial splines of degree  $k > 0$ , defined on a finite interval  $[a, b]$  with the sequence of knots  $\Delta\lambda$ . From isomorphism between  $\mathcal{C}_k^{\Delta\lambda}[a, b]$  and  $\mathcal{Z}_k^{\Delta\lambda}[a, b]$  it holds that  $\dim(\mathcal{C}_k^{\Delta\lambda}[a, b]) = g + k$ . Moreover, from isometric properties of clr transformation it follows that every simplicial spline  $\xi_k(x) \in \mathcal{C}_k^{\Delta\lambda}[a, b]$  in  $B^2(I)$  can be uniquely represented as

$$\xi_k(x) = \bigoplus_{i=-k}^{g-1} c_i \odot \zeta_i^{k+1}(x),$$

where  $\odot$  stands for powering operation in  $\mathcal{B}^2(I)$  [2]

The resulting simplicial splines can be used for representation of densities directly in  $\mathcal{B}^2(I)$ . This is an important step in construction of methods of functional data analysis involving density functions, like for ANOVA modeling or for the SFPCA method.

## 5 Outlook

Once the sample of probability density functions is approximated using optimal smoothing splines in  $L_0(I)$ , any from popular methods of functional data analysis [11] can be applied by considering the zero integral constraint of the clr transformed densities. These methods usually strongly rely just on a proper spline representation of densities. Accordingly, simplicial functional principal component analysis [6] or compositional regression with functional response [13] were developed; they show a clear way how also other methods could be adapted for this important class of functions.

## Acknowledgments

The authors gratefully acknowledge both the support by the grant IGA PrF IGA\_PrF\_2019\_006, Mathematical Models of the Internal Grant Agency of the Palacký University in Olomouc.

## References

- [1] Aitchison J. (1986). *The statistical analysis of compositional data*. Chapman and Hall, London.
- [2] Van den Boogaart K.G., Egozcue J.J., Pawłowsky-Glahn V. (2014). Bayes Hilbert spaces *Australian & New Zealand Journal of Statistics*. Vol. **56**, Num. **2**, pp. 171-194.
- [3] De Boor C. (1978). *A practical guide to splines*. Springer-Verlag, New York.
- [4] Dierckx P. (1993). *Curve and surface fitting with splines*. Oxford University Press, New York.
- [5] Egozcue J.J., Díaz-Barrero J.L., Pawłowsky-Glahn V. (2006). Hilbert space of probability density functions based on Aitchison geometry, *Acta Mathematica Sinica*. Vol. **22**, Num. **4**, pp. 1175-1182.
- [6] Hron K., Menafoglio A., Templ M., Hrušová K., Filzmoser P. (2016). Simplicial principal component analysis for density functions in Bayes spaces. . *Computational Statistics and Data Analysis*. Vol. **94**, pp. 330-350.
- [7] Machalová J., Talská R., Hron K., Gába A. (2019). Simplicial splines for representation of density functions. *arXiv preprint arXiv:1905.06858*.
- [8] Machalová J., Hron K., Monti G. S. (2016). Preprocessing of centred logratio transformed density functions using smoothing splines. *Journal of Applied Statistics*. Vol. **43**, Num. **8**, pp. 1419-1435.
- [9] Machalová J. (2002). Optimal interpolatory splines using *B*-spline representation. *Acta Universitatis Palackianae Olomucensis. Facultas Rerum Naturalium. Mathematica*. Palacký University Olomouc. Vol. **41**, Num. **1**, pp. 105-118.
- [10] Machalová J. (2002). Optimal interpolating and optimal smoothing spline. *Journal of Electrical Engineering*. Vol. **53**, pp. 79-82.
- [11] Ramsay J., Silverman B.W. (2005). *Functional Data Analysis*, second ed. Springer, New York.
- [12] Schumaker L. (2007). *Spline functions: basic theory*. Cambridge University Press.
- [13] Talská R., Menafoglio A., Machalová J., Hron K., Fišerová E. (2018). Compositional regression with functional response. *Computational Statistics & Data Analysis*. Vol. **123**, pp. 66-85.

# FRACTIONAL STOCHASTIC VOLATILITY: F-ORNSTEIN–UHLENBECK AND F-CIR PROCESSES

YU. MISHURA

*Taras Shevchenko National University of Kyiv*

*Kyiv, UKRAINE*

e-mail: myus@univ.kiev.ua

## Abstract

We consider fractional Ornstein–Uhlenbeck process as well as fractional CIR-process with Hurst index  $H \in (0, 1)$ , and several approaches to the exact and approximate option pricing of the asset price model that is described by the geometric linear model with stochastic volatility, where volatility is driven by fractional Ornstein–Uhlenbeck process. We assume that the Wiener process driving the asset price and the fractional Brownian motion driving stochastic volatility are correlated. We consider three possible levels of representation and approximation of option price, with the corresponding rate of convergence of discretized option price to the original one.

We can rigorously treat the class of discontinuous payoff functions of polynomial growth. As an example, our model allows to analyze linear combinations of digital and call options. Moreover, we provide rigorous estimates for the rates of convergence of option prices for polynomial discontinuous payoffs  $f$  and Hölder volatility coefficients, a crucial feature considering settings for which exact pricing is not possible.

**Keywords:** F-Ornstein–Uhlenbeck process, F-CIR process, stochastic volatility, data science

## 1 Model with stochastic volatility driven by fractional Ornstein–Uhlenbeck process

These results are common with K. Ralchenko, V. Piterbarg, V. Bezborodov, L. Di Persio, A. Yurchenko-Titarenko, S. Kuchuk-Jatsenko and partially are published in [1]–[4]. We consider a financial market, characterized by a finite maturity time  $T$ , and composed by a risk free bond, or bank account,  $\beta = \{\beta_t, t \in [0, T]\}$ , whose dynamic reads as  $\beta_t = e^{\rho t}$ , where  $\rho \in \mathbb{R}^+$  represents the risk free interest rate, and a risky asset  $S = \{S_t, t \in [0, T]\}$  whose stochastic price dynamic is defined over the probability space  $\{\Omega, \mathcal{F}, \mathbb{F} = \{\mathcal{F}_t\}_{t \in [0, T]}, \mathbb{P}\}$ , by the following system of stochastic differential equations

$$dS_t = bS_t dt + \sigma(Y_t)S_t dW_t, \quad (1)$$

$$dY_t = -\alpha Y_t dt + dB_t^H, \quad t \in [0, T]. \quad (2)$$

Here  $W = \{W_t, t \in [0, T]\}$  is a standard Wiener process,  $b \in \mathbb{R}$ ,  $\alpha \in \mathbb{R}^+$ , are constants, while  $Y = \{Y_t, t \in [0, T]\}$  characterizes the stochastic volatility term of our model, being the argument of the function  $\sigma$ . The process  $Y$  is Ornstein–Uhlenbeck, driven by a fractional Brownian motion  $B^H = \{B_t^H, t \in [0, T]\}$ , of Hurst parameter  $H \in (0, 1)$ , assumed to be correlated with  $W$ .

We assume that payoff function  $f : \mathbb{R}^+ \rightarrow \mathbb{R}^+$  satisfies the following conditions:

(A)

(i)  $f$  is a measurable function of polynomial growth,

$$f(x) \leq C_f(1 + x^p), \quad x \geq 0,$$

for some constants  $C_f > 0$  and  $p > 0$ .

(ii) Function  $f$  is locally Riemann integrable, possibly, having discontinuities of the first kind.

Moreover we assume that the function  $\sigma : \mathbb{R} \rightarrow \mathbb{R}$  satisfies the following conditions:

(B) there exists  $C_\sigma > 0$  such that

(i)  $\sigma$  is bounded away from 0,  $\sigma(x) \geq \sigma_{\min} > 0$ ;

(ii)  $\sigma$  has moderate polynomial growth, i.e., there exists  $q \in (0, 1)$  such that

$$\sigma(x) \leq C_\sigma(1 + |x|^q), \quad x \in \mathbb{R};$$

(iii)  $\sigma$  is uniformly Hölder continuous, so that there exists  $r \in (0, 1]$  such that

$$|\sigma(x) - \sigma(y)| \leq C_\sigma |x - y|^r, \quad x, y \in \mathbb{R};$$

(iv)  $\sigma$  is differentiable a.e. w.r.t. the Lebesgue measure on  $\mathbb{R}$ , and its derivative is of polynomial growth: there exists  $q' > 0$  such that

$$|\sigma'(x)| \leq C_\sigma(1 + |x|^{q'}),$$

a.e. w.r.t. the Lebesgue measure on  $\mathbb{R}$ .

**Lemma 1.** (i) Equation (2) has a unique solution of the form

$$Y_t = Y_0 e^{-\alpha t} + \int_0^t e^{-\alpha(t-s)} dB_s^H.$$

Moreover, for any  $\alpha > 0$  and any  $\beta < 2$

$$\mathbb{E} \exp\left\{\alpha \sup_{t \in [0, T]} |Y_t|^\beta\right\} < \infty.$$

(ii) Equation (1) has a unique solution of the form

$$S_t = S_0 \exp \left\{ bt + \int_0^t \sigma(Y_s) dW_s - \frac{1}{2} \int_0^t \sigma^2(Y_s) ds \right\}.$$

Moreover, for any  $m \in \mathbb{Z}$  we have  $\mathbb{E}(S_T)^m < \infty$ , and for any  $m > 0$  it holds  $\mathbb{E}(f(S_T))^m < \infty$ .

According to [5], fBm admits a compact interval representation via some Wiener process  $B$ , specifically,

$$B_t^H = \int_0^t k(t, s) dB_s, \quad k(t, s) = c_H s^{\frac{1}{2}-H} \int_s^t u^{H-\frac{1}{2}} (u-s)^{H-\frac{3}{2}} du \mathbf{1}_{s < t},$$

with  $c_H = (H - \frac{1}{2}) \left( \frac{2H\Gamma(\frac{3}{2}-H)}{\Gamma(H+\frac{1}{2})\Gamma(2-2H)} \right)^{1/2}$ . Denote also

$$X(t) = \log S(t) = \log S_0 + bt - \frac{1}{2} \int_0^t \sigma^2(Y_s) ds + \int_0^t \sigma(Y_s) dW_s.$$

**Lemma 2.** (i) *The stochastic derivatives of the fBm  $B^H$  equal to*

$$D_u^W B_t^H = 0, \quad D_u^B B_t^H = k(t, u).$$

(ii) *The stochastic derivatives of  $Y$  equal to*

$$D_u^W Y_t = 0, \quad D_u^B Y_t = c_H e^{-\alpha t} u^{1/2-H} \int_u^t e^{\alpha s} s^{H-1/2} (s-u)^{H-3/2} ds \mathbf{1}_{u < t}.$$

(iii) *The stochastic derivatives of  $X$  equal to*

$$\begin{aligned} D_u^W X_t &= \sigma(Y_u) \mathbf{1}_{u < t}, \\ D_u^B X_t &= \left( - \int_0^t \sigma(Y_s) \sigma'(Y_s) D_u^B Y_s ds + \int_0^t \sigma'(Y_s) D_u^B Y_s dW_s \right) \mathbf{1}_{u < t}. \end{aligned}$$

**Lemma 3.** *The laws of  $S_T$  and  $X_T$  are absolutely continuous with respect to the Lebesgue measure.*

Let us introduce the following notations:  $g(y) = f(e^y)$ ,  $F(x) = \int_0^x f(z) dz$  and let  $G(y) = \int_0^y g(z) dz$ ,  $x \geq 0$ ,  $y \in \mathbb{R}$ . Also, let

$$Z_T = \int_0^T \sigma^{-1}(Y_u) dW_u. \quad (3)$$

Note that  $Z_T$  is well defined because of condition **(B)**, (i).

**Theorem 1.** *Under conditions **(A)** and **(B)** the option price  $\text{E}f(S_T) = \text{E}g(X_T)$  can be represented as*

$$\text{E}f(S_T) = \text{E} \left( \frac{F(S_T)}{S_T} \left( 1 + \frac{Z_T}{T} \right) \right).$$

*Alternatively,*

$$\text{E}g(X_T) = \frac{1}{T} \text{E}(G(X_T) Z_T).$$

Consider the first approach to the numerical approximation of the solution for the option pricing problem. Consider equidistant partition of the interval  $[0, T]$ :  $t_i = \frac{iT}{n}$ ,  $i = 0, 1, 2, \dots, n$ . Then we define the discretizations of Wiener process  $W$  and fractional Brownian motion  $B^H$ :

$$\Delta W_i = W(t_{i+1}) - W(t_i), \quad \Delta B_i^H = B^H(t_{i+1}) - B^H(t_i), \quad i = 0, 1, 2, \dots, n.$$

Discretized processes  $Y$  and  $X$ , corresponding to a given partition have the form

$$\begin{aligned} Y_{t_j}^n &= Y_0 e^{-\alpha t_j} + e^{-\alpha t_{j-1}} \sum_{i=0}^{j-1} e^{\alpha t_i} \Delta B_i^H, \\ X_{t_j}^n &= X_0 + bt_j - \frac{1}{2n} \sum_{i=0}^{j-1} \sigma^2(Y_{t_i}^n) + \sum_{i=0}^{j-1} \sigma(Y_{t_i}^n) \Delta W_i \\ &= X_0 + bt_j - \frac{1}{2} \int_0^{t_j} \sigma^2(Y_s^n) ds + \int_0^{t_j} \sigma(Y_s^n) dW_s, \quad j = 0, \dots, n, \end{aligned}$$

where we put  $Y_s^n = Y_{t_i}^n$  for  $s \in [t_i, t_{i+1})$ . Concerning the discretization of the term  $Z_T$  from (3), it has a form  $Z_T^n = \int_0^T \frac{1}{\sigma(Y_s^n)} dW_s$ . Eventually we define  $S_{t_j}^n = \exp\{X_{t_j}^n\}$ .

**Theorem 2.** *Let conditions (A) and (B) hold. There exists a constant  $C$  not depending on  $n$  such that*

$$\left| \mathbb{E}f(S_T) - \mathbb{E} \left( \frac{F(S_T^n)}{S_T^n} \left( 1 + \frac{Z_T^n}{T} \right) \right) \right| \leq Cn^{-rH}.$$

Let us introduce the following notations: let the covariance matrix reads as follows  $C_{X,Z} = \begin{pmatrix} \sigma_Y^2 & T \\ T & \sigma_Z^2 \end{pmatrix}$ , and let  $\sigma_Y^2 = \int_0^T \sigma^2(Y_s) ds$ ,  $m_Y = X_0 + bT - \frac{1}{2}\sigma_Y^2$ ,  $\sigma_Z^2 = \int_0^T \sigma^{-2}(Y_s) ds$ .

We assume additionally that the following assumption is fulfilled.

(C)  $\Delta = \sigma_Y^2 \sigma_Z^2 - T^2 > 0$  with probability 1.

**Theorem 3.** *Under conditions (A)–(C) the following equality holds:*

$$\begin{aligned} \mathbb{E}g(X_T) &= (2\pi)^{-\frac{1}{2}} \int_{\mathbb{R}} G(x) \mathbb{E} \left( \frac{(x - m_Y)}{\sigma_Y^3} \exp \left\{ -\frac{(x - m_Y)^2}{2\sigma_Y^2} \right\} \right) dx \\ &= (2\pi)^{-\frac{1}{2}} \mathbb{E} \left( (\sigma_Y)^{-1} \int_{\mathbb{R}} G((x + m_Y)\sigma_Y) x e^{-\frac{x^2}{2}} dx \right). \end{aligned} \quad (4)$$

Let  $\sigma_{Y,n} = \int_0^T \sigma^2(Y_s^n) ds$ ,  $m_{Y,n} = X_0 + bT - \frac{1}{2}\sigma_{Y,n}^2$ .

**Theorem 4.** *Under conditions (A), (B), and (C) we have*

$$\left| \mathbb{E}g(X_T) - (2\pi)^{-\frac{1}{2}} \int_{\mathbb{R}} G(x) \mathbb{E} \left( \frac{(x - m_{Y,n})}{\sigma_{Y,n}^3} \exp \left\{ -\frac{(x - m_{Y,n})^2}{2\sigma_{Y,n}^2} \right\} \right) dx \right| \leq Cn^{-rH}.$$

Applying Theorem 3 and equality (4), we clearly see that the option price depends on the random variable  $\sigma_Y^2 = \int_0^T \sigma^2(Y_s) ds$ . Therefore it is natural to derive the density of this random variable. Since  $\sigma_Y^2$  depends on the whole trajectory of the fBm  $B^H$  on  $[0, T]$ , we apply Malliavin calculus in an attempt to find the density.

Now we introduce additional assumptions on the function  $\sigma$ .

(D) The function  $\sigma \in C^{(2)}(\mathbb{R})$ , its derivative  $\sigma'$  is strictly nonnegative,  $\sigma'(x) > 0$ ,  $x \in \mathbb{R}$ , and  $\sigma'$ ,  $\sigma''$  are of polynomial growth.

**Lemma 4.** *Under assumptions (B) and (D) the stochastic process*

$$\frac{D^B \sigma_Y^2}{\|D^B \sigma_Y^2\|_H^2} = \left\{ \frac{D_t^B \sigma_Y^2}{\|D^B \sigma_Y^2\|_H^2}, t \in [0, T] \right\}$$

*belongs to the domain  $\text{Dom } \delta$  of the Skorokhod integral  $\delta$ .*

Denote  $\eta = (\|D^B \sigma_Y^2\|_H^2)^{-1}$ ,  $l(u, s) = c_H e^{-\alpha s} \int_u^s e^{\alpha v} v^{H-1/2} (v-u)^{H-3/2} dv$ ,  $\kappa(y) = \sigma(y)\sigma'(y)$ .

**Theorem 5.** (i) *The density  $p_{\sigma_Y^2}$  of the random variable  $\sigma_Y^2$  is bounded, continuous and given by the following formulas*

$$p_{\sigma_Y^2}(u) = \mathbb{E} \left[ \mathbb{1}_{\sigma_Y^2 > u} \delta \left( \frac{D^B \sigma_Y^2}{\|D^B \sigma_Y^2\|_H^2} \right) \right], \quad (5)$$

*where the Skorokhod integral is in fact reduced to a Wiener integral,*

$$\delta \left( \frac{D^B \sigma_Y^2}{\|D^B \sigma_Y^2\|_H^2} \right) = 2\eta \int_0^T \kappa(Y_s) \left( \int_0^s u^{1/2-H} l(u, s) dB_u \right) ds - \int_0^T D_u^B \eta D_u^B (\sigma_Y^2) du.$$

(ii) *The option price  $\text{Eg}(X_T)$  can be represented as the integral with respect to the density  $p_{\sigma_Y^2}(u)$  defined by (5) as follows:*

$$\begin{aligned} \text{Eg}(X_T) = (2\pi)^{-\frac{1}{2}} T \int_{\mathbb{R}} G(x) \int_{\mathbb{R}} \frac{(x + u/2 - X_0 - bT)}{u^3} \\ \times \exp \left\{ -\frac{(x + u/2 - X_0 - bT)^2}{2u^2} \right\} p_{\sigma_Y^2}(u) du. \end{aligned}$$

## 2 Fractional CIR. Case $k = 0$

Consider the stochastic differential equation of the following form:

$$dX_t = \tilde{a}X_t dt + \tilde{\sigma} \sqrt{X_t} dB_t^H, \quad t \geq 0, \quad \tilde{a} \in \mathbb{R}, \quad X_0, \tilde{\sigma} > 0, \quad (6)$$

$B^H = \{B^H, t \geq 0\}$  is a fractional Brownian motion with  $H > 2/3$ .

It is known that if  $H > 2/3$ , the equation (6) has a unique solution until the first moment of reaching zero, and the integral  $\int_0^t \sqrt{X_s} dB_s^H$  exists as a pathwise Riemann-Stieltjes sums limit. Denote  $\tau_0 := \inf\{t > 0 : X_t = 0\}$  and consider the trajectories

of the process  $\{X_t, t \geq 0\}$  on  $[0, \tau_0)$ . After substitution  $Y_t = \sqrt{X_t}$  and using the Ito formula for integrals with respect to fractional Brownian motion, we obtain:

$$dY_t = \frac{dX_t}{2\sqrt{X_t}} = \frac{\tilde{a}X_t dt}{2\sqrt{X_t}} + \frac{\tilde{\sigma}}{2} dB_t^H.$$

Denoting  $a = \tilde{a}/2$ ,  $\sigma = \tilde{\sigma}/2$ , we get

$$dY_t = aY_t dt + \sigma dB_t^H$$

with the initial condition  $Y_0 = \sqrt{X_0}$ .

So, in the case of  $H > 2/3$ , the solution  $\{X_t, t \in [0, \tau_0)\}$  of the equation (6) is the square of the fractional Ornstein–Uhlenbeck process until it reaches zero.

Let  $H \in (0, 1)$  be an arbitrary Hurst index,  $\{Y_t, t \geq 0\}$  be a fractional Ornstein–Uhlenbeck process, i.e. the solution of the SDE

$$dY_t = aY_t dt + \sigma dB_t^H, \quad t \geq 0, \quad a \in \mathbb{R}, \sigma > 0,$$

and  $\tau$  be the first moment of reaching zero by the latter.

**Definition 1.** The fractional Cox–Ingersoll–Ross process (with zero “mean” parameter) is the process  $\{X_t, t \geq 0\}$  such that for all  $t \geq 0$ ,  $\omega \in \Omega$ :

$$X_t(\omega) = Y_t^2(\omega) 1_{\{t < \tau(\omega)\}}.$$

**Theorem 6.** Let  $\tau$  be the first moment of zero hitting by the fractional Ornstein–Uhlenbeck process with parameters  $a \in \mathbb{R}$  and  $\sigma > 0$ . Then, for  $0 \leq t \leq \tau$ , the corresponding fractional CIR process satisfies the following SDE:

$$dX_t = 2aX_t dt + 2\sigma\sqrt{X_t} \circ dB_t^H,$$

where  $X_0 = Y_0^2 > 0$  and the integral with respect to the fractional Brownian motion is defined as the pathwise Stratonovich integral.

The next natural question regarding the fractional CIR process is finiteness of its zero hitting time moment. It is obvious that it coincides with the respective moment of the corresponding fractional Ornstein–Uhlenbeck process  $\{Y_t, t \geq 0\}$ .

Let  $\{Y_t, t \geq 0\}$  be a fractional Ornstein–Uhlenbeck process, i.e. the solution of the SDE

$$dY_t = aY_t dt + \sigma dB_t^H, \quad t \geq 0, \quad a \in \mathbb{R}, \sigma > 0,$$

and  $\tau$  be the first moment of reaching zero by the latter.

$Y$  can be written explicitly as

$$Y_t = e^{at} \left( Y_0 + \sigma \int_0^t e^{-as} dB_s^H \right),$$

where the integral with respect to fractional Brownian motion is the limit of Riemann–Stieltjes sums and can be defined by integration by parts:

$$\int_0^t e^{-as} dB_s^H = e^{-at} B_t^H + a \int_0^t e^{-as} B_s^H ds.$$

**Proposition 1.** *Let  $t \geq s \geq 0$ . Then covariance function  $R_H(t, s)$  of the fractional Ornstein–Uhlenbeck process  $Y$  can be represented in the following form:*

$$R_H(t, s) = \frac{H\sigma^2}{2} \left( -e^{at-as} \int_0^{t-s} e^{-az} z^{2H-1} dz + e^{-at+as} \int_{t-s}^t e^{az} z^{2H-1} dz - e^{at+as} \int_s^t e^{-az} z^{2H-1} dz + e^{at-as} \int_0^s e^{az} z^{2H-1} dz + 2e^{at+as} \int_0^t e^{-az} z^{2H-1} dz \right).$$

Let  $\tau$  be the first moment of zero hitting by the fractional Ornstein-Uhlenbeck process (and consequently by the corresponding fractional CIR process with zero “mean” parameter).

**Theorem 7.** (1) *If  $a \leq 0$ , then  $\mathbb{P}(\tau < \infty) = 1$ .*

(2) *If  $a > 0$ , then  $\mathbb{P}(\tau < \infty) \in (0, 1)$ , and we have the upper bound*

$$\mathbb{P}(\tau < \infty) \leq C_1 \left( \frac{Y_0}{\sigma} \right)^{\frac{1}{H}-2} \exp \left( -\frac{a^{2H} Y_0^2}{\sigma^2 \Gamma(2H+1)} \right),$$

where  $C_1 > 0$  is a constant.

### 3 Fractional CIR. Case $k > 0$

Consider the process  $Y = \{Y_t, t \geq 0\}$  that satisfies the following SDE until its first zero hitting:

$$dY_t = \frac{1}{2} \left( \frac{k}{Y_t} - aY_t \right) dt + \frac{\sigma}{2} dB_t^H, \quad Y_0 > 0, \quad (7)$$

where  $a, k \in \mathbb{R}$ ,  $\sigma > 0$  and  $\{B_t^H, t \geq 0\}$  is a fractional Brownian motion with the Hurst parameter  $H \in (0, 1)$ .

**Definition 2.** Let  $H \in (0, 1)$  be an arbitrary Hurst index,  $\{Y_t, t \geq 0\}$  be the process that satisfies the equation (7) and  $\tau$  be the first moment of reaching zero by the latter.

The fractional Cox-Ingersoll-Ross process is the process  $\{X_t, t \geq 0\}$  such that for all  $t \geq 0, \omega \in \Omega$ :

$$X_t(\omega) = Y_t^2(\omega) 1_{\{t < \tau(\omega)\}}.$$

Similarly to the case  $k = 0$ , the definition of the fractional CIR process is natural as the following theorem holds:

**Theorem 8.** *Let  $\tau$  be the first moment of hitting zero by  $Y$ . For  $0 \leq t \leq \tau$  the fractional CIR process satisfies the following SDE:*

$$dX_t = (k - aX_t)dt + \sigma \sqrt{X_t} \circ dB_t^H,$$

where  $X_0 = Y_0^2 > 0$  and the integral with respect to the fractional Brownian motion is defined as the pathwise Stratonovich integral.

Just as in the case  $k = 0$ , let us consider the question of finiteness of the zero hitting time moment by the fractional CIR process.

**Theorem 9.** *Let  $k > 0, H > 1/2$ . Then the process  $\{Y_t, t \geq 0\}$ , defined by the equation (7) (and consequently the corresponding fractional CIR process), is strictly positive a.s.*

Let  $\{B_t^H, t \geq 0\}$  be the fractional Brownian motion with  $H < 1/2$  and let  $a \in \mathbb{R}, \sigma > 0$  be fixed. Consider the set of processes

$$\mathbb{Y} := \{Y^{(k)} = \{Y_t^{(k)}, t \geq 0\}, k > 0\},$$

such that

$$Y_t^{(k)}(\omega) = \begin{cases} Y_0 + \frac{1}{2} \int_0^t \left( \frac{k}{Y_s^{(k)}(\omega)} - aY_s^{(k)}(\omega) \right) ds + \frac{\sigma}{2} dB_t^H(\omega), & \text{if } t < \tau^{(k)}(\omega) \\ 0, & \text{if } t \geq \tau^{(k)}(\omega) \end{cases},$$

where  $\tau^{(k)} := \inf\{t \geq 0 | Y_t^{(k)} = 0\}$ .

**Theorem 10.** *For all  $T > 0, \mathbb{P}(\tau^{(k)} > T) \rightarrow 1, k \rightarrow \infty$ .*

## References

- [1] Bezborodov V., Di Persio L., Mishura Yu. (2019) Option pricing with fractional stochastic volatility and discontinuous payoff function of polynomial growth. *Methodology and Computing in Applied Probability* Vol. **21**, Issue 1, pp. 331–366.
- [2] Kuchuk-Iatsenko S., Mishura Y. (2015). Pricing the European call option in the model with stochastic volatility driven by Ornstein–Uhlenbeck process. Exact formulas. *Mod. Stoch. Theory Appl.* Vol. **2**, pp. 233–249.
- [3] Mishura Yu., Piterbarg V., Ralchenko K., Yurchenko-Tytarenko A. (2017). Stochastic representation and pathwise properties of fractional Cox–Ingersoll–Ross process. *Theory Probab. Math. Statist.* Vol. **97**, pp. 157–170.
- [4] Mishura Yu., Yurchenko-Tytarenko A. (2018). Fractional Cox–Ingersoll–Ross process with non-zero “mean” *Mod. Stoch. Theory Appl.* Vol. **5**, pp. 99–111.
- [5] Norros I., Valkeila E., Virtamo J. (1999). An elementary approach to a Girsanov formula and other analytical results on fractional Brownian motions. *Bernoulli*, Vol. **5**, pp. 571–587.

# SOME RESULTS ON THE BROWNIAN MEANDER

E. ORSINGHER  
*Sapienza University*  
*Rome, ITALY*

e-mail: enzo.orsingher@uniroma1.it

## Abstract

Some new results on the Brownian meander are considered.

**Keywords:** data science, Brownian meander, first passage time

A Brownian meander is a Brownian motion evolving under the condition that  $\min_{0 \leq s \leq t} B(s) > v$ . If the starting point  $B(0) = u$  and the critical level  $\min_{0 \leq s \leq t} B(s) > v$  differ one can write down the joint distributions

$$P \left\{ \bigcap_{j=1}^n (B^\mu(s_j) \in dy_j) \mid \min_{0 < z < t} B^\mu(z) > v, B^\mu(0) = u \right\} \quad (1)$$

for  $y_i > v, i = 1, \dots, n, 0 < s_1 < \dots < s_j < \dots < s_n < t$ , as well as

$$P \left\{ \max_{0 \leq z \leq s} B^\mu(z) \leq x \mid \min_{0 < z < t} B^\mu(z) > v, B^\mu(0) = u \right\} \quad (2)$$

for  $s < t, v < u < x$ .

Therefore also the first passage times

$$T_x = \inf\{s < t : B(s) = x\} \quad (3)$$

under the condition that  $\min_{0 \leq s \leq t} B(s) > v$  and  $t < t'$  can be explored.

This analysis becomes more complicated in the case where the Brownian meander has drift, that is constructed by means of a drifted Brownian motion  $B^\mu(t), t > 0, \mu \in \mathbb{R}$ .

For this reason we need some simplifying assumptions such that  $u \downarrow v$  (with eventually  $v = 0$ ).

In this case however we need to analyze the convergence of the sequence of measures (1) and, in particular to check the tightness of these probability measures.

An important result in this context is the proof that

$$\lim_{\delta \downarrow 0} \lim_{u \downarrow v} P \left( \max_{0 \leq z \leq \delta} |B^\mu(z) - B^\mu(0)| < \eta \mid \min_{0 \leq z \leq t} B^\mu(z) > v, B^\mu(0) = u \right) = 1 \quad (4)$$

for all  $\eta > 0$ , which permits us to control the oscillations of the meander in the neighborhood of the starting point.

The analysis of the representation of the meander  $M$  as

$$P \left\{ \left| \frac{B^\mu(T_0^\mu + s(t - T_0^\mu))}{\sqrt{t - T_0^\mu}} \right| \in dy \right\} \quad (5)$$

$$= \frac{1}{2} \left[ P \left\{ M^{-\mu} \sqrt{t - T_0^\mu}(s) \in dy \right\} + P \left\{ M^\mu \sqrt{t - T_0^\mu}(s) \in dy \right\} \right]$$

for  $0 < s < 1$ , as a generalization of the analogous representation for the driftless meander is also considered. The  $T_0^\mu$  random time is defined as

$$T_0^\mu = \sup\{s < t : B^\mu(s) = 0\} \quad (6)$$

The explicit distribution of  $T_0^\mu$  reads

$$P(T_0^\mu \in da)/da = \frac{e^{-\frac{\mu^2 t}{2}}}{\pi \sqrt{a(t-a)}} + \frac{\mu^2}{2\pi} \int_a^t \frac{e^{-\frac{\mu^2 y}{2}}}{\sqrt{a(y-a)}} dy$$

$$= \mathbb{E} \left( \frac{1}{\pi \sqrt{a(W-a)}} I_{(W \geq a)} \right) \quad 0 < a < t.$$

where  $W$  is a truncated r.v. with an absolutely continuous component in  $(0, t)$  with density

$$f_W(w) = \frac{\mu^2}{2} e^{-\frac{\mu^2}{2} w} \quad 0 \leq w \leq t$$

and a discrete component at  $w = t$  with mass

$$P(W = t) = e^{-\frac{\mu^2 t}{2}}.$$

## References

- [1] Iafate F., Orsingher E. (2019). Some results on the Brownian meander with drift. *J. Theor. Probab.*, pp. 1-27.
- [2] Iafate F., Orsingher E. (2019). The last zero crossing of an iterated Brownian motion with drift. *Stochastics*.

# POWER SKEW SYMMETRIC DISTRIBUTIONS: TESTS FOR SYMMETRY

R.N. RATTIHALLI<sup>1</sup>, M. RAGHUNATH<sup>2</sup>

<sup>1</sup>*Department of Statistics, Central University of Rajasthan*

<sup>2</sup>*Department of Statistics, SDSOS, NMIMS (Deemed to be) University  
Bandarsindri, Mumbai, INDIA*

e-mail: <sup>1</sup>rnr5@rediffmail.com, <sup>2</sup>raghumr@gmail.com

## Abstract

In this article a semi-parametric class of skew-symmetric distributions is considered. We call this class as Power-Skew-Symmetric (*PSS*) distributions, being obtained by considering a positive power of a distribution function symmetric about 0. Based on U-statistics we develop two nonparametric tests for symmetry in the *PSS* class. Performances of the proposed tests are evaluated using efficacy and empirical power.

**Keywords:** efficiency, empirical power, semi-parametric class, skew-distributions, U-statistics

## 1 Introduction

In the literature parametric/nonparametric classes of skew-symmetric distributions have been generated by introducing an additional parameter to a class of symmetric distributions. Azzalini (1985) introduced a class of skew-symmetric distributions based on normal distribution and Gómez et. al (2006) have generalized this class by introducing one more addition parameter. Further extensions based on t, Lapalce, Cauchy, Uniform, Logistic distributions have been considered by Gupta et. al (2002) and their distributional properties have been studied by Nadarajah and Kotz (2003, 2006). Mudolkar and Hutson (2000) have proposed Epsilon-Skew normal family by using normal density and a skewness parameter  $\varepsilon$ .

Lehmann (1953) proposed a family of distributions

$$\mathbb{F}_F(x, \alpha) = \{F^\alpha(x), \alpha \in (0, \infty)\} \quad (1)$$

where  $F$  is a distribution function. In the context of testing the null hypothesis that  $F$  is the true distribution one may confine to the class (1) and the subclass of (1) with  $\alpha \neq 1$  is referred to as the class of *Lehmann alternatives*. If  $F$  is absolutely continuous then the corresponding density function is

$$\varphi_F(x, \alpha) = \alpha f(x) \{F(x)\}^{\alpha-1}, x \in \mathbb{R}, \alpha > 0. \quad (2)$$

The class (1) is used for data analysis by considering  $F$  to be a specified parametric family (usually taken to be symmetric), for example Durrans (1992), Gupta and Gupta (2008), Pewsey et. al (2012).

In this article we consider

$$\{F^\alpha(x); F \text{ is symmetric about } 0, \alpha \in (0, \infty)\}. \quad (3)$$

called the *Power Skew Symmetric* family of distributions and is denoted by  $\mathcal{PSS}$ . Thus the family of all distribution functions which are positive powers of a continuous symmetric distribution function symmetric about 0. It is a semiparametric family.

It is to be noted that a member of  $\mathcal{PSS}$  is symmetric if and only if  $\alpha = 1$ . Based on U-statistics theory, We propose two nonparametric tests for testing symmetry in  $\mathcal{PSS}$  class.

In section 2 the class of  $\mathcal{PSS}$  is defined and some of its properties, graphs of Distribution Function (DF), Probability Density Function (PDF) for certain members generated from some well know symmetric models are given. Two U-statistics type statistics for testing symmetry in this class ( $\alpha = 1$ ) are proposed in section 3. Asymptotic null distributions of the proposed statistics are discussed in section 4. The efficacies of the tests are derived in section 5. In section 6, empirical powers of the proposed tests are computed for different subclasses of  $\mathcal{PSS}$  generated from some well known symmetric models.

## 2 The Class of Power-Skew-Symmetric Distributions

In this section we define the class of *Power-Skew-Symmetric*( $\mathcal{PSS}$ ) distributions and study some of its properties.

Let  $F(t) = P(T \leq t)$  be the distribution function of random variable (r.v.)  $Y$  and  $F(t-) = P(Y < t)$ . If  $F(\cdot)$  is continuous at  $t$  the  $F(t) = F(t-)$ . The distribution function  $F$  (or the r.v.  $Y$ ) is said to be symmetric about 0 if  $F(t) = 1 - F(t-)$ ,  $-\infty < t < \infty$ . The class  $\mathcal{PSS}$  is defined as,

$$\mathcal{PSS} = \{F^\alpha(x) : x \in \mathbb{R}, F \text{ is symmetric about } 0\}. \quad (4)$$

In the following we show that  $(F(\cdot), \alpha)$  constitutes the parameter for the class  $\mathcal{PSS}$ . If  $G(\cdot) \in \mathcal{PSS}$  then  $G(x) = F^\alpha(x)$  for some distribution function  $F$  symmetric about 0 and some  $\alpha > 0$ . To be precise  $G(x)$  is  $G_{F,\alpha}(x)$ , but for notational simplicity, unless otherwise required, we write it as  $G(x)$ , The class  $\mathcal{PSS}$  is a semi-parametric family and it can be extend by introducing the location and the scale parameters. In the following we shall show that  $(F(\cdot), \alpha)$  constitutes the parameter for the  $\mathcal{PSS}$  class.

**Lemma 1.**  $(F(\cdot), \alpha)$  constitutes the parameter for the class  $\mathcal{PSS}$

*Proof.* For if,  $F_1^{\alpha_1}(x) = F_2^{\alpha_2}(x), \forall x$ , then we have,

$$F_1(x) = F_2^{\frac{\alpha_2}{\alpha_1}}(x), \forall x. \quad (5)$$

We note that if  $F$  is symmetric about 0 then  $F^\alpha(x)$  is symmetric about 0 if and only if  $\alpha = 0$ . Hence as  $F_1(\cdot)$  and  $F_2(\cdot)$  are symmetric about 0, (4) holds if and only if  $\alpha_1 = \alpha_2$ , which in turn also implies  $F_1(x) = F_2(x), \forall x$ .

Hence the proof. □

In the following we give some of the properties of members of  $\mathcal{PSS}$  class distributions. Let  $X$  be an r.v. with continuous distribution function (DF)  $F^\alpha(x)$  (denoted by  $X \sim F^\alpha(x)$ ).

**P.1:** If  $X \sim F^\alpha(x)$  then  $-X \sim 1 - F^\alpha(-x)$ .

**P.2:** If  $X \sim G(\cdot) \in \mathcal{PSS}$ , then  $G(0) = (1/2)^\alpha$  for any  $F(\cdot)$  symmetric about 0.

**P.3:** Let  $X \sim F^\alpha(\text{say})$ ,  $Y \sim F(\cdot)$  and  $G_\alpha(\cdot)$  be the distribution function of  $X$  then

- i) The probability density function of  $X$  is given by  $g_\alpha(x) = \alpha F^{\alpha-1} f(x)$ . provided it exists.
- ii) The supports of  $G_\alpha(\cdot)$  and  $F(\cdot)$  are the same.
- iii)  $X$  is stochastically larger(sampler) than  $Y$  according as  $\alpha \leq 1$  ( $\alpha \geq 1$ ).
- iv) The inverse function of the CDFs satisfy the relation,

$$G_\alpha^{-1}(u) = F^{-1}(u^{1/\alpha}), 0 < u < 1, \alpha > 0.$$

**P.4:** (Gupta and Gupta (2008)) If the  $X_i \sim PSS(F, \alpha_i), i = 1, 2, \dots, n$  are independent  $X_{(n)} = \max(X_1, X_2, \dots, X_n) \sim PSS(F, \sum_{i=1}^n \alpha_i)$ .

The graphs of DF and PDF of the  $\mathcal{PSS}$  distributions generated from Cauchy, Laplace, Logistic, Normal and Uniform distributions for some values of  $\alpha$  are given in the Appendix.

### 3 Proposed Classes of Tests

Let  $X_1, X_2, \dots, X_n$  be independent identically distributed random variables with common DF  $G \in \mathcal{PSS}$ . The problem of interest is to test the hypothesis  $H_0: G$  is symmetric about 0 against the alternative  $H_1: G$  is not symmetric about 0, that is to test

$$H_0 : \alpha = 1 \text{ against } H_1 : \alpha \neq 1. \quad (6)$$

Here  $F$  is a nuisance parameter.

Motivated from Mehra et. al (1990) and Rattihalli and Raghunath (2012), we propose two U-test-statistics to test the above hypothesis. The kernel function depends on a constant to be chosen so as to maximize the efficacy of the test. This is possible as the efficacies of the tests do not depend upon nuisance parameter  $F(\cdot)$ . The two U-test statistics are given by

$$T_a = \frac{\sum_{C_1} \psi_a(x_i, x_j)}{\binom{n}{2}} \quad (7)$$

$$S_b = \frac{\sum_{C_2} \psi_b(x_i, x_j, x_k)}{\binom{n}{3}} \quad (8)$$

where the summations  $C_1$  and  $C_2$  are respectively over the  $\binom{n}{2}$ ,  $\binom{n}{3}$  combinations of integers from  $\{1, 2, \dots, n\}$  and

$$\psi_a(x_i, x_j) = \begin{cases} a & \text{if } \min\{x_i, x_j\} > 0 \\ 1(-1) & \text{if } x_i x_j < 0, x_i + x_j > (<)0 \\ -a & \text{if } \max\{x_i, x_j\} > 0 \\ 0 & \text{otherwise,} \end{cases} \quad (9)$$

$$\psi_b(x_i, x_j, x_k) = \begin{cases} b & \text{if } x_{(1)} > 0 \\ 1(-1) & \text{if } x_{(1)} < 0 < x_{(2)} (x_{(2)} < 0 < x_{(3)}), x_{(1)} + x_{(3)} > (<)0 \\ -b & \text{if } x_{(3)} < 0 \\ 0 & \text{otherwise,} \end{cases} \quad (10)$$

where  $x_{(i)}$  is the  $r^{\text{th}}$  order statistic from a sub-sample of size 3.

A test rejects  $H_0$  in favour of  $H_1$  for the large absolute value of the corresponding test statistic.

## 4 Asymptotic null distribution of the proposed test statistics

Since the statistics  $T_a$  and  $S_b$  are one sample U-statistics, then from the theorem of Hoeffding (1948), we have the following theorem.

**Theorem 1.** *Let  $\sigma_a^2 = \text{Var}[E_{H_0}(\psi_a(X_1, X_2)|X_1 = x_1)]$ . Then under the  $H_0$   $\sqrt{n}[T_a - E_{H_0}(T_a)]$  converges in distribution as  $n \rightarrow \infty$  to  $N(0, 4\sigma_a^2)$  r.v.*

Thus to obtain the asymptotic null distribution of  $T_a$ , it is enough to find  $E[\psi_a(X_1, X_2)]$ ,  $E_{H_0}[\psi_a(X_1, X_2)|X_1 = x_1]$  and are obtained in the following.

$$\begin{aligned} E[T_a] &= E[\psi_a(X_1, X_2)] \\ &= aP[X_{(1)} > 0] + P[X_{(1)} < 0 < X_{(2)}, X_{(1)} + X_{(2)} > 0] \\ &\quad - P[X_{(1)} < 0 < X_{(2)}, X_{(1)} + X_{(2)} < 0] - ap[X_{(2)} < 0] \\ &= a\{P[E_1] - p[E_4]\} + P[E_2] - P[E_4] \end{aligned}$$

and the probabilities of the above events are,

$$\begin{aligned} P[E_1] &= (1 - 2^{-\alpha})^2 \\ P[E_2] &= 2^{1-\alpha} - 2\alpha \int_0^{1/2} (1-u)^\alpha u^{\alpha-1} du \\ P[E_3] &= 2\alpha \int_0^{1/2} (1-u)^\alpha u^{\alpha-1} du - 2^{1-2\alpha} \\ P[E_4] &= 2^{-2\alpha}. \end{aligned}$$

It is to be noted that, the above probabilities do not depend on the underlying symmetric model  $F(\cdot)$ .

Thus we get,

$$\nu_a(\alpha) = E[\psi_1(X_1, X_2)] = a(1 - 2^{1-\alpha}) + 2^{1-\alpha} + 2^{2\alpha-1} - 4\alpha \int_0^{1/2} (1-u)^\alpha u^{\alpha-1} du. \quad (11)$$

Under  $H_0 : \alpha = 1$ , we have,

$$E_{H_0}[T_a] = 0.$$

Further,

$$E_{H_0}(\psi_a(X_1, X_2)|X_1 = x_1) = \begin{cases} 2F(x_1) - \left(\frac{a+1}{2}\right) & \text{when } x_1 \leq 0 \\ \left(\frac{a-3}{2}\right) + 2F(x_1) & \text{when } x_1 \geq 0 \end{cases} \quad (12)$$

Hence the asymptotic variance  $4\sigma_a^2$  is,

$$\begin{aligned} 4\sigma_a^2 &= 4Var[E_{H_0}(\psi_a(X_1, X_2)|X_1 = x_1)] \\ &= 4 \left\{ \int_0^\infty \left[ \left(\frac{a-3}{2}\right) + 2F(x_1) \right]^2 dF(x_1) + \int_{-\infty}^0 \left[ 2F(x_1) - \left(\frac{a+1}{2}\right) \right]^2 dF(x_1) \right\}. \end{aligned} \quad (13)$$

Thus,

$$4\sigma_a^2 = \left( \frac{1}{3} + a^2 \right). \quad (14)$$

Similarly the asymptotic distribution of  $T_b$  is given by,

**Theorem 2.** Let  $\sigma_b^2 = Var[E_{H_0}(\psi_b(X_1, X_2, X_3)|X_1 = x_1)]$ . Then under  $H_0$   $\sqrt{n}[S_b - E_{H_0}(S_b)]$  converges in distribution as  $n \rightarrow \infty$  to  $N(0, 9\sigma_b^2)$  r. v.

The expectation and asymptotic variance of  $T_b$  are given by,

$$\begin{aligned} \nu_b(\alpha) &= b \left[ (1 - 2^{-\alpha})^3 - 2^{-3\alpha} \right] + 3 \left\{ 2^{-\alpha}(1 - 2^{1-\alpha} + 2^{-2\alpha}) \right. \\ &\quad \left. - \alpha \int_0^{1/2} ((1-u)^\alpha - 2u^\alpha)(1-u)^\alpha u^{\alpha-1} du \right\}. \end{aligned} \quad (15)$$

Under  $H_0 : \alpha = 1$ , we have,

$$E_{H_0}[S_b] = 0.$$

It is easy to verify that,

$$E_{H_0}(\psi_b(X_1, X_2, X_3)|X_1 = x_1) = \begin{cases} 2F(x_1) - 2F^2(x_1) - \left(\frac{b+2}{4}\right) & \text{when } x_1 \leq 0 \\ \left(\frac{b+2}{4}\right) + 2F^2(x_1) - 2F(x_1) & \text{when } x_1 \geq 0 \end{cases} \quad (16)$$

The asymptotic variance  $9\sigma_b^2$  is given by,

$$9\sigma_b^2 = 9 \left( \frac{b^2}{16} + \frac{b}{12} + \frac{1}{20} \right). \quad (17)$$

In the next section we obtain the constants 'a' and 'b', so that the efficacies of the tests are maximal.

## 5 Efficacies of the proposed tests

Let  $T = \{T_n\}$  be a sequence of test statistics for testing the hypothesis that  $H_0 : \theta = \theta_0$  against the suitable alternative. Let  $E(T_n) = \mu_n(\theta)$  and  $Var(T_n) = \sigma_n^2(\theta)$ . Under certain regularity conditions (see Randles and Wolfe (1979)) the efficacy of  $T$  is given by,

$$eff[T] = \lim_{n \rightarrow \infty} \frac{\mu'_n(0)}{\sqrt{n}\sigma_n(0)}. \quad (18)$$

By considering  $T_n = T_a$ ,  $\mu_n(\theta) = \nu_a(\alpha)$ , where  $\nu_a(\alpha)$  is given in (10) and

$$\nu'_a(\alpha)|_{\alpha=1} = (2-a)\ln(1/2) - (3/2) - 4 \int_0^{1/2} (1-u)\ln(u(1-u))du,$$

The efficacy of  $T_a$  is,

$$eff^2[T_a] = \frac{3[(2-a)\ln(1/2) - (3/2) - 4I_1]^2}{(3a^2 + 1)} \quad (19)$$

where  $I_1 = \int_0^{1/2} (1-u)\ln(u(1-u))du$ .

The optimal value  $a^*$  of  $a$  is obtained by solving  $(d/da)eff^2(T_a) = 0$  and verifying  $(d^2/(da^2))eff^2(T_a) < 0$  at the solution obtained. Here the value obtained is,

$$a^* = \frac{2\ln(1/2)}{24I_1 + 9 - 12\ln(1/2)}, \quad (20)$$

where  $I_1$  is define above and by numerical integration it can be shown that  $I_1 = -0.7983$ . Hence from (19) we have,

$$a^* = 0.7528.$$

Thus the efficacy of  $T_{a^*}$  is,

$$eff^2[T_{a^*}] = 0.763.$$

Similarly, the efficacy of the test  $T_b$  is,

$$eff^2[S_b] = \frac{15[8I_2 - (2b+1)3\ln(1/2)]^2}{(60b^2 + 80b + 48)} \quad (21)$$

where  $I_2 = \int_0^{1/2} (1-u)[(3u-1) + 2(2u-1)\ln(1-u) + (5u-1)\ln(u)]du = 0.1122$  (by numerical integration).

The optimal value of  $b^*$  of  $b$  is,

$$b^* = \frac{8I_2 - \ln(1/2)}{2\ln(1/2)}. \quad (22)$$

Substituting the value of  $I_2$  in (21), we get,

$$b^* = 0.1476.$$

and

$$eff^2[S_{b^*}] = 0.7912.$$

The efficacy of the test  $S_{b^*}$  is more than that of  $T_{a^*}$ .

## 6 Monte-Carlo Simulation

In this section we carry out the empirical power study to assess the performances of the proposed test statistics  $T_{a^*}$  and  $S_{b^*}$ . For simulation study samples were drawn from  $G(\cdot)$ , when  $F$  corresponds to Cauchy, Laplace, logistic, normal, triangular and uniform.

Under  $H_0$  test statistics  $T_{a^*}$  and  $S_{b^*}$  are asymptotically normal with mean 0 and variances given in (13) and (16) respectively. Then corresponding to the size  $\gamma$ , the criteria for rejection are

a) to reject  $H_0$  if  $|T_{a^*}| \geq \frac{Z_{(\gamma/2)} 2\sigma_{a^*}}{\sqrt{n}}$

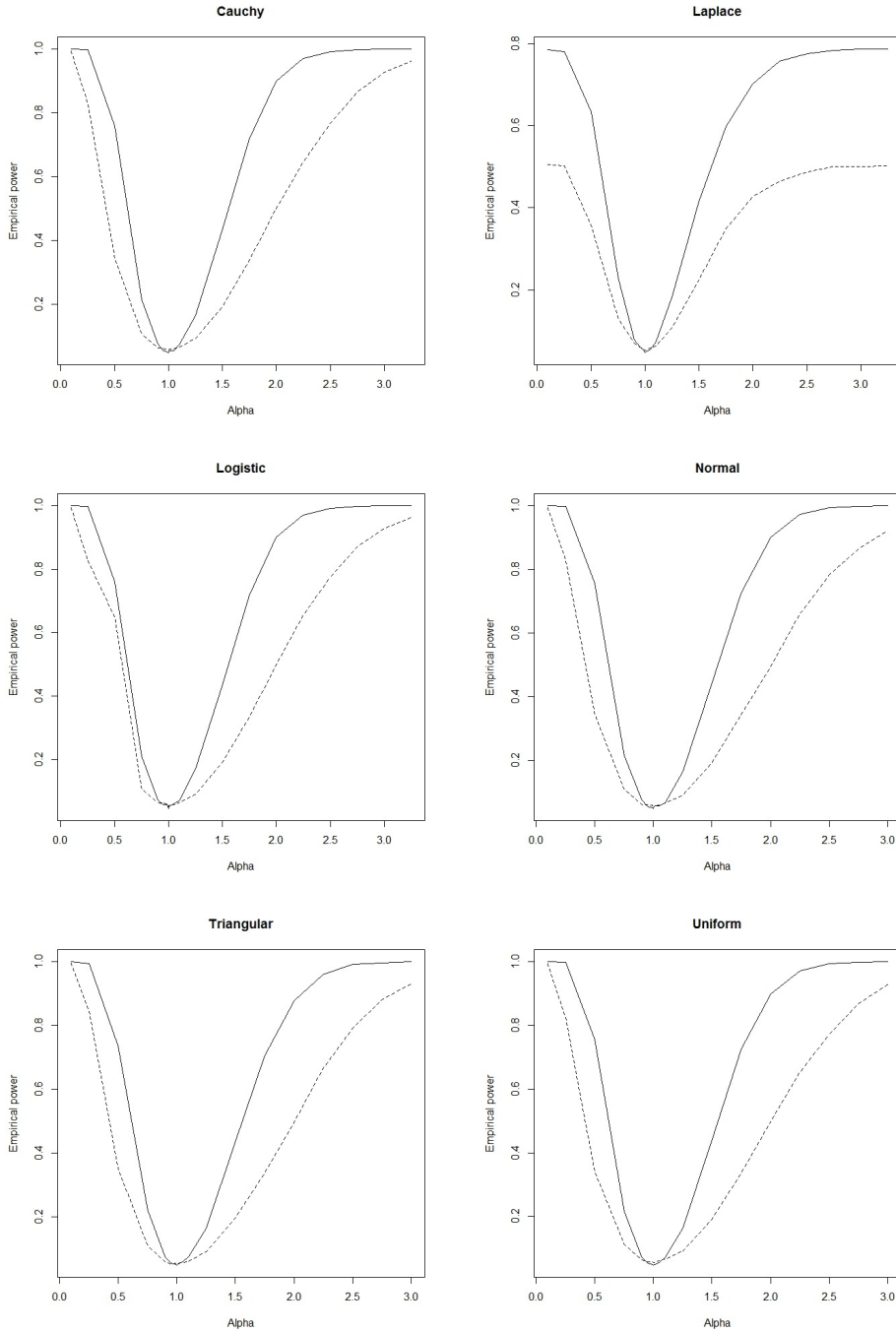
b) to reject  $H_0$  if  $|S_{b^*}| \geq \frac{Z_{(\gamma/2)} 3\sigma_{b^*}}{\sqrt{n}}$

An empirical power study for both the tests was carried out for moderate sample size  $n = 25$  with  $\gamma = 0.05$ . The results based 10000 Monte Carlo simulations are tabulated in Table 1.

Table 1: *Empirical Powers of  $T_{a^*}$  and  $S_{b^*}$  for various values of alpha with  $\gamma = 0.05$  and number of Monte Carlo simulations 10000.*

$\alpha$	Tests	Cauchy	Laplace	Logistic	Normal	Triangular	Uniform
0.1	$T_{a^*}$	1.0	0.7846	1.0	1.0	1.0	1.0
	$S_{b^*}$	0.9943	0.505	0.9949	0.9947	0.9964	0.9951
0.5	$T_{a^*}$	0.7578	0.6319	0.7597	0.756	0.7344	0.7569
	$S_{b^*}$	0.3447	0.3561	0.6493	0.3462	0.3532	0.3425
0.95	$T_{a^*}$	0.0550	0.0617	0.0586	0.0550	0.0558	0.0526
	$S_{b^*}$	0.0610	0.0600	0.0611	0.0610	0.0542	0.0567
0.99	$T_{a^*}$	0.0495	0.0515	0.0587	0.0499	0.0509	0.0488
	$S_{b^*}$	0.0581	0.0549	0.0588	0.0581	0.0561	0.0581
1.0	$T_{a^*}$	0.0488	0.0480	0.0460	0.0495	0.0503	0.0480
	$S_{b^*}$	0.0555	0.0514	0.0508	0.0514	0.0558	0.0549
1.01	$T_{a^*}$	0.0543	0.0493	0.0543	0.0572	0.0530	0.0495
	$S_{b^*}$	0.0587	0.0545	0.0556	0.0569	0.0564	0.0555
1.05	$T_{a^*}$	0.0548	0.0546	0.0601	0.0569	0.0588	0.0548
	$S_{b^*}$	0.0615	0.0589	0.0571	0.0598	0.0573	0.0615
1.5	$T_{a^*}$	0.4329	0.4159	0.4349	0.4410	0.4347	0.4380
	$S_{b^*}$	0.1920	0.2246	0.1919	0.191	0.1957	0.1907
2.0	$T_{a^*}$	0.9002	0.7016	0.9008	0.9016	0.8785	0.8988
	$S_{b^*}$	0.4989	0.4274	0.497	0.4953	0.4984	0.4989
2.5	$T_{a^*}$	0.9928	0.7751	0.9924	0.9932	0.9918	0.9944
	$S_{b^*}$	0.7685	0.487	0.7759	0.7849	0.7913	0.7719
3.0	$T_{a^*}$	1.0	0.7859	1.0	1.0	1.0	1.0
	$S_{b^*}$	0.9273	0.5004	0.9285	0.9225	0.9318	0.9283

Table 2: \*  
*Graphs of the Empirical Powers of  $T_{\alpha}^*$  (solid line) and  $S_b^*$  (longer dashing line) for various values of alpha.*



From the table 1 and the above graphs we observe the following.

- a) The proposed test statistics are maintaining the level of significance.
- b) the empirical powers of  $S_{b^*}$  are larger in the neighborhood of the null.  $T_{a^*}$  performs better when we move away from the null hypothesis.

## 7 Conclusion

In this article we have considered a semi-parametric class of skew-symmetric distributions called Power-Skew-Symmetric ( $\mathcal{PSS}$ ) distributions. We have developed two tests for symmetry, based on the theory of U-Statistics for testing symmetry in this class. The kernel functions depend on arbitrary constants, which are chosen so that efficacies of the test are maximal. Though they are asymptotic tests, based on simulation study, from Table 1, we observe that for each test the attained levels for all the models are almost equal to the nominal level. The efficacy of the test  $S_{b^*}$  is higher than that of  $T_{a^*}$ . As expected the empirical powers of  $S_{b^*}$  are larger in the neighborhood of the null, of course  $T_{a^*}$  is better than  $S_{b^*}$  if the values of  $\alpha$  are much away from the null value 1.

**Remark:** Similar to the class  $\mathcal{PSS}$  of power skew-symmetric distribution functions one can define the  $\mathcal{PSS}^s$  the class of power skew-symmetric survival functions, by considering the survival functions instead of the distribution functions. All the related properties and tests can be obtained in the similar way. Properties related to maximum of random variables will be now related with minimum of random variables.

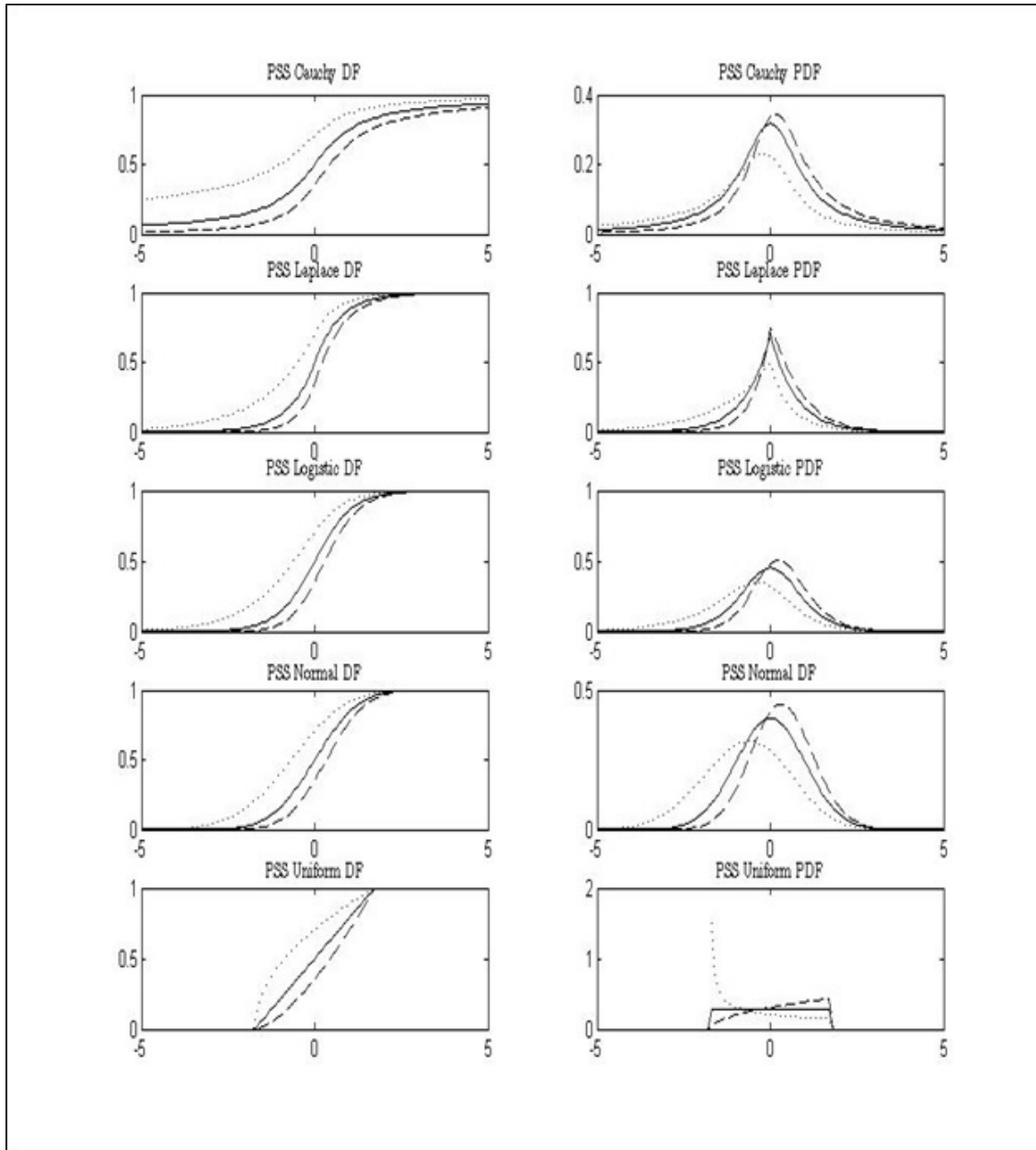
## References

- [1] Azzalini A. (1985). A Class of distributions which includes the normal ones. *Scandinavian Journal of Statistics*. Vol. **12**, pp. 171-178.
- [2] Durrans S. R. (1992). Distributions of fractional order statistics in hydrology. *Water Resources Research*. Vol. **28**, pp. 1649-1655.
- [3] Gupta A. K., Chang F. C., Huang W. J. (2002). Some Skew-Symmetric Distributions. *Random Operators and Stochastic Equations*. Vol. **10**, pp. 133-140.
- [4] Gupta R. D., Gupta R. C. (2006). Analyzing skewed data by power normal model. *Test*. Vol. **17**, pp. 197-210.
- [5] Gomez H. W., Salinas H. S., Bolfarine H. (2006). Generalized skew-normal models: properties and inference. *Statistics*. Vol. **40**, pp. 495-505.
- [6] Hoeffding, W. (1948). A Class of Statistics with Asymptotically Normal Distribution. *Annals of Mathematical Statistics*. Vol. **19**, pp. 223-325.

- [7] Lehmann E. L. (1953). The power of rank tests. *Annals of Mathematical Statistics*. Vol. **24**, pp. 23-43.
- [8] Mehra, K. L., Prasad, N. G. N., Madhava Rao, K. S. (1990). A Class of Non-parametric Tests for the One-Sample Location Problem, *Australian Journal of Statistics*, **32**, pages 373-392.
- [9] Mudholkar, G.S., Hutson, A. D. (2000). The epsilon-skew normal distribution for analyzing near normal data, *Journal of Statistical Planning and Inference*, **83**, pages 291-309.
- [10] Nadarajah, S., Kotz, S. (2006). Skew Distributions Generated from Different Families, *Acta Applicandae Mathematica*, **91**, pages 1-37.
- [11] Pewsey, A., Gomez, H. W., Bolfarine, H. (2012). Likelihood-based inference for power distributions, *Test*, **21**, pages 775-789.
- [12] Randles, R. H., Wolfe, D. A. (1979). *Introduction to the Theory of Nonparametric Statistics*, Wiley, New York.
- [13] Rattihalli, R.N. (2004). *Statistical Models derived from Well-Known distributions: An unpublished Report of a Research Project*, Submitted to University Grant Commission, New Delhi, India.
- [14] Rattihalli, R. N., Raghunath, M. (2012). Generalized Nonparametric Tests for One-Sample Location Problem based on Sub-Samples, *ProbStat Forum*, **05**, pages 112-123.

# Appendix

Graphs of the DF and PDF of Power-skew-symmetric distributions derived from various  $F(\cdot)$ s, with  $\alpha = 1.5$  (longer dashed line),  $\alpha = 0.5$  (dotted line) and  $\alpha = 1$  (solid line).



# INVESTIGATION OF CONDITIONS FOR ASYMPTOTIC NORMALITY OF SPECTRAL ESTIMATES

L.M. SAKHNO

*Taras Shevchenko National University of Kyiv*

*Kyiv, UKRAINE*

e-mail: lms@univ.kiev.ua

## Abstract

We study the question of validity of central limit theorems for empirical spectral functionals of stationary stochastic processes and fields.

**Keywords:** data science, asymptotic normality, spectral estimate

Given observations of a real-valued stationary random field  $X(t)$ ,  $t \in Z^d$ , on a sequence of hypercubes  $L_T = [-T, T]^d = \{t \in Z^d : -T \leq t_i \leq T, i = 1, \dots, d\}$ , we consider spectral functionals

$$J_T(\varphi) = \int_S I_T^h(\lambda) \varphi(\lambda) d\lambda,$$

where  $S = (-\pi, \pi]^d$  and  $I_T^h(\lambda)$  is the second-order periodogram based on the tapered values  $\{h_T(t) X(t), t \in L_T\}$ . We suppose that the taper  $h_T(t)$  factorises and satisfies some standard conditions.

Suppose that all order moments exist and the field  $X(t)$  has spectral densities of all orders  $f_k(\lambda_1, \dots, \lambda_{k-1}) \in L_1(S^{k-1})$ ,  $k = 2, 3, \dots$

To derive central limit theorems for the spectral functionals  $J_T(\varphi)$  we can use the approach based on calculation and evaluation of their cumulants. Within this approach conditions for the asymptotic normality of (appropriately normalized) functional  $J_T(\varphi)$  can be stated in terms of conditions on spectral densities  $f_k(\lambda_1, \dots, \lambda_{k-1})$  and functions  $\varphi$ , in particular, under the conditions of their integrability.

For Gaussian and linear fields, it is possible to state central limit theorems for the functionals  $J_T(\varphi)$  under the conditions of integrability of the following form: the spectral density of the field  $f(\lambda) \in L_p$  and  $\varphi(\lambda) \in L_q$ , where  $\frac{1}{p} + \frac{1}{q} \leq \frac{1}{2}$ .

We state next, for long-range dependent Gaussian random fields, the asymptotic normality result for the functional  $J_T(\varphi)$  under the conditions prescribing behavior of the spectral density at the point of singularity.

**Theorem 1.** *Let  $X(t)$ ,  $t \in Z^d$ , be a zero-mean stationary Gaussian random field with spectral density  $f(\lambda)$ ,  $\lambda \in S$ , such that for some  $0 < \alpha_i < 1$ ,  $i = 1, \dots, d$ ,  $f(\lambda) = O(\prod_{i=1}^d |\lambda_i|^{-\alpha_i})$  as  $\lambda_i \rightarrow 0$ , and  $\varphi(\lambda) = O(\prod_{i=1}^d |\lambda_i|^{\alpha_i})$  as  $\lambda_i \rightarrow 0$ . The sets of discontinuities of functions  $f(\lambda)$  and  $\varphi(\lambda)$  have Lebesgue measure zero, and these functions are bounded for  $\delta \leq |\lambda| \leq \pi$  for all  $\delta > 0$ . Then*

$$T^{d/2}(J_T(\varphi) - EJ_T(\varphi)) \xrightarrow{D} N(0, \sigma^2) \text{ as } T \rightarrow \infty, \quad (1)$$

where  $\sigma^2 = 2(2\pi)^d e(h) \int_S f^2(\lambda) \varphi^2(\lambda) d\lambda$ , and the factor  $e(h)$  depends on the taper function.

We give conditions on the taper under which the statement (1) can be strengthened to the form  $T^{d/2}(J_T(\varphi) - J(\varphi)) \xrightarrow{D} N(0, \sigma^2)$  as  $T \rightarrow \infty$ , where  $J(\varphi) = \int_S f(\lambda) \varphi(\lambda) d\lambda$ .

We state also the conditions of asymptotic normality for nonlinear functionals of the periodogram, namely, for the spectral functionals of powers of a periodogram:

$$J_T^{(k)}(\varphi) = \int_S \varphi(\lambda) (I_T^h(\lambda))^k d\lambda.$$

The main analytic tool used in the proofs in order to evaluate of the asymptotic behaviour of cumulants of spectral functionals is the generalized Hölder inequality.

Statistical analysis based on second-order information (covariance and spectrum) is not always sufficient or not sufficiently good in some situations and one needs to consider higher-order information, higher-order moments/cumulants and higher-order spectra. Statistical techniques based on higher-order moments and spectra are of great demand in many fields of applications, which include: geophysics, astronomy, oceanography, communications, image processing, fluid mechanics, plasma physics, astrophysics, turbulence, economics and finance. In particular, some motivations behind the use of higher-order spectra in signal processing are: to detect and characterize nonlinearities, to detect signal from Gaussian and non-Gaussian noise. The investigation of various statistical problems in the mentioned areas leads to the consideration of functionals of higher order spectral densities

$$J_k(\varphi) = \int_S \varphi_k(\lambda_1, \dots, \lambda_{k-1}) f_k(\lambda_1, \dots, \lambda_{k-1}) d\lambda_1 \cdots d\lambda_{k-1},$$

for an appropriate function  $\varphi_k$ .

We study the estimators for  $J_k(\varphi)$  based on tapered periodograms of higher orders. We introduce also some modifications of such estimators intended to reduce a bias of estimators. And within one more approach we construct the estimators for higher order spectral functionals recursively.

We consider the application of asymptotic results for empirical spectral functionals to the problems of parameter estimation in the spectral domain. Central limit theorems for spectral functionals serve as the main tool to derive asymptotic properties of so-called minimum contrast estimators.

The presentation is partly based on the results obtained jointly with N. Leonenko and F. Avram. Applications for minimum contrast parameter estimation for several models of long-range dependent Gaussian fields are presented in the paper [1].

## References

- [1] Alomari H.M., Frías M.P., Leonenko N.N., Ruiz-Medina M.D., Sakhno L., and Torres A. (2017). Asymptotic properties of parameter estimates for random fields with tapered data. *Electronic Journal of Statistics*. Vol. **11**, pp. 3332-3367.

# ROBUST ANALOGS OF THE $Q_n$ -ESTIMATE OF SCALE FOR THE STUDENT DISTRIBUTIONS

G.L. SHEVLYAKOV, I.S. SHIROKOV, V.G. LITVINOVA  
*Peter the Great St. Petersburg Polytechnic University*  
*St. Petersburg, RUSSIA*  
e-mail: gshevlyakov@yahoo.com

## Abstract

Robust computationally fast Huber's  $MQ_n$ -estimates of scale are designed to approximate the highly robust and efficient  $Q_n$ -estimate of scale proposed by Rousseeuw and Croux (1993). The parameters of this approximation are tuned to provide high robustness and efficiency of these  $M$ -estimates of scale for the Student distributions—the dependencies between the values of the estimate parameter and distribution shape parameter are written out and tabulated. The comparative study of robust estimates is performed by computation of their asymptotic efficiencies and breakdown points. A special attention is paid to the particular cases of the Gaussian and Cauchy distributions.

**Keywords:** data science, robust analog, Student distribution

## 1 Introduction

Estimation of scale is one of the most important problems in statistics (Hampel *et al.*, 1986; Huber, 1981). First of all, there are two natural goals in statistics: constructing measures of distribution location and spread, although the role of scale is secondary as compared to location: generally, the problem of estimation of scale is subordinated to the problem of estimation of location. However, we may enlist a number of important reasons for the direct use of scale estimates: (i) data standardizing, (ii) detection of outliers in the data, (iii) estimation of correlation, and (iv) estimation of regression.

Here, we restrict ourselves to robust estimation of scale. In present, one of the best robust estimates of scale is given by the  $Q_n$ -estimate (Rousseeuw and Croux, 1993). This robust estimate is defined as the first quartile of the pair-wise distances between observations:

$$Q_n = c\{|x_i - x_j|\}_{(k)},$$

where the factor  $c$  provides the consistency of estimation,  $k = C_h^2$ ,  $h = [n/2] + 1$ . The  $Q_n$ -estimate is robust with the breakdown point  $\varepsilon^* = 0.5$  highest possible and high efficiency 82% at the Gaussian. Its drawback is the high asymptotic computational complexity: generally, it takes  $O(n \log n)$  of computational time.

Much more common, Huber's robust  $M$ -estimates  $\hat{S}$  of scale are given by the implicit estimating equation (Huber, 1981)

$$\sum \chi(x_i/\hat{S}) = 0, \tag{1}$$

where  $\chi(x)$  is an estimating (score) function commonly even and nondecreasing for  $x > 0$ . The classical particular cases of  $M$ -estimates of scale are: the standard deviation

$s = \sqrt{n^{-1} \sum x_i^2}$  with  $\chi(x) = x^2 - 1$ , the mean absolute deviation  $d = n^{-1} \sum |x_i|$  with  $\chi(x) = |x| - 1$  and the median absolute deviation  $MAD = \text{med}_i |x_i|$  with  $\chi(x) = \text{sgn}(|x| - 1)$  (the parameter of location is set to zero here).

In this work, we use the approximations of the  $Q_n$ -estimate of scale by low-complexity and computationally fast robust  $MQ_n$ -estimates of scale of high efficiency (Smirnov and Shevlyakov, 2014) with the parameters tuned for the Student distributions. This family of distributions comprises distributions with relatively heavy tails with the important particular cases, such as the Cauchy and Gaussian (the limiting case) distributions.

An outline of the remainder of the paper is as follows. In Section 2, general results on the approximation of the  $Q_n$ -estimate of scale by  $MQ_n$ -estimates of scale are given. In Section 3, the particular case of the Student distributions is considered. In Section 4, some conclusions are drawn.

## 2 Approximation of the $Q_n$ -estimate by $MQ_n$ -estimates

The notion of the influence function  $IF(x; S, F)$  that defines a measure of the sensitivity of an estimate functional  $S = S(F)$  at a distribution  $F$  to the perturbation at a point  $x$  is one of the central in robust statistical analysis (Hampel et al., 1986). It is important that the asymptotic variance  $V(\hat{S}, F)$  of the estimate  $\hat{S}$  is expressed through the influence function

$$V(\hat{S}, F) = \int IF(x; S, F)^2 dF(x).$$

Moreover, in the class of Huber's  $M$ -estimates of scale (1), the influence function  $IF(x; S, F)$  is proportional to the estimating function  $\chi(x)$ :

$$IF(x; S, F) \propto \chi(x).$$

Basing on this result, it is possible to construct an  $M$ -estimate with any admissible influence function, in particular, with the influence function of the  $Q_n$ -estimate of scale. This idea is used for constructing the approximation of the  $Q_n$ -estimate of scale by an  $M$ -estimate of scale.

The sought approximation, namely the estimating function  $\chi(x)$  for  $MQ_n$ -estimates of scale, naturally depends on the underlying distribution density  $f(x)$  shape: the explicit result gives the following form of this connection (Smirnov and Shevlyakov, 2014)

$$\chi_\alpha(x) = c_\alpha - 2f(x) - \frac{1}{3}\alpha^2 f''(x), \quad (2)$$

where the constant  $c_\alpha$  is chosen from the condition of consistency and  $\alpha$  is a tuning parameter. So, we call  $M$ -estimates with estimating function  $\chi_\alpha$  as  $MQ_n$ -estimates.

In what follows, we apply Equation (2) to the Student distribution densities in order to design computationally fast highly robust and efficient  $MQ_n$ -estimates of scale .

### 3 $MQ_n$ -estimates for the Student distributions

#### 3.1 Estimating functions for robust $MQ_n$ -estimates

In order to get the estimating function of  $MQ_n$ -estimates of scale, we substitute the expression for the Student distribution density

$$f(x) = \frac{\Gamma(\frac{k+1}{2})}{\sqrt{k\pi}\Gamma(k/2)(1+x^2/k)^{\frac{k+1}{2}}}, \quad k = 1, 2, \dots,$$

into Equation (2) and compute the constant  $c_\alpha$  determined from the condition of consistency

$$\int \chi_\alpha(x)f(x) dx = 0.$$

The formula for this consistency constant  $c_\alpha(x)$  is given by

$$c_\alpha(x) = \frac{\Gamma^4(\frac{k+1}{2})\Gamma(k+1/2)}{2^{1-2k}\pi^{3/2}k^{3/2}\Gamma^3(k)} \left( 1 - \frac{\alpha^2(k+1)(2k+1)}{24k(k+2)} \right).$$

It can be shown that the tuning parameter  $\alpha$  lies in the interval  $[0, 1/\sqrt{2}]$ . The results of computation are presented in Table 1, so, a potential user may choose a consistency constant and thus with Equation (2) an  $MQ_n$ -estimate.

We skip the general formula for the estimating function  $\chi_\alpha(x)$ —it is rather cumbersome; in the particular case  $\alpha = 0$ , it has the form

$$\chi_0(x) = \frac{\Gamma^4(\frac{k+1}{2})\Gamma(k+1/2)}{2^{1-2k}\pi^{3/2}k^{3/2}\Gamma^3(k)} - \frac{\Gamma^2(\frac{k+1}{2})}{2^{-k}\pi\sqrt{k}\Gamma(k)(1+x^2/k)^{\frac{k+1}{2}}}.$$

The breakdown point of  $MQ_n$ -estimates of scale for the Student distributions with the tuning parameter  $\alpha$  lying in  $[0, 1/\sqrt{2}]$  is given by

$$\varepsilon^* = 1 - \frac{\Gamma^2(\frac{k+1}{2})\Gamma(k+1/2)}{2^{-k}\pi^{1/2}k^{3/2}\Gamma^3(k)} - \frac{\Gamma^2(\frac{k+1}{2})}{2^{-k}\pi^{1/2}k\Gamma^2(k)} \left( 2 - \frac{\alpha^2(k+1)}{3k} \right) \left( 1 - \frac{\alpha^2(k+1)(2k+1)}{24k(k+2)} \right).$$

The maximum possible breakdown point equal to 50% is attained at  $k = 1$  and  $\alpha = 0$  (see Fig. 1). With increasing  $\alpha$ , the breakdown point is decreasing for any  $k$ ; with given  $\alpha$  and increasing  $k$ , the breakdown point also is decreasing.

#### 3.2 Asymptotic efficiency of robust $MQ_n$ -estimates

The asymptotic efficiency  $eff(\widehat{S}_\alpha)$  of  $MQ_n$ -estimates of scale with the estimating function  $\chi_\alpha(x)$  is computed by the following formula

$$eff(\widehat{S}_\alpha) = \frac{1}{V(\widehat{S}_\alpha, F)J(F)},$$

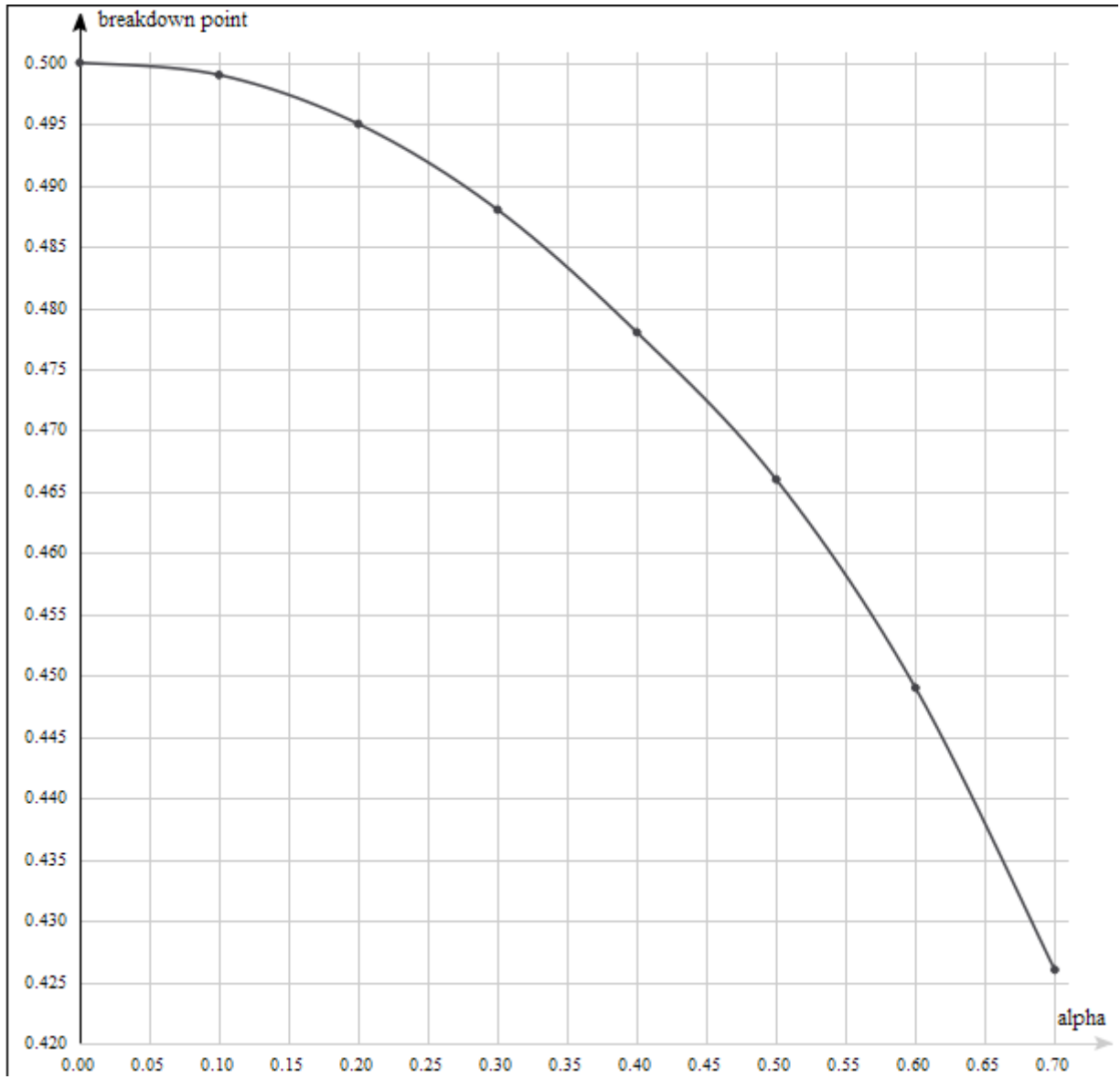


Figure 1: Breakdown Points of  $MQ_n$ -Estimates of Scale,  $k = 1$

Table 1: Consistency Constant  $c_\alpha(x)$  for  $MQ_n$ -Estimates of Scale

$k, \alpha$	0	0.1	0.2	0.3	0.4	0.5	0.6	0.7
1	0.318	0.318	0.317	0.316	0.314	0.312	0.309	0.305
2	0.417	0.416	0.415	0.414	0.411	0.408	0.405	0.401
3	0.459	0.459	0.458	0.456	0.454	0.451	0.447	0.442
4	0.483	0.483	0.482	0.480	0.477	0.474	0.470	0.465
5	0.498	0.498	0.497	0.495	0.492	0.488	0.484	0.479
6	0.509	0.508	0.507	0.505	0.502	0.499	0.494	0.489
7	0.516	0.516	0.515	0.512	0.510	0.506	0.501	0.496
8	0.522	0.522	0.520	0.518	0.515	0.512	0.507	0.502
9	0.526	0.526	0.525	0.523	0.520	0.516	0.511	0.506
10	0.530	0.530	0.528	0.526	0.523	0.519	0.515	0.509
20	0.547	0.546	0.545	0.543	0.540	0.536	0.531	0.525
30	0.553	0.552	0.551	0.549	0.545	0.541	0.536	0.530
40	0.555	0.555	0.554	0.551	0.548	0.544	0.539	0.533
50	0.557	0.557	0.555	0.553	0.550	0.546	0.541	0.535
$\infty$	0.564	0.564	0.562	0.560	0.557	0.552	0.547	0.541

where  $V(\widehat{S}_\alpha, F)$  is the asymptotic variance of  $MQ_n$ -estimates of scale given by Equation (1), which takes the following form

$$V(\widehat{S}_\alpha, F) = \int IF(x; S_\alpha, F)^2 dF(x) = \frac{\int \chi_\alpha^2(x) dF(x)}{[\int x \chi_\alpha'(x) dF(x)]^2},$$

$J(F)$  is the Fisher information for scale

$$J(F) = \int \left[ x \frac{f'(x)}{f(x)} + 1 \right]^2 dF(x) = \frac{2k}{k+3}.$$

The explicit expression for the asymptotic efficiency has been derived, but it is cumbersome and thus not written out; its numerical values are presented in Table 2.

## 4 Conclusions

1. The class of  $MQ_n$ -estimates of computationally fast and highly robust  $M$ -estimates of scale close in efficiency to the highly efficient and robust  $Q_n$ -estimate of scale is thoroughly studied for the Student distributions: explicit formulas are derived for the consistency constants, asymptotic efficiencies and breakdown points of those estimates.
2. The efficiency of the considered  $MQ_n$ -estimates are in the range 80%–100%, their breakdown points lie in the range 25%–50%—this means that  $MQ_n$ -estimates are highly efficient and robust.

Table 2: Asymptotic Efficiency of  $MQ_n$ -Estimates of Scale

$k, \alpha$	0	0.1	0.2	0.3	0.4	0.5	0.6	0.7
1	1.000	1.000	1.000	0.999	0.998	0.995	0.989	0.979
2	0.984	0.985	0.986	0.988	0.991	0.993	0.995	0.996
3	0.962	0.962	0.964	0.967	0.971	0.976	0.981	0.986
4	0.942	0.943	0.945	0.948	0.953	0.958	0.965	0.972
5	0.926	0.927	0.929	0.932	0.937	0.944	0.939	0.948
6	0.913	0.914	0.916	0.920	0.925	0.931	0.939	0.948
7	0.903	0.903	0.906	0.909	0.915	0.921	0.929	0.939
8	0.894	0.895	0.897	0.901	0.906	0.913	0.921	0.931
9	0.887	0.888	0.888	0.890	0.894	0.906	0.914	0.924
10	0.881	0.881	0.884	0.887	0.893	0.900	0.908	0.918
20	0.849	0.849	0.852	0.855	0.861	0.867	0.876	0.886
30	0.836	0.837	0.839	0.843	0.848	0.855	0.863	0.874
40	0.830	0.830	0.832	0.836	0.841	0.848	0.856	0.867
50	0.826	0.826	0.828	0.832	0.837	0.844	0.852	0.862
$\infty$	0.808	0.809	0.811	0.814	0.819	0.825	0.834	0.844

3. The asymptotic complexity of  $MQ_n$ -estimates is of order  $O(n)$ , much smaller than  $O(n \log n)$  of the  $Q_n$ -estimate.
4. Note that in the case of the Cauchy distribution, the  $MQ_n$ -estimate is just the maximum likelihood estimate of scale with efficiency 100% and the breakdown point 50%; in the other limit case, for the Gaussian distribution, the efficiency and breakdown point are equal to 80.8% and 29.3%, respectively.

## References

- [1] Hampel F.R., Ronchetti E.M., Rousseeuw P.J., Stahel W.A. (1986). *Robust Statistics: The Approach Based on Influence Functions*. Wiley, New York.
- [2] Huber P.J. (1981). *Robust Statistics*. Wiley, New York.
- [3] Rousseeuw P.J., Croux C. (1993). Alternatives to the Median Absolute Deviation. *Journal of the American Statistical Association*. Vol. **88**, pp. 1273-1283.
- [4] Smirnov P.O., Shevlyakov G.L. (2014). Fast Highly Efficient and Robust One-Step M-Estimators of Scale Based on  $Q_n$ . *Computational Statistics and Data Analysis*. Vol. **78**, pp. 153-158.

# ON THE UPPER BOUND OF THE RISK IN SELECTION OF THE T BEST ITEMS

E. STOIMENOVA

*Institute of Mathematics and Informatics, Bulgarian Academy of Sciences*

*Sofia, BULGARIA*

e-mail: jeni@math.bas.bg

## Abstract

A fixed sample size procedure for selecting the  $t$  best system components is considered. The probability requirement is set to be satisfied under the indifference zone formulation. In order to minimize the average losses from misclassification, we use loss function which is sensitive to the number of misclassifications. The upper bound of the corresponding risk is derived for location parameter distributions. The risk function for the Least Favorable Configuration is derived in an integral form for a large class of distribution functions.

**Keywords:** data science, risk, least favorable configuration

## 1 Introduction

Consider the following replacement policy. Fixed number of system components should be replaced by new ones. There are given  $k$  competing items and the goal is to select the most reliable  $t$  out of them. The true values of the reliability parameters are not known but they are estimated by a single test. On the basis of test estimates  $X_1, \dots, X_k$ , we want to partition the set of item parameters  $\theta_1, \dots, \theta_k$  into two disjoint subsets such that the first subset contains the  $k - t$  smallest  $\theta_i$ , and the second subset contains the remaining  $t$  largest  $\theta_i$ , where  $1 \leq t < k$ . We denote  $X_{(i)}$  the observation corresponding to  $\theta_{[i]}$ . The parameters in the second subset are called “best”.

The natural single stage procedure selects  $t$  items with largest parameters on the basis of parameter estimators [4]. The usual approach for this problem is in terms of probability of correct selection (PCS). The procedure used should guarantee that the PCS is at least some specified value  $P^*$  whenever the true parameter configuration lies in some subset of parameter space. When the monotonicity property on PCS holds, the problem is to find the parameter configuration for which PCS reaches its minimum.

In a decision theoretic approach, the formulation is in terms of a loss function and associated risk (average loss). Under a 0-1 loss function, the probability of a correct selection and the risk  $\rho$  are connected through,  $PCS = 1 - \rho$ . Thus all decision theoretic formulations in terms of risk can be translated into the “PCS-language”. More sensitive loss functions will be discussed in this paper. Their construction is based on a metric for partial rankings.

The optimum properties of the natural decision procedure for selecting the best single population are derived by Bahadur and Goodman [3]. Lehmann [10], Eaton [7], and Alam [1] have extended the results for more general problems and families of distributions. The problem is further discussed by Gupta and Miescke [8], Gupta and

Panchapakesan [9], Ng et al. [2]. The general partition problem stated by Bechhofer [4] is to classify the set of populations into a fixed number of categories. The general case is treated from a decision theoretic point of view by Sobel [12] and Sobel [13]. If the risk is a monotone function, the problem of its evaluating is reduced to a problem of determining the parameter configuration for which the risk is maximal.

## 2 Decision procedure

### 2.1 Natural Decision Procedure

Let  $X = (X_1, \dots, X_k)$  be estimators of the items unknown reliability parameter vector  $\theta = (\theta_1, \dots, \theta_k)$  in a set  $\Theta$ . It is assumed that  $X_i$  has distribution function  $F(x - \theta_i)$ .

The Natural Decision Procedure divides the coordinate values of  $\theta$  into two disjoint subsets according to the ranking of the observed vector  $X$ . Denote  $\Lambda = \{\lambda\}$  the action space for the selection problem containing all partitions  $\lambda = (\lambda_1, \lambda_2)$  of  $\{1, \dots, k\}$  where  $\lambda_1$  has  $k - t$  elements and  $\lambda_2$  has  $t$  elements.

For each  $\lambda = (\lambda_1, \lambda_2) \in \Lambda$ , let

$$B_\lambda = \{x \in \chi : x_i \leq x_j, \text{ for all } i \in \lambda_1, j \in \lambda_2\}.$$

For each  $x \in \chi$ , let  $H(x) = \{\lambda \in \Lambda : x \in B_\lambda\}$  and  $n(x)$  be the number of elements in the set  $H(x)$  so that  $n(x) \geq 1$ . The decision rule  $\varphi_\lambda^*(x)$  is defined by

$$\varphi_\lambda^*(x) = \begin{cases} 1/n(x) & \text{if } \lambda \in H(x), \\ 0 & \text{if } \lambda \notin H(x). \end{cases}$$

Thus  $\varphi^* = \{\varphi_\lambda^*\}_{\lambda \in \Lambda}$ .

This decision function  $\varphi^*$  divides the parameters  $\theta_1, \dots, \theta_k$  into two ordered subsets. The first subset contains the  $k - t$  smallest parameters, and the second subset contains the remaining  $t$  largest parameters. The procedure does not state any preferences among members of the same subset.

After the  $t$  best parameters have been selected, evaluation of the loss from incorrect partitioning can be made. Let  $\theta_{[1]} \leq \theta_{[2]} \leq \dots \leq \theta_{[k]}$  denote the ordered  $\theta_i$ ,  $i = 1, \dots, k$ . We assume that it is not known which parameter is associated with  $\theta_{[i]}$ .

The parameter  $\theta_{[k-t]}$  divides the parameters into two ordered subsets so that the parameters  $\theta_{[1]}, \dots, \theta_{[k-t]}$  form the first subset, and the parameters  $\theta_{[k-t+1]}, \dots, \theta_{[k]}$  form the second subset. When the parameters are selected using their true (unknown) values, we say that a correct selection has been made. This partition of the parameters is called the true one.

We require the usual type of invariant assumptions regarding sample space,  $\Theta$ ,  $\Lambda$  and  $F(x; \theta)$ . For more explicit treatment of symmetry and invariance see Lehmann [11].

### 2.2 Loss function

Let  $l(\theta, \lambda)$  denote the loss if we terminate selection with action  $\lambda \in \Lambda$  when  $\theta$  is the true value of the parameter vector. Calculate  $n_{ij}$  the number of items which are in the  $i^{\text{th}}$

category according the true partition and in the  $j^{th}$  category according  $\lambda$  ( $i, j = 1, 2$ ). Define the loss function by

$$l(\theta, \lambda) = \sum_{i=1}^2 \sum_{j=1}^2 |c_i - c_j| n_{ij}, \quad (1)$$

where  $c_1 = (k - t)(k - t + 1)/2$  is the mean of the  $k - t$  numbers in the first category and  $c_2 = t(2k - t + 1)/2$  is the mean of the  $t$  numbers in the second category of true partition. Thus the loss function counts the number of misclassified parameters and equals to two times the number of parameters which are among last  $t$  largest and are placed in the first subset by action  $\lambda$ .

The motivation for the use of the loss function (1) comes from a metric for partially ranked data induced by Spearman's footrule. Partial rankings from the same type correspond a set of partitions which is a coset space of the permutation group. Metrics on permutation group induce metrics on its cosets spaces which preserve the invariant properties. Several such metrics for partial rankings are constructed by Critchlow [5]. The idea of using metrics on permutations in the decision theoretic formulation has also been mentioned by Diaconis [6].

The function (1) computes the Spearman's footrule distance between two partial rankings using the "pseudo-ranks"  $c_i$  and  $c_j$  instead the ordinary ranks. The construction of  $l(\theta, \lambda)$  implies that the loss function is a right invariant in the sense

$$l(\theta\tau, \lambda\tau) = l(\theta, \lambda).$$

### 2.3 Expected loss (risk)

Assuming that all partitions of the parameters are equally likely to observe, the risk function for  $\varphi \in D$  is

$$\rho(\varphi^*, \theta) = \mathbf{E}[l(\theta, \lambda)] = \sum_{i=1}^2 \sum_{j=1}^2 |c_i - c_j| \mathbf{E}N_{ij}, \quad (2)$$

where  $N_{ij}$  is the random variable corresponding to  $n_{ij}$ .

**Theorem 1.** *The risk function  $\rho(\varphi^*, \theta)$  defined by could be expressed by*

$$\rho(\varphi^*, \theta) = \sum_{m=k-t+1}^k \sum_{l=1}^{k-t} \mathbf{P}\{X_{(m)} = X_{[l]}\}. \quad (3)$$

### 2.4 Preference Zone and Least Favourable Configuration

The indifference Zone approach, proposed by Bechhofer [4], consists of dividing the parameter space into two regions, the so called Preference Zone (PZ) and its complement the Indifference Zone. We discuss distributions with location parameter.

**Definition 1.** For  $0 < \delta < \infty$ , the subset  $PZ \in \Theta$  defined by

$$PZ = \{\theta \in \Theta : \theta_{[k-t+1]} - \theta_{[k-t]} \geq \delta\} \quad (4)$$

is called the Preference Zone.

The procedure used should guarantee that the risk of decision  $\varphi$  asserted from the observations is at most some specified value  $P^*$  whenever  $\theta$  lies in  $PZ$ . So the Preference Zone represents a subset of parameter values where we have a strong preference for a correct selection. The Indifference Zone approach is directed towards the performance of Natural Decision Procedure for configurations in the  $PZ$ .

The Least Favourable Configuration (LFC) of the parameters is that one from  $PZ$  for which the risk reaches its maximum. For two-category problem with parameter of location we prove in Theorem 3 that

$$LFC : \{\theta_{[k]} - \theta_{[k-t+1]} = 0; \quad \theta_{[k-t+1]} - \theta_{[k-t]} = \delta; \quad \theta_{[k-t]} - \theta_{[1]} = 0\}. \quad (5)$$

The risk  $\rho(\varphi^*, \theta)$  for  $LFC$  is expressed by (3) is

$$\rho(\varphi^*, LFC) = t \sum_{l=1}^{k-t} \mathbf{P}\{X_{(k)} = X_{[l]}\}.$$

### 3 Upper Bound of the Risk Function

Define

$$\gamma_{m,s} = \begin{cases} \theta_{[m]} - \theta_{[s]}, & s = 1, \dots, m-1; \\ \theta_{[s]} - \theta_{[m]}, & s = m+1, \dots, k. \end{cases}$$

Then the following Theorem holds.

**Theorem 2.** For all  $m = k-t+1, \dots, k$ , the risk function  $\rho(\varphi^*, \theta)$  defined in (2) is a strictly decreasing function in  $\gamma_{m,1}, \dots, \gamma_{m,k-t}$  and nonincreasing in  $\gamma_{m,k-t+1}, \dots, \gamma_{m,k}$  for any parameter configuration from the Preference Zone (4), where

**Theorem 3.** With  $LFC$  defined in (5) we have

$$\rho(\varphi^*, \theta) \leq \rho(\varphi^*, LFC)$$

for all parameter configurations from the Preference Zone (4).

Now, the risk function for  $LFC$  is stated for the case  $k-t \leq t$ .

**Theorem 4.** The risk function  $\rho(\varphi^*, LFC)$  for  $LFC$  defined in (5) is

$$\sum_{y=0}^{k-t-1} \int \binom{t-1}{y} [F(x)]^y [1-F(x)]^{t-1-y} \sum_{m=0}^{k-t-y-1} \binom{k-t}{m} [F(x+\delta)]^m [1-F(x+\delta)]^{k-t-m} dF(x).$$

The risk function  $\rho(\varphi^*, \theta)$  is decreasing in  $\delta$ . Thus we can choose  $\delta^*$  to be the smallest  $\delta > 0$  such that  $\rho(\varphi^*, LFC) \leq P^*$ . For all  $\delta > \delta^*$ ,  $\rho(\varphi^*, \theta)$  will be less than  $P^*$  for all parameter configurations (4) specified by  $\delta$ .

## 4 Acknowledgements

This research was supported by the grant DH02-13 of the Bulgarian National Science Fund.

## References

- [1] Alam. K. (1973). On a multiple decision rule. *Annals of Statistics*, Vol. **1**, pp. 750-755.
- [2] Ng H.K.T. , Balakrishnan N., Panchapakesan S. (2007). Selecting the best population using a test for equality based on minimal Wilcoxon rank-sum precedence statistic. *Methodology and Computing in Applied Probability*, Vol. **9**, pp. 263-305.
- [3] Bahadur R., Goodman L. (1952). Impartial decision rules and sufficient statistics. *Annals of Mathematical Statistics*, Vol. **23**, pp. 553-562.
- [4] Bechhofer. R.E. (1954). A single-sample multiple decision procedure for ranking means of normal populations with known variances. *Annals of Mathematical Statistics*, Vol. **25**, pp. 16-39.
- [5] Critchlow. D.E. (1985). *Metric methods for analyzing partially ranked data*. Lecture Notes in Statistics, Springer-Verlag, Berlin-New York.
- [6] Diaconis P. (1988). *Group Representations in Probability and Statistics*. Institute of Mathematical Statistics Lecture Notes – Monograph Series, Hayward.
- [7] Eaton M.L. (1967). Some Optimum Properties of Ranking Procedures. *Annals of Mathematical Statistics*, Vol. **38**, pp. 124-137.
- [8] Gupta S.S., Miescke K.J. (1984). Sequential selection procedures - a decision theoretic approach. *Annals of Statistics*, Vol. **12**, pp.336-350.
- [9] Gupta S.S., Panchapakesan S. (2002). *Multiple decision procedures: theory and methodology of selecting and ranking populations*. Wiley, New York.
- [10] Lehmann E.L.. (1966). On a theorem of Bahadur and Goodman. *Annals of Mathematical Statistics*, Vol. **37**, pp. 1-6.
- [11] Lehmann, E.L., Romano J.P. (2008). *Testing Statistical Hypothesis*. Springer, New York.
- [12] Sobel M.J. (1990). Nonparametric loss functions for partitioning problems. *Statistics & Decisions*, Vol. **8**, pp.71-83.
- [13] Sobel M.J. (1990). Complete ranking procedures with appropriate loss functions. *Commun. Statist. - Theor. Meth.*, Vol. **19**, pp.4525-4544.

# RECENT RESULTS ON THE TOTAL VARIATION DISTANCE

A.M. ZUBKOV

*Steklov Mathematical Institute of RAS*

*Moscow, RUSSIA*

e-mail: zubkov@mi-ras.ru

## Abstract

Let  $(X_1, \dots, X_n)$  and  $(Y_1, \dots, Y_n)$  be two sets of independent discrete random variables. Explicit upper and lower bounds for the total variation distance between distributions of these sets are obtained in terms of some functions of distributions of separate components  $X_k$  and  $Y_k$ ,  $k = 1, \dots, n$ . The cases of identical (inside each set) and arbitrary distributions of random variables are considered. Results may be used to estimate the sample sizes necessary or sufficient for testing two hypotheses with given sum of error probabilities.

**Keywords:** data science, total variation distance, hypotheses testing

## 1 Introduction

Let  $S$  be a countable set; let  $P = \{p_s\}_{s \in S}$  and  $Q = \{q_s\}_{s \in S}$  be probability distributions of random variables  $X$  and  $Y$  with values in  $S$  correspondingly. The total variation distance between probability distributions  $P$  and  $Q$  (or random variables  $X$  and  $Y$ ) is defined by

$$d_{\text{TV}}(P, Q) = d_{\text{TV}}(X, Y) \stackrel{\text{def}}{=} \sup_{A \subseteq S} |P(A) - Q(A)| = \frac{1}{2} \sum_{s \in S} |p_s - q_s|. \quad (1)$$

The value  $1 - d_{\text{TV}}(P, Q)$  is an exact low bound for the sum of error probabilities of two kinds in a problem of testing two simple hypothesis on the observation  $Z$ :

$H_0$  :  $Z$  has distribution  $P$ ,

$H_1$  :  $Z$  has distribution  $Q$ .

So, estimates of total variation distance between distributions of sets of independent random variables  $(X_1, \dots, X_n)$  and  $(Y_1, \dots, Y_n)$  considered as a function on  $n$  may be used to draw objective conclusions on the sample size necessary or sufficient to distinguish simple hypotheses on such distributions.

Recently the upper and lower estimates of the total variation distance between samples  $(X_1, \dots, X_n)$  and  $(Y_1, \dots, Y_n)$  of independent identically distributed observations were obtained in [1, 2]. Under some conditions these estimates has the order  $d_{\text{tv}}(X_1, Y_1)\sqrt{n}$  with coefficients depending on the distributions of  $X_1$  and  $Y_1$ . In the general case the upper bound cannot be smaller than  $d_{\text{tv}}(X_1, Y_1)n$ .

Here we state lower and upper estimates of the total variation distance between the distributions of sets  $(X_1, \dots, X_n)$  and  $(Y_1, \dots, Y_n)$  of independent random variables for cases of identically (within each set) or arbitrary distributed random variables. The domains of applicability of our inequalities are wider than that of [1, 2].

## 2 Identically distributed components

It is easy to see that if  $P$  and  $Q$  are probability distributions on a countable set  $S$  and  $C_{P,Q} = \{x \in S : P(x) > Q(x)\}$ , then  $d_{\text{tv}}(P, Q) = \sum_{x \in C_{P,Q}} (P(x) - Q(x))$ . Put

$$v = v(P, Q) = \min\{P(C_{P,Q}), Q(C_{P,Q}), P(\Omega \setminus C_{P,Q}), Q(\Omega \setminus C_{P,Q})\},$$

then  $0 < v \leq \frac{1}{2}(1 - d_{\text{tv}}(P, Q))$ , and these estimates are best possible.

**Theorem 1.** *Let  $X_1, \dots, X_n$  be independent random variables with the same distribution  $P$  on the countable set  $S$ ,  $Y_1, \dots, Y_n$  be independent random variables with the same distribution  $Q$  on  $S$  and  $d_{\text{tv}}(P, Q) = \varepsilon > 0$ . Then*

$$d_{\text{tv}}((X_1, \dots, X_n), (Y_1, \dots, Y_n)) \geq \frac{e^{-4/nv(1-v)}}{2(1+2/n)} \sqrt{\frac{v}{1-v}} \left( \Phi(2\varepsilon\sqrt{n}) - \frac{1}{2} \right),$$

where  $v = v(P, Q) \in [\frac{2}{n}, \frac{n-1}{2n})$  and  $\Phi(x) = \frac{1}{\sqrt{2\pi}} \int_{-\infty}^x e^{-u^2/2} du$  is a standard normal distribution function.

**Remark 1.** The difference  $\Phi(2\varepsilon\sqrt{n}) - \frac{1}{2}$  does not exceed  $\frac{1}{2}$  and is equivalent to  $\varepsilon\sqrt{2n/\pi}$  for  $\varepsilon\sqrt{n} \rightarrow 0$ . The estimate of theorem 1 cannot be larger than  $\frac{1}{4}$ ; for  $n > 2\varepsilon^{-2} \ln 2$  the known low estimate (see, e. g., [3, 4])

$$d_{\text{tv}}((X_1, \dots, X_n), (Y_1, \dots, Y_n)) \geq 1 - 2e^{-n\varepsilon^2/2},$$

is nontrivial and tends to 1 as  $n \rightarrow \infty$ .

**Theorem 2.** *Let  $X_1, X_2, \dots$  and  $Y_1, Y_2, \dots$  be independent random variables taking values  $1, \dots, N$ :*

$$\mathbf{P}\{X_t = k\} = p_k, \quad \mathbf{P}\{Y_t = k\} = r_k, \quad k \in \{1, \dots, N\}, \quad t = 1, 2, \dots, \quad d_{\text{tv}}(X_1, Y_1) = \varepsilon.$$

Then

$$d_{\text{tv}}((X_1, \dots, X_n), (Y_1, \dots, Y_n)) \leq \varepsilon\sqrt{n} \left( \frac{1}{\sqrt{S_X} + \sqrt{S_X + \varepsilon}} + \frac{1}{\sqrt{S_Y} + \sqrt{S_Y + \varepsilon}} \right),$$

where  $S_X = \sum_{k: p_k < r_k} p_k$ ,  $S_Y = \sum_{k: r_k < p_k} r_k$ .

**Remark 2.** Upper bound may be very large if  $S_X$  or  $S_Y$  is very small, but in such cases the total variation distance between  $(X_1, \dots, X_n)$  and  $(Y_1, \dots, Y_n)$  also may be large. For example, if  $N = 3$ ,  $p_1 = r_2 = \varepsilon$ ,  $p_2 = r_1 = 0$ ,  $p_3 = q_3$ , then  $d_{\text{tv}}(X_1, Y_1) = \varepsilon$ ,  $S_X = S_Y = 0$  and

$$d_{\text{tv}}((X_1, \dots, X_n), (Y_1, \dots, Y_n)) \geq \frac{1}{2} (\mathbf{P}\{\exists k: X_k = 1\} + \mathbf{P}\{\exists k: Y_k = 2\}) \geq n\varepsilon(1 - \varepsilon)^{n-1},$$

upper bound of theorem 2 in this case equals  $2\sqrt{n\varepsilon}$ .

Theorems 1 and 2 were proved in [6]. Another form of theorem 2 may be found in [5].

### 3 Arbitrary distributions of components

**Theorem 3.** Let  $X_1, X_2, \dots$  and  $Y_1, Y_2, \dots$  be independent random variables taking values  $1, \dots, N$ :

$$\mathbf{P}\{X_k = j\} = p_j^{(k)}, \quad \mathbf{P}\{Y_k = j\} = r_j^{(k)}, \quad j \in \{1, \dots, N\}, \quad k = 1, 2, \dots, n,$$

and  $\rho_k = \rho(X_k, Y_k) = \frac{1}{2} \sum_{j=1}^N |p_j^{(k)} - r_j^{(k)}| > 0$  ( $k = 1, \dots, n$ ),  $S = \sum_{k=1}^n \rho_k$ . Then

$$d_{\text{tv}}((X_1, \dots, X_n), (Y_1, \dots, Y_n)) \geq \frac{S}{3(2 + S + \sqrt{2n \ln(n/S)})}.$$

If  $\rho_1 = \dots = \rho_n = \rho < 1$ , then the estimate takes the form

$$d_{\text{tv}}((X_1, \dots, X_n), (Y_1, \dots, Y_n)) \geq \frac{n\rho}{3\left(2 + n\rho + \sqrt{2n \ln\left(\frac{1}{\rho}\right)}\right)} = \frac{\rho\sqrt{n}}{3\left(\frac{2}{\sqrt{n}} + \rho\sqrt{n} + \sqrt{2 \ln\left(\frac{1}{\rho}\right)}\right)}.$$

Modifying the proof it is possible to obtain low bound which is arbitrary close to 1 for fixed  $\rho$  and sufficiently large  $n$ .

**Theorem 4.** Let  $X_1, X_2, \dots$  and  $Y_1, Y_2, \dots$  be independent random variables taking values  $1, \dots, N$ :

$$\mathbf{P}\{X_t = k\} = p_k^{(t)}, \quad \mathbf{P}\{Y_t = k\} = r_k^{(t)}, \quad k \in \{1, \dots, N\}, \quad t = 1, 2, \dots, n,$$

$\rho_t = \rho(X_t, Y_t) = \frac{1}{2} \sum_{k=1}^N |p_k^{(t)} - r_k^{(t)}|$ ,  $t = 1, \dots, n$ , and

$$\min_{1 \leq t \leq n} \min\{S_X^{(t)}, S_Y^{(t)}\} \geq \delta > 0, \quad S_X^{(t)} = \sum_{k: p_k^{(t)} < r_k^{(t)}} p_k^{(t)}, \quad S_Y^{(t)} = \sum_{k: r_k^{(t)} < p_k^{(t)}} r_k^{(t)}.$$

Then

$$\rho((X_1, \dots, X_n), (Y_1, \dots, Y_n)) \leq \frac{1}{\sqrt{2\delta}} \sqrt{\sum_{t=1}^n \rho_t^2}.$$

Condition  $\min_{1 \leq t \leq n} \min\{S_X, S_Y\} \geq \delta > 0$  exclude cases mentioned in Remark 2.

## References

- [1] Reyzin L. (2004). Preprint: A note on the statistical difference of small direct products. *Boston Univ. Computer Science, Techn. Rep. BUCS-TR-2004-032*.
- [2] Renner R. (2005). On the variational distance of independently repeated experiments. *arXiv*.
- [3] Sahai A., Vadhan S. (1999). Manipulating statistical difference. *Randomization Methods in Algorithm Design. Proc. DIMACS Workshop, December 1997. DIMACS Ser. in Discr. Math. and Theor. Comput. Sci. Vol. 43. Amer. Math. Soc. Providence, R.I.* p. 251–270.

- [4] Sahai A., Vadhan S. (2003). A complete problem for statistical zero knowledge. *J. ACM*. Vol. 50, Iss. 2, pp. 196–249.
- [5] Zubkov A. M. (2013). New inequalities for the binomial law and for the total variation distance between iid samples. Proc. 10th Int. Conf. “Computer Data Analysis and Modeling”, v. 2. Publ. center of BSU, Minsk, p. 48–50.
- [6] Zubkov A. M. (2017). New estimates for the variational distance between two distributions of a sample. *Matematicheskie voprosy kriptografii*. Vol. 9, Iss. 3, pp. 45–60.

# CONTRIBUTED PAPERS

# ESTIMATION OF CONDITIONAL SURVIVAL FUNCTION UNDER DEPENDENT RANDOM CENSORED DATA

A.A. ABDUSHUKUROV

*Branch of Moscow State University in Tashkent named after M.V.Lomonosov*

*Tashkent, UZBEKISTAN*

e-mail: a\_abdushukurov@rambler.ru

## Abstract

The aim of paper is considering the problem of estimation of conditional survival function in the case of right random censoring with presence of covariate.

**Keywords:** data science, conditional survival function, right random censoring

Let us consider the case when the support of covariate  $C$  is the interval  $[0, 1]$  and we describe our results on fixed design points  $0 \leq x_1 \leq x_2 \leq \dots \leq x_n \leq 1$  at which we consider responses (survival or failure times)  $X_1, \dots, X_n$  and censoring times  $Y_1, \dots, Y_n$  of identical objects, which are under study. These responses are independent and nonnegative random variables (r.v.-s) with conditional distribution function (d.f.) at  $x_i, F_{x_i}(t) = P(X_i \leq t/C_i = x_i)$ . They are subjected to random right censoring, that is for  $X_i$  there is a censoring variable  $Y_i$  with conditional d.f.  $G_{x_i}(t) = P(Y_i \leq t/C_i = x_i)$  and at  $n$ -th stage of experiment the observed data is  $S^{(n)} = \{(Z_i, \delta_i, C_i), 1 \leq i \leq n\}$ , where  $Z_i = \min(X_i, Y_i)$ ,  $\delta_i = I(X_i \leq Y_i)$  with  $I(A)$  denoting the indicator of event  $A$ . Note that in sample  $S^n$  r.v.  $X_i$  is observed only when  $\delta_i = 1$ . Commonly, in survival analysis independence between the r.v.-s  $X_i$  and  $Y_i$  conditional on the covariate  $C_i$  is assumed. But, in some practical situations, this assumption does not hold. Therefore, in this article we consider a dependence model in which dependence structure is described through copula function. So let

$$S_x(t_1, t_2) = P(X_x > t_1, Y_x > t_2), \quad t_1, t_2 \geq 0,$$

the joint survival function of the response  $X_x$  and the censoring variable  $Y_x$  at  $x$ . Then the marginal survival functions are  $S_x^X(t) = 1 - F_x(t) = S_x(t, 0)$  and  $S_x^Y(t) = 1 - G_x(t) = S_x(0, t), t \geq 0$ . We suppose that the marginal d.f.-s  $F_x$  and  $G_x$  are continuous. Then according to the Theorem of Sclar (see, [1]), the joint survival function  $S_x(t_1, t_2)$  can be expressed as

$$S_x(t_1, t_2) = C_x(S_x^X(t_1), S_x^X(t_2)), \quad t_1, t_2 \geq 0, \quad (1)$$

where  $C_x(u, v)$  is a known copula function depending on  $x, S_x^X$  and  $S_x^Y$  in a general way. We consider estimator of d.f.  $F_x$  which is equivalent to the relative-risk power estimator [2,3] under independent censoring case.

Assume that at the fixed design value  $x \in (0, 1), C_x$  in (1) is Archimedean copula, i.e.

$$S_x(t_1, t_2) = \varphi_x^{-1}(\varphi_x(S_x^X(t_1)) + \varphi_x(S_x^Y(t_2))), \quad t_1, t_2 \geq 0, \quad (2)$$

where, for each  $x$ ,  $\varphi_x : [0, 1] \rightarrow [0, +\infty]$  is a known continuous, convex, strictly decreasing function with  $\varphi_x(1) = 0$ . We assume that copula generator function  $\varphi_x$  is strict, i.e.  $\varphi_x(0) = \infty$  and  $\varphi_x^{-1}$  is an inverse of  $\varphi_x$ . From (2), it follows that

$$\begin{aligned} P(Z_x > t) &= 1 - H_x(t) = \overline{H_x(t)} = S_x^Z(t) = S_x(t, t) = \\ &= \varphi_x^{-1}(\varphi_x(S_x^X(t)) + \varphi_x(S_x^Y(t))), \quad t \geq 0, \end{aligned} \quad (3)$$

Let  $H_x^{(1)}(t) = P(Z_x \leq t, \delta_x = 1)$  be a subdistribution function and  $\Lambda_x(t)$  is crude hazard function of r.v.  $X_x$  subjecting to censoring by  $Y_x$ ,

$$\Lambda_x(dt) = \frac{P(X_x \in dt, X_x \leq Y_x)}{P(X_x \geq t, Y_x \geq t)} = \frac{H_x^{(1)}(dt)}{S_x^Z(t-)}. \quad (4)$$

From (4) one can obtain following expression of survival function  $S_x^X$  :

$$S_x^X(t) = \varphi_x^{-1}\left[-\int_0^t \varphi_x'(S_x^Z(u))dH_x^{(1)}(u)\right], \quad t \geq 0. \quad (5)$$

In order to constructing the estimator of  $S_x^X$  according to representation (5), we introduce smoothed estimators of  $S_x^Z$ ,  $H_x^{(1)}$  and regularity conditions for them. We use the Gasser-Müller weights

$$w_{ni}(x, h_n) = \frac{1}{q_n(x, h_n)} \int_{x_{i-1}}^{x_i} \frac{1}{h_n} \pi\left(\frac{x-z}{h_n}\right) dz, \quad i = 1, \dots, n, \quad (6)$$

with

$$q_n(x, h_n) = \int_0^{x_n} \frac{1}{h_n} \pi\left(\frac{x-z}{h_n}\right) dz,$$

where  $x_0 = 0$ ,  $\pi$  is a known probability density function (kernel) and  $\{h_n, n \geq 1\}$  is a sequence of positive constants, tending to zero as  $n \rightarrow \infty$ , called bandwidth sequence. Let's introduce the weighted estimators of  $H_x$ ,  $S_x^Z$  and  $H_x^{(1)}$  respectively as

$$\begin{aligned} H_{xh}(t) &= \sum_{i=1}^n w_{ni}(x, h_n) I(Z_i \leq t), \quad S_{xh}^Z(t) = 1 - H_{xh}(t), \\ H_{xh}^{(1)}(t) &= \sum_{i=1}^n w_{ni}(x, h_n) I(Z_i \leq t, \delta_i = 1). \end{aligned} \quad (7)$$

Then by pluggin estimators (6) and (7) in (5) we obtained the following intermediate estimator of  $S_x^X$  :

$$S_{xh}^X(t) = 1 - F_{xh}(t) = \varphi_x^{-1}\left[-\int_0^t \varphi_x'(S_{xh}^Z(u))dH_{xh}^{(1)}(u)\right], \quad t \geq 0.$$

In this work we propose the next extended analogue of estimator introduced in [2,3]:

$$\widehat{S}_{xh}^X(t) = \varphi_x^{-1}[\varphi(S_{xh}^Z(t)) \cdot \mu_{xh}(t)] = 1 - \widehat{F}_{xh}(t), \quad (8)$$

where  $\mu_{xh}(t) = \varphi(S_{xh}^X(t))/\varphi(\widetilde{S}_{xh}^Z(t))$ ,  $\varphi(S_{xh}^X(t)) = -\int_0^t \varphi'_x(S_{xh}^Z(u))dH_{xh}^{(1)}(u)$ ,

$\varphi(\widetilde{S}_{xh}^Z(t)) = -\int_0^t \varphi'_x(S_{xh}^Z(u))dH_{xh}(u)$ . In order to investigate the estimate (8) we introduce some conditions. For the design points  $x_1, \dots, x_n$ , denote  $\underline{\Delta}_n = \min_{1 \leq i \leq n} (x_i - x_{i-1})$ ,  $\overline{\Delta}_n = \max_{1 \leq i \leq n} (x_i - x_{i-1})$ .

For the kernel  $\pi$ , let  $\|\pi\|_2^2 = \int_{-\infty}^{\infty} \pi^2(u)du$ ,  $m_\nu(\pi) = \int_{-\infty}^{\infty} u^\nu \pi(u)du$ ,  $\nu = 1, 2$ .

Moreover, we use next assumptions on the design and on the kernel function:

- (A1) As  $n \rightarrow \infty$ ,  $x_n \rightarrow 1$ ,  $\underline{\Delta}_n = O(\frac{1}{n})$ ,  $\overline{\Delta}_n - \underline{\Delta}_n = o(\frac{1}{n})$ .  
(A2)  $\pi$  is a probability density function with compact support  $[-M, M]$  for some  $M > 0$ , with  $m_1(\pi) = 0$  and  $|\pi(u) - \pi(u')| \leq C(\pi)|u - u'|$ , where  $C(\pi)$  is some constant.

Let  $T_{H_x} = \inf\{t \geq 0 : H_x(t) = 1\}$ . Then  $T_{H_x} = \min(T_{F_x}, T_{G_x})$ . For our results we need some smoothness conditions on functions  $H_x(t)$  and  $H_x^{(1)}(t)$ . We formulate them for a general (sub)distribution function  $N_x(t)$ ,  $0 \leq x \leq 1$ ,  $t \in R$  and for a fixed  $T > 0$ .

- (A3)  $\frac{\partial^2}{\partial x^2} N_x(t) = \ddot{N}_x(t)$  exists and is continuous in  $(x, t) \in [0, 1] \times [0, T]$ .  
(A4)  $\frac{\partial^2}{\partial t^2} N_x(t) = N_x''(t)$  exists and is continuous in  $(x, t) \in [0, 1] \times [0, T]$ .  
(A5)  $\frac{\partial^2}{\partial x \partial t} N_x(t) = \ddot{N}'_x(t)$  exists and is continuous in  $(x, t) \in [0, 1] \times [0, T]$ .  
(A6)  $\frac{\partial \varphi_x(u)}{\partial u} = \varphi'_x(u)$  and  $\frac{\partial^2 \varphi_x(u)}{\partial u^2} = \varphi''_x(u)$  are Lipschitz in the  $x$ -direction with a bounded Lipschitz constant and  $\frac{\partial^3 \varphi_x(u)}{\partial u^3} = \varphi'''_x(u)$  exists and is continuous in  $(x, u) \in [0, 1] \times (0, 1]$ .

We derive an almost sure representation result with rate.

**Theorem 1.** Assume (A1), (A2),  $H_x(t)$  and  $H_x^{(1)}(t)$  satisfy (A3)-(A5) in  $[0, T]$  with  $T < T_{H_x}$ ,  $\varphi_x$  satisfies (A6) and  $h_n \rightarrow 0$ ,  $\frac{\log n}{nh_n} \rightarrow 0$ ,  $\frac{nh_n^5}{\log n} = O(1)$ . Then, as  $n \rightarrow \infty$ ,

$$\widehat{F}_{xh}(t) - F_x(t) = \sum_{i=1}^n w_{ni}(x, h_n) \Psi_{tx}(Z_i, \delta_i) + r_n(t),$$

where

$$\begin{aligned} \Psi_{tx}(Z_i, \delta_i) &= \frac{-1}{\varphi'_x(S_x^X(t))} \left[ \int_0^t \varphi''_x(S_x^Z(u))(I(Z_i \leq u) - H_x(u))dH_x^{(1)}(u) - \right. \\ &\quad \left. - \varphi'_x(S_x^Z(t))(I(Z_i \leq t, \delta_i = 1) - H_x^{(1)}(t)) - \right. \\ &\quad \left. - \int_0^t \varphi''_x(S_x^Z(u))(I(Z_i \leq u, \delta_i = 1) - H_x^{(1)}(u))dH_x(u) \right], \end{aligned}$$

and

$$\sup_{0 \leq t \leq T} |r_n(t)| \stackrel{a.s.}{=} O\left(\left(\frac{\log n}{nh_n}\right)^{3/4}\right).$$

The weak convergence of the empirical process  $(nh_n)^{1/2}\{\widehat{F}_{xh}(\cdot) - F_x(\cdot)\}$  in the space  $l^\infty[0, T]$  of uniformly bounded functions on  $[0, T]$ , endowed with the uniform topology is the contents of the next theorem.

**Theorem 2.** Assume (A1), (A2),  $H_x(t)$  and  $H_x^{(1)}(t)$  satisfy (A3)-(A5) in  $[0, T]$  with  $T < T_{H_x}$ , and that  $\varphi_x$  satisfies (A6).

(I) If  $nh_n^5 \rightarrow 0$  and  $\frac{(\log n)^3}{nh_n} \rightarrow 0$ , then, as  $n \rightarrow \infty$ ,

$$(nh_n)^{1/2}\{\widehat{F}_{xh}(\cdot) - F_x(\cdot)\} \Rightarrow \mathbf{W}_x(\cdot) \text{ in } l^\infty[0, T].$$

(II) If  $h_n = Cn^{-1/5}$  for some  $C > 0$ , then, as  $n \rightarrow \infty$ ,

$$(nh_n)^{1/2}\{\widehat{F}_{xh}(\cdot) - F_x(\cdot)\} \Rightarrow \mathbf{W}_x^*(\cdot) \text{ in } l^\infty[0, T],$$

where  $\mathbf{W}_x(\cdot)$  and  $\mathbf{W}_x^*(\cdot)$  are Gaussian processes with means

$$E\mathbf{W}_x(t) = 0, E\mathbf{W}_x^*(t) = a_x(t),$$

and same covariance

$$Cov(\mathbf{W}_x(t), \mathbf{W}_x^*(s)) = Cov(\mathbf{W}_x^*(t), \mathbf{W}_x^*(s)) = \Gamma_x(t, s),$$

with

$$a_x(t) = \frac{-C^{5/2}m_2(\pi)}{2\varphi'_x(S_x^X(t))} \int_0^t [\varphi''_x(S_x^Z(u))\ddot{H}_x(u)dH_x^{(1)}(u) - \varphi'_x(S_x^Z(u))dH_x^{(1)\ddot{}}(u)],$$

and

$$\begin{aligned} \Gamma_x(t, s) &= \frac{\|\pi\|_2^2}{\varphi'_x(S_x^X(t))\varphi'_x(S_x^X(s))} \left\{ \int_0^{\min(t,s)} (\varphi'_x(S_x^Z(z)))^2 dH_x^{(1)}(z) + \right. \\ &+ \int_0^{\min(t,s)} [\varphi''_x(S_x^Z(w))S_x^Z(w) + \varphi'_x(S_x^Z(w))] \int_0^w \varphi''_x(S_x^Z(y))dH_x^{(1)}(y)dH_x^{(1)}(w) + \\ &+ \int_0^{\min(t,s)} \varphi''_x(S_x^Z(w)) \int_w^{\max(t,s)} (\varphi''_x(S_x^Z(y))S_x^Z(y) + \varphi'_x(S_x^Z(y)))dH_x^{(1)}(y)dH_x^{(1)}(w) - \\ &\quad - \int_0^t [\varphi''_x(S_x^Z(y))S_x^Z(y) + \varphi'_x(S_x^Z(y))]dH_x^{(1)}(y) \cdot \\ &\quad \left. \cdot \int_0^s [\varphi''_x(S_x^Z(w))S_x^Z(w) + \varphi'_x(S_x^Z(w))]dH_x^{(1)}(w) \right\}. \end{aligned}$$

## References

- [1] Nelsen R.B. (1999). *An Introduction to Copulas*. Springer, New York.
- [2] Abdushukurov A.A. (1998). Nonparametric estimation of distribution function based on relative risk function. *Commun. Statist.: Theory and Methods*. Vol. **27**, No.8, pp. 1991-2012.
- [3] Abdushukurov A.A. (1999). On nonparametric estimation of reliability indices by censored samples. *Theory Probab. Appl.* Vol. bf 43, No. 1, pp. 3-11.

# PREDICTING THE SUCCESS OF ANTEGRADE CHRONIC TOTAL OCCLUSION RECANALIZATION USING MACHINE LEARNING

M.S. ABRAMOVICH<sup>1</sup>, V.V. KOZLOVSKY<sup>1</sup>, V.I. STELMASHOK<sup>2</sup>,  
O.L. POLONETSKY<sup>2</sup>

<sup>1</sup>*Research Institute for Applied Problems of Mathematics and Informatics*

<sup>2</sup>*Republican Scientific and Practical Centre of Cardiology  
Minsk, BELARUS*

e-mail: Abramovichms@bsu.by

## Abstract

The problem of predicting the success of antegrade coronary arteries chronic total occlusion recanalization, based on X-ray anatomical and clinical markers is considered. The results of comparative analysis of the prediction accuracy based on various machine learning algorithms are presented.

**Keywords:** data science, machine learning, recanalization

## 1 Introduction

Chronic total occlusion (CTO) of the coronary arteries is a frequently detectable type of coronary lesion in patients with ischemic heart disease [1]. Successful restoration of antegrade blood flow by interventional techniques allows to improve the quality of life [2]. However, the indications for interventional CTO recanalization are based on the clinical signs, without taking into account the technical complexity of this procedure and the risk of possible failure of percutaneous coronary intervention.

The most important stage of CTO correction by interventional methods is the CTO crossing by coronary wire; majority of unsuccessfully performed operations are due to the inability to perform this manipulation. Minimization the frequency of unsuccessful CTO crossing by coronary wire will optimize the treatment quality in this group of patients as well as reduce the risk of possible complications.

Analysis of the literature has shown the absence of specific prognostic scales to predict the success of antegrade CTO crossing by coronary wire. This fact as well as the significance of the identified problem mean that it is critically important to develop a system for predicting the success of antegrade coronary arteries CTO recanalization.

Various methods of machine learning such as logistic regression, decision tree and random forest to predicting the success of antegrade chronic total occlusion recanalization are used. Optimal parameters for methods were found and the maximal accuracy was obtained on these parameters.

## 2 Materials and methods

The present study was retrospective, single-center, and included data from 395 patients whom attempts of coronary arteries CTO recanalization were performed during the

period from 2009 to 2018. Based on the success of the coronary wire passage through the CTO zone all of the above-mentioned patients were divided into the 2 groups: patients with successful ( $n_1=292$ ) and failed ( $n_2=103$ ) CTO recanalization.

77 clinical and X-ray anatomical markers are analysed.

First, the sample is divided: train data with 264 patients and test data with 131 patients. Then logistic regression with  $l1$  regularization is trained on test data.

Feature selection was made using LASSO method [3]. Importance features are ones with nonzero weights. The process repeats until the number of features decreases.

Various methods of machine learning such as logistic regression, decision tree and random forest to predicting the success of antegrade chronic total occlusion recanalization are used.

Selection of hyperparameters was made on a grid using cross validation. For evaluating each set of hyperparameters train data is divided into 4 folds. Then model trains on 3 folds and the last fold is used for testing. The process repeats 4 times; finally, each part is used for testing. As a result, we got performance evaluation for given set of hyperparameters with uniform using of data.

In table 1 grid parameters of methods are presented.

Table 1: Grid parameters of methods

Method	Parameter	Values	Description
Logistic regression	penalty	'l2', 'l1'	used to specify regularization
	C	0.8, 0.9, 1, 1.1, 1.2, 1.3, 1.4	inverse of regularization strength
Decision tree	max_depth	2, 4, ..., 18	the maximum depth of the tree
	criterion	'gini', 'entropy'	function to measure the quality of split
	min_samples_split	2, 4, 6, 8	the minimum number of samples to split inner node
	min_samples_leaf	2, 4, 6, 8	the minimum number of samples in leaf node
Random forest	n_estimators	10, 60, 110, 160, 210	number of trees in the forest
	max_depth	2, 3, 4, 5	the maximum depth of each tree
	criterion	'gini', 'entropy'	function to measure the quality of split
	min_samples_split	2, 3, 4	the minimum number of samples to split inner node
	min_samples_leaf	2, 3, 4	the minimum number of samples in leaf node

### 3 Results

In table 2 importance features for classification of patients with successful and failed CTO recanalization are presented. Features are ranked on a 0 – 100 scale in terms of their potential importance.

Table 2: Features importance

Feature	Importance
What coronary artery segment?	100
Blunt CTO stump	71
Soft tapered tip wires as first choice	61
Level of CTO complexity	48
Middle stiffness non-tapered tip wires as a first choice	44
Wire toughening and support	41
Number of wires used for CTO recanalization	35
Is the tortuosity in the CTO zone?	27
If yes, number of side branches	21

In table 3 results of the grid search for machine learning methods and the accuracy patients classification with successful and failed CTO recanalization on train sample are presented.

Table 3: Accuracy patients with successful and failed CTO recanalization

Method	Best parameters	Results on cross validation
Logistic regression	penalty: 'l2' C: 0.8	0.7803
Decision tree	criterion: 'entropy' max_depth: 4 min_samples_leaf: 6 min_samples_split: 2	0.7771
Random forest	n_estimators: 60 criterion: 'gini' max_depth: 2 min_samples_leaf: 3 min_samples_split: 3	0.7924

In figure 1 ROC curves and AUC values for logistic regression, decision tree and random forest on test sample are presented. Logistic regression shows the best result on the test sample.

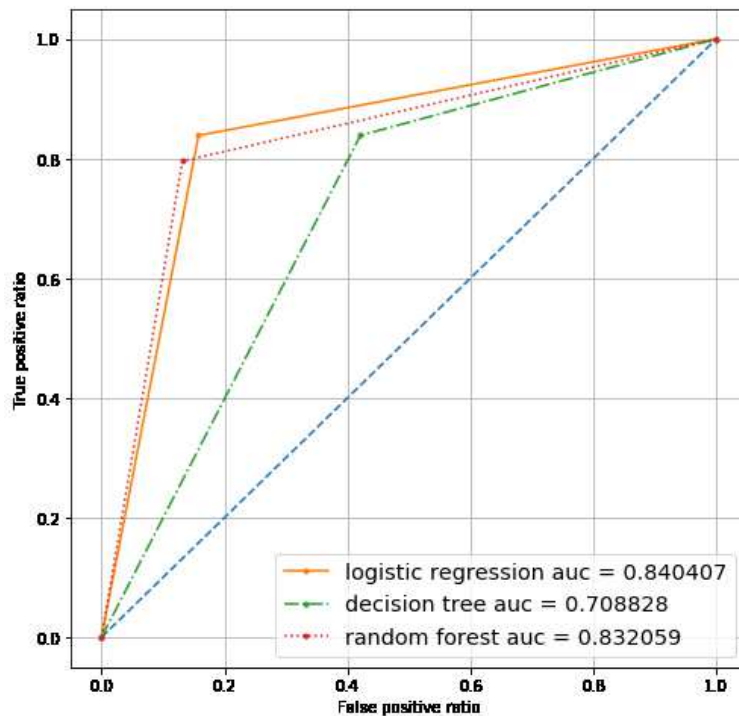


Figure 1: ROC curves

## References

- [1] Di Mario C., Werner G., Sianos G., Galassi A., Büttner J., Dudek D., Chevalier B., Lefevre T., Schofer J., Koolen J., Sievert H., Reimers B., Fajadet J., Colombo A., Gershlick A., Serruys P., Reifart N. (2007). Perspective in the recanalization of Chronic Total Occlusions (CTO): consensus document from the EuroCTO Club. *EuroIntervention*. Vol. **3(1)**, pp. 33-43.
- [2] Werner G., Martin-Yuste V., Hildick-Smith D., Boudou N., Sianos G., Gelev V., Rumoroso J.R., Erglis A., Christiansen E.H., Escaned J., di Mario C., Hovasse T., Teruel L., Bufe A., Lauer B., Bogaerts K., Goicolea J., Spratt J.C., Gershlick A.H., Galassi A.R., Louvard Y. (2018). A randomized multicentre trial to compare revascularization with optimal medical therapy for the treatment of chronic total coronary occlusions. *Eur Heart J*. Vol. **39(26)**, pp. 2484-2493.
- [3] Harrington P. (2012) *Machine Learning in Action*. Manning. New York.

# ON PARAMETER ESTIMATION OF DOUBLE-CENSORED STATIONARY GAUSSIAN TIME SERIES

I.A. BADZIAHIN

*Belarusian State University*

*Minsk, BELARUS*

e-mail: [bodiagin@bsu.by](mailto:bodiagin@bsu.by)

## Abstract

Double-censored stationary Gaussian time series are considered. Statistical estimators of the model parameters are constructed by using the method of moments for special auxiliary time series. Consistency of constructed estimators are proved under some additional general conditions.

**Keywords:** data science, censored data, Gaussian time series, estimation

Consider double-censored Gaussian time series  $x_t$ . It means that instead of the exact values  $x_1, \dots, x_T$  at the time moments  $T_C^+ = \{t : x_t \geq c_+\}$  and  $T_C^- = \{t : x_t \leq c_-\}$  only random events are observed [2, 3]:

$$A_t^+ = \{x_t \in [c_+, +\infty)\}, t \in T_C^+,$$

$$A_t^- = \{x_t \in (-\infty, c_-]\}, t \in T_C^-,$$

where  $c_-$  and  $c_+$  are the lower and upper censoring levels ( $c_- < c_+$ ),  $T$  is the length of the observation process. In other words term “double-censored” means that at the same time we have left and right censoring.

Let  $X = (x_1, \dots, x_T)' \in \mathbf{R}^T$  be the vector of the exact observations. Then for Gaussian time series the vector  $X$  has a normal distribution  $\mathcal{L}(X) = \mathcal{N}(\mu, \Sigma)$ , where the mathematical mean  $\mu$  and the covariance matrix  $\Sigma$  depend on some unknown parameter  $\theta \in \Theta \subseteq \mathbf{R}^m$  of the time series model (e.g. for AR( $p$ ) model  $\theta = (\varphi_1, \dots, \varphi_p, \sigma^2)$ , where  $\varphi_1, \dots, \varphi_p$  are the coefficients of the autoregression and  $\sigma^2$  is the variance of the Gaussian innovation process) [1].

Define the auxiliary time series  $y_t$  for the double-censored time series  $x_t$  [3]:

$$y_t = \begin{cases} x_t, & x_t \in (c_-, c_+), \\ c_-, & x_t \leq c_-, \\ c_+, & x_t \geq c_+. \end{cases}$$

By using the method of moments for auxiliary time series  $y_t$  the  $m$  values of the second moments  $\sigma_\tau = E\{x_t x_{t+\tau}\}$  for the initial time series  $x_t$  can be estimated, i.e. estimators  $\hat{\sigma}_\tau$ , ( $\tau \in \{0, 1, \dots, m-1\}$ ) can be found. By using  $\hat{\sigma}_\tau$  and the method of moments for initial time series  $x_t$  estimators of the model parameters  $\hat{\theta}$  can be calculated. The consistency of the constructed estimators  $\hat{\theta}$  are proved. Proposed procedure obviously can be used for only left or only right censored data.

The example of this estimation procedure is proposed for the AR(2) model. Results of this example is illustrated on figure 1. As we can see empirical variances of the constructed estimators tend to zero and this result is agreed with consistency of the constructed estimators.

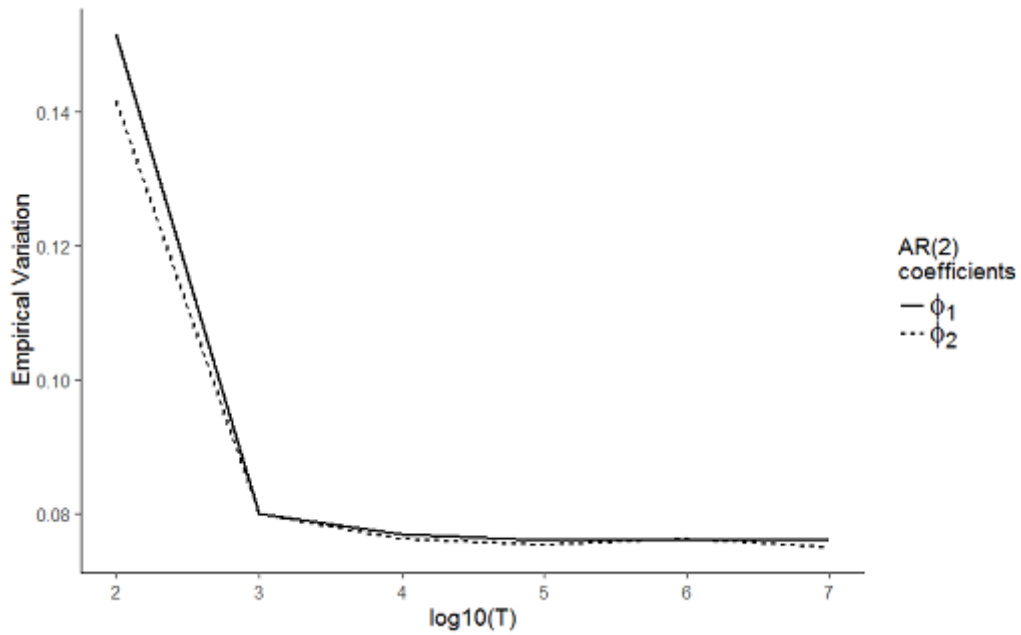


Figure 1: Dependence of empirical variances for the AR(p) coefficients on time series length  $T$  ( $c_- = 0$ ,  $c_+ = 2$ )

## References

- [1] Anderson T.W. (1971). *The Statistical Analysis of Time Series*. John Wiley & Sons, New York.
- [2] Kharin Yu.S. (2013). *Robustness in Statistical Forecasting*. Springer, Heidelberg/Dordrecht/New York/London.
- [3] Park J.W., Genton M.G., Ghosh S.K. (2007). Censored time series analysis with autoregressive moving average models. *The Canadian Journal of Statistics*. Vol. **35**, No. 1, pp. 151-168.

# MODELING BALTIC MARKET INDICES: A COMPARISON OF MODELS

I. BELOVAS

*Vilnius University Institute of Data Science and Digital Technologies*

*Vilnius Gediminas Technical University*

*Vilnius, LITHUANIA*

e-mail: igoris.belovas@mii.vu.lt

## Abstract

In this paper we perform a statistical analysis of the returns of Baltic market indices. We construct symmetric  $\alpha$ -stable, non-standardized Student's  $t$  and normal-inverse Gaussian models, using maximum likelihood method for the estimation of the parameters of the models. The adequacy of the modeling is evaluated with the Kolmogorov tests for composite hypothesis. The results of the study indicate that the normal-inverse Gaussian model provides the best overall fit for the data.

**Keywords:** data science, market index,  $\alpha$ -stable model

## 1 Introduction

Modeling of the returns of stock indices of developed and emerging markets always has been significant and controversial topic, since principal models in financial theory (mean-variance portfolio, capital asset pricing, prices of derivative securities) critically rely on underlying stock returns distribution form. A summary of the literature, covering the history of mainstream models, one may find in [1, 5, 6, 9] and references therein.

In our previous research [2] we have investigated the goodness-of-fit of ten major models (normal, mixture of normals, Student's  $t$ , logistic, exponential power, mixed diffusion-jump model, normal-inverse Gaussian, scaled symmetrized gamma,  $\alpha$ -stable and symmetric  $\alpha$ -stable) to five Standard & Poor's stock market indices. These indices covered the period of ten years (from 2006-04-28 to 2016-05-31). Only  $\alpha$ -stable, Student's- $t$  and normal-inverse Gaussian distributions properly described daily returns of all five Standard & Poor's indices.

In this paper we compare three above mentioned distributions, representing empirical returns of three Baltic market indices. These indices (OMX Tallinn, OMX Riga and OMX Vilnius) are the components of the Nasdaq Baltic index family. They include the shares listed on the Main and Secondary lists of the Baltic exchanges and reflect the current status and changes in each market or the Baltic Market as a whole.

## 2 Candidate models

**Non-standardized Student's  $t$ -distribution (NSS)** is a three-parameter generalization of classical Student's  $t$ -distribution ("arguably the simplest and the most well

known model for stock returns" [1]) with the density function

$$f_{NSS}(x; \nu, \mu, \sigma) = \frac{1}{\sigma} f_S \left( \frac{x - \mu}{\sigma}; \nu \right) = \frac{\Gamma \left( \frac{\nu+1}{2} \right)}{\sqrt{\pi\nu\sigma} \Gamma \left( \frac{\nu}{2} \right)} \left( 1 + \frac{1}{\nu} \left( \frac{x - \mu}{\sigma} \right)^2 \right)^{-\frac{\nu+1}{2}},$$

where  $f_S(x; \nu)$  is Student's  $t$ -distribution (with  $\nu > 0$  degrees of freedom) probability density function,  $\mu$  is a location parameter, and  $\sigma > 0$  is a scale parameter [1].

**Symmetric Normal-Inverse Gaussian distribution** (SNIG) has the density function [5]

$$f_{SNIG}(x; \alpha, \mu, \sigma) = \frac{\alpha\sigma e^{\alpha\sigma}}{\pi\sqrt{\sigma^2 + (x - \mu)^2}} K_1 \left( \alpha\sqrt{\sigma^2 + (x - \mu)^2} \right),$$

where  $K_1(x)$  denotes the modified Bessel function of the third kind,  $\alpha > 0$  is a tail heaviness (shape) parameter,  $\mu$  is a location parameter, and  $\sigma > 0$  is a scale parameter. In order to standardize the NIG distribution, we modify the parametrization of the distribution by setting  $\bar{\alpha} = \alpha\sigma$ . The modified (now scale-invariant) representation (MSNIG) has the density function (cf. [6])

$$f_{MSNIG}(x; \bar{\alpha}, \mu, \sigma) = \frac{1}{\sigma} f_{SMSNIG} \left( \frac{x - \mu}{\sigma}; \bar{\alpha} \right),$$

where  $f_{SMSNIG}(x; \bar{\alpha})$  stands for the standard MSNIG density,

$$f_{SMSNIG}(x; \bar{\alpha}) = \frac{\bar{\alpha} e^{\bar{\alpha}}}{\pi\sqrt{1+x^2}} K_1 \left( \bar{\alpha}\sqrt{1+x^2} \right) = \frac{\bar{\alpha} e^{\bar{\alpha}}}{2\pi} \int_0^\infty t^{-2} e^{-\frac{\bar{\alpha}}{2} \left( t + \frac{1+x^2}{t} \right)} dt.$$

Thus, the cumulative distribution function of SMSNIG distribution can be written in terms of the cumulative distribution function of the standard normal distribution  $\Phi(x)$ ,

$$F_{SMSNIG}(x; \bar{\alpha}) = \sqrt{\frac{\bar{\alpha}}{2\pi}} e^{\bar{\alpha}} \int_0^\infty t^{-3/2} \exp \left( -\frac{\bar{\alpha}}{2} \left( t + \frac{1}{t} \right) \right) \Phi \left( x\sqrt{\frac{\bar{\alpha}}{t}} \right) dt.$$

**Symmetric  $\alpha$ -stable distribution** (S $\alpha$ S) has the density function [4]

$$f_{S\alpha S}(x; \alpha, \mu, \sigma) = \frac{1}{\sigma} f_{SS\alpha S} \left( \frac{x - \mu}{\sigma}; \alpha \right) = \frac{1}{\pi\sigma} \int_0^\infty e^{-t^\alpha} \cos \left( \frac{x - \mu}{\sigma} t \right) dt,$$

where  $\alpha \in (0, 2]$  is a stability parameter,  $\mu$  is a location parameter,  $\sigma > 0$  is a scale parameter and  $f_{SS\alpha S}(x; \alpha)$  stands for the standard S $\alpha$ S density. The cumulative distribution function for the standard S $\alpha$ S distribution is

$$F_{SS\alpha S}(x; \alpha) = \frac{1}{2} + \frac{1}{\pi} \int_0^\infty t^{-1} e^{-t^\alpha} \sin(xt) dt.$$

We estimate parameters of these three models by the maximum likelihood method, maximizing the log-likelihood function (ML),

$$\hat{l}(\Theta) = \frac{1}{n} \sum_{k=1}^n \log f(x_k; \Theta), \quad (1)$$

where  $\Theta$  is a vector of parameters. It is the most accurate (albeit time consuming) method, if applied without parallel computing (cf. [3, 4]).

### 3 Empirical data

The empirical data sets under consideration are daily logarithmic returns of Baltic stock market indices belonging to the Nasdaq Baltic index family. The countries and their representative indices are: Estonia (OMX Tallinn), Latvia (OMX Riga) and Lithuania (OMX Vilnius) [8]. These indices include the shares listed on the Main and Secondary lists of the Baltic exchanges and reflect the current status and changes in each market or the Baltic Market as a whole. The data covers the period of ten years (from 2009-07-01 to 2019-02-19) with the lengths of the series  $n = 4878$ .

### 4 Results

The estimated parameters of the models, obtained by maximizing the log-likelihood function (1), can be found in Table 1. To quantify the goodness-of-fit of the model-

Table 1: Estimated parameters and goodness-of-fit statistics (“\*” means rejected).

2009-2019		Estimated parameters, $\hat{\Theta}$				Goodness-of-fit st.	
Index	Model	Shape	Location	Scale	$\hat{l}(\Theta)$	$D_n(\hat{\Theta})$	$D_P(n, \hat{\Theta})$
OMX Tallinn	S $\alpha$ S	1.3951	0.0004	0.0040	3.4052	0.0152	0.0153
	NSS	2.1349	0.0004	0.0048	3.4139	0.0141	0.0155
	MSNIG	0.2520	0.0004	0.0049	3.4184	0.0092	0.0182
OMX Riga	S $\alpha$ S	1.4922	0.0003	0.0055	3.1593	0.0179*	0.0152
	NSS	2.1035	0.0003	0.0066	3.1686	0.0131	0.0149
	MSNIG	0.3497	0.0003	0.0070	3.1713	0.0108	0.0208
OMX Vilnius	S $\alpha$ S	1.3983	0.0004	0.0031	3.6432	0.0167*	0.0156
	NSS	2.0108	0.0004	0.0037	3.6483	0.0161*	0.0153
	MSNIG	0.1928	0.0003	0.0036	3.6480	0.0162	0.0191

ing, Kolmogorov tests are used. However, for a composite hypothesis testing (a model belongs to a distribution family, and parameters of a model are estimated from the sample we use to quantify the goodness-of-fit) the classical Kolmogorov test is not applicable, since the limiting distribution of the Kolmogorov test statistics no longer distribution-free. It is influenced by the law, corresponding to the null hypothesis, the type and the number of parameters of the law, the method of parameter estimation. Because of that, critical values  $D_P(n, \hat{\Theta})$  of Kolmogorov tests for composite hypotheses are calculated (with the significance level  $P = 0.05$ ) by Monte-Carlo methodology, proposed by Lemeshko et al. [7]. Results of the comparison of the models are summarized in Table 1.

## 5 Conclusions and discussion

As we can see from Table 1, the symmetric  $\alpha$ -stable model performed the worst. Two time it was rejected. We can see that the non-standardized Student's  $t$  and the modified symmetric normal-inverse Gaussian distribution had better goodness-of-fit values.

The normal-inverse Gaussian outperforms alternative heavy-tailed models (note that it corroborates with the recent findings, see [9]), while the non-standardized Student's  $t$  model provides the second best overall fit for the data (cf. [5]).

It should be noted that the four-parameter normal-inverse Gaussian family could be reduced to the three-parameter symmetric normal-inverse Gaussian or modified symmetric normal-inverse Gaussian model without much loss (cf. [9]). The problem of stability of the distribution of returns over different time periods requires special attention.

## References

- [1] Afuecheta E., Chan S., Nadarajah S. (2018) Flexible models for stock returns based on Student's  $t$  distribution. *The Manchester School*, pp. 1–25.
- [2] Belovas I., Sakalauskas L. (2016). Modeling financial data distributions: A comparison of models. In: *Computer Data Analysis and Modeling: Theoretical and Applied Stochastics: Proceedings of the XI International Conference, Minsk, September 6-10, 2016*, pp. 194–197.
- [3] Belovas I., Starikovičius V. (2007). Parallelization of  $\alpha$ -stable modelling algorithms. *Mathematical Modelling and Analysis*. Vol. **12**(4), pp. 409–418.
- [4] Belovas I., Starikovičius V. (2015). Parallel computing for mixed-stable modelling of large data sets. *Information Technology and Control*. Vol. **44**(2), pp. 148–154.
- [5] Corlu C.G., Corlu A. (2015) Modelling exchange rate returns: which flexible distribution to use? *Quantitative Finance*. Vol. **15**(11), pp. 1851–1864.
- [6] Eriksson A., Ghysels E., Wang F. (2009) The normal inverse Gaussian distribution and the pricing of derivatives. *The Journal of Derivatives*. Vol. **16**(3), pp. 23–37.
- [7] Lemeshko B., Lemeshko S., Rogozhnikov A. (2011) Real-Time Studying of Statistic Distributions of Non-Parametric Goodness-of-Fit Tests when Testing Complex Hypotheses. *The International Workshop "Applied Methods of Statistical Analysis. Simulations and Statistical Inference" – AMSA-2011*. Vol. **1**, pp. 19–27.
- [8] Nasdaq Baltic. Mode of Access: <https://www.nasdaqbaltic.com/market/>. Date of Access: 18.05.2019.
- [9] Suárez-García P., Gómez-Ullate D. (2013) Scaling, stability and distribution of the high frequency returns of the IBEX 35 index. *Physica A*. Vol. **392**(6), pp. 1409–1417.

# TOURISM IN BELARUS: INDICATORS, SATELLITE ACCOUNT AND SURVEYS

N. BOKUN

*Belarus State Economic University*

*Minsk, BELARUS*

e-mail: nataliabokun@rambler.ru

## Abstract

The paper describes the tourism satellite account methodology, main tourism trends, problems of introduction of tourism households and establishment surveys in practice of Belarusian official statistics. The sampling frame, sampling design, precision estimation information sources are considered.

**Keywords:** satellite account, tourism, households survey, establishment survey, sample

## 1 Introduction

In recent years, the growing number of destinations worldwide has opened up and invested in tourism turning it into a key driver of socio-economic progress. Tourism is a complex phenomenon which is becoming one of the world's largest economic activities. International tourist arrivals have increased from 25 million globally in 1950 to 1,323 million in 2017. International tourism receipts earned by destinations worldwide have surged from US \$ 2 billion in 1950 to US \$ 1,340 billion in 2017. Tourism represents 7 % of the world's export, has grown faster than world trade for the last five years [1].

The Tourism Statistics (TS) as part of the National System of Statistics is viewed as basic framework for coordination of statistical information on tourism as product by all types of stakeholders. The TS is a set of interconnected components comprising statistical sources, households surveys, tourism industry entities surveys, administrative records, Balance of payments, National Accounts.

The multiplicity of information resources, kinds of tourism activity, indicators have motivated the development of tourism satellite account, methodology for specialized surveys. The first results of their use in Belarus indicated the appearance of significant problems: non-responses, enough high level of sample and non-sample errors, discrepancies between data from these surveys.

This paper has the next parts: 1) main indicators and trends; 2) tourism satellite account and possible information sources; 3) tourism households surveys; 4) tourism establishment surveys.

## 2 Main indicators and trends

In 2014-2017 tourism contributes directly around 2.5 % of GDP, using to 6 % if indirect impacts are also included (Travel and Tourism Economic Impact 2017 Belarus). Export revenues from tourism amount to approximately US \$ 700-800 million annually,

Table 1: Main tourism indicators

Indicators	2010	2015	2016	2017
Total domestic trips, thousand	79.0	836.8	1001.8	976.8
Total international arrivals, thousand	120.1	276.3	217.4	282.7
Trips of Belarus citizens, thousand	7464.2	6962.4	8339.6	9208.6
Tourism receipts, billion rubles	156.7	1129.6	136.6	165.9
Export by "trips", million US \$	440.4	728.7	710.6	789.8
Import by "trips", million US \$	621.5	901.1	806.1	992.2
Number of hotel and similar establishments	693	1014	1052	1072
Total international departures	414.7	736.7	495.8	727.5

equivalent to 1.5-2 % of total exports of goods and services. In 2017 11.1 million people visited Belarus. 40 % of the clients in accommodation establishments were foreign tourists (Table 1).

Main top markets of inbound tourism are Russian Federation, Poland, Lithuania, Latvia, Ukraine. Main destinations of outbound tourism are Turkey, Egypt, Ukraine, Bulgaria, Russian Federation.

The following tourism trends in Belarus are observed:

- the tourism industry has been growing consistently, international tourist arrivals in 2017 grew by 30%;
- travel for holidays, recreation and over half of all international tourist arrivals and departures; some 10 % of all international tourist trips are travel for business and professional purposes;
- one of major tourism spheres is supporting international conferences, cultural and sport events;
- low level of service, low quality of tourism industries, low development rates of alternative kinds of tourism, low tourism efficiency;
- main statistical problems: careless, partial and discordant of information, data.

One of important directions of the tourism estimation is development of tourism satellite account.

### 3 Tourism satellite account and possible information sources

The multiplicity of stakeholders involved in the tourism system (international organizations, national, regional, local administrations) implies different needs in terms of typologies of information: from tourism demand to the economic role and impacts of tourism; from statistical data to quantitative analyses. The final result is an enormous and growing request for information which requires different methodologies. That is

why it is necessary to increase efforts to harmonize methodologies, develop tourism satellite account.

Nowadays the National Statistical Committee of the Republic of Belarus does preparatory work on development of tourism satellite account. In 2017 Methodological Recommendations for construction of Tourism satellite account (TSA) were adopted [2]. Since 2017-2018, the first tables of this account are calculated. Their main aims are:

- to measure the contribution of tourism to the national economy, in line with the National Accounts framework, and thus allowing comparisons with other economic domains (output and value added by tourism industry, employment, tourism consumption, demand);
- to achieve total coverage in terms of visitors, their expenditures, and the industries serving visitors, as well as reasoned reconciliation of different statistical sources involved, in order to ensure consistency among the data derived from them;
- to become part of the system of information in which individual sources are interconnected (for instance annual data are consistent with monthly or quarterly data);

Two aspects of tourism are measured: a) consumption of commodities and services by visitors (demand); b) production of tourist commodities and services by industries (supply).

Tourism expenditures are accounted by kinds of activity: accommodation of visitors, services of public catering entities, transports, tourism industry entities, sporting and others. Consumption consists of visitors consumption, gross fixed capital formation related to tourism and consumption of collective non marked services (education, museums, public health). Supply indicators include tourist product by kinds of activity; observed unit is entity.

TSA consists of seven components: 1) domestic, inbound, outbound, national tourism indicators (tables 1-4); 2) production account by tourism industries (table 5); 3) total domestic demand and supply (table 6); 4) employment (table 7); 5) gross fixed capital formations related to tourism (table 8); 6) collective non marked services (table 9); 7) non-monetary indicators (number of hotels, accommodation capacity, arrivals, departures and others).

TSA based on using of International Recommendations for Tourism Statistics 2008, WTO technical manuals on TSA [3,4], National methodological recommendations, is formed once in two years (since 2017). The main sources and instruments for formation of TSA include tourism industry enterprises censuses and system of different surveys: establishment, households samples.

## 4 Tourism households surveys

The main aim is asking residents in their usual environment about tourism expenditures, trips they have taken, after reference period. Two procedures to measure domestic tourism can be used: 1) specifically designed surveys to estimate tourism activity of the resident population through questionnaires or light telephone surveys (CATI); questions in the latter case need to be simpler and direct; 2) the inclusion of a “tourism module” – a set of interconnected questions to learn more about certain characteristics of visitor behavior – as part of multipurpose surveys. In Belarus the second procedure is used.

Since 1995 *Sample Survey of Households (HH)* is carried out at all country regions and separately in Minsk. It has annually covered 0.2 % or 6000 HH. Territorial probabilistic three-stage sample is used: at the first step sampling units are cities and rural soviets; at the second step – local-polling districts in city and data of the soviet account in rural soviets; at the third – HH. Procedure of selection of administrative and territorial units repeats once in 10 years. Selection of polling districts and HH is carried out annually. The methodology of weighing of the selective data is based on assignment of each finite unit (HH) the corresponding weight:  $B_i = (p_1 p_2 p_3)^{-1}$ , where  $p_1$  is the probability of selection of each city and rural soviet;  $p_2$  is the probability of selection of each polling district in cities, zones in rural soviet;  $p_3$  is the probability of selection of every HH within polling district or a zone.

The sample program assumes filling of some questionnaires (living conditions, education, health, employment) and additional tourism module (trips, duration, tourism expenditures). Daily and quarterly questionnaires include questions about expenses on food and unfood, payment of services [5].

Since 2012 *Labour Force Survey* is conducted. Its purpose is to obtain empirical statistics on the Labour Force, employed by kinds of activity, including tourism. Survey object is the private households in urban and rural areas for each region; resident persons aged 15 – 74 years. Territorial three-stage sampling, basic weights with different probabilities, individual weights, calculated by two iterations, are used. Variables of weighting include sex, age, region, rural/urban. Sampling frame is based on the 2009 census and includes sets of cities, village councils, census enumeration districts in each selected city, villages, the household totality. Non-response weights are calculated using the weighting classic method. There are 25 census enumeration districts in cities and 16 village councils [6].

*Sample Survey of individuals at automobile roads checkpoints across the State border* is conducted (since 2015). Its main aims are to obtain statistical data on the volumes of commodities, imported or exported by individuals and information on the tourism expenditures and tourism trips. Two forms of blanks for inbound and outbound tourism are used; frequency: twice a year in the II and IV quarters [7].

## 5 Tourism establishment surveys

Purpose of the tourist establishment sample surveys is receipt of detailed information on the tourism, production, employment in the informal sector, on the structure of tourism industries.

*Micro-entities Sample Survey* provides information on the tourism micro-entities. Its sampling frames include: 1) micro-entities, represented the state statistical reports on the financial results for basic year (report 1-MP (micro)); 2) set of the private farms. The first file is 80 thousand units; sample fraction depends on a character of the initial information, namely: the size of total population, kind of economic activity, region. The second array includes more than 2 thousand farms; it is observed completely.

The combination of univariate and multivariate samples is used. To receive optimal sample size for  $i$ -th kind of activity and  $j$ -th region the author has developed the next algorithm:

1. The set of observed variables is allocated (for example, the wages fund, volume of production, revenues, profitability). Average, total values, variability of indicators are calculated.
2. Statistician chooses sampling method: univariate or multivariate. It should be executed one of three conditions for applying multidimensional sampling: a) variation coefficient is more than 100 %; b) survey objects are non-uniform on many variables; c) the small size of total population (top limit – 30 – 40 units). Otherwise univariate sampling should be used: random selection without allocation, simple random sample, proportional and optimal allocation.
3. It is expediently to use univariate stratified sample, total population is divided by rather homogenous groups. Then different variants of the sample size are executed (minimal is  $0.05N$ , maximal is  $0.8N$ ). Minimal error is a main criteria of the determination of sample size. The choice of an optimum way of selection for carrying out of particular survey depends on a survey object and character of the auxiliary information, namely: degrees of uniformity, the sample size, presence of the natural isolated groups. It is expedient to approve several sampling designs for the same survey and to choose that from them which gives more precise and unbiased estimates. It is expedient to use multivariate sample, selection is carried out by cluster analysis: total population is partitioned using cluster analysis on homogenous groups to  $k$ -variables, i.e. clustering; in each received group the leading (basic) variable is determined and subsequent random selection of units is performed. Optimal sample population is chosen for each cluster, where standard errors of  $k$ -variables are criterias of productivity. If the error exceeds admissible bounds, three methods of its reduction may be applied: increasing sample population in cluster; additional stratification of the enterprises in cluster to a leading variable; repetition of clustering [8,9].

Sample population is formed once a three-four years, sampling fraction is 20-21 %. Extrapolation of sample data on the total population is carried out by three methods: traditional group weights (HT); calibration (GREG- and SYN-estimators).

Since 2015 *Visitor Survey at collective accommodation establishment (VS)* is conducted. The main purpose is estimation of visitor expenditures: average expenditures per day are measured. These expenditures consist of accommodation, food and beverages, transport, car rental, recreation services, culture, others. Observed units are visitors and accommodation establishments (hotels and similar); sampling frames are collective accommodation establishments, represented in state statistical reports ((4-tur (accommodation)). Establishment stratification is carried out by the main variable – average value of bed-place [2].

## 6 Concluding remarks

The experience of construction of samples in Belarus has shown that the priority is given to inclusion of a “tourism module” as part of multipurpose survey (Sample Survey of Households Living Standards, Labour Force Survey, Micro-entities Sample Survey); main problems are connected with localization of the sample, non-responses (30-40 %), the enough high level of errors. The use of combination of univariate and multivariate samples, quasicausal samples, expert estimates, tertiary sources, increase of sample size of Border surveys, updating existing questionnaires, carrying out special surveys (transport, recreation) will provide more reliable information over larger number of tourism demand and tourism supply indicators.

## References

- [1] UN WTO (2017). *Tourism Highlights*.
- [2] Belstat (2017). Methodological Recommendation for construction of Tourism satellite account (TSA). Minsk (in Russian).
- [3] *International Recommendation for Tourism Statistics 2008. Compl. Guide*. (2010).
- [4] *European Implementation Manual on TSA*. (2014).
- [5] Belstat (2014). Instruction for organization and holding Sample Survey of Households Living Standards. Minsk (in Russian).
- [6] Belstat (2011). Instruction for organization and holding Sample Survey of Households in order to investigate problems of population employment. Minsk (in Russian).
- [7] Belstat (2016). Instruction for organization and holding Sample Survey of individuals at automobile roads checkpoints across the State border of the Republic of Belarus. Minsk (in Russian).
- [8] Belstat (2014). Instruction for organization and holding State Sample Survey for financial activity of micro-entities. Minsk (in Russian).
- [9] Bokun, N. (2016). Micro-entities and small enterprises survey in Belarus. *Proc. XI Intern. Conf. CDAM*, Minsk, Sept. 6-10, 2016, pp. 240–245.

# PROBABILISTIC APPROACH IN FACTORIZATION BY ELLIPTIC CURVE METHOD

I. DERMENZHY, G. VOSTROV  
*Odessa national polytechnic university*  
*Odessa, UKRAINE*

e-mail: ivandermenji97@gmail.com, vostrov@gmail.com

## Abstract

The aim of this work is the analysis of the elliptic curve factorization method by using probabilistic number theory apparatus. Particularly, the relationship between the amount generated curves and the required boundary problem research.

**Keywords:** elliptic curve, factorization, probabilistic number theory

## 1 Introduction

A new probabilistic number theory approach is defined by Erdos-Kac theorem [2] and E. Kowalski point of view about it [3]. Erdos-Kac theorem connects the distribution of the different large numbers prime divisors with the probability theory limit laws formulas.

**Theorem 1.** (*The Erdos-Kac theorem*). For any  $n \geq 1$ , if  $\omega(n)$  is the amount of given number different prime divisors, then for any real numbers  $a < b$ :  $\lim_{N \rightarrow +\infty} \frac{1}{N} |\{1 \leq n \leq N | a \leq \frac{\omega(n) - \log \log N}{\sqrt{\log \log N}} \leq b\}| = \frac{1}{\sqrt{2\pi}} \int_a^b e^{-x^2/2} dx$  is satisfied.

That is, the limit distribution of  $\frac{\omega(n) - \log \log N}{\sqrt{\log \log N}}$ , corresponds to the standard normal distribution [2]. Hence the conclusion, that the amount of natural numbers  $n$  with a small number of divisors is low, and the amount of natural numbers with a great number of divisor is too.

This fact leads us to change the approach of factorization problem consideration. It is possible that, based on the theorem 1, it is necessary to investigate and deepen factorization methods based on probabilistic number theory. This approach, in turn, seems quite natural also due to the fact that the best factorization methods, which belong to the sub-exponential class, have probabilistic character.

## 2 Stochastic elliptic curves method

Among this class of factorization methods, we should single out method based on the elliptic curves theory. This method provides the greatest interest due to a number of features: the dependence of the method computational complexity primarily on the factorized number smallest prime divisor, many ways of optimization, possibility of parallelization.

However ECM has a list of problems, such as the optimal number of curves after using which it would be necessary to increase the method boundary problem. Correct choice of this number can lead to a significant reduction in the time costs of the method software implementation, as shown further.

It is important to estimate the dependence of the method computational complexity as a function of the chosen boundary. First, we need to know the number of primes on a given interval. The prime number theorem does not give exact estimation. Estimating of prime numbers degrees –  $\alpha_i$  values, is not easy task either. All this is complicated by the probabilistic nature of the method.

Proceeding from the foregoing, a theoretical assessment of this relationship, even if it is possible, will be heuristic in view of the huge number of uncertainties. Thus, it makes sense to use an empirical estimate.

Software that modeling the factorization process based on the theory of elliptic curves was implemented. This software is based on the idea of the algorithm proposed by Pomerance [1]. The input of the method software implementation is composite numbers consisting of the two prime numbers product with a size of  $\sim 10^5$ . For the representativeness of the obtained results, for each case, 10 such composite numbers were used as input, each of which was factorized 30 times. The cases with the initial boundary: 100, 30, 6, 2, 1 were considered, these boundaries were chosen empirically respectively to the size of factorized numbers. Obviously we can't get 1-smooth number, however when choosing boundary equal 1, we still got chance to factorize this number by getting divisor as G.C.D. of curve's discriminant and factorized number. Such boundaries were chosen in the research process due to the gradual acceleration of the software with a decrease of the initial boundary. Numbers were taken from the interval, in increments of 500, as the number of curves used, after which the boundary is increased. This is due to the fact that at step 500, obtained results fairly accurately describe the overall efficiency of the method, while this interval length is quite enough for a clear fixation of trend.

The dependence of the time spent on the software implementation work, the final boundary and the number of curves used depending on the number of curves after which the boundary is increased was investigated. Results are reflected in Fig. 1, Fig. 2 and Fig. 3 respectively.

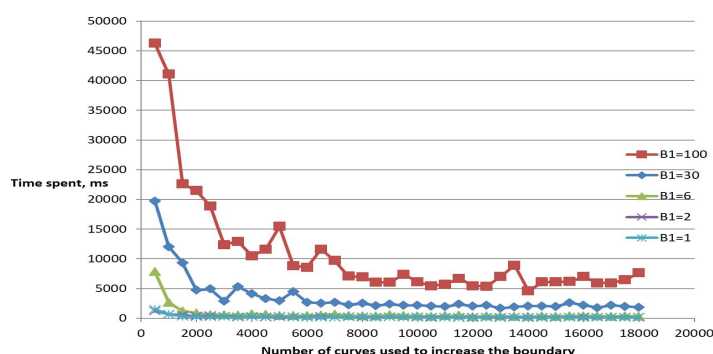


Figure 1: The graph of the time consumed dependence on the number of curves, after which the boundary is increased

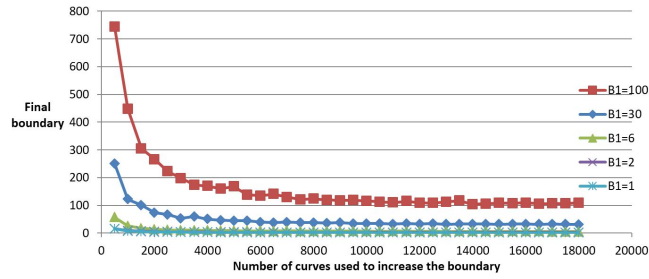


Figure 2: The graph of the final boundary dependence on the number of curves, after which the boundary is increased

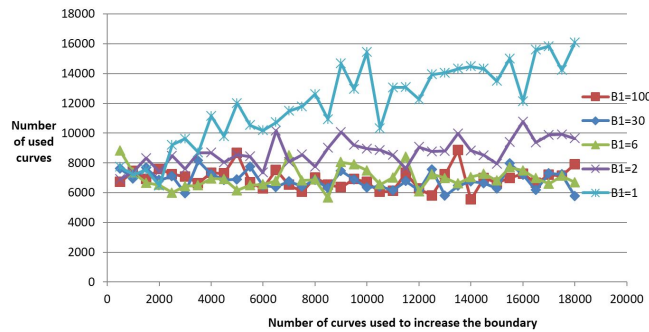


Figure 3: The graph of the curves number used for factorization dependence on the number of curves, after which the boundary is increased

As can be seen from Figures 1 and 2, for all the cases considered, an increase in the number of curves required to change boundary led to a decrease in time costs, as well as to a decrease in the final boundary value. The final boundary with the increase in the number of curves required for changing the boundary converged to its original value. Thus, for numbers whose divisors consist of 5 decimal characters, it is almost always possible to get a curve of  $b_1$ -smooth order, or the fact that in this case  $1 < g < n$ , where  $g = G.C.D.(4a^3 + 27b^2)$  is satisfied. In such case, the discriminant of the generated curve has a common divisor with a composite number  $n$ , different from 1.

It's unlikely to obtain a curve of 1-, 2- or 6-smooth order, since it is a very strict condition. Therefore, most likely for these cases, the second condition was satisfied. Based on this, the percentage of the cases number in which the second condition was satisfied was estimated (Figure 4).

Figure 4 shows, that for boundary  $b_1 = 100$  percentage of such cases fluctuates in a range from 8% to 20%. In case, when  $b_1 = 30$  – from 19% to 34%, when  $b_1 = 6$  – from 28% to 38%. In cases when  $b_1 = 2$  and  $b_1 = 1$  the probability of getting  $b_1$ -smooth order curve is the lowest, as evidenced by the highest percentage of cases when the divisor was detected using the curve discriminant. The percentage of such situations ranges from 31% to 52% and 32% to 83% respectively. In addition, for the last two boundaries the frequency of cases when the divisor was found by using a discriminant increases with the number of curves, after which the boundary increases. This is due

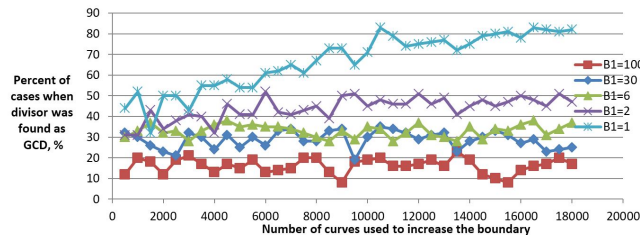


Figure 4: The graph of the finding the divisor by a discriminant of curve dependence on the number of curves, after which the boundary is increased

to the fact that, if these boundaries remain unchanged, the probability that we will get a curve of  $B_1$ -smooth order, is much lower, so we will rather find a curve with the suitable discriminant. This requires the use of a larger curves amount, as shown in Figure 3. Thus, for first three cases, the total number of curves used ranges from 6000 to 9000, and their average value is close for all three cases. In the last two cases, the average number of curves used is much greater.

So, for numbers whose smallest divisor is around  $10^5$  and less, it is much more advantageous to increase the number curves used than the boundary to reduce the time required for factorization process, even in cases of a minimal boundary. This is possible due to the probability that the discriminant of the curve has a common divisor with the specified composite number. This is indicated by the results obtained when  $b_1 = 1$ , was taken as initial boundary. In this case the percentage of these cases was about 80%, while the time costs were the lowest. This is due to a significant increase in the algorithm complexity with the growth of the boundary  $b_1$ , much greater than with increasing of the used curves number for given composite numbers.

However, we cannot exclude the cases when the curves whose order was  $b_1$ - smooth were received. These cases occurred for  $b_1 = 2$ , and for  $b_1 = 1$ , providing a good executing time of program realization. Also despite the result we can't really implement them very far. The reason is that we can't establish the fact that composite number contains divisors less than  $10^5$ .

The represented results are only the first steps in solving of used curves limit after which boundary should be increased problem.

## References

- [1] Crandall R.E., Pomerance C. B. (2006). *Prime numbers: A Computational Perspective*. Springer-Verlag, New-York.
- [2] Erdos P., Kac M. (1940). The Gaussian Law of Errors in the Theory of Additive Number Theoretic Functions. *American J. Math.* Vol. **62**, pp. 738-742.
- [3] Kowalski E., (2018). Arithmetic Randonnee, An introduction to probabilistic number theory. Available at: <https://people.math.ethz.ch/~kowalski/probabilistic-number-theory.pdf>

# APPROXIMATE FORMULAS FOR EXPECTATION OF FUNCTIONALS FROM SOLUTION TO LINEAR SKOROHOD STOCHASTIC DIFFERENTIAL EQUATION

A.D. EGOROV<sup>1</sup>, A.V. ZHERELO<sup>1,2</sup>,

<sup>1</sup>*Institute of Mathematics, National Academy of Sciences of Belarus*

<sup>2</sup>*Belarusian State University*

*Minsk, BELARUS*

e-mail: egorov@im.bas-net.by, ant@im.bas-net.by

## Abstract

Approximate formulas for evaluation of mathematical expectation of nonlinear functionals of solution to linear stochastic differential equation of Skorohod are constructed. The formulas are exact for functional polynomial of second and third degree and converge to the exact value of mathematical expectation.

**Keywords:** data science, Skorohod SDE, nonlinear functional

## 1 Introduction

An approximate calculation of mathematical expectation of nonlinear functionals from solutions to stochastic differential equations is an urgent and, in the general case, extremely difficult task. This is due to the large computational complexity of the algorithms in which the approximations of the trajectories of solutions of stochastic equations and the approximation of integrable functionals from the solutions must be connected, which would ensure the approximation error sufficient for the convergence of the method. In [1,2], an approach to solving this problem for some types of the Ito equations by martingales was considered. The solution of the problem is simplified in cases when a solution of the stochastic equation can be found explicitly, the corresponding approximations are obtained for some kinds of the linear Ito equations in [3-6]. This paper is devoted to the construction of approximate formulas for calculating the expectations of functionals of solution to the linear Skorohod equation.

## 2 The results

Let us consider a stochastic differential equation

$$X_t = X_0 + \int_0^t \sigma(s)X_s \delta W_s, \quad (1)$$

where  $X_0 = g\left(\int_0^1 a(\tau)dW_\tau\right)$ ;  $W_t$ ,  $t \in [0, 1]$ , is canonical Wiener process defined on probability space  $\Omega = C_0([0, 1])$ ,  $W_t(\omega) = \omega(t)$ ;  $\sigma(s)$ ,  $g(u)$ ,  $a(\tau)$  are deterministic

functions,

$\int_0^1 \sigma^2(s)ds < \infty$ ;  $g(u)$  is differentiable necessary number of times,  $a(\tau) \in L_2([0,1])$ ,  $\int_0^1 a(\tau)dW_\tau$  is stochastic Ito-Wiener integral.

The integral in right part of (1) is in the Skorohod sense because  $X_0$  not adapted to the underlying filtration.

It is known [7,8] that the only solution to (1) is given by

$$X_t = X_0(T_t^{-\sigma}) \exp \left\{ \int_0^t \sigma(s)dW_s - \frac{1}{2} \int_0^t \sigma^2(s)ds \right\},$$

where  $T_t^{-\sigma}$  is transformation on  $\Omega$  defined by  $(T_t^{-\sigma})(s) = \omega(s) - \int_0^{t \wedge s} \sigma(\tau)d\tau$ .

In our case we get

$$X_t = g \left( \int_0^1 a(\tau)dW_\tau - \int_0^t a(\tau)\sigma(\tau)d\tau \right) \exp \left\{ \int_0^t \sigma(s)dW_s - \frac{1}{2} \int_0^t \sigma^2(s)ds \right\}.$$

so we can evaluate the moments

$$E[X_t] = E \left[ g \left( \int_0^1 a(\tau)dW_\tau \right) \right],$$

$$E[X_{t_1}X_{t_2}] = \exp \left\{ \int_0^{t_1 \wedge t_2} \sigma^2(\tau)d\tau \right\} \times$$

$$E \left[ g \left( \int_0^1 a(\tau)dW_\tau + \int_0^{t_1} a(\tau)\sigma(\tau)d\tau \right) g \left( \int_0^1 a(\tau)dW_\tau + \int_0^{t_2} a(\tau)\sigma(\tau)d\tau \right) \right] \equiv B(t_1, t_2);$$

$$E \left[ \prod_{k=1}^3 X_{t_k} \right] = \prod_{\{t_i, t_j\}} \exp \left\{ \int_0^{t_i \wedge t_j} \sigma^2(\tau)d\tau \right\} \times$$

$$E \left[ \prod_{\{t_i, t_j\}} g_1 \left( \int_0^1 a(\tau)dW_\tau; t_i, t_j \right) \right] \equiv C(t_1, t_2, t_3),$$

where  $g_1 \left( \int_0^1 a(\tau)dW_\tau; t_i, t_j \right) = g \left( \int_0^1 a(\tau)dW_\tau + \int_0^{t_i} a(\tau)\sigma(\tau)d\tau + \int_0^{t_j} a(\tau)\sigma(\tau)d\tau \right)$ ;  
a couple  $\{t_i, t_j\}$  in the product runs  $\{t_1, t_2\}, \{t_1, t_3\}, \{t_2, t_3\}$ .

Note that in calculating the moments we used the Girsanov transformation on the Wiener space.

Our main result is the next approximate formulas

$$I(F) \equiv E[F(X_{(\cdot)})] \approx I_n(F) - J_n(F) + J(F),$$

where

$$I_n(F) = E \left[ F \left( g \left( \sum_{k=1}^n \xi_k \int_0^1 a(\tau) \alpha_k(\tau) d\tau - \int_0^1 a(\tau) \sigma(\tau) d\tau \right) \times \right. \right. \\ \left. \left. \exp \left\{ \sum_{k=1}^n \xi_k \int_0^1 \sigma(\tau) \alpha_k(\tau) d\tau - \frac{1}{2} \int_0^1 \sigma^2(\tau) d\tau \right\} \right) \right],$$

$\xi_k = \int_0^1 \alpha_k(\tau) dW_\tau$ ;  $\{\alpha_k(\tau)\}, k = 1, 2, \dots$ , is an orthonormal bases in  $L_2([0, 1])$ ;

$$J_n(F) = \sum_{l=1}^4 J_{n,l}(F) + \Lambda F(b_n(\cdot)) + F(0)(1 - B_n(0, 1)),$$

$$J_{n,1}(F) = - \int_0^1 \int_0^1 A_{n,1}(u, v) \Delta F(1_{[0,\cdot]}(u) 1_{[\cdot,1]}(v)) dudv,$$

$$J_{n,2}(F) = \int_0^1 A_{n,2}(u) \Delta F(1_{[0,\cdot]}(u)) du, \quad J_{n,3}(F) = - \int_0^1 A_{n,3}(v) \Delta F(1_{[\cdot,1]}(v)) dv,$$

$$J_{n,4}(F) = f_n(0) f_n(1) h_n(0, 1) G_n(0, 1), \quad A_{n,1}(u, v) = \frac{\partial^2}{\partial u \partial v} B_n(u, v), \\ A_{n,2}(u) = \frac{\partial}{\partial u} B_n(u, 1), \quad A_{n,3}(v) = \frac{\partial}{\partial v} B_n(0, v), \quad B_n(u, v) = f_n(u) f_n(v) G_n(u, v) h_n(u, v),$$

$$G_n(u, v) = E \left[ g \left( \int_0^1 a_n(\tau) dW_\tau + r_n(u, v) \right) g \left( \int_0^1 a_n(\tau) dW_\tau + r_n(v, u) \right) \right],$$

$$r_n(u, v) = \sum_{k=1}^n \left( \int_0^1 a(\tau) \alpha_k(\tau) d\tau \right) \left( \int_0^v \sigma(\tau) \alpha_k(\tau) d\tau \right) +$$

$$\sum_{k=1}^n \left( \int_0^1 a(\tau) \alpha_k(\tau) d\tau \right) \left( \int_0^u \sigma(\tau) \alpha_k(\tau) d\tau \right) - \int_0^u a(\tau) \sigma(\tau) d\tau,$$

$$h_n(u, v) = \exp \left\{ \sum_{k=1}^n \left( \int_0^u \sigma(\tau) \alpha_k(\tau) d\tau \right) \left( \int_0^v \sigma(\tau) \alpha_k(\tau) d\tau \right) \right\},$$

$$f_n(u) = \exp \left\{ \frac{1}{2} \sum_{k=1}^n \left( \int_0^u \sigma(\tau) \alpha_k(\tau) d\tau \right)^2 - \frac{1}{2} \int_0^u \sigma^2(\tau) d\tau \right\};$$

$$a_n(\tau) = \sum_{k=1}^n \int_0^1 a(s) \alpha_k(s) ds \alpha_k(\tau);$$

$$b_n(t) = E \left[ g \left( \int_0^1 a_n(\tau) dW_\tau + \sum_{k=1}^n \int_0^1 a(\tau) \alpha_k(\tau) d\tau \int_0^t \sigma(\tau) \alpha_k(\tau) d\tau - \int_0^t a(\tau) \sigma(\tau) d\tau \right) \right] f_n(t);$$

$$J(F) = \sum_{l=1}^4 J_l(F) + \Lambda F(b(\cdot)) + F(0)(1 - B(0, 1)),$$

$$\text{where } J_1(F) = - \int_0^1 \int_0^1 A_1(u, v) \Delta F(1_{[0,\cdot]}(u) 1_{[\cdot,1]}(v)) dudv,$$

$$J_2(F) = \int_0^1 A_2(u) \Delta F(1_{[0,\cdot]}(u)) du, \quad J_3(F) = - \int_0^1 A_3(v) \Delta F(1_{[\cdot,1]}(v)) dv,$$

$$J_4(F) = h(0, 1) G(0, 1), \quad A_1(u, v) = \frac{\partial^2}{\partial u \partial v} B(u, v), \\ A_2(u) = \frac{\partial}{\partial u} B(u, 1), \quad A_3(v) = \frac{\partial}{\partial v} B(0, v), \quad B(u, v) = G(u, v) h(u, v),$$

$$G(u, v) = E \left[ g \left( \int_0^1 a(\tau) dW_\tau + \int_0^u a(\tau) \sigma(\tau) d\tau \right) g \left( \int_0^1 a(\tau) dW_\tau + \int_0^v a(\tau) \sigma(\tau) d\tau \right) \right],$$

$$h(u, v) = \exp \left\{ \int_0^{u \wedge v} \sigma^2(\tau) d\tau \right\},$$

$$\Delta F(x) = \frac{1}{2}(F(x) + F(-x)), \quad \Lambda F(x) = \frac{1}{2}(F(x) - F(-x)).$$

With some restrictions on  $F(X_{(\cdot)})$ ,  $\sigma(s)$ ,  $g(u)$ ,  $a(\tau)$  we have  $I_n(F) \rightarrow I(F)$ ,  $J_n(F) \rightarrow J$  which implies that  $I_n(F) - J_n(F) + J(F) \rightarrow I(F)$ , while maintaining accuracy for functional polynomials of second degree from the solution to (1).

The same approach we apply to construction of approximate formulas exact for functional polynomial of third degree from solution to (1). Here we give the elementary formula

$$\begin{aligned} J(F(X_{(\cdot)})) &= \int_0^1 \int_0^1 \int_0^1 \left( \frac{\partial^3}{\partial u_1 \partial u_2 \partial u_3} C(u_1, u_2, u_3) \right) \Lambda F(\theta(u_1, u_2, u_3); \cdot) du_1 du_2 du_3 + \\ &\quad 3 \int_0^1 \int_0^1 \left( \frac{\partial^2}{\partial u \partial v} C(u, v, 0) \right) \Lambda F(\theta_1(u, v); \cdot) dudv + \\ &\quad 3 \int_0^1 \left( \frac{\partial}{\partial u} C(u, 0, 0) \right) \Lambda F(a_1 1_{[1, \cdot]}(u) + a_2 + a_3) du - 5C(0, 0, 0) \Lambda F(0), \end{aligned}$$

where  $\theta(u_1, u_2, u_3); t) = \sum_{j=1}^3 a_j 1_{[0, t]}(u_j)$ ,  $\theta_1(u, v); t) = a_1 1_{[0, t]}(u) + a_2 1_{[0, t]}(v) + a_3$ ,

$a_1, a_2, a_3$  – are the roots of the polynomial  $Q_3(x) = x^3 - x^2 + \frac{1}{2}x + \frac{1}{6}$ .

## References

- [1] Egorov A.D., Sobolevsky P.I., Yanovich L.A. (1993). *Functional Integrals. Approximate evaluation and Applications*. Kluwer Academic Publishers, Dordrecht.
- [2] Egorov A.D., Zherelo A.V. (2004). Approximations of functional integrals with respect to measure generated by solutions of stochastic differential equations. *Monte Carlo Methods and Applications*. Vol. **10**, No. 3-4. pp. 257-264.
- [3] Egorov A.D., Zhidkov E.P., Lobanov Yu.Yu. (2006). *Introduction to theory and applications of functional integration*. Fizmatlit Publ., Moscow. (In Russian).
- [4] Egorov A.D., Sabelfeld K.K. (2010). Approximate formulas for expectation of functionals of solutions to stochastic differential equations. *Monte Carlo methods and applications*. Vol. **16**, pp. 95-127.
- [5] Egorov A.D. (2013). Approximate formulas for expectation of functionals from solution to stochastic equation with random measure. . *Proceedings of 10-th International Conference " Computer Data Analysis and Modeling; Theoretical and Applied Stochastic"*. Minsk 10-14 Sept. 2013. Vol. **1**. pp. 206-209.

- [6] Egorov A.D. (2015). On approximate evaluation of mathematical expectation of functionals from solution to linear equation Ito-Levy. . *Doklady NAN Belarusi*. Minsk 10-14 Sept. 2013. Vol. **59**, No. 1. pp. 13-17. (In Russian).
- [7] Buckdahn R. (1991). Linear Skorohod stochastic differential equations. *Probab. Th. Rel. Fields*. Vol. **90**. pp. 223-240.
- [8] Buckdahn R., Nualart D. (1994). Linear stochastic differential equations and Wick products. *Probab. Th. Rel. Fields*. Vol. **99**. pp. 501-526.

# SIMULATION OF ADAPTIVE CONTROL SYSTEM WITH CONFLICT FLOWS OF NON-HOMOGENEOUS REQUESTS

M.A. FEDOTKIN, E.V. KUDRYAVTSEV

*Lobachevsky State University of Nizhni Novgorod*

*Nizhni Novgorod, RUSSIA*

e-mail: fma5@rambler.ru, evgkudryavcev@gmail.com

## Abstract

An adaptive control system with conflict flows of non-homogeneous requests is considered in the paper. A mathematical model of the system is a vector Markov sequence with a countable state space. Components of the Markov sequence satisfy certain functional recurrence relations. The main result of the work is a numerical research of the system by simulation. In particular, some sample estimates for the mean sojourn time of a single request from different queues are presented.

**Keywords:** data science, adaptive control system, conflict flow, non-homogeneity

## 1 Introduction

The adaptive non-cyclic control system with two conflict flows of requests is investigated here using computer-aided simulation. The algorithm controls the input flows using information about queues lengths and the order of requests arrivals. Conflictness of flows means here existence impossibility for the time intervals when requests from different flows are serviced simultaneously. Each flow here consists of requests of different types. In [1, 2], the authors showed the input flows can be approximated by non-ordinary Poisson flows. Thus, two statistically independent flows  $\Pi_1$  and  $\Pi_2$  are serviced. Request arrival moments in the flow  $\Pi_j$  occur with intensity of  $\lambda_j$  (for  $j = 1, 2$ ), and a group with  $k$  requests arrives with probability  $Q_j(k)$  where

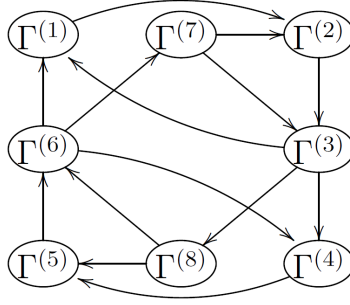
$$Q_j(1) = \left(1 + \alpha_j + \frac{\alpha_j \beta_j}{1 - \gamma_j}\right)^{-1} = p_j, \quad Q_j(2) = \alpha_j \left(1 + \alpha_j + \frac{\alpha_j \beta_j}{1 - \gamma_j}\right)^{-1}$$
$$Q_j(k) = \alpha_j \beta_j \gamma_j^{k-3} \left(1 + \alpha_j + \frac{\alpha_j \beta_j}{1 - \gamma_j}\right)^{-1}, \quad k \geq 3,$$

$\alpha_j$ ,  $\beta_j$  and  $\gamma_j$  are some parameters that have a certain physical meaning [1]. Let the random variable  $\eta_j(t)$  determine the number of requests received by the flow  $\Pi_j$  during the time interval  $[0, t)$ . Denote the probability  $\mathbf{P}(\eta_j(t) = k)$  by the function  $P_j(t, k)$ .

In our previous work the following equality was obtained:

$$P_j(t, k) = e^{-\lambda_j t} \sum_{n=0}^{\lfloor \frac{k}{2} \rfloor} \alpha_j^n \frac{(\lambda_j t p_j)^{k-n}}{n!(k-2n)!} + e^{-\lambda_j t} \sum_{n=0}^{\lfloor \frac{k}{2} \rfloor} \alpha_j^n \sum_{m=1}^{\min\{k-2n, n\}} \beta_j^m \sum_{l=0}^{k-2n-m} \gamma_j^l \frac{(\lambda_j t p_j)^{k-n-m-l} C_{m+l-1}^l}{(n-m)! m! (k-2n-m-l)!}, \quad k \geq 0.$$

The queue for each of the flows is assumed unlimited. The queueing system is assumed lossless. The server state space is  $\Gamma = \{\Gamma^{(1)}, \Gamma^{(2)}, \dots, \Gamma^{(8)}\}$ . The following graph specifies transitions of server states



The state  $\Gamma^{(3j-2)}$  corresponds to the first stage of the service period for the  $j$ -th flow. The service duration for one request from queue  $O_j$  (i.e. from the flow  $\Pi_j$ ) is a constant value  $\mu_{j,1}^{-1}$ . Let  $T_{3j-2}$  be the duration of the state  $\Gamma^{(3j-2)}$ . The state  $\Gamma^{(3j-1)}$  corresponds to the second stage of the service period for the  $j$ -th flow. The service duration of one request in this state is the constant value  $\mu_{j,2}^{-1} < \mu_{j,1}^{-1}$ . The duration of the state  $\Gamma^{(3j-1)}$  is a random variable taking on the values  $kT_{3j-1}$ ,  $k = \overline{1, n_j}$ , where  $n_j$  is the given maximum number of prolongations. The parameter  $K_j$  is the queue size, above which there is the prolongation. The state  $\Gamma^{(3j)}$  corresponds to the server setup after servicing the  $j$ -th flow. The duration of the state is  $T_{3j}$ . The service duration of one request in the state  $\Gamma^{(3j)}$  is  $\mu_{j,2}^{-1}$ . The state  $\Gamma^{(6+j)}$  corresponds to the first stage of the service period for the  $j$ -th flow in the case when an instantaneous transition to the state  $\Gamma^{(3j)}$  is possible. The duration of the state  $\Gamma^{(6+j)}$  is a random variable. Its largest value is  $T_{3j-2}$ . The constant values  $T_k$ ,  $k = \overline{1, 6}$ , are defined by

$$T_{3j-2} = \mu_{j,1}^{-1} + l_{3j-2} \theta_j \mu_{j,1}^{-1}, \quad T_{3j-1} = l_{3j-1} \theta_j \mu_{j,2}^{-1}, \quad T_{3j} = l_{3j} \theta_j \mu_{j,2}^{-1}, \quad (1)$$

where  $l_{3j-2} \in \{0, 1, 2, \dots\} = X$ ,  $l_{3j-1}, l_{3j} \in \{1, 2, \dots\}$  and  $\theta_j$  are parameters. The value  $\theta_j$ ,  $0 < \theta_j \leq 1$ , denotes the portion of the service time which needs pass before the next request can begin its servicing. In case  $\theta_j < 1$ , several requests can be serviced simultaneously. The ratio (1) means that the server changes its state when the service of some request is finished. The maximum possible number of served requests is  $1 + l_{3j-2}$  in the state  $\Gamma^{(3j-2)}$ , one is  $kl_{3j-1}$  for the state  $\Gamma^{(3j-1)}$  and one is the integer part of the number  $1/\theta_j$  for the state  $\Gamma^{(3j)}$ .

## 2 Construction of the mathematical model

We observe the system at random time instants  $\tau_i$ ,  $i = 0, 1, \dots$ , or on intervals  $[\tau_i, \tau_{i+1})$ ,  $i \geq 0$ . Here, the value  $\tau_0$  is the initial moment of time, and  $\tau_i$ ,  $i > 0$ , are the moments of server state change. Set  $y_0 = (0, 0)$ ,  $y_1 = (1, 0)$ ,  $y_2 = (0, 1)$ . For  $i \geq 0$  and  $j = 1, 2$ , we define the following random variables and elements:

1.  $\Gamma_i \in \Gamma$  — the server state during the interval  $[\tau_i, \tau_{i+1})$ ;
2.  $\eta_{j,i} \in X$  is the number of flow  $\Pi_j$  requests that enter the system during the interval  $[\tau_i, \tau_{i+1})$ , and  $\eta_i = (\eta_{1,i}, \eta_{2,i})$ ;
3.  $\eta'_i$  is a random vector. The vector  $\eta'_i$  takes on the value  $y_0$  if no requests have entered the system during the interval  $[\tau_i, \tau_{i+1})$ , otherwise the value  $y_j$  if the request (or requests) of the flow  $\Pi_j$  is the first during the  $i$ -th interval;
4.  $\kappa_{j,i} \in X$  is the number of requests for the flow  $\Pi_j$  in the system at time  $\tau_i$ , and  $\kappa_i = (\kappa_{1,i}, \kappa_{2,i})$ ;
5.  $\xi_{j,i}$  is the maximum possible number of flow  $\Pi_j$  requests that the system can service during the interval  $[\tau_i, \tau_{i+1})$ , and  $\xi_i = (\xi_{1,i}, \xi_{2,i})$ .

An adaptive algorithm for conflict flow control is defined by a function  $u(\cdot, \cdot, \cdot): \Gamma \times X^2 \times \{y_0, y_1, y_2\} \rightarrow \Gamma$  by virtue of the following recurrence relations

$$\begin{aligned} \Gamma_{i+1} &= u(\Gamma_i, \kappa_i, \eta'_i) = \\ &= \begin{cases} \Gamma^{(3j-2)}, & \{[\Gamma_i = \Gamma^{(3s)}] \& [(\kappa_{j,i} > 0) \vee (\kappa_{s,i} \geq K_s) \vee (\eta'_i = y_j)]\} \vee \\ & \vee \{[\Gamma_i = \Gamma^{(3j)}] \& [\kappa_{s,i} = 0] \& [\kappa_{j,i} \leq K_j] \& [\eta'_i = y_j]\}, \\ \Gamma^{(3j-1)}, & \{\Gamma_i = \Gamma^{(3j-2)}\} \vee \{[\Gamma_i = \Gamma^{(6+j)}] \& [\eta'_i = y_j]\}, \\ \Gamma^{(3j)}, & \{\Gamma_i = \Gamma^{(3j-1)}\} \vee \{[\Gamma_i = \Gamma^{(6+j)}] \& [\eta'_i \neq y_j]\}, \\ \Gamma^{(6+j)}, & [\Gamma_i = \Gamma^{(3s)}] \& [\kappa_{j,i} = 0] \& [\kappa_{s,i} < K_s] \& [\eta'_i = y_0], \end{cases} \end{aligned} \quad (2)$$

hereinafter in the work  $j, s = 1, 2$ ,  $j \neq s$ ,  $i \geq 0$ . The queue length dynamics is determined by functions  $v_j(\cdot, \cdot, \cdot, \cdot): \Gamma \times X^2 \times X^2 \times X^2 \rightarrow X$  and the following recurrence relations

$$\kappa_{j,i+1} = v_j(\Gamma_i, \kappa_i, \eta_i, \xi_i) = \begin{cases} \max\{0, \kappa_{j,i} + \eta_{j,i} - \xi_{j,i}\} & \text{if } \Gamma_i \in \Gamma \setminus \{\Gamma^{(3)}, \Gamma^{(6)}\}; \\ \eta_{j,i} + \max\{0, \kappa_{j,i} - \xi_{j,i}\} & \text{if } \Gamma_i \in \{\Gamma^{(3)}, \Gamma^{(6)}\}. \end{cases} \quad (3)$$

Relations (2) and (3) allow to us to study the vector sequence  $\{(\Gamma_i, \kappa_i); i = 0, 1, \dots\}$ . The sequence is a probabilistic model of the queueing system for adaptive control of conflict flows and for service of non-homogeneous requests. The properties of the vector Markov sequence were investigated in [3, 4, 5]. In particular, the conditions for the stationary probability distribution existence were obtained.

Unfortunately, it is not possible to derive analytically the important performance characteristics of the system under study. Therefore, a computer-aided simulation model is built to determine some important characteristics of the system. Simulation results can be interpreted in terms of a transport intersection operation.

### 3 System simulation model

The simulation takes places in the discrete time-scale  $\{\tau_i; i = 0, 1, \dots\}$  and a realization of the sequence  $\{(\Gamma_i, \kappa_i); i = 0, 1, \dots\}$  is generated together with all random objects involved in equations (2) and (3). Besides that, arrival times are stored for all requests, it allow to keep track of sojourn times of every request in the system. Denote by  $\nu_j$  the sample estimate for the mean sojourn time of requests from the flow  $\Pi_j$ . The sample estimate of the sojourn time of an arbitrary request is given by  $\nu = \frac{\lambda_1 M_1 \nu_1 + \lambda_2 M_2 \nu_2}{\lambda_1 M_1 + \lambda_2 M_2}$ . Here  $M_1$  and  $M_2$  are the mathematical expectations of the number of requests in a group and  $M_j = (1 + 2\alpha_j + \alpha_j \beta_j (2/(1 - \gamma_j) + 1/(1 - \gamma_j)^2))p_j$ . The simulation model is implemented as a program written in C++.

As an example, we present the computational results concerning the estimate of the mean sojourn time of an arbitrary request in the system with the following parameters:  $\lambda_1 = 0.4$ ,  $\lambda_2 = 0.3$ ,  $\alpha_1 = 1.1$ ,  $\beta_1 = 0.1$ ,  $\gamma_1 = 0.01$ ,  $\alpha_2 = 1.1$ ,  $\beta_2 = 0.1$ ,  $\gamma_2 = 0.01$ . The parameters of the adaptive algorithm are  $T_1 = T_4 = 5$ ,  $T_2 = T_5 = 1$ ,  $T_3 = T_6 = 2$ ,  $n_1 = n_2 = 7$ ,  $K_1 = K_2 = 10$ ,  $\theta_1 = \theta_2 = 1$ ,  $\mu_{1,1} = \mu_{2,1} = 2/3$ ,  $\mu_{1,2} = \mu_{2,2} = 1$ . The parameters  $T_1, \dots, T_6$  are given in seconds. The parameters  $\lambda_1, \lambda_2, \mu_{1,1}, \mu_{2,1}, \mu_{1,2}, \mu_{2,2}$  have the measurement units of (seconds)<sup>-1</sup>. Other parameters are dimensionless. With these parameters of adaptive flow control the sample estimate of the mean sojourn time is 13.55 seconds.

The work was performed as the basic part of the states tasks in the sphere of scientific activities on the Task No 2014/134 and supported by RFBR (project No 18-413-520005).

## References

- [1] Fedotkin M. A., Fedotkin A. M., Kudryavtsev E. V. (2014) Construction and Analysis of a Mathematical Model of Spatial and Temporal Characteristics of Traffic Flows. *Automatic Control and Computer Sciences*. Vol. **48**, No **6**, pp. 358-367.
- [2] Fedotkin M. A., Fedotkin A. M., Kudryavtsev E. V. (2015) Nonlocal Description of the Time Characteristic for Input Flows by Means of Observations. *Automatic Control and Computer Sciences*. 2015, Vol. **49**, No **1**, pp. 29-36.
- [3] Fedotkin M. A., Kudryavtsev E. V. (2017) Necessary conditions for stationary distribution existence in the adaptive control system of conflict flows. *Proceedings of the International Scientific Conference "Analytical and Comp. Meth. in Probab. Theory and its App. (ACMPT-2017)"*. Moscow. pp. 90-94. (in Russian)
- [4] Kudryavtsev E. V., Fedotkin M. A. (2019) Research of the Mathematical Model of Adaptive Control of Conflict Flows of Inhomogeneous demands. *Herald of Tver State University. Series: Applied Mathematics*. No. **1**, pp. 23-37. (in Russian)
- [5] Kudryavtsev E. V., Fedotkin M. A. (2019) Analysis of a Discrete Model of an Adaptive Control System for Conflicting Nonhomogeneous Flows. *Vestnik Moskovskogo Universiteta, Seriya 15: Vychislitel'naya Matematika i Kibernetika*. No **1**, pp. 33-43. (in Russian)

# BAYESIAN BINOMIAL REGRESSION MODEL WITH A LATENT GAUSSIAN FIELD FOR ANALYSIS OF EPIGENETIC DATA

A. HUBIN<sup>1</sup>, G. STORVIK<sup>2</sup>, P. GRINI<sup>3</sup>, M. BUTENKO<sup>4</sup>  
<sup>1,2,3,4</sup>*University of Oslo*, <sup>1,2</sup>*Norwegian Computing Center*  
*Oslo, NORWAY*

e-mail: <sup>1</sup>[aliaksandr.hubin@nr.no](mailto:aliaksandr.hubin@nr.no), <sup>2</sup>[geirs@math.uio.no](mailto:geirs@math.uio.no),  
<sup>3</sup>[paul.grini@ibv.uio.no](mailto:paul.grini@ibv.uio.no), <sup>4</sup>[m.a.butenko@ibv.uio.no](mailto:m.a.butenko@ibv.uio.no)

## Abstract

Epigenetic observations are represented by the total amount of reads from a particular cell and the amount of methylated reads, making it reasonable to model this data by a binomial distribution. There are numerous factors that can influence probability of success from a particular region. We might also expect spatial dependence of these probabilities. We incorporate dependence on the covariates and spatial dependence of methylation probability for observation from a particular cell by means of a binomial regression model with a latent Gaussian field. We run Mode Jumping Markov Chain Monte Carlo algorithm (MJMCMC) across different choices of covariates in order to obtain the joint posterior distribution of parameters and models. This also allows to find the best set of covariates to model methylation probability within the genomic region of interest.

**Keywords:** Binomial regression, Gaussian field, epigenetic data, data science

## 1 Introduction

Natural epigenetic variation provides a source for the generation of phenotypic diversity, but to understand its contributions to such diversity and its interaction with genetic variation requires further investigation [4]. Epigenetic changes are crucial for the development and differentiation of various cell types in an organism, as well as for normal cellular processes. High-throughput epigenetics experiments have enabled researchers to measure genome-wide epigenetic profiles. Epigenome-wide association studies (EWAS) hold promise for the detection of new regulatory mechanisms that may be susceptible to modification by environmental and lifestyle factors [3]. At the same time, epigenetic data are often spatially correlated with high noise levels, which requires careful spatial-temporal statistical modeling.

A major task today is the development of models and statistical methods for linking epigenetic patterns to genetic and/or environmental variables and interpreting them. Due to the availability of data, our focus will be on the plant *Arabidopsis*. [1] previously analysed *Arabidopsis* data consisting of epigenetic observations on a set of 10 lines, which were separately propagated in a common environment for 30 generations. These were compared with two independent lines propagated for only three generations (because of missing ancestor). Their analysis aimed at global summaries of structures

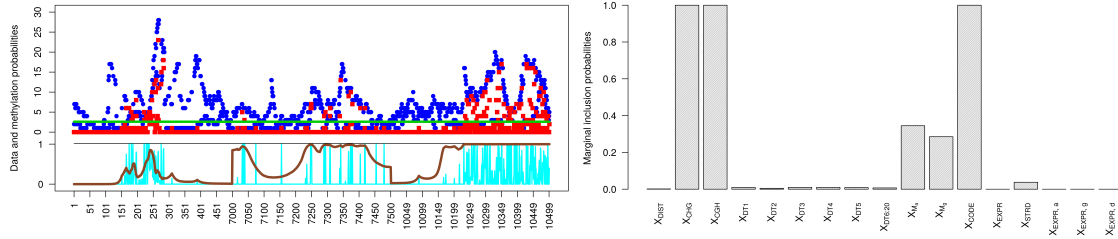


Figure 1: **Left** graph depicts epigenetic observations, where blue dots are total number of reads, red dots - number of methylated reads, green line corresponds to 2 total reads distinguishing the inference and the identification data, light blue line gives naïve probabilities as rates, brown line - probabilities as the posterior mean of the probability of success parameter from the posterior mode model. **Right** graph depicts barplots of RM estimates [2] of marginal inclusion probabilities of the covariates.

but was based on individual and (site-wise) hypothesis testing methods combined with FDR control methodology.

In this paper we limit ourselves to finding a pattern of signals appearing along genome that significantly influences methylation probability. We additionally take into account spatial dependence between the observations as well as the unexplained by the exogenous variables variability of the epigenetic observations. This is done by means of applying the MJMCMC algorithm developed by [2] to the Bayesian binomial regression with a random walk of order one, denoted as  $RW(1)$ , and independent Gaussian, denoted as  $IG$ , latent processes.

## 2 Mathematical model

We model the number of methylated reads  $Y_t \in \{1, \dots, n_t\}$  per position in the genome (nucleobase) to be binomially distributed with the number of trials equal to the number of reads for this position  $n_t \in \mathbb{N}$  and probability of success  $p_t \in \mathbb{R}_{[0,1]}$  modeled via logit link to the covariates  $X_t = \{X_{t1}, \dots, X_{tM}\}, t \in \{t_1, \dots, t_T\}$ , where  $T$  is the total number of genomic positions in the addressed genomic region. These covariates might be a position within a gene, indicator of the underlying genetic structure, and others (our choice of the covariates is given in Section 3). A latent Gaussian  $RW(1)$  process  $\delta_t \in \mathbb{R}$  is included into the model in order to take into account spatial dependence of methylation probabilities along the genome, whilst a latent independent Gaussian process ( $IG$ )  $\zeta_t$  is used to model the variance of the observations, which is not explained

by the covariates. This gives the following model formulation:

$$\Pr(Y_t = y | n_t, p_t) = \binom{n_t}{y} p_t^y (1 - p_t)^{n_t - y}, \quad (1)$$

$$p_t = \frac{e^{\beta_0 + \sum_{i=1}^M \gamma_i \beta_i X_{ti} + \delta_t + \zeta_t}}{1 + e^{\beta_0 + \sum_{i=1}^M \gamma_i \beta_i X_{ti} + \delta_t + \zeta_t}}, \quad (2)$$

$$\delta_t = \delta_{t-1} + \epsilon_t, \epsilon_t \sim N(0, \sigma_\epsilon^2), \quad (3)$$

$$\zeta_t \sim N(0, \sigma_\zeta^2), \quad (4)$$

where  $\beta_i \in \mathbb{R}, i \in \{0, \dots, M\}$  are regression coefficients of the covariates of the model showing whether and in which way the corresponding covariate influences the probability of methylation on average,  $\gamma_i \in \{0, 1\}, i \in \{1, \dots, M\}$  are latent indicators, defining if covariate  $i$  is included into the model ( $\gamma_i = 1$ ) or not ( $\gamma_i = 0$ ),  $\epsilon_t$  are the error terms of  $RW(1)$  process  $\delta_t$ , which are normally distributed with zero mean and variance  $\sigma_\epsilon^2$ . Finally,  $\sigma_\zeta^2$  is the variance term of the  $IG$  process  $\zeta_t$ . We then put the following priors for the parameters of the model:

$$\gamma_i \sim \text{Bernoulli}(q), \beta_i | \gamma_i \sim \mathcal{K}(\gamma_i = 1) N(\mu_\beta, \sigma_\beta^2), \psi_j \sim \log \Gamma(1, 5 \cdot 10^{-5}), j \in \{1, 2\}, \quad (5)$$

where the log Gamma distributed  $\psi_1 = \log \frac{1}{\sigma_{\epsilon,t}^2}$  and  $\psi_2 = \log \frac{1}{\sigma_{\zeta,t}^2}$  are the scaled hyperparameters of the latent models,  $q = 0.5$  is the prior Bernoulli probability of including a covariate into the model. We perform analysis for the model defined by Equations (1)-(5) by means of the MJMCMC algorithm [2]. The algorithm is capable of efficiently moving in the defined model space by means of both accurately exploring the modes of the probability mass and switching between these modes using large jumps combined with local optimization and randomization [2].

### 3 Data description

The addressed data set consists of 1502 observations from the first chromosome of Arabidopsis plant belonging to five predefined groups of genes. This data set was divided into 950 observations (with more than 2 reads, see Figure 1) for inference and 552 observations (with less than 3 reads) for model based identification of methylation probabilities for the positions with the lack of data.

Apart from the observations represented by the methylated versus total amount of reads we have data on various exogenous variables (covariates). Among these covariates we address the factor with 3 levels corresponding to whether the location belongs to CGH, CHH or CHG genetic region, where H is either A, C or T and thus generating two covariates  $X_{CGH}$  and  $X_{CHH}$ . The second group of factors indicates whether the distance to the previous cytosine nucleobase (C) in DNA is 1, 2, 3, 4, 5, from 6 to 20 or greater than 20 inducing six binary covariates  $X_{DT1}, X_{DT2}, X_{DT3}, X_{DT4}, X_{DT5}$ , and  $X_{DT6:20}$ . We also include such 1D distance as a continuous covariate  $X_{DIST}$ . The third addressed group of factors corresponds to whether the location belongs to a gene from a particular group of genes of biological interest. These groups are indicated as

$M_a$ ,  $M_g$  and  $M_d$ , yielding two additional covariates  $X_{M_a}$ ,  $X_{M_g}$ . Additionally we have a covariate  $X_{CODE}$  indicating if the corresponding nucleobase is in the coding region of a gene and a covariate  $X_{STRD}$  indicating if the nucleobase is on a "+" or a "-" strand. Finally, we have a continuous covariate  $X_{EXPR} \in \mathbb{R}^+$  representing expression level for the corresponding gene and interactions between expression levels and gene groups  $X_{EXPR,a}$ ,  $X_{EXPR,g}$ ,  $X_{EXPR,d} \in \mathbb{R}^+$ . Thus multiple predictors with respect to a strict choice of the reference model in our example induced  $M = 17$  potentially important covariates.

## 4 Results and discussion

MJMCMC algorithm was run until around 10000 unique models (7.6% of the model space) were explored. We parallelized the search on 10 CPUs. Default frequencies of large jumps and corresponding local optimizers from [2] were used. Also the default radiuses of proposals of global moves and local moves were addressed.

According to the marginal inclusion probabilities reported in the right graph of Figure 1, only factors  $X_{CHG}$ ,  $X_{CGH}$  and  $X_{CODE}$  are clearly significant for inference on the methylation patterns for the addressed epigenetic region, factors  $X_{M_a}$  and  $X_{M_g}$  also have some significance. In Table 1 one can find marginal posterior model probability and posterior means of the parameters for the best model in the explored subset of models from the model space. Based on the best model we carried out computations of

Table 1: Posterior means for the best model in terms of marginal posterior probability (PMP)

PMP	$\beta_0$	$\beta_{CHG}$	$\beta_{CGH}$	$\beta_{CODE}$	$\sigma_\epsilon^2$	$\sigma_\zeta^2$
0.4276	-8.8255	2.4717	5.2122	6.4240	0.1332	0.8258

methylation probabilities of the locations in both the inference set and the identification set. Furthermore, we compared the results with the naïve approach based on computing the proportion of methylated reads, which is currently addressed in the biological literature as a standard way to evaluate methylation probability of a given nucleobase. These results are summarized in the left graph of Figure 1. The results show that the naïve approach should not be trusted in the presence of spatially correlated data and the corresponding to it probabilities are strongly biased.

In future it would be of interest to obtain additional covariates such as whether the corresponding nucleobase belongs to a particular part of the non-coding gene region like promoter, intron or transposon, and whether the nucleobase is within a CpG island.

## References

- [1] Becker C. [et al.] (2011). Spontaneous epigenetic variation in the arabidopsis thaliana methylome. *Nature*. Vol. 480, No. 7376, pp. 245–249.

- [2] Hubin A., Storvik G. (2018). Mode jumping MCMC for Bayesian variable selection in GLMM. *Computational Statistics and Data Analysis*. Vol. 127, pp. 281–297.
- [3] Michels K. B. [et al.] (2013). Recommendations for the design and analysis of epigenome-wide association studies. *Nature Methods*. Vol. 10, No. 10, pp. 949–955.
- [4] Schmitz R. J. [et al.] (2013). Patterns of population epigenomic diversity. *Nature*. Vol. 495, No. 7440, pp. 193–198.

# EXPECTED ERROR RATE IN LINEAR DISCRIMINATION OF BALANCED SPATIAL GAUSSIAN TIME SERIES

M. KARALIUTĖ<sup>1</sup>, K. DUČINSKAS<sup>1,2</sup>, L. ŠALTYTĖ-VAISIAUSKĖ<sup>2</sup>

<sup>1</sup>*Institute of Data Science and Digital Technologies, Vilnius University*

<sup>2</sup>*Klaipėda University*

*Vilnius, Klaipėda, LITHUANIA*

e-mail: mkaraliute@gmail.com

## Abstract

The problems of discriminant analysis of spatial-temporal correlated Gaussian data were intensively considered previously (see e.g. Saltyte-Benth and Ducinskas (2005)). However, theoretical results were derived under the assumption of statistical independence between observation to be classified and training sample. In the present paper, we avoid this tough restriction. The problem of supervised classifying of the spatial Gaussian time series (SGTS) observation into one of two populations, is specified by different regression mean models and by common covariance function, is considered. In the case of complete parametric certainty and with the fixed training sample locations, the formula of conditional Bayes error rate is derived. In the case of unknown regression parameters and temporal covariance matrix, their ML estimators are plugged into the Bayes discriminant function. The asymptotic approximation of expected error rate is derived. This result is multivariate generalization of previous ones.

**Keywords:** Gaussian random field, Bayes discriminant function, spatial correlation, conditional Bayes error rate, actual and expected error rate

## 1 Introduction

It is known that for completely specified populations an optimal classification rule in the sense of minimum misclassification probability is the Bayesian classification rule (BCR). In practice, however, some or all statistical parameters of populations are unknown. Training sample is used for the estimation of the parameters of both populations. Then the estimators of unknown parameters based on training sample are usually plugged in BCR. The expected error rate are usually considered as performance measure for the plug-in classification rule. To obtain closed-form expressions for the expected error rate are very cumbersome even for the simplest parametric structures of populations. This makes it difficult to build some qualitative conclusions. Therefore, asymptotic expansions of the expected error rate associated with plug-in BCR are especially important.

Many authors have investigated the performance of the plug-in version of the BCR when parameters are estimated from training samples with independent observations, or training samples where observations are temporally dependent (McLachlan(2004)). However, they did not analyze the error rate in classification of spatial-temporal data.

The main objective of this paper is to classify  $T$  observations of spatio-temporal GRF  $\{Z(s, t) : s \in D \subset R^2, t \in [0, \infty)\}$  where  $s$  and  $t$  define spatial and temporal coordinates, respectively.

The model of observation  $Z(s, t)$  in population  $\Omega_l$  is

$$Z(s, t) = \mu_l(s, t) + \varepsilon(s, t),$$

where  $\mu_l(s, t)$  - deterministic spatio-temporal trend,  $l$  - class number.

We modeled large-scale variation as the linear parametric trend

$$\mu_l(s, t) = \beta_l' x(s)$$

where  $x(s) = (x_1(s), \dots, x_q(s))'$  is vector of a spatial covariates and  $\beta_l(t)$  is a  $q$  vector of parameters. The error term is generated by univariate zero - mean stationary GRF  $\{\varepsilon(s, t) : s \in D \subset R^2, t \in [0, \infty)\}$ , with covariance function defined by model for all  $s, u \in D$

$$\text{cov}\{\varepsilon(s, t), \varepsilon(u, r)\} = C(s, u; t, r).$$

*In this paper we restrict our attention to the separable case*

$$C(s, u; t, r) = R(s, u)\Sigma(t, r),$$

where  $R(s, u)$  denotes spatial correlation between observations in locations  $s$  and  $u$  and  $\Sigma(t, r)$  denotes temporal covariance between observations at moments  $t$  and  $r$ .

We consider isotropic spatial correlation belonging to **Matern family (e.g. exponential model)**. Temporal dependence is described **by the AR(p) models**.

Let  $S_n = \{s_i \in D; i = 1, \dots, n\}$  be a set of locations where training observation is taken. Call it the set of training locations (STL). So  $S_n$  is partitioned into the union of two disjoint subsets, i.e.  $S_n = S^{(1)} \cup S^{(2)}$ , where  $S^{(l)}$  is the subset of  $S_n$  where observations of  $Z(\cdot)$  from  $\Omega_l$  are taken  $l = 1, 2$ . Let  $(S^{(l)}) = n_l, l = 1, 2, n = n_1 + n_2$ . The partition of STL denoted by  $\xi = \{S^{(1)}, S^{(2)}\}$  will be called the spatial labels design (SLD) of training sample  $T$ .

Joint training sample  $M$  is stratified training sample, specified by  $n \times T$  matrix  $M = \begin{pmatrix} M_1 \\ M_2 \end{pmatrix}$ , where  $M_l$  is the  $n_l \times T$  matrix of  $n_l$  observations of vectors  $Z_i = (Z(s_i, 1), \dots, Z(s_i, T))'$  from  $\Pi_l = \Omega_l^T$ , where  $\Omega_l^T$  denotes the  $T$ -fold direct product of from  $\Omega_l, l = 1, 2$ . Then for  $l = 1, 2$   $Z_i \sim N_T(B_l' x_i, \Sigma)$ , where  $x_i = x(s_i), i = 0, \dots, n$  and  $B_l = (\beta_l(1), \dots, \beta_l(T))$ .

Let  $B = \begin{pmatrix} B_1 \\ B_2 \end{pmatrix}$  and  $X_1 = (x_1, \dots, x_{n_1})', X_2 = (x_{n_1+1}, \dots, x_n)'$  and  $X = X_1 \oplus X_2$ .

Consider the problem of classification of the vector of  $T$  observations of  $Z$  at location  $s_0$  denoted by  $Z_0 = (Z(s_0, 1), \dots, Z(s_0, T))'$  into one of two populations specified above with the given joint training sample  $M$ .

Then the model of  $M$  is

$$M = XB + E, \tag{1}$$

$E$  is the  $n \times T$  matrix of random errors that has matrix-variate normal distribution i.e.

$$E \sim N_{n \times p}(0, R \otimes \Sigma).$$

Here  $R = (r_{ij}; i, j = 1, \dots, n)$  denotes the spatial correlation matrix among observations in STL.

Denote by  $r_0$  the vector of spatial correlations between  $Z_0$  and observations in STL i.e  $r_0 = (r_{01}, \dots, r_{0n})$ . Set

$$\alpha_0 = R^{-1}r_0, \quad \rho = 1 - r_0' \alpha_0.$$

Notice that in population  $\Omega_l$ , the conditional distribution of  $Z_0$  given  $M = m$  is Gaussian, i.e.

$$(Z_0 | M = m, \Omega_l) \sim N_T(\mu_{lm}^0, \Sigma_{0m}). \quad (2)$$

Then conditional squared Mahalanobis distance between populations for observation taken at location  $s = s_0$  is

$$\Delta_0^2 = (\mu_{1m}^0 - \mu_{2m}^0)' \Sigma_{0m}^{-1} (\mu_{1m}^0 - \mu_{2m}^0) = \Delta^2 / \rho.$$

Let  $H = (I_q, I_q)$  and  $G = (I_q, -I_q)$ , where  $I_q$  denotes the identity matrix of order  $q$ .

Under the assumption that the populations are completely specified and for known prior probabilities of populations  $\pi_1(s)$  and  $\pi_2(s)$  ( $\pi_1(s) + \pi_2(s) = 1$ ), the Bayes discriminant function (BDF) minimizing the probability of misclassification (PMC) is formed by log-ratio of conditional likelihood of distribution specified in (1)-(2), that is

$$W_m(Z_0) = \left( Z_0 - (m - XB)' \alpha_0 - B' H' x_0 / 2 \right)' \Sigma^{-1} B' G' x_0 / \rho + \gamma \quad (3)$$

where  $\gamma = \ln(\pi_1(s_0) / \pi_2(s_0))$ .

In this paper prior probabilities at location  $s_0$  is assumed to be

$$\pi_1(s_0) = \frac{\sum_{i=1}^{n_1} \frac{1}{d(s_0, s_i)}}{\sum_{i=1}^n \frac{1}{d(s_0, s_i)}}, \quad \pi_2(s_0) = 1 - \pi_1(s_0),$$

where  $d(\cdot, \cdot)$  denotes the Euclidean distance function between locations.

This discriminant function is optimal under the criterion of minimum of misclassification probability (see McLachlan, 2004).

The probability of misclassification for  $W_T(Z_0)$  be called the Bayes error rate or optimal error rate. Denote it by  $P_n$ .

**Lemma 1.** *Bayes error rate for  $W_m(Z_0)$  specified in (3) is*

$$P_n = \sum_{l=1}^2 \pi_l \Phi(Q_l), \quad (4)$$

where  $Q_l = -\Delta_0 / 2 + (-1)^l \gamma / \Delta_0$ .

## 2 The error rates for plug-in BDF

When estimators of unknown parameters are plugged into BDF, the plug-in BDF is obtained. In this paper we assume that true values of parameters  $B$  and  $\Sigma$  are unknown. Let  $\hat{B}$  and  $\hat{\Sigma}$  be the estimators of  $B$  and  $\Sigma$  based on  $M$ .

The set of parameters that are to be estimated and the set of their estimators are denoted by  $\Psi = \{B, \Sigma\}$  and  $\hat{\Psi} = \{\hat{B}, \hat{\Sigma}\}$ , respectively.

Then replacing  $\Psi$  by  $\hat{\Psi}$  in (4) we get the plug-in BDF (PBDF)

$$W_M(Z_0; \hat{\Psi}) = \left( Z_0 - (M - X\hat{B})'\alpha_0 - \hat{B}'H'x_0/2 \right)' \hat{\Sigma}^{-1} \hat{B}'G'x_0/\rho + \gamma. \quad (5)$$

**Definition 1.** The actual error rate for BPDF  $W_M(Z_0; \hat{\Psi})$  is defined as

$$P(\hat{\Psi}) = \sum_{l=1}^2 \pi_l P((-1)^l W_M(Z_0; \hat{\Psi}) > 0 | M). \quad (6)$$

**Definition 2.** The expectation of the actual error rate with respect to the distribution of  $M$  designated as  $E_M\{P(\hat{\Psi})\}$ , is called the expected error rate (EER).

So the EER for considered problem of  $Z_0$  classification by BPDF is specified by  $E_M\{P(\hat{\Psi})\}$ .

Let  $\Phi(x)$  be the standard normal distribution function.

**Theorem 1.** Suppose that observation  $Z_0$  to be classified by BPDF specified in (6), then the asymptotic approximation of EER based on second order Taylor expansion is

$$AER = \sum_{l=1}^2 \pi_l \Phi(-\Delta_0/2 + (-1)^l \gamma/\Delta_0) + \pi_1 \varphi(-\Delta_0/2 - \gamma/\Delta_0) \times \\ \{ \Lambda' R_B \Lambda \Delta_0 / k + (T-1)x_0' G R_B G' x_0 / (k\Delta_0) + (2\gamma^2/\Delta_0 + (T-1)\Delta_0) / (n-2q) \} / 2. \quad (7)$$

where  $\Lambda = X'\alpha_0 - (H'/2 + \gamma G'/\Delta_0^2)x_0$ .

## References

- [1] McLachlan G.J. (2004). *Discriminant analysis and statistical pattern recognition*. Wiley, New York.
- [2] Šaltytė-Benth J., Dučinskas K. (2005). Linear discriminant analysis of multivariate spatial-temporal regressions. *Scand. J. Statist.* . Vol. 32, pp. 281–294.

# ON STATISTICAL ESTIMATION OF TRANSITION PROBABILITIES MATRIX FOR MARKOV CHAIN UNDER INCOMPLETE OBSERVATIONS

YU.S. KHARIN, O.V. DERNAKOVA

*Research Institute for Applied Problems of Mathematics and Informatics  
Belarusian State University  
Minsk, BELARUS*

e-mail: kharin@bsu.by, dernakova@bsu.by

## Abstract

A problem of statistical analysis for homogeneous Markov chain is considered for the situation with incomplete observations. The logarithmic likelihood function is constructed when there are multiple series of incomplete observations. A consistent statistical estimator of transition probabilities matrix is constructed using special form of the loglikelihood. A special case of multiple series of missing values is analyzed. Theoretical results are illustrated by computer modelling.

**Keywords:** data science, incomplete observations, transition probabilities matrix, Markov chain, estimation

## 1 Mathematical model

Markov chains are adequate models of discrete-valued time series in many applications: genetics, psychology, finance, information protection [1, 2]. Unfortunately, in practice this data are registered with special type of distortions - incomplete observations, e.g. missing values. This situation is considered in the paper devoted to statistical estimation of transition probabilities matrix.

Let a homogeneous first-order Markov chain  $x_t \in A = \{0, 1, \dots, N-1\}$ ,  $t \in \mathbb{N}$ , with the state space  $A$ , an initial probability distribution  $\pi = (\pi_i)$ ,  $\pi_i = P\{x_1 = i\}$ ,  $i \in A$ , and the one-step transition probability matrix

$$P = (p_{ij}), \quad p_{ij} = P\{x_{t+1} = j \mid x_t = i\}, \quad i, j \in A,$$

be defined on the probability space  $(\Omega, \mathcal{F}, P)$ . This Markov chain is not fully observed for  $T \in \mathbb{N}$  sequential time units: event  $B_t = \{x_t \in A_t\}$  is observed at time point  $t \in \{1, \dots, T\}$ , where  $A_t \subseteq A$  is some given subset. In particular: if the cardinality  $|A_t| = |A| = N$ , then  $x_t$  is a missing value; if  $|A_t| = 1$ , then  $x_t$  is exactly observed (in this case,  $A_t$  is the singleton).

The problem is in construction of a consistent statistical estimator for the matrix of one-step transition probabilities  $P$  based on the observed sequence of events  $X = (B_1, B_2, \dots, B_T)$ .

Introduce the notation:  $I^{(j)} = (B_{f_j}, B_{f_j+1}, \dots, B_{l_j})$  is the  $j$ -th subsequence (series),  $j = 1, \dots, r$ , consisting of  $\tau_j = l_j - f_j + 1 \in \{1, 2, \dots, T\}$  consecutive events that describe incomplete observations, for which  $|A_t| > 1$ ;  $C^{(i)} = (x_{l_{i-1}+1}, x_{l_{i-1}+2}, \dots, x_{f_i-1})$

is the  $i$ -th ( $i = 1, \dots, r + 1$ ) subsequence (series) of  $T_i = f_i - l_{i-1} - 1 \in \{1, 2, \dots, T\}$  complete observations, for which  $|A_t| \equiv 1$ ;  $l_0 ::= 0$ ,  $f_{r+1} ::= T + 1$ . Without loss of generality, let us assume that the observation process begins and ends with complete observations.

**Lemma 1.** *The observed sequence of  $T$  events  $X = (B_1, B_2, \dots, B_T)$  allows the following representation in the form of  $2r + 1$  alternating subsequences  $\{C^{(i)}\}$ ,  $\{I^{(j)}\}$ :*

$$X = (C^{(1)}, I^{(1)}, C^{(2)}, I^{(2)}, \dots, C^{(r)}, I^{(r)}, C^{(r+1)}), \quad (1)$$

where  $r$ ,  $\{T_i\}$ ,  $\{\tau_j\}$  depend on  $T$ .

*Proof.* The representation (1) follows from the definition of the observation model and on the introduced notation.  $\square$

## 2 Construction of the Likelihood Function under incomplete data

As it is known [3], in the case of complete observations, when  $X \equiv C^{(1)} \equiv \{x_1, \dots, x_T\}$ , a consistent, asymptotically unbiased, asymptotically normal and effective estimator of the matrix  $P = (p_{ij})$ ,  $i, j \in A$ , is the maximum likelihood estimator (MLE):

$$\hat{p}_{ij} = \begin{cases} \frac{\sum_{t=1}^{T-1} \mathbb{I}\{x_t=i, x_{t+1}=j\}}{\sum_{t=1}^{T-1} \mathbb{I}\{x_t=i\}}, & \text{if } \sum_{t=1}^{T-1} \mathbb{I}\{x_t=i\} > 0, \\ \frac{1}{N}, & \text{if } \sum_{t=1}^{T-1} \mathbb{I}\{x_t=i\} = 0, \end{cases} \quad (2)$$

where  $\mathbb{I}\{A\}$  is the indicator function of event  $A$ .

**Theorem 1.** *For homogeneous Markov chain  $x_t$  with incomplete observations satisfying Lemma 1, the likelihood function admits the following representation:*

$$\begin{aligned} L(P) &= \pi_{x_1} p_{x_1, x_2} \cdots p_{x_{f_1-2}, x_{f_1-1}} \sum_{i_{f_1} \in A_{f_1}} \cdots \sum_{i_{l_1} \in A_{l_1}} p_{x_{f_1-1}, i_{f_1}} p_{i_{f_1}, i_{f_1+1}} \cdots p_{i_{l_1-1}, i_{l_1}} p_{i_{l_1}, x_{l_1+1}} \times \\ &\times p_{x_{l_1+1}, x_{l_1+2}} \cdots p_{x_{f_2-2}, x_{f_2-1}} \sum_{i_{f_2} \in A_{f_2}} \cdots \sum_{i_{l_2} \in A_{l_2}} p_{x_{f_2-1}, i_{f_2}} p_{i_{f_2}, i_{f_2+1}} \cdots p_{i_{l_2-1}, i_{l_2}} p_{i_{l_2}, x_{l_2+1}} \times \cdots \times \\ &\times p_{x_{l_{r-1}+1}, x_{l_{r-1}+2}} \cdots p_{x_{f_r-2}, x_{f_r-1}} \sum_{i_{f_r} \in A_{f_r}} \cdots \sum_{i_{l_r} \in A_{l_r}} p_{x_{f_r-1}, i_{f_r}} p_{i_{f_r}, i_{f_r+1}} \cdots p_{i_{l_r-1}, i_{l_r}} p_{i_{l_r}, x_{l_r+1}} \times \\ &\times p_{x_{l_r+1}, x_{l_r+2}} \cdots p_{x_{T-1}, x_T}. \end{aligned} \quad (3)$$

*Proof.* Using the Markov property and Lemma 1, we have:

$$\begin{aligned} L(P) ::= P \{ &(x_1, \dots, x_{f_1-1}), (x_{f_1} \in A_{f_1}, \dots, x_{l_1} \in A_{l_1}), (x_{l_1+1}, \dots, x_{f_2-1}), \\ &(x_{f_2} \in A_{f_2}, \dots, x_{l_2} \in A_{l_2}), \dots, (x_{l_{r-1}+1}, \dots, x_{f_r-1}), \end{aligned}$$

$$\begin{aligned}
& (x_{f_r} \in A_{f_r}, \dots, x_{l_r} \in A_{l_r}), (x_{l_r+1}, \dots, x_T) \} = \\
& \pi_{x_1} \cdot p_{x_1, x_2} \cdots p_{x_{f_1-2}, x_{f_1-1}} \cdot P_{x_{f_1-1}, x_{l_1+1}}^{(\tau_1)} (A_{f_1}, \dots, A_{l_1}) \cdot p_{x_{l_1+1}, x_{l_1+2}} \cdots p_{x_{f_2-2}, x_{f_2-1}} \times \\
& \times P_{x_{f_2-1}, x_{l_2+1}}^{(\tau_2)} (A_{f_2}, \dots, A_{l_2}) \cdots p_{x_{l_{r-1}+1}, x_{l_{r-1}+2}} \cdots p_{x_{f_r-2}, x_{f_r-1}} \cdot P_{x_{f_r-1}, x_{r+1}}^{(\tau_r)} (A_{f_r}, \dots, A_{l_r}) \times \\
& \times p_{x_{l_r+1}, x_{l_r+2}} \cdots p_{x_{T-1}, x_T}, \tag{4}
\end{aligned}$$

where

$$\begin{aligned}
P_{x_{f_j-1}, x_{l_j+1}}^{(\tau_j)} (A_{f_j}, \dots, A_{l_j}) = & \sum_{\substack{i_{f_j} \in B_{f_j}, \\ \dots \\ i_{l_j} \in B_{l_j}}} p_{x_{f_j-1}, i_{f_j}} p_{i_{f_j}, i_{f_j+1}} \cdots p_{i_{l_j-1}, i_{l_j}} p_{i_{l_j}, x_{l_j+1}}, \quad j = 1, \dots, r.
\end{aligned} \tag{5}$$

Expressions (4), (5) are equivalent to (3).  $\square$

**Corollary 1.** *The following representation for the loglikelihood function holds:*

$$\begin{aligned}
l(P) = \ln L(P) = & \ln \pi_{x_1} + \ln p_{x_1, x_2} + \cdots + \ln p_{x_{f_1-2}, x_{f_1-1}} + \\
& + \ln \sum_{i_{f_1} \in A_{f_1}} \cdots \sum_{i_{l_1} \in A_{l_1}} p_{x_{f_1-1}, i_{f_1}} p_{i_{f_1}, i_{f_1+1}} \cdots p_{i_{l_1-1}, i_{l_1}} p_{i_{l_1}, x_{l_1+1}} + \\
& + \ln p_{x_{l_1+1}, x_{l_1+2}} + \cdots + \ln p_{x_{f_2-2}, x_{f_2-1}} + \\
& + \ln \sum_{i_{f_2} \in A_{f_2}} \cdots \sum_{i_{l_2} \in A_{l_2}} p_{x_{f_2-1}, i_{f_2}} p_{i_{f_2}, i_{f_2+1}} \cdots p_{i_{l_2-1}, i_{l_2}} p_{i_{l_2}, x_{l_2+1}} + \cdots + \\
& + \ln p_{x_{l_{r-1}+1}, x_{l_{r-1}+2}} + \cdots + \ln p_{x_{f_r-2}, x_{f_r-1}} + \\
& + \ln \sum_{i_{f_r} \in A_{f_r}} \cdots \sum_{i_{l_r} \in A_{l_r}} p_{x_{f_r-1}, i_{f_r}} p_{i_{f_r}, i_{f_r+1}} \cdots p_{i_{l_r-1}, i_{l_r}} p_{i_{l_r}, x_{l_r+1}} + \\
& + \ln p_{x_{l_r+1}, x_{l_r+2}} \cdots + \ln p_{x_{T-1}, x_T}. \tag{6}
\end{aligned}$$

Introduce the notation:

$$\mathcal{I}_\tau = \{I^{(j)} : \tau_j = \tau\} = \bigcup_{j=1, \tau_j=\tau}^r I^{(j)} \tag{7}$$

is a collection of all those subsequences that contain exactly  $\tau \in \{1, 2, \dots, T\}$  incomplete observations;  $L_\tau ::= |\mathcal{I}_\tau|$  is the number of such subsequences,  $0 \leq L_\tau \leq T - 1$ ;

$$C = \bigcup_{i=1}^{r+1} C^{(i)} \tag{8}$$

is a collection of all  $r + 1$  subsequences of complete observations;  $T^{(C)} = |C| = \sum_{i=1}^{r+1} T_i$  is a number of all complete observations;  $T^{(I)} = \sum_{\tau=1}^{r+1} \tau L_\tau = \tau_1 + \cdots + \tau_r$  is a number of all incomplete observations.

The normalization condition follows from the accepted notation (1), (7), (8):

$$\sum_{i=1}^{r+1} T_i + \sum_{j=1}^r \tau_j \equiv T. \quad (9)$$

**Corollary 2.** Under notation (7) – (9) the loglikelihood function allows the following decomposition on  $\tau_+$  layers  $\{\mathcal{I}_\tau\}$ :

$$l(P) = l_0(P) + \sum_{\tau=1}^{\tau_+} l_\tau(P), \quad (10)$$

where  $\tau_+ = \max_{1 \leq j \leq r} \tau_j$  is the maximal length for series  $\{I^{(j)}\}$  of incomplete observations,

$$l_0(P) = \ln \pi_{x_1} + \sum_{i=1}^{r+1} \sum_{t=l_{i-1}+1}^{f_i-2} \ln p_{x_t, x_{t+1}}, \quad (11)$$

$$l_\tau(P) = \sum_{j=1, \tau_j=\tau}^r \ln \sum_{i_1 \in A_{f_1}, \dots, i_\tau \in A_{f_\tau}} p_{x_{f_{j-1}}, i_1} p_{i_1, i_2} \cdots p_{i_\tau, x_{l_{j+1}}}.$$

*Proof.* The expressions (10), (11) are obtained from (6) by grouping of terms, taking into account the notation (7) – (9).  $\square$

### 3 Family of statistical estimators for transition matrix

MLE for  $P$  is defined as a solution of the maximization problem:

$$l(P) \rightarrow \max_P \quad (12)$$

subject to the limitations:

$$0 \leq p_{ij} \leq 1, \quad \sum_{j=0}^{N-1} p_{ij} = 1, \quad i, j \in A. \quad (13)$$

Note, first of all, if  $\tau_+ = 0$  in (10), i.e. incomplete observation among  $x_1, \dots, x_T$  are absent, then solving the problem (12) in this case:

$$l(P) \equiv l_0(P) \rightarrow \max_P,$$

we arrive at the known MLE (2). Consider the case  $\tau_+ = 1$ .

$$l(P) = l_0(P) + l_1(P) \rightarrow \max_P,$$

$$l_1(P) = \sum_{j=1}^r \ln \sum_{i \in A_j} p_{x_{f_{j-1}}, i} p_{i, x_{l_{j+1}}}. \quad (14)$$

We write the Lagrange function for (13), (14):

$$\mathcal{L}(P, \{\lambda_i\}) = l_0(P) + l_1(P) + \sum_{i=0}^{N-1} \lambda_i \left( 1 - \sum_{j=0}^{N-1} p_{ij} \right).$$

We set up a system of equations:

$$\begin{aligned} \frac{\partial \mathcal{L}(\cdot)}{\partial p_{ks}} &= \frac{1}{p_{ks}} \sum_{i=1}^{r+1} \sum_{t=l_{i-1}+1}^{f_i-2} \mathbb{I}\{x_t = k, x_{t+1} = s\} - \lambda_k + \\ &+ \sum_{j=1}^r \frac{\sum_{i \in A_j} \left( \mathbb{I}\{x_{f_j-1} = k, i = s\} p_{i, x_{l_{j+1}}} + p_{x_{f_j-1}, i} \mathbb{I}\{i = k, x_{l_{j+1}} = s\} \right)}{\sum_{i \in A_j} p_{x_{f_j-1}, i} p_{i, x_{f_j-1}}} = 0, k, s \in A. \end{aligned}$$

Consider now the special case when  $A_j \equiv A$ , i.e. each incomplete observation is a missing observation. According to (5), (11), in this case  $l_\tau(\cdot)$  allows the presentation:

$$l_\tau(P) = \sum_{j=1, \tau_j=\tau}^r \ln(P^{\tau+1})_{x_{f_j-1}, x_{l_{j+1}}}. \quad (15)$$

Using (10), (15), to solve maximization problem (12) we consider a series of  $\tau_+ + 1$  auxiliary problems:

$$\hat{P}(\tau) : l_\tau(P) \rightarrow \max_P, \tau = 0, 1, \dots, \tau_+. \quad (16)$$

Solution of the  $\tau$ -th problem in (16) is a matrix  $\hat{P}(\tau)$  satisfying the matrix equation:

$$\begin{aligned} (\hat{P}(\tau))^{\tau+1} &= Q^{(\tau)}, \\ (Q^{(\tau)})_{kl} &= \begin{cases} \frac{\sum_{j=1, \tau_j=\tau}^r \mathbb{I}\{x_{f_j-1}=k, x_{f_j+\tau_j}=l\}}{\sum_{j=1, \tau_j=\tau}^r \mathbb{I}\{x_{f_j-1}=k\}}, & \text{if } \sum_{j=1, \tau_j=\tau}^r \mathbb{I}\{x_{f_j-1} = k\} > 0, \\ \frac{1}{N}, & \text{if } \sum_{j=1, \tau_j=\tau}^r \mathbb{I}\{x_{f_j-1} = k\} = 0, \end{cases} \end{aligned} \quad (17)$$

To solve the matrix equation in (17) we use the Schur decomposition [4].

Finally, by  $\tau_+ + 1$  auxiliary estimators (16) we construct a family of statistical estimators:

$$\check{P} = \sum_{\tau=0}^{\tau_+} a_\tau \hat{P}(\tau). \quad (18)$$

The weight coefficients  $\{a_\tau\}$  in (18) are chosen taking into account the following condition:

$$\sum a_\tau \equiv 1, a_\tau \in [0, 1]. \quad (19)$$

Note, that consistency of the estimator (18), (19) follows [3] from consistency of auxiliary estimators  $\{\hat{P}(\tau) : \tau = 0, 1, \dots, \tau_+\}$ .

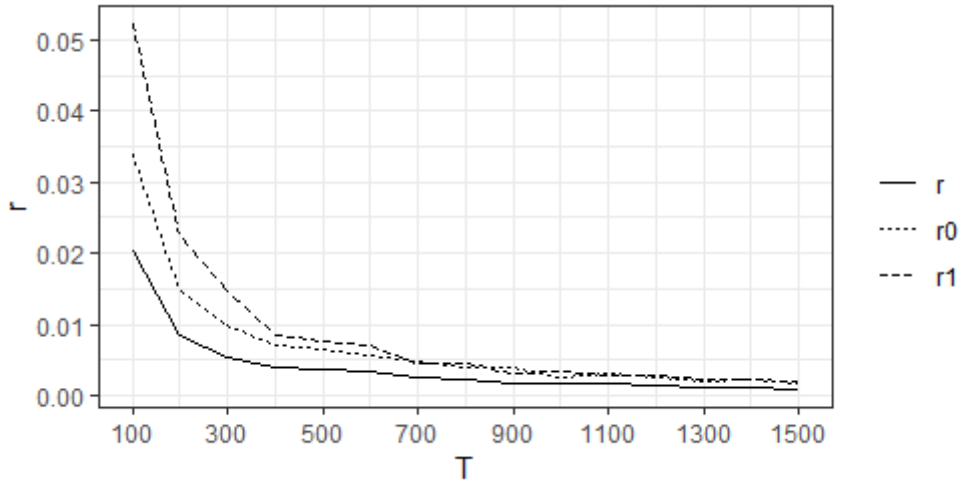


Figure 1: Mean square errors  $r_0, r_1, r$  when  $\alpha = 0.4, \epsilon = 0.6$ .

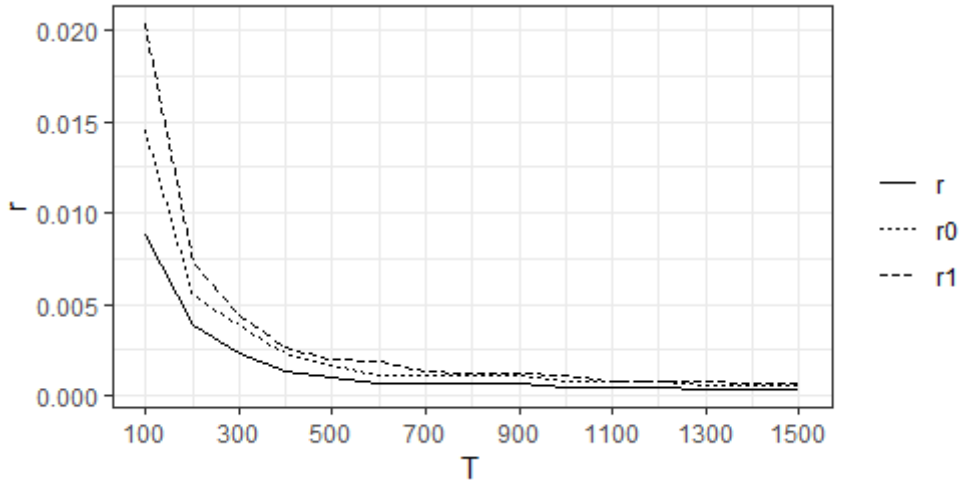


Figure 2: Mean square errors  $r_0, r_1, r$  when  $\alpha = 0.3, \epsilon = 0.9$ .

## 4 Results of computer experiments

Computer experiments were carried out on simulated data. Homogeneous binary Markov chain of the first order  $x_t \in A = \{0, 1\}$ ,  $t \in \mathbb{N}$ , of length  $T$  with the one-step transition matrix

$$P = \frac{1}{2} \begin{pmatrix} 1 + \epsilon & 1 - \epsilon \\ 1 - \epsilon & 1 + \epsilon \end{pmatrix}, \quad -1 \leq \epsilon \leq 1,$$

with series of missing values of length  $\tau \leq 1$  was simulated  $M$  times.

The matrix estimator (18), (19) is

$$\check{P} = a_0 \hat{P}(0) + a_1 \hat{P}(1), \quad a_0 = \frac{T_1 + \dots + T_{r+1}}{r + (T_1 + \dots + T_{r+1})}, \quad a_1 = \frac{r}{r + (T_1 + \dots + T_{r+1})}.$$

In computer experiments we evaluated the mean square errors:

$$r_\tau = E \left\{ \|\hat{P}(\tau) - P\|^2 \right\}, \tau = 0; 1; \quad r = E \left\{ \|\check{P} - P\|^2 \right\}$$

in dependence on the fraction of missing values  $\alpha \in [0, 1]$  and on the parameter  $\epsilon$  for  $M = 100$ . The results of the experiments presented in Figures 1, 2 illustrate consistency of the constructed statistical estimator (18), (19).

## References

- [1] Kharin Yu. (2013). *Robustness in Statistical Forecasting*. Springer, N.Y.
- [2] Weiss C.H. (2018). *On Introduction to Discrete-Valued Time Series*. Wiley, N.Y.
- [3] Billingsley P. (1961) Statistical methods in Markov chains. *The Annals of Mathematical Statistics*. Vol. **32**, no. 1, pp. 12-40.
- [4] Higham N. J. (2008). *Functions of Matrices: Theory and Computation*. SIAM, Philadelphia, PA, USA.

# STATISTICAL ANALYSIS OF COUNT CONDITIONALLY NONLINEAR AUTOREGRESSIVE TIME SERIES BY FREQUENCIES-BASED ESTIMATORS

YU.S. KHARIN, M.I. KISLACH

*Research Institute for Applied Problems of Mathematics and Informatics,  
Belarusian State University  
Minsk, BELARUS*

e-mail: kharin@bsu.by, kislachm@gmail.com

## Abstract

Models of count time series with denumerable states space with conditional probability distributions generated by Bernoulli trial scheme (Poisson (model  $M_1$ ), Geometric (model  $M_2$ ), Negative binomial (model  $M_3$ ), Borel-Tanner (model  $M_4$ )) conditionally nonlinear autoregressive time series are developed. Consistent estimators for parameters of proposed models based on Markov properties are constructed. Algorithms for statistical forecasting of count time series are developed. Results of computer experiments are given.

**Keywords:** data science, count data, nonlinear autoregression, frequencies-based estimator

## 1 Mathematical models of count time series with denumerable state space and their probability properties

Count time series are widely used in different applications: genetics, economics, information protection [1-4]. The case of finite states space is considered in [3]. In this paper we develop our results from [3] to the case of denumerable states space.

Let in probability space  $(\Omega, \mathcal{F}, P)$  a time series  $x_t \in A = \{0, 1, \dots\}$  be defined. We call it the conditionally nonlinear autoregressive time series if the conditional probability distribution of the random value  $x_t$  under its prehistory  $\{x_{t-1}, x_{t-2}, \dots\}$  depends only on  $s$ -prehistory  $X_{t-s}^{t-1} = (x_{t-1}, x_{t-2}, \dots, x_{t-s})' \in A^s$  for some depth  $s \in N$ :

$$P\{x_t = j | x_{t-1} = j_{t-1}, x_{t-2} = j_{t-2}, \dots\} = P\{x_t = j | X_{t-s}^{t-1} = J_1^s\} = \mathbf{Q}(j; J_1^s), \quad (1)$$

where  $j \in A$ ,  $J_1^s \in A^s$ ,  $\mathbf{Q}(\cdot; J_1^s)$  is some discrete probability distribution on  $A$  for each  $J_1^s \in A^s$ . We will assume that this function is parameterized in the following way:

$$\mathbf{Q}(j; J_1^s) ::= \mathbf{q}(j; \theta(J_1^s)), j \in A, J_1^s \in A^s. \quad (2)$$

Here  $q(\cdot; \theta)$  is some fixed (standard) discrete probability distribution with some parameter  $\theta \in R^1$ , and  $\theta = \theta(J_1^s)$  is some function describing dependence of this parameter on the  $s$ -prehistory in the form:

$$\theta = \theta(J_1^s) ::= F \left( \sum_{i=1}^m a_i \psi_i(J_1^s) \right), \quad (3)$$

where  $F(\cdot) : R^1 \rightarrow R^1$  is some known function;  $\Psi(u) = (\psi_1(u), \dots, \psi_m(u))' : A^s \rightarrow R^m$  are some base functions,  $\psi_i(\cdot) : A^s \rightarrow R^1$ ;  $a = (a_i) \in R^m$  is some unknown column-vector of parameters.

Consider four special cases of proposed model (1)–(3) for count time series [2]:

$$\mathbf{q}(j; \theta) = \begin{cases} \theta^j e^{-\theta} / j! & \text{for model } M_1 \\ \theta(1 - \theta)^j, j \in A & \text{for model } M_2, \\ C_{r+j-1}^r \theta^r (1 - \theta)^j, j \geq r & \text{for model } M_3, \\ e^{-j\theta} r \theta^{j-r} j^{j-r-1} / (j-r)!, j \geq r & \text{for model } M_4, \end{cases} \quad (4)$$

where  $r \in N$  is some fixed value.

We use in (3) the function  $F(z) = e^z$  for the model  $M_1$ , and the logistic cumulative distribution function for the models  $M_2 - M_4$ :

$$F(z) = e^z / (1 + e^z), z \in R^1. \quad (5)$$

**Lemma 1.** *Count time series determined by model (1)–(3) is the denumerable homogeneous Markov chain of order  $s$  with the states space  $A$  and the one-step transition probabilities:*

$$P\{x_t = j | X_{t-s}^{t-1} = J_1^s\} = \mathbf{q}(j; \theta(J_1^s)), j \in A, J_1^s \in A^s, \quad (6)$$

where  $\mathbf{q}(\cdot)$  is determined by (4) for the considered special cases.

## 2 Statistical estimation of model parameters

Give two auxiliary results.

**Lemma 2.** *For model (1)–(3) the conditional mean is ( $J_1^s \in A^s$ ):*

$$\mu(J_1^s) ::= E\{x_t | X_{t-s}^{t-1} = J_1^s\} = M(\theta(J_1^s)) = \begin{cases} \theta(J_1^s) & \text{for } M_1, \\ (1 - \theta(J_1^s)) / \theta(J_1^s) & \text{for } M_2, \\ r(1 - \theta(J_1^s)) / \theta(J_1^s) & \text{for } M_3, \\ r / (1 - \theta(J_1^s)) & \text{for } M_4. \end{cases} \quad (7)$$

**Lemma 3.** *For model (1)–(3) the following equations hold:*

$$a' \Psi(J_1^s) = F^{-1}(M^{-1}(\mu(J_1^s))) = \begin{cases} \ln \mu(J_1^s) & \text{for model } M_1, \\ -\ln \mu(J_1^s) & \text{for model } M_2, \\ -\ln(\mu(J_1^s) / r) & \text{for model } M_3, \\ \ln((\mu(J_1^s) - r) / r) & \text{for model } M_4, \end{cases} \quad (8)$$

where  $\mu(\cdot)$  is determined by (7).

To construct statistical estimator for the unknown vector of parameters  $a = (a_i) \in R^m$  in the models (1)–(5) we will use the approach based on the frequencies-based estimators proposed in [3].

Introduce the notation:  $I\{C\}$  is the indicator function of the event  $C$ ;

$$\nu(J_1^s) = \sum_{t=s+1}^T I(X_{t-s}^{t-s} = J_1^s);$$

$$B(X_1^T) = \{J_1^s \in A^s : \nu(J_1^s) > 0\} = \{J_1^{s,(1)}, \dots, J_1^{s,(K)}\},$$

where  $K \leq T - s$  and  $\nu(J_1^{s,(i)}) \geq \nu(J_1^{s,(j)})$  for all  $i < j, (i, j = 1, \dots, K)$ ;  $K_0 = K_0(m, T, s) : N^3 \rightarrow N, m \leq K_0(m, T, s) \leq K$ , is a function nondecreasing w.r.t.  $m$ ;  $B_0 = \{J_1^{s,(1)}, J_1^{s,(2)}, \dots, J_1^{s,(K_0)}\} \subset B(X_1^T)$  with the cardinality  $|B_0| = K_0$ .

**Theorem 1.** For model (1)–(3) under the observed realization  $X_1^T = (x_1, x_2, \dots, x_T)' \in A^T$  the statistical estimator

$$\hat{\mu}(J_1^s) = \sum_{t=s+1}^T x_t I(X_{t-s}^{t-s} = J_1^s) / \nu(J_1^s)$$

is a consistent estimator of  $\mu(J_1^s)$  for  $T \rightarrow +\infty$ .

**Theorem 2.** For model (1)–(5) under the observed realization  $X_1^T = (x_1, x_2, \dots, x_T)' \in A^T$  the statistical estimator

$$\hat{a} = H^{-1}C, \tag{9}$$

is a consistent estimator of vector parameter  $a$ , where  $H = \sum_{J_1^s \in B_0} \Psi(J_1^s) \Psi^T(J_1^s)$ ,

$$C = \sum_{J_1^s \in B_0} F^{-1}(M^{-1}(\mu(J_1^s))) \Psi(J_1^s) = \sum_{J_1^s \in B_0} \begin{cases} \ln(\hat{\mu}(J_1^s)) \Psi(J_1^s) & \text{for } M_1, \\ -\ln(\hat{\mu}(J_1^s)) \Psi(J_1^s) & \text{for } M_2, \\ -\ln(\hat{\mu}(J_1^s)/r) \Psi(J_1^s) & \text{for } M_3, \\ \ln((\hat{\mu}(J_1^s) - r)/r) \Psi(J_1^s) & \text{for } M_4, \end{cases}$$

and  $\{\hat{\mu}(J_1^s)\}$  are from Theorem 1.

### 3 Statistical forecasting of count time series

**Theorem 3.** For the model (1)–(3) under the observed realization  $X_1^T = (x_1, x_2, \dots, x_T)' \in A^T$  and  $|H| \neq 0$  the optimal forecasting statistic for the future state  $x_{T+1} \in A$  that minimizes the mean square error of forecasting [2] is:

$$\hat{x}_{T+1} = \begin{cases} \left[ \hat{\theta} \right] & \text{for model } M_1, \\ \left[ (1 - \hat{\theta}) / \hat{\theta} \right] & \text{for model } M_2, \\ \left[ r(1 - \hat{\theta}) / \hat{\theta} \right] & \text{for model } M_3, \\ \left[ r / (1 - \hat{\theta}) \right] & \text{for model } M_4, \end{cases} \tag{10}$$

where  $\hat{\theta} = F(\hat{a}'\Psi(X_{T-s+1}^T))$ ,  $\lfloor y \rfloor$  means the floor function of  $y$ .

## 4 Results of computer experiments

Experiments were performed in R computer language. Figure 1 for model  $M_1$  illustrates dependence of the Monte-Carlo estimate of the mean square error (MSE) for estimator (9) from  $\log_2 T$  with  $M = 100$  replications.

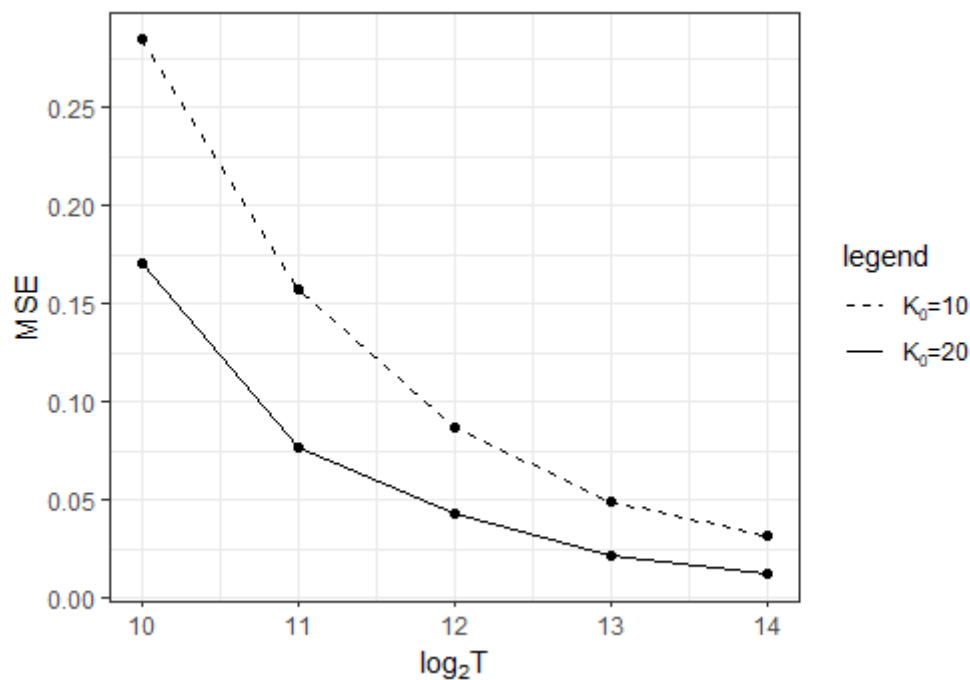


Figure 1: Dependence of the mean square error from  $\log_2 T$

## References

- [1] Frank A.H., Melvin A.B. (1960). The Borel-Tanner distribution. *Biometrika* Vol. **47** (1-2), pp. 143-150.
- [2] Kharin Y.S. (2013). *Robustness in Statistical Forecasting*. Springer, New York.
- [3] Kharin Y.S., Voloshko V.A., Medved E.A. (2018). Statistical estimation of parameters for binary conditionally nonlinear autoregressive time series. *Math Met Stat.* Vol. **17** (2), pp. 103-118.
- [4] Hastings N.A, Peacock J.B. (1979). *Statistical distributions*. John Wiley & Sons Inc, New Jersey.

# PERFORMANCE AND ROBUSTNESS IN SEQUENTIAL TESTING OF HYPOTHESES

A.YU. KHARIN, TON THAT TU

*Belarusian State University; University of Danang*

*Minsk, BELARUS; Danang, VIETNAM*

e-mail: KharinAY@bsu.by; tttu@ued.udn.vn

## Abstract

The problem of sequential testing of parametric hypotheses is considered. Different models of data are analyzed for simple and also for complex hypotheses setting. The approaches to performance characteristics (error probabilities and expected sample sizes) calculation and to robustness analysis (under deviations from the hypothetical model assumptions) of the sequential tests are developed. Within these approaches, asymptotic expansions (w.r.t. the discretization parameter and the distortion levels) of the performance characteristics are obtained, and the robustified sequential procedures are constructed.

**Keywords:** sequential test, stochastic data, error probability, expected number of observations, distortion, robustness

## 1 Introduction

In computer data analysis of stochastic data to solve problems of hypotheses testing the sequential approach [12] is intensively used [11]. In sequential approach the number of observations is not fixed a priori, but is a random variable that depends on observation themselves. Due to the complicated scheme of the sequential inference, the performance characteristics of sequential tests (error probabilities, expected number of observations) are problematic to be calculated with a given accuracy even for basic hypothetical models [10].

The second problem is that the sequential procedures constructed theoretically to be optimal under the hypothetical model, in practice are applied to real data sets that usually do not follow that hypothetical model exactly, the hypothetical model is often distorted [1], [3], [9].

In this paper we present the results on performance and robustness analysis of sequential statistical tests for different models of data, and on robust sequential test construction.

## 2 Performance and Robustness in Case of Simple Hypotheses

### 2.1 Independent homogeneous observations

Let on a probability space  $(\Omega, \mathcal{F}, P)$  discrete random variables  $x_1, x_2, \dots$  be defined,  $\forall t \in \mathbf{N}$ ,  $x_t \in U = \{u_1, u_2, \dots, u_M\}$ ,  $M < \infty$ ,  $u_1 < u_2 < \dots < u_M$ . Let these

random variables be independent identically distributed, from a discrete probability distribution with a parameter  $\theta \in \Theta = \{\theta_0, \theta_1\}$ :

$$P(u; \theta) = P_\theta\{x_t = u\} = a^{-J(u; \theta)}, \quad t \in \mathbf{N}, u \in U, \quad (1)$$

$a \in \mathbf{N} \setminus \{1\}$ ;  $J(u; \theta): U \times \Theta \rightarrow \mathbf{N}_0$  is a function satisfying  $\sum_{u \in U} a^{-J(u; \theta)} = 1$ .

Consider two simple hypotheses w.r.t. the parameter  $\theta$ :

$$H_0 : \theta = \theta_0, \quad H_1 : \theta = \theta_1. \quad (2)$$

Such a problem often appears in applications, where one of the two possible regimes can be realized.

Introduce the notation:

$$\Lambda_n = \Lambda_n(x_1, \dots, x_n) = \sum_{t=1}^n \lambda_t;$$

$$\lambda_t = \log_a (P(x_t; \theta_1)/P(x_t; \theta_0)) = J(x_t; \theta_0) - J(x_t; \theta_1) \in \mathbf{Z}.$$

To test hypotheses (2) by  $n$  ( $n = 1, 2, \dots$ ) observations consider the sequential probability ratio test (SPRT) [12]:

$$d_n = \mathbf{1}_{[C_+, +\infty)}(\Lambda_n) + 2 \cdot \mathbf{1}_{(C_-, C_+)}(\Lambda_n), \quad (3)$$

where  $\mathbf{1}_D(\cdot)$  is the indicator function of the set  $D$ . The decisions  $d_n = 0$  and  $d_n = 1$  mean stopping of the observation process and the acceptance of the appropriate hypothesis. The decision  $d_n = 2$  means that it is necessary to make the  $(n + 1)$ -th observation. In (3) the thresholds  $C_-, C_+ \in \mathbf{R}$ ,  $C_- < C_+$  are the given values (parameters of the test). According to [12], we use

$$C_+ = [\log_a ((1 - \beta_0)/\alpha_0)], \quad C_- = [\log_a (\beta_0/(1 - \alpha_0))], \quad (4)$$

where  $\alpha_0, \beta_0$  are given maximal possible values of the probabilities of type I and type II errors respectively. In fact, the true values  $\alpha, \beta$  for the probabilities of type I and type II errors differ from  $\alpha_0, \beta_0$  [2].

For this model of data, the performance characteristics (error probabilities  $\alpha, \beta$  and the mathematical expectations of the sample size  $t_0, t_1$  under the correspondent hypothesis being true) are calculated in the explicit form in [3].

In the situation, where the assumption 1 does not hold, the approach to calculate the performance characteristics is given in [2].

For the case of distorted observations, the correspondent asymptotic expansions (w.r.t. one more extra parameter – the distortion level) are derived in [4]. The robustified sequential test is constructed in [5].

## 2.2 Heterogeneous observations

Let  $x_1, x_2, \dots$  be observations of time series with a trend:

$$x_t = \theta^T \psi(t) + \xi_t, \quad t = 1, 2, 3, \dots,$$

where  $\psi(t) = (\psi_1(t), \psi_2(t), \dots, \psi_m(t))^T$ ,  $t \geq 1$ , are the vectors of basic functions of trend,  $\theta = (\theta_1, \theta_2, \dots, \theta_m)^T \in \mathbf{R}^m$  is an unknown vector of coefficients, and  $\{\xi_t, t \geq 1\}$  is the sequence of independent identically distributed random variables,  $\xi_t \sim \mathcal{N}(0, \sigma^2)$ .

Consider two simple hypotheses (2).

Denote the accumulated log-likelihood ratio statistic:  $\Lambda_n = \Lambda_n(x_1, x_2, \dots, x_n) = \sum_{t=1}^n \lambda_t$ , where  $\lambda_t = \ln \left( \frac{p_t(x_t, \theta^1)}{p_t(x_t, \theta^0)} \right)$  is the log-likelihood ratio calculated on the observation  $x_t$ , and  $p_t(x, \theta)$  is the probability density function of  $x_t$  provided the parameter value is  $\theta$ .

To test these hypotheses, after  $n$  observations one makes the decision (3).

For this model of data, the approach to calculate the performance characteristics of the sequential test is developed.

The situation where certain observations can be missed, is considered. The sequential test for this situation is constructed and its performance characteristics are evaluated.

### 2.3 Observations forming a Markov chain

In [8] the situation, where observations are forming a homogeneous Markov chain, is considered. For this situation, asymptotic expansions for performance characteristics are derived. The robust sequential tests are constructed in [2] under distortions of the factual values of the one-step transition probabilities matrices.

## 3 Performance and Robustness in Case of Composite Hypotheses

Suppose a sequence  $x_1, x_2, \dots$  of i.i.d. random variables is observed from a continuous distribution with the p.d.f.  $p(x | \theta)$ , where  $\theta \in \Theta \subseteq \mathbf{R}$  is an unknown value of random parameter. Consider two composite hypotheses

$$H_0 : \theta \in \Theta_0, H_1 : \theta \in \Theta_1; \quad (5)$$

$\Theta_0, \Theta_1 \in \Theta$ ,  $\Theta_0 \cap \Theta_1 = \emptyset$ . Assume that the prior p.d.f.  $p(\theta)$  is known.

One of the possible techniques to test the hypotheses (5) is using of weight functions proposed by Wald [12]. Introduce the notation:

$$W_i = \int_{\Theta_i} p(\theta) d\theta, w_i(\theta) = \frac{1}{W_i} \cdot p(\theta) \cdot \mathbf{1}_{\Theta_i}(\theta), \theta \in \Theta, i = 0, 1; \quad (6)$$

$$\Lambda_n = \Lambda_n(x_1, \dots, x_n) = \ln \frac{\int_{\Theta} w_1(\theta) \prod_{i=1}^n p(x_i | \theta) d\theta}{\int_{\Theta} w_0(\theta) \prod_{i=1}^n p(x_i | \theta) d\theta}. \quad (7)$$

For testing hypotheses (5), under the notation (6), (7) the following parametric family of tests is used:

$$N = \min\{n \in \mathbf{N} : \Lambda_n \notin (C_-, C_+)\}, \quad (8)$$

$$d = \mathbf{1}_{[C_+, +\infty)}(\Lambda_N), \quad (9)$$

where (8) gives the stopping rule,  $N$  is the random number of the observation, at which the decision  $d$  is made according to (9);  $d = i$  means that the hypothesis  $H_i$ ,  $i = 0, 1$ , is accepted;  $C_- < 0$ ,  $C_+ > 0$  are parameters of the test, which are usually chosen in practice according to (4).

In [7], expressions in the explicit form are derived for the special case of the data distribution, and asymptotic expansions are constructed in the general case for the performance characteristics, also under distortions. The robust sequential test [6] is constructed by the minimax risk criterion.

## References

- [1] Huber P. J. (2004). *Robust Statistics: Theory and Methods*. Wiley, New York.
- [2] Kharin A. (2013). *Robustness of Bayesian and Sequential Statistical Decision Rules*. BSU, Minsk.
- [3] Kharin A., Galinskij V. (1999). On minimax robustness of Bayesian statistical prediction. *Probability Theory and Mathematical Statistics*. TEV, pp. 259-266.
- [4] Kharin A. (2016). Performance and robustness evaluation in sequential hypotheses testing. *Communications in Statistics – Theory and Methods*. Vol. **45**, No. 3, pp. 1693-1709.
- [5] Kharin A. (2002). On Robustifying of the SPRT for a Discrete Model under “Contaminations”. *Austrian Journal of Statistics*. Vol. **31**, No. 4, pp. 267-277.
- [6] Kharin A. (2008) Robustness Evaluation in Sequential Testing of Composite Hypotheses. *Austrian Journal of Statistics*. Vol. **37**, pp. 51-60.
- [7] Kharin A. (2011) Robustness Analysis for Bayesian Sequential Testing of Composite Hypotheses under Simultaneous Distortion of Priors and Likelihoods. *Austrian Journal of Statistics*. Vol. **40**, pp. 65-74.
- [8] Kharin A. (2013). Robustness of Sequential Testing of Hypotheses on Parameters of M-valued Random Sequences. *Journal of Mathematical Sciences*. Vol. **189**, No. 6, pp. 924-931.
- [9] Kharin A. (2005). Robust Bayesian prediction under distortion of prior and conditional distributions. *Journal of Mathematical Sciences*. Vol. **126** (1), pp. 992-997.
- [10] Lai T. L. (2001). Sequential Analysis: Some Classical Problems and New Challenges. *Statistica Sinica*. Vol. **11**, pp. 303-408.
- [11] Mukhopadhyay N., Datta S., Chattopadhyay S. (2004). *Applied Sequential Methodologies*. Marcel Dekker, New York.
- [12] Wald A. (1947). *Sequential Analysis*. Wiley, New York.

# ON SOME NEW ASPECTS IN ACQUISITION AND ANALYSIS OF BRAIN ELECTRICAL ACTIVITY

A.V. KOLCHIN<sup>1</sup>, H.G. IONKINA<sup>2</sup>

<sup>1</sup>*Moscow Automobile and Road Construction State Technical University (MADI)*

<sup>2</sup>*I.M. Sechenov First Moscow State Medical University (Sechenov University)  
Moscow, RUSSIA*

e-mail: <sup>1</sup>akolchin@madi.ru, <sup>2</sup>helena.ionkina@sechenov.ru

## Abstract

We give a description of a portable system for continuous acquisition of the brain electrical activity based on ARM microcomputers driven by Linux and discuss some problems which arise while developing, implementing, and fine-tuning the system.

**Keywords:** data science, brain electrical activity, ARM microcomputer, continuous acquisition

We developed, implemented, and fine-tuned a portable system for continuous acquisition of the electrical activity of a brain. The key features of the system consist of the following: high sensitivity ( $\mu\text{V}$ ); high-resolution measurement (discretisation up to a hundred kHz per channel); presence of no filters of the input signal in both the analogue-to-digital converter and amplifier modules; this results in the near absence of analogue data loss while acquiring the real time brain bioelectrical activity. The problem to prevent garbling of the input data due to intense electromagnetic pollution of the environment was solved by making use of a multilayer shielding of the analogue part of the system and by using an autonomous direct current power source to feed the whole system.

We investigated the role which the brain cortex plays in formation of the nociceptive reactions by means of analysis of the electroencephalogram and the evoked potentials (EPs) acquired in the somatosensory S<sub>1</sub>HL and the anterior cingulate Cg areas of cerebral cortex in the right hemisphere in immobilised Wistar male rats before the intraperitoneal injection of a lipopolysaccharide (LPS) and at the 1st, 3rd and 7th days after it upon an electrocutaneous stimulation of the tail. The stimulation of the rat tail was by single rectangular current impulses. The EPs were then averaged. In [1, 2], we give an example of dynamics of nociceptive EPs registered in the S<sub>1</sub>HL area of rat's cerebral cortex. We thus came to the classical biostatistics problem to find whether there was an effect of a single administration of a drug or not (see, e.g., [7]); to solve it, we made use of the non-parametric Wilcoxon test; this test uses only the information on the differences between values of the parameters and their signs, and there is no need to make assumptions concerning the laws of distribution of the differences of the parameters under investigation upon the action of the drug. The parametric tests based on the normal approximations appear to be of little use in our case.

If one takes the laboratory animal as a "black box" whose input is some external stimulus while the output yields a high-volume data flow, then the aim of the experiment consists of separating the response to the input stimulus in this flow.

Because of inevitable wear and outdating to which the computer and other laboratory equipment is subject to, we have to go through a severe upgrade and modernisation of the system described in [1, 2, 3, 4, 5].

The stimuli routed to an experimental animal via the constant current isolator unit A365D (World Precision Instruments, Inc.) are now precision-controlled by a Raspberry Pi 3B+ 64-bit quad-core ARM Cortex-A53 microcomputer (shielded in a metal enclosure) by means of its very well documented General Purpose Input/Output (GPIO) interface; we use the `wiringPi` library. The start of acquisition of the electrical activity of the rat brain is triggered by the synchronising impulse issued at a fixed (maybe zero) time interval before the leading front of the stimulus impulse.

The acquisition of electrophysiological data with the use of a 16-channel analogue-to-digital converter `usbdux-fast` (Incite Technology Ltd.), and the visualisation of the acquired electroencephalogram and EPs are now carried out by another Raspberry Pi 3B+ microcomputer loaded with modified Raspbian Stretch Linux with the `COMEDI` project open-source drivers, tools, and libraries for data acquisition implemented as core Linux kernel modules suitable for real-time tasks. This unit is complemented by a high-speed SATA 2.5" hard disk drive of large enough capacity coupled with X820 interface board by SupTronics Ltd. enclosed together in a metal heat-dissipating electromagnetic shielding case.

The Motorola LapDock display/keyboard unit can be successfully used to operate the whole system.

Since the libraries and the firmwares source codes are open source, we succeeded in implementing necessary corrections and revisions in minimal time.

The input electroencephalogram is visually monitored in real time with the use of `xoscope`. In order to capture the data, we use `ktimetrace`; it permits to capture samples from desired channels of our data acquisition device in a given time interval starting either from an arbitrary time instant or from that governed by the external synchronising signal and to save it to a file while providing a real-time graphing display. The data thus obtained form a text file whose each row consists of numerical values captured from the channels at the corresponding time instants. The size of the file can grow to an extremely large value, so we have to use the appropriate file system (`ext4`).

A key feature implemented is visualisation of the electroencephalogram and the results of averaging the EPs as the data are collected in the course of the experiment.

With the use of the `FFTW` library (developed in Massachusetts Institute of Technology) to implement the discrete Fourier transformation and a series of complex wavelet transformations, we are able to observe and analyse the spectrum of the electroencephalogram we acquire.

The complex of solutions we have used while developing and setting up this system allow us to deal with a wide range of problems of electrophysiology, including electromyography, electrocardiography, electroencephalography, and recording of neuronal activity in the brain.

All investigations were carried out on male Wistar rats in compliance with the GLP principles.

The authors express a deep gratitude to Helio Chissini de Castro, Principal Software

Engineer, KDE project <helio@kde.org>, who rewrote `ktimetrace` to make it working on Raspbian Stretch.

## References

- [1] Ionkina E.G., Kolchin A.V. (2013). On acquisition of nociceptive evoked potentials in rats cerebral cortex. *Proc. X International Conference “Computer Data Analysis and Modeling: Theoretical and Applied Stochastics.”* Vol. **1**. Belarusian State Univ. Publ., Minsk, pp. 72–73.
- [2] Ionkina H.G., Kolchin A.V. (2015). Acquisition of the electrical activity of rat cerebral cortex. *Proc. Karelian Sci. Centre Russian Acad. Sci.* №**15**, pp. 62–66.
- [3] Ionkina H.G., Kolchin A.V. (2016). On some aspects in acquisition of brain electrical activity. *Proc. XI International Conference “Computer Data Analysis and Modeling: Theoretical and Applied Stochastics.”* Belarusian State Univ. Publ., Minsk, pp. 285–287.
- [4] Ionkina H.G., Kolchin A.V. (2016). On acquisition of brain electrical activity. *Review Industrial Appl. Math.* **23**, №2, pp. 182–183.
- [5] Ionkina H.G., Kolchin A.V., Krylova E.N. (2016). Some aspects in acquisition of brain electrical activity. *Proc. XII International Interdisciplinary Congress “Neuroscience for Medicine and Psychology.”* MAKS Press, Moscow, pp. 183–184.
- [6] Bezrodnyy B.F., Ionkina H.G., Kolchin A.V. (2019). On some aspects of the registration and processing of low-current electrical signals. *Institute of Engineering Physics Reports* №**2** (**52**), pp. 11–13.
- [7] Glantz S.A. (2012) *Primer of Biostatistics*. McGraw–Hill, N.Y., etc.

# APPLICATION OF OPEN MARKOV NETWORKS WITH VARIOUS FEATURES AT MODELING REAL OBJECTS

D. KOPATS, M. MATALYTSKI

*Grodno State University of Yanka Koupala*

*Grodno, BELARUS*

e-mail: dk80395@mail.ru, m.matalytski@gmail.com

## Abstract

In article investigates an open Markov networks with multiple types of customers at a non-stationary regime. For finding state probabilities of this networks generalized the system of difference-differential equations (DDE) was compiled, for the solution of which a modified method of successive approximations was proposed, combined with the method of the series. The properties of successive approximations are described. Concrete examples of the use of open networks in modeling the behavior of the Internet system when it is attacked by various viruses are also presented.

**Keywords:** Markov network, data science, non-stationarity, difference-differential equation

## 1 Introduction

The method of successive approximations is used to find the probabilities of the states and expected revenues of the network systems in the case when the revenues from transitions are deterministic and depend only on the state of the network. For the first time in the area of queueing such a method was introduced by Harrison in [1] for a closed Jackson network. Then this method was used to analyze other Markov networks with various features [2-3]. As a result of the analysis of various networks, it was noted that the Kolmogorov DDE system for the probabilities of network states in the general case can be written as:

$$\begin{aligned} \frac{P(\vec{d}, \vec{k}, \vec{l}, t)}{dt} = & -\Lambda(\vec{d}, \vec{k}, \vec{l})P(\vec{d}, \vec{k}, \vec{l}, t) + \sum_{i^*, j^*=0}^n \sum_{\alpha, \beta, \gamma, \theta, \eta=0}^{\Psi r} \sum_{m=0}^{\infty} \sum_{b=0}^1 \Phi_{i^* j^* \alpha m \beta b \gamma \theta \eta}(\vec{d}, \vec{k}, \vec{l}) \times \\ & \times P(\vec{d} + I_{i^*} - I_{j^*}, \vec{k} + \tilde{I}_{\alpha} + m\tilde{I}_{\beta} - b\tilde{I}_{\gamma}, \vec{l} + \tilde{I}_{\theta} - \tilde{I}_{\eta}, t), \end{aligned} \quad (1)$$

where  $\tilde{I}_{\alpha}$  - zero-vector of dimension  $\Psi r$ , except for the component with the number  $\alpha$ , which equal 1,  $\Psi$  - some integer positive number,  $r$  - number of type customer,  $I_{\alpha}$  - zero-vector of dimension  $n$ , except for the component with the number  $\alpha$ , which equal 1,  $\vec{d}$  - vector of dimension  $n$  with component  $d_i$ , where  $d_i$  - the number of service lines in the  $i$ -th QS,  $\vec{k}$  - vector of dimension  $\Psi r$  with component  $k_{ic}$ , где  $k_{ic}$  - the number of positive customers of type  $c$  in the  $i$ -th QS,  $\vec{l}$  - vector of dimension  $\Psi r$  with

component  $l_{ic}$ , где  $l_{ic}$  - the number of signals of type  $i$  in the  $i$ -th queueing system (QS),  $i = \overline{1, n}, c = \overline{1, r}$ .

$\Phi_{i^*j^*\alpha m\beta b\gamma\theta\eta}(\vec{d}, \vec{k}, \vec{l})$  - transition intensity of the queueing network (QN) from state  $(\vec{d}, \vec{k}, \vec{l})$  in other, and this transition is characterized by the following parameters:  $i^*, j^*$  characterize the number of QS in which the service line is broken or restored, respectively,  $m$  - size of deleted group,  $\beta$  - number of component of vector  $\vec{k}$ , which there is a removal group of positive customers of the corresponding type from the corresponding QS,  $\alpha$  - number of corresponding component of vector  $\vec{k}$ , in which there was a receipt of a positive customer of the corresponding type in the corresponding QS and in the corresponding queue,  $\gamma$  - number of corresponding component of vector  $\vec{k}$ , in which there was a leave of a positive customer of the corresponding type from the corresponding QS,  $\theta, \eta$  - number of corresponding component of vector  $\vec{l}$  in which arriving or deleting of signal after delete positive customer of corresponding type in corresponding QS,  $\Lambda(\vec{d}, \vec{k}, \vec{l})$  - intensity of exit of state  $(\vec{d}, \vec{k}, \vec{l})$ .  $P(\vec{d}, \vec{k}, \vec{l}, t)$  - state probability  $(\vec{d}, \vec{k}, \vec{l})$  in moment time  $t$ .

Series  $\sum_{i^*, j^*=0}^n \sum_{\alpha, \beta, \gamma, \theta, \eta=0}^{\Psi r} \sum_{m=0}^{\infty} \sum_{b=0}^1 \Phi_{i^*j^*\alpha m\beta b\gamma\theta\eta}(\vec{d}, \vec{k}, \vec{l})$  is converge for all Markov QN.

This follows from that, what network state in all moment time is Markov chain with countable number states, i.e. system of DDE (1) is special case of system of differential equations for states probabilities of the Markov chain with continuous time, in which  $\Lambda(\vec{d}, \vec{k}, \vec{l})$  intensity of exit of state  $(\vec{d}, \vec{k}, \vec{l})$ , and sum of the series - sum of entry intensity of this state.

## 2 Solution of the DDE system

The solution of the system (1) is:

$$\begin{aligned}
 P(\vec{d}, \vec{k}, \vec{l}, t) &= e^{-\Lambda(\vec{d}, \vec{k}, \vec{l})t} \left( P(\vec{d}, \vec{k}, \vec{l}, 0) + \int_0^t e^{\Lambda(\vec{d}, \vec{k}, \vec{l})x} \times \right. \\
 &\times \sum_{i^*, j^*=0}^n \sum_{\alpha, \beta, \gamma, \theta, \eta=0}^{\Psi r} \sum_{m=0}^{\infty} \sum_{b=0}^1 \Phi_{i^*j^*\alpha m\beta b\gamma\theta\eta}(\vec{d}, \vec{k}, \vec{l}) \times \\
 &\times P(\vec{d} + I_{i^*} - I_{j^*}, \vec{k} + \tilde{I}_{\alpha} + m\tilde{I}_{\beta} - b\tilde{I}_{\gamma}, \vec{l} + \tilde{I}_{\theta} - \tilde{I}_{\eta}, x) dx. \tag{2}
 \end{aligned}$$

Denote by  $P_q(\vec{d}, \vec{k}, \vec{l}, t)$  - respectively approximation  $P(\vec{d}, \vec{k}, \vec{l}, t)$  in the  $q$ -th iteration, and  $P_{q+1}(\vec{d}, \vec{k}, \vec{l}, t)$  - solution of system (1) obtained by the method of successive approximations. Then from (2) it follows that

The solution of the system (1) is:

$$P_{q+1}(\vec{d}, \vec{k}, \vec{l}, t) = e^{-\Lambda(\vec{d}, \vec{k}, \vec{l})t} \left( P(\vec{d}, \vec{k}, \vec{l}, 0) + \int_0^t e^{\Lambda(\vec{d}, \vec{k}, \vec{l})x} \times
 \right.$$

$$\begin{aligned} & \times \sum_{i^*, j^*=0}^n \sum_{\alpha, \beta, \gamma, \theta, \eta=0}^{\Psi r} \sum_{m=0}^{\infty} \sum_{b=0}^1 \Phi_{i^* j^* \alpha m \beta b \gamma \theta \eta}(\vec{d}, \vec{k}, \vec{l}) \times \\ & \times P_q(\vec{d} + I_{i^*} - I_{j^*}, \vec{k} + \tilde{I}_\alpha + m\tilde{I}_\beta - b\tilde{I}_\gamma, \vec{l} + \tilde{I}_\theta - \tilde{I}_\eta, x) dx. \end{aligned} \quad (3)$$

We take the stationary solution as the initial approximation  $P_0(\vec{d}, \vec{k}, \vec{l}, t) = \lim_{t \rightarrow \infty} P_q(\vec{d}, \vec{k}, \vec{l}, t) = P(\vec{d}, \vec{k}, \vec{l})$  which satisfies the relation :

$$\begin{aligned} \Lambda(\vec{d}, \vec{k}, \vec{l}) P(\vec{d}, \vec{k}, \vec{l}) &= \sum_{i^*, j^*=0}^n \sum_{\alpha, \beta, \gamma, \theta, \eta=0}^{\Psi r} \sum_{m=0}^{\infty} \sum_{b=0}^1 \Phi_{i^* j^* \alpha m \beta b \gamma \theta \eta}(\vec{d}, \vec{k}, \vec{l}) \times \\ & \times P(\vec{d} + I_{i^*} - I_{j^*}, \vec{k} + \tilde{I}_\alpha + m\tilde{I}_\beta - b\tilde{I}_\gamma, \vec{l} + \tilde{I}_\theta - \tilde{I}_\eta). \end{aligned} \quad (4)$$

For successive approximations, the following statements are valid.

**Theorem 1.** *Successive approximations  $P_q(\vec{d}, \vec{k}, \vec{l}, t)$ ,  $q = 0, 1, 2, \dots$ , converge at  $t \rightarrow \infty$  to the stationary solution of the system of equations (1).*

**Theorem 2.** *The sequence  $P_q(\vec{d}, \vec{k}, \vec{l}, t)$ ,  $q = 0, 1, 2, \dots$ , constructed according to scheme (4), for any zero approximation bounded in  $t$   $P_0(\vec{d}, \vec{k}, \vec{l}, t)$  converge at  $q \rightarrow \infty$  to the unique solution of the system (1).*

**Theorem 3.** *Any approximation  $P_q(\vec{d}, \vec{k}, \vec{l}, t)$ ,  $q \geq 1$  representable as a convergent power series*

$$P_q(\vec{d}, \vec{k}, \vec{l}, t) = \sum_{l=0}^{\infty} g_{ql}(\vec{d}, \vec{k}, \vec{l}) t^l, \quad (5)$$

whose coefficients satisfy the recurrence relations:

$$\begin{aligned} \vec{g}_{q+1l}(\vec{d}, \vec{k}, \vec{l}) &= \frac{-\Lambda(\vec{d}, \vec{k}, \vec{l})^l}{l!} \left\{ P(\vec{d}, \vec{k}, \vec{l}, 0) + \sum_{u=0}^{l-1} \frac{(-1)^{u+1} u!}{\Lambda(\vec{d}, \vec{k}, \vec{l})^{u+1}} D_{qu}(\vec{d}, \vec{k}, \vec{l}) \right\} \\ \vec{g}_{q0} &= P(\vec{d}, \vec{k}, \vec{l}, 0), \vec{g}_{0l} = P(\vec{d}, \vec{k}, \vec{l}, 0) \delta_{l0}. \end{aligned} \quad (6)$$

The proof of Theorems 1-3 is similarly as in [4].

### 3 Example of the queueing network

Consider examples of the QN, the DDE system for has the form (1).

First network is network with signals and batch removal customers. The network description, it parameters and the DDE system for state probability is present in [4]. This system is a special case of the system (1)

$$\Lambda(\vec{d}, \vec{k}, \vec{l}) = \lambda^+ + \lambda^{(s)} + \sum_{i=1}^n \mu_i,$$

$$\begin{aligned} \Phi_{i^*j^* \alpha m \beta b \gamma \theta \eta}(\vec{d}, \vec{k}, \vec{l}) = & \left( \delta_{i^*j^*} \delta_{\vec{d}1^n} \delta_{\theta \eta} \delta_{\vec{l}0} (\delta_{b1} \delta_{\alpha i} \delta_{\gamma j} (\lambda_{0j}^+ u(k_j) + (\mu_j p_{j_i}^+ u(k_i)) (1 - \delta_{ij}) + \right. \\ & + \sum_{s=1}^n (1 - \delta_{si}) (\mu_i p_{i0} + \mu_i p_{is}^- (1 - u(k_s))) + \sum_{j=1}^n (1 - \delta_{ij}) \lambda_{0j}^{(c)} q_{j0} \pi_{jm} + \sum_{s=1}^n (1 - \delta_{js}) \mu_j p_{js}^- q_{s0} \pi_{sm} + \\ & \left. + u(m+1) \mu_i p_{is}^- (1 - u(k_s)) q_{s0} \pi_{sm} + \delta_{b1} \delta_{\alpha i} \delta_{\beta j} \delta_{\gamma s} \mu_i p_{ij}^- q_{js} u(k_s) \right), \end{aligned}$$

where  $\delta_{ij} = \begin{cases} 1, i = j, \\ 0, i \neq j. \end{cases}$ ,  $u(x)$  – Heaviside function.

This network applied at modeling of the operation of the Internet server, which is prone to attacks of exploits. The QS is understood as the processor of user requests in this server. Positive customers – the requests themselves, and signals (act as a negative customer or the exploit) which transfer requests to the phishing site. Signals that act as triggers are developer exploits that move requests from one developer to another.

Second network is G-network with unreliable nodes. The Network description, him parameters and the DDE system for state probabilities is present in [5]. The system is a special case of the system (1) has the form

$$\begin{aligned} \Lambda(\vec{d}, \vec{k}, \vec{l}) = & \sum_{i=1}^n \left( \lambda_{0i}^+ u(k_i) + u(d_i) (\lambda_{0i}^- + \mu_i + \gamma_i) + \beta_i (d_i + 1) \right), \\ \Phi_{i^*j^* \alpha m \beta b \gamma \theta \eta}(\vec{d}, \vec{k}, \vec{l}) = & \delta_{0b} \delta_{0\alpha} \delta_{\theta \eta} \delta_{\vec{l}0} (\delta_{0m} \delta_{0i^*} \gamma_i u(d_j) + \\ & + \delta_{0m} \delta_{0j^*} \beta_i u(1 - d_i)) + \delta_{i^*j^*} (\delta_{0m} \delta_{0\alpha} \delta_{1b} \delta_{\gamma j} \lambda_{0i}^+ u(k_i) + \delta_{0m} \delta_{i\alpha} \delta_{0b} \times \\ & \times u(d_{i^*}) (\mu_i p_{i0} + \lambda_{0i}^- + \mu_i \sum_{j=1}^n p_{ij}^- (1 - u(k_j))) + \delta_{0m} \delta_{i\alpha} \delta_{1b} \delta_{\gamma j} \mu_i u(d_i) p_{ij}^+ u(k_j) + \\ & + \delta_{1m} \delta_{i\alpha} \delta_{0b} \delta_{\beta j} \mu_i u(d_i) p_{ij}^-). \end{aligned}$$

This model is also used at modeling Internet servers. Positive customer are user requests, negative customer are the effect of a Botnet, which destroys the request in the developer's queue. Under the influence of the DDOS-attack the handler fails, and after repair by an engineer it recovers after a random time.

## References

- [1] Harrison P.G. (1961). Transient Behavior of Queueing Networks . *Journal of Applied Probability*. Vol. **18(2)**, pp. 482-490.
- [2] Matalytski M., Tikhonenko O., Kosareva E. (2011). *Queueing system and queueing network: analysis and application* . Publisher center of GrSU, Grodno. (In Russian)

- [3] Matalytski M., Naumenko V. (2016) *Stochastic network with non-standart moving of customers* Publisher center of GrSU, Grodno. (In Russian)
- [4] Matalytski M., Kopats D. (2017) Finding expected revenues in G-network with signals and customers batch removal *Probability in the Engineering and Informational Sciences* Vol. **31(4)**, pp. 561-575.
- [5] Matalytski M., Kopats D. (2019) Analasis of G-network with unrealible line service *Vesnik GrSU. Series 2. Mathematics. Physics. Informatics, Computer Technology and its Control.* Vol. **9(1)**, pp. 140-146.

# ABOUT THE PROCESSES IN THE CHANGING FRACTIONAL DIMENSION SPACE

M.E. KORNET, A.V. MEDVEDEV, E.D. MIHOV  
*Siberian Federal University*  
*Krasnoyarsk, RUSSIA*  
e-mail: edmihov@mail.ru

## Abstract

Processes in which the components of the vector of input actions are in stochastic dependence are considered in the report. Such processes are called H-processes. Computational studies have shown that H-processes occur in a space of fractional dimension. An algorithm for estimating the dimension of the space in which the process proceeds is proposed. Computational experiments were carried out on the basis of the proposed algorithm. Experiments have shown that the dimension of the space in which the H-process proceeds is not only fractional, but also variable.

**Keywords:** data science, fractional dimension space, H-process

## 1 Introduce

While multidimensional memoryless processes are studying,  $\vec{u} \in \Omega(\vec{u}) \subset R^n$  – control variables vector,  $\vec{x} \in \Omega(\vec{x}) \subset R^k$  - output variables vector, the following case can arise. When the model is constructed according to the sample  $x_i, u_i, i = \overline{1, s}$ , as an example  $A^\alpha(\vec{u}(t), \vec{x}(t), \vec{\alpha})$ , then if  $\vec{u} \in \Omega(\vec{u}) \subset R^n$  we can achieve an estimate  $\vec{x}_s \notin \Omega(\vec{x})$ , i.e. outside the technological rules, even physically impossible  $\vec{x}(\vec{u})$  values. This fact can be explained by following considerations.

Let the process proceeds in a single cube  $\Omega(\vec{u}, x) = \Omega(u_1, u_2, x) \subset R^3$ . The process range is  $\Omega^H(\vec{u}, x) \subset \Omega(\vec{u}, x)$ , representing the surface in the area  $\Omega(\vec{u}, x)$  (Fig. 1), we omit the influence of noise  $\xi(t)$  and measurement errors, for simplicity.

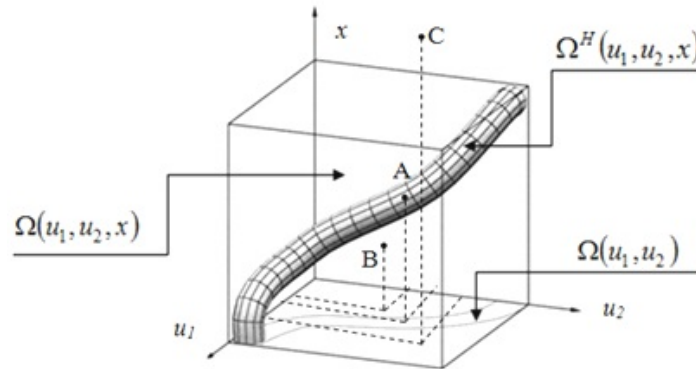


Figure 1: Scheme of the H-process

Real values of the process variables may be known from the technological rules, for example. Thus process takes place in some area  $\Omega(u_1, u_2, x)$ , in particular, a single cube. If there are a stochastic dependence of input variables the process does not take place in the area  $\Omega(u_1, u_2, x)$ , but only in its subarea  $\Omega^H(u_1, u_2, x) \subset \Omega(u_1, u_2, x)$ . True process area  $\Omega^H(\vec{u}, x)$  is always unknown, precisely this is the main complexity when modelling this kind of processes, named H-processes, in other words, pipe process (Fig.1). An example of such processes can be any processes in which the components of the vector of input actions are stochastically dependent.

## 2 The processes in the changing fractional dimension space

Let us give an example is concerned with the identification of the memoryless system. Let the object be described by the equation

$$x(\vec{u}) = f(u_1, u_2, u_3), \quad (1)$$

$f(u_1, u_2, u_3) \in R^3$  – input variable,  $x \in R^1$  – output variable. The traditional way to build a model of this process is to define a class of parametric operator  $\hat{x}(\vec{u}) = \hat{f}(u_1, u_2, u_3, \alpha)$  and further estimate  $\alpha$  parameters using a sample of observations  $(\vec{u}_i, x_i), i = \overline{1, s}$ .  $s$  – sample size.

Let the components of input variables vector  $\vec{u} = (u_1, u_2, u_3)$  are independent. In this case, the process takes place in 4-dimensional space.

We assume that the components of input vector are in function dependence. For example:

$$u_2 = \phi_1(u_1), u_3 = \phi_2(u_2) = \phi_2(\phi_1(u_1)). \quad (2)$$

Obviously, the researcher does not know about dependencies (2). Otherwise, the researcher can make the substitution (2) in (1) and get the dependence of  $x$  on one variable  $u_1$ :

$$x(\vec{u}) = f(u_1, \phi_1(u_1), \phi_2(\phi_1(u_1))). \quad (3)$$

Equation (3) is easily reduced to the two-dimensional (4), when there is no dependence of  $u_3$  on  $u_2$ .

$$x(\vec{u}) = f(u_1, \phi_1(u_1), u_3). \quad (4)$$

From this we can conclude that, in the presence of functional dependencies between the components of the vector, we obtain the dependences of  $x$  on  $u$ , in this case one-, two-, three-dimensional.

Let us analyze the case related to H-processes. Let  $u_3$  and  $u_2$ , have a stochastic dependence. Remind, if the components of input vector are independent, the process is described by a function of three variables. If two components of input vector are functionally dependent, the process is described by a function of two variables. If two

components of input vector are stochastically dependent the process is described by a function of more than two variables, but less than three.

When the stochastic dependence of process input variables exists, it occurs in pipe space with fractional dimension  $F^\lambda$ .

Dimension calculation can be estimated  $F^\lambda$  as (5), for example [1]:

$$\dim F^\lambda = (n + 1) - \sum_{k=1}^{n-1} \lambda_{k,k+1}, \quad \lambda_{k,k+1} = \frac{\sum_{j=1}^s (u_s^k(u_j^{k+1}) - u_j^k)^2}{\sigma^2(u^k)} \quad (5)$$

$n$  – vector  $\vec{u}$  dimension;  $\lambda_{k,k+1}$  is the “strength” of the stochastically dependence between  $u_k$  and  $u_{k+1}$  (for example correlation between  $u_k$  and  $u_{k+1}$ );  $\sigma^2(u^k)$  – random variance  $u^k$ ;  $u_s^k(u_j^{k+1})$  – non-parametric estimation of Nadaraya-Watson  $M\{u^k|u^{k+1}\}$

Dimension calculation  $F^\lambda$  can be estimated other ways.

### 3 The numerical studies of H-processes

The process is described by the function  $x = f(\vec{u})$ . Dimension of the vector  $\vec{u}$  is 10.

The components of the vector of input actions are functionally dependent. It is important to note that the dimension of the space in which the process proceeds depends on the strength of the stochastic connection between the components of the vector of input variables (this is the second term in (5)). To change the strength of the stochastic connection, between the components of the vector of input variables on the components of the vector of input variables is superimposed noise  $\xi(t)$ . Considered 2 cases in the first  $\xi(t) = 0\%$ , and in the second  $\xi(t) = 10\%$ .

We construct a graph of the dependence between the sample size of observations and the estimate of the dimension of the space in which the process takes place.

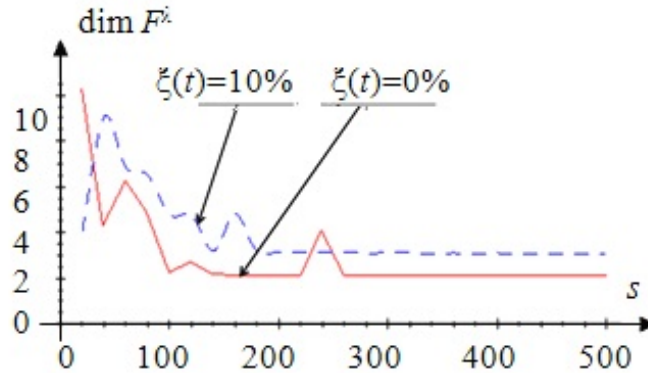


Figure 2: Estimation of  $\dim F^\lambda$  depending on the sample size

As can be seen from figure 2, for small volumes of a sample of observations, the algorithm does not accurately estimate the dimension of the space in which the process

proceeds. With an increase in the sample size of observations  $(\vec{u}_i, x_i), i = \overline{1, s}$ , the estimation accuracy increases, approaching 2, when  $\xi(t) = 0\%$  or 3 when  $\xi(t) = 10\%$ .

We construct a graph of the dependence between the sample size of observations and the estimate of the dimension of the space in which the process takes place for the case when the dimension of the vector  $\vec{u}$  is 2. The components of the vector of input actions are also in a functional dependence.

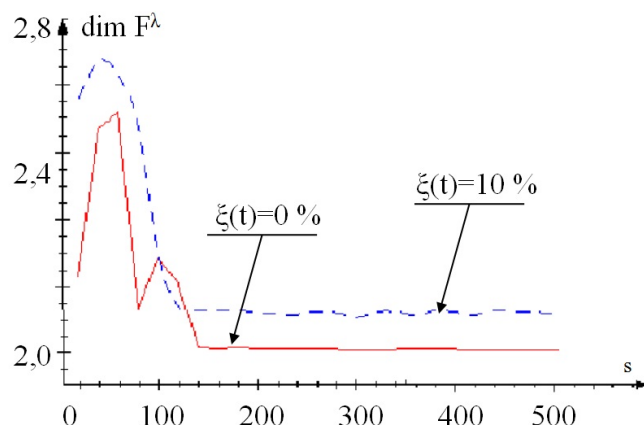


Figure 3: Estimation of  $\dim F^\lambda$  depending on the sample size

Figure 3 also shows that with an increase in the sample size of observations, the accuracy of estimating the dimension of the space in which the process proceeds increases, approaching 2, when  $\xi(t) = 0\%$  or 2,1 when  $\xi(t) = 10\%$ .

It should be noted that it is important for the researcher not the ability to determine the dimension of the space in which such processes take place, but the ability to build models of such processes.

## 4 Conclusion

Numerical researches proved that dimension of the H-process space is a variable quantity. This may mean that in addition to formula (5), other procedures for the dimension calculating can be proposed. Obviously, different formulas will give similar results under identical conditions. This is due to the following factors: the influence of interference, sample sizes, the location of samples in the observation space [1].

## References

- [1] Medvedev A.V.(2018). *Fundamentals of the Theory of Nonparametric Systems*. iz-vo SibGAU, Krasnoyarsk.[Russian] P. 732
- [2] Medvedev A.V.(1995). Data Analysis in Identification Tasks. *Computer Data Analysis and Modeling*. Vol. **2**, pp. 201-206. [Russian]

# PROBABILISTIC DATA ANALYSIS FOR PREDICTING MEAN TIME BEFORE CRITICAL INTEGRITY LOSSES OF COMPLEX SYSTEM WHEN EXPLICIT QUANTITATIVE REQUIREMENTS TO INTEGRITY ARE NOT SPECIFIED

A. KOSTOGRYZOV<sup>1</sup>, A. NISTRATOV<sup>2</sup>, G. NISTRATOV<sup>3</sup>

<sup>1</sup>*Federal Research Center "Computer Science and Control", Russian Academy of  
Sciences*

<sup>2</sup>*Russian Power Agency of Ministry for the Power Generating Industry*

<sup>3</sup>*Research Institute for Applied Mathematics and Certification  
Moscow, RUSSIA*

e-mail: <sup>1</sup>Akostogr@gmail.com

## Abstract

When the requirements to system integrity are not specified (including dangerous manufacture, "smart" equipment, robotic systems, artificial intelligence systems etc.) the questions are appeared: What time can pass before crossing of conditional border of a possible critical loss of integrity? How to define this conditional time border quantitatively (to use preventive countermeasures in real time)? The mathematical approach to solve a problem of predicting mean time before critical integrity losses for complex system, when explicit quantitative requirements to integrity are not specified, is proposed.

**Keywords:** data science, integrity loss, prediction

## 1 Introduction

For modern complex systems there are often problems of predicting mean time before critical integrity losses - it is understood as virtual crossing a conditional border of integrity. System (element) integrity is defined as such system (element) state when system (element) purposes are achieved with the required quality and safety. Reservoirs with water on coal mines may serve an example of system when quantitative requirements to integrity are defined obviously. Filling reservoir above defined upper border is inadmissible because of possible overflow of the reservoir and mine flooding. And filling of the reservoir below defined bottom border is inadmissible from the point of view of readiness to fire-prevention actions. However at systems operation in the conditions of uncertainty (for example, in dangerous manufacture) there are cases when integrity borders are fuzzy or are not specified. So, for enterprise equipment the monitored values parameters are always to be kept within working ranges. But really for some parameters there are deviations not only from working, but also from normative borders. And thus critical integrity losses do not appear (emergencies, failure, quality or safety losses), though long deviations from normative requirements potentially conduct to integrity losses. The questions are: What time can pass before crossing of such conditional border of a possible critical loss of integrity? How to

define this conditional time border quantitatively (to use preventive countermeasures in real time)? Similar questions are not only for dangerous manufacture, but also for “smart”equipment, robotic systems, artificial intelligence systems. Integrity losses of requirements to quality, reliability or safety at systems operation are critical independent on borders which are specified obviously or not specified [1]. It is proposed the mathematical approach to solve such problem.

## 2 Description of idea

The mathematical model, allowing to calculate the probability of integrity during given prognostic period ( $T_{given}$ ) should be selected. Analytical impression should reveal dependability on frequency of dangerous influences (defining the beginning of influencing), mean activation time, mean recovery time, time between the end of diagnostics and the beginning of next diagnostics, diagnostics time. Considering that the prediction is useful for such time  $T_{given}$ , for which it is possible to undertake preventive actions, and this time practically equals to activation time (when “integrity” may be lost after beginning of influencing), we define values of these parameters as unknown and designate these by one unknown “x”.

Further, setting confidence probability of integrity during given prognostic period we solve the analytical equation to find unknown “x”. The maximum value of all revealed solutions “x” gives more wide opportunities for a choice and use of adequate preventive countermeasures against possible losses of integrity. This is the found solution.

## 3 Selected probabilistic model

For every element and whole system the next limited set of two elementary events is proposed: “integrity is provided”(when from integrity point of view no additional actions are needed) and alternatively “integrity is lost”(when some actions are needed for recovering lost integrity).

For calculation in point of given prognostic period  $T_{given}$  the probabilistic model “Protection against dangerous influences”[1] is selected. It allows to estimate technology of periodical system diagnostics. During diagnostics the recovery of lost integrity is initiated (if needed). The next metrics are used for probabilistic prediction: the probability  $P(T_{infl}, T_{activ}, T_{betw.}, T_{diag}, T_{given})$  of integrity during given prognostic period (if all time during this given period element or system will be in elementary event “integrity is provided”) and the probability to lose integrity (if at least once during this given period element or system will be in event “integrity is lost”) - as addition to 1 the probability of integrity.

If element or whole system is presented as “black box”the input data for probabilistic prediction are the next: given prognostic period  $T_{given}$ ; frequency of dangerous influences on “black box”  $\frac{1}{T_{infl}}$  (defining the beginning of influencing); mean activation time  $T_{activ}$  (when “integrity” may be lost after beginning of influencing); time between the end of diagnostics and the beginning of next diagnostics  $T_{betw.}$ ; diagnostics time  $T_{diag}$ .

The next assumption is used: diagnostics time includes recovery time. There are possible the next variants for technologies 1 and 2: variant 1 - the given prognostic period  $T_{given}$  is less than established period between neighboring diagnostics ( $T_{given} < T_{betw.} + T_{diag}$ ) - see Figure 1; variant 2 - the prognostic period  $T_{given}$  is more than or equals to established period between neighboring diagnostics ( $T_{given} \geq T_{betw.} + T_{diag}$ ).

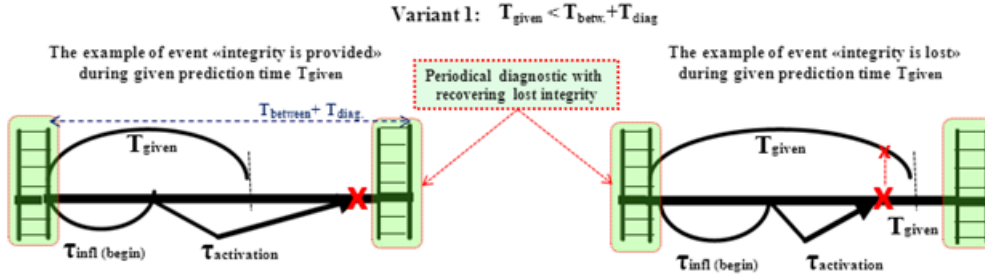


Figure 1: Some elementary events (left - “integrity is provided”, right - “integrity is lost” during  $T_{given}$ )

The next formulas for probability distribution function (PDF) of time between the losses of element or system integrity are proposed under the condition of independence. PDF for the model, variant 1: the probability of integrity is equal to

$$P_{(1)}(t) = 1 - \Omega_{infl}(t) * \Omega_{activ}(t), \quad (1)$$

where  $\Omega_{infl}(t)$  - is the PDF of time between neighboring dangerous influences;  $\Omega_{activ}(t)$  - is the PDF of activation time. These PDF  $\Omega_{infl}(t)$  and  $\Omega_{activ}(t)$  may be exponential PDF,  $\Omega_{infl}(t) = 1 - e^{-\frac{t}{T_{infl}}}$ ,  $\Omega_{activ}(t) = 1 - e^{-\frac{t}{T_{activ}}}$  - see rationale in [1]. For different threats a frequency of dangerous influences for these PDF is the sum of frequencies of every kind of influences.

PDF for the model, variant 2: the probability of integrity is equal to

$$P_{(2)}(T_{given}) = N\left(\frac{T_{betw} + T_{diag}}{T_{given}}\right)P_{(1)}N(T_{betw} + T_{diag}) + \left(\frac{T_{rmn}}{T_{given}}\right)P_{(1)}(T_{rmn}), \quad (2)$$

where  $N = \frac{T_{given}}{T_{betw} + T_{diag}}$ ,  $T_{rmn} = T_{given} - N(T_{betw} + T_{diag})$ . The probability of integrity  $P_{(1)}(t)$  is defined by (1).

## 4 Solution for “Black box”

The proposed method allows to estimate mean time before critical integrity losses of element or system, presented as “black box”, for the given confidence probability to lose integrity  $P_{conf}(T_{given})$ . The found mean time before critical integrity losses is a solution  $x_0$  of equation:

$$P(T_{infl}, x, T_{betw}, T_{diag}, x) = P_{conf}(x) \quad (3)$$

concerning of unknown parameter  $x$ . For calculations the formulas (1) - (2) are used.  $T_{infl}$  is the mathematical expectation of PDF  $\Omega_{infl}(t)$ , it is defined by parameter statistics. The others parameters  $T_{betw.}, T_{diag}$  in (3) are known. According to properties of function  $P(T_{infl}, T_{activ}, T_{betw.}, T_{diag}, T_{given})$  the maximal  $x$  exists when  $0 < P(T_{infl}, x, T_{betw.}, T_{diag}, x) < 1$ . I.e. the mean time before critical integrity losses is equal to maximum  $X_0$  from all defined  $x_0$  as solution of (3).

## 5 Solution for complex system

The model above is applicable to the system presented as one element “Black box”. The main result of such system modelling is the mean time before critical integrity losses  $X_0$  depending on threats, periodic diagnostics and recovery time [1]. For a complex system with parallel or serial structure integrated mean time before critical integrity losses is estimated from  $X_{0i}$ , defined for  $i$ -th element by using method for “Black box”. Let’s consider the elementary structure from two independent parallel elements that means logic connection “OR” or series elements that means logic connection “AND”. The mean time before critical integrity losses  $X_0$  for system combined from two independent elements is equal to  $X_0 = \frac{1}{\frac{1}{x_{01}} + \frac{1}{x_{02}}}$  for series connection and  $X_0 = X_{01} + X_{02} - \frac{1}{\frac{1}{x_{01}} + \frac{1}{x_{02}}}$  for parallel connection.

It is correct for assumption that random values of time before critical integrity losses are distributed exponentially with mean  $X_{0i}$ .

**Example.** Let the frequency of dangerous influences is 1time a month ( $T_{infl} = 1month$ ), time between the end of diagnostics and the beginning of next diagnostics is equal to 8 hours ( $T_{betw} = 8hours$ ). Diagnostics and recovery time is neglected ( $T_{diag} = 0$ ). If confidence probability is about 0.95, prognostic mean time before critical integrity losses is equal to 222 hours for obligatory adequate reaction every 8 hours. For rare events 1time a year the level of probability to lose integrity is about 0.9996.

For confidence probability of integrity about 0.99 estimated mean time before critical integrity losses may be very hard. Therefore confidence probability is recommended to set on level from 0.8 to 0.99 in dependence on system or element importance and possibilities for counteractions or from practice statistics. The approach is implemented by the Joint-Stock Company “Siberian Coal Energy Company” which is the leading coal producer in Russia and one of the world’s largest coal companies [1].

## References

- [1] V. Artemyev, A. Kostogryzov, Ju. Rudenko, O. Kurpatov, G. Nistratov, A. Nistratov (2017). *Probabilistic methods of estimating the mean residual time before the next parameters abnormalities for monitored critical systems.* Proceedings of the 2nd International Conference on System Reliability and Safety (ICSRS- 2017), December 20-22, 2017, Milan, Italy, pp. 368-373.

# STATISTICAL APPROACH TO IMAGE COMPRESSION BASED ON A RESTRICTED BOLTZMANN MACHINE

V.V. KRASNOPROSHIN, V.V. MATSKEVICH

*Belarussian State University*

*Minsk, BELARUS*

e-mail: krasnoproshin@bsu.by

## Abstract

The article deals with the problem of color image compression. A statistical approach based on a restricted Boltzmann machine is investigated. An original algorithm for learning the neural network is proposed. The algorithm implements the annealing method. The effectiveness of training is based on the use of data parallelization technology.

**Keywords:** restricted Boltzmann machine, annealing method, data compression, training

## 1 Introduction

As a result of the rapid development of the information society and the transition to the era of the digital economy the problem of transferring large amounts of data arises. Therefore, for their effective transmission, the problem of information compression becomes urgent.

Compression can be performed without loss, for which different data coding algorithms are used. Or with losses, by constructing various types of informative statistics. The latter allows to achieve a higher compression ratio. In particular, lossy compression can be applied when minor data loss is not critical. For example, in television broadcasting, the blurring of an image or the complete loss of several frames is not significant.

One approach to solving the problem of compressing color images is associated with the use of a restricted Boltzmann machine. However, the effectiveness of the solution in this case essentially depends on the organization of the learning process.

The paper proposes an effective learning algorithm (which implements the ideology of the annealing method), based on the technology of data parallelization.

## 2 Problem analysis

Consider the problem of compressing colored rectangular images. In the most general form, it can be formulated as follows.

Let  $N$  color images be given. Each image is defined by a matrix of dimension  $n \times m$ . The elements of the matrix  $i, j$  are the pixels that describe the brightness value of the

image at a given point

$$\begin{cases} P = \{p_{ij}\}, i = \overline{1, n}, j = \overline{1, m} \\ p_{ij} = (x_{ij}, y_{ij}, z_{ij}) \in ([0, 255])^3 \end{cases} \quad (1)$$

where  $x_{ij}, y_{ij}, z_{ij}$  - the content of the red, green and blue colors in a pixel  $p_{ij}$ .

It is required to develop an algorithm that implements image compression process with minimal loss of information.

Consider the solution of the formulated problem using the restricted Boltzmann machine. It is one of the varieties of recurrent neural networks. Traditionally restricted Boltzmann machine is used to solve problems of compression, semantic search and data cleaning [1]. The process of training such a network requires a lot of time. Therefore, gradient methods (CD-n, PT-n-k and PCD) are usually used to train it. At the same time, the last two are modifications of the base CD method.

Sometimes during sampling, an annealing method is used to improve the accuracy of the gradient estimation [2]. However, the annealing method is not used directly as an algorithm for training a restricted Boltzmann machine. It is considered that the learning process in this case is time consuming. However, with increasing computational power of computers, this problem becomes less significant.

It can be noted that the annealing method has several advantages:

- with an infinitely large number of iterations (with a decrease in temperature exponentially), the method converges almost certainly to the optimal solution, i.e

$$P(\lim_{n \rightarrow +\infty} x_n = x^*) = 1 \quad (2)$$

where  $x_n$  - state at the moment of the n-th iteration,  $x^*$  - optimal solution;

- does not require differentiability of the optimized functional;

- is simple to implement (only meta-parameters and set of transitions are configured);

- the problem of a local minimum is solved in a natural way with the help of high temperatures.

### 3 Architecture of the restricted Boltzmann machine

Let us consider in more detail the architecture and features of the functioning of the restricted Boltzmann machine. At the heart of the machine is the concept of a stochastic neuron. The result of the stochastic neuron is the implementation of a random variable with a certain distribution law. Depending on the distribution law in the neurons of the input and hidden layers, there are several types of restricted Boltzmann machines. In this case, the type Gauss-Bernoulli is considered. This choice was made on the basis of the theorem of the universal approximation. This variant of a restricted Boltzmann machine of Gauss – Bernoulli type is a universal approximator.

Formally, a restricted Boltzmann machine can be represented as a fully connected bipartite graph  $G = (X, U)$ , where  $X$  - vertex set - stochastic neurons,  $U$  - edges set -

synaptic connections.

$$\begin{cases} X = X_1 \cup X_2, X_1 \cap X_2 = \emptyset \\ U = \{u = (x_1, x_2) | \forall x_1 \in X_1, \forall x_2 \in X_2\} \end{cases} \quad (3)$$

vertices of subset  $X_1$  - set the neurons of the input layer,  $X_2$  - output layer neurons.

The number of neurons in the input layer is determined by the size of the input image. Since the input number is eight-bit, then in the hidden layer (for its lossless coding) 8 binary neurons are required. Therefore, the number of neurons in the hidden and the input layer to compress the image in  $k$  times was determined by the formula:

$$\begin{cases} |X_1| = nm \\ |X_2| = \frac{8nm}{k} \end{cases} \quad (4)$$

To each vertex of the input layer we assign a set of parameters  $VB = \{b\}$  - vertex offsets and  $\sigma = \{\sigma\}$  - vertex variances, and to the vertices of the output layer - set of parameters  $HB = \{g\}$  - vertex offsets. The sizes of the sets are equal respectively

$$|VB| = |\sigma| = |X_1|, |HB| = |X_2| \quad (5)$$

Each edge connecting a pair of vertices of the input and output layers will be assigned a set of parameters  $W = \{w\}$  - the weights of the edges.

The size of the set is equal to the following value

$$|W| = |X_1||X_2| \quad (6)$$

Thus, the described family of neural networks can be defined by four types of parameters (see Fig 1):

$$RBM = (W, VB, \sigma, HB) \quad (7)$$

In this case, a specific Boltzmann machine is specified by fixing the values of the parameters from the above sets. In fact, at the training stage, the neural network is set up for an objective task.

Thus, the restricted Boltzmann machine functions in two main modes. In the learning mode, the values of the parameters are calculated, which determine in the family of machines a specific instance for solving an applied problem. In the working mode, compression (encoding) of the image and its recovery (decoding) are performed.

## 4 Training a restricted Boltzmann machine

Consider the approach to the problem of learning a restricted Boltzmann machine using the annealing method.

The following algorithm is proposed that implements the ideology of the method.

At the preliminary stage, initialization (setting the initial values) of the parameters ( $W, VB, HB, \sigma$ ), initial temperature  $T_0$  and cooling coefficient  $\alpha$  is performed.

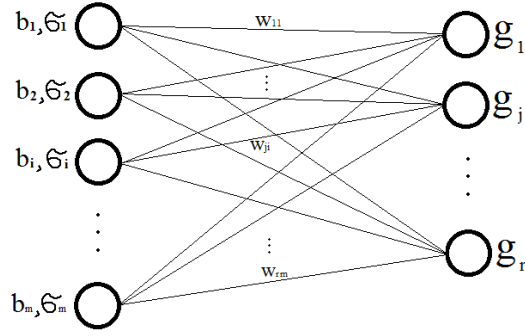


Figure 1: Gauss-Bernoulli RBM architecture

The main stage of the learning algorithm implements a procedure for sequentially updating the values of the specified parameters using a certain quality functional.

Describe the process to update settings in more detail. For simplicity, consider it on the example of the set of parameters  $W$ . For other sets, this procedure is identical.

To the set of parameters  $W$ , we associate a segment  $Lw$  of length  $l$ . After that, each element of the set  $W$  is sequentially placed in the center of the given segment. To determine the direction of change of parameter values, we generate a base random variable. If it is more than 0.5, then the value of the parameter increases, otherwise it decreases.

New parameter values are defined as follows. A random permutation is generated, the number of elements of which is equal to the number of elements of the set  $W$ . We order the elements of the set  $W$  in accordance with the permutation and change the values of the first  $Wp$  elements of the set. The new value of the parameter is determined as a result of the implementation of a uniformly distributed random variable on the segment, the ends of which are the current value of the parameter, and the end of the segment towards which the change is made.

Similarly, actions are sequentially performed for the sets  $VB$ ,  $HB$ ,  $\sigma$ .

For newly obtained parameter values, the quality functional is calculated.

As the latter, it is proposed to use the following function:

$$F(W, VB, HB, \sigma) = \frac{1}{Nnm} \sum_{i=1}^N \sum_{j=1}^{nm} |x_{ij} - f^{-1}(y_{ij})| \quad (8)$$

where  $y_{ij}$  - reconstituted input signal of restricted Boltzmann machine,  $f^{-1}$  - inverse function of the preliminary transformation of input data.

Then a decision is made to move to a new state:

- if the value of the functional is greater than the current one, then we move to the new state with probability:

$$P(y|x) = \exp\left(-\frac{F(y) - F(x)}{T_i}\right) \quad (9)$$

where  $x$  - current state,  $y$  - state selected for transition,  $F$  - minimized objective function,  $T_i$  - temperature of  $i$ -th iteration

- else we always move to a new state.

Further cooling takes place according to the rule:

$$T_{i+1} = \alpha T_i \quad (10)$$

After cooling, the obtained solution is checked for optimality:

the solution is optimal if during the last S iterations there has not been a transition to a new state. If the solution obtained is optimal, then:

- stop algorithm,
- otherwise go to the next iteration.

Thus, as a result of the learning process in the parameter space, describing the family of restricted Boltzmann machines, their specific values are fixed. This builds a specific instance of the machine that best suits the objective task. And in this case, you can go directly to the process of compressing images.

## 5 Experiments and results

The effectiveness of the approach was tested experimentally. For the compression problem, STL-10 dataset from the repository of Stanford University [4] was used. This is one hundred thousand unmarked color images of 96x96 pixels. Each image is described by 27648 integers (in the range from 0 to 255), specifying the content of red, green and blue colors [5].

The experiments were carried out on a computer with a 4 core processor and a nvidia 1060 3gb video card.

Measurement of operations time was performed using the function `gettimeofday`.

Before training, each input image was represented by three components: Red, Green, Blue.

Received three data array dimension  $n \times m \times N$ , where  $n \times m$  – image size,  $N$  - number of objects in the dataset. Arrays were divided into blocks of lower dimension. The blocks described the image from left to right, top to bottom.

Each block was processed by a separate neural network. This gave a number of advantages:

- learning machines are completely independent. Each machine has its own parameters and its own training data. This allowed parallelizing the learning process;
- decomposition reduced the total number of tunable parameters, which reduced the amount of computation.

For each  $i, j$ -th block element ( $i=1, n; j=1, m$ ) arithmetic average was calculated. Then it was subtracted from the initial values of the  $i, j$ -th element. As a result, the data preprocessing was as follows:

$$f(x_{lij}) = \frac{1}{3}(x_{lij} - \mu_{ij}), l = \overline{1, N} \quad (11)$$

where  $\mu_{ij}$  - arithmetic average of coordinate  $(i, j)$ .

For the experiments, the images were divided into blocks of 12x12. The experiments were carried out within the framework of one block by splitting it into mini blocks of

16 elements. To calculate the training time, the experimentally obtained time was multiplied by the number of blocks of 12x12 in the original images.

Each mini-block was processed on a separate Boltzmann machine. The input layer of the machine contained the number of neurons equal to the size of the mini-block.

As a result of the experiments, the following main results were obtained.

At 32-fold compression, the loss was 15%, and the estimated training time was 2.2 days. These results are comparable to similar results obtained using gradient methods: 2 days and 20% loss [7]. This suggests the possibility of practical use of the approach described in this paper for solving the problem of color image compression.

## 6 Conclusion

The article deals with the problem of color image compression. A statistical approach based on a restricted Boltzmann machine is investigated. An original algorithm for learning the neural network is proposed. The algorithm implements the annealing method. The effectiveness of training is based on the use of data parallelization technology.

It was experimentally shown that with proper selection of parameters in the learning algorithm and the use of parallelization technology, the learning process is carried out in a reasonable time [7]. This allows us to make an assumption about the prospects of using the idea of random search in the development of deep learning algorithms. With the rapid development of computer technology, such algorithms can be effectively used to train neural networks and, in particular, for a restricted Boltzmann machine.

## References

- [1] MohanaPriya P., Shalinie S. M. (2017). Restricted Boltzmann machine - based cognitive protocol for secure routing in software defined wireless networks. *IET Networks*. Vol. 6, No. 6, pp. 162–168.
- [2] Lattner S., Grachten M., Widmer G. (2016). Imposing Higher-Level Structure in Polyphonic Music Generation using Convolutional Restricted Boltzmann Machines and Constraints. *J. Creative Music Systems*.
- [3] Adachi S.H., Henderson M.P. (2015). Application of Quantum Annealing to Training of Deep Neural Networks. *arXiv*.
- [4] STL-10 dataset link: [academictorrents.com/details/a799a2845ac29a66c07cf74e2a2838b6c5698a6a](https://academictorrents.com/details/a799a2845ac29a66c07cf74e2a2838b6c5698a6a)
- [5] STL-10 dataset description link: [stanford.edu/~acoates//stl10/](https://stanford.edu/~acoates//stl10/)
- [6] CUDA toolkit link: [developer.nvidia.com/cuda-downloads](https://developer.nvidia.com/cuda-downloads)

- [7] Zhu H., Akrouf M., Zheng B., Pelegris A., Jayarajan A., Phanishayee A., Schroeder B., Pekhimenko G. (2018). Benchmarking and Analyzing Deep Neural Network Training. *arXiv*.

# CLASSIFICATION OF MOTION REGIONS WITH CONVOLUTIONAL NETWORKS, SUPPORT VECTOR MACHINES, AND RANDOM FORESTS IN VIDEO-BASED ANALYSIS OF BEE TRAFFIC

V.A. KULYUKIN<sup>1</sup>, S. MUKHERJEE<sup>1</sup>, P. VATS<sup>1</sup>,

A. TIWARI<sup>1</sup>, Y.B. BURKATOVSKAYA<sup>2</sup>

<sup>1</sup>*Utah State University, Logan, USA*

<sup>2</sup>*Tomsk Polytechnic University, Tomsk, RUSSIA*

e-mail: vladimir.kulyukin@usu.edu, tracey@tpu.ru

## Abstract

Bee traffic is the number of bees moving in a given area in front of a specific hive over a given period of time. Video-based bee traffic analysis has the potential to automate the assessment of bee traffic levels, which, in turn, may lead to the automation of honeybee colony health assessment. In this paper, we evaluate several convolutional networks to classify regions of detected motion as BEE or NO-BEE in videos captured by BeePi, an electronic beehive monitoring system. We compare the performance of several convolutional neural networks with the performance of support vector machines and random forests on the same image dataset.

**Keywords:** convolutional network, support vector machine, random forest, bee traffic, data science

## 1 Introduction

Many beekeepers watch bee traffic to ascertain the state of their honey bee colonies, because bee traffic carries information on colony behavior. Bee traffic patterns change in response to stressors such as failing queens, predatory mites, and airborne toxicants. While experienced beekeepers can tell changes in bee traffic levels in stressed colonies, they may not always be able to determine the exact causes of the changes without hive inspections. Unfortunately, hive inspections disrupt the life cycle of bee colonies and put additional stress on the bees. Since beekeepers cannot monitor their hives continuously due to obvious problems with logistics and fatigue, a consensus is emerging among researchers and practitioners that video-based analysis of bee traffic levels can become an integral component of electronic beehive monitoring and help extract critical information on colony behavior and phenology without invasive beehive inspections and considerable transportation costs.

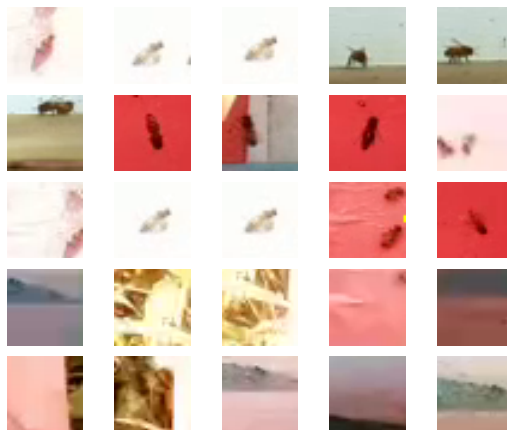


Figure 1: A sample of images from BEE1; the first 3 rows include images classified as BEE; the last 2 rows consist of images classified as NO-BEE.

In this investigation, we focused on training and evaluating three types of classifiers – convolutional networks (ConvNets) [1], random forests [2], and support-vector machines (SVM) [3] – to categorize motion regions detected by the video-processing algorithm of BeePi, a multi-sensor electronic beehive monitoring system we designed and built in 2014 [4], and have been iteratively modifying since then [5].

Once mounted on top of a Langstroth beehive, a BeePi monitor captures a 30-second 360x240 video every 15 minutes from 8:00 to 21:00 at a frame rate of 25 frames per second. Each captured video is processed for motion detection. We experimented with three motion detection algorithms available in OpenCV 3.0.0 ([www.opencv.org](http://www.opencv.org)): KNN, MOG, and MOG2. Although all three algorithms performed on par, we found that MOG worked slightly better than either KNN or MOG2, because it was less sensitive to shadows.

The output of the motion detection module is a set of 32x32 image regions centered around detected motion points. Fig. 1 gives a sample of detected motion regions. Each detected motion region is classified by a trained classifier (e.g., a convolutional neural network, a random forest, or an SVM) into two classes – BEE or NO-BEE. Thus, for each video, the video processing algorithm returns an estimate of the number of bees that moved in a given region in front the beehive over a 30-second period.

## 2 Image Data

The image dataset for this investigation was obtained from the videos captured by four BeePi monitors placed on four Langstroth hives with Italian honeybee colonies. Two monitors were deployed in an apiary in Logan, UT, USA and the other two – in an apiary in North Logan, UT, USA from April 2017 to September 2017.

We randomly selected 40 videos from June and July 2017. The image dataset was then obtained by using the MOG algorithm to automatically extract 54,392 32x32 motion regions from the videos (see Fig. 1). We obtained the ground truth classification by manually labeling the 54,392 32x32 images with two categories - BEE (if it contained

at least one bee) or NO-BEE (if it contained no bees or only a small part of a bee). The image dataset from the apiary in Logan, UT was used for model training and testing. The image dataset from the apiary in North Logan, UT was used for model validation.

We executed the ANOVA and MANOVA analyses on the labeled image dataset to determine whether its training (class 0), testing (class 1), and validation (class 2) images are statistically significantly different. We used the following image features as independent variables in our analysis – contrast, energy, and homogeneity. The dependent variables were class 0, class 1, and class 2. The MANOVA analysis with 1 degree of freedom gave the Pillai coefficient of 0.018588, the  $F$  value of 107.47, and  $Pr(> F) < 2.2e-16$ . The ANOVA analysis on contrast gave the mean squared value of 2.3607, the  $F$  value of 148.2, and  $Pr(> F) < 2e-16$ . The ANOVA analysis on energy gave the mean squared value of 6.237, the  $F$  value of 313.2, and  $Pr(> F) < 2e-16$ . The ANOVA analysis on homogeneity gave the mean squared value of 0.18043, the  $F$  value of 152.2, and  $Pr(> F) < 2e-16$ . Since in all cases the  $P$  value is  $< 0.0005$ , the three training, testing, and validation datasets are significantly different in terms of contrast, energy, and homogeneity.

### 3 Experiments

We performed an exhaustive search for an optimal ConvNet by starting with 1 hidden layer and 1 max pooling layer and varying the filter size, the number of hidden layers, and the number of nodes in each hidden layer. An addition of a hidden layer was always followed with an addition of a max pooling layer with a kernel size of 2. All hidden layers used the ReLU activation function and the adam optimizer. The learning rate was set to 0.001; the loss function was the categorical cross entropy. All models were trained for 50 epochs with a batch size of 50. Table 1 gives a summary of the ConvNet architectures constructed with exhaustive search. Increasing the number of hidden layers above 6 did not improve the results of the best performing 5-hidden layer model.

Table 1: Best ConvNet models discovered through exhaustive search.

Num. HLs	Test Loss	Test Accuracy	Valid Accuracy
1	0.09	97.93%	50.34%
2	0.03	99.31%	74.58%
3	0.03	99.34%	78.29%
4	0.02	99.46%	81.63%
5	0.03	99.32%	86.57%
6	0.03	99.51%	83.29%

We also designed several ConvNets by hand. The best performing manual ConvNet had 8 layers: input, output, and 6 hidden layers. The first 7 layers use ReLU as their activation function. The last layer uses softmax and categorical cross entropy. The first two hidden layers use batch normalization. The last 5 layers use a dropout with a keep

probability of 0.5. Table 2 gives the confusion matrix of this ConvNet on the validation dataset.

Table 2: Confusion matrix of best hand-crafted ConvNet.

	No-Bee	Bee	Accuracy
No-Bee	1677	15	99.11%
Bee	1	1809	99.99%
Total Accuracy			99.54%

To obtain some standard machine learning benchmarks, we trained and tested SVMs and random forests on the same image dataset. All SVMs used the linear kernel with the max-iter parameter varying from 10 to 1000. The best performing SVM on the validation dataset had a max-iter of 1000 and an accuracy of 51.13%. The confusion matrix for this SVM is given in Table 3.

Table 3: Confusion matrix of linear SVM on validation dataset for max-iter 1000.

	No-Bee	Bee	Total	Accuracy
No-Bee	822	896	1718	47.84%
Bee	828	982	1810	54.25%
Total Accuracy				51.13%

We trained and validated random forests with 10, 50, 80, and 100 trees. The best performing random forest on the validation dataset had 50 trees and achieved an accuracy of 93.67%. In summary, random forests performed much better than the SVMs and all the ConvNet models obtained through exhaustive search but were 6% below the hand-crafted ConvNet.

Table 4: Confusion matrix of random forest with 50 trees on validation dataset.

	No-Bee	Bee	Total	Accuracy
No-Bee	1664	54	1718	96.85%
Bee	169	1641	1810	90.66%
Total Accuracy				93.67%

## References

- [1] LeCun, Y., Kavukcuoglu, K., Farabet, C. (2010). Convolutional networks and applications in vision. *Proceedings of IEEE International Symposium on Circuits and Systems*, pp. 253-256.
- [2] Breiman, L. (2001). Random Forests. *Machine Learning*, Vol. **45**, pp. 5-32.
- [3] Hong, J.H., Cho, S.B. (2008). A probabilistic multi-class strategy of one-vs.-rest support vector machines for cancer classification. *Neurocomputing*, Vol. **71**, pp. 3275-3281.

- [4] Kulyukin, V.A., Putnam, M., Reka, SK. (2016). Digitizing buzzing signals into A440 piano note sequences and estimating forage traffic levels from images in solar-powered, electronic beehive monitoring. *Lecture Notes in Engineering and Computer Science: Proceedings of the International MultiConference of Engineers and Computer Scientists*. Vol. **1**, pp. 82-87.
- [5] Kulyukin, V.A., Mukherjee, S., Amlathe, P. (2018). Toward audio beehive monitoring: deep learning vs. standard machine learning in classifying beehive audio samples. *Applied Sciences*, Vol. **8**, pp. 1573-1606.

# ASYMPTOTIC EXPANSIONS OF SOLUTIONS OF MIXED TYPE SDE DRIVEN BY FRACTIONAL BROWNIAN MOTIONS FOR SMALL TIMES

A.A. LEVAKOV, M.M. VASKOUSKI, I.V. KACHAN

*Belarusian State University*

*Minsk, BELARUS*

e-mail: levakov@tut.by, vaskovskii@bsu.by, kachan@bsu.by

## Abstract

In this paper we consider  $n$ -dimensional mixed type stochastic differential equations driven by multivariate fractional Brownian motions with Hurst indices greater than  $\frac{1}{3}$ , standard Brownian motions and a drift term. Using a Taylor type development we obtain an expansion of expectations  $\mathbf{P}_t g = \mathbb{E}g(X_t^x)$  for small  $t$ , where  $X_t^x$  denotes the solution of the mentioned stochastic differential equation with initial value  $x \in \mathbb{R}^n$ , and  $g: \mathbb{R}^n \rightarrow \mathbb{R}$  is a sufficiently smooth function.

**Keywords:** data science, fractional Brownian motion, asymptotic expansion, stochastic differential equation

## 1 Introduction

We consider a mixed type stochastic differential equation

$$dX_t = f(X_t)dt + h(X_t)dW_t + \sigma(X_t)dB_t^H, \quad t \in [0, T], \quad (1)$$

where  $h = (h_1, \dots, h_{d_1})$ ,  $\sigma = (\sigma_1, \dots, \sigma_{d_2})$ ,  $f: \mathbb{R}^n \rightarrow \mathbb{R}^n$ ,  $h_i: \mathbb{R}^n \rightarrow \mathbb{R}^n$ ,  $\sigma_j: \mathbb{R}^n \rightarrow \mathbb{R}^n$ ,  $i = 1, \dots, d_1$ ,  $j = 1, \dots, d_2$  are sufficiently smooth functions with bounded derivatives,  $W_t = (W_t^1, \dots, W_t^{d_1})^T$ ,  $B_t^H = (B_t^{H_1}, \dots, B_t^{H_{d_2}})^T$ ,  $W_t^i$  and  $B_t^{H_j}$ ,  $i = 1, \dots, d_1$ ,  $j = 1, \dots, d_2$ , are independent one-dimensional standard Brownian motions and fractional Brownian motions with Hurst indices  $H_j \in (1/3, 1)$ , respectively. Denote by  $X_t^x$  the solution of the equation (1) with an initial condition  $X_0 = x \in \mathbb{R}^n$ . Here, the solution is understood as the solution of the corresponding integral equation with Ito integral against  $W_t$  and pathwise Gubinelli rough path integral against  $B_t^H$ .

Stochastic differential equations containing a drift term and both fractional Brownian motions and Wiener processes are called mixed type stochastic differential equations. D. Nualart and G. Guerra [2] have proved the existence and uniqueness theorem for equations containing Wiener process  $W_t$  and fractional Brownian  $B_t^H$  motion with Hurst index  $H > 1/2$  combining Ito and Young integrals theory. Y. Mishura and G. Shevchenko [8] have generalized the existence theorem for such equations to the case when  $W_t$  and  $B_t^H$  are not necessary independent. Reader can also find some generalizations of existence theorems and some properties of mixed stochastic differential equations and inclusions in the papers [3, 4, 5, 6, 7, 10].

The goal of this article is to study for small times the family of operators

$$(\mathbf{P}_t g)(x) = \mathbb{E}(g(X_t^x)) \quad (2)$$

corresponding to the solutions of general equations (1) assuming that a function  $g$  is sufficiently smooth and has bounded derivatives. Asymptotic expansions of the family (2) for the Stratonovich's type equation (1) have been studied in an article [11]. It is worth noting that the mentioned expansions for small times can be used to get partial differential equations of Kolmogorov's type for the expectations of the solutions of the equation (1) in some particular cases, see [11, Section 6].

## 2 Main results

On a probability space  $(\Omega, \mathcal{F}, \mathbb{P})$  define multivariate fractional Brownian motion  $B_t = (B_t^{(0)}, \dots, B_t^{(d)})^T$ , where  $B_t^{(0)} = t$  and  $B_t^{(1)}, \dots, B_t^{(d)}$ ,  $d = d_1 + d_2$  are the components of  $W_t$  and  $B_t^H$  taken in some fixed order. Let us define a function  $F: \mathbb{R}^n \rightarrow \mathbb{R}^{n \times (d+1)}$ ,  $F = (F_0, F_1, \dots, F_d)$  where  $F_1, \dots, F_d$  are the components of  $h$  and  $\sigma$ , respectively, taken in the same fixed order. The equation (1) can be formally re-written in new terms as follows:

$$dX_t = F(X_t)dB_t, \quad t \in [0, T].$$

Note that the  $B_t^{(1)}, \dots, B_t^{(d)}$  are all the independent one-dimensional fractional Brownian motions. Let us denote their Hurst indices as  $H_1, \dots, H_d \in (1/3, 1)$ , respectively. Also let  $H_0 = 1$  and  $H_{\min}$  be the minimal value over all  $H_i$ ,  $i = 0, \dots, d$ . We choose and fix some  $H \in (1/3, 1/2]$  such that  $H < H_{\min}$ .

In the Chapter 4 of [1] the reader can find basic facts of rough path theory including Gubinelli's derivative  $Y'$ , the space  $\mathcal{D}_Z^{2H}$  of pairs  $(Y, Y')$  such that  $Y$  is controlled by  $Z$  and rough path integral.

**Definition 1.** We call a second order process over  $B$  the random process  $\mathbb{B}: [0; T]^2 \times \Omega \rightarrow \mathbb{R}^{(d+1) \times (d+1)}$  defined by the following equations:

$$\begin{aligned} \mathbb{B}_{s,t} &= \left( \mathbb{B}_{s,t}^{(i,j)} \right)_{i,j=0}^d, \\ \mathbb{B}_{s,t}^{(i,j)} &\stackrel{L^2}{=} \lim_{|\mathcal{P}| \rightarrow 0} \int_{\mathcal{P}} B_{s,r}^{(i)} dB_r^{(j)}, \quad \int_{\mathcal{P}} B_{s,r}^{(i)} dB_r^{(j)} = \sum_{t_k, t_{k+1} \in \mathcal{P}} B_{s,t_k}^{(i)} B_{t_k, t_{k+1}}^{(j)}, \quad 1 \leq i < j \leq d, \\ \mathbb{B}_{s,t}^{(0,j)} &= \int_s^t B_{s,r}^{(j)} dr \stackrel{a.s.}{=} \lim_{|\mathcal{P}| \rightarrow 0} \sum_{t_k, t_{k+1} \in \mathcal{P}} B_{s,t_k}^{(j)} (t_{k+1} - t_k), \quad 1 \leq j \leq d, \\ \mathbb{B}_{s,t}^{(i,i)} &= \frac{1}{2} \left( B_{s,t}^{(i)} \right)^2 - \frac{1}{2} (t - s) \mathbf{1}_{\{H_i=1/2\}}, \quad 0 \leq i \leq d, \\ \mathbb{B}_{s,t}^{(i,j)} &= -\mathbb{B}_{s,t}^{(j,i)} + B_{s,t}^{(i)} B_{s,t}^{(j)}, \quad 0 \leq j < i \leq d \end{aligned}$$

for each pair  $(s, t) \in [0, T]^2$ , where  $\mathcal{P} = \{s = t_0 < t_1 < \dots < t_l = t\}$  is an arbitrary partition of the segment  $[s, t]$ ,  $|\mathcal{P}| = \max |t_{k+1} - t_k|$ ,  $\mathbf{1}_{\{H_i=1/2\}} = 1$  if  $H_i = 1/2$  and 0 otherwise, and all the limits assumed to be independent of the sequence of  $\mathcal{P}$ . Here, the notations  $\stackrel{L^2}{=}$ ,  $\stackrel{a.s.}{=}$  are used to show that the mentioned limits are understood in the sense of  $L^2(\Omega, \mathcal{F}, \mathbb{P})$  and  $\mathbb{P}$ -almost surely, respectively.

*Remark 1.* For  $1 \leq i < j \leq d$  the  $\mathbb{B}_{s,t}^{(i,j)}$  is the Ito integral which in fact coincides with Stratonovich integral in view of the independence of  $B^{(i)}$  and  $B^{(j)}$ , see [1, Section 5.2]. In turn, the  $\mathbb{B}^{(i,i)}$  corresponds to the Stratonovich integral  $\int_s^t B_{s,r}^{(i)} dB_r^{(i)}$  if  $H_i \neq 1/2$  and to the Ito integral otherwise. Finally, the formula  $\mathbb{B}_{s,t}^{(i,j)} = -\mathbb{B}_{s,t}^{(j,i)} + B_{s,t}^{(i)} B_{s,t}^{(j)}$  comes from the integration by parts formula accurate for the Stratonovich integrals.

*Remark 2.* It is easy to see that  $\text{Sym}(\mathbb{B}_{s,t} + \frac{1}{2}(t-s)I_{\overline{H}}) = \frac{1}{2}B_{s,t} \otimes B_{s,t}$  where  $I_{\overline{H}} = I_{(H_0, \dots, H_d)} = \text{diag}(\mathbf{1}_{\{H_0=1/2\}}, \dots, \mathbf{1}_{\{H_d=1/2\}})$ .

The correctness of the definition above was clarified in [11]. Also, as it was shown in the Proposition 2 in [11],  $(B, \mathbb{B})$  is a rough path and we can define the rough path integral against it.

**Definition 2.** A process  $X_t$  is called a solution of equation (1) if  $(X, X') \in \mathcal{D}_B^{2H}([0, T], \mathbb{R}^n)$  a.s. and the equality

$$X_t = X_0 + \int_0^t F(X_s) dB_s, \quad t \in [0, T],$$

holds a.s., where the integral on the right-hand side is understood as the rough path integral against  $(B, \mathbb{B})$ . Let  $x \in \mathbb{R}^n$ . A solution  $X_t$  of equation (1) with the initial condition  $X_0 = x$  is called unique a.s. if for any other solution  $Y_t$  of equation (1) with the initial condition  $Y_0 = x$  there holds  $\mathbb{P}(X_t = Y_t \forall t \in [0, T]) = 1$ .

*Remark 3.* In case all the components of  $B_t^H$  introduced in the equation (1) are sharing the same Hurst index  $H > 1/2$ , the definition above coincides with the definitions of the solutions of the mixed type equations (1) considered in the articles [3, 2, 8, 4, 5, 6, 7, 10]. This fact follows from the Proposition 5.1 of [1].

For any Banach spaces  $U_1$  and  $U_2$  denote by  $C_b^k(U_1, U_2)$  the set of functions  $\varphi: U_1 \rightarrow U_2$  which have continuous and bounded derivatives (in Frechet sense) up to  $k$ -th order.

The following statement is a reformulation of the Theorem 2.1 from [9].

**Proposition 1.** *Let  $F \in C_b^2(\mathbb{R}^n, \mathbb{R}^{n \times (d+1)})$ , then for any  $x \in \mathbb{R}^n$  there exists a unique solution  $X_t$  of equation (1) with the initial condition  $X_0 = x$ . Additionally, if  $H_i > H^* \geq 1/2$  for any  $i = 0, \dots, d$ , then  $X_t$  is Hölder continuous with an exponent  $H^*$  a.s. and the integral in the definition of solution of equation (1) can be defined as the Young pathwise integral.*

**Theorem 1.** *Let  $F \in C_b^3(\mathbb{R}^n, \mathbb{R}^{n \times (d+1)})$ ,  $g \in C_b^3(\mathbb{R}^n, \mathbb{R})$ . Then for any  $s, t \in [0, T]$  the following Ito's type formula holds a.s.*

$$g(X_t) = g(X_s) + \int_s^t Dg(X_r) F(X_r) dB_r + \int_s^t \frac{1}{2} \text{tr}((F(X_r) I_{\overline{H}})^T D^2 g(X_r) (F(X_r) I_{\overline{H}})) dr,$$

where  $X_t$  is the solution of equation (1) with the initial condition  $X_0 = x$ .

The proof of the theorem easily follows from the proof of the Theorem 2 in [11], the Definition 1 and the Remark 2.

Let us denote  $B_t^{(d+1)} = t$  and follow the agreement that the integrals against  $B_t^{(d+1)}$  should be understood in Lebesgue's sense. We will use the following notations

$$\begin{aligned} \Delta^k[0, t] &= \{(t_1, \dots, t_k) \in [0, 1]^k : 0 \leq t_1 < \dots < t_k \leq t\}, \quad k \in \mathbb{N}, \\ \int_{\Delta^k[0, t]} dB^{(I_k)} &= \int_0^t \int_0^{t_k} \dots \int_0^{t_2} dB_{t_1}^{(i_1)} \dots dB_{t_{k-1}}^{(i_{k-1})} dB_{t_k}^{(i_k)}, \\ I_k &= (i_1, \dots, i_k) \in \mathbb{N}_{d+1}^k := \{0, \dots, d+1\}^k, \\ D_F^{(i)} &= \sum_{j=1}^n F_{ji}(\cdot) \frac{\partial}{\partial x_j}, \quad i \in \{0, \dots, d\}, \\ D_F^{(d+1)} &= \frac{1}{2} \sum_{k=0}^d \mathbf{1}_{\{H_k=1/2\}} \sum_{i,j=1}^n F_{ik}(\cdot) F_{jk}(\cdot) \frac{\partial^2}{\partial x_i \partial x_j}, \\ D_F^{(I_k)} &= D_F^{(i_1)} \dots D_F^{(i_k)}, \\ \mathbf{P}_t g(x) &= \mathbb{E}g(X_t^x), \quad t \geq 0, \end{aligned}$$

where  $X_t^x$  is the unique solution of equation (1) with the initial condition  $X_0 = x \in \mathbb{R}^n$ .

**Theorem 2.** *Let  $F \in C_b^{2N+2}(\mathbb{R}^n, \mathbb{R}^{n \times (d+1)})$ ,  $g \in C_b^{2N+3}(\mathbb{R}^n, \mathbb{R})$ ,  $N \in \mathbb{N}$ . Then for any fixed  $H \in (1/3, 1/2]$  such that  $H < H_{\min} = \min_{i=0, \dots, d} H_i$  the following asymptotic decomposition holds*

$$\mathbf{P}_t g(x) = g(x) + \sum_{k=1}^N \sum_{I_k \in \mathbb{N}_{d+1}^k} t^{|H_{I_k}|} (D_F^{(I_k)} g)(x) \mathbb{E} \left( \int_{\Delta^k[0, 1]} dB^{(I_k)} \right) + O(t^{(N+1)H}),$$

as  $t \rightarrow 0$ , where  $|H_{I_k}| = H_{i_1} + H_{i_2} + \dots + H_{i_k}$  is the sum of the Hurst indices of the processes  $B^{(i_1)}, B^{(i_2)}, \dots, B^{(i_k)}$ .

The proof of the theorem is totally analogous to the proof of Theorem 3 in [11]. The key idea of that proof is to apply the Ito formula recursively  $N+1$  times and then to estimate the obtained remainder term by using the classic estimate for rough path integrals stated in the Theorem 4.10 of [1] and the finiteness of the  $(B, \mathbb{B})$  moments, see [11, Proposition 2].

## References

- [1] Friz P., Hairer M. (2014). *A Course on Rough Paths with an introduction to regularity structures*. Springer International Publishing AG, Cham.
- [2] Guerra G., Nualart D. (2002). Stochastic differential equations driven by fractional Brownian motion and standard brownian motion. *Stochastic analysis and their Applications*. Vol. **26**, pp. 1053-1075.

- [3] Kubilius K. (2002). The existence and uniqueness of the solution of an integral equation driven by a p-semimartingale of special type. *Stochastic Processes and their Applications*. Vol. **98**, pp. 289-315.
- [4] Levakov A.A., Vas'kovskii M.M. (2014). Existence of weak solutions of stochastic differential equations with standard and fractional Brownian motions and with discontinuous coefficients. *Differential Equations*. Vol. **50**, pp. 189-202.
- [5] Levakov A.A., Vas'kovskii M.M. (2014). Existence of weak solutions of stochastic differential equations with standard and fractional Brownian motion, discontinuous coefficients, and a partly degenerate diffusion operator. *Differential Equations*. Vol. **50**, pp. 1053-1069.
- [6] Levakov A.A., Vas'kovskii M.M. (2015). Existence of solutions of stochastic differential inclusions with standard and fractional Brownian motions. *Differential Equations*. Vol. **51**, pp. 991-997.
- [7] Levakov A.A., Vas'kovskii M.M. (2016). Properties of solutions of stochastic differential equations with standard and fractional Brownian motions. *Differential Equations*. Vol. **52**, pp. 972-980.
- [8] Mishura Y.S., Shevchenko G.M. (2011). Stochastic differential equation involving Wiener process and fractional Brownian motion with Hurst index  $H > 1/2$ . *Comm. Statist. Theory Methods*. Vol. **40**, pp. 3492-3508.
- [9] Neuenkirch A., Nourdin I., Rößler A., Tindel S. (2009). Trees and asymptotic expansions for fractional stochastic differential equations. *Annales de l'Institut Henri Poincaré Probabilités et Statistiques*. Vol. **45**, pp. 157-174.
- [10] Vas'kovskii M.M. (2017). Stability and attraction of solutions of nonlinear stochastic differential equations with standard and fractional Brownian motions. *Differential Equations*. Vol. **53**, pp. 157-170.
- [11] Vaskouski M.M., Kachan I.V. (2018). Asymptotic expansions of solutions of stochastic differential equations driven by multivariate fractional Brownian motions having Hurst indices greater than  $1/3$ . *Stochastic Analysis and Applications*. Vol. **36**, pp. 909-931.

# STATISTICAL PROPERTIES OF PARAMETER ESTIMATORS IN THE FRACTIONAL VASICEK MODEL

S.S. LOHVINENKO

*Taras Shevchenko National University of Kyiv  
Kyiv, UKRAINE*

e-mail: stanislav.lohvinenko@gmail.com

## Abstract

We study the fractional Vasicek model, described by the stochastic differential equation  $dX_t = (\alpha - \beta X_t) dt + \gamma dB_t^H$ , where  $B^H$  is a fractional Brownian motion. We assume that the parameters  $x_0 \in \mathbb{R}$ ,  $\gamma > 0$  and  $H \in (0, 1)$  are known and consider a problem of estimating  $\alpha$  and  $\beta$ . Least squares, maximum likelihood and alternative estimators are constructed, and their asymptotic properties are established.

**Keywords:** data science, fractional Vasicek model, stochastic differential equation

## 1 Introduction

The standard Vasicek model was proposed and studied by O. Vasicek [6] in 1977 for the purpose of interest rate modeling. It is described by the following stochastic differential equation

$$dX_t = (\alpha - \beta X_t) dt + \gamma dW_t, \quad (1)$$

where  $\alpha, \beta, \gamma \in \mathbb{R}_+$ , and  $W$  is a standard Wiener process. From the financial point of view,  $\beta$  corresponds to the speed of recovery, the ratio  $\alpha/\beta$  is the long-term average interest rate, and  $\gamma$  represents the stochastic volatility. Now the Vasicek model is widely used not only in finance, but also in various scientific areas such as economics, biology, physics, chemistry, medicine and environmental studies.

In our research we deal with the fractional Vasicek model of the form

$$dX_t = (\alpha - \beta X_t) dt + \gamma dB_t^H, \quad (2)$$

where the Wiener process  $W$  is replaced with  $B^H$ , a fractional Brownian motion with Hurst index  $H \in (0, 1)$ . This generalization of the model (1) enables one to model processes with long-range dependence. Such processes appear in finance, hydrology, telecommunication, turbulence and image processing.

## 2 Model description

Let  $(\Omega, \mathfrak{F}, \mathbf{P})$  be a complete probability space. Let  $B^H = \{B_t^H, t \geq 0\}$  be a fractional Brownian motion on this probability space, that is, a centered Gaussian process with covariance function

$$\mathbb{E}B_t^H B_s^H = \frac{1}{2} (s^{2H} + t^{2H} - |t - s|^{2H}).$$

We consider the continuous (and even Hölder up to order  $H$ ) modification of  $B_t^H$  that exists due to the Kolmogorov theorem.

We study the fractional Vasicek model, described by the stochastic differential equation

$$X_t = x_0 + \int_0^t (\alpha - \beta X_s) ds + \gamma B_t^H, \quad t \geq 0. \quad (3)$$

We assume that the parameters  $x_0 \in \mathbb{R}$ ,  $\gamma > 0$  and  $H \in (0, 1)$  are known. Such assumption can be made due to existence of many methods to estimate parameters  $\gamma$  and  $H$  (for example, see [1] and [3, Remark 2.1]). The main goal is to estimate parameters  $\alpha \in \mathbb{R}$  and  $\beta > 0$  by continuous observations of a trajectory of  $X$  on the interval  $[0, T]$ .

Following [2], for  $0 < s < t \leq T$ , define

$$\begin{aligned} \kappa_H &= 2H\Gamma(3/2 - H)\Gamma(H + 1/2), & \lambda_H &= \frac{2H\Gamma(3 - 2H)\Gamma(H + 1/2)}{\Gamma(3/2 - H)}, \\ k_H(t, s) &= \kappa_H^{-1} s^{1/2-H} (t-s)^{1/2-H}, & w_t^H &= \lambda_H^{-1} t^{2-2H}. \end{aligned}$$

Define also next stochastic processes

$$\begin{aligned} M_t^H &= \int_0^t k_H(t, s) dB_s^H, & P_H(t) &= \frac{1}{\gamma} \frac{d}{dw_t^H} \int_0^t k_H(t, s) X_s ds, \\ S_t &= \frac{1}{\gamma} \int_0^t k_H(t, s) dX_s, & Q_H(t) &= \frac{1}{\gamma} \frac{d}{dw_t^H} \int_0^t k_H(t, s) (\alpha - \beta X_s) ds = \frac{\alpha}{\gamma} - \beta P_H(t). \end{aligned}$$

### 3 Main results

Let us introduce the least squares estimators of the unknown parameters:

$$\widehat{\alpha}_T^{(1)} = \frac{(X_T - X_0) \int_0^T X_t^2 dt - \int_0^T X_t dX_t \int_0^T X_t dt}{T \int_0^T X_t^2 dt - \left( \int_0^T X_t dt \right)^2}, \quad (4)$$

$$\widehat{\beta}_T^{(1)} = \frac{(X_T - X_0) \int_0^T X_t dt - T \int_0^T X_t dX_t}{T \int_0^T X_t^2 dt - \left( \int_0^T X_t dt \right)^2}. \quad (5)$$

**Theorem 1** ([5, Theorem 2.1]). *Let  $H \in [\frac{1}{2}, 1)$ . Then the estimators  $\widehat{\alpha}_T^{(1)}$  and  $\widehat{\beta}_T^{(1)}$  are strongly consistent.*

Since the discretization and simulation of  $\widehat{\alpha}_T^{(1)}$  and  $\widehat{\beta}_T^{(1)}$  when  $H \neq 1/2$  is quite difficult, we introduce alternative estimators:

$$\widehat{\beta}_T^{(2)} = \left( \frac{1}{\gamma^2 H \Gamma(2H) T^2} \left( T \int_0^T X_t^2 dt - \left( \int_0^T X_t dt \right)^2 \right) \right)^{-\frac{1}{2H}}, \quad (6)$$

$$\widehat{\alpha}_T^{(2)} = \frac{\widehat{\beta}_T^{(2)}}{T} \int_0^T X_t dt. \quad (7)$$

**Theorem 2** ([5, Theorem 2.2]). *Let  $H \in (0, 1)$ . Then the estimators  $\widehat{\alpha}_T^{(2)}$  and  $\widehat{\beta}_T^{(2)}$  are strongly consistent.*

In applications usually the observations cannot be continuous. The estimators  $\widehat{\alpha}_T^{(2)}$  and  $\widehat{\beta}_T^{(2)}$  can be discretized as follows.

Let  $h > 0$ . Assume that a trajectory of  $X$  is observed at times  $t_k = kh$ ,  $k = 0, 1, \dots, n$ . Define

$$\widehat{\beta}_n^{(3)} = \left( \frac{1}{\gamma^2 H \Gamma(2H) n^2} \left( n \sum_{k=0}^{n-1} X_{kh}^2 - \left( \sum_{k=0}^{n-1} X_{kh} \right)^2 \right) \right)^{-\frac{1}{2H}}, \quad (8)$$

$$\widehat{\alpha}_n^{(3)} = \frac{\widehat{\beta}_n^{(3)}}{n} \sum_{k=0}^{n-1} X_{kh}. \quad (9)$$

**Theorem 3** ([5, Theorem 2.3]). *Let  $H \in (0, 1)$ . Then the estimators  $\widehat{\alpha}_n^{(3)}$  and  $\widehat{\beta}_n^{(3)}$  are strongly consistent.*

Applying the analog of the Girsanov formula for a fractional Brownian motion (see [2, Theorem 3]), we obtain next likelihood ratio:

$$\begin{aligned} \Lambda_H(T) &= \exp \left\{ \int_0^T Q_H(t) dS_t - \frac{1}{2} \int_0^T (Q_H(t))^2 dw_t^H \right\} \\ &= \exp \left\{ \frac{\alpha}{\gamma} S_T - \beta \int_0^T P_H(t) dS_t - \frac{\alpha^2}{2\gamma^2} w_T^H \right. \\ &\quad \left. + \frac{\alpha\beta}{\gamma} \int_0^T P_H(t) dw_t^H - \frac{\beta^2}{2} \int_0^T (P_H(t))^2 dw_t^H \right\}. \end{aligned} \quad (10)$$

Now we can construct maximum likelihood estimators.

**Theorem 4** ([4, Theorem 3.1]). *Let  $H > 1/2$  and  $\beta$  is known. The MLE for  $\alpha$  is*

$$\widehat{\alpha}_T^{(4)} = \frac{S_T + \beta \int_0^T P_H(t) dw_t^H}{w_T^H} \gamma. \quad (11)$$

*It is unbiased, strongly consistent and normal:*

$$T^{1-H} \left( \widehat{\alpha}_T^{(4)} - \alpha \right) \stackrel{d}{\rightarrow} \mathcal{N}(0, \lambda_H \gamma^2).$$

**Theorem 5** ([4, Theorem 3.2]). *Let  $H > 1/2$  and  $\alpha$  is known. The MLE for  $\beta$  is*

$$\widehat{\beta}_T^{(5)} = \frac{\frac{\alpha}{\gamma} \int_0^T P_H(t) dw_t^H - \int_0^T P_H(t) dS_t}{\int_0^T (P_H(t))^2 dw_t^H}. \quad (12)$$

*It is strongly consistent and asymptotically normal:*

$$\sqrt{T} \left( \widehat{\beta}_T^{(5)} - \beta \right) \stackrel{d}{\rightarrow} \mathcal{N}(0, 2\beta).$$

**Theorem 6** ([4, Theorem 3.4]). Let  $H > 1/2$ . The MLEs for  $\alpha$  and  $\beta$  equal

$$\begin{aligned}\widehat{\alpha}_T^{(6)} &= \frac{\int_0^T P_H(t) dS_t \int_0^T P_H(t) dw_t^H - S_T \int_0^T (P_H(t))^2 dw_t^H}{\left(\int_0^T P_H(t) dw_t^H\right)^2 - w_T^H \int_0^T (P_H(t))^2 dw_t^H} \gamma, \\ \widehat{\beta}_T^{(6)} &= \frac{w_T^H \int_0^T P_H(t) dS_t - S_T \int_0^T P_H(t) dw_t^H}{\left(\int_0^T P_H(t) dw_t^H\right)^2 - w_T^H \int_0^T (P_H(t))^2 dw_t^H}.\end{aligned}\tag{13}$$

They are consistent and asymptotically normal:

$$T^{1-H} \left( \widehat{\alpha}_T^{(6)} - \alpha \right) \xrightarrow{d} \mathcal{N}(0, \lambda_H \gamma^2), \quad \sqrt{T} \left( \widehat{\beta}_T^{(6)} - \beta \right) \xrightarrow{d} \mathcal{N}(0, 2\beta).$$

**Theorem 7** ([3, Theorem 4.2]). Let  $H > 1/2$ . The vector maximum likelihood estimator  $(\widehat{\alpha}_T^{(6)}, \widehat{\beta}_T^{(6)})$  for vector parameter  $(\alpha, \beta)$  is asymptotically normal:

$$\begin{bmatrix} T^{1-H} \left( \widehat{\alpha}_T^{(6)} - \alpha \right) \\ \sqrt{T} \left( \widehat{\beta}_T^{(6)} - \beta \right) \end{bmatrix} \xrightarrow{d} \mathcal{N} \left( \begin{bmatrix} 0 \\ 0 \end{bmatrix}, \begin{bmatrix} \lambda_H \gamma^2 & 0 \\ 0 & 2\beta \end{bmatrix} \right), \quad T \rightarrow \infty,\tag{14}$$

hence estimators  $\widehat{\alpha}_T^{(6)}$  and  $\widehat{\beta}_T^{(6)}$  are asymptotically independent.

## 4 Acknowledgements

I would like to thank K. Ralchenko for constant support throughout whole my research.

## References

- [1] Berzin C., Latour A., León J.R. (2014). *Inference on the Hurst Parameter and the Variance of Diffusions Driven by Fractional Brownian Motion*. Springer.
- [2] Kleptsyna M., Le Breton A., Roubaud M.-C. (2000). Parameter estimation and optimal filtering for fractional type stochastic systems. *Stat. Inference Stoch. Process.* Vol. **3**, pp. 173-182.
- [3] Lohvinenko S.S., Ralchenko K.V. (2018). Asymptotic distribution of maximum likelihood estimator in fractional Vasicek model. *Teor. Imovir. Mat. Stat.* Vol. **99**, pp. 134-151 (In Ukrainian).
- [4] Lohvinenko S.S., Ralchenko K.V. (2017). Maximum likelihood estimation in the fractional Vasicek model. *Lithuanian J. Statist.* Vol. **56(1)**, pp. 77-87.
- [5] Lohvinenko S.S., Ralchenko K.V., Zhuchenko O.M. (2016). Asymptotic properties of parameter estimators in fractional Vasicek model. *Lithuanian J. Statist.* Vol. **55(1)**, pp. 102-111.
- [6] Vasicek O. (1977). An equilibrium characterization of the term structure. *J. Finance Econ.* Vol. **5(2)**, pp. 177-188.

# ANALYSIS OF FINANCIAL STABILITY OF THE BELARUSIAN ECONOMY BASED ON MICRODATA AND EXPERT INFORMATION

V.I. MALUGIN<sup>1</sup>, A.YU. NOVOPOLTSEV<sup>1</sup>, N.V. HRYN<sup>2</sup>

<sup>1</sup>*Belarusian State University, Minsk, BELARUS*

<sup>2</sup>*Yanka Kupala State University, Grodno, BELARUS*

e-mail: malugin@bsu.by, novopsacha@gmail.com, lebnat@tut.by

## Abstract

In the practice of a central bank, prudential indicators based on aggregated macroeconomic and financial data [1] are used to analyze financial stability of the banking system. There is an evidence that it's may be not enough to use aggregated macroeconomic and financial data to identify situations of growing systemic risks threatening economic and financial stability [2]. Obviously, the financial stability of the banking sector and the economy as a whole essentially depends on the financial state (creditworthiness) of certain categories of enterprises, as well as the level of credit risk for various sectors of the economy. For this reason, firm-level data is going to be more appealing for central banks. It's reported that, in contrast to aggregated economic and financial data, microdata allow for more flexible and differential analysis. This makes the statistical indicators of solvency and financial stability based on microdata a useful complementary tool for analysis of actual economic and financial processes.

**Keywords:** data science, financial stability, microdata, expert information

## 1 Issues of traditional methodology

In international practice microdata and macroeconomic indicators are used in various applications related to the estimation of statistical credit risk models and probability of default at the macro level and for individual companies. Depending on data and indicators used, the following set of models may be applied [3]: 1) models based on balance sheet data of companies; 2) models based on microdata and stock market statistics; 3) models based on macroeconomic and stock market indicators; 4) credit scoring models; 5) hybrid models that allow using both microdata and macroeconomic indicators.

In [3] some of the models listed above are estimated on Belarusian data, and the issues related to their application are reported. The most critical issues related to practical application of the models proposed are the following: 1) lack of a mechanism for formation stock prices that comes from insufficient development of the financial market; 2) lack of credit ratings for the majority of Belarusian companies.

All this does not allow applying models based on indicators of a stock market and credit ratings. Another obstacle for the effective application of the models proposed is a priori endogenous-exogenous structure dictated by the developed economies. Problems can arise from taking into account the properties of the Belarusian economy,

as well as possible changes in the economic policy, for example, a gradual reduction in issuing new loans for state programs. In this regard, the most promising type of model for assessing the financial stability of the Belarusian economy is one based on balance sheets microdata, as well as hybrid models incorporating macroeconomic and prudential indicators.

The process of construction models based on microdata, however, is associated with a number of specific issues. As noted above, microdata allow for more flexible and differentiated analysis. Differentiated analysis of solvency involves the partitioning of the set of companies from a particular sector of the economy into classes corresponding to different levels of credit risk. In this case, the most important issue is to identify correctly the class corresponding to the state of default. To distinguish the companies in the default, statistics on the defaults derived for the model estimation period is necessary. The first issue related to models based on financial statements of companies is the lack of actual statistics on the defaults. That makes it difficult to unambiguously formalize the definition of default and forces the researchers to replace actual statistics with some proxies such as unprofitable companies frequency that cannot always be justified [3].

To solve this problem from the point of international experience, it is recommended to use the data of the Credit Register of the National Bank of the Republic of Belarus. The data are compiled on a daily basis and include the credit histories of the majority of companies. In particular, it is may be used for construction of statistical indicators of credit risk based on widely used criteria of default. An example of such indicator is an estimate of probability of default as relative frequency of accounts with past due payments. In the Basel framework default is defined as: "90 days past due on debt or interest payment by a contract" [4].

The application of generally accepted criteria of default on microdata requires estimation of creditworthiness for different categories of companies. For example, large state-owned enterprises (SOE) have soft budget constraints with their positive (high probability of financial support by government) and negative consequences (strengthening the relationship between the insolvency risk of enterprises, credit risk for banks and fiscal risks for the government) [3]. As SOE constitute a large part of the real sector of the economy, these features like "soft budget constraints", which are not taken into account, may significantly bias the estimates of credit risk measures derived according to international standards. Therefore, along with the generally accepted default criteria, it is recommended to use alternative "expert" criteria taking into account the specific features of credit risk assessment process in the Belarusian economy. To illustrate that, Figure 1 shows line plots of expert indicators of financial stability estimated on a sample of companies in each quarter: an average integral statistical credit rating based on cluster analysis (`ind_rating`, right scale) is compared with one indicator that is purely statistical combination of some expert criteria (`ind_best`) and another one estimated by IMF methodology (`ind_imf`) [7]. Obviously, both indicators have similar dynamics to statistical rating, but IMF indicator differs in larger extent after the crisis period of the 2016 year that shows that expert information may help to introduce some corrections to statistical methodology.

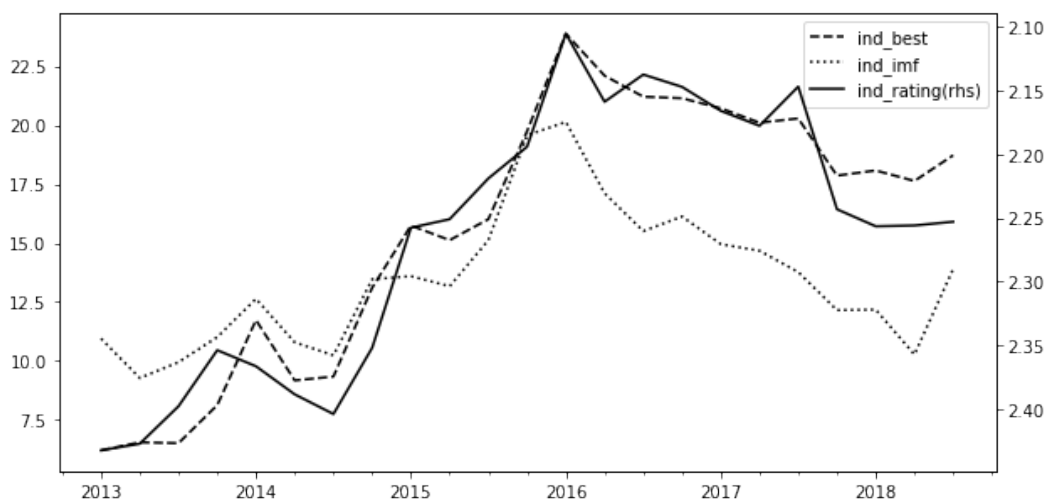


Figure 1: Comparative analysis of aggregated indicators of financial stability

## 2 Developed methodology and software

To assess the financial stability of the economy using microdata on a regular basis, it is necessary to take into account the features of the Belarusian economy and possible risk factors, as well as to develop methodology, modeling tools and software for calculating economic and financial indicators, and applying for that statistical, machine learning, and big data techniques.

As a part of this study, methodological, model and software tools intended to build statistical indicators of the creditworthiness of the real sector of the economy and the financial stability of the banking sector based on the financial statements of companies and available expert information. To build these indicators, we used representative sample of enterprises from the real sector of the economy that are mainly SOE and generate a large part of revenues and profits in Belarusian economy.

Unlike earlier studies [5, 6], in this research we also utilized available expert information in a form of economically reasonable criteria used in real practice to assess financial state of the Belarusian enterprises based on their balance sheets statements.

Statistical indicators of creditworthiness at the micro and macro levels include the following: statistical credit ratings of companies corresponding to the credit risk groups (from 1 to 4); average credit rating for an economic activity; average credit rating for the whole sample of companies which represent integral indicator of the creditworthiness for the economy as a whole [6]. For a given set of expert criteria of default and the proposed integral criteria, which take into account expert information, statistical indicators of financial stability are calculated as estimates of the probability of default. The proposed statistical methodology is implemented using statistical and machine learning algorithms in Python programming language.

A joint econometric analysis of prudential and financial stability indicators of the banking sector and the indicators based on microdata shows their significant correla-

tions, both at the level of the main industries, as well as at the level of the real sector of the economy. In particular, the leading nature of the integral indicator of the creditworthiness of the economy is revealed in relation to the capital adequacy ratio. An estimate of the probability of default for the dominant integral criterion (covers over 50% of enterprises that are vulnerable according to at least one expert criteria proposed) also demonstrates the leading dynamics with respect to the problem debt share from borrowers (at the level of the banking sector). The discovered relations are important for validation of the proposed statistical indicators and their further practical application. The advanced features of the proposed statistical indicators allow them to be used as exogenous variables in more complex econometric models on extended data sets. In case of fast retrieval of initial data, it can be used as independent indicators for the vulnerabilities diagnostics of the banking sector with an aim of early warning of systemic risks that threaten economic and financial stability.

## References

- [1] Pashkevich A.V., Vlasenko M.N. (2017). Instruments of macroprudential policy: European experience, perspectives for Belarus. National Bank of Belarus. Bank Bulletin. No. **12**, pp. 11-18. (in Russian)
- [2] Bank for International Settlements (2017). Uses of central balance sheet data offices' information. *IFC-ECCBSO-CBRT Conference on "Uses of Central Balance Sheet Data Offices information"*. Ozdere-Izmir, Turkey, 26 September 2016.
- [3] Vlasenko M.N., Tkachev A.I. (2017). Estimation of probability of default for the enterprises of a real sector of economy. National Bank of Belarus. Bank Bulletin. No. **1**, pp. 18-26. (in Russian)
- [4] Bank for International Settlements (2005). Basel II: Revised international capital framework.
- [5] Malugin V., Hryn N., Novopoltsev A. (2014). Statistical analysis and econometric modelling of the creditworthiness of non-financial companies. *International Journal of Computational Economics and Econometrics*. Vol. **4** (1/2), pp. 130-147.
- [6] Malugin V.I., Novopoltsev A.Yu., Hryn N.V., Milevsky P.S. (2018). Statistical analysis of creditworthiness of real sector of Belarusian economy with microdata *Bank Bulletin. – A special issue "Bank Research"*. No. **14**. (in Russian)
- [7] Information portal of International Monetary Fund. Mode of Access: <https://www.imf.org/>. Date of Access: 20.10.2018.

# INFLUENCE OF THE TRAINING SET ON THE PREDICTION STABILITY IN ESTIMATION OF ACUTE PANCREATITIS SEVERITY

E. MANGALOVA, O. CHUBAROVA, D. MELEKH  
*LLC RD Science, Siberian Federal University*  
*Krasnoyarsk, RUSSIA*  
e-mail: e.s.mangalova@hotmail.com

## Abstract

The small sample size problem is often encountered in data analysis, especially for medical applications. It leads to unstable predictions when including or excluding several observations could change prediction significantly. Prediction stability visualization and measure were proposed and applied to estimation of acute pancreatitis severity. A simulation experiments were carried out to study the stability of ridge-regression, SVM, random forest trained with various subsets.

**Keywords:** data science, small sample, prediction, acute pancreatitis severity

## 1 Introduction

Analysts in medicine face two contradictory problems due to the prohibition on disclosure and dissemination of personal data. Usually medical analysts deal with either large amounts of poorly matched data (health facilities have a different set of equipment with various accuracy, also medical institutions can depersonalize data in different ways) or small amounts of data (from one medical institution).

When training predictive models on a small data set is required, the analyst deals with the following challenges:

- Overfitting. With only a few data, the risk to overfit model is higher.
- Outliers. If you have millions of data, a couple of outliers will not be a problem. But with only a few, they will definitely skew your results.

The work is devoted to the research of the influence of the training set on the prediction results. As example, acute pancreatitis severity classification task is considered.

## 2 Classification task

Acute pancreatitis severity is classified as mild, moderate or severe. Mild acute pancreatitis, the most common form, has no organ failure, local or systemic complications and usually resolves in the first week. Moderately severe acute pancreatitis is defined by the presence of transient organ failure, local complications or exacerbation of co-morbid disease. Severe acute pancreatitis is defined by persistent organ failure [1].

The study was based on a retrospective analysis of 130 cases of acute pancreatitis: 47 cases from “Krasnoyarsk Regional Clinical Hospital” and 83 cases from RSBHI

“Regional Interdistrict Clinical Hospital no. 20 named after I.S. Berzon” in the period from 2015 to 2017.

The task is to estimate of acute pancreatitis severity by using patient clinical examination data  $D = \{(\bar{x}_i, y_i), i = 1, \dots, 130\}$ , where  $\bar{x} = \{x^1, \dots, x^{27}\}$  is set of features (Clinical Blood Analysis, Biochemical Blood Analysis, Ultrasound of pancreas, the results of the examination of the patient) measured in 130 patients,  $y$  is acute pancreatitis severity determined by medical expert based on patient clinical examination data defined by integer (1 - mild, 2 - moderate, 3 - severe).

The existing multi-class classification task can be transformed to binary classification task. One-vs.-rest strategy involves training a single classifier per class, with the samples of that class as positive samples and all other samples as negatives. One-vs.-rest strategy requires the base classifiers to produce a real-valued class probability; class labels alone can lead to ambiguities, where multiple classes are predicted for a single observation.

Thus, there are two problems of binary classification:

- 1vsR: mild acute pancreatitis vs moderate and severe acute pancreatitis.
- 3vsR: severe acute pancreatitis vs mild and moderate acute pancreatitis.

The task 2vsR is excluded, since the moderate class is intermediate that requires the construction of a more complex separating surface, which is not desirable in small sample size conditions. For the study, three algorithms were chosen that allow the construction of simple separating surfaces: Ridge Regression, SVM and Random Forest.

### 3 Algorithm description

For  $i$ -th observation from the initial training set we estimate prediction stability of classification method using the following algorithm:

1. A set of  $T$  training subsets is created such that each subset contains  $m$  different observations and do not contains  $i$ -th observation:

$$S_i = \{S_{i,1}, \dots, S_{i,T}\}, S_{i,t} = ((\bar{x}_{j_{t,k}}, y_{j_{t,k}}), k = 1, \dots, m : j_{t,k} \neq i), t = 1, \dots, T. \quad (1)$$

The  $m/n$  ratio can range from 0.5 to  $(n - 2)/(n - 1)$ :

- If  $m/n$  is equal to  $(n - 2)/(n - 1)$ , we deal with some analogue of the leave-one-out cross-validation. Each pair of subsets is distinguished by one observation. This variant allows to show how one observation can change classifier prediction and identify specific observations that are similar to outliers.
- If  $m/n$  is smaller than  $(n - 2)/(n - 1)$ , the impact of sample size can be estimated. Changes in the classifier predictions trained on subsets with significant differences show how much information is contained in observations. The smaller the changes, the less information the observations contain. And the greater the changes, the greater the need to increase the training set.

It is also possible to vary the parameter  $T$  (number of subsets):

- If  $m/n$  is equal to  $(n-2)/(n-1)$  training subsets contain  $(n-2)$  observations and only  $(n-2)$  different subsets can be formed. And accordingly, for small initial training set (number of observations  $n$  allows to build  $n^2$  classifiers in limited time) it is possible to form a complete set of subsets.
  - If ratio  $m/n$  is smaller then the number of possible variants becomes much larger (even for sufficiently small training set size). It means that the number  $T$  should be limited to some reasonable value, and  $T$  training samples for  $i$ -th observation should be chosen randomly. At the same time, we note that because the decision rule is tested for stability to a training set of observations, there is no need to ensure the preservation of the different classes objects proportion in the training subsets and the initial training set.
2.  $T$  models  $M_i, i = 1, 2, \dots, T$  are built using the training subsets  $S_i$  to obtain matrix of  $T$  predictions  $P_i = \{p_{t,z}^i, t = 1, \dots, T, z = 1, \dots, Z\}$ , where  $Z$  is the number of classes.
  3. A convex hull of a set  $P_i$  of points is constructed according to the predictions of the classifiers  $M_i$ .

If the problem of binary classification is solved, then there is a segment  $H_i$  containing all predictions of classifiers for the  $i$ -th observation. The beginning of the segment is the minimum prediction, the end of the segment is the maximum prediction  $H_i = [a_i, b_i] = [\min P_i, \max P_i]$ .

If the problem of multiclass classification is solved, then there is such a convex hull  $H_i$  containing all predictions of classifiers (rows of the matrix  $P_i$ ). In mathematics, the convex hull of a set  $P_i$  of points in the Euclidean space is the smallest convex set that contains  $P_i$ . Computing the convex hull means constructing an unambiguous, efficient representation of the required convex shape.

Chan's algorithm [2] is an optimal output-sensitive algorithm to compute the convex hull of a set  $P_i$  of  $T$  points in two- and three-dimensional space. The algorithm takes  $O(T \log h)$  time, where  $h$  is the number of vertices of the output (the convex hull). In the planar case, Chan's algorithm combines Graham scan algorithm with time complexity  $O(T \log T)$  with Jarvis march algorithm with time complexity  $O(Th)$ , in order to obtain an optimal  $O(T \log h)$  time.

The convex hull allows to display on a two-dimensional graph (for three classes) all possible classifier predictions based on different training subsets. Figure 1 illustrates the stability of various classifiers predictions (Ridge Regression, Support Vector Machine, Random Forest) for new observation. For this observation a set of  $T = 500$  training subsets ( $n = 130, m = 117$ ) was generated to fit classifiers. All three machine learning algorithms do not classify the patient as a severe acute pancreatitis, but there is ambiguity regarding classification as mild acute pancreatitis. Random forest estimates probability of mild class in the range  $[0.4, 0.7]$ , it is significantly less than the predictions of the two other algorithms.

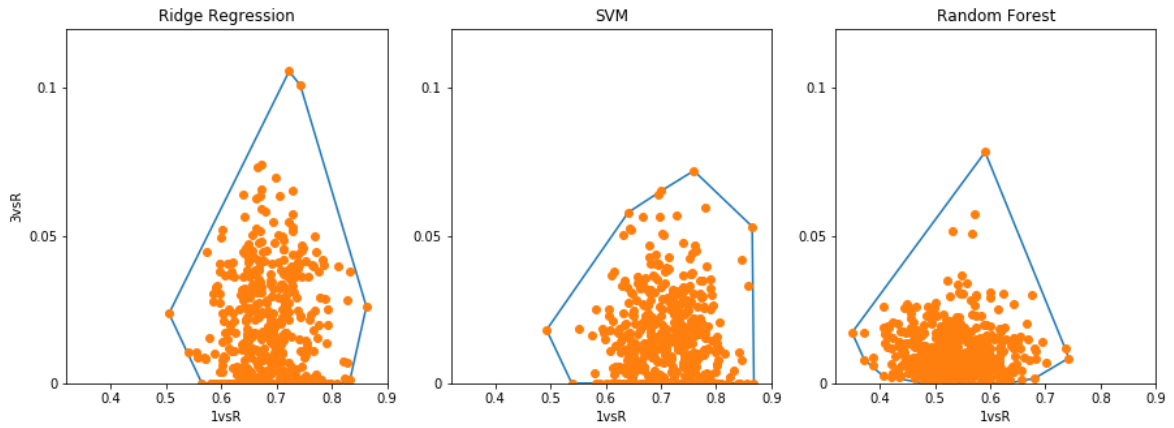


Figure 1: The stability of predictions for new observation: points are predictions of classifiers trained on different subsets of the training data, polygon is the convex hull constructed by these points

## 4 Experimental results

The proposed visualization algorithm allows to view the spread of predictions for multiple observations on a single graph. Figure 2 shows the stability of classifiers predictions for set of observations. In general random forest turns out to be a less stable algorithm, in other words, the convex hull area is larger for most observations. At the same time there is more compact area of observations with severe acute pancreatitis than in case of Ridge Regression and SVM. The wide scatter of the some predictions for the Ridge Regression and Random Forest indicates the presence of outliers. Note that the predictions scatter for patients with severe acute pancreatitis is higher than in others cases.

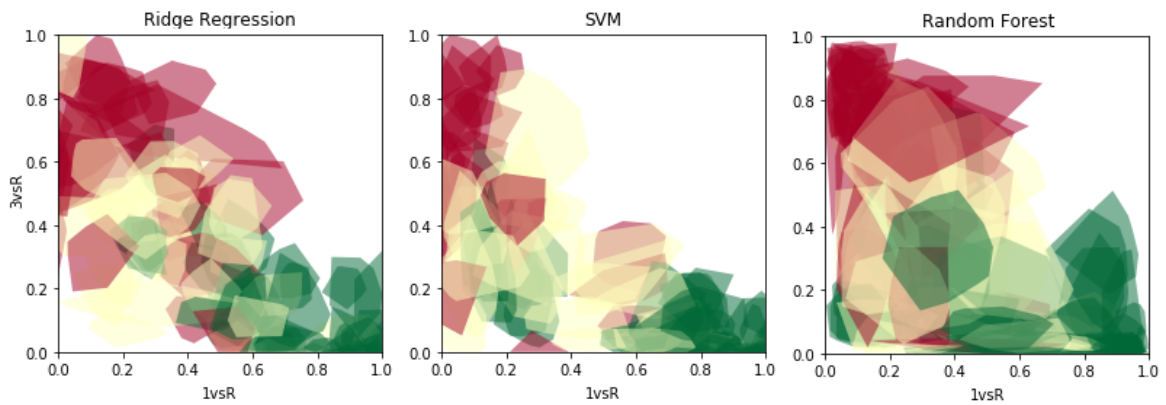


Figure 2: The stability of predictions for set of observations. The severity estimated by doctors are marked by the following colors: mild acute pancreatitis (green), moderate acute pancreatitis (yellow), severe acute pancreatitis (red)

## 5 Conclusion

Prediction stability visualization and measure were proposed and applied to estimation of acute pancreatitis severity. Visualization allows to evaluate the spread of predictions for multiple observations on a single graph and compare various machine learning algorithms. This study can be useful to estimate the current dataset quality and to justify the need dataset increasing.

Also the study shows the need for a combination of several algorithms for the final forecast because different methods have their advantages and disadvantages for different observations from various classes.

## References

- [1] Banks P.A., Bollen T.L., Dervenis C., et al (2013). Classification of acute pancreatitis—2012: revision of the Atlanta classification and definitions by international consensus. *Gut*. Vol. **62**, pp. 102–111.
- [2] Chan T.M. (1996). Optimal output-sensitive convex hull algorithms in two and three dimensions. *Discrete & Computational Geometry*. Vol. **16**, pp. 361–368.

# NONPARAMETRIC MODELLING OF MULTIDIMENSIONAL MEMORYLESS PROCESSES

A.V. MEDVEDEV, A.V. TERESHINA, D.I. YARESHENKO

*Siberian Federal University*

*Krasnoyarsk, RUSSIA*

e-mail: yareshenkodi@yandex.ru

## Abstract

The report considers the case when multidimensional memoryless objects have an unknown stochastic dependence between output variables, a training sample is available. Such processes are called T-processes. Constructing a model for such a process leads to solve a system of implicit functions. Moreover, the form of these functions is unknown up to parameters. Therefore, practical application of generally accepted parametric identification theory is not possible. In this case, we will use a piecemeal approach to predict output variables from known input variables.

**Keywords:** data science, memoryless process, nonparametric modeling

## 1 Introduction

Suppose the object input variables vector is  $\vec{u} = (u_1, u_2, \dots, u_m)$ , output vector is  $\vec{x} = (x_1, x_2, \dots, x_n)$  and training sample  $\{u_i, x_i, i = \overline{1, s}\}$ . In this case, mathematical description of the object can be represented as analogue of an implicit functions system  $F_j(u, x) = 0, j = \overline{1, n}$ . The main feature of this case is that the dependency  $F(\cdot)$  form is unknown. In this way, it is advisable to use nonparametric methods [1]. Thus, the identification is reduced to solving a system of nonlinear equations  $F_j(u, x) = 0, j = \overline{1, n}$ , where  $\vec{u}_s, \vec{x}_s$  - time vectors of components  $x = (x_1, x_2, \dots, x_n)$  with known  $u$ .

## 2 T-process nonparametric identification

In general, the studied multidimensional system that implements a T-process can be represented in Figure 1.

In Figure 1, the following notations are used:  $u(t) = (u_1(t), \dots, u_m(t))$  - m-dimensional vector of input variable,  $x(t) = (x_1(t), \dots, x_n(t))$  - n-dimensional vector of output variables,  $\xi(t)$  - random noise acting on the object,  $t$  - time. For various interaction channels, the dependence of j-th component vector  $x$  can be represented as some dependence on certain components of the vector  $u$ .

A feature of the T-process modelling is that it is described by a system of implicit stochastic equations 1:

$$F_j(u(t - \tau), x(t), \xi(t)) = 0, j = \overline{1, n}, \quad (1)$$

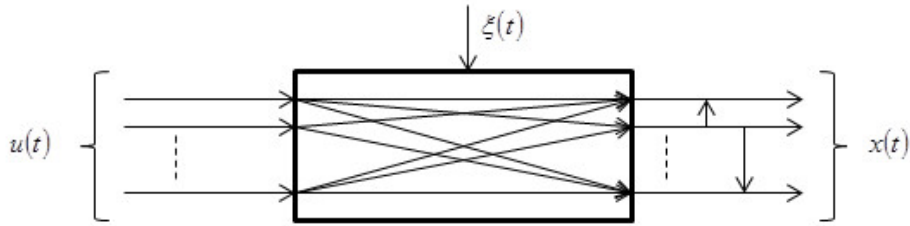


Figure 1: T-process

where  $F_j(\cdot)$  – unknown,  $\tau$  – delay of a multidimensional system's various channels. Since the delay vector is different through various channels, but it is known, we will omit it for simplicity.

Note that when constructing the models of a real technological and production processes (complexes), we often deal with the vectors  $x$  and  $u$  in a form of certain compound vectors [1]. Compound vector means a vector composed of some components of the corresponding vector, in particular  $u^{<j>} = (x_2, x_5, x_7, x_8)$ , or another set. In this case, the system of equations takes the form  $\hat{F}_j(u^{<j>}, x^{<j>}) = 0, j = \overline{1, m}$

### 3 T-models

Analyzing the previous considerations, it is easy to see that mathematical description of the process, shown on figure 1, can be taken as a system of implicit functions:

$$F_j(u^{<j>}, x^{<j>}) = 0, j = \overline{1, m} \quad (2)$$

where  $u^{<j>}, x^{<j>}$  - compound vectors. The main feature concerned with modelling such a process in the conditions of nonparametric uncertainty, is the fact that the type of functions (2) is unknown. The system of models can be represented as follows:

$$\hat{F}_j(u^{<j>}, x^{<j>}, \vec{u}_s^{<j>}, \vec{x}_s^{<j>}) = 0, j = \overline{1, m} \quad (3)$$

where  $\vec{u}_s^{<j>}, \vec{x}_s^{<j>}$  - time vectors (data array received at the  $s$ -th time point), in particular  $\vec{x}_s = (x_1, \dots, x_s) = (x_{11}, x_{12}, \dots, x_{1s}, \dots, x_{21}, x_{22}, \dots, x_{2s}, \dots, x_{m1}, x_{m2}, \dots, x_{ms})$ , but  $\hat{F}_j(\cdot), j = \overline{1, m}$  also unknown. In the identification theory, such problems are not only considered, but also not posed. Usual way is choosing the parametric structure (3), but, unfortunately it takes a long time to determine the parametric structure.

So, let input variables be inputted to the object  $u'$ . In this case, the evaluation of the components of output variables vector  $x$  with known values  $u=u'$ , as it was already noted, leads to solving the system of equations (3). Since the dependence of output variables  $x$  on the components of input variables vector is not known, it is reasonable to apply the methods of non-parametric estimation [1].

The problem is reduced to the fact that for a given value of input variables vector  $u=u'$ , it is necessary to solve the system (3) with respect to output variables vector. The general scheme for solving such a system:

- first, the residual is calculated by the formula:

$$\varepsilon_{ij} = F_j(u^{<j>}, x^{<j>}(i), \vec{u}_s^{<j>}, \vec{x}_s^{<j>}), j = \overline{1, m} \quad (4)$$

where  $F_j(u^{<j>}, x^{<j>}(i), \vec{u}_s^{<j>}, \vec{x}_s^{<j>})$  is taken in the form:

$$\varepsilon_j(i) = F_{sj}(u^{<j>}, x_j(i)) = x_j(i) - \frac{\sum_{i=1}^s x_j[i] \prod_{k=1}^{<n>} \Phi\left(\frac{u'_k - u_k[i]}{c_{su_k}}\right)}{\sum_{i=1}^s \prod_{k=1}^{<n>} \Phi\left(\frac{u'_k - u_k[i]}{c_{su_k}}\right)}, \quad (5)$$

where  $j = \overline{1, m}$ ,  $<n>$  is dimension of a compound vector  $u_k$ . Further, this notation is used for other variables.

- next step is to evaluate the mathematical expectation:

$$x_j = M\{x|u^j, \varepsilon = 0\}, j = \overline{1, m} \quad (6)$$

As an estimate (6), we take non-parametric Nadaraya-Watson regression:

$$\hat{x}_j = \frac{\sum_{i=1}^s x_j[i] \prod_{k_1=1}^{<n>} \Phi\left(\frac{u_{k_1} - u_{k_1}[i]}{c_{su}}\right) \prod_{k_2=1}^{<m>} \Phi\left(\frac{\varphi_{k_2}[i]}{c_{s\varphi}}\right)}{\sum_{i=1}^s \prod_{k_1=1}^{<n>} \Phi\left(\frac{u_{k_1} - u_{k_1}[i]}{c_{su}}\right) \prod_{k_2=1}^{<m>} \Phi\left(\frac{\varphi_{k_2}[i]}{c_{s\varphi}}\right)}, j = \overline{1, m} \quad (7)$$

where kernel functions  $\Phi(*)$  satisfy certain conditions [1].

Realizing this procedure, we obtain the values of output variables  $x$  when input action on the object is  $u=u'$ . This is the main purpose of the constructed model, which can be applicable in various control systems.

## 4 Application of the developed method

An object was taken, with five input variables  $u(t) = (u_1(t), u_2(t), u_3(t), u_4(t), u_5(t))$ , taking random values in the interval  $u(t) \in [0, 3]$ , and three output variables  $x(t) = (x_1(t), x_2(t), x_3(t))$  [2]. For this object, let us generate a sample of input and output variables based on the system of equations, that are unknown to the researcher (they are necessary only to obtain training samples):

$$\begin{cases} x_1(t) - 2u_1(t) + 1.5\sqrt{u_2(t)} - u_5^2(t) - 0.3x_3(t) = 0; \\ x_2(t) - 1.5u_4(t) - 0.3\sqrt{u_5(t)} - 0.6 - 0.3x_1(t) = 0; \\ x_3(t) - 2u_2(t) + 0.9\sqrt{u_3(t)} - 4u_5(t) - 6.6 + 0.5x_1(t) - 0.6x_2(t) = 0. \end{cases} \quad (8)$$

As a result, we obtain a sample of measurements  $\vec{u}_s, \vec{x}_s$ , where  $\vec{u}_s, \vec{x}_s$  - are time vectors.

Let us present the results of a computing experiment with 5% noise acting on the object output. In this case, the elements of training sample  $\vec{u}_s, \vec{x}_s$  are used in

the algorithms (5) and (6), and for exam input variables values  $u'_k$  from the training sample are submitted to the object input. The kernel smoothing  $c_s$  will be an adjustable parameter, which in this case we take equal to 0.3 (the value was determined as a result of numerous experiments in order to reduce a quadratic error between an output of the model and object), the kernel smoothing will be the same when calculated in formulas (5) and (6), sample size is  $s=2000$ . Below figures show the object outputs  $x_1(t), x_2(t)$  and  $x_3(t)$ .

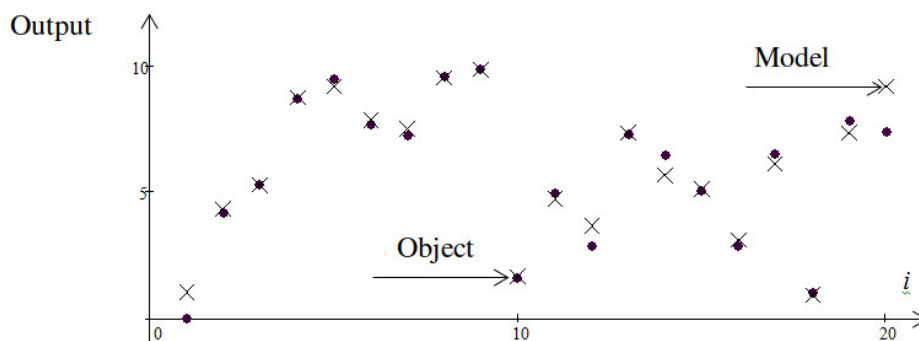


Figure 2: Predicted output  $x_1$  , without noise

In Figure 2 the “point” denotes the output variables values, and the “cross” denotes the model output value. The figures demonstrate a comparison of the true output vector components values of the test sample and their predicted values obtained using the algorithm (5) - (7) (For convenience, the first 20 sample points were shown in the figures).

## 5 Conclusion

In this paper, we considered the identification problem of memoryless multidimensional objects with delay while components of the output vector have unknown stochastic interactions. Such features are characteristic of complex technological processes with many output variables. The identification algorithm here is the above described procedures, which allows one to predict the output variables with known input variables.

The performed computing experiments showed high efficiency of T-modeling in the presence of random noise acting both on the object and in the measurement channels.

## References

- [1] Medvedev A.V.(2018). *Fundamentals of the Theory of Nonparametric Systems*. iz-vo SibGAU, Krasnoyarsk.[Russian] P. 732

- [2] Tereshina A. V., Yareshenko D. I. (2018). About nonparametric modelling of the memoryless systems with delay. *Siberian Journal of Science and Technology*. Vol. **19**, No. **3**, [Russian] pp. 452–461.

# FINDING SIGNIFICANT VARIABLES IN THE PROBLEMS OF MODELLING LESS MEMORY PROCESSES

E.D. МИНОВ  
*Siberian Federal University*  
*Krasnoyarsk, RUSSIA*  
e-mail: edmihov@mail.ru

## Abstract

The report is devoted to the task of identifying significant variables. There are many algorithms for the selection of significant variables, but they all have their weaknesses. A new algorithm for extracting significant variables based on non-parametric algorithms has been proposed. The result of the proposed algorithm is shown in the report.

**Keywords:** data science, memoryless process, significant variable

## 1 Introduction

The identification of many stochastic objects is often reduced to the identification of static systems [3]. The general scheme of the discrete-continuous process under study is presented in the Figure 1:

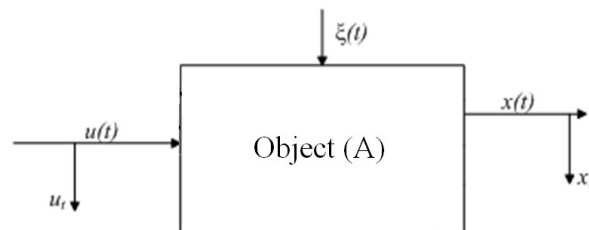


Figure 1: The general scheme of the process under study

In figure 1, the following notations:  $A$  is the unknown operator of the object,  $x(t)$  is the output characteristic of the process,  $\vec{u}$  is the vector of control actions,  $\xi(t)$  is the interference (interference affects the accuracy of the reading of the output variables, for example, if the interference is 5%, then this means that the read output variable contains an error of up to 5%).

The need to find significant input variables that affect  $x(t)$  often arises in the study of such processes. The process of diagnosing diseases can be cited as an example.

If a technique for diagnosing any disease is not developed, then it is important to understand which factors will be of greater importance for diagnosis.

This is the reason to recognize the relevance of research in this area.

There are two ways to assess the significance of variables, direct and indirect [2].

A direct way to assess significantly variables is discussed in the report. It is important to note that the article discusses inertialess processes. For other types of processes, the allocation of significant variables may require additional actions.

The direct one is that it is necessary to find the vector of variables  $\vec{u} = (u_1, u_2, \dots, u_n)$ ,  $R(\vec{u}, \vec{c}_s) \rightarrow 0$ ,  $R(\vec{u}, \vec{c}_s)$  – average model error.

The task is to select  $m$  ( $m < n$ ) of the  $n$  variables. Several algorithms exist to accomplish this task.

## 2 Del algorithm

The researcher should exclude  $u_1$  and calculate  $R(u_2, \dots, u_n)$  the model constructed using variables  $u_2, \dots, u_n$  where  $R(u_2, \dots, u_n)$  is the average classification error. Then  $R(u_2, \dots, u_n)$  excluded in the same way and  $R(u_1, u_3, \dots, u_n), \dots, R(u_1, \dots, u_{n-1})$  are calculated. The variable with the least degree of significantly is by the rule:  $\max R(u_1, \dots, u_i, \dots, u_n) \rightarrow \min I(u_i)$ ,  $u_i$  is the variable with the least degree of significantly. This variable is excluded from the modelling process.  $n - 1$  variables remains after that. The algorithm must be repeated until there are  $m$  significant variables left.

The number of iterations (L) performed for the selection of significant variables is calculated by the formula (1) with this approach.

$$L = n + (n - 1) + (n - 2) + \dots + (m + 1) = \sum_{i=1}^{n-m} (n - i) \quad (1)$$

## 3 Algorithm Ad

According to this algorithm is necessary estimate  $R(u_i)$  for every  $u_i$ . The significant variable is selected by the rule:  $\min R(\cdot) \rightarrow \max I(\cdot)$ , where  $R$  is the error of variable ( $\cdot$ ) based model,  $I$  is the significant of variable. Thus the first significant variable will be found. Variables  $u_1, \dots, u_{i-1}, u_{i+1}, \dots, u_n$  are alternately added to the variable found. As a result, the researcher receives the appropriate sets of variables  $(u_i, u_1), \dots, (u_i, u_n)$  on the basis of which he calculates  $R(u_i, u_1), \dots, R(u_i, u_n)$ . The essential set of variables is selected by the above rule again. This operation must be repeated until a set of  $n$  variables is typed. The number of iterations done to select significant variables is equal to the number of iterations in the Del algorithm for this approach.

## 4 AdDel Algorithm

The considered algorithms of selection of essential variables are included in the class of the so-called "greedy" algorithms. The problem with such algorithms is that when

an optimal solution is obtained at each step, they do not provide a global optimum.

To partially eliminate the shortcomings of these algorithms, use the algorithm Ad-Del. According to this algorithm, the researcher first finds  $a_1$  the significant variables using the Ad algorithm. Next, the researcher using the algorithm Del excludes  $a_2(a_2 < a_1)$  variables from the selected ones. This algorithm is repeated until a set consisting of  $n$  variables is found.

It was proved that the presented algorithms for finding significant variables do not always lead to a satisfactory result [1].

## 5 Algorithm for finding significant variables based on the setting of the blur coefficient parameter

A new method for finding significant variables was proposed - an algorithm for evaluating significantly of variables based on the setting of the blur coefficient parameter.

Before using the algorithm for evaluating significantly of variables based on the setting of the blur coefficient parameter, it is necessary to center and normalize the elements of the vector  $u$  from the training set.

The nonparametric evaluation of the regression function from observations is (2) [3]:

$$x_s(\vec{u}) = \frac{\sum_{i=1}^s x_i \prod_{j=1}^n \Phi\left(\frac{u_j - u_{ji}}{c_{sj}}\right)}{\sum_{i=1}^s \prod_{j=1}^n \Phi\left(\frac{u_j - u_{ji}}{c_{sj}}\right)}, \quad (2)$$

$x_s(\vec{u})$  is a non-parametric function estimate  $x_s(\vec{u})$  in the point  $\vec{u}$ ;  $\Phi(\cdot)$  is bell-shaped function;  $s$  is the sample size of observations;  $\vec{c}_s$  is blur parameter vector.

The corresponding component of the vector  $\vec{c}_s$  is associated with each component of the vector  $\vec{u}$  as can be seen from (2). Further, based on the available training set, it is necessary to find the optimal  $\vec{c}_{s1}^*, \vec{c}_{s1}^* \dots \vec{c}_{sn}^*$  from the minimum condition (3):

$$\sigma(\vec{c}_s) = \sqrt{\frac{1}{s} \sum_{i=1}^s (x_s(\vec{u}_i, \vec{c}_s) - x_k)^2} \rightarrow \min, \quad (3)$$

and  $k \neq i$ .

After finding the vector  $\vec{c}_s^*$ , sorting vector elements  $c_s^*$  from lowest to highest to highest should be produced. The chain of inequalities will turn out this way, for example:  $|c_{s2}^*| < |c_{s9}^*| < |c_{s1}^*| < \dots < |c_{s4}^*| < |c_{s3}^*|$ . The component of the vector  $\vec{u}$  for which the corresponding element of the vector  $\vec{c}_s^*$  was the largest, is the candidate for the exception from the nonparametric estimation, as the least significant.

Computational experiment. The object under study has 10 input variables and 1 output variable. The impact of interference is 5%. The sample size of observations is 1000. Optimization is performed using the Neddler – Midd algorithm (a deformable polyhedron). The output variable is affected by two non-essential variables.

The object is described by the formula (4):

$$x(\vec{u}) = 3.62u_1 + 3.69u_2 + 3.79u_3 + 0.75u_4 + 3.73u_5) + \quad (4)$$

$$3.61u_6 + 3.79u_7 + 3.78u_8 + 0.62u_9 + 3.61u_{10}$$

Note that the formula describing the object is unknown to the researcher. This formula is used only for generating the sample.

The variables  $u_4$  and  $u_9$  are non-informative. Therefore, they should be excluded according to the rule formulated above.

The results of the calculations are presented below.

At the tact 1 was found so components of vector:

$\vec{c}_s = \{0.59; 0.55; 0.53; 1.26; 0.87; 0.56; 0.70; 0.69; 2.72; 0.51\}$ , modeling error = 5.5%.

At the tact 2 was found so components of vector:

$\vec{c}_s = \{0.83; 0.91; 0.43; 1.23; 0.90; 0.55; 0.53; 0.87; -; 0.75\}$ , modeling error = 5.0%.

At the tact 3 was found so components of vector:

$\vec{c}_s = \{0.70; 0.64; 0.58; -; 0.63; 0.69; 0.67; 0.65; -; 0.57\}$ , modeling error = 4.3%.

At the tact 4 was found so components of vector:

$\vec{c}_s = \{-; 0.76; 0.48; -; 0.69; 0.67; 0.59; 0.72; -; 0.58\}$ , modeling error = 4.3%.

The symbol "-" denotes the absence of the components of the vector  $u$  when describing the process under study. Non-essential variables were excluded in the first two tacts as shown in experiment. The elimination of the significant variable  $u_1$ , in the third tact, led to an increase in the simulation error. Thus, the above method of finding significant variables in the problems of identification seems encouraging. This is confirmed by the results of numerous computational experiments.

## 6 Conclusion

A method for evaluating the significantly of process variables has been proposed. The results of using this method, which prove its effectiveness, were presented. The complexity of the method lies in optimizing the vector of blur factors.

This variable selection method allows reducing the number of modelling errors and eliminating non-essential variables. Studies can be applied in medicine for the diagnosis of diseases or in little-studied technical processes.

*This work was supported by the Ministry of Education and Science of the Russian Federation in the framework of the Federal target program «Research and development on priority directions of development of the scientific-technological complex of Russia for 2014-2020» (agreement № 14.578.21.0247, unique ID project RFMEFI57817X0247)*

## References

- [1] Francuz A.G. (1964). Adaptation and training in automatic systems. *Izv. AN SSSR. Ser. Tekhn. Kibernetika.* Vol. 4, pp. 68-77.
- [2] Zagorujko N.G. (2013). *Cognitive data analysis*. Geo, Novosibirsk.
- [3] Tsypkin Ya.Z.(1968). *Adaptation and training in automatic systems*. Nauka, Moskva.

# IDENTIFICATION OF MINERALIZATION IN GEOCHEMISTRY BASED ON THE SPATIAL CURVATURE OF LOG-RATIOS

D. MIKŠOVÁ, C. RIESER, P. FILZMOSEK

*TU Wien*

*Vienna, AUSTRIA*

e-mail: dominika.miksova@tuwien.ac.at

## Abstract

Detecting subcropping mineralizations but also deeply buried mineralizations is one important goal in geochemical exploration. The identification of useful indicators for mineralization is a difficult task as mineralization might be influenced by many factors, such as location, investigated media, depth, etc. We propose a statistical method which indicates chemical elements related to mineralization. The identification is based on GAM models for the element concentrations across the spatial coordinate(s). The log-ratios of the GAM fits are taken to compute the curvature, where high curvature is supposed to indicate mineralization. By defining a measure for the quantification of high curvature, the log-ratios can be ranked, and elements can be identified that are indicative of the anomaly patterns.

**Keywords:** data science, spatial curvature, mineralization

## 1 Introduction

Identifying geochemical processes as mineralization is defined as the presence of higher concentrations of particular chemical elements compared to the background concentration. In other words, one would expect a rapid spatial change in the concentration on top of the mineralization, depending on the type and extent of the mineralization. Data coming from geochemistry are naturally compositional data, which are strictly non-negative values, forming parts of a whole. Therefore, using log-ratios seems to be an appropriate approach for constructing meaningful features that indicate mineralization. The important information is reflected in the ratios between the variables rather than in the absolute values. Relative information might lead to a proper understanding of the data.

The problem of identifying mineralization is of major interest in the project Up-Deep [2], where TU Wien is the project partner responsible for developing statistical methods. The exploration techniques might then even lead to suggestions considering ore discoveries. In this project several data sets are available, and for the development and illustration of the method we use a geochemical data set originating from Finland. The data have been sampled along a linear transect, and concentrations of various chemical elements have been measured in different sample media.

The presented method is based upon the behavior of the curvature of log-ratios. A big (absolute) value of the curvature corresponds to a rapid change of the log-ratio in the area of interest, and this may indicate mineralization. In order to suppress

the effect of measurement uncertainties, we use as a first step GAM models (see, e.g., [4], [5]) to smooth the absolute concentrations ensuring sufficient smoothness. Based on the curvature of the log-ratio of the smoothed concentrations, we then employ an unsupervised learning method leading to a hitlist of log-ratios most suitable for finding mineralization.

The proposed method has been tested on the mentioned real data set, where the mineralizations are even known, and the results seem to be reliable and promising.

## 2 Methodology

Smoothing splines, as developed by [3], are nowadays an indispensable tool in the modern days statistician's toolbox. They have been used with great success in a variety of areas and continue to this day to be a very active field of research.

Usually as a starting point one considers, for given data  $(x_1, y_1), \dots, (x_n, y_n)$ , the following non-parametric model with Gaussian i.i.d. errors,

$$y_i(x_i) = f(x_i) + \epsilon_i, \quad (1)$$

$\epsilon_i \sim \mathcal{N}(0, \sigma^2)$ , with  $i = 1, \dots, n$ . The presumably smooth linear predictor  $f$  is estimated by solving the problem given by

$$\max_f \sum_{i=1}^n \omega_i l(y_i | x_i; f) - \lambda \int (f''(x))^2 dx, \quad (2)$$

where  $f(x) = \mathbf{h}(x)^t \boldsymbol{\beta}$  for  $\mathbf{h}$  being a B-spline basis, and  $l$  stands for log-likelihood of the Gamma distribution, which is appropriate in this context since we deal with positive concentrations of elements. Note,  $\omega_i$  represent predefined weights enforcing the higher concentrations. The part  $\lambda \int (f''(x))^2 dx$  in (2) is important for controlling the smoothness via the number of basis functions. The parameter  $\lambda$  is the smoothing parameter controlling the trade-off between fitting the data closely and having a smooth model, and finally  $f''$  is the second derivative of  $f$ .

Using log-ratios of the obtained fitted values from the GAM model for a pair of variables, we calculate the absolute curvature, denoted as  $\kappa(x)$ . A big value of the curvature indicates clear peaks in the log-ratio.

A further step is to define a measure to rank the log-ratios according to their curvature. For this purpose, we define a threshold as mean plus standard deviation of the curvature, marked as  $\tau := \mu + \sigma$ . This allows to determine the number  $J$  of separated regions, obtained as half of number of points  $N$  crossing a threshold of its curvature, as well as the length  $I_j$  of the interval of each region. A measure for the quantification of high curvature of particular log-ratio can be then defined as

$$c = \frac{1}{J} \sum_{j=1}^J \max_{x \in I_j} (\kappa(x) - \mathcal{T})_+^2, \quad (3)$$

where  $\max_{x \in I_J} (\kappa(x) - \mathcal{T})_+^2$  is the highest distance of curvature subtracted from threshold for  $J$ th interval. The log-ratios of all pairs of variables can now be ranked according to this value  $c$ , and log-ratios on top of the hitlist indicate the locations of potential mineralization.

In the presentation we will show results from our data set, and also results from other geochemical data sets. All these results indicate that the method indeed is able to identify pathfinder elements for mineralization. Note that our proposed approach is unsupervised – thus it is not necessary to know the locations of the potential mineralization.

## References

- [1] Friedman J., Hastie T., Tibshirani R. (2001). *The Elements of Statistical Learning*. Springer Series in Statistics, New York.
- [2] KAVA Reference: 16329, UpDeep, Upscaling deep buried geochemical exploration techniques into European business (2017–2020).
- [3] Reinsch C.H. (1967). Smoothing by spline functions. *Numerische Mathematik*. Vol.10, pp. 177-183.
- [4] Wood S.N. (2017). *Generalized Additive Models: An Introduction With R*. Chapman and Hall/CRC, Boca Raton, USA.
- [5] Yee T.W. (2015). *Vector Generalized Linear and Additive Models: With an Implementation in R*. Springer, New York.

# FLUID LIMITS FOR THE WAITING TIME OF A CUSTOMER IN MULTIPHASE QUEUES

S. MINKEVIČIUS

*Institute of Data Science and Digital Technologies, Vilnius University*

*Vilnius, LITHUANIA*

e-mail: minkevicius.saulius@gmail.com

## Abstract

The object of this research in the queueing theory is the Functional-Strong-Law-of-Large-Numbers (FSLLN) under the conditions of heavy traffic in Multiphase Queueing Systems (MQS). FSLLN is known as a fluid limit or fluid approximation. In this paper, FSLLN is proved for the values of important probabilistic characteristics of MQS investigated as well for the total waiting time of a customer and the waiting time of a customer.

**Keywords:** data science, multiphase queueing system, fluid limit

## 1 Introduction

At first FSLLN is considered when investigating the total waiting time of a customer in MQS. The interest in the field of multiphase queueing systems was stimulated by the theoretical values of the results as well as by their possible applications in information and computing systems, communication networks, and automated technological processes. The methods of investigation of single phase queueing systems are considered in [2], [3], etc. The asymptotic analysis of models of queueing systems in heavy traffic is of special interest (see, for example, [4], [5], etc.). Papers [4], [5] and others described the beginning of the investigation of diffusion approximation to queueing networks. Intermediate models - multiphase queueing systems - are considered rarer due to serious technical difficulties (see, for example, book [3]).

We present some definitions in the theory of metric spaces (see, for example, [1]). Let  $C$  be a metric space consisting of real continuous functions in  $[0, 1]$  with a uniform metric

$$\rho(x, y) = \sup_{0 \leq t \leq 1} |x(t) - y(t)|, \quad x, y \in C.$$

Let  $D$  be a space of all real-valued right-continuous functions in  $[0, 1]$  having left limits and endowed with the Skorokhod topology induced by the metric  $d$  (under which  $D$  is complete and separable). Also, note that  $d(x, y) \leq \rho(x, y)$  for  $x, y \in D$ .

In this paper, we will constantly use an analog of the theorem on converging together (see, for example, [1]):

**Theorem 1.** *Let  $\varepsilon > 0$  and  $X_n, Y_n, X \in D$ . If  $P(\lim_{n \rightarrow \infty} d(X_n, X) > \varepsilon) = 0$  and  $P(\lim_{n \rightarrow \infty} d(X_n, Y) > \varepsilon) = 0$ , then  $P(\lim_{n \rightarrow \infty} d(Y_n, X) > \varepsilon) = 0$*

We investigate here a  $k$ -phase queue (i.e., after a customer has been served in the  $j$ -th phase of the queue, he goes to the  $j + 1$ -th phase of the queue, and, after the customer has been served in the  $k$ -th phase of the queue, he leaves the queue). Let us denote by  $t_n$  the time of arrival of the  $n$ -th customer; by  $S_n^{(j)}$  – the service time of the  $n$ -th customer in the  $j$ -th phase;  $z_n = t_{n+1} - t_n$ ; by  $\tau_{j,n+j}$  – departure of the  $n$ -th customer from the  $j$ -th phase of the queue,  $j = 1, 2, \dots, k$ . Let interarrival times ( $z_n$ ) to MQS and service times ( $S_n^{(j)}$ ) in each phase of the queue for  $j = 1, 2, \dots, k$  be mutually independent identically distributed random variables. Next, denote by  $W_n^{(j)}$  the waiting time of the  $n$ -th customer in the  $j$ -th phase of the queue; here  $Y_n^{(j)} = \sum_{i=1}^j W_n^{(i)}$  stands for the total waiting time of the  $n$ -th customer until the  $j$ -th phase of the queue,  $j = 1, 2, \dots, k$ . Suppose that the waiting time of the customer in the  $j$ -th phase of the queue is unlimited, the service principle of customers is "first come, first served". All random variables are defined on the common probability space  $(\Omega, \mathcal{F}, P)$ . Let us define  $\delta_{j,n+1} = S_{n-(j-1)}^{(j)} - z_n$ ,  $S_{j,n} = \sum_{i=1}^{n-1} \delta_{j,i}$ ,  $S_{0,n} \equiv 0$ ,  $\hat{S}_{j,n} = S_{j-1,n} - S_{j,n}$ ,  $x_{j,n} = \tau_{j,n} - t_n$ ,  $x_{0,n} \equiv 0$ ,  $\hat{x}_{j,n+1} = x_{j,n} - \delta_{j,n+1}$ ,  $\hat{x}_{0,n} \equiv 0$ ,  $S_n^{(0)} = z_n$ ,  $Dz_n = \hat{\sigma}_0^2$ ,  $DS_n^{(j)} = \hat{\sigma}_j^2$ ,  $j = 1, 2, \dots, k$ . Also, let us denote  $\beta_j = (\mathbf{E}S_n^{(j)})^{-1}$ ,  $\beta_0 = (\mathbf{E}z_n)^{-1}$ ,  $\alpha_j = \beta_0 - \beta_j$ ,  $\alpha_0 = 0$ ,  $\tilde{\sigma}_j^2 = \hat{\sigma}_0^2 + \hat{\sigma}_j^2$ ,  $\sigma_j^2 = \hat{\sigma}_j^2 + \hat{\sigma}_{j-1}^2$ ,  $j = 1, 2, \dots, k$ . Assume the following condition to be fulfilled  $\beta_0 > \beta_1 > \dots > \beta_k > 0$ . Then

$$\alpha_k > \alpha_{k-1} > \dots > \alpha_1 > 0. \quad (1)$$

## 2 Main results

First of all, we present one of the main results of the paper, a theorem on FSLLN for the total waiting time of a customer in MQS.

**Theorem 2.** *If conditions (2) are fulfilled, then*

$$\left( \frac{Y_n^{(1)}}{\tilde{\sigma}_1 \cdot n}; \frac{Y_n^{(2)}}{\tilde{\sigma}_2 \cdot n}; \dots; \frac{Y_n^{(k)}}{\tilde{\sigma}_k \cdot n} \right) \Rightarrow (\alpha_1; \alpha_2; \dots; \alpha_k)$$

*Proof.* Using the following equation presented in [6], p. 718, we derive

$$\hat{x}_{j-1,n} = \max_{0 \leq l \leq n} (\hat{x}_{j-1,l} - S_{j,l}) + S_{j,n}, \quad \hat{x}_{0,n} \equiv 0, \quad (2)$$

$j = 1, 2, \dots, k$  and  $n \geq k$ .

So, we obtain that, for each fixed  $\varepsilon > 0$ ,

$$\lim_{t \rightarrow \infty} P \left( \frac{|Y_n^{(j)} - \hat{x}_{j,n}|}{n} > \varepsilon \right) = 0, \quad j = 1, 2, \dots, k \text{ and } n \geq k. \quad (3)$$

Next, using (2) we prove that for each fixed  $\varepsilon > 0$

$$\lim_{t \rightarrow \infty} P \left( \frac{|\hat{x}_{j,n} - S_{j,n}|}{n} > \varepsilon \right) = 0, \quad j = 1, 2, \dots, k \text{ and } n \geq k. \quad (4)$$

Thus, we derive (see (3))

$$\hat{x}_{j,n} - S_{j,n} = \max_{0 \leq l \leq n} (x_{j-1,l} - S_{j,l}) \geq 0, \quad j = 1, 2, \dots, k, \quad n \geq k, \quad \hat{x}_{0,n} \equiv 0.$$

Then,

$$\hat{x}_{j,n} \geq S_{j,n}, \quad j = 1, 2, \dots, k. \quad (5)$$

Hence, (see again (3)) for  $j = 1, 2, \dots, k$

$$\begin{aligned} \hat{x}_{j,n} &\leq \max_{0 \leq l \leq n} (\hat{x}_{j-2,l} - \hat{S}_{j-1,l}) + \max_{0 \leq l \leq n} \hat{S}_{j,l} + S_{j,n} \leq \hat{x}_{j,n} + \max_{0 \leq l \leq n} \hat{S}_{j,l} - \hat{S}_{j,n} \\ &\leq \dots \leq \sum_{i=1}^j \{ \max_{0 \leq l \leq n} (\hat{S}_{i,l} - S_{i,n}) \} = \sum_{i=1}^j \{ \max_{0 \leq l \leq n} (\hat{S}_{i,l}) \} + S_{j,n} \\ &\leq \sum_{i=1}^k \{ \max_{0 \leq l \leq n} (\hat{S}_{i,l}) \} + S_{j,n}, \quad j = 1, 2, \dots, k, \quad n \geq k. \end{aligned} \quad (6)$$

Finally, according to (7), we have

$$\hat{x}_{j,n} \leq \sum_{i=1}^j \{ \max_{0 \leq l \leq n} (\hat{S}_{i,l}) \} + S_{j,n}, \quad j = 1, 2, \dots, k, \quad n \geq k. \quad (7)$$

Next, denote  $c_n = \sum_{i=1}^k \{ \max_{0 \leq l \leq n} (\hat{S}_{i,l}) \}$ . We assume that  $S_{j,0} \equiv 0$ ,  $j = 1, 2, \dots, k$ . So,  $c_n \geq 0$ . From (6) and (8) we get

$$|\hat{x}_{j,n} - S_{j,n}| \leq c_n, \quad j = 1, 2, \dots, k, \quad n \geq k. \quad (8)$$

Therefore, using (9) we achieve, for each fixed  $\varepsilon > 0$ , that

$$P \left( \frac{|\hat{x}_{j,n} - S_{j,n}|}{n} > \varepsilon \right) \leq P \left( \frac{c_n}{n} > \varepsilon \right) \leq \sum_{j=1}^k P \left( \frac{\max_{0 \leq l \leq n} \hat{S}_{j,l}}{n} > \frac{\varepsilon}{k} \right), \quad (9)$$

$j = 1, 2, \dots, k$ ,  $n \geq k$ .

Now we prove that, if conditions (2) are satisfied, then for each fixed  $\varepsilon > 0$ ,

$$\lim_{n \rightarrow \infty} P \left( \frac{\max_{0 \leq l \leq n} \hat{S}_{j,l}}{n} > \varepsilon \right) = 0, \quad j = 1, 2, \dots, k, \quad n \geq k. \quad (10)$$

$\frac{\max_{0 \leq l \leq n} \hat{S}_{j,l}}{n}$ ,  $j = 1, 2, \dots, k$ ,  $n \geq k$  have a negative drift (see conditions (2)). Thus, (11) follows from the strong law for  $\hat{S}_{j,n}$ ,  $n \geq 1$ ,  $j = 1, 2, \dots, k$  (see [4]). Consequently, (11) is proved. However, we obtain for each fixed  $\varepsilon > 0$ , that

$$\lim_{n \rightarrow \infty} P \left( \left| \frac{S_{j,n}}{n} - \alpha_j \right| > \varepsilon \right) = 0, \quad j = 1, 2, \dots, k, \quad n \geq k. \quad (11)$$

So, for each fixed  $\varepsilon > 0$

$$P\left(\left|\frac{Y_n^{(j)}}{n} - \alpha_j\right| > \varepsilon\right) \leq P\left(\left|\frac{Y_n^{(j)}}{n} - \frac{\hat{x}_{j,n}}{n}\right| > \frac{\varepsilon}{3}\right) + P\left(\left|\frac{\hat{x}_{j,n}}{n} - \frac{S_{j,n}}{n}\right| > \frac{\varepsilon}{3}\right) \\ + P\left(\left|\frac{S_{j,n}}{n} - \alpha_j\right| > \frac{\varepsilon}{3}\right), \quad j = 1, 2, \dots, k. \quad (12)$$

Using (10)-(12) we prove that, for each fixed  $\varepsilon > 0$ ,

$$\lim_{n \rightarrow \infty} P\left(\left|\frac{Y_n^{(j)}}{n} - \alpha_j\right| > \varepsilon\right) = 0, \quad j = 1, 2, \dots, k. \quad (13)$$

The proof is complete.  $\square$

Next, the theorem of FSLLN on the waiting time of a customer is proved similarly as Theorem 2.1.

**Theorem 3.** *If conditions (2) are fulfilled, then*

$$\left(\frac{W_n^{(1)}}{\sigma_1 \cdot n}; \frac{W_n^{(2)}}{\sigma_2 \cdot n}; \dots; \frac{W_n^{(k)}}{\sigma_1 \cdot n}\right) \Rightarrow (\alpha_1; \alpha_2 - \alpha_1; \dots; \alpha_k - \alpha_{k-1}).$$

*Proof.* Using (14), we get that

$$P\left(\left|\frac{|W_n^{(j)}}{n} - \alpha_j - \alpha_{j-1}\right| > \varepsilon\right) \leq P\left(\left|\frac{Y_n^{(j)}}{n} - \alpha_j\right| > \frac{\varepsilon}{2}\right) + \\ + P\left(\left|\frac{Y_n^{(j-1)}}{n} - \alpha_{j-1}\right| > \frac{\varepsilon}{2}\right), \quad j = 1, 2, \dots, k, \quad n \geq k. \quad (14)$$

Thus, a further proof of Theorem 2.2 is similar to that of Theorem 2.1. The proof is complete.  $\square$

## References

- [1] Billingsley P. (1968). *Convergence of probability measures*. Wiley, New York.
- [2] Borovkov A. (1972). *Stochastic processes in queueing theory*. Nauka, Moscow (in Russian).
- [3] Borovkov A. (1980). *Asymptotic methods in theory of queues*. Nauka, Moscow (in Russian).
- [4] Iglehart D.L., Whitt W. (1970a). Multiple channel queues in heavy traffic. I. *Advances in Applied Probability*, **2**, 150-177.
- [5] Iglehart D.L., Whitt W. (1970b). Multiple channel queues in heavy traffic. II. Sequences, networks and batches. *Advances in Applied Probability*, **2**, 355-369.
- [6] Minkevičius S. (1986). Weak convergence in multiphase queues. *Lietuvos Matematikos Rinkinys*, **26**, 717-722 (in Russian).

# INTEGRALS RELATED TO THE MULTIDIMENSIONAL-MATRIX GAUSSIAN DISTRIBUTION

V.S. MUKHA<sup>1</sup>, N.F. KAKO<sup>2</sup>

*Belarusian State University of Informatics and Radioelectronics  
Minsk, BELARUS*

e-mail: <sup>1</sup>mukha@bsuir.by, <sup>2</sup>kako.nancy@gmail.com

## Abstract

The three integrals, total probability formula and Bayes' formula connected with the multidimensional-matrix Gaussian distribution are presented. These results can be used in the various tasks of the statistical decision theory, particularly in the dual control theory.

**Keywords:** data science, multidimensional-matrix Gaussian distribution, dual control theory

## 1 Introduction

Integrals related to the probability distributions are the part of the statistical decision theory. One example of using of the statistical decision theory is the dual control [4], [2]. Some integrals related to the vector Gaussian distribution are developed in the paper [2]. More complicated problems in the framework of the statistical decision theory require generalizations of the results of the paper [2] in various directions. In this paper, such generalizations for the multidimensional-matrix Gaussian distribution are developed. The three integrals, total probability formula and Bayes' formula related to the multidimensional-matrix Gaussian distribution are presented.

## 2 The integrals related to the multidimensional-matrix Gaussian distribution

The random  $q$ -dimensional matrix  $\xi = (\xi_{\bar{i}_q})$ ,  $\bar{i}_q = (i_1, i_2, \dots, i_q)$ ,  $i_\alpha = 1, 2, \dots, m_\alpha$ ,  $\alpha = 1, 2, \dots, q$ , is distributed according to the normal or Gaussian law if its probability density is defined by the following expression [3]:

$$f(\xi) = \frac{1}{\sqrt{(2\pi)^{r_q} |d_\xi|}} \exp\left(-\frac{1}{2} {}^{0,2q} (d_\xi^{-1} (\xi - \nu_\xi)^2)\right), \quad \xi \in E^{r_q}, \quad (1)$$

where:  $\nu_\xi$ ,  $d_\xi$  are the parameters of the Gaussian multidimensional-matrix distribution, herewith  $\nu_\xi = (\nu_{\xi, \bar{i}_q})$ ,  $\bar{i}_q = (i_1, i_2, \dots, i_q)$ ,  $i_\alpha = 1, 2, \dots, m_\alpha$ ,  $\alpha = 1, 2, \dots, q$ , is the mathematical expectation of the random  $q$ -dimensional matrix  $\xi$  and  $d_\xi = (d_{\xi, \bar{i}_q; \bar{j}_q})$ ,  $\bar{i}_q = (i_1, i_2, \dots, i_q)$ ,  $\bar{j}_q = (j_1, j_2, \dots, j_q)$ ,  $i_\alpha, j_\alpha = 1, 2, \dots, m_\alpha$ ,  $\alpha = 1, 2, \dots, q$ , is the dispersion matrix of the random  $q$ -dimensional matrix  $\xi$ ;  $d_\xi^{-1}$  is the matrix  $(0, q)$ -inverse to

the matrix  $d_\xi$ ;  $|d_\xi|$  is the determinant of the matrix  $d_\xi$ ;  $r_q = \prod_{i=1}^q m_i$  is the number of the elements of the matrix  $\xi$ ;  $E^{r_q}$  is the  $r_q$ -dimensional Euclidean space;  $\bar{i}_q = (i_1, i_2, \dots, i_q)$ ,  $\bar{j}_q = (j_1, j_2, \dots, j_q)$  are the multi-indexes either of which contains  $q$  indexes.

The mathematical expectation of the random  $q$ -dimensional matrix  $\xi$  is the  $q$ -dimensional matrix with the same size as the matrix  $\xi$ . It is defined by the expression

$$\nu_\xi = E(\xi) = (E(\xi_{\bar{i}_q})) = (\nu_{\xi, \bar{i}_q}), \bar{i}_q = (i_1, i_2, \dots, i_q), i_\alpha = 1, 2, \dots, m_\alpha, \alpha = 1, 2, \dots, q,$$

so that  $\nu_{\xi, \bar{j}_q} = E(\xi_{\bar{j}_q})$ ,  $E$  is the symbol of the mathematical expectation [3].

The dispersion matrix  $d_\xi$  of the random  $q$ -dimensional matrix  $\xi$  is the  $2q$ -dimensional matrix defined by the expression

$$d_\xi = E((\xi - \nu_\xi)^2) = (E((\xi_{\bar{i}_q} - \nu_{\xi, \bar{i}_q})(\xi_{\bar{j}_q} - \nu_{\xi, \bar{j}_q}))) = (d_{\xi, \bar{i}_q, \bar{j}_q}),$$

$$\bar{i}_q = (i_1, i_2, \dots, i_q), \bar{j}_q = (j_1, j_2, \dots, j_q), i_\alpha, j_\alpha = 1, 2, \dots, m_\alpha, \alpha = 1, 2, \dots, q,$$

so that  $d_{\xi, \bar{i}_q, \bar{j}_q} = E((\xi_{\bar{i}_q} - \nu_{\xi, \bar{i}_q})(\xi_{\bar{j}_q} - \nu_{\xi, \bar{j}_q}))$ ,  $E$  is the symbol of the mathematical expectation, and  $(\xi - \nu_\xi)^2 = ((\xi_{\bar{i}_q} - \nu_{\xi, \bar{i}_q})(\xi_{\bar{j}_q} - \nu_{\xi, \bar{j}_q}))$  is the  $(0, 0)$ -rolled square of the matrix  $\xi$  [3].

The determinant  $|d_\xi|$  of the matrix  $d_\xi$  is defined as the determinant of the two-dimensional matrix  $\tilde{d}_{\xi, q, 0, q}$  that is the  $(q, 0, q)$ -associated matrix with the  $2q$ -dimensional matrix  $d_\xi$  [3].

We have proved the following equalities connected with the function (1):

$$\begin{aligned} \int_{E^{r_q}} \exp\left(-\frac{1}{2} {}^{0,2q}(A\xi^2) + {}^{0,q}(B\xi)\right) d\xi &= \sqrt{(2\pi)^{r_q} |A^{-1}|} \exp\left(\frac{1}{2} {}^{0,2q}(A^{-1}B^2)\right), \\ \int_{E^{r_q}} {}^{0,q}(C\xi) \exp\left(-\frac{1}{2} {}^{0,2q}(A\xi^2) + {}^{0,q}(B\xi)\right) d\xi &= \\ &= \sqrt{(2\pi)^{r_q} |A^{-1}|} \exp\left(\frac{1}{2} {}^{0,2q}(A^{-1}B^2)\right) {}^{0,q}(C {}^{0,q}(A^{-1}B)), \\ \int_{E^{r_q}} {}^{0,2q}(U\xi^2) \exp\left(-\frac{1}{2} {}^{0,2q}(A\xi^2) + {}^{0,q}(B\xi)\right) d\xi &= \\ &= \sqrt{(2\pi)^{r_q} |A^{-1}|} \exp\left(\frac{1}{2} {}^{0,2q}(A^{-1}B^2)\right) {}^{0,2q}(U(A^{-1} + {}^{0,0}({}^{0,q}(A^{-1}B))^2)), \end{aligned}$$

where:  $\xi = (\xi_{\bar{i}_q})$ ,  $\bar{i}_q = (i_1, i_2, \dots, i_q)$ , is the  $q$ -dimensional  $(m_1 \times m_2 \times \dots \times m_q)$ -matrix;  $r_q = \prod_{i=1}^q m_i$  is the number of the elements of the matrix  $\xi$ ;  $B = (b_{\bar{i}_q})$ ,  $C = (c_{\bar{i}_q})$  are the  $q$ -dimensional  $(m_1 \times m_2 \times \dots \times m_q)$ -matrices of the parameters;  $A = (a_{\bar{i}_q, \bar{j}_q})$ ,  $U = (u_{\bar{i}_q, \bar{j}_q})$  are the  $2q$ -dimensional  $(m_1 \times m_2 \times \dots \times m_q \times m_1 \times m_2 \times \dots \times m_q)$ -matrices of the parameters that are positive-definite and symmetric relative their  $q$ -multi-indexes  $\bar{i}_q$ ,  $\bar{j}_q$ ;  $A^{-1}$  is the matrix  $(0, q)$ -inverse to the matrix  $A$ ;  $|A^{-1}|$  is the determinant of the matrix  $A^{-1}$ .

### 3 The total probability formula for the multidimensional-matrix Gaussian distributions

**Theorem 1.** (the total probability formula for multidimensional-matrix Gaussian distributions). Let  $\xi$  is the  $q$ -dimensional  $(m_1 \times m_2 \times \dots \times m_q)$ -matrix,  $x$  is the  $p$ -dimensional  $(s_1 \times s_2 \times \dots \times s_p)$ -matrix,  $r_q = \prod_{i=1}^q m_i$  is the numbers of the elements of the matrix  $\xi$ ,  $r_p = \prod_{i=1}^p s_i$  is the numbers of the elements of the matrix  $x$ ,  $f(\xi)$  is the probability density of the matrix  $\xi$ ,  $f(x/\xi)$  is the conditional probability density of the matrix  $x$ ,  $R^{r_q}$  is the  $r_q$ -dimensional Euclidean space. If in the total probability formula

$$f(x) = \int_{E^{r_q}} f(x/\xi) f(\xi) d\xi \quad (2)$$

the probability density  $f(x/\xi)$  is represented in the form

$$f(x/\xi) = \frac{1}{\sqrt{(2\pi)^{r_p} |d_x|}} \exp \left( -\frac{1}{2} {}^{0,2q}(S\xi^2) + {}^{0,q}(V\xi) - \frac{1}{2} W \right),$$

and probability density  $f(\xi)$  is represented in the form

$$f(\xi) = \frac{1}{\sqrt{(2\pi)^{r_q} |d_\xi|}} \exp \left( -\frac{1}{2} {}^{0,2q}(d_\xi^{-1}\xi^2) + {}^{0,q}({}^{0,q}(d_\xi^{-1}\nu_\xi)\xi) - \frac{1}{2} {}^{0,2q}(d_\xi^{-1}\nu_\xi^2) \right),$$

then the probability density  $f(x)$  (2) (total probability formula) determine by the expression

$$f(x) = \frac{1}{\sqrt{(2\pi)^{r_p} |d_x| |d_\xi| |A|}} \exp \left( -\frac{1}{2} {}^{0,2q}(A^{-1}B^2) - \frac{1}{2} C \right),$$

where

$$A = d_\xi^{-1} + S,$$

$$B = {}^{0,q}(d_\xi^{-1}\nu_\xi) + V,$$

$$C = {}^{0,2q}(d_\xi^{-1}\nu_\xi^2) + W,$$

$|d_x|$ ,  $|d_\xi|$ ,  $|A|$  are the determinants of the corresponding multidimensional matrices, and  $A^{-1}$  is the matrix  $(0, q)$ -inverse to the matrix  $A$ .

We denote that the matrices  $d_\xi$ ,  $d_\xi^{-1}$ ,  $S$ ,  $A$ ,  $A^{-1}$  are  $2q$ -dimensional symmetrical relative their  $q$ -multi-indexes,  $\nu_\xi$ ,  $V$ ,  $B$  are  $q$ -dimensional,  $d_x$  is the  $2p$ -dimensional symmetrical relative its  $p$ -multi-indexes,  $W$ ,  $C$  are zero-dimensional (scalars).

## 4 The Bayes' formula for the multidimensional-matrix Gaussian distributions

**Theorem 2.** (*Bayes' formula for multidimensional-matrix Gaussian distributions*). Let  $\xi$  is the  $q$ -dimensional  $(m_1 \times m_2 \times \dots \times m_q)$ -matrix,  $x$  is the  $p$ -dimensional  $(s_1 \times s_2 \times \dots \times s_p)$ -matrix,  $r_q = \prod_{i=1}^q m_i$  is the numbers of the elements of the matrix  $\xi$ ,  $r_p = \prod_{i=1}^p s_i$  is the numbers of the elements of the matrix  $x$ ,  $f(\xi)$  is the probability density of the matrix  $\xi$ ,  $f(x/\xi)$  is the conditional probability density of the matrix  $x$ ,  $R^{r_q}$  is the  $r_q$ -dimensional Euclidean space. If in the Bayes' formula

$$f(\xi/x) = \frac{f(x/\xi)f(\xi)}{\int_{E^{r_q}} f(x/\xi)f(\xi)d\xi} \quad (3)$$

the probability density  $f(x/\xi)$  is represented in the form

$$f(x/\xi) = \frac{1}{\sqrt{(2\pi)^{r_p}|d_x|}} \exp\left(-\frac{1}{2} {}^{0,2q}(S\xi^2) + {}^{0,q}(V\xi) - \frac{1}{2} W\right),$$

and the probability density  $f(\xi)$  is represented in the form

$$f(\xi) = \frac{1}{\sqrt{(2\pi)^{r_q}|d_\xi|}} \exp\left(-\frac{1}{2} {}^{0,2q}(d_\xi^{-1}\xi^2) + {}^{0,q}({}^{0,q}(d_\xi^{-1}\nu_\xi)\xi) - \frac{1}{2} {}^{0,2q}(d_\xi^{-1}\nu_\xi^2)\right),$$

then the posteriori probability density  $f(\xi/x)$  of the random vector  $\xi$  determined by the Bayes' formula (3), has the following form

$$f(\xi/x) = \frac{1}{\sqrt{(2\pi)^{r_q}|A^{-1}|}} \exp\left(-\frac{1}{2} {}^{0,2q}\left(A\left(\xi - {}^{0,q}(A^{-1}B)\right)^2\right)\right),$$

where  $A = d_\xi^{-1} + S$ ,  $B = {}^{0,q}(d_\xi^{-1}\nu_\xi) + V$ .

## References

- [1] Mukha V.S., Sergeev E.V. (1976). Dual control of the regression objects. *Proceedings of the LETI*. Issue **202**, pp. 58-64. (In the Russian).
- [2] Mukha V.S. (1974). Calculation of integrals connected with the multivariate Gaussian distribution. *Proceedings of the LETI*. Issue **160**, pp. 27-30. (In the Russian).
- [3] Mukha V.S. (2004). *Analysis of multidimensional data*. Technoprint, Minsk, 368 p. (In the Russian).
- [4] Feldbaum A.A. (1965). *Optimal Control Systems*. Academic Press, New York and London, 452 p.

# OVERVIEW OF SPEECH SYNTHESIS USING LSTM NEURAL NETWORKS

G. NAVICKAS, G. KORVEL, J. BERNATAVIČIENĖ

*Vilnius University, Institute of Data Science and Digital Technologies*

*Vilnius, LITHUANIA*

e-mail: `gediminas.navickas@mii.vu.lt`

## Abstract

Currently, the most popular speech recognition systems are based on unit selection – decision tree algorithms. In literature, new speech synthesis methods based on Recurrent Neural Networks (RNN) and Long Short Term Memory (LSTM) are proposed. In this paper, an overview of speech synthesis and their realization called LSTM is given. Directions for further investigations are highlighted.

**Keywords:** data science, speech synthesis, neural network

## 1 Introduction

Much effort is given by scientists and engineers for human speech modelling at least for half of a century. The state-of-the-art methods applied to speech modelling are a concatenative synthesis, formant synthesis, articulatory synthesis, HMM-based synthesis, sine-wave synthesis. The literature review reveals that speech synthesis beyond the typically used techniques is extended towards exploring Deep Neural Networks (DNNs). Deep learning-based synthesizers use Artificial Neural Networks (ANNs), which are trained on recorded human speech data. One of the types of DNN is Recurrent Neural Network (RNN) architecture called Long Short Term Memory (LSTM) network [1]. These days RNN and LSTM networks are used by researchers for speech synthesis. They are used for English and several other languages and show good results. The goal of this research is the overview of these results. A comparison of the effectiveness of using LSTM networks for speech synthesis collected from the literature for different languages is given in this paper. Neural networks are not used for Lithuanian speech synthesis. Lithuanian speech synthesis systems are implemented using unit selection - decision tree algorithms that are one of the concatenative synthesis methods. In this paper, the possibilities of using LSTM networks for Lithuanian speech synthesis are discussed.

## 2 Recurrent Neural Networks and LSTM

Recently ANNs and especially DNNs are successfully used for solving machine speech problems [2], [3], [4]. RNN is a type of neural network designed for capturing information from sequential or time series data [2]. RNN is the repetition of simple units, which takes as an input the past, new input and produces a new prediction and connects to the future. Due to the fact that this network has short term memory, it does not work

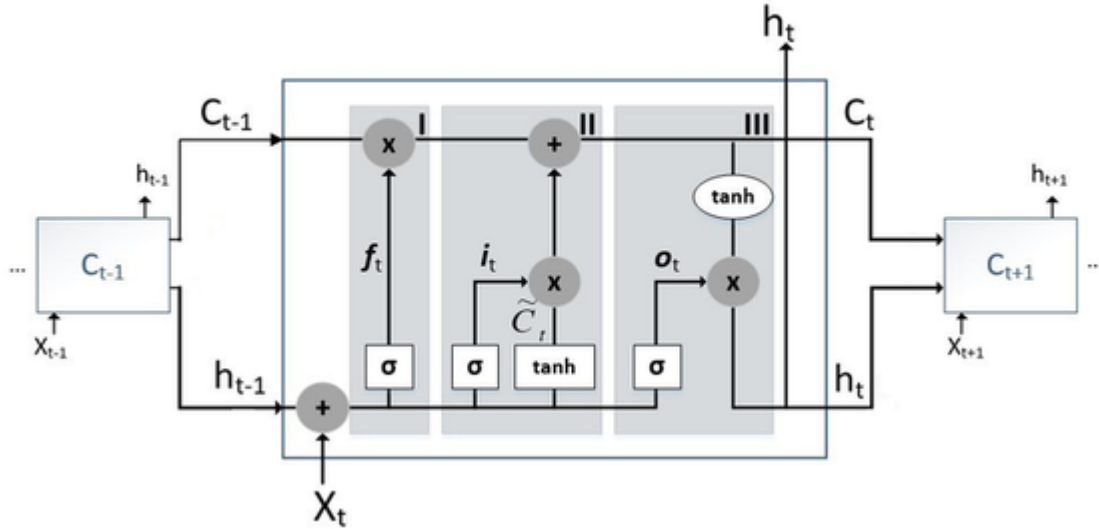


Figure 1: Concept Scheme of Vanilla LSTM network

well for longer sequences. This disadvantage is known as the Vanishing Gradient Problem [5]. One of the most common RNN architectures which solve this problem is the LSTM network. It is the type of RNN designed to work with long data sequences. It uses a mechanism called gates. Gates are used for learning which information to forget or add to the hidden state. LSTM network was presented in 1997 [1]. These days it is the most used RNN architecture. This architecture is also called Vanilla LSTM. The graphical representation of the LSTM network is given in Fig. 1.

The Vanilla LSTM network is RNN network where a repeating module contains three interacting gates. The module is called the LSTM cell. Denote state of LSTM cell of current time by  $C_t$ , input of current time by  $X_t$ , output of previous time by  $h_{t-1}$ . First gate of the LSTM cell is called forget gate  $f_t$ , and is given by:  $f_t = \sigma(W_f \cdot X_t + R_f \cdot h_{t-1} + b_f)$ , where  $W_f$  - input weights,  $R_f$  - recurrent weights,  $b_f$  - bias. It is a *sigmoid* layer with outputs between 0 and 1. It takes  $h_{t-1}$  and  $X_t$  and for each number in the cell state  $C_{t-1}$  returns a number where 0 means completely forget and 1 means completely keep the value.

Second gate is called input gate  $i_t$ . It decides what new information we will store in the cell state. At first, this *sigmoid* layer decides which values will be updated according to formula  $i_t = \sigma(W_i \cdot X_t + R_i \cdot h_{t-1} + b_i)$ , then *tanh* layer creates a vector of new candidate values  $\tilde{C}_t = \tanh(W_C \cdot X_t + R_C \cdot h_{t-1} + b_C)$ . At this step previously calculated values are combined by multiplying old state by  $f_t$  (forgetting the values), then  $i_t * \tilde{C}_t$  is added (the new candidate values scaled by how much we decided to update each state value)  $C_t = f_t * C_{t-1} + i_t * \tilde{C}_t$ .

Third gate is called output gate  $o_t$ . At first, *sigmoid* layer decides which parts of the cell state will go to output  $o_t = \sigma(W_o \cdot X_t + R_o \cdot h_{t-1} + b_o)$ . Before outputting the cell state is run through *tanh* layer and values are pushed between -1 and 1. Finally,

Table 1: Speech Synthesis using different DNN architectures

Reference	Network architecture	Data Set	Results
Salah Al-Radhi et al. [9], 2017	LSTM: 4 feed-forward hidden lower layers of 1024 hyperbolic tangent units each, followed by a single LSTM hidden top layer with 512 units.	US English female (SLT); speaker from the CMU-ARCTIC database.	Improved naturalness of the speech synthesized significantly over DNN baseline. Object of synthesis: sentences.
Wu and King [8], 2016	Simplified LSTM architecture (uses only the forget gate, has significantly fewer parameters than the vanilla LSTM). 256 units (e.g., LSTM blocks) in the recurrent layer.	A corpus from a British male speaker divided into three subsets: training, development and testing (2400, 70 and 72 utterances).	Forget gate can learn the temporal structure of speech; its activations have a high correspondence with phone boundaries. For this task, the forget gate is the only critical component of the LSTM; other components can be omitted with no reduction in naturalness. Object of synthesis: sentences.
Zen and Sak [10], 2015	Unidirectional LSTM RNNs with a recurrent output layer. The architecture of the LSTM: 1 forward-directed hidden LSTM layer with 256 memory blocks.	US English speech data from a female professional speaker. The training and development data sets consisted of 34 632 and 100 utterances, respectively.	LSTMs produced significantly better speech than DNNs. Object of synthesis: Utterances.
Zen et al. [7], 2016	LSTM-RNNs was 1 x 128-unit ReLU layer followed by 3 x 128-cell LSTM layers with 64 recurrent projection units with a linear recurrent output layer.	Speech data from a female professional speaker, 26 languages.	The LSTM-RNN-based SPSS systems with proposed optimizations surpassed the HMM-based SPSS systems in speed, latency, disk footprint, and naturalness on modern mobile devices. Experimental results also showed that the LSTM-RNN-based SPSS system with the optimizations could match the HMM-driven unit selection TTS systems in naturalness in 13 of 26 languages. Object of synthesis: Utterances.
Fan et al. [6], 2014	Hybrid system of DNN and BLSTM (Bidirectional LSTM): lower hidden layers with a feed-forward structure which is cascaded with upper hidden layers with a BLSTM.	Female, American English, native speaker, both phonetically and prosodically rich. The corpus consisted of 5,000 training utterances (around 5 hours) and 200 extra utterances were used for testing.	Hybrid system can outperform either the conventional, decision tree-based HMM, or a DNN TTS system, both objectively and subjectively. Object of synthesis: sentences.

*sigmoid* layer and *tanh* layer values are multiplied and we output only the parts which were decided  $h_t = o_t * \tanh(C_t)$ . More detailed LSTM description is presented in [11].

### 3 LSTM for Speech synthesis

LSTM is successfully used for different speech synthesis applications. In this section overview of using LSTM networks for speech synthesis is given. Overview is presented in Table 1.

Based on analysed references we can make the following conclusions: 1) it is difficult to compare the quality of synthesis among different experiments because they use different evaluation systems and criteria (both objective and subjective), 2) it is obvious that most of the experiments and LSTM applications are made for the English language.

## 4 Further investigations

Speech synthesis using LSTM networks according to recent articles outperforms statistical methods and traditional Neural Network implementations. In addition, it gives more flexibility for signal transformations, and most significant among them are: adding the emotions to synthesized speech and voice conversion. In further investigations, LSTM networks will be used for Lithuanian speech synthesis and later for adding intonation and emotions to synthesized speech.

## References

- [1] Hochreiter S., Schmidhuber J. (1997). Long short-term memory. *Neural computation*, Vol. **9(8)**, pp. 1735-1780.
- [2] Graves A., Mohamed A. R., Hinton G. (2013). Speech recognition with deep recurrent neural networks. *In 2013 IEEE international conference on acoustics, speech and signal processing*, pp. 6645-6649.
- [3] Korvel G., Treigys P., Tamulevicius G., Bernataviciene J., Kostek B. (2018). Analysis of 2D Feature Spaces for Deep Learning-Based Speech Recognition. *Journal of the Audio Engineering Society*, Vol. **66(12)**, pp. 1072-1081.
- [4] Tkachenko M., Yamshinin A., Lyubimov N., Kotov M., Nastasenko M. (2017). Speech Enhancement for Speaker Recognition Using Deep Recurrent Neural Networks. *In International Conference on Speech and Computer*, pp. 690-699.
- [5] Hochreiter S., et al. (2001). Gradient flow in recurrent nets: the difficulty of learning long-term dependencies.
- [6] Fan Y., Qian Y., Xie F. L., Soong F. K. (2014). TTS synthesis with bidirectional LSTM based recurrent neural networks. *In Fifteenth Annual Conference of the International Speech Communication Association*.
- [7] Zen H., Agiomyrgiannakis Y., Egberts N., Henderson F., Szczepaniak P. (2016). Fast, compact, and high quality LSTM-RNN based statistical parametric speech synthesizers for mobile devices. arXiv preprint arXiv:1606.06061.
- [8] Wu Z., King S. (2016). Investigating gated recurrent networks for speech synthesis. *In 2016 IEEE International Conference on Acoustics, Speech and Signal Processing (ICASSP)*, pp. 5140-5144.
- [9] Al-Radhi M. S., Csapó T. G., Németh G. (2017). Deep Recurrent Neural Networks in Speech Synthesis Using a Continuous Vocoder. *In International Conference on Speech and Computer*, Springer, Cham, pp. 282-291.

- [10] Zen H., Sak H. (2015). Unidirectional long short-term memory recurrent neural network with recurrent output layer for low-latency speech synthesis. *In 2015 IEEE International Conference on Acoustics, Speech and Signal Processing (ICASSP)*, pp. 4470-4474.
- [11] Wu Y., Yuan M., Dong S., Lin L., Liu Y. (2018). Remaining useful life estimation of engineered systems using vanilla LSTM neural networks. *Neurocomputing*, Vol. **275**, pp. 167-179.

# COMPARATIVE ANALYSIS OF OPTIMAL ALGORITHMS TREATMENT OF STATIONARY POISSON FLUXES

V.I. NIKITIONAK<sup>1</sup>, S.S. VETOKHIN<sup>2</sup>, A.M. BAKHAR<sup>1</sup>, E.V. TERESHKO<sup>2</sup>

<sup>1</sup>*Belarusian State University*

<sup>2</sup>*Belarusian State Technological University  
Minsk, BELARUS*

e-mail: <sup>1</sup>nikitsionakvi@mail.ru, <sup>2</sup>serega49@mail.ru

## Abstract

Two Poisson signals detectors that use the results of number of events' accounts accounting or time intervals between the neighboring events measurements are described. It is displayed the both detectors could provide the close detection characteristics.

**Keywords:** data science, Poisson flux, decision theory

## 1 Introduction

It is in common practice to describe different random fluxes by Poisson distribution. The most applicable they are for the tasks in applied physics, radio physics, radio and optical location where they are usually named as a simplest flux of homogenous events or a stationary (constant distribution parameter) Poisson flux (SPF). Depending the sample values being analyzed, the SPF could be represented by Poisson law of accounts' distribution or the exponential law of the distribution of intervals between neighboring events. It can be assumed that both ideas have the right to practical application. Indeed, the constant intensity  $\lambda$  of the SPF:

$$\lambda = \frac{m}{T}, \quad (1)$$

where  $m$  is the number of events that are detected within the interval  $T$ . So, it is possible to select  $m$  or  $T$  as a variable fixing the alternative that leads to obvious equivalency of two interpretations of the same random process. If we fix  $T$  counting of events will be terminated just at the moment  $T$  [1, 2]. In the opposite case the time measurement procedure should be stopped by  $m$  events registration [3].

The theory and practice of hypotheses testing use the first idea in common. Nevertheless, the second one was grounded enough for practical use [4]. Moreover, it was offered to explore the testing of a simple hypothesis about the parameter of an exponential distribution to build an optimized detector [5] for the goals of super weak optical signals at the level of single photons that are just the events of the Poisson process. Such a procedure is considered below.

## 2 Main part

It is known that the decision-making algorithm consists in comparing likelihood ration or its logarithm with a definite threshold. In this case, we have the series of intervals  $t_1, \dots, t_m$  between the consecutive events that are independent sample values belonging to the exponential distribution

$$f(t) = \lambda e^{-\lambda t}, \quad t > 0, \quad \lambda > 0. \quad (2)$$

To make a decision, a simple hypothesis  $H_0$  that  $\lambda = \lambda_0$  is verified, against a simple alternative  $H_1$ , that the distribution parameter  $\lambda = \lambda_1 > \lambda_0$ . The logarithm of the likelihood ratio in this case is [5]:

$$\ln l(t_1, \dots, t_m) = \sum_{k=1}^m \ln \frac{\lambda_1 e^{-\lambda_1 t_k}}{\lambda_0 e^{-\lambda_0 t_k}} = m \ln \frac{\lambda_1}{\lambda_0} - (\lambda_1 - \lambda_0) \sum_{k=1}^m t_k. \quad (3)$$

This gives us the rule of a decision selection

$$\ln \frac{\lambda_1}{\lambda_0} - (\lambda_1 - \lambda_0) \sum_{k=1}^m t_k \geq \ln c_0 \quad (4)$$

or

$$\frac{1}{m} \sum_{k=1}^m t_k \leq \frac{1}{\lambda_1 - \lambda_0} \left( \ln \frac{\lambda_1}{\lambda_0} - \frac{1}{m} \ln c_0 \right) = \frac{1}{\lambda_1 - \lambda_0} \ln \frac{\lambda_1}{\lambda_0 c_0^{1/m}} = c, \quad (5)$$

where  $c_0$  and  $c$  are the thresholds of decision making.

In accordance with (5) the rule of a decision selection for fixed in advance the size of the retrieval could be given in the next way: the hypothesis  $H_1$  is true ( $\lambda = \lambda_1$ ) if [6]

$$S_{0.1} = \frac{1}{m} \sum_{k=1}^m t_k \leq \frac{1}{\lambda_1 - \lambda_0} \ln \frac{\lambda_1}{\lambda_0 c_0^{1/m}} = c, \quad (6)$$

otherwise the hypothesis  $H_0$  is true ( $\lambda = \lambda_0$ ).

Thus, the algorithm for testing the hypothesis on the parameter of the exponential probability distribution is reduced to comparing the arithmetic mean of sample values with the decision rule threshold

$$c = \frac{1}{\lambda_1 - \lambda_0} \ln \frac{\lambda_1}{\lambda_0 c_0^{1/m}}, \quad (7)$$

where value of  $c$  should be stated in accordance with the selected quality criterion of the decision rule.

To find such criteria it is necessary to determine conditional probabilities of errors of the first and second kind (noting that the optimal decision-making algorithm (6) contains the sum of  $m$  independent exponentially distributed random variables). It is known that the sum of  $m$  independent exponentially distributed random variables has a  $\chi^2$  distribution with  $2m$  degrees of freedom [5] and its parameter  $\lambda = \frac{1}{2}$ . Because

$\lambda > 0$  and the hypothesis  $H_0(\lambda = \lambda_0)$  is under checking in contra the simple hypothesis  $H_1(\lambda = \lambda_1)$ , in the considering case the random variable  $2\lambda \sum_{k=1}^m t_k$  is  $\chi^2$  distributed with  $2m$  degrees of freedom. Thus, the errors of the first ( $\alpha$ ) and second ( $\beta$ ) kinds could be calculated as

$$\alpha = P\left\{2\lambda_0 \sum_{k=1}^m t_k \leq 2m\lambda_0 c | H_0\right\} = \frac{\Gamma(m, 2m\lambda_0 c)}{\Gamma(m)}, \quad (8)$$

$$\beta = P\left\{2\lambda_1 \sum_{k=1}^m t_k > 2m\lambda_1 c | H_1\right\} = 1 - \frac{\Gamma(m, 2m\lambda_1 c)}{\Gamma(m)}, \quad (9)$$

where  $\Gamma(m)$  is a gamma function and  $\Gamma(m, 2m\lambda_i c)$  is incomplete gamma function.

It is necessary to outline that the random variables  $\sum_{k=1}^m t_k$  and  $2\lambda \sum_{k=1}^m t_k$  are both distributed with the law  $\chi^2$  with  $2m$  degrees of freedom but they have different parameters. And arithmetic mean is not apparently presents in (8) and (9) that could make the practical realization more complete.

For the Neumann-Pierson criterion under defined error of the first kind (8) could be conversed in the threshold ( $\chi_{1-\alpha}^2$  is a percent point of  $\chi^2$  distribution with  $2m$  degrees of freedom)

$$c = \frac{1}{2m\lambda_0} \chi_{1-\alpha}^2. \quad (10)$$

The threshold (10) is independent from  $\lambda_1$ .

If  $m \gg 1$  and taking into account asymptotic normality of  $\chi^2$  distribution it is possible to represent the errors (8) and (9) in the view:

$$\alpha \approx \Phi(2\sqrt{2m\lambda_0 c} - 2\sqrt{m}), \quad (11)$$

$$\beta \approx 1 - \Phi(2\sqrt{2m\lambda_1 c} - 2\sqrt{m}), \quad (12)$$

where  $\Phi(x) = \frac{1}{\sqrt{2\pi}} \int_{-\infty}^x e^{-\frac{z^2}{2}} dz$  is the integral of probability.

The power of the decision selection rule:

$$D = 1 - \beta \approx \Phi(2\sqrt{2m\lambda_1 c} - 2\sqrt{m}). \quad (13)$$

The expression (12) gives us the threshold of decision that is dependent on the known  $m$  and  $\lambda_0$ :

$$c \approx \frac{(\sqrt{m} - \frac{1}{2}\Phi^{-1}(1 - \alpha))^2}{2m\lambda_0}. \quad (14)$$

Then, the power of the decision selection rule will be

$$D \approx \Phi(2\sqrt{m}(\sqrt{k_\lambda} - 1) - \sqrt{k_\lambda}\Phi^{-1}(1 - \alpha)), \quad (15)$$

where  $\Phi^{-1}$  is the reverse function of the integral of probability, and  $k_\lambda = \frac{\lambda_1}{\lambda_0}$  is the ratio of parameters of the exponential law meeting alternative of hypothesis (distance between the hypothesis and alternative).

It is possible to find the indicators of decision making quality in different way using the asymptotic normality of arithmetic mean distribution of samples. In this case the indicators could be calculated through the integrals of probability [6] (sinistral decision). In this way the error of the first kind is

$$\alpha = P(-\infty < S_{0.1} < c) = \Phi\left\{\frac{c - \frac{1}{\lambda_0}}{\frac{1}{\lambda_0\sqrt{m}}}\right\} = \Phi\{c\lambda_0\sqrt{m} - \sqrt{m}\}. \quad (16)$$

And the threshold of decision depends on the level of the given error of the first kind, number of events, and intensity  $\lambda_0$ :

$$c = \frac{1}{\lambda_0}\left(1 - \frac{1}{\sqrt{m}}\Phi^{-1}\{1 - \alpha\}\right). \quad (17)$$

In the same way the power of the rule of decision selection could be defined as

$$D = \Phi\{\sqrt{m}(k_\lambda - 1) - k_\lambda\Phi^{-1}\{1 - \alpha\}\}. \quad (18)$$

It is necessary to stress the difference in the  $D$  expressions for  $\chi^2$  distribution (15) and for Gauss distribution (18).

Now, let's consider the optimal algorithm of decision making when in the rule (4) dividing by  $m$  abandoned [3], and the rule (4) transmit in

$$m \ln \frac{\lambda_1}{\lambda_0} - (\lambda_1 - \lambda_0) \sum_{k=1}^m t_k \geq \ln c_0 \quad (19)$$

$$\sum_{k=1}^m t_k \leq \frac{m \ln \frac{\lambda_1}{\lambda_0} - \ln c_0}{\lambda_1 - \lambda_0} = c. \quad (20)$$

According (20) the rule for fixed sample volume  $m$  is the following: the alternative  $H_1$  is true and  $\lambda = \lambda_1$  if

$$S_{0.2} = \sum_{k=1}^m t_k \leq c, \quad (21)$$

and hypothesis  $H_0$  is true and  $\lambda = \lambda_0$  if the opposite to (21) inequity is held. Thus, the considering algorithm of hypothesis on the parameter of the exponential distribution checking reduces to comparison of the sum of the sample values with the threshold of the decision rule.

Because the sum of independent random variables that fluctuate in accordance with exponential law with parameter  $\lambda$  is subordinated to gamma distribution with the parameters  $\lambda$  and  $m$ , the error of the first kind for  $m \gg 1$  when gamma distribution runs to Gauss distribution and integrals of probability [6] are applicable (sinistral decision)

$$\alpha = P(-\infty < S_{0.2} < c) = \Phi\left\{\frac{c - \frac{m}{\lambda_0}}{\frac{\sqrt{m}}{\lambda_0}}\right\} = \Phi\left\{\frac{c\lambda_0}{\sqrt{m}} - \sqrt{m}\right\}. \quad (22)$$

The threshold of decision will be equal to

$$c = \frac{\sqrt{m}}{\lambda_0}(\sqrt{m} - \Phi^{-1}\{1 - \alpha\}) = \frac{\sqrt{m}}{\lambda_0}(1 - \frac{1}{\sqrt{m}}\Phi^{-1}\{1 - \alpha\}). \quad (23)$$

Its value depends on the stated error of the first kind, sample volume, and parameter of the exponential distribution. For these conditions power of decision is the same as it was earlier (18).

### 3 Conclusion

The comparative analysis of two algorithms displayed that for close enough hypothesis and alternative the difference of powers of the decision making rules are absent or acceptable. For big distance the difference could become inadmissible. At ones, under direct application of Gaussian approximation to gamma distribution the power of rule doesn't exceed one for Gaussian approximation of  $\chi^2$  distribution.

### References

- [1] Matveev I.N. (1984). *et al. Laser location*. Mashinostroenie, Moscow. 272 p. (In Russian)
- [2] Trishenkov M.A. (1992) *Photo receiving devices and Charge-Coupled Device. Detection of weak optical signals*. Radio and Connection, Moscow. 400 p. (In Russian)
- [3] Nikitionok V.I., Vetokhin S.S. (2015). On optimal detection of weak optical signals. *Proceedings of BSTU*. No. 6, pp. 88-91. (In Russian)
- [4] Nikitionok V.I. (2010). *Fast nonparametric algorithms of signal detection*. BSU, Minsk. 131 p. (In Russian)
- [5] Levin B.R. (1968). *Theoretical backgrounds of statistical radio technique*. Soviet Radio, Moscow. Ch. 2. 504 p. (In Russian)
- [6] Ventcel Y.S. (2001). *The theory of probability*. Higher School, Moscow. 575 p. (In Russian)

# USING CREDIT HISTORY DATA TO MONITOR FINANCIAL STABILITY OF THE BELARUSIAN ECONOMY

A.YU. NOVOPOLTSEV  
*Belarusian State University*  
*Minsk, BELARUS*  
e-mail: novopsacha@gmail.com

## Abstract

Data on credit histories may be very helpful for analysis of vulnerability of private sector to monitor financial stability in central banks. In National Bank of Belarus, there are credit register including vast database of credit histories of most companies and individuals on daily basis. These data may be used for estimating some useful risk measures such as Probabilities of Default (PD), Loss Given Default (LGD), etc. To construct aggregated measures from daily data special algorithms are developed. The event of default is defined according to Basel methodology. Some issues related to estimation of the risk measures are solved through analysis of the data distribution. The constructed measures can be further used for analytical reporting and statistical models estimation using supervised learning techniques.

**Keywords:** data science, credit history, financial stability

## 1 The issues and the data

This study is devoted to a problem of assessment financial vulnerability and credit risk of nonfinancial companies on microdata. Some research projects based on analysis of companies' balance sheets data have been already conducted in National Bank of Belarus [1, 2, 3]. In these projects some analytical and program tools to estimate companies financial risks were proposed. Statistical credit ratings were estimated on a set of financial ratios with cluster analysis algorithm. Unsupervised learning technique was applied because of the lack of real data on defaults. Estimated credit ratings showed close connections with various expert financial indicators used in financial stability reports. But still it was hard to validate the results of classification due to the lack of actual outcomes on defaults.

On contrarily, credit register data may be used to construct credit risk measures entirely based on data. For example, probability of default may be derived as a frequency of accounts with overdue payments that excess certain limit [4]. This approach implies a definition of default in sense of Basel framework [5]. According to the Basel definition, the event of default is defined as 90 days past due in the debt or interest payments by a contract.

The credit register database collects information on credit contracts and collaterals. All changes in contract information or in the history of payments, including debt outstanding, overdue payments (by debt and interest) and group risks for reserves accumulation, are promptly reported by banks to the credit register of National Bank.

All contracts are grouped by borrower (company or individual), type of credit contract, currency, bank that issued the credit.

## 2 Aggregated measures of default

Now describe the structure of credit register data and corresponding aggregated measures of credit risk which are proposed in this research.

Let  $J(i, t) \subset J$  be the set of active credit contracts of a company with number  $i$  on date  $t$  where  $J$  is a set of all credit contracts;  $I(t) \subset I$  be the set of companies that has at least one active contract on date  $t$  where  $I$  is all set of companies in a sample;  $a(i) \in \{1, \dots, A\}$  be the major economic activity of a company  $i$ ;  $b(j) \in \{1, \dots, B\}$  be a bank number that issued the credit with number  $j \in J$ .

There are indicators which changes are tracked by credit history:  $s_{jt}$  is debt outstanding,  $p_{jt}$  is payments overdue. Given the information of the date of last change for each indicator and corresponding amount, we may calculate a number of days overdue for credit contract  $j$  on date  $t$ , that is denoted as  $d_{jt}$ . Actually, it's defined as a number of days in the period when overdue payments  $p_{jt}$  were greater than zero from particular date in the past to the last observed date. Also, there are data specific to a credit contract which are currency, amount of credit issued  $s_j^0$ . Further on, let  $s_{jt}$  represent so called Exposure at Default (EAD) on a contract  $j$  on date  $t$ .

Now define the rule of default according to the Basel framework for a single contract  $j$ :

$$bd_{jt} = 1 \text{ if } d_{jt} > 90, \quad \text{else } bd_{jt} = 0 \quad (1)$$

which may be adopted for a company level by using a rule of maximum overdue days by all contracts of a company  $i$ , that is  $d_{it} = \max_{j \in J(i,t)} \{d_{jt}\}$ , and subsequent substitution to formula (1). Note that here the overdue days are calculated based on overdue payments as a whole including overdue payments by debt, interest and service. In fact, the rule (1) means that there is a technical default on a contract, because the actual default can only be a result of judicial procedure.

In reality, the rule (1) should be modified to take into account an amount of overdue payments: if they are too small or if the level of debt outstanding is too low, the positive decision about default according to the rule (1) should be rejected. We can formulize some additional conditions of default, for example, by requiring that overdue payments  $p_{jt}$  be greater than a particular amount or ratio of overdue payments  $p_{jt}$  to amount of credit  $s_j^0$  be greater than some threshold  $\eta$  that can be expressed by a formula  $p_{jt}/s_j^0 > \eta$ . For the thresholds expert assessments are usually taken, but we use data driven approach with an aim to get these from distribution of the actual data.

Using the indicators derived above we can calculate Probability of Default (PD) on date  $t$  on a level of a company  $i$ , an industry  $a$  or a bank  $b$  that are denoted as  $pd_{it}$ ,  $pd_{at}$ ,  $pd_{bt}$ , by calculating relative frequency of default occurrences on the data according to the rule like (1).

Another one important characteristic we address is Loss Given Default (LGD) that is, again, calculated on the data. For this task data on collaterals are used. Let  $K$

is a set of all available collateral contracts in database,  $K(i, t) \subset K$  is a set of active collaterals that belong to company  $i$  as a pledger on date  $t$ . For each collateral contract  $k$  on date  $t$  there are the following indicators:  $r_{kt}$  – requirements on the collateral,  $u_{kt}$  – the amount of requirement that were reimbursed,  $v_k^0$  – value of collateral. Again, let  $b(k) \in \{1, \dots, B\}$  be a bank that issued a collateral contract  $k$ . Then, using the data on collaterals we can calculate an approximation of LGD by applying a formula:

$$LGD_{kt} = 1 - u_{kt}/r_{kt}, \quad (2)$$

which provides LGD on a level of a contract. Also we may generalize (2) by calculating LGD on a level of a company, type of industry or a bank. Usually it's done on a level of industry that could be get by aggregating  $u_{kt}$ ,  $r_{kt}$  on a subset of active contracts  $K(a, t) \subset K$  on date  $t$  that belong to companies which are from industry  $a$ .

To generalize, let define aggregated indicators  $pd_{lt}$ ,  $lgd_{lt}$ ,  $ead_{lt}$ , which are PD, LGD, EAD on date  $t$  on a level of aggregation  $l \in \{i, a, b\}$ , that is on a level of a company, an industry of a bank. The proposed indicators may be used for calculating expected losses from credit portfolio that is expressed by a formula:

$$EL_t = \sum_l PD_{lt} \times LGD_{lt} \times EAD_{lt}, \quad (3)$$

where the sum is done on a set of different industries, types of credit contracts (products), or different types of borrowers.

### 3 Applications of proposed measures

Credit register data may be very promising for monitoring financial stability of real and banking sectors [6]. This research aims to apply data driven approach to uncover vulnerabilities in real time. Some traditional modeling techniques for panel and macroeconomic data may also be applied on proposed risk measures derived from the data.

We can propose further applications of the risk measures outlined above.

1. Analytical reporting for monitoring financial stability. It was the first intention to do this research. It's expected that the methodology of calculating risk measures developed on a test sample would be applied to the whole database to get timely reports on the current situation.

2. Mathematical modeling of credit risk measures. For example, a logit model to forecast probability of default of companies at one-year horizon could be developed based on classification variable derived from the data on overdue payments. The developed scoring model may help to validate scoring models of commercial banks.

## References

- [1] Malugin V., Hryn N., Novopoltsev A. (2014). Statistical analysis and econometric modelling of the creditworthiness of non-financial companies. *International Journal of Computational Economics and Econometrics*. Vol. 4 (1/2), pp. 130-147.

- [2] Malugin V.I., Novopoltsev A.Yu., Hryn N.V., Milevsky P.S. (2018). Statistical analysis of creditworthiness of real sector of Belarusian economy with microdata *Bank Bulletin. – A special issue "Bank Research"*. No. **14**. (in Russian)
- [3] Malugin V.I., Novopoltsev A.Yu., Hryn N.V., Pashkevich A.V. (2019). Development of model tools for assessing and predicting the credit risk of banks at the micro level *Bank Bulletin. – A special issue "Bank Research"*. No. **17**. (in Russian)
- [4] Antunes A., Gonçalves H., Prego P. (2016) Firm default probabilities revisited. *IFC-ECCBSO-CBRT Conference on "Uses of Central Balance Sheet Data Offices information"*. Ozdere–Izmir, Turkey, 26 September 2016. Mode of Access: <https://www.bis.org/ifc/publ/ifcb45i.pdf>. Date of Access: 11.03.2019.
- [5] Basel II: Revised international capital framework. Bank of International Settlements. Mode of Access: <https://www.bis.org/publ/bcbsca.htm>. Date of Access: 11.03.2019.
- [6] Navapoltseu A.Yu. (2018) Using microdata on companies to monitor financial stability. *The conference of young researchers in economics and finance*. Minsk, Belarus, December 22, 2018. Mode of access: <http://eng.beroc.by/conference/conference-of-young-researches/2018/>. Date of Access: 11.03.2019.

# USE OF VARIABILITY OF THE HEART RHYTHM FOR PREDICTING THE SUCCESS OF THE OPERATOR'S WORK WHEN USING HUMAN-MACHINE INTERFACES

V.A. PODOLSKIY<sup>1,a</sup>, YA.A. TUROVSKIY<sup>1,2,b</sup>, A.V. ALEKSEEV<sup>2,c</sup>,  
A.I. MIKHALSKII<sup>1,d</sup>

<sup>1</sup>*Trapeznikov Institute of Control Sciences, Russian Academy of Sciences*

<sup>2</sup>*Voronezh State University*

*Moscow, Voronezh, RUSSIA*

e-mail: <sup>a</sup>vladimirsk2007@yandex.ru, <sup>b</sup>yroslav\_turovsk@mail.ru,  
<sup>c</sup>a\_v\_alekseev@bk.ru, <sup>d</sup>ipuran@yandex.ru

## Abstract

In the modern world, systems providing human-machine interaction, human-machine interfaces, are becoming increasingly important. The quality of operation of such interfaces consists of two components: the quality of the performance of the hardware content and the efficiency of the algorithms for processing incoming information. This paper discusses the possibility to use operator heart rate variation signal to predict errors in the task completion.

**Keywords:** human-machine interface, machine learning, biomedical information

## 1 Introduction

The widespread introduction of human-machine interfaces (HMI) raised a number of tasks, for solution of which it is necessary to develop new approaches for analyzing and interpreting the information received from the operator. The range of application of modern HMIs extends from medical applications for disabled people support, to military systems, assisting the operator to perform tasks with high accuracy. Examples of HMI based on different principles are:

- non-invasive brain-computer interface;
- neuromuscular interface;
- oculographic interface.

Different interfaces use registration of various physical parameters of a human operator body: electroencephalograms, electromyograms, pupil movements, and form device control signals based on these signals. Different interfaces are subject to various disturbing signals and facts. While the influence of technical disturbances can be reduced using various filters, disturbances associated with the operator psycho-emotional state require implementation of special methods. This report discusses the possibility to use operator heart rate variation (HRV) signal to estimate the operator psycho-emotional state in terms of number of errors made during the task fulfilment. All experiments on moving object control were using oculographic interface.

## 2 Accounting for individual information in the oculo-graphic interface

The work uses data obtained from the oculo-graphic interface, based on contactless recording of eye movement. Tracking the eye movement, the device defines which objects the user's attention is focused on, the position of the pupil and analyzing the patterns of the movements, forms commands for performing the necessary actions by managing technical system. In motor disorders rehabilitation of various etiologies this can be a willed chair or exoskeleton. Management of interaction between a patient and electronic-mechanical devices, light switches and so on is possible using oculo-graphic interface as well.

The specific components that interfere with the operation of the oculo-graphic interface, in addition to technical reasons, are refocus operator's attention to outsider objects; involuntary eye movements. Psycho-emotional and psychosomatic state of the operator can be determined with the help of appropriate tests and instrumental observations at the stage of building the command generation algorithm. This information can be used to increase performance of the task completion. Psycho-emotional and psychosomatic state can be controlled on-line by recording HRV or other informative signal. In this case, performance of the task completion can be improved on-line.

## 3 Heart rate variability as a predictor of the management process performance

HRV is an important indicator characterizing the psychosomatic state of a person. In this work, we study dependence between changes in HRV and number of errors made by the operator.

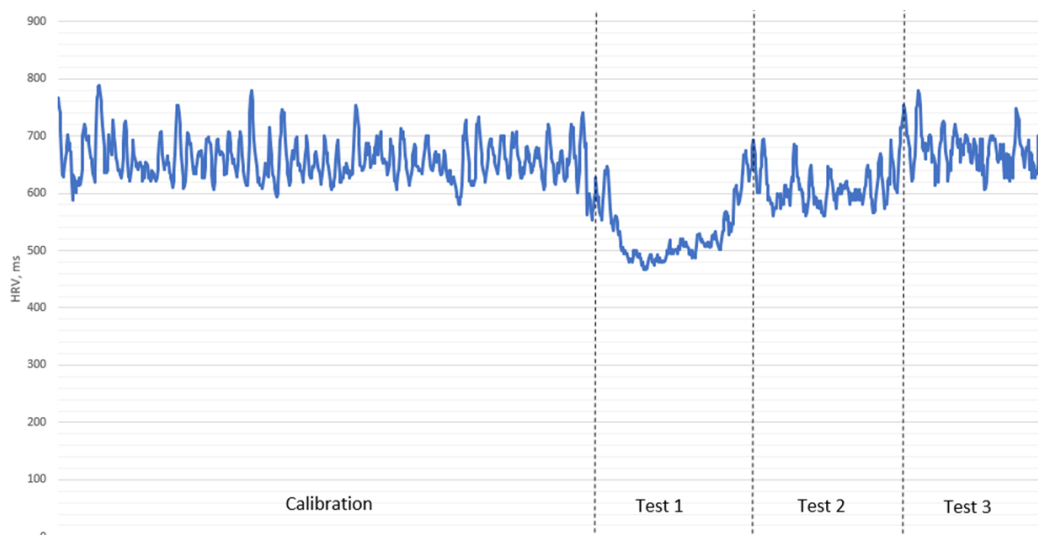


Figure 1: Individual HRV in dynamics

Figure 1 shows an individual HRV signal, recorded for operator who made one mistake in Test 1. Calibration is the period when an operator gives different commands without managing the system to tune oculographic interface. One can see a pronounced increase in the heart rate during the Test 1 stage with the gradual stabilization of HRV at the control level in the 3rd test. We assume that the HRV can serve as a predictor of successful performance of the task.

An important property of ergatic systems is human adaptation during the interaction of the software and hardware of the complex and the operator [3-4]. To identify the individual characteristics of the user's HRV during the task completion, an analysis of time periods was performed during which non-stationary signal fragments were detected. This indicator was chosen primarily as reflecting the total time during which active changes in the HRV parameters. The data were preprocessed to zero mean and unit variance. The spectral power of HRV in low frequency (LF) and in high frequency (HF) ranges were estimated for different stages of the task completion. These estimations were made separately for three groups of operators: operators, who made no mistakes during the task completion – “without errors” group (11 operators), operators, who made one mistakes during the task completion – “1 error” group (10 operators), and operators, who made two mistakes during the task completion – “2 errors” group (10 operators). The results are presented in Figure 2.

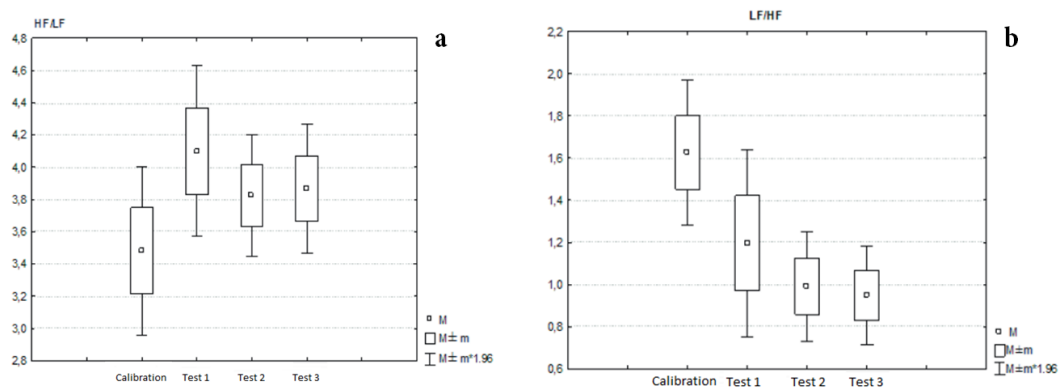


Figure 2: a) Dynamics of the SPM HF / LF ratio during the experiments; b) The ratio of the lifetime of nonstationary fragments of HRV in the LF and HF ranges

From Figure 2b one can see, that the ratio of LF / HF for the time period during which non-stationary fragments of HRV were identified for the 2nd and 3rd tests was significantly lower than in the control, not differing for the first test. In other words, from arrival to arrival, there was an increase in activity in the HF range relative to the initial state.

The dynamics of the ratio of the total power of non-stationary fragments reflected reduction in their severity in the LF components during the first test. For the subsequent tests, no differences were identified, which reflects the restoration of the balance between HF and LF regulatory influences.

Figure 3 shows mean HRV values with 95 % confidence intervals at different stages for operators in three groups mentioned above. One can observe that at calibration

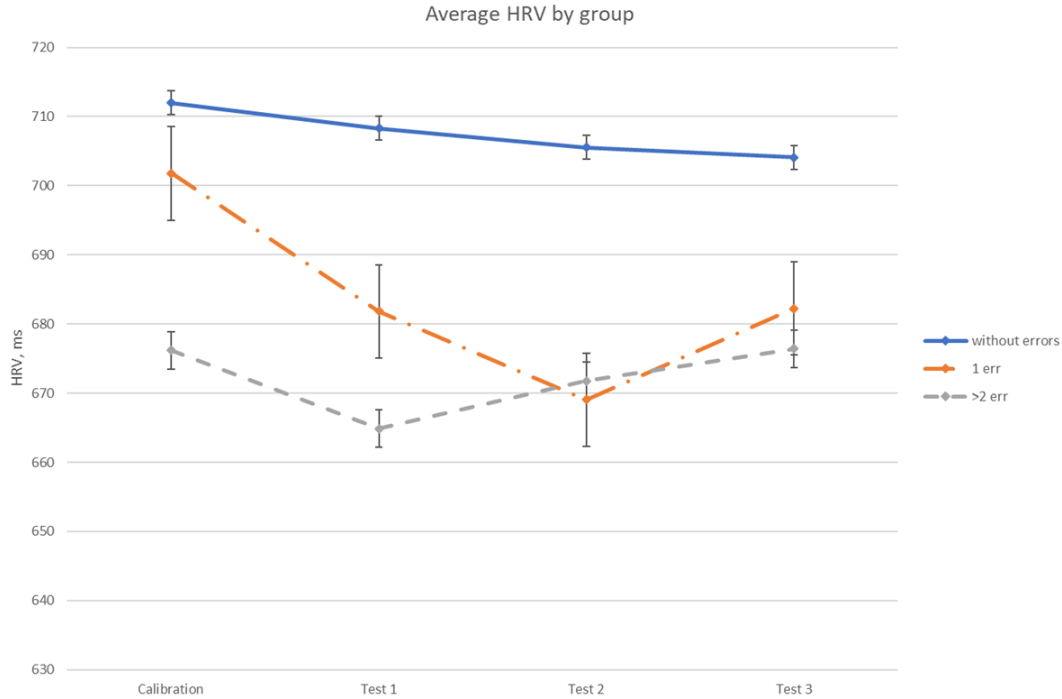


Figure 3: The results of the analysis of the average HRV for three groups of operators

stage all three groups have different mean HRV values. For the group “without mistakes”, the mean HRV is stable with small in group variance. This group does not demonstrate significant deviations in psycho-emotional state. In group “1 error” one can observe sharp decrease in the mean values of HRV at test stages. Decrease in HRV values characterizes the acceleration of the heart rate. The third “more than 2 errors” confirms the trend found in the group “1 error”.

In the last two groups HRV variance is higher than in group “without mistakes” as at calibration stage, so at three test stages. Because in all groups number of subjects are practical the same, the difference in variance justifies the links between mean VHR value and quality of the task performance.

## 4 Conclusion

In the report, we discuss the possibility to use HRV signal to predict individual performance of the task completion. Data obtained in experiments with oculographic interface were used. Stratification of operators by the number of errors made during the task completion helped to demonstrate links existing between VHR value and quality of the task performance.

According to the analysis of the parameters of HRV, a decrease in the power spectral density in the HF and LF ranges is shown. The ratio of LF / HF for the time period during which non-stationary fragments of HRV were identified for the 2nd and 3rd tests was significantly lower than in the control, not different for Test 1.

This work was supported by the Russian Foundation for Basic Research (No. 19-07-01037).

## References

- [1] Vapnik V., Vashist A. (2009). A new learning paradigm: learning using privileged information. *Neural Networks*. Vol. 22, pp. 544–557.
- [2] Turovskiy Ya.A., Kurgalin S.D., Alekseev A.V. (2017). Analysis of the movement of human eyes in the management of self-propelled chassis using the system videookulograficheskogo interface. *SENSOR SYSTEMS*. Vol. 31, No. 1, pp. 51–58.
- [3] Turovskiy Ya. A., Alekseev A. V. (2017). Heart rate variability of users by the video-coluographic interface in the process of learning to control a self-propelled chassis. *VORONEZH STATE UNIVERSITY. SERIES: CHEMISTRY. BIOLOGY. PHARMACY*. No. 1, pp. 118–124.
- [4] Turovskiy Ya. A., Borzunov S. V., Vakhtin A. A. (2017). An additional channel for assessing the emotional dynamics of a person when working with neuro-computer and oculographic interfaces. *BIOMEDICAL RADIO ELECTRONICS*. No. 6, pp. 17–26.

# PROBLEMS OF THE FORMATION OF THE SYSTEM OF ENVIRONMENTAL-ECONOMIC ACCOUNTING

E.A. POLESHCHUK

*National Statistical Committee of the Republic of Belarus*

*Minsk, BELARUS*

e-mail: [ekapoleshchuk@gmail.com](mailto:ekapoleshchuk@gmail.com)

## Abstract

The paper identifies the necessary steps in preparing for the formation of a satellite environmental-economic account: an analysis of the legislative, methodological, institutional and information bases. The possible difficulties in their analysis are considered.

**Keywords:** data science, environmental-economic accounting, system formation

## 1 Introduction

Today it is not enough just to analyze economic, social, or environmental systems separately. Requirements for the results of analysis at the macro level are complex. In turn, the introduction of the system of environmental-economic accounting (SEEA) contributes to the expansion of the system of national accounts through additional satellite accounts of environmental topics, that is, the integration of economic and environmental data.

For the formation of a satellite account of SEEA, it is necessary to analyze the legislative, methodological, institutional and information bases.

## 2 Legislative base

The significance of the legislative base cannot be denied. Despite the fact that scientists can work autonomously, the presence of legislative justification, the consolidation of the need for such information greatly facilitate public understanding of the work done by the researcher.

The legislative base is considered in accordance with the thematic area within which it is planned to form a satellite account. And if, for example, the Law on Environmental Protection and the Law on State Statistics are present in the practice of most countries of the world, then legislative consolidation of SEEA accounts is mainly observed only in developed countries. In particular, the Regulation of the European Parliament and the European Council No. 691/2011 “On European environmental economic accounts” works in the EU countries. In Belarus, the issue of forming the SEEA is reflected in the Strategy for the development of state statistics for the period up to 2022, which can be attributed to the first step on the way to legislative fixation of this issue.

### 3 Methodological base

The methodological base is the international statistical standard “System of Environmental-Economic Accounting Central Framework” (SEEA-CF), other methodological guidelines developed by international organizations in various areas of SEEA (for example, water resources, energy resources, agriculture, forestry and fisheries), scientific researches.

Based on SEEA-CF [1], as the leading document in the field of environmental-economic accounting, it should be noted that all the accounts of SEEA are divided into three groups: physical flow accounts; asset accounts; environmental activity accounts and related flows. Each of the groups represents the issues of accounting for natural resources and related activities.

Physical flow accounts characterize the involvement of a resource from the environment in economic activity. In SEEA-CF, accounts of flows of energy resources, water resources and flows of materials are defined. Methodologically, physical flow accounts can be called quite affordable, since their coverage is limited to involvement in the economy. Therefore, with the quality of primary accounting and proper consolidation of information, their formation, both in physical and in monetary terms, is more possible.

Asset accounts are formed for the purpose of accounting for a specific natural asset, for example, mineral and energy resources, land resources, timber resources and other biological resources. The fundamental difference in this case is the physical and monetary estimate for the components of the account. The asset account in physical terms is wider than the asset account in monetary terms for the amount of an asset that is not involved in commercial activities.

Environmental activity accounts and related flows capture issues of environmental expenditure analysis, environmental taxes and subsidies, environmental goods and services. This group of accounts is the “most economic”. They are formed only in monetary terms. Their formation is directly linked to the system of national accounts and depends largely on the quality of the SNA.

Despite the fact that SEEA-CF is the leading methodological document in the formation of environmental-economic accounts, it does not limit the actions of researchers to the question of its expansion and the addition of new satellite accounts. For example, FAO as the leading international organization in the area of agriculture, forestry and fisheries along with recommendations from SEEA-CF offers to produce an account of the physical flows of timber resources [2].

At the same time, if you intend to introduce SEEA accounts into the national practice and use a structure that is comparable at the international level, special care must be taken, since the structure of the accounts in different methodological sources may be different. In particular, compared to SEEA-CF, FAO offers a slightly different structure for the forest land asset account and the timber asset account. Also, as compared with SEEA-CF, significant differences are observed in the structure of the water resource flow account recommended in the additional UN guideline SEEA-water [3].

A very urgent task in the present development of SEEA methodology is ecosystem

accounts. Ecosystem accounts, unlike SEEA-CF accounts, characterize environmental services and assets from the point of the ecosystem as a whole, rather than a specific resource.

The definition of ecosystem services offered in the guideline on experimental ecosystem accounting [4] is rather diffuse and characterizes them as a contribution to the benefits used by society in economic and other activities.

In 2013, the first full version of the Common International Classification of Ecosystem Services (CICES), according to which all ecosystem services fall into three categories: provisioning services, regulating services and cultural services. On the example of forest resource accounts, provisioning services include picking berries and preying of game animals; regulating services – carbon dioxide absorption, protection from wind erosion; cultural services – the use of forest for aesthetic, research and educational purposes.

Ecosystem assets include complex systems consisting of both biotic and abiotic components.

In contrast to the accounts formed in accordance with SEEA-CF, methodological approaches to the formation of ecosystem accounts are not currently accepted as a standard because of the multiplicity of existing approaches to their formation and are additionally called experimental.

Analyzing the methodological base recommended at the international level, in order to further introduce into national practice, it is also necessary to keep in mind its nationalization, that is, harmonization with the current national legislation and accounting system. It is also recommended to develop and approve national methodology for the formation of accounts in order to make the future results of the construction of natural economic accounts transparent.

## 4 Institutional base

The analysis of the institutional base is another important step in exploring the possibilities of forming the SEEA. Depending on the complexity and thematic direction, a SEEA account may be formed within the same department or interdepartmental working group.

The issue of interdepartmental communications never loses its relevance, despite its clarity. Thematic interdepartmental working group is a convenient platform for discussing methodological features, searching for new information sources, as well as verifying results. In addition, it facilitates the exchange of experience and the dissemination of the results obtained. At the same time, world practice shows that the national statistical office acts as a coordinator of work in such interdepartmental working groups. Despite the wide involvement of various organizations in the process of forming the SEEA, this area in most countries is still considered to be more statistical and requires precise coordination and popularization. In Belarus today there are two interdepartmental working groups for the SEEA implementation in national practice: on water accounts and on forest accounts.

## 5 Information base

Finally, the analysis of the information base is the final stage on the way of preparing for the formation of the SEEA. Information sources for the formation of a satellite account can be thematic official statistical information or administrative data (data from departmental reporting, monitoring, inventories, registries, etc.). When analyzing the existing information base, it is necessary to determine the sources of information, their quality and assess the coverage of the account with the obtained data.

Sources and quality of data are determined through interdepartmental interaction using approximate account layouts. Questions of inadequate data quality often emerge during the formatting of accounts, with the result that measures should be taken to improve them. At the same time, the duration of the data quality improvement process can reach up to a year or more.

After determining the sources, the coverage of the account by data is estimated. As a result of such an assessment, the researcher understands where additional evaluation is required to form an account in full. Methods for additional evaluation are determined by the researcher independently and subsequently reflected in the national methodological paper.

When assessing the information base, it is necessary to note the particular difficulty in compiling of physical flow and asset accounts in monetary terms. Most often, the valuation of natural resources in monetary terms requires additional research and, accordingly, the involvement of additional sources of information.

The considered stages of the analysis of the legislative, methodological, institutional and information bases are a necessary basic work in the formation of the satellite account of the system of environmental-economic accounting. They are universal for any SEEA satellite account. The only difference is the time spent studying them, depending on the complexity of the area being researched.

## References

- [1] System of Environmental-Economic Accounting 2012. Central Framework (2014). United Nations, New York.
- [2] System of Environmental-Economic Accounting for Agriculture, Forestry and Fisheries: SEEA AFF White Cover version (pending final UNSD editorial clearance) (2016). FAO, UNSD.
- [3] System of Environmental-Economic Accounting for Water (2012). United Nations, New York.
- [4] System of Environmental Economic Accounting 2012 – Experimental Ecosystem Accounting (2014). United Nations, New York.

# STRUCTURAL DISTRIBUTION ESTIMATION

M. RADAVIČIUS

*Institute of Data Science and Digital Technologies, Vilnius University  
Vilnius, LITHUANIA*

e-mail: marijus.radavicius@mii.vu.lt

## Abstract

We consider count data models in case of sparse asymptotics. Then a consistent estimator of expected frequencies does not exist for any reasonable metric. Moreover, a plug-in estimator of a structural distribution is also inconsistent. Assuming that some auxiliary information on expected frequencies is available, we construct a consistent estimator of the structural distribution.

**Keywords:** data science, count data, sparse asymptotics, structural distribution

## 1 Introduction

Let us consider multinomial sampling scheme

$$Y = (y_1, \dots, y_n), \quad Y \sim \text{Multinomial}_n(N, P), \quad P = (p_1, \dots, p_n) \in \mathcal{P}_n,$$

in case of sparse asymptotics:  $n \rightarrow \infty$  and  $P = P(n)$ ,  $N = N(n) \rightarrow \infty$ . Here  $\mathcal{P}_n$  is the unit  $(n - 1)$ -simplex of probabilities  $P$ .

Define *occupation statistics*:

$$V_m = V_m(n) := \sum_{j=1}^n I\{y_j = m\}, \quad m = 0, 1, \dots$$

Here and in the sequel  $I\{\cdot\}$  denotes an indicator function.

The statistic  $V_0$  ( $V^+ = V^+(n) := n - V_0$ ) is the number of *empty* (respectively, *nonempty*) boxes. In linguistics,  $V^+$  ( $V_0$ ) is the size of a vocabulary or the number of observed (respectively, unseen) word tokens.

Khmaladze (1988) [3] proposed specifications of sparse asymptotics by introducing sampling schemes with *large number of rare events* (LNRE). They are based on the following assumptions:

$$\lim_{n \rightarrow \infty} \frac{V_1(n)}{N(n)} > 0, \tag{1}$$

and

$$V^+(n) \rightarrow \infty, \quad \lim_{n \rightarrow \infty} \frac{V_1(n)}{V^+(n)} > 0. \tag{2}$$

**Definition.** ([3]) A multinomial sampling scheme with *large number of rare events* is said to be in zone (d1) (in zone (d2)) iff condition (1) (respectively, (2)) is satisfied.

Note that (1) implies (2).

In the LNRE model, a consistent estimator of probabilities  $P$  does not exist for any reasonable metric [3, 5, 2]. Sometimes much less informative characteristics of a model are sufficient for inference. For instance, if the cell numbering is irrelevant for statistical inference, all useful information about the cell probabilities  $P$  is contained in their *structural distribution*. Structural distributions are widely used in quantitative linguistics.

Klaassen and Mnatsakanov (2000) [5] (cf. Khmaladze & Chitashvili (1989) [4] and Khmaladze (1988) [3]) defined the (empirical) *structural distribution*  $G_n$  as the empirical distribution of the "observations"  $N \cdot P$ ,

$$G_n := \frac{1}{n} \sum_{j=1}^n \delta_{Np_j}. \quad (3)$$

Here and in what follows  $\delta_a$  denotes the Dirac measure centered at  $a$ . The basic assumption is that  $G_n$  (weakly) converges to a probability distribution  $G$ , i.e.,

$$G_n \xrightarrow{w} G, \quad n \rightarrow \infty. \quad (4)$$

From the viewpoint of latent distribution modelling it is more natural to reserve the term *structural distribution* for the distribution  $G$  and to refer to  $G_n$  as the *empirical structural distribution*.

Khmaladze (1988) [3] has noticed that a natural (plug-in) estimator of  $G$  obtained by substituting  $y_j$  for  $Np_j$  ( $j = 1, \dots, n$ ) in (3) generally yields an inconsistent estimator. Consistent estimators of structural distribution based on grouping or kernel smoothing are provided by Klaassen & Mnatsakanov (2000) [5], van Es & Koliou (2003) [2] and van Es et al. (2003) [1] under some smoothness conditions, see assumption (U) below.

**Assumption (U)** ([5, 1]). The sequence of distribution densities

$$f_n(u) := \sum_{j=1}^n np_j I \left\{ \frac{j-1}{n} < u \leq \frac{j}{n} \right\}, \quad u \in (0, 1],$$

uniformly converges to a continuous distribution density  $f$ .

Assumption (U) implies an approximate *latent distribution model* with a latent variable  $Z \sim f$ :

$$p_j = \int_{(j-1)/n}^{j/n} f(u) du + \frac{\epsilon_j}{n}, \quad j = 1, \dots, n, \quad \max_j |\epsilon_j| \rightarrow 0.$$

In this study, we deal with a *Poisson sampling* scheme and construct a consistent estimator of structural distribution of expected cell frequencies.

## 2 Consistent estimator of structural distribution

We consider a *sparse hierarchical Poisson (independent) sampling* scheme with a sparsity rate  $\tau$ :

$$[Y|\Lambda] \sim \text{Poisson}_n(\tau\Lambda), \quad \Lambda \sim Q^{(n)}, \quad \Lambda := (\lambda_1, \dots, \lambda_n),$$

where  $\tau = \tau(n)$  is a positive convergent sequence, the components of  $Y = (y_1, \dots, y_n)$  are mutually independent, the conditional distribution of  $y_j$  given  $\Lambda$  is  $\text{Poisson}(\tau\lambda_j)$ , the components of  $\Lambda$  are also mutually independent with  $\lambda_j \sim Q_j = Q_j^{(n)}$ ,  $j = 1, \dots, n$ , and  $\lambda_+ = n$ ,  $\lambda_+ := \sum_{j=1}^n \lambda_j$ .

Actually, we are interested in cases where  $\tau \rightarrow 0$ .

The Poisson sampling scheme is used as an approximation to that of multinomial under the LNRE condition and can be obtained from the latter via Poissonization [2, 1]. When  $Q_j \equiv Q_1$  and  $\tau \equiv 1$ , we get a Poisson mixture model considered in [6].

Similarly as in (3), define

$$G_n := \frac{1}{n} \sum_{j=1}^n Q_j^{(n)} \tag{5}$$

and assume (4), i.e.,  $G_n \xrightarrow{\mathcal{W}} G$  as  $n \rightarrow \infty$ . The limiting distribution  $G$  is called *structural distribution for the rate  $\tau$* . In the Poisson mixture model,  $G = Q_1$ .

**Assumptions (P):**

(P1) Let  $\{\Delta_\ell, \ell = 1, \dots, L\}$  be a partition of  $\{1, \dots, n\}$  such that  $n_\ell := |\Delta_\ell| \geq n_{\min}$  where  $\tau n_{\min} \rightarrow \infty$ , and, for some parametric family of distributions  $F(\Theta) := \{F_\theta, \theta \in \Theta\}$ ,  $\Theta \subset \mathbb{R}^k$ ,

$$\frac{1}{n_\ell} \sum_{j \in \Delta_\ell} Q_j^{(n)} \xrightarrow{\mathcal{W}} F_{\theta_\ell}, \quad \theta_\ell \in \Theta,$$

as  $n \rightarrow \infty$  uniformly with respect to  $\ell = 1, \dots, L$ . Moreover, for some distribution  $H$  on  $\Theta$ ,

$$\frac{1}{n} \sum_{\ell=1}^L n_\ell \delta_{\theta_\ell} \xrightarrow{\mathcal{W}} H.$$

(P2) Distributions of the family  $F(\Theta)$  are uniformly continuous in weak topology with respect to  $\theta \in \Theta$ .

(P3) There exist estimators  $\hat{\theta}_\ell := \hat{\theta}(y(j), j \in \Delta_\ell)$  of  $\theta_\ell$  which are consistent uniformly over  $\{\ell = 1, \dots, L\}$ , i.e., for each  $\varepsilon > 0$ ,

$$\left\{ \max_{\ell=1, \dots, L} |\hat{\theta}_\ell - \theta_\ell| > \varepsilon \right\} \rightarrow 0.$$

**Proposition.** Let assumptions (P) be satisfied. Then

$$\hat{G} := \sum_{\ell=1}^L F_{\hat{\theta}_\ell} \frac{n_\ell}{n}$$

is a consistent estimator of the structural distribution (for the sparsity rate  $\tau$ )

$$G = \int_{\Theta} F_{\theta} H(d\theta).$$

**Examples:**

(a) *Latent distribution model* (cf. assumption (U)):

$$\lambda_j = n \int_{(j-1)/n}^{j/n} f(u) du, \quad Q_j^{(n)} = \delta_{\lambda_j}, \quad j = 1, \dots, n,$$

$f$  is a continuous probability density on  $[0, 1]$ .

(b) *Poisson regression and related models.* When  $\lambda_j = \mu(j/n)$ ,  $j = 1, \dots, n$ , where  $\mu(u), u \in [0, 1]$ , is a nonnegative continuous function that integrate to 1, we have a nonparametric Poisson regression model with the explanatory variable  $x, x_j := j/n, j = 1, \dots, n$ . For a negative binomial regression model, one can take  $Q_j \sim \text{Gamma}(\mu(j/n), \nu)$ , where  $\text{Gamma}(a, \nu)$  denotes *Gamma* distribution with the mean  $a$  and the shape parameter  $\nu$ , and  $\mu(u), u \in [0, 1]$ , is the same as above (cf. [8]).

In [7], zero inflated negative binomial regression model and the empirical Bayes method have been applied to estimate the structural distribution of words in Lithuanian texts.

## References

- [1] van Es B., Klaassen C.A.J., Mnatsakanov R.M. (2003). Estimating the structural distribution function of cell probabilities. *Austrian Journal of Statistics*, **32**, pp. 85-98.
- [2] van Es B., Kolios S. (2002). Estimating a structural distribution function by grouping. *Mathematics ArXiv* PR/0203080.
- [3] Khmaladze E.V. (1988). The statistical analysis of a large number of rare events. *CWI Report MS-R8804*.
- [4] Khmaladze E.V., Chitshvili R.J. (1989). The statistical analysis of a large number of rare events the related problem. *Proc. Tbilisi Mathematical Institute* **92**, pp. 196-245.
- [5] Klaassen C.A.J., Mnatsakanov R.M. (2000). Consistent estimation of the structural distribution function, *Scand. J. Statist.*, **27** (4), pp. 733-746.
- [6] Mnatsakanov R.M., Klaassen C.A.J. (2003). Estimation of the mixing distribution in the Poisson mixture models: uncensored and censored samples. In: *Proceedings of Hawaii International Conference on Statistics and Related Fields*, Honolulu, Hawaii, June 4-8, 2003, pp. 1-18.  
Available at <http://www.hicstatistics.org/2003StatsProceedings>.

- [7] Piaseckienė K., Radavičius M. (2014). Empirical Bayes estimators of structural distribution of words in Lithuanian texts. *Nonlinear Analysis: Modelling and Control*, **19** (4), pp. 611-625.
- [8] Radavičius M., Samusenko P. (2012). Nonparametric testing for sparse nominal data. *Nonlinear analysis: modeling and control*. **17** (4), pp. 489-501.

# DRIFT PARAMETER ESTIMATION IN GAUSSIAN REGRESSION MODEL BY CONTINUOUS AND DISCRETE OBSERVATIONS

K. RALCHENKO

*Taras Shevchenko National University of Kyiv*

*Kyiv, UKRAINE*

e-mail: k.ralchenko@gmail.com

## Abstract

The paper is devoted to the maximum likelihood estimation in the regression model of the form  $X_t = \theta G(t) + B_t$ , where  $B$  is a Gaussian process,  $G(t)$  is a known function, and  $\theta$  is an unknown drift parameter. The estimation techniques for the cases of discrete-time and continuous-time observations are presented. As examples, models with fractional Brownian motion, sub-fractional Brownian motion and two independent fractional Brownian motions are considered.

**Keywords:** data science, fractional Brownian motion, discrete observation, continuous observation, drift parameter

## 1 Introduction

We study rather general model where the noise is represented by a centered Gaussian process  $B = \{B_t, t \geq 0\}$  with known covariance function,  $B_0 = 0$ . We assume that all finite-dimensional distributions of the process  $\{B_t, t > 0\}$  are multivariate normal distributions with nonsingular covariance matrices. We observe the process  $X_t$  with a drift  $\theta G(t)$ , that is,

$$X_t = \theta G(t) + B_t,$$

where  $G(t) = \int_0^t g(s) ds$ , and  $g \in L_1[0, t]$  for any  $t > 0$ . The paper is devoted to the estimation of the parameter  $\theta$  by observations of the process  $X$ . We consider the MLEs for discrete and continuous schemes of observations. The results presented are based on the recent articles [2, 1, 3].

## 2 Drift parameter estimator for discrete-time observations

Let the process  $X$  be observed at the points  $0 < t_1 < t_2 < \dots < t_N$ . Then the vector of increments

$$\Delta X^{(N)} = (X_{t_1}, X_{t_2} - X_{t_1}, \dots, X_{t_N} - X_{t_{N-1}})^\top$$

is a one-to-one function of the observations. We assume in this section that the inequality  $G(t_k) \neq 0$  holds at least for one  $k$ .

Evidently, vector  $\Delta X^{(N)}$  has Gaussian distribution  $\mathcal{N}(\theta \Delta G^{(N)}, \Gamma^{(N)})$ , where

$$\Delta G^{(N)} = (G(t_1), G(t_2) - G(t_1), \dots, G(t_N) - G(t_{N-1}))^\top.$$

Let  $\Gamma^{(N)}$  be the covariance matrix of the vector

$$\Delta B^{(N)} = (B_{t_1}, B_{t_2} - B_{t_1}, \dots, B_{t_N} - B_{t_{N-1}})^\top.$$

Then one can take the density of the distribution of the vector  $\Delta X^{(N)}$  for a given  $\theta$  w.r.t. the density for  $\theta = 0$  as a likelihood function:

$$L^{(N)}(\theta) = \exp \left\{ \theta (\Delta G^{(N)})^\top (\Gamma^{(N)})^{-1} \Delta X^{(N)} - \frac{\theta^2}{2} (\Delta G^{(N)})^\top (\Gamma^{(N)})^{-1} \Delta G^{(N)} \right\}.$$

The corresponding MLE equals

$$\hat{\theta}^{(N)} = \frac{(\Delta G^{(N)})^\top (\Gamma^{(N)})^{-1} \Delta X^{(N)}}{(\Delta G^{(N)})^\top (\Gamma^{(N)})^{-1} \Delta G^{(N)}}. \quad (1)$$

**Theorem 1** (Properties of the discrete-time MLE [2]). *1. The estimator  $\hat{\theta}^{(N)}$  is unbiased and normally distributed:*

$$\hat{\theta}^{(N)} - \theta \simeq \mathcal{N} \left( 0, \frac{1}{(\Delta G^{(N)})^\top (\Gamma^{(N)})^{-1} \Delta G^{(N)}} \right).$$

*2. Assume that*

$$\frac{\text{var } B_t}{G^2(t)} \rightarrow 0, \quad \text{as } t \rightarrow \infty.$$

*If  $t_N \rightarrow \infty$ , as  $N \rightarrow \infty$ , then the discrete-time MLE  $\hat{\theta}^{(N)}$  converges to  $\theta$  as  $N \rightarrow \infty$  almost surely and in  $L_2(\Omega)$ .*

### 3 Drift parameter estimator for continuous-time observations

In this section we suppose that the process  $X_t$  is observed on the whole interval  $[0, T]$ . We investigate MLE for the parameter  $\theta$  based on these observations.

Let  $\langle f, g \rangle = \int_0^T f(t)g(t) dt$ . Assume that the function  $G$  and the process  $B$  satisfy the following conditions.

(A) There exists a linear self-adjoint operator  $\Gamma = \Gamma_T : L_2[0, T] \rightarrow L_2[0, T]$  such that

$$\text{cov}(X_s, X_t) = \mathbb{E} B_s B_t = \int_0^t \Gamma_T \mathbf{1}_{[0, s]}(u) du = \langle \Gamma_T \mathbf{1}_{[0, s]}, \mathbf{1}_{[0, t]} \rangle.$$

(B) The drift function  $G$  is not identically zero, and in its representation  $G(t) = \int_0^t g(s) ds$  the function  $g \in L_2[0, T]$ .

(C) There exists a function  $h_T \in L_2[0, T]$  such that  $g = \Gamma h_T$ .

Note that under assumption (A) the covariance between integrals of deterministic functions  $f \in L_2[0, T]$  and  $g \in L_2[0, T]$  w. r. t. the process  $B$  equals

$$\mathbb{E} \int_0^T f(s) dB_s \int_0^T g(t) dB_t = \langle \Gamma_T f, g \rangle.$$

**Theorem 2** (Likelihood function and continuous-time MLE [2]). *Let  $T$  be fixed, assumptions (A)–(C) hold. Then one can choose*

$$L(\theta) = \exp \left\{ \theta \int_0^T h_T(s) dX_s - \frac{\theta^2}{2} \int_0^T g(s) h_T(s) ds \right\} \quad (2)$$

as a likelihood function. The MLE equals

$$\hat{\theta}_T = \frac{\int_0^T h_T(s) dX_s}{\int_0^T g(s) h_T(s) ds}. \quad (3)$$

It is unbiased and normally distributed:

$$\hat{\theta}_T - \theta \simeq \mathcal{N} \left( 0, \frac{1}{\int_0^T g(s) h_T(s) ds} \right).$$

**Theorem 3** (Consistency of the continuous-time MLE [2]). *Assume that assumptions (A)–(C) hold for all  $T > 0$ . If, additionally,*

$$\liminf_{t \rightarrow \infty} \frac{\text{var } B_t}{G(t)^2} = 0,$$

then the estimator  $\hat{\theta}_T$  converges to  $\theta$  as  $T \rightarrow \infty$  almost surely and in mean square.

**Theorem 4** (Relations between discrete and continuous MLEs [2]). *Let the assumptions of Theorem 2 hold. Construct the estimator  $\hat{\theta}^{(N)}$  from (1) by observations  $X_{T_k/N}$ ,  $k = 1, \dots, N$ . Then*

- 1) the estimator  $\hat{\theta}^{(N)}$  converges to  $\hat{\theta}_T$  in mean square, as  $N \rightarrow \infty$ ,
- 2) the estimator  $\hat{\theta}^{(2^n)}$  converges to  $\hat{\theta}_T$  almost surely, as  $n \rightarrow \infty$ .

## 4 Application of estimators to various models

### 4.1 Model with fractional Brownian motion and power drift

Let  $0 < H < 1$  and  $\alpha > -1$ . Consider the process

$$X_t = \theta t^{\alpha+1} + B_t^H, \quad (4)$$

where  $B^H = \{B_t^H, t \geq 0\}$  is a fractional Brownian motion with Hurst index  $H$ .

**Theorem 5** ([2]). *If  $\alpha > H - 1$ , the model (4) satisfies the conditions of Theorem 1. The estimator  $\hat{\theta}^{(N)}$  in the model (4) is  $L_2$ -consistent and strongly consistent (provided that  $\lim_{N \rightarrow \infty} t_N = +\infty$ ). If  $\alpha > 2H - \frac{3}{2}$ , the conditions of Theorems 2, 3 and 4, are satisfied. The estimator  $\hat{\theta}_T$  is  $L_2$ -consistent and strongly consistent. For fixed  $T$ , it can be approximated by discrete-sample estimator in mean-square sense.*

## 4.2 Model with subfractional Brownian motion

Let  $0 < H < 1$ . Consider the model

$$X_t = \theta t + \tilde{B}_t^H, \quad (5)$$

where  $\tilde{B}^H = \{\tilde{B}_t^H, t \geq 0\}$  is a subfractional Brownian motion with Hurst parameter  $H$ .

**Theorem 6** ([2]). *Under condition  $t_N \rightarrow +\infty$  as  $N \rightarrow \infty$ , the estimator  $\hat{\theta}^{(N)}$  in the model (5) is  $L_2$ -consistent and strongly consistent. If  $\frac{1}{2} < H < \frac{3}{4}$ , then the random process  $\tilde{B}^H$  satisfies Theorems 2, 3, and 4. As the result,  $L(\theta)$  defined in (2) is the likelihood function in the model (5), and  $\hat{\theta}_T$  defined in (3) is the MLE. The estimator is  $L_2$ -consistent and strongly consistent. For fixed  $T$ , it can be approximated by discrete-sample estimator in mean-square sense.*

## 4.3 The model with two independent fractional Brownian motions

Consider the following model:

$$X_t = \theta t + B_t^{H_1} + B_t^{H_2}, \quad (6)$$

where  $B^{H_1}$  and  $B^{H_2}$  are two independent fractional Brownian motion with Hurst indices  $H_1, H_2 \in (\frac{1}{2}, 1)$ .

**Theorem 7** ([3]). *Under condition  $t_N \rightarrow +\infty$  as  $N \rightarrow \infty$ , the estimator  $\hat{\theta}^{(N)}$  in the model (6) is  $L_2$ -consistent and strongly consistent. If  $H_1 \in (1/2, 3/4]$  and  $H_2 \in (H_1, 1)$ , then the random process  $B^{H_1} + B^{H_2}$  satisfies Theorems 2, 3, and 4. As the result,  $L(\theta)$  defined in (2) is the likelihood function in the model (6), and  $\hat{\theta}_T$  is the maximum likelihood estimator. The estimator is  $L_2$ -consistent and strongly consistent. For fixed  $T$ , it can be approximated by discrete-sample estimator in mean-square sense.*

## References

- [1] Mishura Y., Ralchenko K., Shklyar S. (2017). Maximum likelihood drift estimation for Gaussian process with stationary increments. *Austrian J. Statist.* Vol. **46**, pp. 67–78.
- [2] Mishura Y., Ralchenko K., Shklyar S. (2018). Maximum likelihood estimation for Gaussian process with nonlinear drift. *Nonlinear Anal. Model. Control.* Vol. 23(1), pp. 120 - 140, - 2018 *Nonlinear Anal. Model. Control* Vol. **23**, pp. 120–140.
- [3] Mishura Y., Ralchenko K., Shklyar S. (2018). Parameter estimation for Gaussian processes with application to the model with two independent fractional Brownian motions. In *Stochastic Processes and Applications, SPAS2017, Vol. 271 of Springer Proceedings in Mathematics & Statistics*, Springer, Cham, pp. 123–146.

# A SET OF ASYMPTOTICALLY INDEPENDENT STATISTICS OF POLYNOMIAL FREQUENCIES CONTAINING THE PEARSON STATISTIC

M.P. SAVELOV

*Lomonosov Moscow State University  
Moscow, RUSSIA*

e-mail: savelovmp@gmail.com

## Abstract

Consider a multinomial scheme with  $N$  outcomes. We suggest a set of  $N - 2$  new statistics which along with the Pearson statistic are jointly asymptotically independent. Limit distributions of these statistics are found.

**Keywords:** data science, Pearson statistic, multinomial scheme

## 1 Introduction

Suppose that independent identically distributed trials with  $N$  outcomes having probabilities  $p_1, \dots, p_N$  ( $p_1 + \dots + p_N = 1$ ,  $p_i > 0$ ) are performed. Denote by  $\nu_i = \nu_i(n)$  the frequency of the  $i$ -th outcome in the first  $n$  trials. The Pearson statistics  $X(n) := \sum_{i=1}^N \frac{(\nu_i - np_i)^2}{np_i}$  is widely used to test the hypothesis  $H()$ : “probabilities of outcomes constitute a vector  $(p_1, \dots, p_N)$ ”, because the distribution of  $X(n)$  for  $n \rightarrow \infty$  converges to the standard chi-square distribution with  $N - 1$  degrees of freedom denoted here by  $\chi_{N-1}^2$  [1]. We suggest a set of  $N - 2$  new statistics (polar coordinates of the vector of frequencies in some basis) which along with the Pearson statistic are jointly asymptotically independent. Limit distributions of these statistics are found.

## 2 Main results

**Theorem 1.** *Suppose that vector  $p = (\sqrt{p_1}, \sqrt{p_2}, \dots, \sqrt{p_N})$  and  $v_1, v_2, \dots, v_{N-1}$  form an orthonormal basis of  $\mathbb{R}^N$ . Put*

$$Y_i = \left( \left( \frac{\nu_1 - np_1}{\sqrt{np_1}}, \frac{\nu_2 - np_2}{\sqrt{np_2}}, \dots, \frac{\nu_N - np_N}{\sqrt{np_N}} \right), v_i \right), 1 \leq i \leq N - 1$$

$$\alpha_{N-2}(n) = \operatorname{arctg} \frac{Y_{N-1}}{\sqrt{Y_1^2 + \dots + Y_{N-2}^2}} = \arccos \frac{Y_{N-1}}{\sqrt{Y_1^2 + \dots + Y_{N-1}^2}},$$

$$\alpha_{N-3}(n) = \operatorname{arctg} \frac{Y_{N-2}}{\sqrt{Y_1^2 + \dots + Y_{N-3}^2}} = \arccos \frac{Y_{N-2}}{\sqrt{Y_1^2 + \dots + Y_{N-2}^2}},$$

$$\alpha_{N-4}(n) = \operatorname{arctg} \frac{Y_{N-3}}{\sqrt{Y_1^2 + \dots + Y_{N-4}^2}} = \arccos \frac{Y_{N-3}}{\sqrt{Y_1^2 + \dots + Y_{N-3}^2}},$$

...

$$\alpha_2(n) = \operatorname{arccctg} \frac{Y_3}{\sqrt{Y_1^2 + Y_2^2 + Y_3^2}} = \arccos \frac{Y_3}{\sqrt{Y_1^2 + \dots + Y_4^2}},$$

$$\alpha_1(n) = 2 \operatorname{arccctg} \frac{Y_2 + \sqrt{Y_1^2 + Y_2^2}}{Y_2} = \begin{cases} \arccos \frac{Y_2}{\sqrt{Y_1^2 + Y_2^2}}, & Y_1 \geq 0, \\ 2\pi - \arccos \frac{Y_2}{\sqrt{Y_1^2 + Y_2^2}}, & Y_1 < 0, \end{cases}$$

and if the denominator of the formula for  $\alpha_i$  is zero we put  $\alpha_i = 0$ . Then the limit distribution of  $(X(n), \alpha_1(n), \dots, \alpha_{N-2}(n))$  is a distribution of a random vector  $\rho^2, \alpha_1, \dots, \alpha_{N-2}$  with independent components such that  $\rho^2 \sim \chi_{N-1}^2$ ,  $\alpha_1 \sim U[0, 2\pi]$  and for all  $i \in \{2, \dots, N-2\}$  a density  $p_{\alpha_i}(x)$  of a random variable  $\alpha_i$  distribution is defined by

$$p_{\alpha_i}(x) = \begin{cases} \frac{\Gamma\left(\frac{i+1}{2}\right)}{\sqrt{\pi}\Gamma\left(\frac{i}{2}\right)} \sin^{i-1} x, & 0 \leq x \leq \pi. \\ 0. \end{cases}$$

For  $N \geq 3$  put

$$T_1(n) = \operatorname{arctg} \left( \frac{\sqrt{p_3}(p_1 + p_2 + p_3)}{\sqrt{p_1 p_2}} \cdot \frac{\nu_2 p_1 - \nu_1 p_2}{(\nu_1 + \nu_2)p_3 - (p_1 + p_2)\nu_3} \right),$$

$$T_2(n) = \arccos \frac{\nu_N - np_N}{(1 - p_N)\sqrt{np_N X(n)}}.$$

**Example 1.** If  $N \geq 3$  then  $\alpha_1$  is defined and  $T_1(n) = \arctan(\tan(\alpha_1(n)))$ . Hence the limit distribution of a vector  $(X(n), T_1(n))$  is a distribution of a vector  $(\zeta_1, \zeta_2)$  with independent components such that  $\zeta_1 \sim \chi_{N-1}^2$ ,  $\zeta_2 \sim U[-\frac{\pi}{2}, \frac{\pi}{2}]$ . If  $N \geq 4$  then  $\alpha_1$  and  $\alpha_{N-2} = \pi - T_2(n)$  are defined, and the limit distribution of a vector  $(X(n), T_1(n), T_2(n))$  is a distribution of a vector  $(\zeta_1, \zeta_2, \zeta_3)$  with independent components such that  $\zeta_1 \sim \chi_{N-1}^2$ ,  $\zeta_2 \sim U[-\frac{\pi}{2}, \frac{\pi}{2}]$ . The density of  $\zeta_3$  is equal to  $\frac{\Gamma\left(\frac{N-1}{2}\right)}{\sqrt{\pi}\Gamma\left(\frac{N-2}{2}\right)} \sin^{N-3} x$  for  $x \in [0, \pi]$  and 0 otherwise.

### 3 Acknowledgments

The author is grateful to A.M. Zubkov for the constant attention.

### References

- [1] Borovkov A.A. (1984). *Mathematical statistics (in Russian)*. Nauka, Moscow.

# TESTING THE NIST STATISTICAL TEST SUITE ON ARTIFICIAL PSEUDORANDOM SEQUENCES

A.A. SEROV, A.M. ZUBKOV

*Steklov Mathematical Institute of RAS*

*Moscow, RUSSIA*

e-mail: serov@mi.ras.ru, zubkov@mi.ras.ru

## Abstract

We discuss the results of experiments with the well-known NIST Statistical Test Suite designed for testing the hypothesis on the uniformity and independence of binary sequence elements. In particular, we investigate conditions on the parameters of piecewise merging of two linear recurrent sequences under which such combined sequences successfully pass all tests of the NIST package.

**Keywords:** data science, pseudorandom sequence, statistical test

## 1 Introduction

Generators of random and pseudo-random sequences are used in different fields of science and technology, including the cryptography. The most strict conditions on the quality of generated sequences are used in cryptography: to ensure the information security it is necessary for the generated sequences to be indistinguishable (or to be difficult to distinguish) from the equiprobable Bernoulli sequences. So the development and investigation of methods to test the closeness of the binary sequence properties to that of the equiprobable Bernoulli sequence is an actual problem.

## 2 Statistical test packages

In practice the testing of statistical qualities of random sequences (the quality is the higher the closer the characteristics of the tested sequence are to that of random equiprobable sequence) begins with the application of some statistical test packages. There are several popular packages of statistical tests which are distributed with open source codes (e.g. TESTU01 see [4], DIEHARD see [1], NIST see [3], SPRNG see [2]), or with closed source codes (e.g. Crypt-X [http://www.isrc.qut.edu.au /resource/cryptx/](http://www.isrc.qut.edu.au/resource/cryptx/)). These packages allow to perform the analysis and testing of random sequences and have significant intersections in the sets of tests.

## 3 Main results

From the statistical test packages listed above, the NIST statistical tests package was selected as one of the most popular, fully documented and actively used for generator certifications.

The NIST Statistical Test Suite consists of 15 tests “developed for the randomness testing of the binary sequences” (word-for-word from the manual). These 15 tests are listed in Table 1.

Table 1: List of NIST Statistical Tests

Number	Test Name
1	Frequency
2	Block Frequency
3	Runs
4	Longest Run
5	Binary Matrix Rank
6	Discrete Fourier Transform
7	Non-overlapping Template Matching
8	Overlapping Template Matching
9	Universal
10	Linear Complexity
11	Serial
12	Approximate Entropy
13	Cumulative Sums
14	Random Excursions
15	Random Excursions Variant

For testing the sequence it is divided into several sufficiently long blocks and for each statistical test a set of  $P$ -values corresponding to these blocks are produced. The sequence is considered as *accepted by the test* if the corresponding  $P$ -values look like independent random variables with the uniform distribution on  $[0, 1]$ , in particular, satisfy some statistical test of uniformity, and is considered as *rejected by the test* otherwise.

The critical values of statistics in the NIST Statistical Test Suite were computed by means of limit theorems, and it was recommended that analysed sequences should have sufficiently large lengths. All segments sequences that we have tested were of  $33,554,431 = 2^{25} - 1$  bit length. The significance level  $\alpha = 0.01$  determining the rule of acceptance/rejection of the hypothesis was selected by default.

We have tested the following types of pseudo-random sequences by the NIST Test Suite (a brief description of the test results are given in brackets):

- pseudo-random sequences generated by linear shift registers of the maximal period with feedbacks given by the following primitive polynomials of degrees 25 and 27 over  $\text{GF}(2)$ :

$$\begin{aligned}
 f(x) &= x^{25} + x^3 + 1, \\
 g(x) &= x^{27} + x^5 + x^2 + x + 1, \\
 h(x) &= x^{27} + x^{19} + x^{18} + x^{17} + x^{11} + x^6 + 1, \\
 m(x) &= x^{27} + x^{26} + x^{25} + x^{24} + x^{23} + x^{22} + x^{21} + x^{20} + x^{19} + x^{17} \\
 &\quad + x^{15} + x^{13} + x^{11} + x^9 + x^7 + x^5 + x^3 + x + 1
 \end{aligned}$$

(the segments of the pseudorandom sequences obtained by the linear shift registers with the  $g(x)$ ,  $h(x)$  and  $m(x)$  polynomials have successfully passed all the

tests from the NIST Test Suite except for The Binary Matrix Rank Test, The Discrete Fourier Transform Test and The Linear Complexity Test, where the  $P$ -values were less than  $10^{-6}$ , with the significance level  $\alpha = 0.01$ , the sequence corresponding to the polynomial  $f(x)$ , in addition to the listed tests, did not pass the Tests for the Longest Run-of-Ones in a Block ( $P$ -value  $6 \cdot 10^{-6}$ ) and Maurer's "Universal Statistical Test" ( $P$ -value  $1.91 \cdot 10^{-4}$ )

- pseudo-random sequences generated by the linear shift registers with additive noise (the only test from the NIST Test Suite that detects nonrandomness in the disjoint  $2^{25} - 1$  bit segments of output sequences of linear shift registers with polynomials  $f(x)$ ,  $g(x)$ ,  $h(x)$ ,  $m(x)$  perturbed by the Bernoulli noise sequence with parameter  $\frac{1}{4}$ , turned out to be The Discrete Fourier Transform Test (the corresponding  $P$ -values were smaller  $10^{-6}$ );
- filtered output sequences of linear shift registers of the maximal period (failed to pass a number of tests of NIST Test Suite, corresponding  $P$ -values in many cases were smaller than  $10^{-6}$ );
- pseudo-random sequences obtained by merging of outputs of two linear shift registers of maximal periods: A) the output sequence of the first register  $\{x_1, x_2, \dots\}$  corresponding to the polynomial  $f(x)$  was divided into adjacent segments of  $L_1 = 25$  bits, the output sequence of the second register  $\{y_1, y_2, \dots\}$  corresponding to the polynomial  $g(x)$  was similarly divided into segments of  $L_2 = 27$  bits; the tested sequence  $\{z_1, z_2, \dots\}$  of the first type was constructed by merging of obtained segments of two sequences:

$$\{z_k\}_{k=0}^{2^{L_1-1} + \lceil \frac{2^{L_1-1}}{L_1} \rceil L_2} = \{x_1, \dots, x_{L_1}, y_1, \dots, y_{L_2}, x_{L_1+1}, \dots, x_{2L_1}, y_{L_2+1}, \dots\};$$

B) the output register sequences were divided into adjacent segments of a variable lengths according to the following rule:

$$\{w_1, w_2, \dots\} = \{x_1, \dots, x_{L_1}, y_1, \dots, y_{L_1^*}, x_{L_1+1}, \dots, x_{L_2}, y_{L_1^*+1}, \dots, y_{L_2^*}, \dots\},$$

where  $L_1 = 25$ ,  $L_k^* = 16 + 2^3 x_{L_k-3} + 2^2 x_{L_k-2} + 2x_{L_k-1} + x_{L_k}$ ,  $L_{k+1} = 16 + 2^3 y_{L_k^*-3} + 2^2 y_{L_k^*-2} + 2y_{L_k^*-1} + y_{L_k^*}$ ,  $k \geq 1$  (the A type sequences had passed all tests with the exception of Discrete Fourier Transform Test: for this test  $P$ -values were smaller than  $10^{-6}$ , while the B type sequences had passed all the tests with  $P$ -values being as a rule essentially larger than  $\alpha = 0.01$ );

- pseudo-random sequence generated by AES, each byte of the encrypted sequence was replaced by the corresponding bit depending on the byte value (four non-overlapping segments of the length  $2^{25} - 1$  bits of the initial sequence of the length  $2^{27} - 4$  bits passed all the tests from the NIST Test Suite in the aggregate);
- output sequence of shrinking generators composed of two linear shift registers; two tested sequences were obtained by extracting from the output sequence of the first linear shift register (with feedback polynomial  $g(x)$ ) all bits corresponding to the nonzero bits in the output sequence of the second linear shift register (with

feedback polynomial  $f(x)$  for the first type test sequence and the polynomial  $h(x)$  for the second one). The first type sequence passed all the tests from the NIST Test Suite with the significance level  $\alpha = 0.01$ . The second type sequence passed all the tests except for the Serial Test: for this test  $P$ -values turned out to be smaller than  $10^{-6}$ . Maybe this is the consequence of coincidence of orders of the source and control sequences.

Also three series of experiments for following binary sequences having some different probabilistic structures were performed:

- pseudo-random sequences generated by AES, these sequences are considered as almost perfect;
- output sequences of linear shift register with primitive polynomial of degree 32 filtered by the equiprobable Boolean function corresponding to the first bit of nonlinear substitution in AES;
- non-equiprobable sequences obtained from the AES pseudo-random sequences by replacement each byte with bit such that the probability of 1 is  $\frac{127}{256}$ .

In each series of experiments 128 binary sequences of length  $2^{20}$  were generated, the above 15 tests of the NIST package were applied to each sequence and the statistics values of these tests were saved, after which sample correlation statistics matrices were constructed.

Large correlations of statistics of Frequency, Cumulative Sums, Random Excursions, Random Excursions Variant, Runs tests were observed. So, these tests cannot be considered as independent.

## 4 Conclusions

The set of experiments with different non-random pseudo-random sequences showed that the NIST Test Suite may detect some deviations of properties of analyzed sequences from that of ideal Bernoulli sequences, but may fail to detect non-randomness of deterministic sequences with not very complex artificial irregularities.

## References

- [1] Marsaglia G. (1996). *DIEHARD: a battery of tests of randomness*.
- [2] Mascagni M. (2000). Algorithm 806: SPRNG: A scalable library for pseudorandom number generation. *ACM Trans. Math. Soft.* Vol. 26, pp. 436–461.
- [3] Rukhin A. et al. (2010). *A statistical test suite for the validation of random number generators and pseudo random number generators for cryptographic applications*. NIST Special Publ. 800-22 Revision 1a. 27 April 2010. NIST, ed.: L. E. Bassham III.
- [4] L'Ecuyer P., Simard R. (2013). *TestU01*. D'epartement d'Informatique et de Recherche Op'erationnelle Universit'e de Montr'eal.

# ADAPTIVE METHODS FOR FORECASTING CURRENCY COURSES

L.A. SOSHIKOVA  
*Belarus State Economic University*  
*Minsk, BELARUS*  
e-mail: ludmila\_sosh@mail.ru

## Abstract

The paper discusses the use of adaptive models for short-term forecasting of currency rates. As a criterion for the randomness of the movement of the levels of the dynamic range of currency rates, the criterion of turning points was used.

**Keywords:** data science, adaptive method, currency course

## 1 Introduction

One of the objectives of a statistical study of macroeconomic indicators is to analyze the dynamics of the rates of major foreign currencies. This is due, first of all, that the valuation of assets in the corresponding period of time, the indicators of their dynamics depend on the emerging exchange rates. This paper discusses the methodology and main results of the analysis and prediction of market fluctuations in exchange rates using adaptive methods [1].

The work was performed on the basis of the data of the National Bank of the Republic of Belarus for 2016–2017. about the daily exchange rates of the US dollar, euro and Russian ruble to the Belarusian denominated ruble. At first glance, the dynamics of national currencies seems to the researcher a chaotic process, in which there is no regularity. In such conditions, it is very important to find statistical methods and forecasting methods that, if they do not quantify the foreign currency exchange rate for the upcoming period (for example, a day), then at least indicate the direction of its dynamics (growth, decrease or stabilization). As the analytical practice in this area shows, the use of traditional approaches to modeling the dynamics does not give good results.

Before embarking on the mechanism of the relationship between successive values of the exchange rate, an attempt was made to find out if the original series are not completely random. As criteria of randomness, the criterion of turning points was used. The number of turning points in the test row is compared with their number in a completely random row, and on this basis it is concluded whether the row is random or not.

## 2 Techniques for building a predictive model

There were 124 turning points in the range of the Belarusian ruble / euro exchange rate under study from July 1, 2016 to September 13, 2017. The test showed that for

all the considered rows the observed number of turning points is significantly less than it should theoretically be for a random series. Criterion for turning points:

$$P_{forecasted}(n) = 2(n - 2/3 - 1.96\sqrt{(16n - 29)/90}),$$

$$P_{forecasted}(440) = 274 > P_{real} = 124.$$

Consequently, the random nature of changes in the levels of this series is not confirmed. For a number of dynamics of the Belarusian ruble exchange rate, there were 113 turning points for the same period against the dollar, and 120 turning points for the Russian ruble. In other words, this criterion indicates that these series are not entirely random: they can conceal some pattern of movement forward. When building a predictive model, the choice was made in favor of the class of adaptive models. In this connection, we will make some transformations of the initial series. First, from the initial levels of the dynamic series we move on to their first differences. Secondly, we replace the differences by the values  $k_t = \text{sign}(\Delta y_t)$  according to [2].

Further analysis of the series is reduced to the analysis of alternation or preservation of characters. Three options are possible:

- supply and demand contribute to the preservation of the mark of the growth rate;
- expectation of a change in the direction of movement of the course causes a change in the sign of growth;
- future course direction is completely random.

The model should catch which of the three situations prevails recently, and give a forecast for the next moment. To build a model, we use the values  $M_t = k_t k_{t-1}$ . In order to find out which situation is more often encountered recently, one can apply the exponential smoothing method of the series  $M_t$ :

$$S_t = \alpha M_t + (1 - \alpha)S_{t-1} = S_{t-1} + \alpha(M_t - S_{t-1}).$$

Here,  $S_t$  can be considered as a forecast one step further, i.e. as a prediction of the value of  $M_t$  made at time  $t - 1$ , then the value of  $M_t - S_{t-1}$  is a prediction error, and the new forecast  $S_t$  is obtained by adjusting the previous forecast taking into account its error. This is the adaptation of the predictive model.

The value of  $M_t = \Delta y_t \Delta y_{t-1} / |\Delta y_t \Delta y_{t-1}|$  is a modified correlation coefficient, so  $S_t$  is an adaptive correlation coefficient [2]. Therefore, the value of  $S_t$  resulting from the averaging of ones and zeros will be a fractional number from the interval  $[-1, 1]$ , therefore, the value  $M_t$  at the moment  $t + 1$  will be defined as  $M_{t+1} = \text{sign}(S_t)$ . A positive  $M_{t+1}$  means the preservation of the sign of the increment that occurred at time  $t$ , and the negative one means a change. The forecast of the sign of the currency exchange rate increase at the moment  $t + 1$  is defined as  $\text{sign}(\Delta y_{t+1}) = \text{sign}(M_{t+1} k_t)$ . This model is capable at different times to reflect either positive or negative correlation of neighboring increments. It from time to time adapting to the observations, as if changes its properties to the opposite.

### 3 Evaluation of forecast results

If the prediction turned out to be correct, the payoff is equal to the difference  $|x_{t+1} - x_t|$ , and if the prediction is wrong, then  $|x_{t+1} - x_t|$  will be the size of the damage.

The criterion for estimating the results of forecasting is the average gain (or loss) from currency operations per unit of time (that is, per day) per dollar or cumulative gain for a certain period of model operation. In addition, a series of absolute and relative indicators are calculated:

- $L$  is the number of the winnings (predictions of the sign of a currency rate increase);
- $M$  is the number of erroneous predictions of the growth sign, i.e. the number of losses;
- $PL = L/(L + M)$  is the portion of the predictions of the growth mark that came true;
- $PM = M/(L + M)$  is the portion of erroneous predictions of the growth sign;
- $SPR$  is the sum of winnings (i.e., only winnings are summed up) in foreign exchange transactions for the entire study period of the forecast model functioning, which will be denoted by  $T$  (measured in national currency);
- $SLOS$  is the amount of losses in foreign exchange transactions for the period  $T$  (in national currency);
- $SPR - SLOS$  is balance, net winnings (in national currency);
- $R = SPR/SLOS$  is the ratio of the amount of winnings to the amount of losses;
- $REL = SPR/(SPR + SLOS)$  is the portion of the realized opportunities ( $SPR + SLOS$  is the maximum possible gain).

### 4 Findings

Thus, we showed that even the simplest statistical model can be useful for solving such a difficult task as forecasting currency rates. The proposed approach to short-term forecasting allows you to quickly make a decision on current currency transactions.

### References

- [1] Kantorovich G. G. (2002). Lectures: time series analysis. *Economic Journal of the Higher School of Economics*. Vol. 6, No. 1, pp. 85–116.
- [2] Lukashin Yu. P. (2003). *Adaptive short-term forecasting methods*. Finance and Statistics, Moscow.

# STATISTICAL CLASSIFICATION OF THE STATES OF BIOLOGICAL CELLS TREATED WITH CARBON NANOTUBES BASED ON AFM-IMAGES OF CELL SURFACE

I.E. STARODUBTSEV<sup>1,2</sup>, YU.S. KHARIN<sup>1,2</sup>, M.N. STARODUBTSEVA<sup>3,4</sup>

<sup>1</sup> *Research Institute for Applied Problems of Mathematics and Informatics*

<sup>2</sup> *Belarusian State University*

<sup>3</sup> *Gomel Medical State University*

<sup>4</sup> *Institute of Radiobiology National Academy of Sciences of Belarus*

*Minsk, Gomel, BELARUS*

e-mail: [istarodubtsev.science@gmail.com](mailto:istarodubtsev.science@gmail.com)

## Abstract

The method of statistical classification of biological cells, treated with carbon nanotubes, based on images of cell surface obtained with an atomic force microscope (AFM) is proposed. Each scan line of the original AFM image is considered as a random sequence realization, and the discrete Fourier transform is applied to compute its spectral features. After smoothing, the map of spectral estimates is formed. The informative features are computed as the medians for the set of the spectrogram values. Classification of four classes of cells (control and treated with carbon nanotubes, after 1 hour and 24 hours of incubation) was carried out by the obtained informative features using the decision trees method. The proposed method provides a sufficiently high accuracy classification of cell states after the treatment with carbon nanotubes.

**Keywords:** data science, AFM-image, carbon nanotube, cell surface, classification

## 1 Introduction

Atomic force microscopy (AFM) is a modern method of biomedical research which allows studying the relief and the physicommechanical properties of biological cell surfaces at nanoscale level, it makes possible the determination of their type and condition based on complex statistical data [1,2,3].

The aim of this paper is to solve the problem of the statistical classification of AFM-images (the microscale maps of cell surface mechanical properties) of biological cells (glial cells) treated with carbon nanotubes.

The samples of rat glioma cell (C6 cell line) treated with the DNA-single-walled carbon nanotube (NT) complex (incubation time was 1 and 24 hours) were kindly provided by the Biophysics Department of Physics Faculty of Belarusian State University. The structure and distribution of mechanical properties over the cell surface change in time dependent on treatment of cells with NT. Images of cell surfaces were recorded using AFM NT-206 in Research Laboratory of the Gomel State Medical University. For the analysis, the maps of lateral forces of the cell surface of size of  $2.5 \mu m \times 2.5 \mu m$  ( $256 \times 256$  points) were used. AFM-images were processed by the software developed by us using the `fftw` library [4].

## 2 Mathematical model

The AFM-image of cell surface is a two-dimensional array  $z=z(x,y)$ , where  $x$  is the vertical coordinate,  $y$  is the horizontal coordinate,  $x,y \in \{1,2,\dots,N\}$ ;  $z$  is the value of the sliding friction force at the point  $(x, y)$ . An AFM-image of size of  $N \times N$  points can be considered as a set of  $N$  one-dimensional arrays  $z = z^{(y)}(x)$  of  $N$  points each, located at a distance of a scanning step along the  $y$  axis ( $N$  is an even number, in experiments  $N=256$ ).

Original AFM-images were normalized by dividing the values  $z(x,y)$  by  $10^3$ . Instead of the initial values of  $z$  at each  $y$  were considered  $z'$  is the differences between adjacent values along the  $x$  axis, divided by the value of the standard deviation for each line:

$$z'(x,y) = \frac{z(x+1,y) - z(x,y)}{\sqrt{D(y)}}, \quad x \in \{1,2,\dots,N-1\}.$$

The data obtained in this way corresponds to four classes:  $\Omega_1$  - NT-1h (with NT, after 1 hour),  $\Omega_2$  - control-1h (without NT, after 1 hour),  $\Omega_3$  - NT-24h (with NT, after 24 hours),  $\Omega_4$  - control-24h (without NT, after 24 hours).

## 3 Informative features

Each one-dimensional array  $z = z^{(y)}(x)$  with fixed  $y$  can be considered as an realization of a random sequence  $z = z_x^{(y)}$ ,  $x \in \{1,2,\dots,N\}$ , for which a discrete Fourier transform can be applied:

$$X^{(y)}(\omega_k) = \sum_{n=1}^N (z_n^{(y)} - \bar{z}^{(y)}) e^{-j \frac{2\pi kn}{N}}, \quad k = 0, 1, \dots, N-1,$$

where  $\bar{z}_n^{(y)} = \frac{1}{N} \sum_{n=1}^N z_n^{(y)}$  is the sample mean on the  $x$  axis with fixed  $y$ ,  $\omega_k = 2\pi \frac{k}{L}$  is frequency,  $L$  is the length of analyzed interval along the  $x$  axis.

Based on the sample spectrum  $X^{(y)}(\omega_k)$ , we calculated the periodogram

$$r^{(y)}(\omega_k) = |X^{(y)}(\omega_k)|^2,$$

and, smoothing it using the Daniel window with a width of  $m$  ( $m=5$ ), we obtained spectral density estimates  $R^{(y)}(\omega_k)$  [5]. Estimates  $R^{(y)}(\omega_k)$  at  $k=\frac{N}{2}+1,\dots,N-1$  were excluded from our consideration as they repeated the values at  $k=0,\dots,\frac{N}{2}-2$ .

For each frequency  $\omega_k$  we calculated the medians of the spectral density using  $N$  values along the  $y$  axis:

$$\tilde{R}(\omega_k) = Med\{R^{(1)}(\omega_k), \dots, R^{(N)}(\omega_k)\}, \quad k = 0, \dots, \frac{N}{2} - 1,$$

that were used as informative features of the original AFM image. We will call  $\tilde{R}(\omega_k)$  :  $k = 0, \dots, \frac{N}{2} - 1$  as the spectrogram of AFM image of cell surface under this study. Values  $\tilde{R}(\omega_k)$  :  $k = 71, \dots, 128$  were excluded from our consideration because the corresponding periods  $T_k = \frac{2\pi}{\omega_k}$  were smaller than the scanning step.

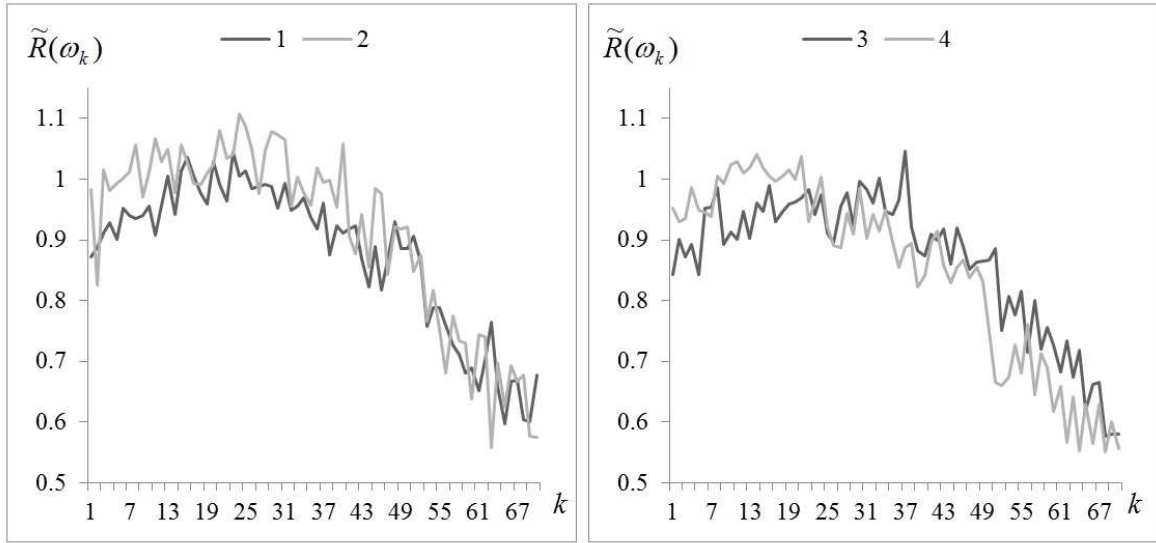


Figure 1 –Averaged over entire sample spectrograms of AFM images of surfaces for classes  $\Omega_1$  (1),  $\Omega_2$  (2),  $\Omega_3$  (3) and  $\Omega_4$  (4).

## 4 Statistical classification

We used the decision trees algorithm for classification, to build decision trees we used the C&RT algorithm [6]. The choice of features for constructing a decision tree was carried out using the Gini criterion [6]. Since the training sample is not large enough, the choice of the optimal size of the classification tree was determined using cross-validation [7]. The examination sample size was 30% of the entire sample size.

## 5 Numerical results

The training sample size was consist of 51 observations (the AFM images of  $256 \times 256$  dots). Examples of averaged spectrograms for pairs of classes  $\{\Omega_1, \Omega_2\}$  and  $\{\Omega_3, \Omega_4\}$  are shown in Figure 1.

Table 1 presents the values of the accuracy of correct classification.

## 6 Conclusion

The proposed statistical classification method based on spectral features of the AFM images presenting the maps of mechanical properties of rat glioma cells provides a sufficiently high classification accuracy of cell states after the treatment with carbon nanotubes. The results can be used in the study of the effects of carbon nanotubes on biological cells.

Table 1. Accuracy of correct classification of cell states using the decision trees algorithm, %

Classification for pair of classes $\{\Omega_1, \Omega_2\}$	$\Omega_1$	$\Omega_2$
	<b>93.33%</b>	<b>75.00%</b>
Classification for pair of classes $\{\Omega_3, \Omega_4\}$	$\Omega_3$	$\Omega_4$
	<b>72.73%</b>	<b>92.31%</b>
Classification for pair of classes $\{\Omega_1, \Omega_3\}$	$\Omega_1$	$\Omega_3$
	<b>80.00%</b>	<b>100.00%</b>
Classification for pair of classes $\{\Omega_2, \Omega_4\}$	$\Omega_2$	$\Omega_4$
	<b>66.67%</b>	<b>92.31%</b>

## References

- [1] Starodubtseva M.N., Starodubtsev I.E. , Starodubtsev E.G. (2017). Novel fractal characteristic of atomic force microscopy images. *Micron*. Vol. **96**, pp. 96-102.
- [2] Starodubtseva M.N., Mitsura E.F., Starodubtsev I.E., Chelnokova I.A., Yegorenkov N.I., Volkova L.I., Kharin Yu.S. (2018). Nano- and microscale mechanical properties of erythrocytes in hereditary spherocytosis. *J. Biomech*. Vol. **83**, pp. 1-8.
- [3] Kharin Yu.S. (1996). *Robustness in Statistical Pattern Recognition*. Kluwer, Dordrecht.
- [4] FFTW package: <http://www.fftw.org/> (accessed 10 April 2019).
- [5] Anderson T. W. (1971). *The Statistical Analysis of Time Series*. J. Wiley, N. Y.
- [6] Harrington P. (2012). *Machine Learning in Action*. Manning, N. Y.
- [7] Hastie T., Tibshirani R., Friedman J. H. (2009). *The Elements of Statistical Learning* . Springer Publ., N. Y.

# INTERNALLY HOMOGENEOUS RANDOM FIELDS ANALYSIS

T.V. TSEKHAVAYA, N.N. TROUSH  
*Belarusian State University*  
*Minsk, BELARUS*  
e-mail: Tsekhavaya@bsu.by

## Abstract

An internally homogeneous random field and the variogram are introduced, and their properties are analyzed.

**Keywords:** internal homogeneity, random field, data science

## 1 Introduction

A number of publications is devoted to the analysis of internally stationary random processes, e.g. [1] – [4]. The variogram is a major characteristic of internally stationary random processes. The results of its properties studies and statistical properties of its estimators are presented in [5] – [6]. Here the variogram analysis for internally homogeneous random fields is performed.

## 2 The variogram and an internally stationary random field

Let  $X(t)$ ,  $t \in R^n$ , be a real valued homogeneous random field with the mathematical expectation  $m = MX(t) = 0$ ,  $t \in R^n$ , the covariance function  $R(t)$ ,  $t \in R^n$ , the spectral density  $f(\lambda)$ ,  $\lambda \in R^n$ , and the correspondent spectral function  $F(\lambda)$ ,  $\lambda \in R^n$ .

**Definition 1.** A random field  $X(t)$ ,  $t \in R^n$ , is called internally homogeneous, if

$$M\{X(t+h) - X(t)\} = 0,$$

$$D\{X(t+h) - X(t)\} = 2\gamma(h),$$

for all  $t$ ,  $h \in R^n$ , function  $2\gamma(h)$  is called the variogram, and  $\gamma(h)$  is the semivariogram.

Note that a homogeneous random field is also an internally homogeneous with

$$\gamma(h) = 0, 5(DX(t+h) - 2\text{cov}\{X(t+h), X(t)\} + DX(t)) = R(0) - R(h).$$

Although, an internally homogeneous random field is not necessary to be homogeneous.

An internally homogeneous random field  $X(t)$ ,  $t \in R^n$ , that satisfies the condition

$$M\{X^2(t)\} = D = \text{const} < \infty,$$

is also a homogeneous random field.

For the real Gaussian random field, homogeneity and internal homogeneity are equivalent.

**Theorem 1.** If  $R(t)$ ,  $t \in R^n$ , is the covariance function of an homogeneous random field, then  $R(t)$ ,  $t \in R^n$ , is non-negatively defined function. Vice versa, if  $R(t)$ ,  $t \in R^n$ , is an even non-negatively defined function, then there exist the only one Gaussian random field with zero mean and covariance function  $R(t)$ ,  $t \in R^n$ .

If  $R(t)$ ,  $t \in R^n$ , is an integrable covariance function, then the spectral function  $F(\lambda)$ ,  $\lambda \in R^n$ , is absolutely continuous, and the spectral density

$$f(\lambda) = \frac{1}{(2\pi)^n} \int_{R^n} R(\tau) e^{-i(\lambda, \tau)} d\tau,$$

where  $(\lambda, \tau)$  is the scalar product of vectors  $\lambda, \tau \in R^n$ .

Note that the sums, the products and the limits of the non-negatively defined functions are non-negatively defined; the sumes, the products and the limits of the covariance functions are still covariance functions.

**Definition 2.** The function  $\gamma(t)$ ,  $t \in R^n$ , is called conditionally negatively defined, if for any natural  $m$ ,  $m \geq 1$ , arbitrary  $t_i \in R^n$ ,  $i = \overline{1, m}$ , and any non-zero real vector  $(a_1, \dots, a_m)$ , such that  $\sum_{i=1}^m a_i = 0$ , the inequality holds

$$\sum_{i=1}^m \sum_{j=1}^m a_i a_j \gamma(t_i - t_j) \leq 0.$$

Let  $X(t)$ ,  $t \in R^n$ , be real internally homogeneous random field with a finite second order moment and semivariogram  $\gamma(t)$ ,  $t \in R^n$ .

**Theorem 2.** The semivariogram  $\gamma(t)$ ,  $t \in R^n$ , of an internally homogeneous random field  $X(t)$ ,  $t \in R^n$ , is a conditionally negatively defined function.

*Proof.* From the variogram definition we have

$$\begin{aligned} \sum_{i=1}^m \sum_{j=1}^m a_i a_j \gamma(t_i - t_j) &= \sum_{i=1}^m \sum_{j=1}^m a_i a_j \frac{1}{2} D\{X(t_i) - X(t_j)\} = \\ &= \frac{1}{2} \sum_{i=1}^m \sum_{j=1}^m a_i a_j (D\{X(t_i)\} - 2R(t_i, t_j) + D\{X(t_j)\}) = \\ &= \frac{1}{2} \left( \sum_{i=1}^m a_i D\{X(t_i)\} \sum_{j=1}^m a_j - 2 \sum_{i,j=1}^m a_i a_j R(t_i, t_j) + \sum_{i=1}^m a_i \sum_{j=1}^m a_j D\{X(t_j)\} \right). \end{aligned}$$

As  $\sum_{i=1}^m a_i = 0$ , then

$$\sum_{i=1}^m \sum_{j=1}^m a_i a_j \gamma(t_i - t_j) = - \sum_{i,j=1}^m a_i a_j R(t_i, t_j) \leq 0.$$

The last inequality is valid due to Theorem 1. □

Note that

$$D \left( \sum_{i=1}^m a_i X(t_i) \right) = - \sum_{i=1}^m \sum_{j=1}^m a_i a_j \gamma(t_i - t_j).$$

**Theorem 3.** Let  $\gamma_1(t), \gamma_2(t)$  be the semivariograms of internally homogeneous random fields  $X_1(t), X_2(t)$ ,  $t \in R^n$ , respectively. Then the function  $\gamma(t) = \gamma_1(t) + \gamma_2(t)$ ,  $t \in R^n$ , is also the semivariogram of an internally homogeneous random field.

*Proof* of the theorem follows from Theorem 2.

**Theorem 4.** Let  $\gamma(t)$ ,  $t \in R^n$ , be the semivariogram of an internally homogeneous random field  $X(t)$ ,  $t \in R^n$ . Then for any  $b > 0$  the function  $b\gamma(t)$  is the semivariogram of the internally homogeneous random field  $\sqrt{b}X(t)$ ,  $t \in R^n$ .

*Proof* of the theorem is based on the Theorem 2 statement.

**Theorem 5.** Let an arbitrary real function  $m(t) = m$ ,  $t \in R^n$ , and an even conditionally negatively defined real function  $\gamma(t)$ ,  $t \in R^n$  exist. Then there exist a probability space and a real Gaussian random field defined on it  $X(t)$ ,  $t \in R^n$ , so that  $M\{X(t)\} = m$  and  $D\{X(t+h) - X(t)\} = 2\gamma(h)$  for all  $h \in R^n$ .

*Proof* is analogous to the proof of Theorem 1 in [1] for random processes.

**Corollary 1.** The class of even conditionally negatively defined real functions coincides with the class of real Gaussian homogeneous random fields semivariograms.

**Theorem 6.** The continuous function  $\gamma(t)$ ,  $t \in R^n$ , is a semivariogram of an internally homogeneous random field  $X(t)$ ,  $t \in R^n$ , with a finite second order moment, if and only if for any  $a > 0$  the function  $e^{-a\gamma(t)}$ ,  $t \in R^n$ , is non-negatively defined.

*Proof. Necessity.* From Theorem 5 there exist a probability space and a real Gaussian random field  $X(t)$ ,  $t \in R^n$ , defined on it with  $M\{X(t)\} = 0$  and  $D\{Y(t) - Y(s)\} = 2\gamma(t - s)$  for all  $t, s \in R^n$ . Note that the field  $X(t)$  is internally homogeneous.

Put  $Z(s) = e^{-i\sqrt{a}X(s)}$  and find the correlation function for this field.

$$R_Z^0(s, s+t) = M \left\{ Z(s) \overline{Z(s+t)} \right\} = M \left\{ e^{i\sqrt{a}(X(s+t) - X(s))} \right\}. \quad (1)$$

From the characteristic function definition, and the field  $X(t)$  properties, the right-hand side of (1) for any  $t \in R^n$  equals

$$\Psi_{X(s+t) - X(s)}(\sqrt{a}) = e^{-\frac{a}{2}D\{X(s+t) - X(s)\}} = e^{-a\gamma(t)}, \quad a > 0.$$

Hence, for any  $a > 0$  the function  $e^{-a\gamma(t)}$ ,  $t \in R^n$ , is a characteristic function. From the Bokhner–Khinchin Theorem [7],  $e^{-a\gamma(t)}$  is non-negatively defined.

*Sufficiency.* Let  $e^{-a\gamma(t)}$ ,  $a > 0$ ,  $t \in R^n$ , be a non-negatively defined function. Then from the Bokhner–Khinchin Theorem this function is a characteristic function. Further proof duplicates the sufficiency proof of Theorem 1 in [6].  $\square$

**Corollary 2.** Let  $\gamma(t)$ ,  $t \in R^n$ , be the semivariogram of an internally homogeneous random field  $X(t)$ ,  $t \in R^n$ , satisfying the condition:  $M\{X^2(t)\} < \infty$  for any  $t \in R^n$ . Then for any  $a > 0$  the function  $e^{-a\gamma(t)}$ ,  $t \in R^n$  is a correlation function of a random field.

**Theorem 7.** If the semivariogram  $\gamma(t)$ ,  $t \in R^n$ , of the internally homogeneous random field  $X(t)$ ,  $t \in R^n$ , with a finite second order moment is a continuous function, then the following statements are equivalent:

1.  $\gamma(t)$  is a conditionally negatively defined function;
2.  $e^{-a\gamma(t)}$  is a non-negatively defined function for any  $a > 0$ ,  $t \in R^n$ .

*Proof* follows from Theorem 6 in this paper and Theorem 1 in [6].

### 3 Semivariogram asymptotics

For homogeneous random fields the covariance function  $R(t)$  goes to zero at  $|t| \rightarrow \infty$ . That is why the semivariogram  $\gamma(t) \rightarrow R(0)$ , when  $|t| \rightarrow \infty$ .

For internally homogeneous random fields that do not have finite second moment, the semivariogram  $\gamma(t) \rightarrow \infty$  at  $|t| \rightarrow \infty$ , and the covariance function does not exist.

Let further  $\gamma(t)$ ,  $t \in R^n$ , be the semivariogram of an internally homogeneous random field, that has no finite moments of the second order. Analyze the asymptotics of the semivariogram  $\gamma(t)$  at  $t \rightarrow \infty$ .

**Theorem 8.** The semivariogram  $\gamma(t)$ ,  $t \in R^n$ , of an internally homogeneous random field  $X(t)$ ,  $t \in R^n$ , can not increase at the infinity faster than the function  $At^2$ , where  $A$  is a positive constant,  $t \in R^n$ .

*Proof.* Using the variogram definition, for any  $n \in N$  we have:

$$\begin{aligned} 2\gamma(t) &= M\{(X(t) - X(0))^2\} = M\left\{\left(\sum_{i=1}^n \left[X\left(\frac{it}{n}\right) - X\left(\frac{(i-1)t}{n}\right)\right]\right)^2\right\} = \\ &= \sum_{i=1}^n \sum_{j=1}^n M\left\{\left[X\left(\frac{it}{n}\right) - X\left(\frac{(i-1)t}{n}\right)\right] \left[X\left(\frac{jt}{n}\right) - X\left(\frac{(j-1)t}{n}\right)\right]\right\}. \end{aligned}$$

From the Cauchy–Bunyakovsky inequality we get:

$$\begin{aligned} &2\gamma(t) \leq \\ \leq &\sum_{i=1}^n \sum_{j=1}^n \sqrt{M\left\{\left[X\left(\frac{it}{n}\right) - X\left(\frac{(i-1)t}{n}\right)\right]^2\right\}} \sqrt{M\left\{\left[X\left(\frac{jt}{n}\right) - X\left(\frac{(j-1)t}{n}\right)\right]^2\right\}} = \\ &= n^2 \cdot 2\gamma\left(\frac{t}{n}\right). \end{aligned}$$

Hence,

$$\frac{\gamma(t)}{t^2} \leq \frac{\gamma(t/n)}{(t/n)^2}$$

Denote by  $A$  the maximum of the function  $\gamma(t)/t^2$  with  $t \geq 1$ , then  $\gamma(t) \leq At^2$ ,  $t \geq 1$ . From here we get the result of the Theorem.  $\square$

## References

- [1] Tsekhavaya T. V. (2017). Internally stationary random processes properties. *Journal of the Belarusian State University. Mathematics. Informatics*. Vol. **1**, p. 28-33. (In Russian)
- [2] Tsekhavaya T. V. (2017). Variogram analysis of random processes. *Journal of the Belarusian State University. Mathematics. Informatics*. Vol. **2**, p. 23-27. (In Russian)
- [3] Tsekhavaya T. V. (2015). Semivariogram and stochastic analysis of random processes. *Probability Theory, Random Processes, Mathematical Statistics and Applications: International Conference Proceedings*. Minsk: RIHS, p. 360-365. (In Russian)
- [4] Cressie N. (1991). *Statistics for Spatial Data*. New York.
- [5] Trough N. N., Tsekhavaya T. V. (2001). Analysis of statistical properties of the variogram and covariance function estimators. *Proc. of the NAS of Belarus. Phys. and Math. Series.* Vol. **2**, p. 24-29. (In Russian)
- [6] Tsekhavaya T. V. (2004). Properties of the internally stationary random processes variogram. *Probability Theory, Mathematical Statistics and Applications: Proceedings of the Int. Conf.* Minsk, p. 181-186. (In Russian)
- [7] Shiryaev A. N. (1989). *Probability*. Moscow. (In Russian)

# METEOROLOGICAL DATA INFLUENCE ON MISSING VESSEL TYPE DETECTION USING DEEP MULTI-STACKED LSTM NEURAL NETWORK

J. VENSUS, P. TREIGYS  
*Vilnius University*  
*Vilnius, LITHUANIA*  
e-mail: `julius.venskus@mii.vu.lt`

## Abstract

Highly-loaded seaports have extremely complex and intensive marine vessel traffic, which generates large volumes of traffic data. Meteorological conditions and maritime vessel type influence maritime traffic and they must also be taken into account in order to train the model capable of recognizing the abnormal movement of the sea transport. Real data often misses some data values, such as type of vessel or its status. This paper reviews method of obtaining vessel traffic and meteorological data and filling missing vessel type data in Rotterdam port region. A deep multi-stacked LSTM neural network model is trained to fill the missing vessel type data. This model is trained with available vessel type data and used to predict missing values. This paper describes creation and evaluation of this model. Results of the experiment show it is expedient to use traffic data of a vessel in conjunction with meteorological data.

**Keywords:** data science, LSTM neural network, Vessel type detection, meteorology

## 1 Introduction

Maritime transport is one of the most important and intense sectors of human activity, accounting for about 90% of total trade. The high volume of vessel traffic generates large amounts of data, which overload various information systems and sensors [3]. Assistive systems are developed to facilitate the task, which extract the necessary information from the big data. One of the systems is an unusual traffic detection system, which requires full data for accurate detection. Unfortunately, the data that comes from different systems such as AIS, radars or satellite systems, is not full at all times [1]. The lack of such data prevents the creation of a sufficiently accurate model for detection of unusual vessel traffic. It is therefore necessary to develop smart systems for filling in the missing data, especially with the increased development of new methods for the detection of unusual traffic, which is essential for safety at sea [5]. This article offers a way to fill in the missing data for missing vessel types, which would allow for improved prediction of abnormal maritime traffic. The first part of the article introduces the developed method used to fill in the missing vessel type information in the data, and the second part describes the experiments with this method using vessel traffic data in the Rotterdam harbour. This research is continuous work in field of abnormal maritime traffic detection [4].

## 2 Proposed Method

**Deep neural neural network:** The main purpose of the model being developed is to determine the type of vessel by the available or received sets of vessel positions so that the missing information fields can be filled. The model input consists of a sequence of vessel position vectors, and the model predicts the type of vessels sailing under these sets. The model for vessel type prediction uses historical sets of vessel position vectors sorted by time, which can be represented as follows:  $X_T = [X_{T-(n-1)}, X_{T-(n-2)}, \dots, X_{T-1}, X_T]$ , where  $X_T$  is the set of the vessel's positions,  $T$  is the sequence number of a vessel set, which was received at a certain time,  $n$  is the predefined length of the set. The input vector  $X$  consists of the positioning elements of the vessel, such as the latitude, longitude, heading, speed, time, state reported by the vessel, weather conditions in the geographical location. We can describe the full input vector as a matrix:

$$X_T^p = \begin{bmatrix} X^1 \\ X^2 \\ \vdots \\ X^p \end{bmatrix} = \begin{bmatrix} X_{T-(n-1)}^1 & X_{T-(n-2)}^1 & \dots & X_{T-1}^1 & X_T^1 \\ X_{T-(n-1)}^2 & X_{T-(n-2)}^2 & \dots & X_{T-1}^2 & X_T^2 \\ \vdots & \vdots & \ddots & \vdots & \vdots \\ X_{T-(n-1)}^p & X_{T-(n-2)}^p & \dots & X_{T-1}^p & X_T^p \end{bmatrix},$$

Where  $p$  is the number of elements in the vessel's position vector. The output vector consists of the predicted distribution of probability classes of vessel types calculated by Softmax function. LSTM Deep Neural Network [2] with fully connected multilayer perceptron is used to train the model at work. The simplified network architecture is shown in Figure 1. The deep network architecture diagram shows a network structure consisting of 6 constituent layers. The first layer is input layer In with a number of inputs that equals to the length of the vessel's position sequence  $n$ . The input layer is connected in series to the first  $n$  cells from A1 to an in LSTM (A) layer. The LSTM layer may have more than  $n$  cells. The total number of cells is expressed in  $k$  when  $k = n$ . LSTM (A) layer is connected in series to the LSTM (B) layer. Each output of layer A is connected to Layer B inputs. The total number of cells in LSTM (B) is expressed in  $k$ . Both LSTM layers use ReLu activation function. The last cell in B is connected to the multilayer fully connected layer of perceptron. The layer of perceptron consists of two hidden layers of neurons and one output layer. The hidden layers use ReLu activation function. A number  $j$  of outputs constitutes an output layer where each output describes the probability of a particular class classification, which is calculated by Softmax function. Adam's stochastic optimizer with a training factor  $\alpha = 0.001$  and a decay factor  $\delta = 10^{-6}$  are used for network training. The termination of epoch training cycles is set in accordance with the validation set. The training uses the Sparse Categorical Cross Entropy [2] for loss function. **Data preparation:** Duplicate position entries are cleared out and then data is parsed based on desired data types. The same actions are performed to meteorological data. Technical data fields of a vessel are assigned to each position vector of a vessel based on vessel MMSI identifier. Meteorological data is assigned to a position data vector by using the method of the closest neighbor, depending on the closest time and geolocation of the forecast. Model train-

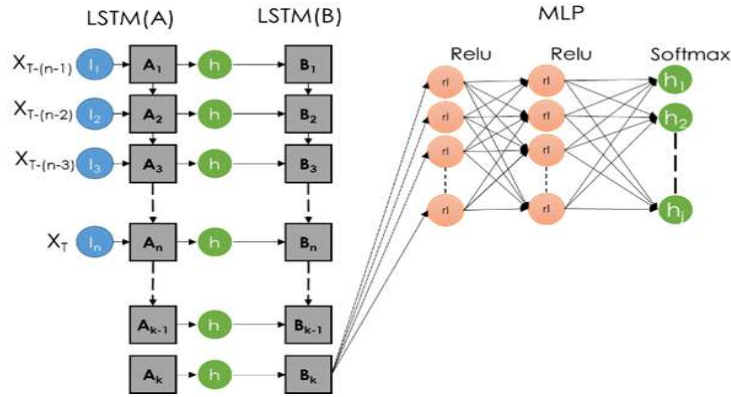


Figure 1: Multi-Stacked LSTM deep neural network architecture

ing data is formed by joining all the data to one vector. **Creation of Vector Sets:** After the preparation of data the vector sets that will be provided to train, validate and test the model, are further formed. The data sets must correspond to the model input matrix, which is described by formula above. To do this, the available vessel data is grouped by their MMSI identifier. All consecutive position of a vessel is cut in sequences of 12 positions by step of 3 positions. All these formed sequences are used to construct training matrix described in this article above.

### 3 Experiment and Results

To test proposed method Rotterdam harbour area was chosen. The data for model training are collected from several sources such as AIS vessel traffic monitoring system, vessel parameter information system, meteorological observation system, and geographic information system. This information comes from several data sources. The marine traffic data was collected from shipfinder.co: Collected data is: geolocation, speed, direction and type of vessel, length, width, draft, etc. The Meteorological data collected from worldweatheronline.com, provides meteorological data in given geolocations: wind direction and speed, wave, swell and other data of a particular location in 3h intervals. Two separate set was formed to test influence of meteorological data. One set with meteo data, another without. A total of  $2.90 * 10^7$  vessel traffic vectors were collected in one set from the Rotterdam harbour from November 1, 2018 till November 30, 2018, of which  $2.78 * 10^7$  do not have information about vessel type. This represents 95.88% of all available data. A set with vessel type information consists of  $1.195 * 10^6$  vessel traffic vectors from Rotterdam harbour. These vectors were collected and created using the methods mentioned above, and they constitute 4.12% of all data. The data are randomly divided into three sets: 50% of the data are used for training, 30% for validation, and 20% for testing. Training data set is used to train models. Validation Set - is designed to select the number of LSTM layers in the model and LSTM cells in the layer. The test set is used to evaluate accuracy of the final model. In this

Table 1: Trend of classification accuracy for different network settings

	Meteorological data excluded		Meteorological data included	
Layers	Cells	Accuracy	Cells	Accuracy
2	245	0.78	290	0.78
3	215	0.79	265	0.81
4	195	0.77	250	<u>0.93</u>

article precision, recall, and accuracy are calculated using a test set in order to evaluate the accuracy of the classifier for different numbers of deep multi-stacked LSTM neural network layers and cells. Table 1 first part shows the results of the experiment for different values of the model parameters without meteorological data. We see that the best result was achieved using 3 LSTM layers made of 215 cells. Table 1 second part shows the results of the experiment with meteorological data. Best result was achieved using 4 LSTM layers with 250 cells.

## 4 Conclusion

According to the results of the experiment, the proposed method of combining vessel traffic data with meteorological data leads to an improved classification. Based on the results the best model configuration is chosen, then checked using continued data with classification accuracy 0.93, recall 0.92, and precision 0.93.

## References

- [1] Alvarez A.A. et al. (2016). Mining Vessel Tracking Data for Maritime Domain Applications. *Data Mining Workshops (ICDMW), 2016 IEEE 16th International Conference*. pp. 361-367.
- [2] Ergen T., Kozat S.S. (2018). Online Training of LSTM Networks in Distributed Systems for Variable Length Data Sequences. *IEEE Transactions on Neural Networks and Learning Systems*. Vol. **29**. pp. 5159-5165.
- [3] Sun F., Deng Y., and Deng F. (2015). Unsupervised maritime traffic pattern extraction from spatio-temporal data. 11th International Conference on Natural Computation (ICNC). pp. 1218-1223.
- [4] Venskus J. et al. (2017) Integration of a self-organizing map and a virtual pheromone for real-time abnormal movement detection in marine traffic. *Informatica. Vilnius Universitetas*. Vol. **28**. pp. 359-374.
- [5] Zhen R., et al. (2017). Maritime Anomaly Detection within Coastal Waters Based on Vessel Trajectory Clustering and Naïve Bayes Classifier. *The Journal of Navigation*., pp. 1-23.

# ON SOME UPPER BOUNDS FOR NONCENTRAL CHI-SQUARE CDF

V.A. VOLOSHKO<sup>1</sup>, E.V. VECHERKO<sup>2</sup>

<sup>1,2</sup>*Research Institute for Applied Problems of Mathematics and Informatics  
Minsk, BELARUS*

e-mail: <sup>1</sup>valeravoloshko@yandex.ru, <sup>2</sup>vecherko@bsu.by

## Abstract

Some new upper bounds for noncentral chi-square cdf are derived from the basic symmetries of the multidimensional standard Gaussian distribution. The proposed new bounds have analytically simple form compared to analogues available in the literature, and may be useful both in theory and in applications: for proving inequalities related to noncentral chi-square cdf, and for bounding powers of Pearson's chi-squared tests.

**Keywords:** data science, noncentral chi-square distribution, upper bound

## 1 Introduction

Let  $d \in \mathbb{N}$ ,  $\mu = (\mu_i)_{i=1}^d \in \mathbb{R}^d$ ,  $\lambda = \|\mu\|^2 = \sum_{i=1}^d \mu_i^2$ . Then the cumulative distribution function (cdf) of the noncentral chi-square distribution with  $d$  degrees of freedom and noncentrality parameter  $\lambda$  is defined as follows:

$$f(x, d, \lambda) ::= \mathbf{P} \{ \|\xi - \mu\|^2 \leq x \}, \quad x \geq 0. \quad (1)$$

Here  $\xi \in \mathbb{R}^d$  is a standard normally distributed random  $d$ -vector. For the central chi-square cdf ( $\lambda = 0$ ) we use brief notation  $f(x, d) ::= f(x, d, 0)$ .

The function (1) plays an important role in mathematical statistics. In particular, consider the classical problem of statistical hypothesis testing of null-hypothesis  $H_0 : \mathcal{L}\{y_t\} = p = (p_i)_{i=1}^K$  against point alternative hypothesis  $H_1 : \mathcal{L}\{y_t\} = q = (q_i)_{i=1}^K$ , where  $\{y_t\}_{t=1}^T$  are  $T$  observed i.i.d. random variables. If the significance level  $\alpha \in (0, 1)$  is fixed, and  $H_1$  is contiguous to  $H_0$ , i.e.  $T \sum_{i=1}^K \frac{(p_i - q_i)^2}{p_i} \rightarrow \lambda > 0$  as  $T \rightarrow \infty$ , then the probability  $\beta$  of type II error of the standard Pearson's chi-squared test converges to the value (1) with  $d = K - 1$  and  $x = F_{\chi_d^2}^{-1}(1 - \alpha)$ . Hence the upper bounds for (1) provide the lower bounds for asymptotic power of chi-squared test under contiguous alternatives.

The function (1) is well studied analytically, being closely related to the generalized Marcum functions [1, 2] and modified Bessel function of the first kind [3]. Various upper and lower bounds for (1) are also available in the literature [1, 4]. These bounds, however, are analytically as complex as (1) itself, being based on complex transcendental functions like modified Bessel function [1] or the moments of truncated normal distribution [4]. We present here some new upper bounds for (1). These bounds are of a relatively simple analytical form and may be useful both in theory (proving inequalities related to (1)) and in applications (bounding powers of chi-squared tests).

## 2 Upper bounds for noncentral chi-square cdf

Since the value (1) is a standard Gaussian measure of a ball  $B_{\mu, \sqrt{x}}$  of radius  $\sqrt{x}$  with center  $\mu$ , our idea is to construct upper bounds of the form

$$f(x, d, \lambda) \leq \mathbf{P} \{ \xi \in A \}, \quad B_{\mu, \sqrt{x}} \subset A \subset \mathbb{R}^d. \quad (2)$$

Let  $\Pi_1, \Pi_2 \subset \mathbb{R}^d$  be orthogonally complemented subspaces. Minkowski sums  $A_i = B_{\mu, \sqrt{x}} + \Pi_i$  are cylindric sets containing  $B_{\mu, \sqrt{x}}$ . Due to properties of standard normal distribution, the events  $\xi \in A_i$  are independent and  $\mathbf{P} \{ \xi \in A_i \} = f(x, d_i, \lambda_i)$ , where  $d_i = \dim \Pi_i$  and  $\lambda_i$  is a squared norm of an orthogonal projection of  $\mu$  onto  $\Pi_i$ . The set  $A = A_1 \cap A_2$  in (2) leads to the following upper bound.

**Lemma 1.** *Let  $d = d_1 + d_2$ ,  $\lambda = \lambda_1 + \lambda_2$ ,  $\lambda_i \geq 0$ ,  $d_i \in \mathbb{N}$ ,  $i = 1, 2$ . Then the following inequality holds:*

$$f(x, d, \lambda) \leq f(x, d_1, \lambda_1) f(x, d_2, \lambda_2). \quad (3)$$

Since  $f(x, 1, \lambda) = \Phi \left| \frac{\sqrt{\lambda} + \sqrt{x}}{\sqrt{\lambda} - \sqrt{x}} \right|$ , where  $\Phi(\cdot)$  is the standard Gaussian cdf, we get from (3):

$$f(x, d, \lambda) \leq f(x, d-1) \cdot \Phi \left| \frac{\sqrt{\lambda} + \sqrt{x}}{\sqrt{\lambda} - \sqrt{x}} \right|. \quad (4)$$

Repeated application of (3) also gives the following bounds:

$$f(x, d, \lambda) \leq \left( \Phi \left| \frac{\sqrt{\lambda/d} + \sqrt{x}}{\sqrt{\lambda/d} - \sqrt{x}} \right| \right)^d, \quad (5)$$

$$f(x, d, \lambda) \leq \left( \Phi \left| \frac{\sqrt{x}}{-\sqrt{x}} \right| \right)^{d-1} \Phi \left| \frac{\sqrt{\lambda} + \sqrt{x}}{\sqrt{\lambda} - \sqrt{x}} \right|. \quad (6)$$

Another way to construct covering set  $A$  in (2) is based on unitary invariance of standard normal distribution. Namely, let us assume  $d \geq 2$ ,  $x \leq \lambda$ , and define  $A_1 = \{w \in \mathbb{R}^d : |||w|| - \sqrt{\lambda}| \leq \sqrt{x}\}$ ,  $A_2 = \{c \cdot w : c \geq 0, w \in B_{\mu, \sqrt{x}}\}$ . According to mentioned unitary invariance, the events  $\xi \in A_i$  are independent as well. It is easy to see that  $\mathbf{P} \{ \xi \in A_1 \} = f(\cdot, d) \left| \frac{(\sqrt{\lambda} + \sqrt{x})^2}{(\sqrt{\lambda} - \sqrt{x})^2} \right|$ , while  $A_2$  is a cone and  $\mathbf{P} \{ \xi \in A_2 \}$  equals normalized Lebesgue measure of a spherical ball  $A_2 \cap \mathbb{S}^{d-1}$  of radius  $\arcsin(\sqrt{x/\lambda})$  (in spherical metric). Hence we get:

**Lemma 2.** *The following inequality holds for  $d \geq 2$ ,  $x \leq \lambda$ :*

$$f(x, d, \lambda) \leq f(\cdot, d) \left| \frac{(\sqrt{\lambda} + \sqrt{x})^2}{(\sqrt{\lambda} - \sqrt{x})^2} \right| \cdot \frac{\Gamma(\frac{d}{2})}{\Gamma(\frac{d-1}{2})\sqrt{\pi}} \int_0^{\arcsin(\sqrt{x/\lambda})} (\sin \rho)^{d-2} d\rho. \quad (7)$$

Using the inequalities  $\mathbf{P} \{ \xi \in A_2 \} \leq \frac{1}{2}$ ,  $\Gamma(z + \frac{1}{2})/\Gamma(z) \leq \sqrt{z}$ ,  $z > 0$ , and

$$\int_0^{\rho_*} (\sin \rho)^{d-2} d\rho \leq \int_0^{\rho_*} (\sin \rho)^{d-2} \frac{d \sin \rho}{\cos \rho_*} = \frac{(\sin \rho_*)^{d-1}}{(d-1) \cos \rho_*},$$

we obtain a weakened version of (7) having more explicit form:

$$f(x, d, \lambda) \leq f(\cdot, d) \Big|_{(\sqrt{\lambda}+\sqrt{x})^2}^{(\sqrt{\lambda}-\sqrt{x})^2} \cdot \min \left\{ \frac{1}{2}, \sqrt{\frac{(x/\lambda)^{d-1}}{2\pi(d-1)(1-x/\lambda)}} \right\}, \quad d \geq 2, \quad x \leq \lambda. \quad (8)$$

For even  $d$  the bound (7) has completely explicit form since central chi-square pdf is integrable.

**Corollary 1.** *The following inequalities hold for  $x \leq \lambda$ :*

$$f(x, 2, \lambda) \leq \frac{2}{\pi} e^{-\frac{1}{2}(\lambda+x)} \sinh(\sqrt{\lambda x}) \arcsin(\sqrt{x/\lambda}), \quad (9)$$

$$f(x, 4, \lambda) \leq \frac{2}{\pi} e^{-\frac{1}{2}(\lambda+x)} \left( \left( 1 + \frac{\lambda+x}{2} \right) \sinh(\sqrt{\lambda x}) - \sqrt{\lambda x} \cosh(\sqrt{\lambda x}) \right) \\ \times \left( \arcsin(\sqrt{x/\lambda}) - \lambda^{-1} \sqrt{x(\lambda-x)} \right). \quad (10)$$

Combining (3) with (9), we get the following bounds for even  $d = 2k$  and  $x \leq \lambda/k$ :

$$f(x, 2k, \lambda) \leq e^{-\frac{1}{2}(\lambda+kx)} \left( \frac{2}{\pi} \sinh(\sqrt{\lambda x/k}) \arcsin(\sqrt{kx/\lambda}) \right)^k, \quad (11)$$

$$f(x, 2k, \lambda) \leq \frac{2}{\pi} e^{-\frac{1}{2}(\lambda+kx)} \sinh^{k-1}(x) \sinh(\sqrt{\lambda_* x}) \arcsin(\sqrt{x/\lambda_*}), \quad (12)$$

where  $\lambda_* = \lambda - (k-1)x$ . The bounds similar to (11), (12) can be obtained from (10) for  $d = 4k$ .

### 3 Computer experiments

The four plots on the Figure 1 illustrate the upper bounds for (1) proposed in the paper. On the plots A, B and D we see that the corresponding upper bounds are strictly ordered for the chosen  $d$  and  $\lambda$ . This observation allows us to formulate the following.

**Conjecture 1.** *The upper bounds for (1) are ordered as follows:*

1. “(6)≤(5)” for any  $x \geq 0$ ,  $d \in \mathbb{N}$ ,  $\lambda \geq 0$ ;
2. “(11)≤(12)” for any  $0 \leq x \leq \lambda/k$ ,  $d = 2k$  (even),  $\lambda \geq 0$ ;
3. “(10)≤(6)≤(11)” for any  $0 \leq x \leq \lambda/2$ ,  $d = 4$ ,  $\lambda \geq 0$ .

The inequality “(4)≤(6)” is not included in Conjecture 1, because it obviously follows from (5). The plot C allows to conjecture that for  $d \geq 2$  the upper bound (8) is better than (4) for small  $x \leq x_*$  up to some  $x_* \leq \lambda$ , and vice versa for  $x_* \leq x \leq \lambda$ .

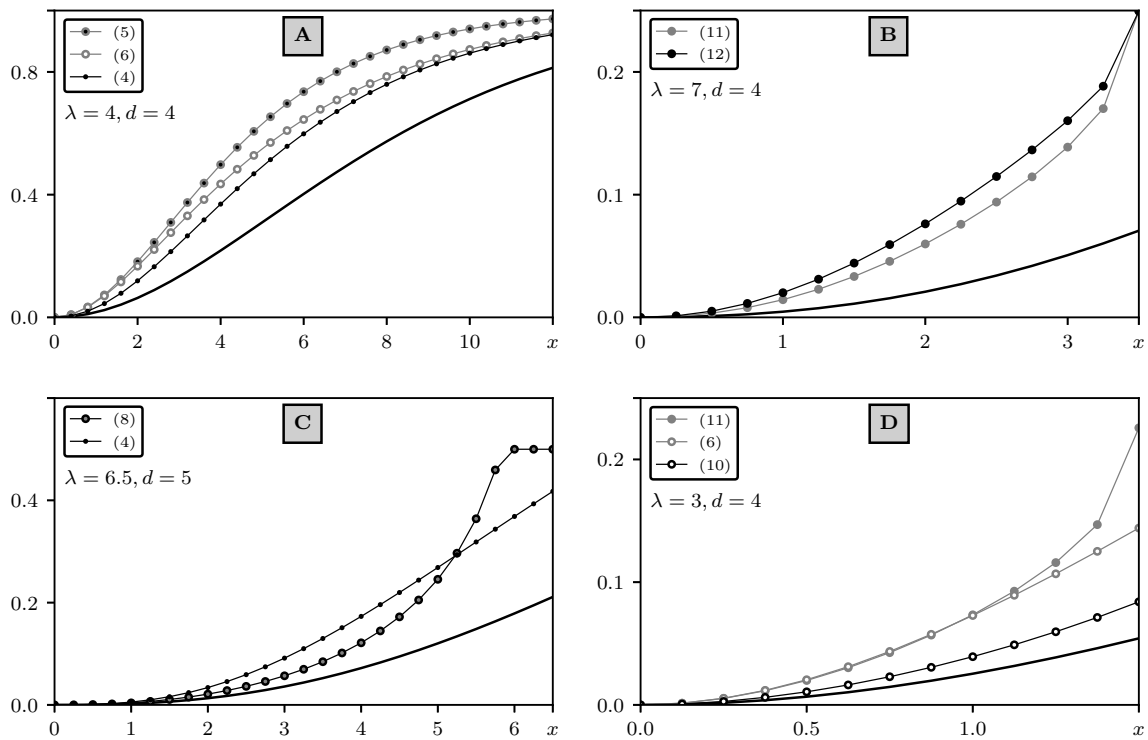


Figure 1: Noncentral chi-square cdf (1) (lower black lines) and its upper bounds (upper broken lines)

## References

- [1] Segura J. (2014). Monotonicity Properties and Bounds for the Chi-square and Gamma Distributions. *Applied Mathematics and Computation*. Vol. **246**, pp. 399-415.
- [2] Andras Sz., Baricz A., Sun Y. (2011). The Generalized Marcum Q-function: an Orthogonal Polynomial Approach. *Acta Universitatis Sapientiae, Mathematica*. Vol. **3**, Num. **1**, pp. 60-76.
- [3] Bateman H., Erdelyi A. (1953). *Higher Transcendental Functions, Vol. 2*. McGraw-Hill, New York.
- [4] Cook J.D. (2010). Upper Bounds on Non-central Chi-squared Tails and Truncated Normal Moments. *UT MD Anderson Cancer Center Department of Biostatistics Working Paper Series*. Working Paper **62**, pp. 1-4.

# NON-ASYMPTOTIC CONFIDENCE ESTIMATION OF THE AUTOREGRESSIVE PARAMETER IN AR(1) PROCESS WITH AN UNKNOWN NOISE VARIANCE

S.E. VOROBAYCHIKOV, YU.B. BURKATOVSKAYA  
*Tomsk State University, Tomsk Polytechnic University*  
*Tomsk, RUSSIA*  
e-mail: sev@mail.tsu.ru, tracey@tpu.ru

## Abstract

The paper considers the problem of estimating the autoregressive parameter in the first-order autoregressive with Gaussian noises, when the noise variance is unknown. We propose the non-asymptotic technique for compensating the unknown variance, and then, for constructing an estimator. The results of Monte-Carlo simulations are given.

**Keywords:** data science, confidence estimation, autoregression

## 1 Introduction

The problem of estimation with prescribed accuracy of the parameter of first-order autoregressive process was considered in [1]. An approach on the base of sequential analysis with a special choice of stopping time was proposed. The mean square accuracy of the estimator was determined by the parameter of the procedure. To construct this estimator, one needs to know the variance of the noises. In paper [3], authors proposed a two-stage procedure to construct the estimator of an unknown parameter if the noise variance is unknown. The first stage is used to obtain the upper bound of the variance. It should be noted that if the absolute value of the autoregressive parameter is close to unity then the estimate [3] exceeds manifold the variance. It implies increasing of estimation time.

In [2], a modification of the sequential estimation procedure ([1]) was proposed. It allows one to obtain an estimator of the autoregressive parameter with non-asymptotic Gaussian distribution. We propose to use this estimator to construct a modified two-stage estimation procedure for AR(1) process with unknown noise variance.

## 2 Problem statement

Consider the first-order autoregressive model AR(1) defined as follows:

$$x_k = \theta x_{k-1} + b\varepsilon_k, \varepsilon_k \text{ i.i.d. } \mathcal{N}(0, 1), k = 1, 2, \dots \quad (1)$$

where  $\theta$  and  $b$  are unknown real parameters. The problem is to construct an estimator for  $\theta$  with a prescribed mean-square deviation on the basis of observations  $\{x_k\}$ .

### 3 Two-stage sequential point estimator

We propose a modified two-stage procedure to estimate parameter  $\theta$  in model (1). At the first stage, we construct the following statistics to compensate the unknown noise variance

$$\Gamma_l(h) = \frac{h}{2(l-2)} \sum_{i=1}^l \left( \hat{\theta}_{2i}(h) - \hat{\theta}_{2i-1}(h) \right)^2. \quad (2)$$

We use here as  $\{\hat{\theta}_j(h)\}$  the improved sequential point estimates proposed in [2]. These estimates represent a special modification of the least squares (maximum likelihood) estimates. For each  $h > 0$  we introduce the sequence of stopping instances

$$\tau_j = \tau_j(h) = \inf \left\{ n \geq 1 : \sum_{k=\tau_{j-1}+1}^n x_{k-1}^2 \geq h \right\}, \quad \tau_0 = 0, \quad (3)$$

and define the sequence of sequential estimates by the formula

$$\hat{\theta}_j(h) = \frac{1}{\tilde{h}_j} \sum_{k=\tau_{j-1}+1}^{\tau_j} \sqrt{\beta_k} x_{k-1} x_k, \quad (4)$$

where  $\beta_k = 1$  if  $k < \tau_j$  and  $\beta_{\tau_j} = \alpha_{\tau_j}$ ,  $\alpha_{\tau_j}$  is the correction factor,  $0 < \alpha_{\tau_j} \leq 1$ , uniquely defined by the equation

$$\sum_{k=\tau_{j-1}+1}^{\tau_j-1} x_{k-1}^2 + \alpha_{\tau_j} x_{\tau_j-1}^2 = h,$$

and

$$\tilde{h}_j = \sum_{k=\tau_{j-1}+1}^{\tau_j} \sqrt{\beta_k} x_{k-1}^2.$$

According to [2],

$$m_j(h) = \frac{\tilde{h}_j}{\sqrt{h}} (\hat{\theta}_j(h) - \theta)$$

has Gaussian distribution  $N(0, b^2)$ , which, together with the inequality  $\tilde{h}_j \geq h$  let one to construct the confidence interval for  $\hat{\theta}_j(h) - \theta$  if  $b^2$  is known. Besides,  $\{m_j(h)\}$  are independent. It allows us to use  $\Gamma_l(h)$  as an estimator for  $b^2$  in model (1).

At the second stage, we construct an estimator for parameter  $\theta$ . First, we introduce a stopping time

$$\tau = \tau(H) = \inf \left\{ n \geq 1 : \sum_{k=\tau_{2l}+1}^n \frac{x_{k-1}^2}{\Gamma_l(h)} \geq H \right\} \quad (5)$$

and define a sequential estimator by the following formula

$$\hat{\theta}(h, l, H) = \frac{1}{\tilde{H}} \sum_{k=\tau_{2l}+1}^{\tau} \sqrt{\beta_k} \frac{x_{k-1} x_k}{\Gamma_l(h)}, \quad (6)$$

where  $\beta_k = 1$  if  $k < \tau_j$  and  $\beta_\tau = \alpha_\tau$ ,  $\alpha_\tau$  is the correction factor,  $0 < \alpha_\tau \leq 1$ , uniquely defined by the equation

$$\sum_{k=\tau_{2l}+1}^{\tau-1} \frac{x_{k-1}^2}{\Gamma_l(h)} + \alpha_\tau \frac{x_{\tau-1}^2}{\Gamma_l(h)} = H,$$

and

$$\tilde{H} = \sum_{k=\tau_{2l}+1}^{\tau} \sqrt{\beta_k} \frac{x_{k-1}^2}{\Gamma_l(h)}.$$

Note that, at the first stage, the parameter  $h$  can be small compared with  $H$ . As for the parameter  $l$ , according to [3], it should be not less than 3, to provide the limited expectation of the multiplier  $1/\Gamma_l(h)$ . However, we recommend to take  $l \geq 10$ , which makes estimator (2) more stable, even if we use small values of  $h$ .

**Theorem 1.** *The stopping instant (5) is finite with the probability one; the mean square deviation of estimator (6) is bounded from above*

$$E \left( \hat{\theta}(h, l, H) - \theta \right)^2 \leq \frac{1}{H}. \quad (7)$$

## 4 Simulation results

In this section, we report and discuss the results of Monte Carlo experiments. Selected data obtained by the simulations are tabulated in Table 1. For our study, we set  $\theta = 0.1, 0.3, 0.5, 0.7, 0.9, 0.99$ . For each  $\theta$ , 100 replications were run. The quantities recorded in Table 1 are:  $h$  – threshold in the sequential sampling rule at the first stage;  $H$  – threshold in the sequential sampling rule at the second stage;  $\theta$  – the autoregressive parameter;  $\Gamma$  – the mean estimator for the parameter  $b^2$  obtained at the first stage;  $\tilde{\theta}$  – the mean estimator for the parameter  $\theta$  obtained at the second stage;  $\tilde{\sigma}^2$  – the mean square deviation for  $\tilde{\theta}$ ;  $N_1$  and  $N_2$  – the mean numbers of observations at the first and at the second stages, correspondingly. The noise variance  $b^2 = 0.81$  in all cases. We also compared our results with the estimator described in [3], here  $D$  – the mean estimator for the parameter  $b^2$  obtained at the first stage;  $\hat{\theta}$  – the mean estimator for the parameter  $\theta$  obtained at the second stage;  $\hat{\sigma}^2$  – the mean square deviation for  $\hat{\theta}$ ;  $T$  – the mean number of observations at the second stage; at the first stage, the number of observation was always taken equal to  $N_1$ . The threshold parameter of the procedure is equal to  $H$ .

The simulation demonstrates, that, for both procedures, the estimators of  $\theta$  are in good agreement with the real value of the parameter; the mean square deviation is about  $1/H$ , as Theorem 1 states. But the estimators of the noise variance  $b^2$  behave differently: for our algorithm, they are in the interval  $[0.78, 1.1]$ , while the real value is 0.81; for the algorithm described in [3], the interval is  $[0.85, 180.7]$ , so, the estimator exceeds the real value more than 200 times if the autoregressive parameter is close to the bound of the stability region. It implies the grows of the number of observations in the same proportion. If the autoregressive parameter is close to zero then estimator [3]

Table 1: Parameter estimation for AR(1) (the noise variance 0.81)

$h$	$H$	$\theta$	$\Gamma$	$\hat{\theta}$	$\hat{\sigma}^2$	$N_1$	$N_2$	$D$	$\hat{\theta}$	$\hat{\sigma}^2$	$T$
50	500	0.1	0.848	0.102	0.0016	1239	516	0.923	0.113	0.0008	522
50	500	0.3	0.969	0.297	0.0020	1174	540	0.915	0.297	0.0011	535
50	500	0.5	1.069	0.492	0.0025	965	501	1.082	0.499	0.0014	505
50	500	0.7	1.085	0.706	0.0020	675	341	1.603	0.704	0.0010	501
50	500	0.9	1.068	0.894	0.0026	259	128	4.459	0.899	0.0003	534
50	500	0.99	0.782	0.998	0.0017	40	12	180.7	0.989	3.9612	2380
100	1000	0.1	1.069	0.095	0.0010	3467	1306	0.822	0.102	0.0010	1000
100	1000	0.3	1.065	0.300	0.0009	2275	1205	0.887	0.304	0.0010	1003
100	1000	0.5	1.010	0.497	0.0011	1876	939	1.081	0.499	0.0011	1008
100	1000	0.7	0.968	0.701	0.0011	1279	616	1.592	0.703	0.0005	998
100	1000	0.9	0.990	0.897	0.0012	505	240	4.465	0.901	0.0002	1047
100	1000	0.99	0.765	0.998	0.0008	65	25	147.4	0.990	1.4631	3622

slightly outperforms estimator (6); the number of observations  $T$  is less than  $N_2$  for about 25-30 per cent (1000 vs 1306).

So, our procedure can be used for the estimation of the autoregressive parameter in AR(1). It should be noted that it can be applied even if the process is not stable, unlike estimator [3].

## Acknowledgement

This study was supported by The Ministry of Education and Science of the Russian Federation, Goszadanie No 2.3208.2017/4.6

## References

- [1] Borisov V.Z., Konev V.V. (1977). On sequential parameter estimation in discrete time processes. *Automat. Remote Control*. Vol. **38**, pp. 58-64.
- [2] Konev V.V., Vorobeychikov S.E. (2017). Non-asymptotic confidence estimation of the parameters in stochastic regression models with Gaussian noises. *Sequential Analysis – Design Methods and Applications*. Vol. **36**, pp. 55-75.
- [3] Dmitrienko A.A., Konev V.V. (1994). On a Guaranteed Estimation of Autoregressive Parameters for an Unknown Variance of Noise. *Automat. Remote Control*. Vol. **55**, pp. 218-228.

# A GENERALIZED PROBABILISTIC MODEL OF COMPUTER PROOF OF THE ARTIN HYPOTHESIS

G. VOSTROV, R. OPIATA

*Odessa national polytechnic university*

*Odessa, UKRAINE*

e-mail: [vostrov@gmail.com](mailto:vostrov@gmail.com), [roma.opyata@gmail.com](mailto:roma.opyata@gmail.com)

## Abstract

The analysis of the probabilistic approach to solving the problem of the distribution of primes in the generalized Artin's hypothesis is given. The foundations of a computer approach to solving problems in the field of pure and applied number theory are formulated. On the basis of the generalized Artin's hypothesis, it is shown how probabilistic methods of nonlinear dynamic systems can be obtained with sufficiently accurate solutions.

**Keywords:** data science, Artin hypothesis, computer proof

## 1 Introduction

An important problem in the theory of numbers is the description of the law of the distribution of primes. This problem was solved by Hadamard and Valle-Poussin, independently of each other, in 1896 [1]. They proved that the number of primes ( $\pi(x)$ ) is less than or equal to  $x$  is determined by the expression:

$$\pi(x) = \int_2^x \frac{dt}{\ln t} + O\left(xe^{-\frac{c}{2}\sqrt{\ln x}}\right) \quad (1)$$

where  $c$  is an absolute constant. This analytically proved form of representation of the law of distribution of prime numbers has already become universally recognized in the mathematical world. Yet two things should be noted. First, it was obtained on the basis of the analytic zeta-Riemann function, which, until it is proved, adequately describes the distribution of primes in a complex space. According to the Riemann hypothesis, all the zeros of the zeta function are on the line passing through the point equal to  $1/2$ . This millennium hypothesis has not yet been proved. And this fact is the basis for criticizing all the results obtained on the basis of the zeta-Riemann function.

The second circumstance is that simultaneously with this fact the dynamics of the change of  $O\left(xe^{-\frac{c}{2}\sqrt{\ln x}}\right)$  [2] is investigated. In [1, 5], an estimate of the entropy of this estimate is obtained and it is proved that it is fractal in nature. These facts are the basis for the formation of proposals on the need to study other models for the distribution of prime numbers. Another problem related to the distribution of prime numbers appeared in 1927, when the well-known mathematician Artin formed a hypothesis about the distribution of prime numbers for which the natural number  $a > 1$  is given is their primitive root [1, 5].

According to the Artin conjecture [5], the set of such prime numbers has the distribution law  $\pi(x, a)$  in the form of the expression:

$$\pi(x, a) = c(a)\pi(x) \quad (2)$$

where  $\pi(x)$  is the distribution of primes, and  $c(a)$  is a constant depending on  $a$ . So far, despite numerous studies, this hypothesis has not been resolved. At the same time, it is not known whether this is true for any values of  $a$ . If the hypothesis is correct, the question remains how to evaluate the constant  $c(a)$  for each particular  $a$  and what properties of the number  $a$  affect its value. Answers to these questions are still lacking. In [1, 5] a detailed analysis of all research results in the field of the Artin hypothesis solution is given.

It should be noted that the proof of Artin's hypothesis is important both from a theoretical point of view in number theory, and from an applied rehenium point, because its positive solution is important in cryptography, coding theory, and the theory of dynamical systems. In [6], a generalized Artin hypothesis was formed for any  $a > 1$ , i.e. and at the same time  $a$  may not be a primitive root. According to Artin's generalized theory, the following equality is true:

$$\pi(x, a, i) = c(a, i)\pi(x) \quad (3)$$

where  $a > 1$ ,  $i$  is the index of the subgroup of the group  $(Z/pZ)^*$  of primes in the classification of prime numbers generated by the numbers  $a$ ,  $c(a, i)$  is a constant. According to the classification built in [6]:

$$\mathcal{P}(a, i) = \left\{ p \in \mathcal{P} \mid \frac{(p-1)}{\text{card}_a(p)} = i \right\} \quad (4)$$

where  $\text{card}_a(p)$  is the length of the recursion  $x_{n+1} \equiv ax_n \pmod{p}$  at  $x_0 = 1$ ,  $\mathcal{P}$  is the set of all primes.

It is not difficult to show that for any  $a > 1$  the equality:

$$\sum_{i=1}^{\infty} c(a, i) = 1 \quad (5)$$

This means that primes are evenly distributed in classes  $\mathcal{P}(a, i)$  for any  $a$ . By uniformity is meant that within each class of primes  $\mathcal{P}(a, i)$  a logarithmic law of the distribution of primes is preserved. The constant  $c(a, i)$  determines the measure of puncturing prime numbers based on the value  $a$ . If  $i = 1$  then  $a$  is the primitive root of all primes  $\mathcal{P}(a, 1)$ . For an arbitrary natural number  $x$ , the equality:

$$\pi(x, a, i) = c(a, i, x)\pi(x) \quad (6)$$

Moreover, if  $x \rightarrow \infty$ , then  $c(a, i, x)$  tends to the limit value  $c(a, i)$ . If we put  $i = 1$  then  $c(a, 1)$  will be Artin's constant for primitive roots. In this case  $a \neq \pm 1$ , and  $a \neq k^2$  for none  $k \in N$ . This is true according to Fermat's theorem [3,4]. Wherein,  $a$  is the primitive root of the group of residues  $(Z/pZ)^*$  for any  $p \in \mathcal{P}$  such that:

$$\mathcal{P}(a, 1) = \left\{ p \in \mathcal{P} \mid \frac{(p-1)}{\text{card}_a(p)} = 1 \right\} \quad (7)$$

It is important to investigate the classes of primes  $\mathcal{P}(a, i)$  for  $i > 1$  since in this case the positive integer  $a$  will be the primitive root for the subgroups of the group  $(Z/pZ)^*$  with the index defined by the relations:

$$\mathcal{P}(a, i) = \left\{ p \in \mathcal{P} \mid \frac{(p-1)}{\text{card}_a(p)} = \text{ind}_a(p) \right\} \quad (8)$$

where  $\text{ind}_a(p) = i$  is the index of the subgroup of  $(Z/pZ)^*$ . The classes of primes  $\mathcal{P}(a, i)$  have not yet been studied and the distribution of primes in these classes is not known. In [1], an assumption was made that  $\mathcal{P}(a, i)$  at  $i > 1$  is proportional to  $\mathcal{P}(a, 1)$  with a factor of  $1/i^2$ . Since  $i > 1$  is considered, in this case it is important to know the distribution of prime numbers for the value  $a = k^2$ . This is an important generalization of Artin's hypothesis. At the same time, the probability of:

$$P(p \in \mathcal{P}(a, i)) = \left\{ p \in \mathcal{P} \mid \frac{|\mathcal{P}(a, i)|}{|\mathcal{P}|} = c(a, i) \right\} \quad (9)$$

membership agrees exactly with the provisions of the theory of probability, and therefore, estimating  $c(a, i)$  on the basis of successive statistical tests and the law of large numbers is parity.

The determination of  $c(a, i)$  for any  $a, i$  using analytical methods is unlikely in the near term. However, the formation and development of experimental mathematics [1, 2] opens up another way to solve this problem by using computer simulation of nonlinear dynamic processes for the formation of classes of prime numbers.

## 2 Modeling of dynamic processes of distribution of simple numbers in the generalized artin hypothesis

The process of modeling the distribution of primes in classes  $\mathcal{P}(a, 1), \mathcal{P}(1, 2), \dots, \mathcal{P}(a, k)$  was reduced to choosing a set of consecutive primes from a set of a sufficiently large sample of these classes. The number of primes analyzed at each interval of natural numbers was chosen to be 500,000. This choice was largely due to the fact that it was previously established that reducing this value leads to more significant fluctuations in estimates, although convergence to the limit over the entire set of any intervals, even if they are not placed consistently, has the same character.

The process of statistical testing of  $p \rightarrow \mathcal{P}$  primes for checking their belonging to class  $\mathcal{P}(a, i)$  was reduced to calculating for the selected number  $p$  the recursive procedure  $x_0 = 1, x_{n+1} = ax_n \pmod{p}$  until the pairs  $ax_l \equiv 1 \pmod{p}$  were reached at some step  $i$ . Then  $\text{card}_a(p) = i$  and according to Fermat's theory and the cyclic group theorem the number  $p - 1$  is divisible by  $i$  and then  $\text{ind}_a(p) = (p - 1)/\text{card}_a(p) = i$ , and therefore  $p \in \mathcal{P}(a, i)$  and if  $i = 1$ , then  $a$  is the primitive root of the cyclic group  $(Z/pZ)^*$ , and otherwise it is the primitive root of some subgroup. At  $i > 1$ , we obtain the primitive roots of the subgroups of the  $(Z/pZ)^*$  residue group with the index  $i > 1$ .

The study of the distribution law of prime numbers  $p$  on their belonging to  $\mathcal{P}(a, i)$  had the character of consistent statistical tests on the set of natural numbers contain-

ing the first 500,000 primes. At the first stage, primes  $p$  were chosen from the set  $p_1, \dots, p_{500000}$ . With this  $x = p_{500000}$ .

For each  $n \in \{2, \dots, x\}$ , we had to solve two problems: check  $n$  for simplicity, and if  $n = p \in \mathcal{P}$ , then  $p - 1$  was decomposed into simple factors, i.e. systematically solved two non-simple problems of checking numbers for simplicity and decomposition into simple factors. An effective algorithm for solving them was created based on probabilistic methods in the theory of elliptic curves.

As a result of analyzing  $a \in \{2, \dots, x\}$ ,  $\mathcal{P}(a, 1), \dots, \mathcal{P}(a, l)$  sets were obtained for some  $l < x$  and absolutely exact values of their powers were calculated, i.e.  $|\mathcal{P}(a, 1)|, \dots, |\mathcal{P}(a, l)|$ , and then estimates of  $c(a, 1) = \frac{|\mathcal{P}(a, 1)|}{\pi(x)}, \dots, c(a, l) = \frac{|\mathcal{P}(a, l)|}{\pi(x)}$  were obtained.

At the next stage, work was also carried out for primes from the interval as  $\{p_{500001}, \dots, p_{1000000}\}$  interval and the values of the  $c(a, 1), \dots, c(a, l)$  constants were calculated using the same scheme. At the same time  $l$  increases. The  $\{p_1, \dots, p_{500000}\}$  and  $\{p_{500001}, \dots, p_{1000000}\}$  sequences were combined, and the estimates of the generalized Artin constants were again calculated and the process of their refinement was studied on the basis of the theory of large numbers in probability theory. This procedure continued until  $x = p = 179424673$  and this is a ten million prime numbers. It was found that  $c(a, 1), \dots, c(a, k)$  in probability converges to some values, the exact values of which are irrational and possibly transcendental numbers. In the process of estimating the  $c(a, i)$  constants, two important theorems were proved:

**Theorem 1.** *For any  $a \in \{2, 3, \dots, k, \dots\}$  that is not a square, i.e.  $a \neq k^2$  The number of non-empty classes of primes tends to infinity at  $x \rightarrow \infty$ .*

**Theorem 2.** *For any  $a \in \{2, 3, \dots, k, \dots\}$  that is not a square, i.e.  $a \neq k^2$  The number of prime numbers in  $\mathcal{P}(a, i)$  tends to infinity at  $x \rightarrow \infty$ .*

These theorems are the basis of the convergence of a sequence of statistical tests to marginal values. Since for any  $x \in N$  it is obvious that  $\bigcup_{i=1}^k \mathcal{P}(a, i) = \pi(x)$  and

$\mathcal{P}(a, i) \cap \mathcal{P}(a, j) = \emptyset$  at  $i \neq j$ , it follows from this that  $\sum_{i=1}^k c(a, i) = 1$  and this is

true for all values of  $x \rightarrow \infty$ . The review [5] provides an estimate of  $c(2, 1)$ , which is identified by  $c(2, 1)$  in our sense, but  $c(2, 1)$  differs from the estimate of  $c(2, 1)$  starting from the fifth decimal place and this is a theoretical error of the survey works.

For different  $a \in \{2, 3, 5, 6, 7, 8, 10, 11\}$ , the behavior of the  $c(a, i)$  constants is complex group-theoretic and number-theoretic. The study of their dynamic properties is beyond the scope of this work. It should be noted that the results of computer simulation of the processes of distribution of primes are calculated with an accuracy of the eleventh decimal place for estimates of  $c(2, 1), c(3, 1), c(5, 1), c(6, 1), \dots$  values. This cannot be asserted for classes by the  $i \geq 2$  index. To achieve the same accuracy with  $i \geq 2$ , it is necessary to significantly increase the number of prime numbers. With an increase in the  $i$  class index  $\mathcal{P}(a, i)$  more than three requirements and the volume of the analyzed primes increases in accordance with the unexplored laws.

### 3 Statistical analysis of the distribution of prime numbers in classes

Probability-theoretic interpretation of the constant  $c(a) = \frac{\pi(x,a)}{\pi(x)}$  at  $x \rightarrow \infty$ . Consider the probability space  $(\Omega, F, P)$  based on  $\Omega = \{\omega_1, \dots, \omega_n, \dots\} = \{p_1, \dots, p_n, \dots\}$ . Obviously at  $x \rightarrow \infty$  the numbers are  $\pi(x) \rightarrow \infty$ ,  $\pi(x, a) \rightarrow \infty$ , but  $\pi(x, a) = |\mathcal{P}(a, 1, x)|$ ,  $\pi(x) = |\mathcal{P}(x)|$ ,  $c(a, 1, x) = \frac{|\mathcal{P}(a, 1, x)|}{|\mathcal{P}(x)|}$  and at  $x \rightarrow \infty$  it is obvious that  $\frac{|\mathcal{P}(a, 1, x)|}{|\mathcal{P}(x)|} \rightarrow c(a, 1)$  is where  $x \in \mathcal{P}$ ,  $\mathcal{P} \rightarrow \infty$ ,  $\mathcal{P}(a, i, x) = \left\{ p | p \leq x \& \frac{(p-1)}{\text{card}_a(p)} = i \right\}$  is at  $x \rightarrow \infty$   $\mathcal{P}(a, i, x) \rightarrow \mathcal{P}(a, i)$ . Thus  $c(a) = \lim_{x \rightarrow \infty} \frac{\pi(x,a)}{\pi(x)}$ .

It follows from Artin's hypothesis that with  $c(a, 1)$  there is precisely the probability of a random event  $\mathcal{P}(a, 1)$  consisting of a choice of  $\Omega = \{p_1, \dots, p_n, \dots\}$  of a prime number  $p$  for which  $a$  is an original root of the cyclic group  $(Z/pZ)^*$ . To estimate this probability, the law of large numbers and the method of successive statistical tests were used. The essence of the method is that the first test group was reduced and calculated for  $\{p_1, p_2, \dots, p_{500000}\}$  for each  $a \in \{2, 3, \dots, 16\}$  evaluation of the values of  $c(a, i, x)$  at  $x = p_{500000}$  for all possible values of  $i \in \{1, 2, \dots, k, \dots\}$ , that is,  $\tilde{c}_1(a, 1, x), \dots, \tilde{c}_1(a, k, x), \dots$  was calculated on the next iteration, the same tests were performed for the second iteration on the set  $\{p_{500001}, \dots, p_{1000000}\}$ .  $\tilde{c}_1(a, 1, x), \dots, \tilde{c}_k(a, 1, x), \dots$  Estimates were obtained at the same time  $\tilde{c}_1(a, 1, x), \dots, \tilde{c}_k(a, k, x), \dots$ , provided that the first and second samples were combined and computed values and were determined by  $|\tilde{c}(a, i, x) - \tilde{c}(a, k, x)| \leq \varepsilon$  for all  $x$ . The main focus was on  $c(a, 1, x)$ . As a result of some iterations, it was found that for all  $a$  the estimates obtained:

$$\mathcal{P}(x) = \{p | p \leq x\} \tag{10}$$

$$\mathcal{P}(a, i, x) = \left\{ p | p \leq x \& \frac{(p-1)}{\text{card}_a(p)} = i \right\} \tag{11}$$

the order of the cyclic group of the subgroup  $(Z/pZ)^*$ . If  $l = p-1$ , then  $a$  is an original root, and if  $l < p-1$  is the original form of the  $c(a)$  Artin measure,  $c(a, i)$  is a measure of classes by  $\mathcal{P}(a, i)$  in  $\mathcal{P}$ . At that  $c(a, i) = \frac{|\mathcal{P}(a, i)|}{|\mathcal{P}|}$  and  $\sum_{i=1}^{\infty} c(a, i) = 1$ .

This applies only to classes with indexes  $i = 1$ . For  $i \geq 2$  it is necessary to increase the number of statistical tests. This is naturally due to the fact that the classes  $\mathcal{P}(a, i, x)$  for  $i \geq 2$  from numerical theorems contain less than prime numbers. In [1] it is stated that this decrease should be of the order of  $1/i^2$ , but this is an erroneous assertion. The degree of decline essentially depends on the properties of  $a$  and requires a separate study. Case  $a \in \{4, 9, 16\}$  requires separate investigations, because these numbers cannot be primitive roots of that number  $p$ , in accordance with the Fermat theorem [3]. cannot be generating elements of groups  $(Z/pZ)^*$ . However, they are generating elements of the subgroups of the group  $(Z/pZ)^*$  with even indices. All classes with odd indices are empty sets. Table 1 shows the constants for  $c(a, 1)$  for all  $a$  except  $\{4, 9, 16\}$ . Analysis of the table. The table contains over a thousand

columns. The analysis of these data is numerically theoretical and group-specific and goes beyond the scope.

The simulation process of the dynamics of the formation of prime numbers was constructed on the following assumptions. Suppose that an ordered set of prime numbers  $\mathcal{P} = \{p_1, p_2, \dots, p_k, \dots\}$  is given, whose elements are ordered in ascending order. All this set was split into a subset of 500,000 primes. The number of 500,000 is due to the limitations of MS Excel, as a statistical analysis tool, on a number of characteristics of the process of generating prime numbers. Only one restriction is important. We always select 500,000 consecutive primes of the set  $\mathcal{P}$ . In the current version of Excel, this number can be increased to one million. If you use a powerful computer, you can choose a larger number instead of a million.

The implemented version of the study of dynamic processes for the formation of primes includes the following indicators: the number of a simple number in the  $p$  in the ordered set of  $\mathcal{P}$ , the value of a simple number of  $p$ , the value of the recursion length of the numbers  $card_a(p)$  at the same value of  $a$  for all prime numbers  $\mathcal{P}$ , the index  $ind_a(p)$  of the index of the class,  $ind_a(p) = \frac{(p-1)}{card_a(p)}$ , the value of the residues modulo any natural module  $n > 1$ , for all classes and any other analytic properties of primes or factors of the decomposition of the number of  $p - 1$  into simple factors. For each simple multiplier  $p_i$  in the  $p - 1 = \prod_{i=1}^n p_i^{a_i}$  decomposition, one parameter of the dynamic process of generating primes is presented, with separate indicators that can be analyzed for any other indicators, the values for them are deducted by the modulus of the natural number  $n > 1$ . The only exception is  $ind_a(p)$ . The number of controlled indicators analyzed in the Excel environment can be expanded.

According to the idea of experimental mathematics on the first iteration, we proceed from hypothetically known data. But it is also the basis for obtaining experimental information on the basis of which the analytical methods of the theory of numbers yield an expanded representation of the hypothesis in the form  $H_i$ . It is possible that at the same time the hypothesis can be corrected or even rejected as not true. From the point of view of information technology in mathematics, the hypothesis  $H_i$  is used to develop from the point of view of deepening the experimental mathematics of the model of in-depth studies at the level  $I_1$ .

The iterations process is continued until an analytically based solution of the generated hypothesis is obtained. Since the Artin generalized hypothesis is considered in the paper, we present the results of the estimation of the constant  $c(a, i)$  for the case  $a = 4$  and  $i = 2$ . The number  $a = 4$  is a perfect square, and therefore it cannot be a primitive root. In terms of Artin's generalized hypothesis, this is as interesting and important as in the case when  $a$  is an original root.

Based on the data presented in [6], we obtained estimates for  $c(a, i)$  for  $a = 2, \dots, 10$  and  $i = 1, 2, \dots, 9, \dots$ . It is shown that their values are stable for class  $\mathcal{P}(4, 2)$  ie class with  $ind_4(p) = 2$  to within a fourth decimal place. They are presented in the table 1.

An analysis of the data in the tables shows that for these numbers Artin's hypothesis is true on the set of primes  $|\mathcal{P}| = 10^9$ .

Table 1: The distribution of prime numbers in 1 to 9 classes in the generalized artin conjecture

a	$\mathcal{P}(a, 1)$	$\mathcal{P}(a, 2)$	$\mathcal{P}(a, 3)$	$\mathcal{P}(a, 4)$	$\mathcal{P}(a, 5)$	$\mathcal{P}(a, 6)$	$\mathcal{P}(a, 7)$	$\mathcal{P}(a, 8)$	$\mathcal{P}(a, 9)$
2	0.3740	0.2805	0.0664	0.0467	0.0189	0.0498	0.0089	0.0351	0.0074
3	0.3739	0.2992	0.0666	0.0561	0.0190	0.0332	0.0089	0.0140	0.0074
4	0	0.5609	0	0.0935	0	0.0997	0	0.0701	0
5	0.3937	0.2657	0.0700	0.0664	0	0.0473	0.0094	0.0166	0.0078
6	0.3741	0.2805	0.0665	0.0748	0.0189	0.0498	0.0089	0.0140	0.0074
7	0.3741	0.2827	0.0664	0.0684	0.0188	0.0503	0.0089	0.0170	0.0074
8	0.2243	0.1683	0.1995	0.0281	0.0114	0.1496	0.0054	0.0211	0.0222
9	0	0.5983	0	0.1122	0	0.0666	0	0.0281	0
10	0.3741	0.2804	0.0665	0.0713	0.0189	0.0499	0.0089	0.0166	0.0074

## 4 CONCLUSIONS

The results of experimental mathematics in table 1 of the first iteration confirm that Artin's hypothesis is correct. The estimates of the constants are obtained with the accuracy of the third decimal place. These tables confirm Artin's generalized hypothesis for  $a = 2, \dots, 8$  and the assumption that  $\sum_{i=1}^{\infty} c(a, 2i) = 1$ . The results obtained are the basis for constructing an analytical proof of Artin's hypothesis and its generalization.

## References

- [1] Ambrose D. (2014). *On Artin's Primitive Root Conjecture*. der Georg-August-Universität Gottingen.
- [2] Artin E. (1982). *Collected papers*. Edited by Serge, Lang and T. John, Springer-Verlag, New York.
- [3] Crandall R., Pomerance C. (2005). *Prime Numbers A Computational Perspective*. Springer, Portland.
- [4] Manin Yu. I., Panchishkin A. A. (2009). *Introduction to the modern theory of numbers*. MTSNMO, Moscow.
- [5] Moree P. (2012). Artin's Primitive root conjecture a survey, *Journal*. Vol. **12**, pp. 1305-1416.
- [6] Vostrov G., Opiata R. (2018). Computer modeling of dynamic processes in analytic number theory, *Jornal* Vol, **26**, pp. 240-247.

# STOCHASTIC ANALYSIS OF THE SMOOTH NUMBER PROPERTIES AND THEIR SEARCH

G. VOSTROV, O. PONOMARENKO  
*Odessa national politechnic university*  
*Odessa, UKRAINE*

e-mail: [vostrov@gmail.com](mailto:vostrov@gmail.com), [ponomarenkoelena1997@gmail.com](mailto:ponomarenkoelena1997@gmail.com)

## Abstract

The paper introduces the concept of smooth primes and their classification, depending on the properties of their simple factors, into perfectly smooth and partially smooth. It is shown that in order to search for smooth primes and their analysis, it is necessary to know how primes are distributed depending on the number of simple factors ( $p - 1$ ). The problem of constructing a measure of smoothness is considered. Results are shown showing how the first 10 million numbers ( $p - 1$ ) are distributed by the number of simple factors.

**Keywords:** smooth number, data science, stochastic analysis

## 1 Introduction

At the moment, in number theory, there are many open problems that have not been solved for decades or centuries. Unsolved problems in number theory significantly limit the development of mathematics in theoretical and applied aspects. One of the fundamental problems is unproven hypotheses about prime numbers. According to which law the numbers ( $p - 1$ ) are distributed according to the number of simple factors, is still unknown.

Prime numbers are widely used in public key cryptography, as well as directly related to the problem of discrete logarithm, which is currently not solved either. There are no efficient algorithms that allow solving a problem with polynomial complexity. Silver, Pohlig, and Hellman in [5] proposed an algorithm that promises polynomial complexity when using numbers of a special type, called “smooth”. A more accurate description of the algorithm is given in [1]. However, the authors begin the description of the algorithm with a remark that it is not known that, for simplicity, we assume that the prime number  $p$  is smooth, and  $b$  is its primitive root. Such an assumption greatly simplifies the solution of the problem. At the same time, the authors completely ignore the rationale for such an assumption from the point of view, but how to find such numbers and how great is the probability of their being in a certain interval and what is the most important and what is the probability of such an option in the entire problem of the discrete logarithm. In modern number theory there is no clear definition of “smooth” numbers and their classification, and the laws of their distribution are completely unknown. This is especially important in modern cryptography. Along with this, it is necessary to solve the problem of finding smooth numbers of sufficiently large dimension.

## 2 The definition of the concept of smoothness of numbers and their classification

The general form of the discrete logarithm equation is represented by the expression:  $c \equiv b^x \pmod{m}$  and  $c, b, x, m \in N$ . There are four possible solutions to this equation: 1) set  $b, x, m$ , find  $c$ ; 2) set  $c, b, m$ , find  $x$ ; 3) set  $c, b, x$ , find  $m$ ; 4) set  $c, x, m$ , find  $b$ .

The first equation is solved relatively simply, but it should be noted that if  $c = 1$ ,  $m$  is a prime number,  $m \in P$ ,  $b$  is its primitive root and it is necessary to find the distribution law of primes having the same primitive root  $b$ , then we come to the solution of Artin's hypothesis (1927),  $\pi(x, a) = c(b) \cdot \pi(x)$ , where  $\pi(x, a)$  is the number of primes  $p \leq x$  with a primitive root  $b$ ,  $c(b)$  is Artin's constant, and  $\pi(x)$  is the general number of primes  $p \leq x$ . However, this is true if  $x \rightarrow \infty$ .

The second problem is the discrete logarithm problem. As stated in [1] in general, the problem may turn out to be algorithmically unsolvable. If  $m$  is a prime number, that is  $m = p \in P$ , then the algorithm exists, but its complexity depends on the complexity of factorization  $p - 1 = \prod_{i=1}^k p_i^{\alpha_i}$ , where  $p_i$  are prime factors,  $k$  their number. In case if the number to be factorized is a Sophie Germain number  $p = 2\tilde{p} + 1$  or  $p = 2^\alpha \tilde{p} + 1$ , where  $\tilde{p}$  there is also a prime number, the solution of the discrete logarithm problem becomes very complex in terms of computational costs. Note that if  $m$  the composite number and does not belong to the final fields  $F(2^p)$  or  $F(p^k)$ , then non-simple algorithmic problems arise in [2]. Cases 3 and 4 are practically not considered in the literature. It is easy to show that they are more complex than the discrete logarithm problem.

Pohlig and Hellman [5] proposed an algorithm for solving the problem of the discrete logarithm, provided that it  $p$  is a simple smooth number. In [3], the problem of smoothness is discussed. The authors note that there is still no clear interpretation of the concept of smoothness. One option is that the decomposition  $p - 1 = \prod_{i=1}^k p_i^{\alpha_i}$  has the property that  $p_k < \tilde{p}$ , where the  $\tilde{p}$  given prime number.

As noted above in the work [1], the author literally write: "for simplicity, we suppose that  $(p - 1)$  is smooth and  $b$  its primitive root". This is where a really complicated problem arises. Since  $p$  can be arbitrarily large, it is not known how smooth primes are distributed. A search algorithm is needed for a smooth prime number of arbitrarily large size, and then to find its primitive root satisfying certain conditions. This is especially important if it is related to cryptographic tasks. But this is no less important from the point of view of the whole variety of problems formulated in the "MathOverflow" project for the discrete logarithm. For this reason, the problem of the distribution of smooth primes on the set of all primes was considered. In the work of E. Kowalski [6] the Erdős-Kac theorem is given, which states that for any natural number  $n \in [1; N]$ , for any real  $a < b$ , the following holds: 
$$\lim_{N \rightarrow \infty} \frac{1}{N} |\{1 \leq n \leq N | a \leq \frac{\omega(n) - \log \log N}{\sqrt{\log \log N}} \leq b\}| = \frac{1}{\sqrt{2\pi}} \int_a^b e^{-\frac{x^2}{2}} dx$$
, where  $\omega(n)$  the number of prime dividers, without taking into account their degrees.

From the theorem it follows that by the number of simple factors in their factorization on the set of natural numbers by the frequency of their appearance the natural numbers  $n$  obey the normal distribution law. But the question arises to what extent

is this true for numbers like  $(p - 1)$ , where  $p \in P$ . On the basis of data related to the solution by computer and analytical methods of the generalized Artin hypothesis, it was established [7] that for smooth prime numbers  $p - 1 = \prod_{i=1}^k p_i^{\alpha_i}$  with increasing  $k$ , the value  $\omega(p - 1)$  obeys most likely the lognormal distribution law. It is possible that this may turn out to be another distribution law, similar to a lognormal one. This fact requires clarification. From the experimental data on the set of the first 10 million primes it follows that smooth numbers are very rare. Therefore, Koblitz's statement [1] "for simplicity, we suppose that  $(p - 1)$  is smooth ..." is completely incorrect, since the search for such a simple number may be more difficult than solving the problems of the discrete logarithm. In addition, to find a primitive root for  $p$  from  $\varphi(p - 1)$  (Euler function) possible variants from the set of natural numbers  $\{2, \dots, p - 1\}$  is not at all easy, it follows from the theorem on the cyclic group [4]. For this reason, the study of this problem is no less relevant than the solution of the problem of the discrete logarithm. We present the results of a statistical analysis of the first 10 million primes and decomposition  $(p - 1)$  into prime factors. On the horizontal axis, the number

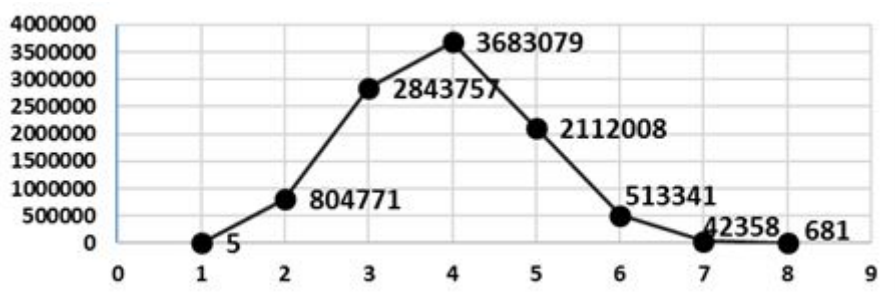


Figure 1: Results of decomposition  $(p - 1)$  into simple factors

of simple factors is plotted, on the vertical, the number of the corresponding prime numbers. Based on the obtained results, it can be seen that with increasing values of prime numbers, the number of factors increases, from which it can be concluded that the set of numbers  $(p - 1)$  does not obeys a normal distribution law. Figure 1 confirms that the lognormal form of distribution is clear.

Depending on the sequence of increasing simple factors, smooth numbers can be classified as follows:

1) Perfectly smooth primes - such numbers as for  $p - 1 = \prod_{i=1}^k p_i^{\alpha_i}$ ,  $p_i = 2, 3, 5, \dots, p_k$ . This means that all prime factors are consecutive prime numbers.

Pohlig and Hellman argue that such a type of smooth numbers will allow solving the discrete logarithm problem using an algorithm with polynomial complexity [5]. However, along with the definition of a perfectly smooth number, the question arises as to the number of such numbers. It may happen that the search for a smooth number of large dimensionality will have a high algorithmic complexity, which in turn makes the use of the Silver-Pohlig-Hellman algorithm impractical.

2) Partially smooth prime numbers. It is assumed that for such numbers the sequence of simple factors is not necessarily consecutive prime numbers, but the difference between the consecutive factors should not be too large. Partially smooth primes can

also be used for the algorithm of Silver, Pohlig, and Hellman, but its effectiveness will depend on a measure of the smoothness of such numbers.

Among the first 10 million  $(p - 1)$ , perfectly smooth numbers with more than 6 factors, there are no more than a few dozen. From this we can conclude that the assumption of smoothness does not simplify the solution of the discrete logarithm problem, but even complicates if we take into account the iterations for each factor  $p_i^{\alpha_i}$  with  $\alpha_i$  substantially more than 1 and systematic use of the Chinese theorem on residuals with a large number of simple factors.

In conclusion, we note that this paper shows that when solving the problem of a discrete logarithm, it is necessary to take into account the properties of some types of prime numbers. To solve the problem of discrete logarithm using the Silver-Pohlig-Hellman algorithm, an important point is the use of smooth numbers that must satisfy  $(p - 1) > 10^{300}$ . However, it is still not known how to find such numbers. This makes the task difficult to compute.

The next important factor in solving the discrete logarithm problem is a measure of the smoothness of a prime number, since the speed of the algorithm execution directly depends on this. The construction of a measure of smoothness and an analysis of the algorithm depending on the smoothness of the number is a topic for further study. The problem of constructing a measure of smoothness must be considered from two sides: from the point of view of the difference between adjacent factors of simple smooth numbers and depending on the exponent of each of the factors.

## References

- [1] Koblitz N. (2001). *Course of number theory and cryptography*. Scientific publishing house PTA, Moscow.
- [2] Pomerance C. (2008). Elementary thoughts on discrete logarithms. *Algorithmic Number Theory, MSRI Publications*. Vol. 44
- [3] Crandall R., Pomerance C. (2001). *Prime numbers: A Computational Perspective*. Springer-Verlag, New York.
- [4] Lidl R., Niederreiter G. (1997). *Finite Fields*. Cambridge University Press.
- [5] Pohlig S.C., Hellman M.E. (1978). An Improved Algorithm for Computing Logarithms Over  $GF(p)$  and its Cryptographic Significance. *IEEE Transactions on Information Theory*. Vol. 1, pp. 106-110.
- [6] Kowalski E. (2018). Arithmetic Randomness. An introduction to probabilistic number theory. Available at: <https://people.math.ethz.ch/~kowalski/probabilistic-number-theory.pdf>
- [7] Vostrov G., Opiata R. (2018). Generalized Artina hypothesis and computer information model its solutions. *ELTECS*. Vol. 29, pp. 120-126.

# SOME FORMULAS OF OPERATOR INTERPOLATION ON THE SET OF RANDOM PROCESSES

L.A. YANOVICH, M.V. IGNATENKO

*National Academy of Sciences, Institute of Mathematics; Belarus State University  
Minsk, BELARUS*

e-mail: yanovich@im.bas-net.by; ignatenkomv@bsu.by

## Abstract

For operators defined on the Cartesian product of random and deterministic continuous functions the interpolation polynomials of arbitrary fixed degree, coinciding at the given points with the original operator, are constructed. Formulas of the linear interpolation and their applications for the approximation of specific random operators, nonlinear with respect to the Wiener process, are considered.

**Keywords:** data science, random process, operator interpolation

## 1 Introduction

Let us denote by  $\Xi = \{\xi(t, \omega), t \in T, \omega \in \Omega\}$  the set of random processes, defined on the probability space  $\{\Omega, \mathcal{F}, P\}$ , by  $C(T)$  the space of the deterministic functions  $x(t)$ ,  $t \in T$ , continuous on  $T$ , where  $T$  is the time interval on  $\mathbb{R}^+ = [0, \infty)$ .

Let the operator  $F(\xi, x) = F(\xi(t, \omega), x(t))$  be defined on the Cartesian product of  $\Xi \times C(T)$  and  $F : \Xi \times C(T) \rightarrow Y$ , where  $Y$  is a set, whose elements have random or deterministic nature.

We introduce vectors of the form  $r_l(\xi, x) = \{\xi - \xi_l, x - x_l\}$  and  $r_{lk}(\xi, x) = \{\xi_k - \xi_l, x_k - x_l\}$ , where  $\xi, \xi_k$  are elements of the set  $\Xi$ , and  $x = x(t)$ ,  $x_k = x_k(t)$ ,  $x_l = x_l(t)$  are functions continuous on  $T$ ,  $0 \leq l, k \leq n$ . Let us denote by  $(r_l, r_{lk})$  the scalar product of  $r_l$  and  $r_{lk} : (r_l, r_{lk}) = (\xi - \xi_l)(\xi_k - \xi_l) + (x - x_l)(x_k - x_l)$ . Correspondingly  $(r_{lk}, r_{lk})$  is the square of vector length of  $r_{lk} : (r_{lk}, r_{lk}) = (\xi_k - \xi_l)^2 + (x_k - x_l)^2$ .

We associate the operator  $F(\xi, x)$  and the points  $(\xi_k, x_k)$  ( $k = 0, 1, \dots, n$ ) with a random algebraic operator polynomial  $L_n(F; \xi, x)$  of the form

$$L_n(F; \xi, x) = F(\xi_0, x_0) + \sum_{k=1}^n \int_0^1 l_{nk}(\xi(\tau), x(\tau)) d_\tau F(\xi_0 + \tau(\xi_k - \xi_0), x_0 + \tau(x_k - x_0)), \quad (1)$$

where the integral on the variable  $\tau$  in the equality (1) is understood as the Riemann-Stieltjes integral for trajectories of random processes in this integral, and

$$l_{nk}(\xi, x) = \frac{(r_0, r_{0k})(r_1, r_{1k}) \cdots (r_{k-1}, r_{k-1 k})(r_{k+1}, r_{k+1 k}) \cdots (r_n, r_{nk})}{(r_{0k}, r_{0k})(r_{1k}, r_{1k}) \cdots (r_{k-1 k}, r_{k-1 k})(r_{k+1 k}, r_{k+1 k}) \cdots (r_{nk}, r_{nk})}. \quad (2)$$

## 2 Operator interpolation formulas of other form

Now we consider another version of the polynomial of the form (1) for the operator  $F(\xi, x)$  that is differentiable by Gateaux. We denote by  $\delta F[\xi, x; h]$  the Gateaux differential of this operator at the point  $(\xi, x)$  in the direction  $h = (h_0, h_1)$ , where  $h_0 = h_0(\omega, t)$  is a random process from the set  $\Xi$ ,  $h_1 = h_1(t) \in C(T)$ . The Gateaux differential  $\delta F[\xi, x; h]$  of the operator  $F(\xi, x)$  in the direction  $h = (h_0, h_1)$  is defined by the equality  $\delta F[\xi, x; h] = \frac{d}{d\lambda} F(\xi + \lambda h_0, x + \lambda h_1)_{\lambda=0}$ ,  $\lambda \in [0, 1]$ . This differential is used below only at the points  $(\xi, x) = (\xi_0 + \tau(\xi_k - \xi_0), x_0 + \tau(x_k - x_0))$ ,  $\tau \in [0, 1]$  and in the directions  $h_{0k} = (\xi_k - \xi_0)l_{nk}(\xi, x)$  and  $h_{1k} = (x_k - x_0)l_{nk}(x)$ , where

$$l_{nk}(x) = \frac{(x - x_0) \cdots (x - x_{k-1})(x - x_{k+1}) \cdots (x - x_n)}{(x_k - x_0) \cdots (x_k - x_{k-1})(x_k - x_{k+1}) \cdots (x_k - x_n)} \quad (k = 1, 2, \dots, n),$$

and here we suppose that in (2) and in the fraction  $l_{nk}(x)$ , none of the factors in the denominator vanish.

Let us denote by  $\tilde{L}_n(F; \xi, x)$  the operator polynomial of the following form

$$\tilde{L}_n(F; \xi, x) = F(\xi_0, x_0) + \sum_{k=1}^n \int_0^1 \delta F[\xi_0 + \tau(\xi_k - \xi_0), x_0 + \tau(x_k - x_0); h_{0k}, h_{1k}] d\tau. \quad (3)$$

**Theorem.** *Random operator polynomials (1) and (3) are interpolational for the operator  $F(\xi, x)$  and nodes  $(\xi_k, x_k)$ , i.e.*

$$L_n(F; \xi_k, x_k) = \tilde{L}_n(F; \xi_k, x_k) = F(\xi_k, x_k) \quad (k = 0, 1, \dots, n).$$

During applied problems solving are often limited by the formulas of the linear and quadratic interpolation. In the linear case we use two nodes  $(\xi_0(t), x_0(t))$ ,  $(\xi_1(t), x_1(t))$  and the formulas (1) and (3) take the form correspondingly

$$L_1(F; \xi, x) = F(\xi_0, x_0) + \int_0^1 l_{11}(\xi(\tau), x(\tau)) d_\tau F[\xi_0 + \tau(\xi_1 - \xi_0), x_0 + \tau(x_1 - x_0)], \quad (4)$$

$$\begin{aligned} & \tilde{L}_1(F; \xi, x) = F(\xi_0, x_0) + \\ & + \int_0^1 \delta F[\xi_0 + \tau(\xi_1 - \xi_0), x_0 + \tau(x_1 - x_0); (\xi_1 - \xi_0)l_{11}(\xi, x), (x_1 - x_0)l_{11}(x)] d\tau, \quad (5) \end{aligned}$$

where

$$l_{11}(\xi(\tau), x(\tau)) = \frac{(\xi(\tau) - \xi_0(\tau))(\xi_1(\tau) - \xi_0(\tau)) + (x(\tau) - x_0(\tau))(x_1(\tau) - x_0(\tau))}{(\xi_1(\tau) - \xi_0(\tau))^2 + (x_1(\tau) - x_0(\tau))^2},$$

$$l_{11}(x(\tau)) = \frac{x(\tau) - x_0(\tau)}{x_1(\tau) - x_0(\tau)}.$$

It is obvious that for linear on  $\Xi \times C(T)$  operators (4) and (5) the interpolation conditions  $L_1(F; \xi_i, x_i) = \tilde{L}_1(F; \xi_i, x_i) = F(\xi_i, x_i)$  ( $i = 0, 1$ ) hold true.

In the case, when the approximated operator  $F$  depends only on random process  $\xi(t)$  the formulas (4) and (5) take the form

$$L_1(F; \xi) = F(\xi_0) + \int_0^1 \frac{\xi(\tau) - \xi_0(\tau)}{\xi_1(\tau) - \xi_0(\tau)} d_\tau F(\xi_0 + \tau(\xi_1 - \xi_0)),$$

$$\tilde{L}_1(F; \xi) = F(\xi_0) + \int_0^1 \delta F[\xi_0 + \tau(\xi_1 - \xi_0); \xi - \xi_0] d\tau. \quad (6)$$

### 3 Some applications of formulas of the linear interpolation

We construct the formulas of the linear interpolation for certain types of random processes. Let

$$F(\xi, x) = X_0 e^{\sigma \xi(t) + (r - \frac{1}{2} \sigma^2) x(t)}, \quad (7)$$

where  $X_0$  is a random variable independent on  $\xi(t) = \xi(\omega, t)$ ;  $r$  and  $\sigma$  are arbitrary given numbers,  $t \in T$ . When  $\xi(t)$  is a standard Wiener process  $W(t)$  and  $x(t) = t$ , then  $F(W, t) = X(t)$  (see, for example [2], p. 524 or [3]) is the solution of the stochastic differential equation with linear drift and linear volatility  $dX(t) = rX(t)dt + \sigma X(t)dW(t)$ ,  $X(0) = X_0$ .

For the random process (7) we construct the polynomial of the form (5) at the nodes  $(\xi_0(t), x_0(t))$  and  $(\xi_1(t), x_1(t))$ , where  $\xi_i(t)$  is a stochastic process defined on the space  $\{\Omega, \mathcal{F}, P\}$ , and  $x_i(t)$  is a deterministic function continuous on  $T$  ( $i = 0, 1$ ). The Gateaux differential of the operator (7) at the point  $(\xi, x)$  in the direction  $h = (h_0, h_1)$  can be calculated by the formula  $\delta F[\xi, x; h_0, h_1] = F(\xi, x) [\sigma h_0 + (r - \frac{1}{2} \sigma^2) h_1]$ . In this case the integral in (5), when  $h_0 = (\xi_1 - \xi_0)l_{11}(\xi, x)$ ,  $h_1 = (x_1 - x_0)l_{11}(x)$ , can be calculated exactly, and the formula (5) can be transformed to the form

$$\tilde{L}_1(F; \xi, x) = F(\xi_0, x_0) + [F(\xi_1, x_1) - F(\xi_0, x_0)] \times$$

$$\times \frac{\sigma(\xi_1(t) - \xi_0(t))l_{11}(\xi, x) + (r - \frac{1}{2} \sigma^2)(x_1(t) - x_0(t))l_{11}(x)}{\sigma(\xi_1(t) - \xi_0(t)) + (r - \frac{1}{2} \sigma^2)(x_1(t) - x_0(t))}. \quad (8)$$

Since for the operator (7) at every fixed function  $x(t)$  the Gateaux differential  $\delta F[\xi, x; h_0]$  with respect to variable  $\xi$  is defined by the formula  $\delta F[\xi, x; h_0] = \sigma h_0(t)F(\xi, x)$ , then the integral in (6) can be also calculated exactly and this interpolation formula with the nodes  $\xi_0$  and  $\xi_1$  takes the form

$$\tilde{L}_1(F; \xi, x) = F(\xi_0, x) + [F(\xi_1, x) - F(\xi_0, x)] \frac{\xi(t) - \xi_0(t)}{\xi_1(t) - \xi_0(t)}. \quad (9)$$

Interpolation formulas (8) and (9) can be used for the linear approximation of the random processes  $F(\xi, x)$  of the form (7).

Similarly we are constructing the interpolation formulas of the form (8), (9) and for the operator  $F(W; t) = Y(t) = X^\alpha(t)$ ,  $\alpha \in \mathbb{R}$ , where  $X(t) = X_0 e^{\sigma W(t) + (r - \frac{1}{2} \sigma^2)t}$  and  $X_0$

is a random value or a given number. The mathematical expectation of this operator in the case of stochastic independence of the initial condition  $X_0$  and the Wiener process  $W(t)$  (see [3], [4]) is given by  $E\{Y(t)\} = E\{X_0^\alpha\} e^{\alpha[r - \frac{1}{2}\sigma^2(1-\alpha)]t}$ .

The requirements of coincidence of the mathematical expectation and the variance of the interpolated operator with the expectation and the variance of the corresponding interpolation polynomial in the approximation problem of random functions are natural. Let us illustrate the construction of such class of interpolation formulas on the simplest examples.

We consider the interpolation polynomial (6) for the random process  $F(W) = W^2(t)$ . We take two deterministic functions  $x_0(t)$  and  $x_1(t)$  as interpolation nodes. In this case

$$\tilde{L}_1(F; W) = \tilde{L}_1(W) = -x_0(t)x_1(t) + [x_0(t) + x_1(t)]W(t). \quad (10)$$

We choose the functions  $x_0(t)$  and  $x_1(t)$  such that the mathematical expectation and dispersion of both  $F(W)$  and  $\tilde{L}_1(W)$  coincide. Since  $E\{F(W)\} = E\{W^2(t)\} = t$  and the dispersion of this process  $D\{F(W)\} = 2t^2$ , then with the requirement of coincidence of the mean values and dispersions of the random processes  $W^2(t)$  and  $\tilde{L}_1(W)$  the nodes  $x_0(t)$  and  $x_1(t)$  have to be determined from the system of equations  $E\{\tilde{L}_1(W)\} = t$ ,  $D\{\tilde{L}_1(W)\} = 2t^2$ . From the equality (10) we obtain, that  $E\{\tilde{L}_1(W)\} = -x_0(t)x_1(t)$ . Hence,  $x_1(t) = -\frac{t}{x_0(t)}$  and correspondingly the formula (10) has the form  $\tilde{L}_1(W) = t + \left[x_0(t) - \frac{t}{x_0(t)}\right]W(t)$ , where  $x_0(t)$  is arbitrary function which does not vanish on  $T$ . Since  $E\{\tilde{L}_1^2(W)\} = t^2 + \left[x_0(t) - \frac{t}{x_0(t)}\right]^2 t$ , then for the dispersion of the process (10) we obtain the equality  $D\{\tilde{L}_1(W)\} = \left[x_0(t) - \frac{t}{x_0(t)}\right]^2 t$ . Thus,  $x_0(t)$  has to be determined from the equation  $\left[x_0(t) - \frac{t}{x_0(t)}\right]^2 = 2t$ , solving which we get two pairs of nodes  $x_0(t) = \frac{\sqrt{2t}(1 \pm \sqrt{3})}{2}$ ,  $x_1(t) = -\frac{\sqrt{2t}}{1 \pm \sqrt{3}}$ , and correspondingly the equality (10) at these nodes takes the following simple form

$$\tilde{L}_1(W) = t + \sqrt{2t}W(t). \quad (11)$$

As a consequence equalities  $E\{F(W)\} = E\{\tilde{L}_1(W)\} = t$ ,  $D\{F(W)\} = D\{W^2(t)\} = 2t^2$ , in some problems the approximate replacing of the square of the Wiener process with the linear process relative to  $W(t)$  of the form (11).

The interpolation formula (1) and (2) are the basis for construction of approximation and for other random processes of the form considered here. In particular, as interpolation nodes can be used only deterministic functions.

## References

- [1] Trenogin V.A. (1980). *Functional analysis*. Nauka, Moscow.

- [2] Matalytski M.A. (2006). *Probability and stochastic processes: theory, examples, problems*. Grodno State University, Grodno.
- [3] Pugachev V.S. and Sinitsyn I.N. (1990). *Stochastic differential systems. Analysis and filtration*. Nauka, Moscow.
- [4] Kharin Yu.S., Zuev N.M. and Zhuk E.E. (2011). *Probability theory, mathematical and applied statistics*. BSU, Minsk.

# EMPIRICAL LIKELIHOOD CONFIDENCE INTERVALS FOR CENSORED INTEGRALS

D.G. ZAKHIDOV, D.KH. ISKANDAROV  
*Andijan branch of Tashkent Agrar University*  
*Andijan, UZBEKISTAN*  
 e-mail: a\_abdushukurov@rambler.ru

## Abstract

The problem of finding empirical likelihood confidence intervals is considered for censored integrals.

**Keywords:** data science, empirical likelihood, censored integral

Let  $X_1, X_2, \dots$  ( survival times) and  $Y_1, Y_2, \dots$  (censoring times) be two independent sequences of random variables (r.v.-s) on the real line with marginal distribution function (d.f.-s)  $F$  and  $G$  respectively. Under the right random censoring model, instead of observing  $X_i$ , we observe the pairs  $(Z_i, \delta_i), i = 1, 2, \dots, n$  where  $Z_i = \min(X_i, Y_i)$  and  $\delta_i = I(X_i \leq Y_i)$  with  $I(\cdot)$  the indicator function. Let  $H$  denote d.f. of  $Z_i$ . Then  $H(t) = 1 - (1 - F(t))(1 - G(t))$ . Let  $F$  and  $G$  are continuous. We are interested in constructing a nonparametric confidence interval for a integral functional of the form

$$\theta = \theta(F) = \int \varphi(t)dF(t)$$

where  $\varphi$  is some given Borel measurable function. Let  $F_n$  denote the Relative Risk Power estimator of  $F$  proposed [1] as

$$F_n(t) = 1 - [1 - H_n(t)]^{R_n(t)}, t \in R, \tag{1}$$

where  $H_n(t) = \frac{1}{n} \sum_{i=1}^n I(Z_i \leq t)$  be empirical estimator of  $H(t)$  and

$$R_n(t) = \sum_{i=1}^n \delta_i(Z_i \leq t) \left[1 - H_n(Z_i) + \frac{1}{n}\right]^{-1} \left\{ \sum_{i=1}^n I(Z_i \leq t) \left[1 - H_n(Z_i) + \frac{1}{n}\right]^{-1} \right\}^{-1}$$

is the relative-risk function estimator. Note that estimator (1) is a correct estimator of d.f.  $F(t)$  than the Product-Limit estimator of Kaplan-Meier and Exponential-Hazard estimator of Altschuler-Breslow (see[2]). Since estimator (1) have same good properties such that representation as sum of independent and identically distributed (i.i.d) r.v.-s up to point  $T < T_H = \inf \{t : H(t) = 1\}$ , then instead of  $\theta(F)$  we consider  $\theta_T(F) = \int \varphi^*(t)dF(t)$  where  $\varphi^*(t) = \varphi(t)I(t \leq T)$ . We prove for plug-in estimator of  $\theta_T(F)$  the asymptotic representation

$$\theta_T(F_n) = \int \varphi^*(t)dF_n(t) = \frac{1}{n} \sum_{i=1}^n U_i + O_p\left(n^{-\frac{1}{2}}\right) \tag{2}$$

where  $U_i = U_i(F, G)$  are i.i.d. r.v.-s. with  $EU_i = \theta_T(F)$ . Following Owen's [3] idea we propose empirical likelihood confidence interval for truncated integral functional  $\theta_T(F)$ .

## References

- [1] Abdushukurov A.A. (1998). Nonparametric estimation of distribution function based on relative risk function. *Commun. Statist.: Theory and Methods*. Vol. **27**, No.8, pp. 1991-2012.
- [2] Abdushukurov A.A. (2009). Nonparametric estimation based on incomplete observations. *In: international Enciclopedia of Statistical Sciences*.(Prof. Miodrag Lovric ED.) Springer. 2009. Pt.14, pp. 962-964.
- [3] Owen A. (2001). *Empirical likelihood*. Chapman and Hall /CRC.

# PRINCIPLE COMPONENTS METHOD IN STATISTICAL CLASSIFICATION AND ITS EFFICIENCY

E.E. ZHUK

*Belarusian State University*

*Minsk, BELARUS*

e-mail: zhukee@mail.ru

## Abstract

The problem of reducing the dimensionality in statistical classification is studied. The case of the well-known Fisher model of multivariate normal (Gaussian) distribution mixture is considered. The average decrease of interclass distances square is presented as a new criterion of feature selection directly connected with the classification error probability. The stepwise discriminant analysis procedure based on this criterion is proposed.

**Keywords:** principal component, statistical classification, data science

## 1 Introduction

Let a sample of  $n$  jointly independent random observations  $x_1, \dots, x_n$  from  $L \geq 2$  classes  $\{\Omega_1, \dots, \Omega_L\}$  be registered in the feature space  $R^N$  and  $d_t^o \in S = \{1, \dots, L\}$  be an unknown random class index to which  $x_t$  belongs:

$$\{d_t^o = i\} = \pi_i > 0, \quad i \in S \quad (\pi_1 + \dots + \pi_L = 1), \quad (1)$$

where  $\{\pi_i\}_{i \in S}$  are prior class probabilities [1, 3]. Under fixed  $d_t^o = i$  ( $i \in S$ ) the observation  $x_t \in R^N$  is described by the conditional probability density function:  $p_i(x) \geq 0$ ,  $x \in R^N$ :  $\int_{R^N} p_i(x) dx = 1$ ,  $i \in S$ .

The classes  $\{\Omega_i\}_{i \in S}$  are completely determined by the introduced characteristics  $\{\pi_i, p_i(\cdot)\}_{i \in S}$ . Often in practice [1, 2, 3] these characteristics are unknown, however the vector of true classification indices  $D^o = (d_1^o, \dots, d_n^o)^T \in S^n$  ("T" is the transposition symbol) for the sample  $X = \{x_1, \dots, x_n\}$  is observed (so-called training sample). The discriminant analysis problem [1, 2, 3] consists in construction of decision rule (DR)  $d = d(x; X, D^o) \in S$  for classifying a random observation  $x \in R^N$  with true class index  $d^o \in S$ .

However, often in practice the initial feature space is redundant. It means that its dimensionality  $N$  is too large [1, 2] and new sample  $Y = \{y_1, \dots, y_n\}$  must be constructed from sample  $X$ :  $y_t = f(x_t) \in R^{N^*}$ ,  $N^* < N$  ( $t = \overline{1, n}$ ), so as classification  $\bar{d} = \bar{d}(y; Y, D^o) \in S$  ( $y = f(x) \in R^{N^*}$ ,  $x \in R^N$ ) remains acceptable.

## 2 Fisher model and Bayesian classification

Let the well-known Fisher model [1, 2, 3] of multivariate normal (Gaussian) distribution mixture be investigated:

$$p_i(x) = n_N(x|\mu_i, \Sigma), \quad x \in R^N, \quad i \in S, \quad (2)$$

where  $n_N(x|\mu_i, \Sigma)$  is  $N$ -variate Gaussian probability density function [3] with mean vector  $\mu_i = \{x | d^o = i\} \in R^N$  (class "center") and non-singular covariance ( $N \times N$ )-matrix  $\Sigma$  ( $\det(\Sigma) \neq 0$ ), common for all classes:  $\Sigma = \{(x - \mu_i)(x - \mu_i)^T | d^o = i\}$ .

The Bayesian DR corresponds to the Fisher model (1), (2) is

$$d_o(x) = \arg \max_{i \in S} \{\pi_i n_N(x|\mu_i, \Sigma)\} = \arg \max_{i \in S} \{\delta_i(x)\}, \quad x \in R^N, \quad (3)$$

where  $\delta_i(x) = \mu_i^T \Sigma^{-1} x - \frac{1}{2} \mu_i^T \Sigma^{-1} \mu_i + \ln \pi_i$ ,  $i \in S$ , are linear (per  $x \in R^N$ ) discriminant functions [1, 2, 4].

The DR (3) has the minimal error probability  $r_o = \{d_o(x) \neq d^o\}$  [1, 3] at estimating unknown true class index  $d^o \in S$  to which classified observation  $x \in R^N$  belongs. For efficiency characteristic  $r_o$  named by risk [1, 3] the following estimation from above is true [4]:

$$r_o \leq \sum_{i \in S} \pi_i \sum_{i \neq j \in S} \Phi \left( -\frac{1}{2} \Delta_{ij} - \Delta_{ij}^{-1} \ln(\pi_i/\pi_j) \right), \quad (4)$$

where  $\Phi(z) = \frac{1}{\sqrt{2\pi}} \int_{-\infty}^z \exp\left(-\frac{w^2}{2}\right) dw$ ,  $z \in R$ , is the standard Gaussian distribution function, and

$$\Delta_{ij} = \sqrt{(\mu_i - \mu_j)^T \Sigma^{-1} (\mu_i - \mu_j)}, \quad i \neq j \in S, \quad (5)$$

are so-called Mahalanobis interclass distances [1, 3]. Note that only in the case of two classes ( $L = 2$ ) in (4) exact equality is true [1, 3].

From (4) it is seen that interclass distances (5) determine efficiency of classification: the more distances, the risk value there is less.

### 3 The principle components method and interclass distances

According to principle components method [1, 2]  $N$ -vector  $x = (\tilde{x}_1, \dots, \tilde{x}_N)^T \in R^N$  with the covariance ( $N \times N$ )-matrix  $\Sigma$  is linearly transformed:

$$\tilde{y}_k = \tilde{y}_k(x) = \Psi_k^T x, \quad k = \overline{1, N}, \quad (6)$$

where  $\{\Psi_k\}_{k=1}^N$  are orthonormalized eigenvectors of matrix  $\Sigma$ :

$$\Sigma \Psi_k = \lambda_k \Psi_k, \quad \Psi_k^T \Psi_l = \delta_{k,l} = \{1, \text{ if } k = l; 0, \text{ if } k \neq l\}, \quad k, l = \overline{1, N}, \quad (7)$$

and  $\{\lambda_k\}_{k=1}^N$  are descent ordered eigenvalues of matrix  $\Sigma$ :  $\lambda_1 \geq \lambda_2 \geq \dots \geq \lambda_N > 0$ .

Obtained values  $\tilde{y}_1, \dots, \tilde{y}_N$  are called principle components for initial observation  $x = (\tilde{x}_1, \dots, \tilde{x}_N)^T$ . The dispersion values of principle components are equal to appropriate eigenvalues and  $tr \Sigma = \sum_{k=1}^N \{\tilde{x}_k\} = \sum_{k=1}^N \{\tilde{y}_k\} = \sum_{k=1}^N \lambda_k$ . To detect informative principle components the criterion of large variability of these components is applied. Components with small dispersion are rejected and  $N^*$  first principle components  $\tilde{y}_1, \dots, \tilde{y}_{N^*}$  are used ( $N^* \leq N$ ). The number of informative components  $N^*$  is defined by the following rule [1, 2]:

$$N^*(\varepsilon) = \min\{k : 1 - \nu(k) \leq \varepsilon, k = \overline{1, N}\}, \quad \nu(k) = \sum_{l=1}^k \lambda_l / \sum_{l=1}^N \lambda_l, \quad (8)$$

where  $\varepsilon \in [0, 1)$  is a predetermined value,  $0 < \nu(k) \leq 1$  is the relative summarized dispersion fraction of first  $k$  principle components ( $\nu(N) = 1$ ).

Let new sample  $Y = \{y_1, \dots, y_n\}$  be constructed from  $X = \{x_1, \dots, x_n\}$  using principle components method (6), (7):  $y_t = f(x_t) = \Psi^N x_t$ ,  $t = \overline{1, n}$ , where  $\Psi^N = (\Psi_1 \dots \Psi_N)^T$  is  $(N \times N)$ -matrix composed of eigenvectors of matrix  $\Sigma$ . Observations  $\{y_t\}_{t=1}^n$  from  $Y$  are described by the Fisher model with the following parameters  $\{m_i\}_{i \in S}$  and  $\Sigma_y$ :

$$m_i = (m_{i,1}, m_{i,2}, \dots, m_{i,N})^T = \Psi^N \mu_i, \quad i \in S; \quad \Sigma_y = \text{diag}\{\lambda_1, \dots, \lambda_N\}. \quad (9)$$

Let  ${}_{N^*}\Delta_{yij}$  be the Mahalanobis interclass distance between classes  $\Omega_i, \Omega_j$  in the space of first  $N^*$  principle components:

$${}_{N^*}\Delta_{yij} = \sqrt{(m_i(N^*) - m_j(N^*))^T (\Sigma_y(N^*))^{-1} (m_i(N^*) - m_j(N^*))}, \quad i \neq j \in S, \quad (10)$$

where  $\{m_i(N^*) \in R^{N^*}\}_{i \in S}$  and  $\Sigma_y(N^*)$  are obtained from (9) by removal of last  $N - N^*$  rows and columns. The following theorem is true.

**Theorem.** *The Mahalanobis interclass distance  ${}_{N^*}\Delta_{yij}$  in the space of first  $N^*$  principle components ( $N^* < N$ ) is related to appropriate interclass distance  ${}_N\Delta_{yij}$  in the space of all  $N$  principle components by expression:*

$${}_{N^*}\Delta_{yij}^2 = {}_N\Delta_{yij}^2 - \sum_{l=N^*+1}^N (m_{i,l} - m_{j,l})^2 / \lambda_l, \quad i \neq j \in S, \quad (11)$$

and the inequality is true:

$${}_N\Delta_{yij}^2 - {}_{N^*}\Delta_{yij}^2 \leq |\mu_i - \mu_j|^2 \sum_{l=N^*+1}^N 1/\lambda_l, \quad i \neq j \in S, \quad (12)$$

where  $|z| = \sqrt{z^T z}$  is the Euclidean norm of vector  $z \in R^N$ .

Under  $N = N^*$  the distance (10) coincides with the appropriate distance (5) in the initial space:  ${}_N\Delta_{yij} = \Delta_{ij}$ ,  $i \neq j \in S$ .

The obtained results (11), (12) allow to investigate the efficiency of the classical procedure of principle components selection based on the rule (8). It is seen that the interclass distances decrease when features are rejected from the space of  $N$  principle components:  ${}_{N^*}\Delta_{yij} \leq {}_N\Delta_{yij}$ ,  $i \neq j \in S$ , and the value of this decreasing is inversely proportional to dispersions  $\{\tilde{y}_l\} = \lambda_l > 0$ ,  $l = \overline{N^* + 1, N}$ . Therefore the rejection of principle components with small dispersions as in (4) can cause the acute increase of the classification error probability.

## 4 Effective classification in the space of principle components

The results (11), (12) of Theorem allows to introduce new (directly connected with the classification error probability) criterion of principle component rejection. The

rejected component number  $k$  ( $k \in \{1, \dots, N\}$ ) should minimize the average decrease of interclass distances square:

$$\delta\Delta_y^2(k) = \frac{1}{L^2 - L} \sum_{i \in S} \sum_{\substack{j \in S \\ j \neq i}} ({}_N\Delta_{yij}^2 - {}_{N \setminus k}\Delta_{yij}^2) = \frac{2}{L(L-1)} \sum_{i \in S} \sum_{\substack{j \in S \\ j > i}} \frac{(m_{i,k} - m_{j,k})^2}{\lambda_k}, \quad (13)$$

where  ${}_{N \setminus k}\Delta_{yij}$  is the Mahalanobis interclass distance (10) in the space of  $N-1$  principle components after rejecting the component number  $k$ .

If under the Fisher model (1), (2) the class characteristics  $\{\pi_i, \mu_i\}_{i \in S}$ ,  $\Sigma$  are unknown then observed sample  $X = \{x_1, \dots, x_n\}$  and true classification vector  $D^o = (d_1^o, \dots, d_n^o)^T \in S^n$  allows to use their statistical estimates [1, 4]:

$$\hat{\pi}_i = \frac{n_i}{n}, \quad \hat{\mu}_i = \frac{1}{n_i} \sum_{t=1}^n \delta_{d_t^o, i} x_t, \quad i \in S; \quad \hat{\Sigma} = \frac{1}{n-L} \sum_{t=1}^n (x_t - \hat{\mu}_{d_t^o})(x_t - \hat{\mu}_{d_t^o})^T, \quad (14)$$

where  $n_i = \sum_{t=1}^n \delta_{d_t^o, i}$ . In the criterion (13) the statistical estimates  $\{\hat{m}_i\}_{i \in S}$  are calculated by applying (9):  $\hat{m}_i = \hat{\Psi}^N \hat{\mu}_i$  ( $i \in S$ ), where  $\hat{\Psi}^N = (\hat{\Psi}_1, \dots, \hat{\Psi}_N)^T$  is  $(N \times N)$ -matrix composed of eigenvectors and  $\hat{\lambda}_1 \geq \dots \geq \hat{\lambda}_N$  are eigenvalues of matrix  $\hat{\Sigma}$  from (14).

The proposed stepwise discriminant analysis procedure based on the criterion (13) transforms an initial observation  $x = (\tilde{x}_1, \dots, \tilde{x}_N)^T$  to principle components  $\tilde{y}_1^*, \dots, \tilde{y}_N^*$ :

$$\tilde{y}_j^* = \tilde{y}_{i_j}, \quad j = \overline{1, N} : \hat{\delta}\Delta_y^2(i_1) \leq \dots \leq \hat{\delta}\Delta_y^2(i_N); \quad \hat{\delta}\Delta_y^2(k) = \frac{2}{L(L-1)} \sum_{i \in S} \sum_{\substack{j \in S \\ j > i}} \frac{(\hat{m}_{i,k} - \hat{m}_{j,k})^2}{\hat{\lambda}_k},$$

where  $\tilde{y}_1, \dots, \tilde{y}_N$  are classical principle components (6), (7).

## References

- [1] Aivazyan S.A., Buchstaber V.M., Yenyukov I.S., Meshalkin L.D. (1989). *Applied Statistics: Classification and Dimensionality Reduction*. Finansy i Statistika, Moskow.
- [2] Fukunaga K. (1990). *Introduction to Statistical Pattern Recognition*. Academic Press, New York.
- [3] Kharin Yu.S., Zuev N.M., Zhuk E.E. (2011). *Probability Theory, Mathematical and Applied Statistics*. BSU, Minsk.
- [4] Zhuk E.E., Serikova E.V. (2007). "Compression" of the Multivariate Probability Mixtures with Keeping the Interclass Distances. *Computer Data Analysis and Modeling: Complex Stochastics Data and Systems: Proc. of the Eighth Intern. Conf.* Vol. 1, pp. 190-193.

# IMPLEMENTATION OF GENERALIZED ADDITIVE MODELS FOR SPATIAL BETA REGRESSION

E. ZIKARIENĖ, K. DUČINSKAS

*Institute of Data Science and Digital Technologies, Vilnius University  
Vilnius, LITHUANIA*

e-mail: egle.zikariene@gmail.com, k.ducinskas@gmail.com

## Abstract

Beta regression models are proposed by [1] to model the continuous variates that assume values in the standard unit interval, e.g. rates, proportions or concentration, or inequality indices. These models belong to the class of generalized linear mixed models (GLM) or more general generalized additive models (GAM) with responses belonging to the exponential family. In present study we use GAM to model spatial Beta data. We develop the Monte Carlo version of EM algorithm for obtaining of penalized maximum likelihood estimators of model parameters. This method is applied to real data set on Black carrageen concentration index to obtain a model of its distribution over the southeastern Baltic Sea.

**Keywords:** spatial Beta regression, generalized additive model, data science

## 1 Introduction

GLM [3] and GAM [4] have become one of the standard tools for analyzing the impact of covariates on possibly non-Gaussian response variables. The only difference between GAM and GLM is that GAM permits the including nonlinear smooth functions in the model. A crucial question in setting up a spatial GAM for a particular application is how to model various spatial covariate effects. We focus on spatial GAM. The spatial dependence in this type of models can be taken into account by the introducing covariance functions of location specific random effects or/and by implementing smooth spatial functions in the mean structure. We develop the latter one.

We will restrict our attention to the linear effects represented by regressors and nonlinear smoothed spatial effects. In present study we apply GAM for modeling the distribution of particular species of algae (Black carrageen) over southeastern Baltic sea. Reddish-brown to nearly black in colour Black carrageen belongs to the red algae group. They are widely used in the food industry for their thickening, gelling, and stabilizing properties. In the Lithuanian coastal waters between Palanga and Šventoji, the black carrageen forms extensive zones of dense meadows attached to different substrates of the underwater slope, such as gravel, cobble or boulders. The meadows of black carrageen are the main spawning grounds of the Baltic herrings which reproduce in spring [2] .

## 2 Model and Methods

The model is defined as follows:

(1) For any spatial location  $s$ , let  $Z(s)$  denote the response variable with marginal Beta distribution i.e.  $Z(s) \sim B(p(s), q(s))$  with reparametrized p.d.f.

$$f(z; \mu(s), \phi(s)) = \frac{\Gamma(\phi(s))}{\Gamma(\mu(s), \phi(s))\Gamma((1 - \mu(s))\phi(s))} z^{\mu(s)\phi(s)-1} (1-z)^{(1-\mu(s))\phi(s)-1}, 0 < z < 1$$

with mean and precision parameter  $\mu(s) = p(s)/p(s) + q(s)$  and  $\phi = p(s) + q(s)$ .

(2)  $x(s)$  is  $q \times 1$  vector of non-random regressors and  $\beta$  is  $q \times 1$  vector of parameters and nonlinear effect is defined by  $f(s)$  - smooth function of  $s$  (practically, smooth bivariate surface).

(3) conditionally on  $\mu(s)$ ,  $\{Z(s) : s \in D\}$  is an independent RF with marginal Beta distribution and for some link function  $h(\mu(s)) = x'(s)\beta + f(s)$ .

Suppose that  $\{s_i \in D; i = 0, 1, \dots, n\}$  is the set of spatial sites where the observations of RF are taken. The set of training sites is denoted by indexing spatial sites using integers, i.e.  $s_i = i, i = 0, 1, \dots, n$ , denote the set of training sites by. In what follows we use notations  $Z(s_i) = Z_i, x(s_i) = x_i, \mu(s_i) = \mu_i, \phi(s_i) = \phi_i$  and  $Z = (Z_1, Z_2, \dots, Z_n)'$ .

Then log-likelihood function based on  $Z$  is

$$L(z; \beta) = \sum_{i=1}^n l_i(z_i; \mu_i, \phi_i),$$

where

$$l_i(z_i; \mu_i, \phi_i) = \ln\Gamma(\phi_i) - \ln\Gamma(\mu_i, \phi_i) - \ln\Gamma((1 - \mu_i)\phi_i) \\ + (\mu_i\phi_i - 1)\ln z_i + ((1 - \mu_i)\phi_i - 1)\ln(1 - z_i)$$

The objective function is based on penalized likelihood

$$p(z; \beta, \lambda) = -L(z; \beta) + g(\lambda, \beta),$$

where  $g(\lambda, \beta)$  is smooth penalty function.

Model parameters are estimated by minimization of this objective function, algorithm realized in function GAM of package mgcv for statistical system R.

### 3 Applications

Black carrageen concentration data used in this paper was sampled at 318 (1m×1m) plots in the southeastern Baltic Sea. We apply GAM with the concentration index of Black carrageen as Beta response variable with p.d.f. specified above with logit link function i.e.

$$h(\mu(s)) = \ln(\mu(s)/(1 - \mu(s)))$$

Regressors, which are used in the model as a term of link function specified above are assumed to be the following:

- $x_1$  - Secchi depth,
- $x_2$  - wave generated orbital near-bottom velocity,

Table 1: Parameter values and significance

	Estimate	Std	Error z value	Pr(>  z )
$\beta_0$	-2.18300	0.08208	-26.596	$< 2e - 16$
$\beta_1$	-0.11162	0.03929	-2.841	0.0045
$\beta_2$	-0.14281	0.04796	-2.978	0.0029
$\beta_3$	0.21161	0.09401	2.251	0.0244

$x_3$  - distance to sand.

Due to the large differences in the scales of the regressors and the response variable we decide to standardise the regressors. Geographic coordinates longitude and latitude are considered as components of location  $s$ .

After preliminary peerwise analysis of variants we conclude that regressors  $x_1$  and  $x_2$  need to be replaced by  $x_1^2$  and  $x_2^2$ . So the model of link function at location  $s$  has the form:

$$\ln\{\mu(s)/(1 - \mu(s))\} = \beta_0 + x_1^2(s)\beta_1 + x_2^2(s)\beta_2 + x_3(s)\beta_3 + f(s).$$

Stationary isotropic bivariate Gaussian RF with exponential covariance function is used for smoothing. Using methods implemented in GAM we obtain REML estimates of parameters and their significance that is presented in Table 1.

High significance of these and pseudo R-squared 0,584 give us strong argument to use the proposed method for mapping the algae distribution over the whole area of interest.

## References

- [1] Ferrari S.L.P., Cribari-Neto F. (2004). Beta Regression for Modelling Rates and Proportions. *Journal of Applied Statistics*. Vol. **31**, pp. 799–815.
- [2] Morkvėnas Ž., Daunys D. (2015). *The Book of the Sea. The Realms of the Baltic Sea*. Baltic Environmental Forum, Vilnius.
- [3] Zhang Y. (2002). On Estimation and Prediction for Spatial Generalized Linear Mixed Models. *Biometrics*. Vol. **58**, pp. 129-136.
- [4] Wood S.N. (2017). *Generalized Additive Models: An Introduction with R (2nd Edition)*. Chapman and Hall/CRC, Boca Raton.

# REGENERATIVE SIMULATION OF TIME-SHARING QUEUEING SYSTEM IN RANDOM ENVIRONMENT

A.V. ZORINE

*N.I. Lobachevsky State University of Nizhni Novgorod*

*Nizhni Novgorod, RUSSIA*

e-mail: `andrei.zorine@itmm.unn.ru`

## Abstract

Time-sharing queueing systems in random environments allow only a limited-depth analytical study. In particular, the coinciding necessary and sufficient conditions for the stationary probability distribution existence and an optimization problem for mean total sojourn cost per working tact can be solved only under much stricter assumptions about the time structure of input flows. In this talk a regenerative method is discussed in its application to Monte-Carlo simulation of the class of queueing systems.

**Keywords:** data science, random environment, regenerative simulation

## 1 Introduction

Time-sharing queueing systems [1] is a family of multi-class queueing system with Bernoulli feedback. In the more modern queueing theory language they can be described as polling systems with state-dependent routing and Bernoulli feedback. Two main questions are of fundamental interest about such queueing systems, namely the stability conditions and the optimal control policy. In the seminal works [1, 2] it was assumed that the input flows are Poisson. Such assumption, typical for an early stage of study of almost any queueing model, made it feasible to obtain a simple condition, both necessary and sufficient at the same time, for the existence of a stationary probability distribution of the queueing process. The authors employed different techniques to obtain stationarity conditions. In [1] it was a combination of the the mean-drift test due to Moustafa and a limit theorem for regenerative processes. In [2], only an embedded chain was considered, and an original iterative-dominating approach was applied. Furthermore, in the cited papers two different optimization objectives were considered: a long-run time-average for sojourn cost of all jobs, and the stationary mean sojourn cost of all customers per one operational tact of the server. But the so-called Klimov's priority indices were shown to minimize both objectives.

In [3], a time-sharing queueing system was considered whose input flows were modulated by a two-state Markov chain. Some stationarity conditions were found, some of them were sufficient, and the others were necessary, and the stationary mean sojourn cost of all customers was chosen as an objective for the optimization problem. A rigorous proof for the optimality of Klimov's indices was possible only under certain stricter assumptions on the batch sizes distributions together with service times and setup times distribution functions. So, a computer-aided simulation was needed to

investigate the optimality properties of Klimov's indices. An approach with burn-in period and a quasi-stationary period was used that time. The purpose of the present research is to redo experimental study using the regenerative simulation.

## 2 Time-sharing system in random environment and optimal control problem

There are  $m < \infty$  input flows (of jobs)  $\Pi_1, \Pi_2, \dots, \Pi_m$  in the system. Jobs from these flows are called *primary jobs*. The flows are modulates by a random environment with two states,  $e^{(1)}$  and  $e^{(2)}$ . During the time the environment is in  $e^{(k)}$  the flow  $\Pi_j$  ( $j = 1, 2, \dots, m$ ) is a Poisson flow of batches, with the intensity  $\lambda^{(k)}$  of batch arrivals, and the probability  $p_x^{(j,k)}$  of batch size  $x = 1, 2, \dots$ . Jobs from  $\Pi_j$  join an infinite capacity FIFO buffer  $O_j$ . The server has  $n = m + 1$  states:  $\Gamma^{(1)}, \Gamma^{(2)}, \dots, \Gamma^{(n)}$ . In the state  $\Gamma^{(r)}$  only a job from  $O_r$  is serviced,  $r = 1, 2, \dots, m$ . In the state  $\Gamma^{(n)}$  the server doesn't serve jobs but performs inner setup. The server selects a queue for service according to some 'switching function'  $h(\cdot)$  as follows: if the queue sizes make a nonzero vector  $x = (x_1, x_2, \dots, x_m)$  at the decision moment, then the service starts for the queue  $O_j$  with  $j = h(x)$ . Here  $h(\cdot)$  denotes a mapping of the  $m$ -dimensional non-negative integer lattice  $X = \{0, 1, \dots\}^m$  onto  $\{1, 2, \dots, n\}$ , and  $h(x) = j$  implies  $x_j > 0$  for  $j = 1, 2, \dots, m$ . Only the zero vector  $\bar{0} = (0, 0, \dots, 0) \in X$  is mapped to  $n$ . But if the queues are empty at the decision moment, the first arriving job will occupy the server. Jobs are serviced without interruption. A service time for a job from queue  $O_j$  has a probability distribution function  $B_j(t)$  ( $B_j(0) = 0$ ). Besides ordinary service, the server needs some sort of setup times after each service. No job is serviced during setup intervals. The probability distribution function for a setup time after a queue  $O_j$  was serviced is  $\bar{B}_j(t)$  ( $\bar{B}_j(0) = 0$ ). Service durations and setup durations are mutually independent and independent of the input flows. After service, the job from queue  $O_j$  can be instantly transferred to a queue  $O_r$  with probability  $p_{j,r}$ , thus forming a *secondary* flow, or leave the system with probability  $p_{j,n} = 1 - \sum_{r=1}^m p_{j,r}$ , where ( $n = m + 1$ ). So, both primary and secondary flows enter the system. The external random environment is synchronous with the service-and-setup process. It can change states only at service termination epochs and setup termination epochs. Let the environment state be a homogeneous irreducible aperiodic Markov chain. The probability for this Markov chain to go from the state  $e^{(k)}$  to the state  $e^{(l)}$  in one step is  $a_{k,l}$ .

Let  $I_m$  be the  $m \times m$  identity matrix,  $Q = (p_{j,r})_{j,r} = \overline{1, m}$ . It will be assumed throughout this paper that:

- 1) a matrix  $(I_m - Q)$  is invertible;
- 2) the moments  $\beta_{j,s} = \int_0^\infty t^s dB_j(t)$ ,  $\bar{\beta}_{j,s} = \int_0^\infty t^s d\bar{B}_j(t)$  are finite for  $s = 1, 2$ ;
- 3) batch size moments  $\mu_{j,s}^{(k)} = \sum_{x=1}^\infty x^s p_x^{(j,k)}$  are finite for  $s = 1, 2$ .

Let  $\tau_0 = 0$  and  $\tau_i$  be the end of the  $i$ -th working tact (these are both service periods and setup periods). Denote by  $\Gamma_0 \in \Gamma = \{\Gamma^{(1)}, \Gamma^{(2)}, \dots, \Gamma^{(n)}\}$  the initial server

state at time  $\tau_0$ , by  $\Gamma_i \in \Gamma$  the server state during the time interval  $(\tau_{i-1}, \tau_i]$ , by  $\kappa_i = (\kappa_{1,i}, \kappa_{2,i}, \dots, \kappa_{m,i})$  the vector of queues sizes at time instant  $\tau_i$ , by  $\chi_i$  the random environment state during the time interval  $(\tau_i, \tau_{i+1}]$ . Then, under the model assumptions, the stochastic sequence  $\{(\Gamma_i, \kappa_i, \chi_i), i = 0, 1, \dots\}$  is a periodic homogeneous irreducible Markov chain.

Denote by  $Q^{(r,k)}(x)$  the stationary probability of the event  $\{\Gamma_i = \Gamma^{(r)}, \kappa_i = x, \chi_i = e^{(k)}\}$ . It was also proven by direct computation, that the stationary probabilities

$$\sum_{x \in X} (Q^{(r,1)}(x) + Q^{(r,2)}(x)), r = 1, 2, \dots, m, \text{ and } \sum_{k=1}^2 Q^{(n,k)}(\bar{U}) \left( \lambda_1^{(k)} + \dots + \lambda_m^{(k)} \right)^{-1}$$

are independent of the switching function  $h(\cdot)$  under either of the two conditions: *i*)  $a_{1,2} = a_{2,2}$ , or *ii*)  $a_{1,2} \neq a_{2,2}$  and  $\lambda_j^{(1)} \mu_{1,j}^{(1)} = \lambda_j^{(2)} \mu_{1,j}^{(2)}$  for all  $j = 1, 2, \dots, m$ .

Now, let  $\zeta_{j,i}$  be the total time sojourn time of all jobs in the queue  $O_j$  during the time interval  $(\tau_i, \tau_{i+1}]$ . Further, let the sojourn cost  $c_j$  per time unit be given for the queue  $O_j$ ,  $j = 1, 2, \dots, m$ . We consider the mean sojourn cost

$$\mathcal{J}_i(h) = \sum_{j=1}^m (c_j \zeta_{j,i}) \quad (1)$$

as a measure of the control quality. In the stationary case  $\mathcal{J}_i(h) = \mathcal{J}(h)$ . Again, it was proved that Klimov's priority indices are optimal with respect to the objective function  $\mathcal{J}(h)$  when either *i*)  $a_{1,2} = a_{2,2}$ , or *ii*)  $a_{1,2} \neq a_{2,2}$ ,  $\lambda_j^{(1)} \mu_{1,j}^{(1)} = \lambda_j^{(2)} \mu_{1,j}^{(2)}$  and  $\lambda_j^{(1)} \mu_{2,j}^{(1)} = \lambda_j^{(2)} \mu_{2,j}^{(2)}$  for all  $j = 1, 2, \dots, m$

### 3 Regenerative simulation of time-sharing queueing system

A computer-aided simulation model was constructed using the cybernetic approach [5]. Simulation takes place in discrete time scale  $\{\tau_i, i = 0, 1, \dots\}$ . A multivariate stochastic sequence  $\{Y_i, i = 1, 2, \dots\}$  with  $Y_i = (\tau_i - \tau_{i-1}, \Delta_i, \Gamma_i, \chi_i, \kappa_i, \tilde{\eta}_{i-1}; \tilde{\zeta}_{1,i-1}, \dots, \tilde{\zeta}_{m,i-1})$  is generated where  $\Delta_i$  is the server idle time during the tie interval  $(\tau_{i-1}, \tau_i]$ ,  $\tilde{\eta}_i = (\tilde{\eta}_{1,i}, \dots, \tilde{\eta}_{m,i})$ ,  $\tilde{\eta}_{j,i} = 1$  if a job from  $O_r$ ,  $\Gamma^{(r)} = \Gamma_i$ , is placed into  $O_j$  after having been serviced in the time interval  $(\tau_{i-1}, \tau_i]$ , otherwise  $\tilde{\eta}_{j,i} = 0$ ,  $\tilde{\zeta}_{j,i} = (\zeta_{j,i}(1), \dots, \zeta_{j,i}(\kappa_{j,i}))$ ,  $\tilde{\zeta}_{j,i}(x)$  is the total amount of time spent in the queueing system by the  $x$ -th job in the queue  $O_j$  by the time  $\tau_i$ . Then

$$\zeta_{j,i} = \sum_{x=1}^{\kappa_{j,i}} \min\{\tau_i - \tau_{i-1}, \tilde{\zeta}_{j,i}\} \quad (2)$$

and  $\mathcal{J}_i(h) = (f(Y_i))$  with  $f(\cdot)$  defined by (1) and (2).

The sequence  $\{Y_i, i = 0, 1, \dots\}$  is a general Markov chain and at the same time a discrete-time regenerative process with a corresponding sequence  $T_1 = \min\{i \geq 0: \kappa = \bar{U}, \Gamma_i = \Gamma^{(n)}, \chi_i = e^{(1)}\}$ ,  $T_{s+1} = \min\{i \geq T_s: \kappa = \bar{U}, \Gamma_i = \Gamma^{(n)}, \chi_i = e^{(1)}\}$ ,  $s = 1, 2, \dots$  of regeneration epochs [4]. Let  $Y_\infty$  be a random vector with the same probability

distribution as the stationary probability distribution of  $\{Y_i, i = 1, 2, \dots\}$ . In ergodic case,  $N^{-1}(f(Y_1) + f(Y_2) + \dots + f(Y_N)) \rightarrow f(Y_\infty)$  a.s. The regenerative method consists in using  $\left(\left[\sum_{i=T_s}^{T_{s+1}-1} f(Y_i)\right]\right)((T_{s+1} - T_s))^{-1}$  to evaluate  $f(Y_\infty)$ . This approach also allows to obtain a confidence interval for  $f(Y_\infty)$  based on a sequence  $(V_1, \alpha_1), (V_2, \alpha_2), \dots, (V_N, \alpha_N)$  of i.i.d. vectors, where  $V_s = \sum_{i=T_s}^{T_{s+1}-1} f(Y_i)$  and  $\alpha_s = T_{s+1} - T_s$  is the regenerative cycle length.

Let us consider now the load  $\rho$  of the queuing system, i.e. the fraction of time the queuing system is non-empty. Since in ergodic case  $1 - \rho$  equals

$$\lim_{N \rightarrow \infty} \left(\sum_{i=1}^N g_1(Y_i)\right) \left(\sum_{i=1}^N g_2(Y_i)\right)^{-1} = \frac{g_1(Y_\infty)}{g_2(Y_\infty)} = \left(\left[\sum_{i=T_s}^{T_{s+1}-1} g_1(Y_i)\right]\right) \left(\left[\sum_{i=T_s}^{T_{s+1}-1} g_2(Y_i)\right]\right)^{-1}$$

where the mapping  $g_1(t, d, \Gamma^{(r)}, e^{(e)}, x, w; z_1, z_2, \dots, z_m)$  for  $x = (x_1, \dots, x_m)$ ,  $z_j = (z_j(1), \dots, z_j(x_j))$  equals  $(t - d)$  if  $r \neq n$ , it equals 0 otherwise, and the mapping  $g_2(t, \Gamma^{(r)}, e^{(e)}, x, w; z_1, \dots, z_m) = t$ , the regenerative method is also applicable to evaluate the ration of means along a cycle and to obtain a confidence interval for the ratio estimator when one sets  $V_s = \sum_{i=T_s}^{T_{s+1}-1} g_1(Y_i)$  and  $\alpha_s = \sum_{i=T_s}^{T_{s+1}-1} g_2(Y_i)$  instead of the cycle length.

Results of the computational experiments will be included in the talk.

## References

- [1] Klimov G.P. (1974). Time-sharing queueing systems. I. *Probability theory and its applications*. Vol. **XIX**, No. 3, pp. 558-576.
- [2] Fedotkin M.A. (1999) Optimal control for conflict flows and marked point processes with selected discrete component. II. *Lietuvos matematikos rinkibys*. Vol. **29**, No. 1, pp. 148-159. (in Russian)
- [3] Zorine A.V., Fedotkin M.A. (2005). Optimization of control of doubly stochastic nonordinary flows in time-sharing systems. *Automation and remote control*. Vol. **66**, No. 7, pp. 1115-1124.
- [4] Crane M.A., Lemoine A.J. (1977) *An introduction to the regenerative method for simulation analysis*. Springer-Verlag, Berlin Heidelberg New York.
- [5] Zorine A.V. (2014) A Cybernetic Model of Cyclic Control of Conflicting Flows with an After-Effect. *Uchenye Zapiski of Kazan University. Physics and Mathematics Series*. Vol. **156**, No. 3, pp. 66-73 (in Russian).

# NUMBER OF PAIRS OF IDENTICALLY MARKED TEMPLATES IN $q$ -ARY TREE

A.M. ZUBKOV, V.I. KRUGLOV

*Steklov Mathematical Institute of Russian Academy of Sciences*

*Moscow, RUSSIA*

e-mail: zubkov@mi-ras.ru, kruglov@mi-ras.ru

## Abstract

Let the vertices of a complete  $q$ -ary tree be assigned independent random marks having uniform distribution on a finite alphabet. We consider pairs of identically marked embeddings of a given subtree template. An asymptotic formula for the expectation of the number of such pairs is obtained and the Poisson limit theorem for this number is proposed.

**Keywords:** data science,  $q$ -ary tree, template, Poisson limit theorem

## 1 Introduction

Repetitions of unusual events are often perceived as manifestations of hidden regularities. Therefore, it is important to have information on the possible values of probabilities of complex events repetition in sets of independent random variables (that is, in cases if there are no any regularities).

The problems associated with repetitions of patterns in trees with randomly marked vertices were investigated by many authors. Distribution of the numbers of given subtrees in random trees were studied in [4, 5]. Problems of such kind arise in computer science, e. g. [6] and [7].

Results on the random number of coincidences of marks for chains of vertices in a randomly marked binary or  $q$ -ary tree were obtained by the authors in [1] and in [3]. In the present paper we consider distribution of the number of pairs of identically marked subtree in the  $q$ -ary tree with random independent marks of vertices.

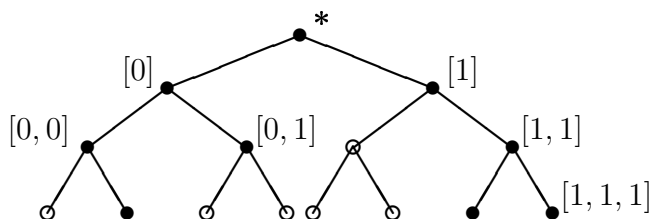
## 2 Main results

Let  $T_q^n$  be a complete  $q$ -ary tree of height  $n$ . We will denote the root of the tree by the symbol  $*$  and assume that it forms the layer  $I^{(0)}$  of vertices. For any  $k = 1, \dots, n$  the layer  $I^{(k)}$  consists of  $q^k$  vertices  $\alpha = [i_1, i_2, \dots, i_k]$ , where  $i_1, i_2, \dots, i_k \in \{0, 1, \dots, q-1\}$ . The root  $*$  is connected by  $q$  outgoing edges with vertices  $[0], [1], \dots, [q-1] \in I^{(1)}$ , for  $k = 1, \dots, n-1$  any vertex  $\alpha = [i_1, i_2, \dots, i_k]$  of layer  $I^{(k)}$  is connected by  $q$  outgoing edges with vertices  $[\alpha, j] = [i_1, i_2, \dots, i_k, j]$ ,  $j = 0, 1, \dots, q-1$  of layer  $I^{(k+1)}$ . Any vertex  $\alpha = [i_1, i_2, \dots, i_k]$  with  $k > 1$  is connected by incoming edge with vertex  $\alpha^- = [i_1, i_2, \dots, i_{k-1}]$ , and if  $k = 1$ , then it is connected by incoming edge with the root  $* = [0]^- = [1]^- = \dots = [q-1]^-$ . For vertex  $\alpha \in I^{(k)}$  we define its *height* as  $h(\alpha) = k$ . If  $\alpha = [i_1, i_2, \dots, i_k]$ ,  $\beta = [j_1, j_2, \dots, j_m]$ , then  $[\alpha, \beta] \stackrel{\text{def}}{=} [i_1, i_2, \dots, i_k, j_1, j_2, \dots, j_m]$ ,  $[\alpha, *] \stackrel{\text{def}}{=} [i_1, i_2, \dots, i_k]$ .

We define natural lexicographical order on the set of vertices of  $T_q^n$ :  $\prec$  if either  $h(\cdot) < h(\cdot)$  or  $h(\cdot) = h(\cdot) = k \in \{1, 2, \dots, n\}$ ,  $\cdot = [i_1, \dots, i_k]$ ,  $\cdot = [j_1, \dots, j_k]$  and  $\sum_{m=1}^k i_m q^{k-m} < \sum_{m=1}^k j_m q^{k-m}$ .

**Definition 1.** A *template* is a subtree  $B$  of the tree  $T_q^n$  with the root  $*$  and  $|B|$  vertices  ${}^{[B]}_0 = * \prec {}^{[B]}_1 \prec \dots \prec {}^{[B]}_{|B|-1}$ . The *height*  $h(B)$  of the template  $B$  is the value  $h$  such that  ${}^{[B]}_{|B|-1} \in I^{(h)}$ . For  $\cdot \in I^{(k)}$ ,  $0 \leq k \leq n - h(B)$ , the *embedding*  $B(\cdot)$  of the template  $B$  into the tree  $T_q^n$  is the subtree of the tree  $T_q^n$  with vertices  $\cdot = [{}^{[B]}_0] \prec [{}^{[B]}_1] \prec [{}^{[B]}_2] \prec \dots \prec [{}^{[B]}_{|B|-1}]$ .

**Example:** the figure for  $q = 2$  shows the template  $B$  with  $h(B) = 3$ ,  $|B| = 9$  and vertices  ${}^{[B]}_0 = * \prec {}^{[B]}_1 = [0] \prec {}^{[B]}_2 = [1] \prec {}^{[B]}_3 = [0, 0] \prec {}^{[B]}_4 = [0, 1] \prec {}^{[B]}_5 = [1, 1] \prec {}^{[B]}_6 = [0, 0, 1] \prec {}^{[B]}_7 = [1, 1, 0] \prec {}^{[B]}_8 = [1, 1, 1]$ .



Let any vertex  $\cdot$  of the tree  $T_q^n$  be assigned a random mark  $m(\cdot)$  taking values in the set  $\{1, \dots, d\}$  such that random variables  $m(\cdot)$ ,  $\cdot \in T_q^n$ , are independent and  $\{m(\cdot) = j\} = \frac{1}{d}$ ,  $j \in \{1, \dots, d\}$ , for all  $\cdot \in T_q^n$ . For any embedding  $B(\cdot)$  of template  $B$  we have the ordered set  $M(B(\cdot)) = (m([{}^{[B]}_k]), k = 0, 1, \dots, |B| - 1)$  of random marks on subtree  $B(\cdot)$  vertices.

Obviously, if for some vertices  $\cdot, \dots$ , subtrees  $B(\cdot), \dots, B(\cdot)$  are pairwise nonintersecting, then the corresponding sets of marks  $M(B(\cdot)), \dots, M(B(\cdot))$  are independent and have equiprobable distribution on the set  $\{1, \dots, d\}^{|B|}$ .

In the present paper we consider distributions of the number of pairs of identically marked embeddings of a given template  $B$  (depending on  $n$ ) that cannot be extended to the root, i.e. distributions of sums of indicators

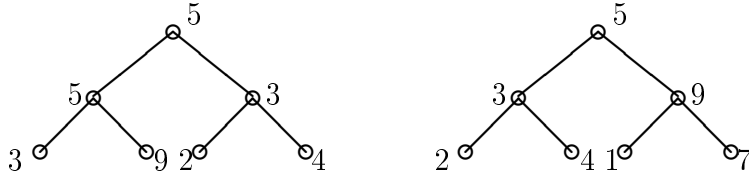
$$X_{\cdot, B} = \{M(B(\cdot)) = M(B(\cdot)), m(\cdot) \neq m(\cdot)\}, \quad \cdot \in \bigsqcup_{k=0}^{n-h(B)+1} I^{(k)}, \prec$$

(for  $\cdot = * \prec$  the condition  $m(\cdot) \neq m(\cdot)$  is considered to be valid automatically).

**Example:** let us consider for a binary tree a template  $B$  with  $h(B) = 1$  and  $|B| = 3$



and two fragments of the binary tree marked as follows:



here we suppose that the vertex preceding the root of the right fragment has the mark not equal to 5. Then in these fragments there are one non-extendable to the root coincidence of labels on the template  $B$  embeddings with marks 5, 3, 9, and another coincidence of the template  $B$  embeddings formed by the vertices with marks 3, 2, 4, the latter coincidence may be extended to the root and therefore is not accounted.

For any natural  $n$  and template  $B = B_n$  of height  $h_n = h(B_n)$  we consider random variables

$$V_{n,B_n} = \sum_{\cdot \in T_q^{n-h_n} : \prec} X_{\cdot, B_n} \quad \text{and} \quad \tilde{V}_{n,B_n} = \sum_{(\cdot) \in \mathcal{P}_{n,B_n}} X_{\cdot, B_n},$$

where

$$\mathcal{P}_{n,B_n} = \{(\cdot): \cdot \in T_q^{n-h_n}, * \prec \prec, \neq [\cdot] \forall: h(\cdot) \leq h_n + 1\}.$$

Somewhat artificial restrictions (fixed template  $B_n$ , the condition  $m(\cdot) \neq m(\cdot)$ , the definition of the set  $\mathcal{P}_{n,B_n}$ ) are made to simplify the statement and the proof of the weak convergence of sums  $V_{n,B_n}$  and  $\tilde{V}_{n,B_n}$  to the Poisson distribution as  $n \rightarrow \infty$ .

Lexicographical order on the set of vertices of the tree  $T_q^n$  has, in particular, the following property: if  $\prec$ , then the same relation is valid for any two corresponding vertices of embeddings  $B(\cdot)$  and  $B(\cdot)$  of the template  $B$ :  $[\cdot]_k^{[B]} \prec [\cdot]_k^{[B]}$ ,  $1 \leq k < |B|$ . Thus in the sequence  $m(\cdot) \neq m(\cdot)$ ,  $m([\cdot]_k^{[B]}) = m([\cdot]_k^{[B]})$ ,  $k = 0, 1, \dots, |B| - 1$ , each equality contains at least one new vertex of the subtree  $B(\cdot)$ . From this observation and assumption on independence and uniformity of distribution of marks it follows that for each equality in the sequence the conditional probability that it is valid (conditionally on the validity of all previous equalities) equals to the unconditional probability of its validity, i. e. that for  $\prec$

$$X_{\cdot, B} = \{X_{\cdot, B} = 1\} = \begin{cases} \frac{d-1}{d^{|B|+1}}, & \text{if } \neq *, \\ \frac{1}{d^{|B|}}, & \text{if } = *. \end{cases}$$

**Theorem 1.** *If  $n, h_n = h(B_n) \rightarrow \infty$  in such a way that  $n - h_n \rightarrow \infty$ , then*

$$V_{n,B_n} = \frac{d-1}{d^{|B_n|+1}} \frac{q^{2(n-h_n+1)}}{2(q-1)^2} (1 + o(1)),$$

$$0 \leq V_{n,B_n} - \tilde{V}_{n,B_n} = o(V_{n,B_n}).$$

**Corollary 1.** *If  $n, h_n = h(B_n) \rightarrow \infty$  in such a way that  $n - h_n \rightarrow \infty$  and  $V_{n,B_n}$  is bounded, then  $\{\tilde{V}_{n,B_n} = V_{n,B_n}\} \rightarrow 1$ .*

We will use the following notation:  
 $\mathcal{L}(V)$  is the distribution of random variable  $V$ ,  
 $\text{Pois}(\lambda)$  is the Poisson distribution with parameter  $\lambda$ ,  
 $d_{\text{tv}}(P, Q)$  is the total variation distance between distributions  $P$  and  $Q$ .

**Theorem 2.** *If  $n, h_n = h(B_n) \rightarrow \infty$  in such a way that  $n - 2h_n \rightarrow \infty$ , then for some function  $\varepsilon(n) = o(1), n \rightarrow \infty$ , the following inequality is valid:*

$$d_{\text{tv}}(\mathcal{L}(\tilde{V}_{n,B_n}), \text{Pois}(\tilde{V}_{n,B_n})) \leq \frac{16 \left(1 - \exp(-\tilde{V}_{n,B_n})\right) \tilde{V}_{n,B_n}}{q^{n-2h_n-1}} (1 + \varepsilon(n));$$

if we also have  $q^n = o(d^{|B_n|})$ , then

$$d_{\text{tv}}(\mathcal{L}(\tilde{V}_{n,B_n}), \text{Pois}(\tilde{V}_{n,B_n})) \rightarrow 0.$$

Proofs of these theorems may be found in [2].

## References

- [1] Zubkov A.M., Kruglov V.I. (2016). On coincidences of tuples in a binary tree with random labels of vertices. *Discrete Math. Appl.* Vol. **26:3**, pp. 145-153.
- [2] Kruglov V., Zubkov A. (2017). Number of Pairs of Template Matchings in q-ary Tree with Randomly Marked Vertices. *Analytical and Computational Methods in Probability Theory, Lecture Notes in Comput. Sci.* Vol. **10684**, pp. 336-346.
- [3] Kruglov V.I. (2018). On coincidences of tuples in a q-ary tree with random labels of vertices. *Discrete Math. Appl.* Vol. **28:5**, pp. 293-307.
- [4] Hoffmann C.M., O'Donnell M.J. (1982). Pattern matching in trees. *J. ACM* Vol. **29:1**, pp. 68-95.
- [5] Steyaert J.-M., Flajolet P. (1983). Patterns and pattern-matching in trees: an analysis. *Inf. and Control* Vol. **58:1**, pp. 19-58.
- [6] Singh G., Smolka S.A., Ramakrishnan I.V. (1988). Distributed algorithms for tree pattern matching. *Lect. Notes Comput. Sci.* Vol. **312**, pp. 92-107.
- [7] Tahraoui M.A., Pinel-Sauvagnat K., Laitang C., Boughanem M., Kheddouci H., Ning L. (2013). A survey on tree matching and XML retrieval. *Computer Science Review.* Vol. **8**, pp. 1-23.

# A FORMULA FOR EUROPEAN OPTIONS COSTS CALCULATION

N.M. ZUEV

*Belarusian State University*

*Minsk, BELARUS*

e-mail: ZuevNM@bsu.by

## Abstract

The problem of European options calculation is considered. The recursive equations for the major characteristics are obtained.

**Keywords:** European option, recursive equations, starting capital

## 1 Main Result

Consider a  $(B,S)$ -market [1].

Let  $S_n$  be the cost of a risky active unit at the time moment  $n$ . Suppose it follows the model:

$$S_n = S_0(1 + \rho_1) \dots (1 + \rho_n),$$

where  $\rho_k$ ,  $k = 1, \dots, n$ , are the interest rates that are changing stochastically. Let  $B_n$  be the cost of a non-risky active unit at the time moment  $n$ :

$$B_n = B_0(1 + r_1) \dots (1 + r_n),$$

where  $r_k$ ,  $k = 1, \dots, n$  are supposed to be constant further. that depends on the random variables  $\rho_1, \dots, \rho_{n-1}$  only. Denote by  $\pi_n = (\beta_n, \gamma_n)$  the portfolio at the time moment  $n$ , where  $\beta_n$  is the number of non-risky active units at the time moment  $n$ ,  $\gamma_n$  is the number of risky active units at the time moment  $n$ ,  $n = 1, \dots, N$ ;  $N$  is the terminal moment, at this moment the option is executed. Denote by  $f_N$  the payment function that depends on random variables  $\rho_1, \dots, \rho_N$  only. In case of a standard purchase of the European option,  $f_N = (S_N - K)^+$  are the losses of the option seller for a risky active unit. Let  $K$  be the contract price for the purchase of a risky active unit at the time moment  $N$ . The variables  $\beta_n, \gamma_n$  are under prediction, and are supposed to depend on  $\rho_1, \dots, \rho_{n-1}$  only. Let  $X_n = \beta_n B_n + \gamma_n S_n$  be the portfolio cost at the time moment  $n$ .

The problem of calculation of a European option is concentrated on the choice of the starting capital  $X_0 > 0$  (the option cost) and the portfolio  $\pi_n = (\beta_n, \gamma_n)$ ,  $n = 1, \dots, N$ , so that  $E\{X_N - f_N\} = 0$  and  $D\{X_N - f_N\}$  would be minimal.

Denote for convenience:  $\tilde{X}_n = X_n/B_n$ ,  $\tilde{S}_n = S_n/B_n$ ,  $\bar{\rho}_n = (\rho_1, \dots, \rho_n)$ ,  $\tilde{f}_n = f_n/B_n$ .

**Theorem 1.** [2] For the self-financing portfolio  $\pi_n = (\beta_n, \gamma_n)$ ,  $n = 1, \dots, N$ , the values  $X_0, \beta_n, \gamma_n$  are calculated recursively from the following equations:

$$\gamma_n = \frac{E\{\Delta(\tilde{S}_n)\tilde{f}_m \mid \bar{\rho}_{n-1}\} - E\{\Delta(\tilde{S}_n) \mid \bar{\rho}_{n-1}\}E\{\tilde{f}_m \mid \bar{\rho}_{n-1}\}}{D\{\Delta(\tilde{S}_n) \mid \bar{\rho}_{n-1}\}}, \quad (1)$$

$$\begin{aligned} \tilde{f}_{n-1} &= E\{\tilde{f}_n \mid \bar{\rho}_{n-1}\} - \gamma_n E\{\Delta(\tilde{S}_n) \mid \bar{\rho}_{n-1}\}, \\ \beta_n &= \beta_{n-1} - \tilde{S}_{n-1}(\gamma_n - \gamma_{n-1}), \quad \tilde{X}_0 = \tilde{f}_0, \quad n = 1, \dots, N. \end{aligned}$$

In (1) the expectation is taken conditionally w.r.t.  $\bar{\rho}_{n-1}$ .

**Theorem 2.** *If random variables  $\rho_1, \dots, \rho_N$  are independent, then*

$$X_0 = B_0 E \left\{ \tilde{f}_N \prod_{k=1}^N N \left( 1 - \frac{(\rho_k - a_k)(a_k - r_k)}{b_k^2} \right) \right\},$$

where  $a_k = E\{\rho_k\}$ ,  $b_k^2 = D\{\rho_k\}$ .

**Proof** follows from Theorem 1.

## References

- [1] Shiryaev A.N. (1998). *Financial Mathematics*. Vol. 2. Moscow: Phasis. P. 482–1106.
- [2] Zuev N.M. (2014). Calculation of European and American type options. *Proceedings of the International Conference on Probability Theory, Random Processes, Mathematical Statistics and Applications*. Minsk: RIHS, pp. 64-66.

## Index

- Šaltytė-Vaisiauskė, 172
- Abdushukurov, 133  
Abramovich, 138  
Aleksëev, 271
- Badziahin, 142  
Bakhar, 262  
Barbiero, 13  
Belovas, 144  
Bernatavičienė, 257  
Bokun, 148  
Breitender, 32  
Brodinová, 32  
Burg, 43  
Burkatovskaya, 214, 315  
Butenko, 167
- Chubarova, 232
- Datta, 37  
Dermenzhy, 154  
Dernakova, 176  
Dreiziene, 17  
Dučinskas, 17, 172, 341  
Dzemyda, 29  
Dürre, 21
- Egorov, 158
- Fedotkin, 163  
Filzmoser, 32, 246  
Fried, 21
- Gammerman, 33  
Grimes, 37  
Grini, 167  
Groenen, 43
- Hron, 87  
Hryn, 228  
Hubin, 167
- Ignatenko, 330
- Ilmonen, 79  
Ionkina, 191  
Iskandarov, 335
- Kachan, 219  
Kako, 253  
Karaliutė, 172  
Kharin, 51, 176, 183, 298  
Kharin A., 187  
Kislach, 183  
Kolchin, 191  
Kollo, 65  
Kopats, 194  
Kornet, 199  
Korvel, 257  
Kostogryzov, 203  
Kozlovsky, 138  
Krasnoproshin, 207  
Kruglov, 348  
Kubilius, 68  
Kudryavtsev, 163  
Kulyukin, 214
- Levakov, 219  
Li, 71  
Lietzén, 79  
Litvinova, 117  
Lohvinenko, 224
- Machalová, 87  
Maiti, 71  
Malugin, 228  
Mangalova, 232  
Matalytski, 194  
Matskevich, 207  
Medvedev, 199, 237  
Melekh, 232  
Mihov, 199, 242  
Mikšová, 246  
Mikhalskii, 271  
Minkevičius, 249  
Mishura, 94

Mukha, 253  
Mukherjee, 214  
  
Navickas, 257  
Nikitionak, 262  
Nistratov, 203  
Nordhausen, 79  
Novopoltsev, 228, 267  
  
Opiata, 319  
Orsingher, 102  
Ortner, 32  
  
Podolskiy, 271  
Poleshchuk, 276  
Polonetsky, 138  
Ponomarenko, 326  
  
Radavičius, 280  
Raghunath, 104  
Ralchenko, 285  
Rattihalli, 104  
Rieser, 246  
Rohm, 32  
Rosen, 65  
  
Sabaliauskas, 29  
Sakhno, 115  
Savelov, 289  
Serov, 291  
Shevlyakov, 117  
Shirokov, 117  
Soshnikova, 295  
Starodubtsev, 298  
Starodubtseva, 298  
Stelmashok, 138  
Stoimenova, 123  
Storvik, 167  
  
Talská, 87  
Tereshina, 237  
Tereshko, 262  
Tiwari, 214  
Ton, 187  
Treigys, 307  
Trough, 302  
Tsekhavaya, 302  
  
Turovskiy, 271  
  
Valge, 65  
Vaskouski, 219  
Vats, 214  
Vecherko, 311  
Venskus, 307  
Vetokhin, 262  
Virta, 79  
Voloshko, 311  
Vorobeychikov, 315  
Vostrov, 154, 319, 326  
  
Yanovich, 330  
Yareshenko, 237  
  
Zakhidov, 335  
Zhereło, 158  
Zhuk, 337  
Zikarienė, 341  
Zorine, 344  
Zubkov, 128, 291, 348  
Zuev, 352

Scientific edition

**COMPUTER DATA ANALYSIS AND MODELING:  
STOCHASTICS AND DATA SCIENCE**

Proceedings of the Twelfth International Conference  
September 18–22, 2019, Minsk

In the author's edition

Responsible for Issue V. A. Voloshko

Signed in print August 16, 2019. Format 60x84 1/8. Offset paper.  
Digital printing. Conventional printed sheets 41.85. Publisher's signatures 40.6.  
Circulation of        copies. Order

Belarusian State University.  
Certificate of state registration of the publisher, manufacturer,  
distributor of printed publications No. 1/270 of 03.04.2014.  
4 Nezavisimosti Ave., 220030, Minsk.

Republican Unitary Enterprise  
“Publishing Center of the Belarusian State University”.  
Certificate of state registration of the publisher, manufacturer,  
distributor of printed publications No. 2/63 of 19.03.2014.  
6 Krasnoarmeyskaya St., 220030, Minsk.